annual progress report

2009

ADVANCED COMBUSTION ENGINE RESEARCH AND DEVELOPMENT

U.S. DEPARTMENT OF ENERGY | Energy Efficiency & Renewable Energy

U.S. Department of Energy
1000 Independence Avenue, S.W.
Washington, D.C. 20585-0121

FY 2009 PROGRESS REPORT FOR ADVANCED COMBUSTION ENGINE RESEARCH AND DEVELOPMENT

Energy Efficiency and Renewable Energy
Office of Vehicle Technologies

Approved by Gurpreet Singh
Team Leader, Advanced Combustion Engine R&D
Office of Vehicle Technologies

December 2009

Acknowledgement

We would like to express our sincere appreciation to Alliance Technical Services, Inc. and Oak Ridge National Laboratory for their technical and artistic contributions in preparing and publishing this report.

In addition, we would like to thank all the participants for their contributions to the programs and all the authors who prepared the project abstracts that comprise this report.

Table of Contents

I. Introduction

I. Introduction

DEVELOPING ADVANCED COMBUSTION ENGINE TECHNOLOGIES

On behalf of the Department of Energy's Vehicle Technologies Program (VTP), we are pleased to introduce the Fiscal Year 2009 Annual Progress Report for the Advanced Combustion Engine Research and Development (R&D) subprogram. The mission of the VTP Program is to develop more energy-efficient and environmentally friendly highway transportation technologies that will meet or exceed performance expectations, enable the United States to use significantly less petroleum, and reduce greenhouse gas and other regulated emissions. The Advanced Combustion Engine R&D subprogram supports this mission by removing the critical technical barriers to commercialization of advanced internal combustion engines (ICEs) for passenger and commercial vehicles that meet future Federal emissions regulations. Dramatically improving the efficiency of ICEs and enabling their introduction in conventional as well as hybrid electric vehicles is the most promising and cost-effective approach to increasing vehicle fuel economy over the next 30 years. Improvements in engine efficiency alone have the potential to increase passenger vehicle fuel economy by 25 to 40 percent, and commercial vehicle fuel economy by 30 percent with a concomitant reduction in greenhouse gas emissions, more specifically, carbon dioxide emissions. These improvements are expected to be even greater when coupled with advanced hybrid electric powertrains.

The following are representative goals of the Advanced Combustion Engine R&D subprogram that can contribute to meeting national energy security, environmental, and economic objectives:

- Passenger vehicles: After successfully meeting the peak engine thermal efficiency goal of 45 percent for passenger vehicles, the goal will emphasize the use of these engines to improve vehicle fuel economy over a real-world driving cycle. More specifically, the goal is to increase the efficiency of ICEs resulting in vehicle fuel economy improvements of 25 percent for gasoline vehicles and 40 percent for diesel vehicles by 2015.
- Commercial vehicles: Increase the efficiency of ICEs from 42 percent (2010 baseline) to 50 percent (20 percent improvement) by 2015, and further improve engine efficiency to 55 percent by 2018 with demonstrations on commercial vehicle platforms.
- Solid State Energy Conversion: Increase the efficiency of thermoelectric generators to convert waste heat to electricity from eight percent to greater than 15 percent by 2015.

The passenger and commercial vehicle goals will be met while utilizing advanced fuel formulations that can incorporate a non-petroleum-based blending agent to reduce petroleum dependence and enhance combustion efficiency.

R&D activities include work on combustion technologies that increase efficiency and minimize in-cylinder formation of emissions, aftertreatment technologies that enable implementation of high-efficiency engines and further reduce exhaust emissions, as well as the impacts of these new technologies on human health. Research is also being conducted on approaches to produce useful work from engine waste heat through the development and application of thermoelectrics, electricity generation from exhaust-driven turbines, and incorporation of energy-extracting bottoming cycles. The subprogram also supports the development of critical enabling technologies such as sensors, controls, and air-handling components.

This introduction serves to outline the nature, recent progress, and future directions of the Advanced Combustion Engine R&D subprogram. The research activities of this subprogram are planned in conjunction with the FreedomCAR and Fuel Partnership and the 21st Century Truck Partnership and are carried out in collaboration with industry, national laboratories, and universities. Because of the importance of clean fuels in achieving high efficiency and low emissions, R&D activities are closely coordinated with the relevant activities of the Fuels Technologies subprogram, also within VTP.

CURRENT TECHNICAL FOCUS AREAS AND OBJECTIVES

The Advanced Combustion Engine R&D subprogram focuses on developing technologies for all highway transportation ICEs. Fuel efficiency improvement is the overarching focus of this activity, but resolving the interdependent emissions challenges is a critical integrated requirement. (Penetration of even current-technology diesel engines into the light-duty truck market would reduce fuel use by 30-40% per gasoline vehicle replaced.) The reduction of engine-out emissions is key to managing the extra cost of exhaust aftertreatment devices that can be a barrier to market acceptance. Accordingly, research has been emphasizing advanced combustion modes including homogeneous charge compression ignition (HCCI), pre-mixed charge compression ignition (PCCI), lean-burn gasoline, and other modes of low-temperature combustion (LTC) which will increase efficiency beyond current state-of-the-art engines and reduce engine-out emissions of nitrogen oxides (NOx) and particulate matter (PM) to near-zero levels. In parallel, research on those emission control systems is underway to increase their performance and durability for overall emissions compliance at an acceptable cost. Projects to stretch engine efficiency via innovative combustion methods and thermal energy recovery (such as compound cycles) are in progress as well. In response to the challenges of realizing and implementing higher efficiency engines, the Advanced Combustion Engine R&D subprogram is working toward achieving the following objectives:

- Further the fundamental understanding of advanced combustion processes which simultaneously exhibit low emissions and high efficiency. This will be used in the development of cleaner, more efficient engines which will operate predominately in low-temperature or HCCI combustion modes. These technology advances are expected to reduce the size and complexity of emission control hardware and minimize potential fuel efficiency penalties. A fuel-neutral approach is also being taken, with research addressing gasoline- and diesel-based advanced engines, including renewable fuels. The effects of fuel properties on combustion are addressed in the Fuels Technologies subprogram. Hydrogen engine R&D is underway as well.
- Improve the effectiveness, efficiency, and durability of engine emission control devices to enable increased penetration of advanced combustion engines in the light-duty market and maintain and/or expand application to heavy-duty vehicles.
- Extend robust engine operation and efficiency through the development and implementation of high-speed predictive models for improvements in combustion control and thermal management.
- Further the development of advanced thermoelectric technologies for recovering engine waste heat and directly converting it to useful energy that will significantly increase vehicle fuel economy.
- Advance engine technologies such as turbo-machinery, flexible valve systems, variable compression ratio, and fuel system components to achieve a reduction in parasitic losses and other losses to the environment to maximize engine efficiency.
- Develop key enabling technologies for advanced engines such as sensors and control systems, diagnostics for engine development, and components for thermal energy recovery.
- Improve the integration of advanced engine/emissions technologies with hybrid-electric systems for improved efficiency with lowest possible emissions.
- In cooperation with the Fuels Technologies subprogram, accelerate industry development of a next generation of E85 flexible-fuel engines that exploit ethanol properties for higher efficiency.
- Identify that any potential health hazards associated with the use of new vehicle technologies being developed by VTP will not have adverse impacts on human health through exposure to toxic particles, gases, and other compounds generated by these new technologies.

The Advanced Combustion Engine R&D subprogram maintains close communication with industry through a number of working groups and teams, and utilizes these networks for setting goals, adjusting priorities of research, and tracking progress. Examples of the cooperative groups are the Advanced Combustion Memorandum of Understanding (including auto manufacturers, engine companies, fuel suppliers, national laboratories, and others) and the CLEERS (Cross-Cut Lean Exhaust Emission Reduction Simulation) activity for the Diesel Cross-Cut Team.

TECHNOLOGY STATUS AND KEY BARRIERS

Significant advances in combustion, emission controls, fuel injection, turbo-machinery, and other advanced engine technologies continue to increase the thermal efficiency of ICEs with simultaneous reductions in emissions. With these advances, gasoline and diesel engines continue to be an attractive option as prime movers for conventional and hybrid-electric vehicles. These engines offer outstanding driveability, fuel economy, and reliability with low combustion noise and extremely clean exhaust.

Spark-ignition (SI) gasoline engines serve as the primary movers for the majority of the U.S. light-duty vehicle fleet. Substantial progress in gasoline engine efficiency in recent years has been the result of advances in engine technologies including direct fuel injection, flexible valve systems, improved combustion chamber design, and reduced mechanical friction. While all gasoline engines sold in the U.S. operate with stoichiometric combustion, other areas in the world are seeing the introduction of lean-burn gasoline engines. These engines are characterized by higher efficiencies at part load, but require more costly lean-NOx emission controls that are likely not adequate for U.S. emissions regulations. Advances in lean-gasoline emission controls are critical for meeting U.S. regulations and ultimately the introduction of this efficiency technology in the U.S. market. In addition, the direct injection technology utilized for most advanced gasoline engines produces particulate emissions that although smaller in mass than the diesel engine still represent significant emissions in terms of particulate number counts. Recent laboratory research into highly-diluted, stoichiometric gasoline-based engines has produced efficiencies approaching diesels. This path will receive additional attention to address the challenges of moving the combustion “recipes” to multi-cylinder platforms. Being able to achieve high boost levels, achieve and control very highly cooled exhaust gas recirculation (EGR), and maintain the research-scale efficiency are major hurdles.

Attaining the high efficiency potential of lean-burn gasoline technology will require better understanding of the dynamics of fuel-air mixture preparation and other enabling technologies. Consistently creating combustible mixtures near the spark plug and away from walls in an overall lean environment is a challenge requiring improved understanding of fuel-air mixture preparation and modeling tools that embody the information. A comprehensive understanding of intake air flows and fuel sprays, as well as their interaction with chamber/piston geometry over a wide operating range is needed. Generating appropriate turbulence for enhancement of flame speed is a further complexity requiring attention. The wide range of potential intake systems, piston geometries, and injector designs makes the optimization of lean-burn systems dependent on the development of the improved simulation tools. Furthermore, reliable ignition and combustion of lean (dilute) fuel-air mixtures remains a challenge. Lean and possibly boosted conditions require a more robust, high-energy ignition system that, along with proper mixture control, is needed to reduce combustion variability. Several new ignition systems have been proposed (high-energy plugs, plasma, corona, laser, etc.) and need to be investigated.

Diesel engines are also well-suited for light-duty vehicle applications, delivering fuel economy considerably higher than comparable SI engines. Key developments in combustion and emission controls, plus low-sulfur fuel have enabled manufacturers to achieve the necessary emissions levels and introduce additional diesel-powered models to the U.S. market. DOE research contributed to all of these areas. Primarily due to the cost of the added components and diesel fuel price, diesels in passenger cars have limited U.S. market penetration. Hence the Advanced Combustion Engine R&D subprogram continues to address paths to reduce the cost of emission compliance.

The heavy-duty diesel is the primary engine for commercial vehicles because of its high efficiency and outstanding durability. However, the implementation of increasingly stringent heavy-duty engine emission standards over the last decade held efficiency gains to a modest level. Current heavy-duty diesel engines have efficiencies in the 42-43% range. With stability in NOx and PM regulations in 2010, further gains in efficiency are now seen as achievable. Continued aggressive R&D to improve boosting, thermal management, and the reduction and/or recovery of rejected thermal energy are expected to enable efficiencies to reach 55%. Heavy-duty vehicles using diesel engines have significant potential to employ advanced combustion regimes and a wide range of waste heat recovery technologies that will improve engine efficiency and reduce fuel consumption.

Emissions of NOx (and PM) are a significant challenge for all lean-burn technologies including conventional and advanced diesel combustion strategies, both light-and heavy-duty, as well as lean-burn gasoline. Numerous technologies are being investigated to reduce vehicle NOx emissions while minimizing the fuel penalty associated with operating these devices. These technologies include post-combustion emissions control devices as well as advanced combustion strategies which make use of high levels of dilution to reduce in-cylinder NOx formation.

In early 2007, the U.S. Environmental Protection Agency (EPA) finalized the guidance document for using selective catalytic reduction (SCR) which makes use of urea for regeneration (urea-SCR) technology for NOx control in light-duty and heavy-duty diesel vehicles and engines. This guidance allows for the introduction of SCR technology in Tier 2 light-duty vehicles, heavy-duty engines, and in other future diesel engine applications in the U.S. Strategies to supply the urea-water solution (given the name "diesel exhaust fluid") for vehicles have been developed and are being implemented. Using urea-SCR, light-duty manufacturers have been able to meet Tier 2, Bin 5 which is the "gold standard" at which diesel vehicle sales do not have to be offset by sales of lower emission vehicles. Most heavy-duty diesel vehicle manufacturers are adopting urea-SCR since it has a broader temperature range of effectiveness than competing means of NOx reduction and allows the engine/emission control system to achieve higher fuel efficiency. Although urea-SCR is a relatively mature catalyst technology, more support research is needed to aid formulation optimization and minimize degradation effects such as hydrocarbon fouling.

Another technology being used to control NOx levels in diesel engines and potentially lean-burn gasoline engines is lean-NOx traps (LNTs), which are also referred to as NOx adsorbers. An example application is that Volkswagen has certified its 2009 diesel Jetta to Tier 2, Bin 5 and California LEV-II using an LNT in conjunction with EGR, an oxidation catalyst and diesel particulate filter (DPF). The use of this technology in the U.S. is the direct result of regulation to reduce fuel sulfur content and R&D to develop advanced emission control technologies. LNTs are also used on lean-burn SI engines in Europe, but this form of SI engine is not available in U.S. emission certified autos. While LNTs have a larger impact on fuel consumption than urea-SCR, light-duty vehicle manufacturers appear to prefer LNTs since overall fuel efficiency is less of a concern and urea replenishment is more of a challenge for light-duty customers as compared to heavy-duty vehicle users. While aggressive research on LNTs has substantially decreased the LNT fuel "penalty," the penalty is still in the range of five percent of total fuel flow. This problem is exacerbated by the need to periodically drive off accumulated sulfur (even using ultra-low-sulfur fuel) by heating the adsorber to high temperatures, again by using fuel (desulfation). In addition, the high temperature of regeneration and desulfation has been shown to cause deterioration in catalyst effectiveness. LNTs additionally require substantial quantities of platinum group metals, and the cost of these materials is high and the world sources are limited. An improvement for LNT technology is to pair them with SCR catalysts. The advantage is that the SCR catalyst uses the NH_3 produced by the LNT so no urea is needed. Formulation and system geometries are being researched to reduce the overall precious metal content of LNT+SCR systems which reduces cost and makes the systems more feasible for light-duty vehicles.

A highly attractive solution to reducing vehicle emissions is to alter the combustion process such that engine-out emissions are at levels which remove or reduce the requirements for auxiliary devices while maintaining or improving engine efficiency. This is the concept behind advanced combustion processes such as HCCI, PCCI and other modes of LTC, which exhibit high efficiency with significant reductions in NOx and PM emissions. Note that emissions of hydrocarbons (HCs) and carbon monoxide (CO) are often higher and require additional controls which are often a challenge with the low exhaust temperature characteristic of these combustion modes. Significant progress continues for these advanced combustion systems, and the operational range continues to be expanded to better cover the speed/load combinations consistent with light-duty and heavy-duty drive cycles. In recent years, DOE adopted the term "high-efficiency clean combustion" (HECC) as an all encompassing term which includes a range of combustion modes which are focused on improvements in efficiency with lowest possible emissions. The major R&D challenges include fuel mixing, intake air conditioning, combustion timing control, and expansion of the operational range. To meet these challenges, there has been significant R&D on allowing independent control of the intake/exhaust valves relative to piston motion and on improvements in air-handling and engine controls. Many of these technologies are transitioning to the vehicle market.

High dilution operation through advanced EGR is a key element of HECC and can be a major contributor to meet the 2010 EPA heavy-duty engine emission standards and is also applicable to light-duty diesel and gasoline engines. There are numerous advantages of advanced EGR compared to urea-SCR and LNT packages including lower vehicle weight, less maintenance, and lower operating cost. The disadvantages relative to post-combustion emission controls include increased heat rejection load on the engine and the potential for increased fuel consumption due to more frequent DPF active regeneration. In 2009 the Diesel Cross-Cut Team formed a working group to study the widespread issues of fouling and corrosion in the EGR systems. The DOE Propulsion Materials subprogram is a co-sponsor.

Complex and precise engine and emission controls require sophisticated feedback systems employing new types of sensors. A major advancement in this area for light-duty engines has been the introduction of in-cylinder pressure sensors integrated into the glow plug. Start-of-combustion sensors (other than the aforementioned pressure sensor) have been identified as a need, and several development projects are nearing completion. Sensors are also beneficial for the emission control system. NOx and PM sensors are under development and require additional advances to be cost-effective, accurate, and reliable. Upcoming regulations with increased requirements for on-board diagnostics will also challenge manufacturers trying to bring advanced fuel efficient solutions to market. The role of sensors and catalyst diagnostic approaches will be a key element of emission control research in the next few years.

Advanced combustion engines must be compatible with, if not optimized, for renewable fuels. The Energy Independence and Security Act of 2007 calls for 36 billion gallons of renewable fuels by 2022, which would be mostly ethanol for SI engines, biodiesel for diesels, and second-generation renewable fuels for both. Research has confirmed the basic compatibility of these fuels with various interpretations of HECC. The impact of these fuels on emission controls is also under study, principally in the Fuels Technologies area. Recent tests have shown that biodiesel lowers the regeneration temperature of particulate traps and increases the rate of regeneration with the potential for avoiding or reducing the need for active regeneration and its associated fuel economy penalty.

Waste heat recovery is being implemented in heavy-duty diesel vehicles and explored for light-duty diesel and gasoline applications. New engines being introduced by Daimler Trucks include turbo-compounding technology that uses a turbine to extract waste energy and add to engine power output. The addition of turbo-compounding and other engine changes result in a claimed 5% improvement in vehicle fuel economy. Experiments have shown that waste heat recovery has the potential to improve vehicle fuel economy by as much as 10%.

Another form of waste heat recovery is a thermoelectric generator. Vehicular thermoelectric generators directly convert engine waste heat to electricity and are on a path to commercialization. BMW intends to introduce thermoelectric generators in their 5 and 7 Series cars in the 2010-2014 timeframe in both Europe and North America. The system currently tested by BMW generates 750 W during highway driving, equivalent to a 5% improvement in fuel economy, and about half of that amount in city driving. Thermoelectric devices are also used for zonal cooling systems in vehicles.

FUTURE DIRECTIONS

ICEs have a maximum theoretical fuel conversion efficiency that is similar to that of fuel cells and considerably higher than the mid-40% peak values seen today. The primary limiting factors to approaching these theoretical limits of conversion efficiency start with the high irreversibility in traditional premixed or diffusion flames, but more practically the limits are imposed by heat losses during combustion/expansion, structural limits that constrain peak pressures, untapped exhaust energy, and mechanical friction. To achieve reductions in internal combustion powered vehicle fuel consumption, we must focus on not only the peak efficiency, but place much emphasis on enabling the engine to operate near peak efficiency most of the time. The revised goals for the subprogram were described previously in this section. For SI engines this means reducing the throttling losses with technologies such as lean-burn, high dilution, and variable geometry. Exhaust losses are being addressed by analysis and development of compound compression and expansion cycles achieved by valve timing, use of turbine expanders, regenerative heat recovery, and application of thermoelectric generators. Employing

such cycles and devices has been shown to have the potential to increase heavy-duty engine efficiency to as high as 55%, and light-duty vehicle fuel economy by 25%. In 2010, VTP plans to issue new requests for proposals and award new contracts for engine efficiency R&D within the vehicle context.

Analyses of how "advanced combustion regimes" might impact the irreversibility losses have indicated a few directions to moderate reductions of this loss mechanism, but converting the preserved availability to work will require compound cycles or similar measures of exhaust energy utilization. The engine hardware changes needed to execute these advanced combustion regimes include variable fuel injection geometries, turbo- and super-charging to produce very high manifold pressures, compound compression and expansion cycles, variable compression ratio, and improved sensors and control methods. Larger reductions in combustion irreversibility will require a substantial departure from today's processes but are being examined as a long-range strategy.

Most of the basic barriers to high engine efficiency hold true for both gasoline- and diesel-based engines. Recognizing the dominance of gasoline-type SI engines in the U.S., VTP intends to increase emphasis on their improvement. Gasoline-based engines, including E85 flexible-fuel, can be made at least 20-25% more efficient through direct injection, boosting/downsizing, and lean-burn. Real-world fuel savings might be even higher by focusing attention on the road-load operating points.

Hydrogen engine efficiencies of roughly 45% have been demonstrated based on single-cylinder engine data. The underlying reasons for these impressive levels suggest a case study for applicability to other fuels. Work will continue on increasing the power density of hydrogen fueled engines while maintaining low NOx.

Meeting anticipated future emission standards will be challenging for high efficiency diesel and lean-burn gasoline engines. To address this issue, research on innovative emission control strategies will be pursued through national laboratory and university projects designed to reduce cost and increase performance and durability of NOx reduction and PM oxidation systems. Project areas include development of low-cost base metal catalysts (to replace expensive platinum group metals), lighter and more compact multifunctional components, new control strategies to lessen impact on fuel consumption, and improved sensors and on-board diagnostics for meeting upcoming regulations. Furthermore, simulations of the catalyst technologies are being developed to enable industry to perform more cost-effective system integration during vehicle development. As advanced combustion approaches evolve and engine-out emissions become cleaner, the requirements of emission controls are expected to change as well.

The majority of lean-NOx emission controls development has been focused on diesel engines. With the potential introduction of high efficiency lean-gasoline engines, these technologies will require further research and development as well emission controls for managing HC/CO emissions. Engine-out PM emissions from lean-gasoline engines, although lower in mass than the diesel engine, are also a concern and may require new processes due to differences in particle size and morphology.

Enabling technologies being developed by the Combustion and Emission Control R&D activity will address fuel systems, engine control systems, and engine technologies. Fuel systems R&D focuses on injector controls and fuel spray development. Engine control systems R&D focuses on developing engine controls that are precise and flexible for enabling improved efficiency and emission reduction in advanced combustion engines. These control system technologies will facilitate adjustments to parameters such as intake air temperature, fuel injection timing, injection rate, variable valve timing, and EGR to allow advanced combustion engines to operate over a wider range of engine speed/load conditions. Engine technologies development will be undertaken to achieve the best combination that enables advanced combustion engines to meet maximum fuel economy and performance requirements. These include variable compression ratio, variable valve timing, variable boost, advanced sensors and ignition systems, and exhaust emission control devices (to control hydrocarbon emissions at idle-type conditions) in an integrated system. Upcoming EPA onboard diagnostic requirements will be addressed through research on advanced sensors, improved understanding of emission control aging, and development of models that are integral to the diagnostic method.

The Solid State Energy Conversion activity will continue on developing advanced thermoelectric generators for converting waste heat from engines directly into useful electrical energy to improve

overall vehicle energy efficiency and reduce emissions. Effective use of waste heat from combustion engines would significantly increase vehicle fuel economy. In current production passenger vehicles, roughly over 70% of the fuel energy is lost as waste heat from an engine operating at full power. About 35 to 40 percent is lost in the exhaust gases and another 30 to 35 percent is lost to the engine coolant. There is an opportunity to recover some of the engine's waste heat using thermoelectric materials that will convert it directly to electricity for operating vehicle auxiliaries and accessories. Improving the energy conversion efficiency of thermoelectric materials directly supports the overall goals of improving the fuel economy of passenger and commercial vehicles. Achieving the vehicle-based performance goals requires reduction in the cost of thermoelectrics, scaling them up into practical devices, and making them durable enough for vehicle applications. Contracts with Ford and General Motors will pursue the concept of a zonal, dispersed thermoelectric cooling system which will cool an occupant with 630 W compared with the 3,500 to 4,000 W used by conventional mobile air conditioning systems. Air conditioning power reductions of greater than 7% are possible.

The Combustion and Emission Control R&D activity performs the critical role of elevating potential health issues related to advanced combustion engine technologies to the attention of industry partners and DOE/VTP management. This portion of the activity will continue to ensure that the development of new vehicle technologies, rather than just enabling compliance with existing standards, also considers the possibility of causing negative health impacts:

- To provide a sound scientific basis underlying any unanticipated potential health hazards associated with the use of new powertrain technologies, fuels and lubricants in transportation vehicles.
- To ensure that vehicle technologies being developed by VTP for commercialization by industry will not have adverse impacts on human health through exposure to toxic particles, gases, and other compounds generated by these new technologies.

PROJECT HIGHLIGHTS

The following projects highlight progress made in the Advanced Combustion Engine R&D subprogram during FY 2009.

Advanced Combustion and Emission Control Research for High-Efficiency Engines

A. Combustion and Related In-Cylinder Processes

The objective of these projects is to identify how to achieve more efficient combustion with reduced emissions from advanced technology engines.

- Argonne National Laboratory (ANL) made a significant discovery that demonstrates how the movement of the needle as the injector opens affects the structure of the spray as it emerges from the nozzle. This is the first time that needle motion has been directly correlated with spray structure, and the data represents a comprehensive view of nozzle flow that will be invaluable to computational modeling. Additional accomplishments include development of a new experimental station at the Advanced Photon Source dedicated to transportation research and finalization of a new collaboration with Delphi Diesel Systems. (Powell, ANL)
- Sandia National Laboratories (SNL) refined and extended a deep-ultraviolet laser-induced

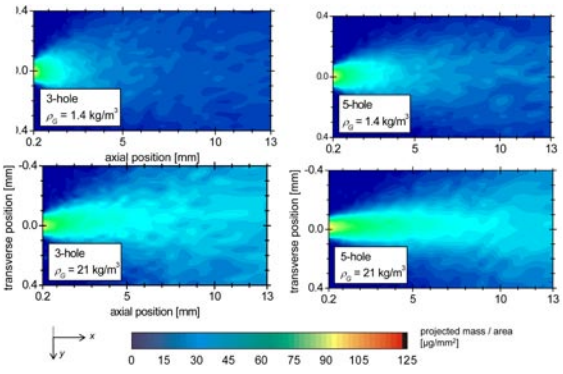

A comparison of the fuel distribution for two different nozzles at two different ambient densities. X-ray measurements in collaboration with Bosch showed that the number of holes affect the fuel distribution from injectors with otherwise identical orifices. (Powell, ANL)

fluorescence technique to provide two-dimensional images of the in-cylinder distributions of CO, unburned hydrocarbons (UHC), and partial oxidation products. The technique was applied to several operating conditions representative of different LTC strategies, and has successfully identified the dominant sources of engine-out UHC and CO. Comparisons of the experimental data with the predictions of numerical models have identified discrepancies caused by inaccurate predictions of the fuel-air mixing processes. Fundamental studies of the performance of reduced chemical kinetic mechanisms in homogeneous engine environments have identified shortcomings in their predictions of CO and UHC yields. Improved reduced kinetic mechanisms have been developed which significantly improve the accuracy of the predicted emissions, without significant impact on computational cost. (Miles, SNL)

- SNL improved the understanding of in-cylinder LTC spray, combustion, and pollutant-formation processes required by industry to build cleaner, more efficient, heavy-duty engines. The entrainment wave concept developed by SNL explains many LTC phenomena, and provides additional building blocks for an extension to LTC conditions of Sandia's conceptual model for conventional diesel combustion. It was also discovered that if residual soot from the main injection remains in the squish region, which typically occurs for late main injections, then a late post injection may interact with and oxidize the squish region soot, thereby reducing exhaust soot emissions for LTC conditions. Improved computer models with reduced grid dependency agree with and supplement experimental measurements were also developed. (Musculus, SNL)

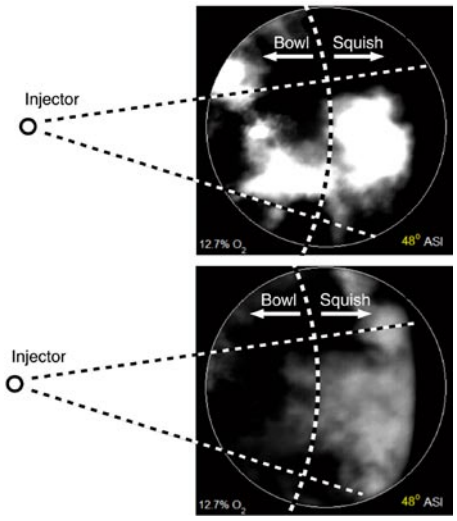

Soot luminosity images in the squish region above the piston for a main-injection only (top) and with a post injection (bottom) acquired through the cylinder head window. (Muculus, SNL)

- SNL's development of a simultaneous Mie-scatter, chemiluminescence, soot luminosity, and shadowgraph/schlieren high-speed imaging has shown to be a useful tool for interpretation of diesel combustion. In addition to liquid and vapor penetration, the technique detects cool-flame progression by a "disappearance" of the shadowgraph effect and high-temperature combustion by strong radial expansion and a smooth texture in the shadowgraph image. The contrast between high-temperature combustion regions, visible in the shadowgraph images downstream of the injector, and fuel vapor regions near the injector, allows identification of sources of UHC in a diesel spray. Results show that LTC conditions tend to leave significant regions of UHC near the injector, while high-temperature combustion propagates back to the injector for conventional diesel combustion. (Pickett, SNL)
- Oak Ridge National Laboratory (ORNL) was successful at providing new insight into the implementation of advanced combustion operation on multi-cylinder engines and demonstrating 2010 FreedomCAR efficiency and emissions milestones on light-duty diesel engines. Substantial improvements in the engine dynamometer setup including expanded control of engine thermal boundary conditions and a second flexible control system for independent operation and control of all engine actuators and systems were made. The effect of intake charge temperature and combustion chamber wall temperature on emissions, efficiency, and cyclic dispersions on a General Motors (GM) 1.9-L diesel engine was characterized: (1) A shorter ignition delay was observed with increasing intake charge temperature and combustion chamber wall temperature; (2) Both CO and hydrocarbon (HC) emissions exhibit a strong sensitivity to the variations of combustion chamber wall temperature; (3) The HECC operating range was expanded with the extended intake charge temperature range enabled by a higher heat rejection capacity EGR cooler; and (4) Robust HECC operation can be achieved and its operating range can be expanded by precisely controlling thermal conditions of both intake charge and combustion chamber wall without paying penalties in efficiency and emissions. (Wagner, ORNL)

- SNL completed development of improved high-pressure multiphase models for time-accurate treatment of direct-injection processes in diesel and LTC engines. High-fidelity simulations of the optical hydrogen-fueled engine in collaboration with Kaiser et al. were continued, and collaboration with Dec et al. was continued to systematically work toward modeling HCCI combustion. The performance and usability of Oefelein's massively-parallel large eddy simulation solver ("RAPTOR") for engine-related calculations as part of the DOE Office of Science innovative and novel computational impact on theory and experiment (INCITE) program was improved. (Oefelein, SNL)
- Lawrence Livermore National Laboratory (LLNL) has greatly improved execution speed for CHEMKIN multizone modeling by using an iterative solver with an appropriate preconditioner. Modeling of ORNL experiments demonstrates transition between stable spark ignition (SI) operation at low EGR, chaotic SI-HCCI transition at intermediate EGR, and stable HCCI conditions at high EGR. The KIVA multizone model accurately predicts PCCI combustion in an engine with optical access running with considerable negative valve overlap (NVO) and partial fuel injection during NVO. (Aceves, LLNL)
- SNL determined the evolution of naturally occurring thermal stratification in an HCCI engine, including the distribution of thermal inhomogeneities and their magnitude at a typical operating condition. They showed that intake-pressure boosting has a strong potential for extending the high-load limit for gasoline-fueled HCCI, at a representative 1,200 rpm condition. They also determined the behavior of ethanol as an HCCI fuel over a range of operating conditions, and worked cooperatively with M. Sjöberg of the Advanced SI-Engine Fuels Lab. A detailed exhaust-speciation analysis was initiated for the primary reference fuel blend (80% iso-octane and 20% n-heptane, PRF80) as a representative two-stage ignition fuel in cooperation with L. Davisson at LLNL. Chemical-kinetic and computational fluid dynamics (CFD) modeling work was supported at LLNL which provided data and analysis for: 1) improving chemical-kinetic mechanisms, and 2) CFD modeling of fuel stratification to improve low-load combustion efficiency and emissions. (Dec, SNL)

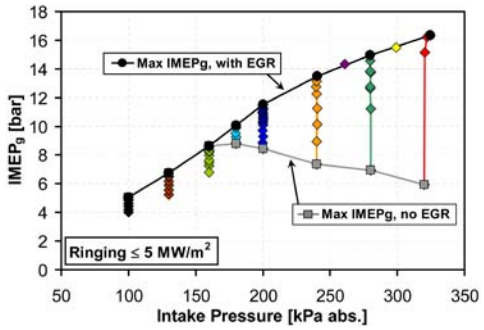

Maximum $IMEP_g$ at the knock/stability limit for various intake pressures, both with EGR and without. (Dec, SNL)

- SNL developed an algorithm for computing NVO cycle temperatures from experimental data. The tool was validated using planar laser induced fluorescence (PLIF) temperature measurements, GT-Power model estimates, and published iso-octane ignition data. Engine experiments were conducted with and without NVO fueling to characterize low-load operation while varying main combustion phasing. The two types of fueling were compared using computed cycle temperatures in order to distinguish thermal and chemical effects of NVO fueling. Bench-top tests of a CO laser-absorption diagnostic were performed for characterizing the extent of reactions during NVO reformation. Stanford's two-wavelength PLIF diagnostic was applied to capture cycle temperatures during fired NVO operation. Continued collaboration with the University of Wisconsin and LLNL to develop modeling tools for automotive HCCI application. (Steeper, SNL)
- ORNL progressed toward the development, implementation, and demonstration of technologies for meeting and possibly exceeding Vehicle Technologies engine and efficiency milestones. Specific accomplishments included: (1) The FY 2009 FreedomCAR milestone of 44% peak brake thermal efficiency on a light-duty diesel engine was demonstrated; (2) An organic Rankine cycle was developed and evaluated through simulation and experiments on-engine; (3) Thermal energy recovery was investigated on-engine and with transient-realistic models using GT-Drive; (4) New insight into the thermodynamic availability of engine systems (e.g., exhaust system, exhaust gas recirculation, etc.) across the speed/load operational range of a light-duty diesel engine was gained and potential fuel economy improvements over the Federal Test Procedure drive cycle

were estimated; and (5) The path forward to demonstration of FY 2010 efficiency and emissions milestones was finalized. (Wagner, ORNL)

- Los Alamos National Laboratory (LANL) completed the alpha KIVA-4 parallel version with the full version release planned for late fall 2009. Piston-ring crevice modeling in domains with piston rings on highly refined grids with bowls above the ring-walls and crevice regions was highly refined and is working for two-dimensional (2-D) and three dimensional (3-D) sector and full 3-D grids and is included for the parallel KIVA-4 release. KIVA-4 capability has been extended to predict heat conduction in solids, that is, the combustion chamber. Cut-cell grid generation to create 3-D grids in hours, in contrast to days for complex geometries has been partially achieved. KIVA-4 now has support and capability to use Cubit-generated unstructured grids and an h-adaptive characteristic-based split finite element method for incompressible and compressible flows was developed. (Carrington, LANL)

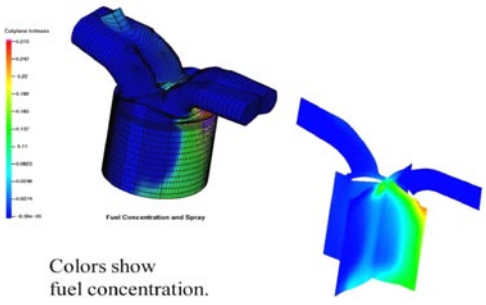

Parallel solution of a 4-valve (slanted) engine with hemi-head on four processors. (Carrington, LANL)

- LLNL developed and validated for the first time, a chemical kinetic model for 2,2,4,4,6,8,8-heptamethylnonane, a primary reference fuel for diesel, for low- and high-temperature chemistry regimes. This model is also available to represent iso-alkanes in diesel fuel. The predictive capabilities of detailed chemical kinetic mechanisms for critical components in gasoline (n-heptane, iso-octane and toluene) were improved at conditions found in engines, and chemical kinetic models for binary and tertiary mixtures of gasoline components were tested and compared well to experimental data in rapid compression machines. (Pitz, LLNL)

- SNL continued development of a free-piston generator with a projected fuel-to-electricity conversion efficiency of 50% at 30 kW output using hydrogen as the fuel. The major components needed for the research prototype, including engine combustion chamber, intake and exhaust manifolds, pistons, magnets, linear alternators, and other associated hardware were fabricated and assembled. The research experiment for stability of piston coupling via a prototype resistive load circuit was analyzed with a Mathematica-based model. The piston lock-and-release mechanism intended to lock pistons in place for starting and to release pistons simultaneously to ensure piston synchronization on the first stroke was designed and fabricated. (Van Blarigan, SNL)

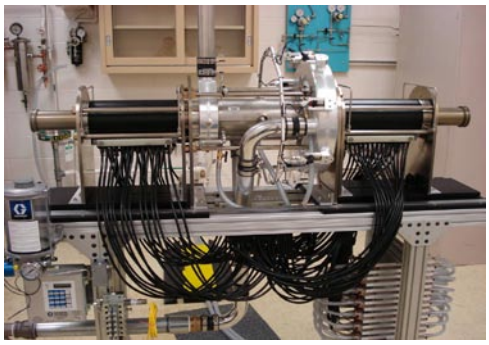

The Hydrogen Free-Piston Engine Prototype (Van Blarigan, SNL)

- ANL found that employing a multiple injection strategy in a hydrogen direct injection engine allows maintaining the same engine efficiency as achieved with single injection while reducing NOx emissions by as much as 85%. The potential of EGR was evaluated for NOx emissions reduction and found that an emissions reduction of up to 70% is feasible with an efficiency loss of approximately 1%. Tests using a single-hole nozzle injector showed that in general injection towards the spark plug is beneficial for engine efficiency but results in higher NOx emissions. 3-D CFD simulation was integrated in the analysis and optimization process in close coordination with the optical experiments performed at SNL. (Wallner, ANL)

- SNL assembled an extensive database on fuel/air mixing in a direct-injection hydrogen-fueled engine that is being used for physical understanding and simulation validation. For all injector configurations and all but the latest injection timings, extensive jet/wall interaction determines the details of pre-spark fuel distribution. The momentum from the injection dominates the in-cylinder convection. Drastic increase in intake-induced tumble flow can change this somewhat

for early injection timings. For intermediate injection timings, all injector configurations investigated yield an unfavorable pre-spark stratification. Improvements may include using a shaped piston top. Depending on the jet divergence-angle in multi-hole nozzles, jet merging may not occur at all, may yield complete merging, or may cause injection-to-injection instabilities. Initial comparisons of optical results to CFD modeling performed at ANL show that end-of-injection transients need improved treatment in the simulation. (Kaiser, SNL)

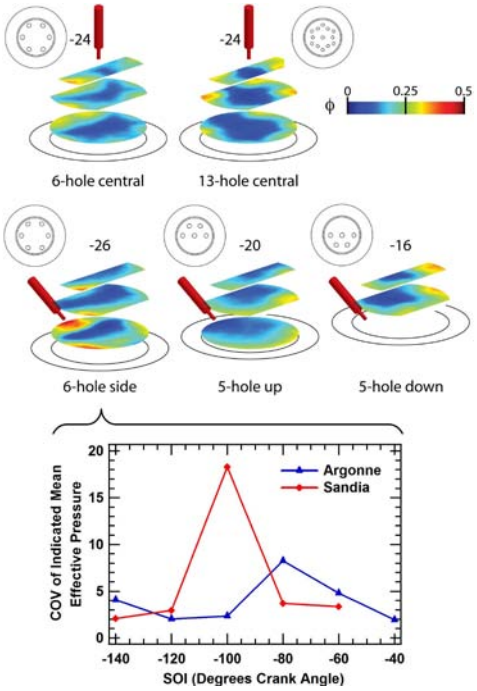

Top: Hydrogen distribution towards the end of the compression stroke for five different injector configurations with intermediately retarded injection (SOI = -80°CA). Bottom: Coefficient of variation for the 6-hole injector in side location as a function of injection timing. (Kaiser, SNL)

- Cummins is engaged in developing and demonstrating advanced diesel engine technologies to significantly improve engine thermal efficiency while meeting U.S. EPA 2010 emissions. The essence of this effort is focused on HECC in the form of low-temperature, highly-premixed combustion in combination with lifted flame diffusion controlled combustion. Reduced equivalence ratio, premix charge in combination with high EGR dilution has resulted in low engine-out emission levels while maintaining high expansion ratios for excellent thermal efficiency. The various embodiments of this technology require developments in component technologies such as fuel injection equipment, air handling, EGR cooling, combustion, and controls. Recent efforts have focused on integration of the engine technology with aftertreatment systems to maximize fuel efficiency improvements. In addition to the engine technologies, Cummins is evaluating the impact of diesel fuel variation on the thermal efficiency, emissions, and combustion robustness of HECC technology. Biofuels are also being evaluated as part of the fuels study to determine if the thermal efficiency improvements and emissions compliance can be maintained. (Stanton, Cummins)
- Caterpillar continued their efforts to identify and develop technologies to enable low-temperature, high-efficiency combustion to achieve a 10% reduction in fuel consumption while meeting Environmental Protection Agency 2010 on-highway and Tier 4 non-road emissions requirements. An interaction between combusting sprays of 10-hole and 14-hole injector nozzles was identified that affects flame lift-off length and may partially explain high soot emissions from such nozzles at high engine loads. Testing of PCCI combustion using gasoline and diesel fuel blends was completed. The fuel blend did not significantly increase the PCCI operating range, but did show smoke emissions reduction across the entire operating range. A wells-to-wheels energy audit for three heavy-duty diesel engine applications and four combustion system/fuel configurations was completed. (Fiveland, Caterpillar)
- Navistar Engine demonstrated the application of LTC on their 6.4L V8 engine by use of EGR, charge temperature control and the use of a multiple injection strategy. Engine testing yielded engine NOx levels below 0.2 g/bhp-hr and soot levels manageable by a diesel particular filter. Overall, tests demonstrated a gain in the engine break thermal efficiency of up to 5% with respect to the base. Further improvements in the engine efficiency were sought by the installation of a variable valve actuation (VVA) system. The VVA system was validated in a dedicated test rig, accumulating over 400 hours of testing before engine installation. The fuel injection and VVA controls were integrated into the electronic control unit (ECU) with the previously developed cylinder pressure feedback system. VVA proved capable to extend the LTC regime with extraordinary results over soot reduction and improved engine thermal efficiency. For operating loads up to 5 bar brake mean effective pressure (BMEP), at engine-out 0.2 g NOx/bhp-hr, soot was

reduced to levels below 0.01 g/bhp-hr. The engine brake specific fuel consumption (BSFC) was reduced by nearly 5%. (de Ojeda, International)

- ORNL continued their efforts to analyze and define specific pathways to improve the energy conversion efficiency of ICEs from nominally 40% to as high as 60%. Their initial thermodynamic investigation of thermochemical recuperation (TCR) indicates that it could result in substantial boosts in ICE efficiency (as measured in terms of single-stage work output) for a range of fuels. For an ideal stoichiometric engine fueled with methanol, TCR can increase the estimated ideal engine efficiency by about 5% of the original fuel exergy. For ethanol and isooctane the estimated efficiency increases for constant volume reforming are 9% and 11% of the original fuel exergies, respectively. The efficiency improvements from TCR are due to lower exhaust exergy losses and reduced combustion irreversibility with the reformed fuels, but are offset to some extent by entropy generation in the reformer and heat released from the intercooler. (Daw, ORNL)

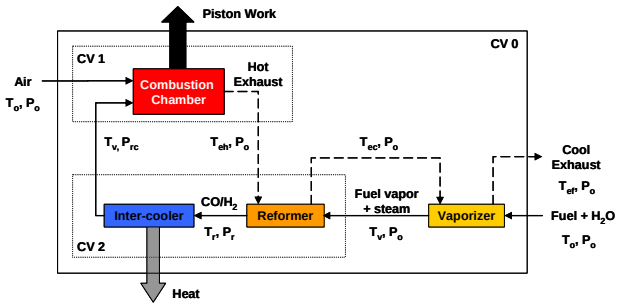

Schematic of Conceptual Ideal Piston Engine Utilized for TCR Study (Daw, ORNL)

- Detroit Diesel Corporation (DDC) experimentally demonstrated up to 5% thermal efficiency improvement through PCCI combustion optimization on a multi-cylinder engine by using analytical simulations to drive experimental investigations. A transient control methodology on a transient cycle was experimentally demonstrated to achieve up to 2.5% thermal efficiency improvement compared to the baseline engine with simultaneous significant engine-out NOx reduction. Combustion chamber features for optimal emissions and combustion were identified including a piston design with significant soot reduction, and a path to piston designs with potential thermal efficiency improvements was identified. (Zhang, DDC)

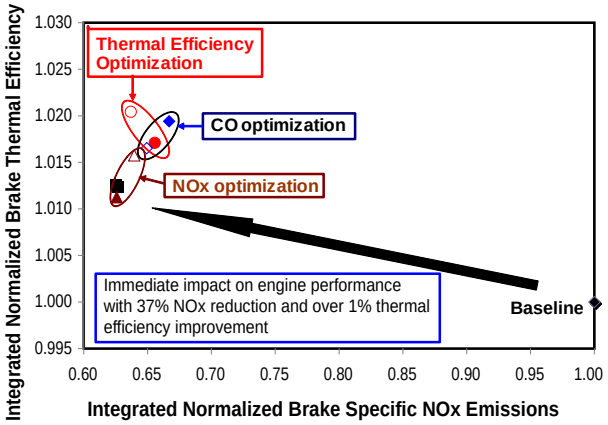

Controller Optimization over Transient Cycle (Zhang, DDC)

- GM continued their efforts to develop of high efficiency clean combustion engine designs for spark-ignition and compression-ignition ICEs. A gasoline-fueled HCCI engine has been demonstrated in the lab and in a vehicle. One continuing specific challenge is the durability and robustness of production-feasible and cost-effective in-cylinder pressure sensing subsystems and mode-switching from spark ignition (SI)-to-HCCI and HCCI-to-SI regimes. One continuing specific challenge is the noise and vibration performance of the engine in HCCI mode and during mode-switching. Fuel efficiency benefits of 8-20% have been measured during HCCI operation. A VVA system was installed on a multi-cylinder diesel engine and a fully flexible valve actuation system was installed on a single-cylinder engine. The benefits and limitations of internal EGR for controlling exhaust temperatures was assessed and the design and implementation of a two-stage turbocharging system for charging requirements of VVA in a multi-cylinder diesel engine were completed. Using these technologies, an estimated 50% reduction in unburned hydrocarbons and 34% reduction in carbon monoxide emissions during the first 200 sec of the FTP cycle were estimated based on weighted emission factors. (Patton and Gonzalez, GM)

- Cummins developed and calibrated an engine cycle simulation model for their light-duty diesel engine. They estimated fuel efficiency improvement for an in-cylinder NOx emissions solution is 11.5%, which exceeds the project goal of 10.5%. However, the most significant risk associated with an in-cylinder solution is that it will not be capable of meeting the emissions requirements required by the potential SFTP2 regulation. Hence, a high-efficiency SCR NOx aftertreatment solution is also being investigated. The estimated efficiency improvement for the SCR architecture, relative to the baseline LNT architecture, is similar to the in-cylinder solution. However, since the SCR solution enables high engine-out NOx over much of the drive cycle, closed-cycle efficiency improvement is expected to be slightly greater. Due to urea consumption and thermal management, efficiency improvements associated with aftertreatment are expected to be slightly less than the in-cylinder solution. During the next phase of the project efficiency improvements with be validated and optimized experimentally. (Stanton, Cummins)

- Ford is developing optimal system solutions to address boost system challenges, such as efficiency degradation and compressor surge, etc., in diesel combustion/emission control system development to enable commercialization of advanced diesel combustion technologies. The first round of design, analysis and flow bench tests have demonstrated efficiency improvement on both the compressor and turbine, especially at low compressor mass flow and low turbine speed ratio areas where most customer driving will be done. The test data also identified areas for further improvement. The test data guided design optimization for better efficiency and wider flow range. The final design and analyses of the compressor and turbine will be completed in the near future. The strategy will focus on compressor impeller improvement and casing treatment optimization, rather than variable compressor inlet guide vane and variable diffuser vane as previously suggested. The next steps will include: fabrication of the redesigned compressor and turbine wheel, using fewer moving parts in the compressor to achieve wider operation range with efficiency improvement, and flow bench test validation. (Sun, Ford)

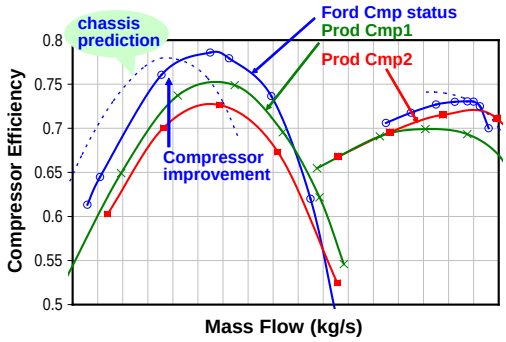

Turbocharger Compressor Efficiency 70,000 RPM, Bench Test and Simulation Results (Sun, Ford)

- ANL is using low-cetane fuels to create a combustion system that relies on premixed, but not well-mixed, fuel/air mixtures to control power output and emissions. A 1.9-L GM diesel engine was successfully operated using "Next Cycle" control which was able to self-optimize each cylinder's injection timing to provide tremendous consistency of operation despite uneven cylinder-to-cylinder EGR distribution. It is anticipated that this strategy will also work well for LTC operation, since EGR distribution will likely be rather uneven and at very high levels. (Ciatti, ANL)

- ORNL demonstrated spark ignition, spark assisted (SA)-HCCI, and HCCI on a multi-cylinder production engine at the Delphi research facility in Rochester, NY. The multi-cylinder engine platform for this study is providing new data in support of expanding the operational range of HCCI-like combustion. These data in combination with modeling are expected to continue to provide new insight into engine control strategies as well as advance the fundamental understanding of cyclic and cylinder dispersion issues commonly associated with these types of combustion processes. A patent on HCCI combustion mode transition control concepts was awarded to ORNL based on this work. (Wagner, ORNL)

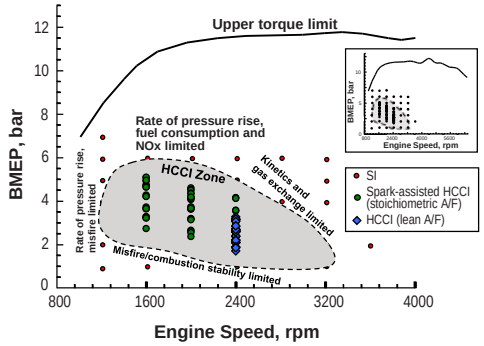

Operating Limits Explored to Date with the Multi-Cylinder Engine. (Wagner, ORNL)

B. Energy-Efficient Emission Controls

The following project highlights summarize the advancements made in emission control technologies to both reduce emissions and reduce the energy needed for emission control system operation.

- PNNL is conducting three fundamental research projects as part of the CLEERS activities. The projects include DPFs, SCR catalysts and LNTs. Accomplishments during the year include: (1) Processed multiple 3-D digital maps of pore structures obtained from micro X-ray scans of commercial cordierite and silicon carbide DPF substrates; (2) Used digital DPF pore structures to study resolution and sample size necessary for representative predictions; (3) Developed and validated the Fe-zeolite urea-SCR catalyst model based on steady-state bench reactor tests. Validated NH_3 storage, NH_3 oxidation and standard SCR kinetic models using the thermal transient micro-reactor tests; (4) Measured the inhibition effect of H_2O and toluene on NO oxidation over Fe-zeolite catalyst through steady-state and thermal-transient reactor tests, and developed kinetics-based and neural networks-based inhibition models to describe the experimental observations; (5) Demonstrated that the common catalyst metal, Pt, is dispersed on the γ-alumina support surface by anchoring to penta-coordinated Al sites using ultra-high field nuclear magnetic resonance spectroscopy coupled with ultra-high resolution transmission electron microscopy (TEM); and (6) Performed computational studies of the adsorption of NOx on a variety of alkaline earth oxide surfaces to compare with our experimental results, including calculations of NOx adsorption on supported BaO surfaces as a function of the BaO particle size. (Herling, PNNL)

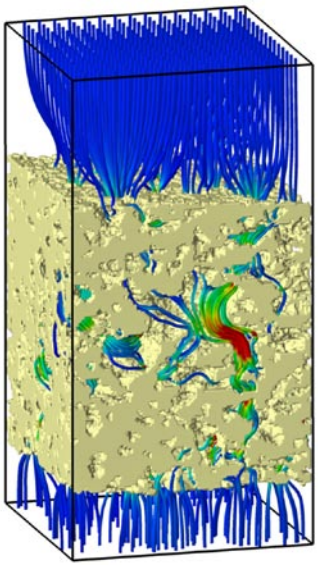

Three-dimensional flow field simulation through reconstructed cordierite filter wall. (Herling, PNNL)

- PNNL and its Cooperative Research and Development Agreement (CRADA) partners from Cummins Inc. and Johnson Matthey have initiated a new CRADA project aimed at improving the higher temperature performance and stability of LNT technology. Results obtained this year demonstrate that the presence of CO_2 promoted the desulfation steps by inhibiting the formation of the BaS phase. By using in situ characterization techniques, it can be deduced that the sulfur species formed on Pt-BaO/CeO_2 sample is less likely to be removed and has more tendency to stay in the catalyst, even after desulfation up to 800°C. This result implies that the desulfation mechanism totally depends on the support material. Overall, these approaches are expected to give invaluable information to overcome the critical stability issues in LNT catalysts. (Peden, PNNL)

- ORNL is researching the complex chemistry that occurs during the regeneration processes for LNTs through experiments conducted on a full-size engine-LNT catalyst system; supplemental research in a more controlled experiment is also conducted on a bench flow reactor for comparison. The temporal profiles of reductant emissions during LNT regeneration were measured with in-line ultraviolet (UV) adsorption spectroscopy; NH_3 release occurs after the initial NOx release as observed in bench flow reactor studies. The quantity of NH_3 formation as a function of rich duration of the LNT regeneration event has been measured, and furthermore, the NOx reduction gained by using the NH_3 on the downstream SCR catalyst has been characterized. NOx reduction efficiencies of 90% from the LNT alone have been increased to >98% from the LNT+SCR combination for equivalent fuel penalty. (Parks, ORNL)

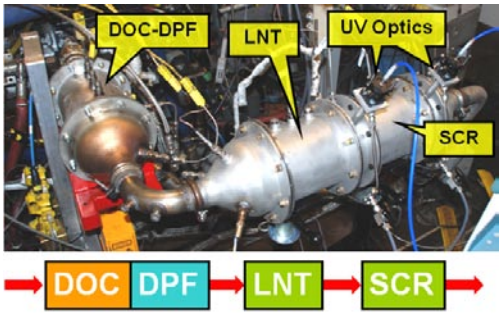

Picture and schematic of the LNT+SCR catalyst system on the light-duty diesel engine. (Parks, ORNL)

- SNL is developing an elementary reaction mechanism that describes both phases of LNT operation, i.e., trapping and storing NOx via adsorption on high-capacity catalytic sites, and periodically this stored NOx is released and reduced to harmless N_2 on precious metal sites by imposing rich conditions for a short time. They modified their previously developed mechanism for chemistry on the precious metal sites, and re-optimized the corresponding kinetic parameters, in response to the realization that transient effects and NOx storage were not always negligible during the comprehensive set of steady flow temperature sweep experiments. They made further refinements to their previously developed mechanism for chemistry on the NOx and oxygen storage sites, combined this with the modified precious metal mechanism, and performed a global optimization of the kinetic parameters in the overall mechanism by fitting simultaneously data for all of the steady flow and long cycle experiments. Their thermodynamically consistent mechanism for sulfation and desulfation was streamlined, and used the standard optimization methodology to fit semi-quantitatively some published data for gas production during high-temperature desulfation. (Larson, SNL)
- ORNL has been assisting Navistar to develop insights into aftertreatment device operation which can be used to develop emissions control systems models. A transient evaluation protocol that measures the NH_3 storage capacity and reaction kinetics of key processes occurring over a urea-SCR catalyst was developed. The transient evaluation protocol was refined based on feedback from our partners at Michigan Technological University. An automated bench-scale flow reactor was used to exercise the revised protocol on core samples cut from fresh and engine-aged SCR catalysts provided by Navistar. The data from the protocol experiments have been transferred to MTU for use in development, calibration, and validation of a urea-SCR control model. ORNL fully analyzed the protocol data to draw conclusions about the surface chemistry of urea-SCR catalysts and the mechanisms by which aging reduces catalyst performance. (Pihl, ORNL)
- ORNL is studying the fundamentals of sulfation/desulfation of LNTs. They confirmed the improvement in performance and desulfation properties with 5%mol Ca introduction into the BaO storage phase of an LNT catalyst; the improvement is due to a synergistic effect as Ca-only catalyst results in higher desulfation temperatures. The sulfur stability and desulfation characteristics of individual components of a commercial LNT catalyst were determined. Results were presented at the 12th CLEERS Workshop, 21st North American Catalysis Society Meeting, and the 2009 DOE Vehicle Technologies Merit Review. A paper was prepared for submission to Applied Catalysis B. (Toops, ORNL)
- ORNL is developing and applying minimally invasive advanced diagnostic tools to resolve spatial and temporal variations within operating diesel engines and catalysts. They developed an instrument for detecting cylinder-to-cylinder combustion variations within a single engine cycle through direct, on-engine measurements in undiluted exhaust. The nature of how sulfur degrades the water-gas shift (WGS) reaction during LNT regeneration was characterized, and the relationship between sulfur degradation of WGS, NOx storage and reduction (NSR) and oxygen storage capacity catalyst functions; this detailed information enables advanced catalyst control strategies to improve system cost, fuel economy and durability. A tool for rapid, on-engine measurements of oil dilution by fuel was licensed to Da Vinci Emissions Services, Ltd. (Partridge, ORNL)
- ORNL demonstrated the benefits of HECC in conjunction with an LNT to achieve low emissions with only a slight drop in fuel efficiency as compared with conventional combustion modes. They found that advanced combustion modes such as HECC have lower PM emissions and can greatly reduce the frequency of desoot operations of the DPF which leads to lower fuel consumption from the desoot process. The lower NOx emissions from HECC also help to reduce PM emissions and desoot fuel penalty for the case when LNT aftertreatment is used since the frequency of the PM-rich LNT regeneration is also reduced by HECC. On a system fuel consumption basis, the lower fuel penalty from desoot operation with HECC better enables HECC to compete with conventional combustion on a system fuel consumption basis. (Parks, ORNL)
- ORNL continued co-leading the CLEERS Planning Committee and facilitation of the SCR, LNT, and DPF Focus Group telecoms with strong domestic and international participation. Key R&D priorities from the 2007 and 2008 CLEERS surveys were identified and analyzed, and the current DOE national lab projects to identify potential gaps in current emissions control R&D portfolio.

The 12th CLEERS workshop was organized and held at the University of Michigan, Dearborn on April 28-30, 2009. The CLEERS Web site (www.cleers.org) was maintained including functionalities, security, and data to facilitate Web meetings and serve focus group interactions. Regular update reports to the DOE Diesel Cross-Cut Team were provided and co-leadership of the LNT Focus Group and refinement of the standard LNT materials protocol was continued. (Daw, ORNL)

- ORNL has been conducting experimental LNT research to identify roles that different sulfur types play in overall LNT performance. Detailed spatio-temporal measurements of the CLEERS LNT reference catalyst have confirmed that multiple sulfur compounds form during sulfation. These compounds form and decompose at different rates and have distinct roles in altering LNT performance, implying that LNT formulation needs to be coordinated with the lean-rich cycling and desulfation strategies. Hydrocarbon poisoning of the CLEERS reference SCR catalyst appears to occur by blocking active sites critical for one or more surface reaction steps in the SCR reaction rather than by blocking ammonia adsorption. Questions remain about the detailed reaction steps needed to successfully model both short- and long-cycle LNT behavior with a single set of reaction parameters. Results continue to indicate that intra-solid diffusion still needs to be a critical part of any successful model. Simplified kinetic models are now being successfully used to simulate vehicle systems with LNT lean NOx controls. (Daw, ORNL)
- ANL is evaluating pressure drop across DPF membranes during PM filtration processes and developing technologies to reduce pressure drops across the DPF membrane. It was found that the pressure drop in a modified DPF membrane increased as the front plug position was shifted to the membrane exit, mainly due to the increase of wall-through losses, while the frictional losses and inertial losses were not significant in magnitude. The optimum position of plug shift was determined by examining parametric relations between permeability and plug position. Thermogravimetric analysis experiments successfully evaluated the oxidation rates of diesel PM and amount of soluble organic compounds and ashes contained in the PM samples. Differential scanning calorimeter experiments were successfully conducted to measure the specific heat of diesel PM as a function of temperature, showing a significantly different magnitude than those of diesel soot artifacts. (Lee, ANL)
- PNNL is adapting the micro-modeling capabilities developed by CLEERS to investigate substrate characteristics and spatial location of catalyzed washcoats on back pressure, soot regeneration and LNT function. LNT kinetics were identified and incorporated into a one-dimensional wall-flow micro-model. A multi-channel reactor experiment was conducted to determine the 'flow-through' versus 'wall flow 'performance. Single-channel reactor experiments to document NOx uptake of DOW's LNT washcoat were conducted and the effect of soot loading on NOx uptake was investigated. (Stewart, PNNL)
- PNNL is investigating fresh, laboratory- and engine-aged DOC and SCR catalysts to lead to a better understanding of various aging factors that impact the long-term performance of catalysts used in the urea-SCR technology, and improve the correlation between laboratory and engine aging in order to reduce development time and cost. Results demonstrate that the growth of platinum group metal in a DOC catalyst is a primary cause of deactivation. For the case of the urea-SCR catalyst, both the collapse of zeolite structure and the growth of active metal particles are observed for a heavily aged sample and attributed to the main reason for the activity loss. (Peden, PNNL)
- PNNL is developing a novel oxidation catalyst applicable for the HCCI engine which has lower engine exhaust temperature profiles than conventional diesel engines. PNNL demonstrated (via novel oxidation catalyst development) the ability to

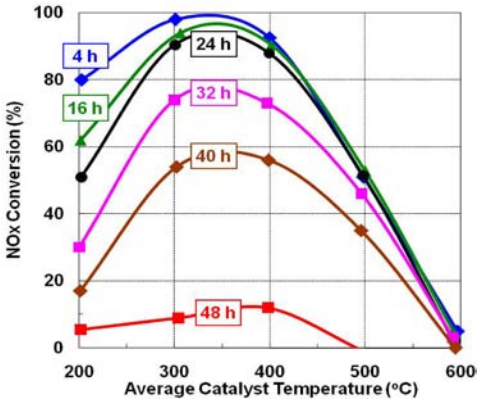

Changes in NOx Conversion over Aged Urea-SCR Catalysts as a Function of Aging Time (Peden, PNNL)

mitigate the inherent and unique engine emission challenges that currently face HCCI combustion strategies, helping to facilitate its applicability and ultimate implementation. Engine testing performed at Caterpillar shows that this can be accomplished with less platinum group metal requirements versus comparable supplier catalysts, helping to achieve engine cost requirements in addition to emission target requirements. (Rappe, PNNL)

C. Critical Enabling Technologies

Variable valve actuation (VVA), variable compression ratio, and combustion sensors are enabling technologies for achieving more efficient engines with very low emissions. The following highlights show the progress made during FY 2009.

- Cummins Inc. is improving heavy-duty diesel engine fuel efficiency by 10% through the recovery of waste heat energy, reducing the need for additional cooling capacity in Class 8 trucks, and providing conditioning (cooling) for combustion charge air. The engine and on-engine, R245fa-based, ORC energy recovery system were successfully operated. The system's predicted 8% fuel economy benefit from EGR and exhaust gas energy recovery was demonstrated. The project goal of 10% fuel efficiency improvement through the recovery of waste heat energy when combined with the benefit of electric engine parasitics was also demonstrated. This system mitigates the need for increased cooling capacity in Class 8 trucks and provides conditioning of combustion charge air. Effective controls to operate the energy recovery system through all engine operating conditions were developed and the energy recovery system components and subsystems were refined to minimize cost, complexity, and improve performance. (Nelson, Cummins)
- Caterpillar Inc. is developing technologies that will reduce all forms of exhaust energy loss, including: blowdown losses, aero machinery losses, fluid frictional losses, losses due to pulsating exhaust flow, heat transfer losses, and losses of energy out the exhaust stack to achieve a 10% improvement in engine thermal efficiency. The results of components tests, component design and analysis, and engine simulation has resulted in high confidence that the project goal of a 10% improvement in engine thermal efficiency can be achieved. A predicted system-level benefit of 8.0% is solidly based on a combination of: (1) Components for which performance has been demonstrated via bench tests of prototype hardware; and (2) Components for which performance has been predicted from design/analysis tools. In these cases confidence is bolstered by the similarity of these components to prototypes that have been demonstrated in hardware as part of prior research projects. Additional technologies are under investigation and show promise for further improvements, thus leading to the conclusion that the 10% target can be met. (Kruiswyk, Caterpillar)
- Volvo is developing a highly efficient engine system, including mild hybridization, to reduce carbon dioxide emissions from a long haul truck by >10%, in comparison to current production technology, while meeting U.S. 2010 emission levels. This engine platform would also be tolerant of biodiesel specifications. A narrow-speed turbocompound engine was simulated and showed a reduction in fuel consumption of 5 g/kW-hr over a typical European long haul cycle. Ultra-high injection pressure was found to produce lower soot emissions but higher NOx emissions. Optimization of the combustion system for a turbocompound, narrow-speed engine was found to yield a small but measurable improvement in the fuel consumption characteristics of the engine. Diesel operation at stoichiometry was found, in principle, to simplify the emission control system required for U.S. 2010 emission standards but significant issues concerning exhaust system component temperatures, DPF regeneration strategy and higher fuel consumption present formidable barriers. The use of fatty acid methyl ester and other similar biofuel blends in diesel fuel was found to be feasible from a combustion standpoint and produces lower soot emissions at comparable efficiency and NOx emissions. (Tai, Volvo)
- TIAX LLC is developing an accelerometer-based start of combustion (SOC) sensor which provides adequate SOC event capture to control an HCCI engine in a feedback loop. Three engines of the same model line/different serial number were installed to verify engine-to-engine repeatability of the SOC sensor system (a potential drawback of accelerometer-based systems), including two dynamometer setups and one vehicle setup. An initial real-time version of the SOC algorithm

has been developed to optimize the algorithm for accuracy and processing speed. Data over the operating range of interest (the expected HCCI operating envelope of low to medium speed, low to medium load) has been recorded. Twenty-two original equipment manufacturers and Tier 1 suppliers to push this technology out into the marketplace, ten of which have requested further information. (Smutzer, TIAX LLC)

- Westport Power, Inc. is developing an accelerometer-based SOC sensing system including a method to minimize sensor-to-sensor variation. The average sensor-to-sensor variation over all modes was reduced to 0.36 crank angle degree (CA°) at the 98.9% confidence level which exceeds the initial target of sensor-to-sensor variation of 0.5 CA°. The mode-averaged total error (based on one standard deviation) was reduced to 0.41 CA° which exceeded the initial target to achieve total error of measured SOC timing of 0.5 CA°. The capability of the accelerometer-based combustion sensing system was extended to capture not only the SOC timing but also the complete in-cylinder pressure trace. Significant improvement in the robustness of the processing method indicates as few as three knock sensors are required for a six-cylinder engine. On-road testing has demonstrated that the knock-sensor based combustion sensing method and the algorithm developed from the test cell studies are applicable to on-road application without major modification. (Mumford, Westport Power, Inc.)
- Envera LLC reduced the hydraulic pressures in the actuator system of its variable compression ratio (VCR) system by 86% through system optimization. The reduction in pressure significantly relaxes the demands that will be placed on the hydraulic system and enables cost to be reduced. Test results indicated that compression ratio can be reduced from 18:1 to 8.5:1 in ~0.35 seconds, and increased from 8.5:1 to 18:1 in ~0.70 seconds. On average 0.074 seconds is projected to elapse for each point increase in compression ratio. Finite element analysis of the production-intent 4-cylinder VCR engine predicts that the crankcase meets all stiffness, robustness and durability requirements for mass production. Production-intent design optimization of the VCR engine crankcase with imbedded VCR actuator system was completed and the upper crankcase has been optimized for low-cost mass production. (Mendler, Envera LLC)

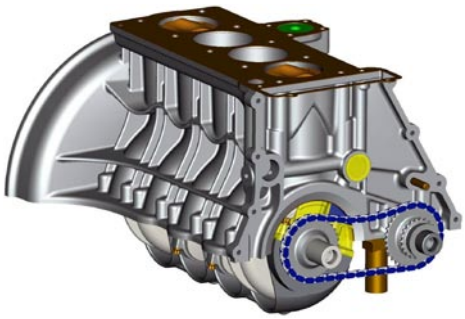

VCR Crankcase, with Hydraulic Cylinder located Vertically next to the 3rd Engine Cylinder (Mendler, Envera)

D. Health Impacts

The Health Impacts activity studies potential health issues related to new powertrain technologies, fuels, and lubricants to ensure that they will not have adverse impacts on human health. The following are highlights of the work conducted in FY 2009.

- ORNL is seeking to understand the potential impact of developing fuel, combustion, and aftertreatment technologies on air quality, quantify mobile source air toxic (MSAT) emissions from advanced technologies, and link emissions measured in the laboratory to air quality impact, and thereby, health impact. MSATs were measured from several light-duty vehicles operating on intermediate blends of ethanol (E10, E15 and E20). It was found that higher ethanol blends decrease emissions of benzene, toluene, ethylbenzene, and xylenes (BTEX) over a driving cycle and that the decrease is proportionally higher than what would be expected from simple mixtures with ethanol which does not contain

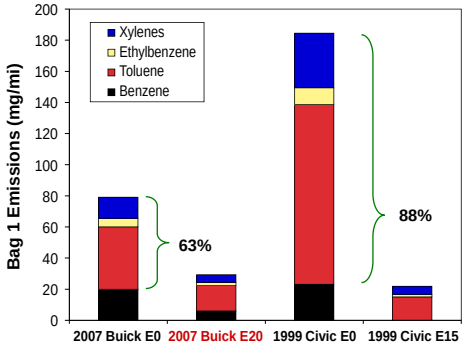

Intermediate ethanol blends substantially lower MSATs such as benzene, toluene, ethylbenzene and xylenes. (Storey, ORNL)

BTEX. An intensive campaign to measure the morphology and effective density of diesel PM from conventional and PCCI operation was completed. It was found that the difference in effective density of conventional diesel and PCCI PM depended on particle diameter. TEM analysis of diesel particle morphology was conducted and compared to the particles generated using HECC modes. Particle size and number concentration emissions from an HCCI engine operating on surrogate gasoline fuels was characterized and it was found that combustion phasing for reduced fuel consumption and particle number concentration emissions was affected by fuel chemical composition. (Storey, ORNL)

- The National Renewable Energy Laboratory (NREL) is quantifying the role of engine lubricating oil on PM and semi-volatile organic compound emissions from in-use motor vehicles fueled with gasoline, 10% ethanol in gasoline (E10), diesel, biodiesel, and compressed natural gas while operating on fresh and used crankcase lubricants. Both "normal" and "high-emitting" vehicles are being tested. To date, vehicle testing has been completed on the light-duty and medium-duty "normal" and "high-emitters" – heavy-duty vehicle testing will begin in October 2009. This project will be completed by August 2010, and results will be available at that time. (Lawson, NREL)
- The Health Effects Institute (HEI) is conducting a cooperative, multi-party effort to characterize the emissions and assess the safety of advanced heavy-duty diesel engine and aftertreatment systems and fuels designed to meet the 2007 and 2010 emissions standards for PM and NOx. The Phase 1 report was published and disseminated in June 2009. Characterization of emissions and exposure atmosphere in Phase 3 has made important progress and the main health effects testing will go forward by the end of 2009. (Greenbaum, HEI)

Solid State Energy Conversion

Several projects are being pursued to capture waste heat from advanced combustion engines in both light- and heavy-duty vehicles using thermoelectrics (TEs). Following are highlights of the development of these technologies during FY 2009.

- General Motors Research & Development Center (GM) is studying the basic physics and chemistry of new and breakthrough TE materials, conducting modeling and design of a waste heat recovery device for automotive applications and, completion of engineering and assembly of a working TE generator. The TE generator design has been finalized, various parts and components have been ordered, and fabrication is underway. A generator and power conversion topology was selected and initial circuit simulation models were developed to examine high-level performance. A functioning prototype module has been fabricated and is now being tested. A method for improving the TE properties of type I clathrates by transition metal doping on the Ga sites has been developed. (Meisner, GM)

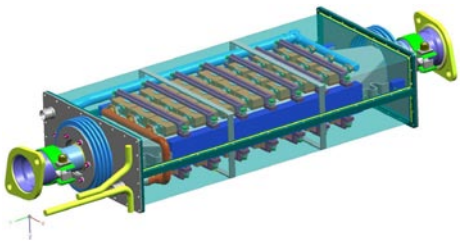

Side view of the GM TE Generator Design (Meisner, GM)

- BSST is designing and testing a full-scale, high-temperature (600°C) thermoelectric generator (TEG) integrated with a BMW 6-cylinder engine in conjunction with BMW, Ford, Visteon, and Emcon Technologies LLC. High-temperature TEG subassemblies are in the final stages of build and test and dynamometer testing is planned to occur in January 2010. A significant TEG redesign has occurred, in which the planar form has been succeeded by a cylindrical shape, offering significantly improved manufacturability and, as a result, accelerated readiness for commercialization. The cylindrical TEG has been designed to provide a nominal 500 watts electric power during a 130 kph driving condition. Emcon has joined the BSST-BMW-Ford team for the 5th and final phase and has designed the TEG into BMW X6 (manufactured in South Carolina) and Ford Fusion exhaust systems. (LaGrandeur, BSST)

- Michigan State University (MSU) is conducting an in-depth effort aimed at determining the viability of using advanced TE materials implemented in an electric generator to recover waste heat from an over-the-road (Class 8) truck. A batch of Skutterudite unicouples were fabricated, and the unicouples were used to build modules. The modules were used to construct a TEG and a specialized test facility was constructed to test the TEG. The retail price of a 5-kW system was estimated to be $19,276.13 and pay-back on a typical Class 8 truck is projected to be three years. (Schock, MSU)

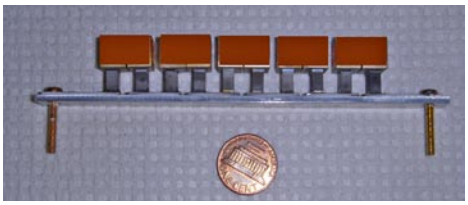

10-Leg Thermoelectric Module Capable of Producing 5 W (Schock, MSU)

University Research

- University of Michigan (UM) is investigating the fundamental processes that determine the practical boundaries of LTC engines. Over the past year, UM found the following: (1) The experimental high load limit established last year by supercharging has been extended by more than 2 bar NMEP to 8.7 bar in multi cylinder tests; (2) Extending the low-load limit to near 1 bar net mean effective pressure was shown to be achievable through fuel injection during NVO; (3) A multi-mode combustion diagram has been established to delineate the characteristic regimes of combustion including spark ignition, HCCI and spark-assisted compression ignition (SAIC); (4) A comprehensive analytical exploration of flame propagation at spark assist conditions has been carried out; the study supports the experimental engine observations that viable flame propagation is possible at SACI conditions not normally encountered in conventional SI engines; and (5) Previous ignition delay studies of small biofuels esters carried out in the UM Rapid Compression Facility have been extended to include speciation studies of the intermediates formed during ignition of methylbutanoate and air mixtures. (Assanis, UM)
- The University of Houston is utilizing a combination of experimental and theoretical tools to advance LNT technology. Isotopic temporal analysis of products (TAP) studies were conducted which show that the transport of stored NOx is an important rate limiting process during regeneration/reduction. Comprehensive cyclic studies using H_2 were completed which reveal a significant effect of the Pt dispersion on the storage and reduction rates as well as product distribution. A global reaction-based LNT model was developed which predicts most of the spatio and temporal data using H_2 as the reductant. A crystallite level description was incorporated that accounts for stored NOx gradients and predicts most of the trends in the dependence of conversion and selectivity on Pt/BaO catalysts with a wide range of Pt dispersions. A microkinetic model of NOx storage was developed which predicts most of the trends including the effect of Pt loading. Construction of a second bench-scale reactor system was completed which enables the use of actual diesel engine exhaust feeds. Low-dimensional models were developed that can be used for real time simulations of catalytic after-treatment systems. (Harold, University of Houston)
- The University of Kentucky is examine the effect of washcoat composition on LNT catalyst aging characteristics. Steady-state data for NOx reduction over fresh and aged model LNT catalysts have been obtained and analytical data have been acquired for the fresh and aged catalysts which provide insights into the physico-chemical changes that occur in the washcoat during aging. A detailed high resolution transmission electron microscopy study has been performed on the fresh and aged catalysts which revealed that two main factors can be held responsible for the degradation in LNT performance, viz., (i) Pt particle sintering and (ii) sulfur accumulation in the washcoat (associated with the Ba phase) resulting from repeated sulfation-desulfation cycles. Spectacular improvement in LNT durability through the incorporation of CeO_2 or CeO_2-ZrO_2 in the washcoat has been demonstrated and the factors responsible for this improvement elucidated. (Crocker, University of Kentucky)
- The University of Texas (UT) Engine Combustion Laboratory is refining and completing development of an on-board PM sensor, bringing it to a point where it can be commercialized

Typical EmiSense electronic soot sensor with electrode and shrouds on the left, M18 threads, and sensor body on the right. (Hall, UT at Austin)

and marketed. New sensor designs were developed that make use of new manufacturing technologies that bond electrodes directly to ceramic support posts which are electrically isolated in metal bases. Testing in a 2008 model year Cummins 6.7 liter diesel engine showed that at least for some operating conditions, it has the sensitivity to detect DPF failures and the time resolution for feedback control applications. Sensitivity decreased with increasing EGR levels. The sensor was found to be most sensitive to the number density of the smallest (nucleation mode) particles. Because of this the sensor's sensitivity it is affected by any engine operating condition that changes the particle size distribution, particularly of the smallest particles. These conditions may include engine load, EGR level and downstream location in the exhaust. The effect of gas velocity on sensor sensitivity is complex and may be compensated for by sensor orientation. Commercialization efforts are proceeding with Emisense. (Hall, UT at Austin)

FUTURE DIRECTIONS

Advanced Combustion and Emission Control Research for High-Efficiency Engines

A. Combustion and Related In-Cylinder Processes

The focus in FY 2010 for combustion and related in-cylinder processes will continue to be on advancing the fundamental understanding of combustion processes in support of achieving efficiency and emissions goals. This will be accomplished through modeling of combustion, in-cylinder observation using optical and other imaging techniques, and parametric studies of engine operating conditions.

- ANL will begin a new collaboration with Delphi Diesel Systems. Over the next few years, Delphi will deliver modern fuel system hardware to ANL to be studied using several X-ray diagnostics. These measurements will focus on the study of how different nozzle geometries affect the fuel distribution in the combustion chamber. The relevance of the measurements will be enhanced by studying sprays under conditions even closer to those of modern diesel engines. Measurement improvements will be made including faster data acquisition, processing, and analysis, improved X-ray detector systems, increased X-ray intensity, finer spatial resolution, and greater automation. Collaborations with modeling groups will be increased to increase the fundamental understanding of the mechanics of the spray event, while collaborations with industry will guide development of a technique that is useful as a diagnostic for injection system manufacturers. (Powell, ANL)
- SNL will investigate fuel property effects on combustion efficiency and associated UHC and CO emissions, varying both fuel volatility and ignition quality. The impact of biofuel blends on the fuel preparation, combustion, and emissions formation and oxidation processes will be examined. UHC imaging studies will be extended to the horizontal plane to capture lack of symmetry in squish volume UHC sources associated with piston top valve pockets and head features. Horizontal plane flow field data will be obtained to support the interpretation of UHC images, to examine asymmetries in the squish flow patterns, and to characterize the attenuation of angular momentum in the squish volume. (Miles, SNL)
- SNL has shown that diesel jet interactions are critical for soot reductions with multiple injections. Based on this observation, SNL will: (1) Use planar laser diagnostics (laser-induced incandescence, hydroxyl radical planar laser-induced fluorescence) to learn how soot formation dynamics can be controlled; (2) Use planar-laser diagnostics (fuel tracer PLIF, formaldehyde PLIF) to understand mixing, ignition, and combustion dynamics of multiple injections; (3) Understand how post-injection interactions with main-injection soot are affected by targeting: vary the injection spray angle and/or swirl; and (4) Use other injections schemes (split-main, pilot, three or more

injections). SNL will also consolidate insights from multiple institutions and try to build a consensus on the chemical and mixing processes of LTC to develop and refine conceptual model extension for LTC. (Musculus, SNL)

- SNL will continue their investigation of fundamental causes of UHC and CO formation in LTC. They will develop a quantitative dataset of penetration, mixing, combustion, and soot formation for neat biodiesel and diesel. The extent of liquid penetration at problematic post-injection conditions, injections which are now used for diesel particulate filter regeneration will be quantified. Direct measurements of mixing (equivalence ratio) at the time of the premixed burn in constant-injection-duration diesel fuel jets for various EGR levels will be performed. Mixing and combustion measurements will also be performed at the Engine Combustion Network working group conditions and jet-jet interaction effects on flame lift-off will be investigated. (Pickett, SNL)
- ORNL will further explore HECC strategies on a GM 1.9-L engine. The effect of thermal boundary conditions on HECC operation with expanded control of the thermal boundary conditions will be explored. The efficiency/emissions potential of advanced gasoline-diesel combustion concepts on the GM 1.9-L engine will be characterized. Support of efficiency and emission controls activities will be continued to ensure collaborative path toward FY 2010 DOE FreedomCAR milestones. (Wagner, ORNL)
- SNL will continue development of their state-of-the-art simulation capability based on the LES technique. Future analysis will focus on multidimensional turbulence-chemistry interactions and related cycle-to-cycle variations in the actual engine geometry. In addition, they will begin to focus on high-pressure injection of liquid hydrocarbon fuels at thermodynamically near-critical and supercritical conditions. The multiphase injection dynamics associated with these conditions are common to state-of-the-art engines and dominate all subsequent modes of combustion. SNL will focus on the transient evolution of the injection process with different fuels to determine the mixture state and flow topology just prior to, and during, combustion. In addition, they will perform a series of simulations that identically match the hierarchy of direct injection experiments of Pickett (see www.ca.sandia.gov/ECN) using n-heptane as our initial fuel. This work will be complemented by extending the Subgrid-Scale model development efforts in combustion to high-pressure regimes in collaboration with Barlow et al. as an extension of the flames studies as part of the Turbulent Nonpremixed Flames workshop (www.ca.sandia.gov/TNF). (Oefelein, SNL)
- LLNL will continue their combustion modeling development in the coming year. Further CHEMKIN multizone execution will be accelerated by software and hardware implementations that will further reduce fluid mechanics and chemical kinetics calculations. Analysis tools under partially stratified conditions will be validated by working with engine researchers at Sandia Livermore (John Dec and Dick Steeper) to validate KIVA multi-zone code at partially stratified conditions. Fast modeling of partially stratified combustion with an artificial neural network-based chemical kinetics model will be demonstrated. (Aceves, LLNL)
- SNL will continue HCCI combustion development by determining how natural thermal stratification develops in an HCCI engine, including its magnitude and distribution, which is critical for high-load HCCI operation. The investigation of intake boosting at a representative 1,200 rpm condition will be completed and the investigation of boosted HCCI to a wider range of operating conditions will be expanded. The natural thermal stratification and its potential for extending the high-load limit of HCCI over a wider range of conditions will be investigated. Collaboration with J. Oefelein et al. (SNL) to apply LES modeling to determine the main mechanisms producing thermal stratification, and how they might be enhanced will be explored. Additional studies of the performance of ethanol over a wider range of operating parameters, including: EGR, load, and intake-boost will be conducted and collaboration with LLNL on improving chemical-kinetic mechanisms and on combined CFD and kinetic modeling will be continued. (Dec, SNL)
- SNL will continue optical-engine investigations designed to enhance our understanding of in-cylinder processes in automotive-scale HCCI engines. In the coming year, SNL will apply infrared absorption and laser-induced fluorescence optical diagnostics to characterize reforming reactions during the NVO period; apply optical diagnostics to quantify piston wetting during NVO fuel injection to understand its effect on NVO- and main-combustion reactions; and validate

the University of Wisconsin CFD model of our automotive HCCI engine using optical and conventional measurements over a range of NVO operating conditions. (Steeper, SNL)

- ORNL will continue achieving and demonstrating Vehicle Technologies engine fuel efficiency goals. A peak brake thermal efficiency of 45% on a light-duty diesel engine will be demonstrated and the potential of an ORC or other recovery technology for recovering exhaust energy under conditions consistent with road-load operation will be evaluated. A prototype turbo-compounding system being developed and supplied to ORNL by VanDyne SuperTurbos will be tested. Vehicle systems level simulations with an integrated transient-capable ORC model using GT-Drive and/or PSAT will be performed to estimate the potential benefits of and manage implementation issues associated with thermal energy recovery on light-duty vehicle applications. (Wagner, ORNL)
- LANL will continue development of KIVA-4 for release as a parallel version. Specific activities will include (1) Comparing Sandia's diesel engine data with an LES turbulence model in KIVA-4 on the complex diesel engine geometry in collaboration with Iowa State University; (2) Continue cut-cell grid generation development to include more complex geometries and demonstration of solution on both a few general benchmarks and on a KIVA-engine test case, and continue the development of the moving grid system, and make use of more of the unstructured grid constructions in this process; (3) Develop an hp-adaptive characteristic based split finite element method for multiphase incompressible and compressible flows and begin implementing this method to perform KIVA-type (ICE), other engine, and also general combustion modeling. (Carrington, LANL)
- LLNL will continue to develop detailed chemical kinetic models for fuel components used in surrogate fuels for diesel and HCCI engines. A high- and low-temperature mechanism for selected higher molecular weight iso-alkanes will be developed, an important chemical class in diesel fuel. A high- and low-temperature mechanism for a high molecular weight alkyl-benzene will be developed, to represent aromatics in diesel fuel. An improved mechanism for toluene and benzene and efficient software to create reduced mechanisms for use in multidimensional engine simulation codes will be developed. (Pitz, LLNL)
- SNL will continue fabrication and assembly of a two-stroke, opposed free-piston hydrogen engine. In the coming year, assembly of the research prototype engine, bounce chamber air control system, and piston lock-and-release mechanism will be completed and associated support and data acquisition hardware will be acquired. The engine will be initially run under air injection motoring mode only to test the stabilizing capability of the linear alternator coupling. Combustion experiments will then be performed and indicated thermal efficiency will be measured at various compression ratios and equivalence ratios with both conventional and alternative fuels: hydrogen, natural gas, ethanol, biofuels, propane, gasoline, and other renewables. (Van Blarigan, SNL)
- ANL plans to continue their optimization of direct injection hydrogen combustion engine performance. In the coming year, ANL will upgrade their research engine to an optimized bore-stroke ratio and expand the efficient operating regime to higher speeds using Piezo-driven injectors. Improved injector nozzle designs will be developed for specific operation conditions (injector location, injection strategy) supported by optical engine results (Sandia National Laboratories) and 3-D CFD simulation. Optimized mixture formation strategies with in-cylinder NOx emissions reduction measures will be combined. (Wallner, ANL)
- SNL will continue to provide the science base for the development of high-efficiency hydrogen-fueled vehicle engines. A database on hydrogen/air mixture preparation with in-cylinder velocity measurements for selected injection strategies will be completed. A new engine head, supplied by Ford, will be installed featuring central or side injection and central ignition. Supplement quantitative laser-based techniques with qualitative high-speed Schlieren measurements to understand temporal development mixture formation. Planar laser-induced fluorescence of hydroxyl radicals will be used to investigate combustion with multiple injections per cycle. (Kaiser, SNL)
- Cummins will continue to design and develop advanced engine architectures capable of achieving U.S. EPA 2010 emission regulations while improving brake thermal efficiency by 10% compared to current production engines. The structural analysis of the final combustion system for the 15L ISX engine and the commercial viability assessment of HECC technologies for the 15L ISX and the

6.7L ISB engines will be completed. Vehicle packaging studies for the engine and aftertreatment components will also be completed. Transient fuel consumption improvements over a variety of vehicle duty cycles will be confirmed using a combination of test cell and software analysis. The development of the SCR dosing system controls strategy to maximize engine efficiency will be finalized and the cost of the ammonia slip catalyst will be optimized and the size of the SCR system catalyst will be reduced. The DOC formulation that thrifts the precious metal content will be optimized and on-board diagnostics associated with the implementation of the new HECC subsystem technology will be developed to achieve proper functioning during in-use operation. (Stanton, Cummins)

- Caterpillar will continue their efforts to identify and develop technologies to enable low-temperature, high-efficiency combustion. They will identify an air system configuration that delivers the EGR needed for PCCI combustion and meets engine performance requirements. They will also develop an alternative fueling strategy to extend the thermodynamic advantages of PCCI to full load. (Fiveland, Caterpillar)
- Navistar will continue their efforts to apply LTC to their 6.4L V8 engine. An electro-hydraulic VVA system developed during the course of this project was installed and used to explore the impact of valve timing on effective compression ratio and improved engine thermal efficiency. KIVA simulations captured the combustion process, matching experimental pressure and heat release traces and will be used to further optimize combustion boundary conditions provided by VVA to extend the operation of LTC. The engine will be re-run through the federal transient heavy-duty cycle with VVA hardware and the electronic control unit will be expanded to use valve timing control. (de Ojeda, Navistar)
- ORNL will continue their efforts to analyze and define specific pathways to improve the energy conversion efficiency of ICEs. Construction of the regenerative air preheating with thermochemical recuperation (RAPTR) bench-top constant volume combustor will be completed and low-irreversibility combustion in the RAPTR bench-top apparatus will be experimentally demonstrated. Data from RAPTR experiments to determine efficiency implications and appropriate ways to model exergy losses under different operating modes will be analyzed. Better ways for recuperating exhaust heat and utilizing compound cycles for extracting work will continue to be explored. They will continue exercising engine and combustion models to identify combustion modifications that would mitigate exergy losses. (Daw, ORNL)
- DDC will continue their efforts to explore advancements in engine combustion systems using HECC techniques to improve thermal efficiency while minimizing cylinder-out emissions. They plan to continue evaluation of advanced combustion concepts with advanced fuel injection systems and development of closed-loop real-time combustion control using novel in-cylinder sensors. Fuel injection strategy and multiple combustion modes will be consolidated to maximize thermal efficiency while maintaining or reducing engine-out emissions compared to baseline. Transient combustion and control development using next generation model based control technology will be continued, and optimized sub-components and optimized combustion strategy will be integrated into a system targeting 10% thermal efficiency improvement. (Zhang, DDC)
- GM will demonstrate a fully-flexible gasoline-fueled HCCI engine. They will use the engine as the test bed for production-style cylinder pressure sensing subsystems. Experimental testing of a concentric camshaft mechanism for variable effective compression ratio in a multi-cylinder diesel engine will be conducted, a review of variable valve actuation profiles for functionalities at key conditions of engines in driving cycles will be completed, and the design of purpose-built mechanisms for specific functionalities on cold- and hot-engine operation will be done. Further study of the synergy of intake and exhaust camshaft valve actuation mechanisms on steady-state and transient engine in-cylinder conditions will be conducted and emissions and fuel efficiency benefits with single-cylinder and multi-cylinder engine development will be validated. (Patton and Gonzalez, GM)
- Cummins will develop an advanced combustion system that meets EPA Tier 2, Bin 5 emissions standards while demonstrating a 10.5% improvement in fuel economy over the Federal Test Procedure (FTP) city drive cycle. In the coming year, emphasis on simulation will be reduced and

experimental development and validation will become the primary focus. Multi-cylinder engine testing using the Phase 2 hardware (revised 2-stage sequential turbo, piezo fuel system, high-capacity EGR, controls, and aftertreatment) will be performed and a detailed engine calibration using the Phase 2 technology to meet FTP75 and SFTP2 emissions certification will be developed. A new SCR system design with full engine and aftertreatment calibration will be incorporated and VVA testing and design refinement will be continued. Technology to enhance aftertreatment thermal management will be explored and transient assessment of fuel efficiency improvements will be completed using test cell and software analysis procedures. Biofuel blends will be tested to demonstrate compatibility. (Stanton, Cummins)

- Ford will continue their development of advanced engine boosting through development of advanced turbocharger technology. In the coming year, the final design and analyses of the compressor and turbine will be completed. The strategy will focus on compressor impeller improvement and casing treatment optimization, rather than variable compressor inlet guide vane and variable diffuser vane as previously suggested. The next steps will include: fabrication of the redesigned compressor and turbine wheel, using fewer moving parts in the compressor to achieve wider operation range with efficiency improvement, and flow bench test validation. (Sun, Ford)
- ANL will continue to utilize in-cylinder combustion imaging to expand the operational limits of LTC in a production automotive engine. In the coming year, ANL will evaluate the operation of their GM 1.9-L turbodiesel using "Next Cycle" control using stock piston crowns (17.5:1) and iso-paraffinic kerosene fuel and naptha-type fuel. The performance and emissions signature obtained by operating these fuels, especially NOx emissions and brake specific fuel consumption will be analyzed. Additional experiments using lower compression ratio piston crowns will be conducted. (Ciatti, ANL)
- ORNL will continue to demonstrate a practical application of HCCI in a production-level, light-duty gasoline engine. During the coming year, ORNL will (1) Continue hardware evaluation and integration of valve mechanism for controlling intake/exhaust valve lift and timing; (2) Calibration of the spark-assisted HCCI model with data from the single- and multi-cylinder engines; and (3) Implement and evaluate control strategy for multi-mode operation on the multi-cylinder HCCI engine which is now located at the Delphi research facility in Auburn Hills, Michigan. (Wagner, ORNL)

B. Energy-Efficient Emission Controls

In FY 2010, work will continue on LNTs and urea-SCR to reduce NOx emissions. The focus of activities will be on making these devices more efficient, more durable, and less costly. For PM control, the focus will be on more efficient methods of filter regeneration to reduce impact on engine fuel consumption.

- PNNL will continue to lead and contribute to CLEERS activities. Activities in the coming year include: (1) Conduct fundamental filtration experiments with samples of commercial filter substrates using lab-generated soot and simple aerosols; (2) Validate discrete particle filtration project by comparison to theoretical unit collector models; (3) Further examine the hydrocarbon poisoning of SCR catalysts using engine-out hydrocarbon and fuel-component hydrocarbon species, and incorporate the inhibition model into the Fe-zeolite SCR model; (4) Examine the SCR catalyst deactivation through reactor testing and spectroscopic analysis, and develop a model to describe the performance degradation behavior; (5) Investigate the hydrolysis of HNCO over an Fe-zeolite SCR catalyst; (6) Examine the interaction between LNT and SCR catalysts in the integrated LNT-SCR system through reactor testing and modeling; (7) Develop a new model to describe the NOx reduction performance of SCR/DPF technology; and (8) Continue studies of CO_2 and H_2O effects on BaO morphology changes and NOx storage properties. (Herling, PNNL)
- PNNL will continue to identify approaches to significantly improve the high-temperature performance and stability of LNT technology. Activities during the coming year include: (1) Complete studies of sulfur-loading levels on the desulfation behavior of model BaO-based LNT materials to develop a fundamental understanding of these effects; (2) Determine the effects of

H_2O and CO_2 on the desulfation of ceria-supported BaO LNT materials; (3) Compare behavior of ceria-supported and ceria-doped, alumina supported BaO LNT materials; and (4) Initiate studies to determine performance limitations, sulfur sensitivity and desulfation behavior of candidate alternative support materials that provide improved high-temperature performance. (Peden, PNNL)

- ORNL will continue their efforts to understand the complex chemistry that occurs during the regeneration processes for LNTs through experiments conducted on a full-size engine-LNT catalyst system. In the coming year, they will evaluate the performance of the LNT+SCR approach at higher space velocities (reduced catalyst size and cost), and conduct experiments relative to lean gasoline engine applications of LNTs. (Parks, ORNL)
- SNL will continue their efforts to develop chemical kinetics models for LNTs. They will account for the role of hydrocarbons and partial oxidation products as alternate reductant species during normal catalyst regeneration; enhance the transient plug flow reactor code with a complete energy balance equation, and use this to simulate more conventional short storage/regeneration cycles, in which temperature excursions cannot be neglected or easily measured; and use the validated reaction mechanisms to investigate coupling between an LNT and other devices in the aftertreatment train. (Larson, SNL)
- ORNL continue NOx abatement research and development with Navistar, Inc. It is planned to optimize the transient evaluation protocol to identify a minimal set of sufficient steps and operating conditions required for model calibration and validation. The protocol will be transferred to the CLEERS SCR focus group as a starting point for development of a standard CLEERS transient SCR protocol. Soot oxidation kinetics of engine-generated soot loaded in miniature DPF samples will be measured for use in a DPF regeneration control model. (Pihl, ORNL)
- ORNL will continue their fundamental sulfation/desulfation studies of LNTs. The stability of the Ca in the Ba lattice will be determined to understand if the observed performance improvements withstand aging. A key material impact from Ca insertion will be confirmed and work with modelers at the ORNL Center for Nanophase Materials Science undertaken to understand how the improvement is occurring. Modeling will be used to identify other dopants and appropriate concentrations to investigate. (Toops, ORNL)
- ORNL will continue to improve diesel engine-catalyst system efficiency through better combustion uniformity, engine calibrations and catalyst control. They will quantify engine combustion non-uniformities and develop mitigation strategies, and enable development of self-diagnosing smart catalyst systems through: (1) Detailed characterization of the spatiotemporal relationship between natural and indicator chemical functions and catalyst properties throughout the catalyst operation and ageing; and (2) Develop methods for in situ, on-engine-system assessment of catalyst state. (Partridge, ORNL)
- ORNL will continue their efforts to assess the relative merits of efficient emissions control for multi-mode lean direct injection engines. In the coming year they will investigate synergies between SCR and advanced combustion (HECC), and study the potential of on-board diagnostics for reducing the fuel penalty of DPFs. (Parks, ORNL)
- ORNL will continue co-leading the CLEERS planning committee and co-leading the LNT Focus Group, and support the DPF and SCR Focus Groups as needed. ORNL will also continue providing standard reference LNT materials and data for Focus Group evaluation and continue assisting in refinement of CLEERS technical priorities, especially in regard to the balance between LNT and urea-SCR R&D and synergies between these two technology areas. ORNL will organize and conduct the 2010 CLEERS workshop in the spring of 2010. Basic data and model exchange between CLEERS and other VT projects will be expanded and maintenance and expansion of the CLEERS Web site will be continued. Regular update reports to the DOE Diesel Crosscut team will be provided. (Daw, ORNL)
- ORNL will continue supporting the CLEERS joint development of benchmark kinetics by confirming primary chemical mechanisms and kinetics of sulfation and desulfation, implementing a combined LNT model that includes NOx capture and reduction and sulfation and desulfation in a

form that can be used for systems drive cycle simulations and shared with the CLEERS community, and investigation of urea-SCR kinetics. Additional activities will include: (1) Understanding the detailed structures and mechanistic implications of the different LNT sulfur species identified in Fiscal Year 2009; (2) Broaden the understanding of LNT NH_3 chemistry by evaluating performance as a function of the nature of reductant (H_2, CO, HCs); and (3) Perform detailed identification of surface spectral features of CLEERS reference urea SCR catalyst under relevant operating conditions to refine mechanistic understanding of HC fouling. (Daw, ORNL)

- ANL will evaluate pressure drop across DPF membranes during PM filtration processes, develop technologies to reduce pressure drop across the DPF membrane, and measure the thermo-physico-chemical properties of diesel PM emissions for future numerical calculations. (Lee, ANL)
- PNNL will adapt the micro-modeling capabilities developed by the CLEERS Program to investigate substrate characteristics and spatial location of catalyzed washcoats on back pressure, soot regeneration and LNT function. They will also incorporate simplified LNT kinetics into the PNNL micro-model and exercise the model to answer key questions regarding DOW's acicular ceramic material substrate attributes. (Gallant, PNNL)
- PNNL will continue to develop an understanding of the deactivation mechanisms of and interactions between the DOC and the urea-SCR catalyst used in light-duty diesel aftertreatment systems. Upcoming activities include revising the initial laboratory aging protocol used, and continuing to evaluate of the most effective characterization tools in order to provide additional crucial information about materials changes in the active catalytic phases. (Peden, PNNL)
- PNNL will end their efforts to develop a novel oxidation catalyst applicable for HCCI engines. Significant control challenges currently face the HCCI engine development platform. Once rectified, a novel after-treatment oxidation catalysis platform such as this system needs to be demonstrated on an HCCI-configured engine over a range of transient and steady-state conditions to demonstrate both activity and durability. (Stewart, PNNL)

C. Critical Enabling Technologies

The critical enabling technologies activities in FY 2010 include work on VVA, VCR systems, and combustion sensors.

- Cummins will improve engine fuel efficiency by 10% through the recovery of waste heat energy, reduce the need for additional cooling capacity in Class 8 trucks, and provide conditioning (cooling) for combustion charge air. In the coming year, Cummins will continue development of an effective and efficient organic Rankine cycle waste heat recovery system. They will proceed with second-generation system hardware testing and demonstration that incorporates production-intent design features. Additional fuel economy benefits from recovering heat from the compressed fresh charge air will be demonstrated. (Nelson, Cummins)
- Caterpillar will continue their study of waste heat recovery systems to demonstrate significant progress toward the goal of a 10% improvement in thermal efficiency using prototype components. In the coming year, an on-engine demonstration of a 5 to 7% improvement in thermal efficiency using advanced turbocharger technologies, intercooling, insulated exhaust ports, and mechanical turbocompound will be demonstrated. Parallel developments of technologies for future integration into the system solution, including the mixed flow turbine and electric turbocompound will be pursued. (Kruiswyk, Caterpillar)
- Volvo is developing a highly efficient engine system, including mild hybridization, to reduce carbon dioxide emissions from a long haul truck by >10%, in comparison to current production technology, while meeting U.S. 2010 emission levels. The major areas of focus include the development of a very high efficiency powertrain system, including an optimized narrow-speed turbocompound engine, an automated powershift transmission and mild hybridization. An additional area of focus is the adaptation of the diesel engine for the use of biofuels, primarily fatty acid methyl ester (FAME) fuels, and blends of FAME biofuels with conventional petroleum-based diesel fuel. All these efforts will see further development in the coming year. (Tai, Volvo)

- TIAX LLC has developed a pre-production prototype accelerometer-based SOC sensor which provides adequate SOC event capture to control an HCCI engine in a feedback loop. Twenty-two original equipment manufacturers (OEMs) and Tier 1 suppliers were contacted to push this technology out into the marketplace, ten of which have requested further information. Further project progress depends on the responses from OEMs and Tier 1 suppliers. (Smutzer, TIAX LLC)
- Westport Power, Inc. completed development of an accelerometer-based SOC sensing system. Significant improvement in the robustness of the processing method indicates as few as three knock sensors are required for a six-cylinder engine. On-road testing has demonstrated that the knock-sensor based combustion sensing method and the algorithm developed from the test cell studies are applicable to on-road application without major modification. (Mumford, Westport Power, Inc.)
- Envera LLC is developing a proof of concept variable compression ratio (VCR) actuator system and will optimize the design to be suitable for production. Envera will optimize the hydro-mechanical system crankcase for improved performance and manufacturability and rig-test the VCR actuator and demonstrate low-cost, fast response and mass production practicality. (Mendler, Envera LLC)

D. Health Impacts

The focus of the activities in Health Impacts is to identify and quantify the health hazards associated with exhaust from advanced combustion engines and put them in proper context with other air quality hazards, and to assess the relative hazards of emissions from different fuel, engine, and emission reduction technologies.

- ORNL will continue their study of health effects from advanced combustion and fuel technologies by characterizing particulate emissions from a direct-injection spark ignition vehicle operating on gasoline and intermediate blends of ethanol, examining mixed-mode DPF/LNT/SCR catalytic effects on mobile source air toxics, and reconciling idealized aggregate theory with PM samples collected under conventional and HECC conditions. (Storey, ORNL)
- NREL will continue their collaborative lubricating oil study on emissions project by testing heavy-duty vehicles over different driving test cycles at room (72°F) temperature on chassis dynamometers. The fuels used will be diesel fuel and natural gas. The complete vehicle and emissions testing project will be completed during FY 2010. (Lawson, NREL)
- HEI will continue management of the Advanced Collaborative Emissions Study. The Phase I final report will be published in a peer-reviewed journal. Phase 3A emissions and exposure chamber characterization will be completed. The chronic bioassay in rats and associated biological screening studies in rats and mice will be started. (Greenbaum HEI)

Solid State Energy Conversion

Research will continue in FY 2010 on thermoelectrics for converting waste heat from advanced combustion engines directly to electricity. Research will focus on development of practical systems that are suitable for future production.

- GM will continue to develop TE technology for automotive waste heat recovery. In the coming year, GM will: (1) Complete construction and assembly of the TE generator subassemblies; (2) Complete fabrication of PbTe modules and validation of their performance; (3) Assemble and integrate TE generator into a vehicle exhaust system; (4) Integrate TE generator into the controls and electrical system of the test vehicle, and conduct preliminary testing; (5) Collect and analyze performance data for TE generator in a test vehicle; and (6) Develop metal contact layers for skutterudites by completing prototype TE module construction, starting performance tests of prototype TE modules, completing TE exhaust waste heat recovery subsystem prototype construction, and completing vehicle modification for TE generator performance testing. (Meisner, GM)
- BSST is planning to complete dynamometer testing of a high-temperature TEG at NREL to validate the vehicle fuel efficiency performance model and to gain experience operating the TEG with an ICE. By June 2010, BSST, together with Emcon, will install high temperature TEGs into

BMW and Ford demonstration vehicles to gain further experience and to show concept readiness. (LaGrandeur, BSST)

- MSU will continue their study of TE conversion of waste heat to electricity in an ICE-powered vehicle. They will establish the modes of failure experienced during operation of the generators and engineer a solution to correct these issues. The hot pressing operation to allow for production of a 75 mm diameter n and p type thermoelectric material billets will be scaled up. Significant barriers relevant to implementation of TEGs in transportation systems will be identified. The operation of a 1 kW TEG will be demonstrated. (Schock, MSU)

University Research

In FY 2010, our university partners will continue their fundamental research into combustion and the chemistry of emission control devices.

- UM will to carry out extensive thermodynamic and system analyses of new mixed combustion modes and their potential benefit for lean-burn, high-pressure engine operation. They will explore fuel and thermal stratification and its interaction with fuel properties and heat transfer for improving and controlling combustion; investigate advanced multi-mode ignition and combustion under lean, high-pressure conditions; and explore opportunities for improved engine efficiency through novel fuel chemistry. (Assanis, UM)
- The University of Houston will continue their efforts to study regeneration kinetics of LNT catalysts. During a six month no-cost extension, efforts will be focused on completing the microkinetic and crystallite-level models of NOx storage and reduction, bench-scale studies of Pt/Rh/BaO/CeO_2 catalysts, isotopic Temporal Analysis of Products experiments to quantify the extent of rate limitations associated with stored NOx transport, bench-scale studies of model NOx storage and reduction catalysts using actual diesel vehicle exhaust and development of software for real time simulations of catalytic after-treatment systems. (Harold, University of Houston)
- The University of Kentucky will continue their examination of the effect of washcoat composition on LNT catalyst aging characteristics by performing additional high resolution transmission electron microscopy studies aimed at visualization of Pt-Ba phase segregation during LNT thermal aging, and deriving a quantitative model that describes LNT catalyst performance as a function of aging time. (Crocker, University of Kentucky)
- UT at Austin will continue efforts to design, develop, and commercialize an on-board engine exhaust PM sensor for HCCI and conventional diesel engines. They will continue evaluating sensor response, durability and velocity sensitivity for the commercially manufactured sensors and electronics, and will work to support trials of the PM sensor. Future work measuring particle size and morphology using transmission electron microscopy to accompany the existing sensitivity data will shed more light on the sensor response and allow quantification of its sensitivity to particle size. (Hall, UT at Austin)

HONORS AND SPECIAL RECOGNITIONS

1. Salvador Aceves of LLNL invited to serve as an opponent in Ph.D. exam, Chalmers University, Gothenburg, Sweden, September 2008.

2. Nick Killingsworth of LLNL invited to deliver a seminar at the "Advanced Engine Control Symposium," Tianjin, China, November 2008.

3. Invited topical keynote talk by W.P. Partridge of ORNL at the 21st North American Catalysis Society Meeting (NAM), San Francisco, California, June 7–12, 2009.

4. Invited topical talk by W.P. Partridge of ORNL at the GE Emissions Aftertreatment Symposium, GE Global Research Laboratories, September 17, 2009.

5. Paul Miles of SNL, Invited Speaker: University of Wisconsin Engine Research Center Symposium : Reducing Fuel Consumption: Solutions and Prospects, June 10–11, 2009, Madison, WI.

6. Invited presentation: Bill Partridge, Jae Soon Choi, Jim Parks, Josh Pihl, Todd Toops, Nathan Ottinger, Alex Yezerets, Neal Currier (ORNL), "Elucidating Lean NOx Trap Catalyst Regeneration & Degradation Chemistry: Insights from Intra-Catalyst, Spatiotemporally Resolved Measurements," Keynote Lecture, Catalysis for Environmental Protection topical area, North American Catalysis Society, 21st North American Meeting, San Francisco, California, June 9, 2009.

7. Invited presentation: Bill Partridge, Jae-Soon Choi, Jim Parks, Sam Lewis, Neal Currier, Mike Ruth, Robert Smith, George Muntean, John Stang, Alex Yezerets (ORNL), "Measuring Transient Chemistry Distributions Inside Automotive Catalyst & Engine Systems," General Electric Global Research Center's Symposium on Emissions and After Treatment, Niskayuna, New York, September 17, 2009.

8. The ORNL CRADA-developed SpaciMS received the 2009 National Award for Excellence in Technology Transfer presented annually by the Federal Laboratory Consortium for Technology Transfer (FLC). The award recognizes laboratory employees who have accomplished outstanding work in the process of transferring a technology developed by a federal laboratory to the commercial marketplace.

9. Lyle Pickett of SNL was awarded the SAE Excellence in Oral Presentation Award (2009 World Congress, Paper 2009-01-0658).

10. SCIENCEWATCH© identified Charles Westbrook and William Pitz of LLNL as in the top 25 most cited authors in the area of energy and fuels for the period of 1998 to 2008.

11. William Pitz of LLNL received an award as co-author on the best paper of the year from the Japanese Combustion Society. The paper is "A Kinetic Modeling Study on the Oxidation of Primary Reference Fuel-Toluene Mixtures Including Cross Reactions between Aromatics and Aliphatics", Y. Sakai, A. Miyoshi, M. Koshi, W.J. Pitz, Proceedings of the Combustion Institute, 2009.

12. Richard Steeper of SNL was awarded the 2009 Forest McFarland Award for outstanding contributions to SAE Engineering Meetings Board.

INVENTION AND PATENT DISCLOSURES

1. "High Efficiency Transition-Metal-Doped Type I Clathrate Thermoelectric Materials", J. Yang, X. Shi, Jiong, Yang, S. Bai, W. Zhang, and L. Chen, P-008791, 3/6/2009 (pending).

2. "High Efficiency Multiple-Element-Filled Skutterudite Thermoelectric Materials", J. Yang, X. Shi, S. Bai, W. Zhang, and L. Chen, P-008792, 3/7/2009 (pending).

3. "Formation of thermoelectric (TE) elements by net shape sintering for improved mechanical property performance", James R. Salvador, J. Yang, and A. R. Wereszczak, P009885, 7/10/2009 (to be filed).

4. Graves, Ronald L., West, Brian H., Huff, Shean P., Parks, II, James E., "Advanced engine management of individual cylinders for control of exhaust species", US Patent 7,469,693 (December 30, 2008).

5. US Appl. No.: 12/326,223; L.C. Maxey, W.P. Partridge, S.A. Lewis, J.E. Parks "Optically Stimulated Differential Impedance Spectroscopy," ORNL Ref. No.: 1861.0, Filed 12/2/2008.

6. US Appl. No.: 12491781; J.E. Parks, W.P. Partridge "Optical Backscatter Probe for Sensing Particulate in a Combustion Gas Stream," ORNL Ref. No.: 2130.0, Filed June 25, 2009.

7. Pacific Northwest National Laboratory has submitted an invention disclosure report, titled, "Low Temperature Oxidation Catalyst for Homogeneous Charge Compression Ignition Emission Reduction."

8. U.S. Patent Application, Title: WASTE HEAT RECOVERY SYSTEM, U.S. Application No.: 61/228,528, Filed: July 24, 2009 (BSST).

9. Manuel Angel Gonzalez Delgado; Rober J. Moran; Sameer Bhargava; Ronald Jay Pierik, "Engine including valve lift assembly for internal EGR control" U.S. and international patent application (GM).

LICENSED TECHNOLOGIES

The CRADA-developed Fuel-in-Oil Diagnostic (US Appl. No.: 12/137,964, "Laser Induced fluorescence fiber optic probe measurement of oil dilution by fuel," ORNL Ref. No.: 1940.0, Filed 6/13/2008) was licensed by UT-Battelle (ORNL Contractor) to Da Vinci Emissions Services, Ltd. (www.davinci-limited.com) on 10-13-2009.

The remainder of this report highlights progress achieved during FY 2009 under the Advanced Combustion Engine R&D subprogram. The following 63 abstracts of industry, university, and national laboratory projects provide an overview of the exciting work being conducted to tackle tough technical challenges associated with R&D of higher efficiency, advanced ICEs for light-duty, medium-duty, and heavy-duty vehicles. We are encouraged by the technical progress realized under this dynamic subprogram in FY 2009, but we also remain cognizant of the significant technical hurdles that lay ahead, especially those to further improve efficiency while meeting the EPA Tier 2 emission standards and heavy-duty engine standards for the full useful life of the vehicles.

Gurpreet Singh
Team Leader,
Advanced Combustion Engine R&D
Office of Vehicle Technologies

Roland M. Gravel
Office of Vehicle Technologies

Kenneth C. Howden
Office of Vehicle Technologies

John W. Fairbanks
Office of Vehicle Technologies

James Eberhardt
Chief Scientist,
Office of Vehicle Technologies

II. Advanced Combustion and Emission Control Research for High-Efficiency Engines

II.A.1 Light-Duty Diesel Spray Research Using X-Ray Radiography

Christopher F. Powell (Primary Contact),
Jin Wang
Argonne National Laboratory
9700 S. Cass Ave.
Argonne, IL 60439

DOE Technology Development Manager:
Gurpreet Singh

Objectives

- Study the mechanisms of spray atomization by making detailed, quantitative measurements in the near-nozzle region of sprays from light-duty diesel injectors.
- Perform these measurements under conditions as close as possible to those of modern engines.
- Utilize the results of our unique measurements in order to advance the state-of-the-art in spray modeling.
- Provide industrial partners in the spray and engine community with access to a unique and powerful spray diagnostic.

Accomplishments

- In Fiscal Year 2009 we made a significant discovery that demonstrates how the movement of the needle as the injector opens affects the structure of the spray as it emerges from the nozzle. This is the first time that needle motion has been directly correlated with spray structure, and the data represents a comprehensive view of nozzle flow that will be invaluable to computational modeling.
- A new experimental station at the Advanced Photon Source dedicated to transportation research was completed in FY 2009. Significant progress has been made, with the first measurements from the facility were taken in June 2009. This facility will allow for more experimental time, greater X-ray intensity, and more precise spray measurements than have been previously achievable.
- In FY 2009, Argonne began a new collaboration with Delphi Diesel Systems. This collaboration will give a U.S.-owned injector manufacturer access to Argonne's unique suite of X-ray-based fuel injection and spray diagnostics.
- In FY 2008 we arranged a new collaboration with the computational modeling group at the University of Wisconsin's Engine Research Center (ERC). In FY 2009, Prof. Christopher Rutland sent one of his Ph.D. students, Nidheesh Bharadwaj, to work at Argonne for two months. During this time, we performed several measurements that are of interest to both Argonne and the ERC. Nidheesh will use the X-ray data to validate ERC's KIVA computational spray model, with the goal of improving the droplet drag modeling. This is a significant new development, as it has the potential to improve the industry's leading computational models.
- An Argonne staff member spent two weeks performing spray measurements at the corporate research labs of Robert Bosch GmbH in Stuttgart, Germany, at the invitation of Bosch. During this visit, the staff member performed laser spray imaging, and learned some of the techniques that Bosch uses in its spray labs for engine and spray research. This visit resulted in a joint publication by Argonne and Bosch.

Future Directions

- We have begun a new collaboration with Delphi Diesel Systems. Over the next few years, Delphi will deliver modern fuel system hardware to Argonne to be studied using several X-ray diagnostics. These measurements will focus on the study of how different nozzle geometries affect the fuel distribution in the combustion chamber. This will provide a U.S. fuel systems company with access to the most advanced spray and injector diagnostics.
- Increase the relevance of our measurements by studying sprays under conditions even closer to those of modern diesel engines. We have made steady progress over the course of the project, continually increasing the ambient pressure and enabling the use of production nozzles. We have now acquired a fuel system that is identical to the one in the General Motors-Fiat 1.9 liter engine running in Argonne's Engine and Emissions Research group. This will enable us to study sprays under conditions that mimic those in the engine, and use the results to understand the impact that sprays have on engine emissions, efficiency, and performance.
- Improve the measurement technique. While we produce useful results today, improvements to the measurement technique will increase its applicability and accessibility in the future. Such improvements include faster data acquisition, processing, and analysis, improved X-ray detector systems, increased X-ray intensity, finer spatial resolution, and greater automation.

- Increase the impact of our work by fostering collaboration with outside groups. Our collaborations with modeling groups allow our work to increase the fundamental understanding of the mechanics of the spray event, while our collaborations with industry enable us to develop a technique that is useful as a diagnostic for injection system manufacturers. Both of these expand the impact of our research, and help to meet the program objectives of decreased emissions and increased efficiency.

Introduction

Fuel injection systems are one of the most important components in the design of combustion engines with high efficiency and low emissions. A detailed understanding of the fuel injection process and the mechanisms of spray atomization can lead to better engine design. This has spurred considerable activity in the development of optical techniques (primarily using lasers) for measurements of fuel sprays. Some of these optical techniques have become commercially available and can be readily applied to the testing and development of modern injection systems. Despite significant advances in spray diagnostics over the last 30 years, scattering of light from the large number of droplets surrounding the spray prevents penetration of visible light and limits such measurements to the periphery of the spray. This is especially true in the near-nozzle region of the spray, which is considered to be the most important region for developing a comprehensive understanding of spray behavior. Existing models of spray structure have only been compared with data acquired in the region relatively far from the nozzle. It is unknown how well these models apply in the crucial near-nozzle region. The limitations of visible light in the near-nozzle region of the spray have led us to develop X-ray diagnostics for the study of fuel sprays. X-rays are highly penetrative, and measurements are not complicated by the effects of scattering. The technique is non-intrusive, quantitative, highly time-resolved, and allows us to make detailed measurements of the spray, even in the densely-packed region very near the nozzle.

Approach

This project studies the sprays from commercially-available light-duty diesel fuel injectors. Our approach is to make detailed measurements of the sprays from these injectors using X-ray absorption. This will allow us to map the fuel distribution in these sprays, extending the existing knowledge into the near-nozzle region. The X-ray measurements are performed at the Advanced Photon Source at Argonne National Laboratory. A schematic of the experimental setup is shown in Figure 1; detailed descriptions of the experimental methods are given in [1] and [2]. The technique is straightforward; it is similar to absorption or extinction methods commonly used in optical analysis. However, X-ray radiography has a significant advantage over optical techniques in the measurement of sprays: because the measurement is not complicated by the effects of scattering, there is a simple relation between the measured X-ray intensity and the mass of fuel in the path of the X-ray beam. For a monochromatic (narrow wavelength bandwidth) X-ray beam, this relationship is given by

$$I/I_0 = \exp(-\mu_M M)$$

where I and I_0 are the transmitted and incident intensities, respectively; μ_M is the mass absorption constant; and M is the mass of fuel. The constant μ_M is measured in a standard cell, and the incident and transmitted intensities are measured as a function of time by the X-ray detector. This allows direct determination of the mass of fuel at any position in the spray as a function of time. It is the goal of our work to use X-ray radiography to measure sprays from light-duty fuel injectors at different injection pressures, different ambient pressures, and using different nozzle geometries. This will enable us to quantify how each of these variables affects the structure of the spray. We will collaborate with industrial partners including engine and fuel injection system manufacturers so that they will have access to these diagnostics for improvement of their products. We will also collaborate with spray modelers to incorporate this previously unknown information about the near-nozzle region of the spray into new models. This will lead to an increased understanding of the mechanisms of spray atomization and will facilitate the development of fuel injection systems designed to improve efficiency and reduce pollutants.

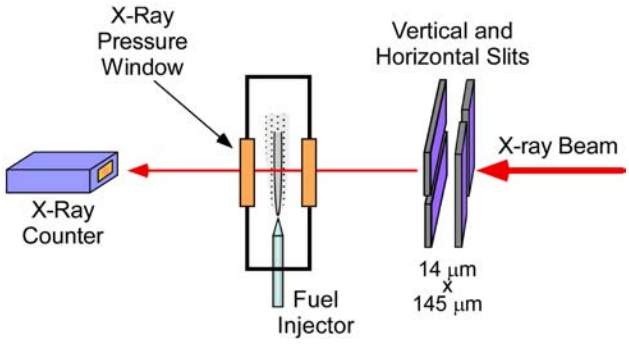

FIGURE 1. Schematic of the Experimental Setup

Results

In FY 2009 we made a significant discovery that demonstrates how the movement of the mechanical components inside the injector affects the distribution of the fuel as it emerges from the nozzle. For this discovery, we combined X-ray radiography with high-speed X-ray imaging of the mechanical components inside the fuel injector. We were able to image the opening and closing of the needle valve inside the injector, and tracked the motion of the needle over time in three dimensions. It was discovered that rather than a simple opening and closing motion, the needle valve travels an eccentric, spiraling path. It is clear from the images that this eccentric motion changes the shape of the flow passages inside the injector, and we speculated that this might affect the fuel distribution. In order to investigate this possibility, we used X-ray radiography to measure the fuel distribution as it first emerges from the nozzle. We found oscillations in the fuel density that are synchronized with the eccentric motion of the needle valve (Figure 2). This is the first time that needle motion has been directly correlated with spray structure, and the data represents a comprehensive view of nozzle flow that will be invaluable to computational modeling.

In FY 2009, a new experimental station at the Advanced Photon Source dedicated to transportation research was completed (Figure 3). This facility was built with both Basic Energy Sciences and Energy Efficiency and Renewable Energy funds, and signifies the important collaboration between basic and applied research. The first measurements at the new beamline were performed in March 2009 as part of collaboration among Argonne, Sandia National Laboratories, and the University of Wisconsin-Madison's ERC. The new beamline represents a significant advance in our ability to perform measurements, as we are guaranteed access to the X-ray source and have a dedicated space for our experimental equipment. In the past we have had very limited access to time at the C-ray source; the new beamline will allow us to expand our collaborations with both industrial partners and other researchers. The new facility also enables several technical improvements, including increased X-ray flux and a better beam focus, which improves the spatial resolution of spray measurements. This facility will allow for more experimental time, greater X-ray intensity, and more precise spray measurements than have been previously achievable.

In mid-FY 2009, Argonne began a new collaboration with Delphi Diesel Systems. Delphi and Argonne have agreed to begin studying some of Delphi's fuel injection hardware, and DOE has agreed to fund the project. Delphi will make in-kind contributions including a custom-built spray chamber, fuel system hardware, and technical support. Argonne will perform measurements on injector designs that are of interest to Delphi. Measurements will include Argonne's full suite of X-ray diagnostics, including spray radiography, edge-enhanced imaging of sprays, and high-speed imaging of the internal components of the injector. Progress to date includes a concept drawing of a custom-designed pressure vessel for this work, and an agreement on specifications of an injector driver. Delphi

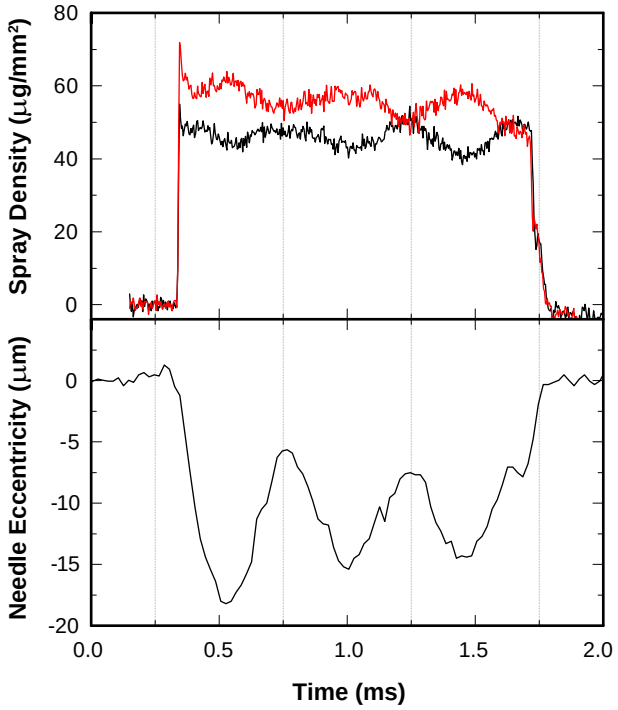

FIGURE 2. Off-axis position of the injector needle versus time (bottom) and spray density versus time at the top and bottom edges of the spray (top). The needle motion and spray density are synchronized, so that off-axis motion of the needle leads to oscillations in the density of the spray.

FIGURE 3. Photo of the entrance to the new beamline at the Advanced Photon Source dedicated to transportation research. This new facility will allow us greater time for experiments, higher precision measurements, and an expanded list of collaborators.

will deliver hardware in FY 2010, and Argonne will begin measurements. The current economic climate has prevented Delphi from signing a Cooperative Research and Development Agreement, but they plan to do so in FY 2010. This collaboration will give a U.S.-owned injector manufacturer access to Argonne's unique suite of X-ray-based fuel injection and spray diagnostics.

In FY 2009, Prof. Christopher Rutland of the University of Wisconsin-Madison's ERC sent one of his Ph.D. students, Nidheesh Bharadwaj, to work at Argonne for two months. During this time, Mr. Bharadwaj took part in several spray measurements, including measurements that are part of collaboration among Argonne, Sandia, and ERC. Mr. Bharadwaj will use the X-ray data to validate ERC's KIVA computational spray model, with the goal of improving its ability to predict spray behavior. This is a significant new development, as it rejuvenates a previously dormant collaboration with ERC, with the potential to improve the industry's leading computational models.

As part of our ongoing collaboration with Bosch, we completed a series of measurements designed to study how changing the number of holes in an injector nozzle affects the fuel distribution. Bosch provided two nozzles with identical orifice geometries, but one had three holes and one had five. A series of measurements at different ambient densities showed that the three hole nozzle consistently produces sprays with a wider cone angle (Figure 4). These results are being used by Bosch to improve their computational modeling of injector flow.

Conclusions

- The X-ray measurements can be used to understand how internal nozzle flows affect the structure of the fuel spray. Such measurements are not possible using other imaging techniques, and represent a powerful data set for validating computational models of fuel flow.
- The time-dependent mass measurements provide unique information to spray modelers, and allow them to test their models in the near-nozzle region of the spray, something that was impossible previously. This data is crucial for the development of accurate spray models and for the detailed understanding of spray behavior. The quantitative measurements that we have provided may help to elucidate the mechanisms of spray atomization. This could ultimately lead to the design of cleaner, more efficient engines.
- The impact of our work on the engine community is shown by the expanding list of collaborators and by the significant in-kind contributions to our

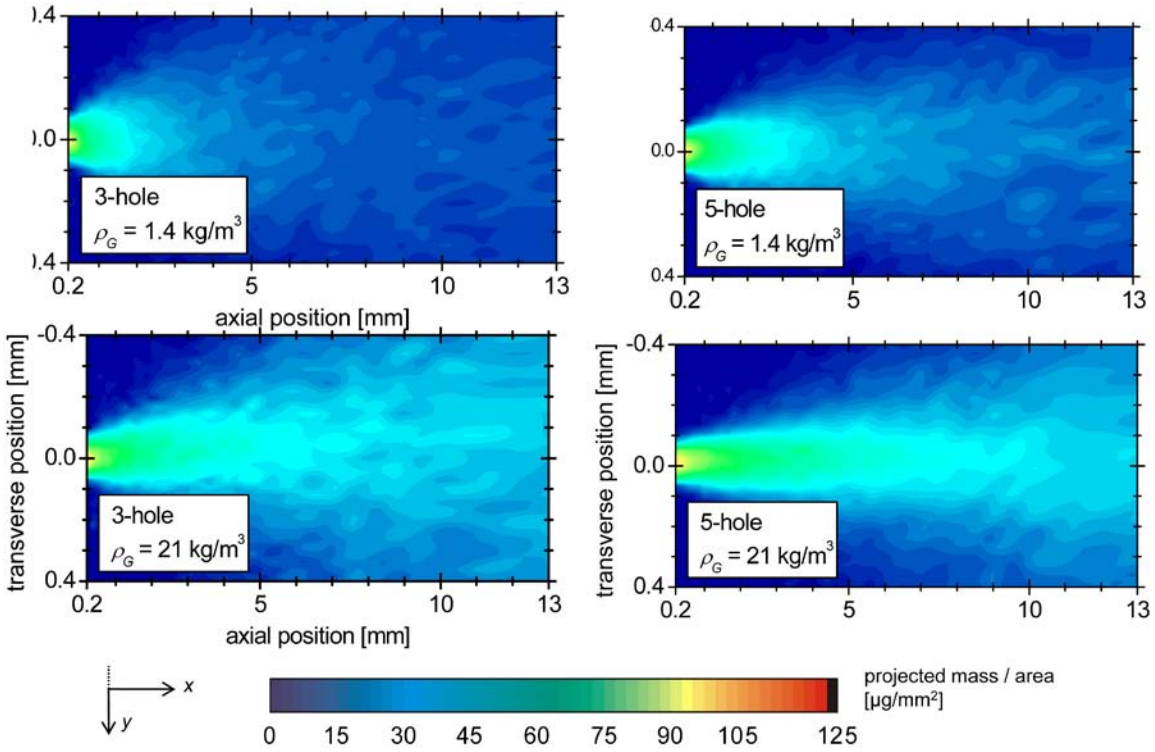

FIGURE 4. A comparison of the fuel distribution for two different nozzles at two different ambient densities. X-ray measurements in collaboration with Bosch showed that the number of holes affect the fuel distribution from injectors with otherwise identical orifices.

work that are being made by fuel system and engine manufacturers.

References

1. C.F. Powell, Y. Yue, R. Poola, and J. Wang, J. Synchrotron Rad. 7:356-360 (2000).

2. C.F. Powell, Y. Yue, R. Poola, J. Wang, M.-C. Lai, J. Schaller, SAE 2001-01-0531, (2001).

FY 2009 Publications

1. "The Effects of Diesel Injector Needle Motion on Spray Structure", C.F. Powell, A.L. Kastengren, Z. Liu, K. Fezzaa. American Society of Mechanical Engineers ICEF2009-14076, September 2009.

2. "Effect of nozzle transients and compressibility on the penetration of fuel sprays", J. Kostas, D. Honnery, J. Soria, A. Kastengren, Z. Liu, C.F. Powell, and J. Wang. Appl. Phys. Lett. 95, 024101, July 2009.

3. "Measurement of Biodiesel Blend and Conventional Diesel Spray Structure Using X-Ray Radiography", A.L. Kastengren, C.F. Powell, K.–S. Im, Y.-J. Wang, J. Wang. Journal of Engineering for Gas Turbines and Power Vol. 131, Iss. 6, July 2009.

4. "X-Ray Measurements of Mass Distributions in the Near-Nozzle Region of Sprays from Standard Multi-Hole Common-Rail Diesel Injection Systems", P. Leick, A.L. Kastengren, Z. Liu, J. Wang and C.F. Powell. Eleventh International Conference on Liquid Atomization and Spray Systems, Vail, CO, July 2009.

5. "High-Speed X-Ray Imaging of Diesel Injector Needle Motion", A.L. Kastengren, C.F. Powell, Z. Liu, K. Fezzaa, J. Wang. American Society of Mechanical Engineers ICES2009-76032, May 2009.

6. "Time Resolved, Three Dimensional Mass Distribution of Diesel Sprays Measured with X-Ray Radiography", A.L. Kastengren, C.F. Powell, Z. Liu, J. Wang. Society of Automotive Engineers, Paper 2009-01-0840 (2009).

7. "Characterizing Spray Behavior Differences between Common Rail and Unit Injection Systems Using X-Ray Radiography", A.I. Ramírez, S. Som, S.K. Aggarwal, A.L. Kastengren, E. El-Hannouny, D.E. Longman, C.F. Powell. Society of Automotive Engineers, Paper 2009-01-0649 (2009).

8. "Development and Extensive Validation of a Primary breakup model for Diesel Engine Applications", S. Som, A.I. Ramirez, S.K. Aggarwal, A. Kastengren, E. El-Hannouny, D.E. Longman, C.F. Powell. Society of Automotive Engineers, Paper 2009-01-1838 (2009).

FY 2009 Presentations

1. "Fuel Spray Characterization Using X-Ray Diagnostics at High Temperature and Pressure", C.F. Powell, Advanced Photon Source Renewal Workshop, Naperville, IL, 20 October 2009.

2. "Fuel Spray Research on Light-Duty Injection Systems", Christopher Powell, Alan Kastengren, Zunping Liu, Jin Wang, 2009 OVT Merit Review, 19 May 2009, Crystal City, VA.

3. "X-Ray Measurements of Mass Distributions in the Near-Nozzle Region of Sprays from Standard Multi-Hole Common-Rail Diesel Injection Systems", P. Leick, A.L. Kastengren, Z. Liu, J. Wang and C.F. Powell. Eleventh International Conference on Liquid Atomization and Spray Systems, Vail, CO, July 2009.

4. "Diesel Injector and Spray Characterization Using X-Ray Diagnostics", A.L. Kastengren, C.F. Powell, Z. Liu, K. Fezzaa, J. Wang. ACEC Meeting, USCAR, 12 March 2009.

5. "High-Speed X-Ray Imaging of Diesel Injector Needle Motion", A.L. Kastengren, C.F. Powell, Z. Liu, K. Fezzaa, J. Wang. American Society of Mechanical Engineers Internal Combustion Engine Division Spring Meeting, May 2009.

6. "The Effects of Diesel Injector Needle Motion on Spray Structure", C.F. Powell, A.L. Kastengren, Z. Liu, K. Fezzaa. American Society of Mechanical Engineers Internal Combustion Engine Division Spring Meeting, September 2009.

7. "Diesel Injector and Spray Characterization Using X-Ray Diagnostics", C. F. Powell, AEC MOU Meeting, Sandia National Laboratories, 10 February 2009.

II.A.2 Low-Temperature Automotive Diesel Combustion

Paul Miles
Sandia National Laboratories
P.O. Box 969
Livermore, CA 94551-0969

DOE Technology Development Manager:
Gurpreet Singh

Subcontractor:
University of Wisconsin Engine Research Center,
Madison, WI

Objectives

- Provide the physical understanding of the in-cylinder combustion processes needed to minimize the fuel consumption and the carbon footprint of automotive diesel engines while maintaining compliance with emissions standards.
- Develop efficient, accurate computational models that enable numerical optimization and design of fuel-efficient, clean engines.
- Provide accurate data obtained under well-controlled and characterized conditions to validate new models and to guide optimization efforts.

Accomplishments

- Extended spectrally-resolved laser-induced fluorescence diagnostic technique to obtain mean, two-dimensional images of the spatial distribution of carbon monoxide (CO) in high-background (*e.g.* sooting) environments and to detect unburned hydrocarbons (UHC) embedded in the products of moderately rich combustion.
- Developed liquid fuel imaging capability to examine injector nozzle dribble and liquid fuel penetration into the squish volume leading to piston-top film formation and ring-land crevice UHC.
- Applied multiple diagnostics to examine and contrast the evolution of the in-cylinder distributions of UHC and CO for both early- and late-injection low-temperature combustion regimes.
- Employed design of experiments concepts to examine the impact of squish height and spray targeting on combustion and on UHC and CO emissions, measuring both engine-out emissions and in-cylinder spatial distributions of these species.
- Compared in-cylinder distributions of UHC and CO predicted with multi-dimensional simulations to experimental results, and identified critical areas for model improvement.
- Performed homogeneous reactor simulations in a simulated engine environment to evaluate several reduced kinetic mechanisms for hydrocarbon oxidation. Contrasted results with detailed mechanisms and identified shortcomings in reduced mechanisms leading to excessive UHC emissions. Developed and tested improved mechanisms, resulting in ~50% improvement in the prediction of engine-out UHC emissions.

Future Directions

- Investigate fuel property effects on combustion efficiency and associated UHC and CO emissions, varying both fuel volatility and ignition quality.
- Examine the impact of biofuel blends on the fuel preparation, combustion, and emissions formation and oxidation processes.
- Extend UHC imaging studies to the horizontal plane to capture lack of symmetry in squish volume UHC sources associated with piston top valve pockets and head features.
- Obtain horizontal plane flow field data to support the interpretation of UHC images, to examine asymmetries in the squish flow patterns, and to characterize the attenuation of angular momentum in the squish volume.

Introduction

Direct-injection diesel engines have the highest fuel conversion efficiency and the lowest carbon dioxide (CO_2) emissions of any reciprocating internal combustion engine technology. However, conventional diesel engines produce elevated emissions of both soot and oxides of nitrogen (NO_x). To address this shortcoming, low-temperature combustion techniques that prevent the formation of these pollutants within the engine are being developed. These techniques generally rely on high levels of charge dilution with recirculated exhaust gases to keep in-cylinder temperatures low. High dilution levels with attendant low charge oxygen concentrations make it difficult to mix the fuel with sufficient oxygen to achieve complete combustion, and the low combustion temperatures also slow the kinetic rates of oxidation. Hence, incomplete combustion–characterized by high UHC and CO emissions–can lead to a significant fuel economy penalty. A major focus of this work is to understand the main causes

of combustion inefficiency through examination of the in-cylinder sources of UHC and CO emissions. Identifying these sources is insufficient, however: an ability to accurately predict these sources and how they vary with different engine design parameters is required to enable the design of clean, more efficient engines. Consequently, we also focus on careful comparison of the experimentally measured CO and UHC fields with the results of numerical simulations, and, through this comparison, we refine computer models and improve predictions of efficiency and emissions.

Approach

The research approach involves carefully coordinated experimental, modeling, and simulation efforts. Detailed measurements of in-cylinder flows, fuel and pollutant spatial distributions, and other thermo-chemical properties are made in an optical engine facility with geometric and thermodynamic characteristics that allow it to closely match the combustion and engine-out emissions behavior of a traditional, all-metal test engine. These measurements are closely coordinated and compared with the predictions of numerical simulations.

The experimental and numerical efforts are mutually complementary. Detailed measurements of the in-cylinder variables permit the evaluation and refinement of the computer models, while the model results can be used to obtain a more detailed understanding of the in-cylinder flow and combustion physics–a process that is difficult if only limited measurements are employed. Jointly, these efforts address the principal goals of this project: development of the physical understanding to guide and the modeling tools to refine the design of optimal, clean, high-efficiency combustion systems.

Results

A central aspect of our research this year was the extension and adaptation of our deep-ultraviolet laser-induced fluorescence (UV LIF) diagnostic to provide two-dimensional in-cylinder spatial distributions of CO, and to detect UHC embedded within the partial oxidation products of moderately rich mixtures. This improved diagnostic additionally allows visualization of UHC and CO distributions in environments with significant interference from soot, where background subtraction techniques have proven difficult to apply.

The diagnostic is illustrated in Figure 1. A deep-UV laser beam is focused into a small sheet, approximately 0.5 mm thick and 3 mm high. Light from this sheet is imaged onto the entrance slit of a spectrograph, which spectrally-resolves the light collected from each radial location along the sheet. From the individual spectra, the signal corresponding to CO, C_2, and polycyclic aromatic hydrocarbon (PAH)-like UHC is extracted by applying a signal modeling approach to separate the various contributions. The result is a radial profile of each species, as shown in the upper-left inset of Figure 1. By making these measurements at various heights in the clearance volume, we are able to build two-dimensional mean spatial distributions, as shown in the lower-left portion of the figure.

Interpretation of the CO signal is unambiguous; however, interpretation of the C_2 signal is less certain. C_2 can be formed by photo-fragmentation of combustion intermediates such as C_2H_3 or C_4H_6 [1]. It thus indicates the presence of partially-oxidized fuel. More importantly, however, it can be formed from photo-fragmentation of C_2H_2, one of the dominant UHC species present in the products of moderately rich combustion (fuel/air equivalence ratio, $\phi \sim 1.5$). In this equivalence ratio range, the UHC is dominated by CH_4, C_2H_4, and C_2H_2–species which are not detectable using more conventional laser-induced fluorescence diagnostics. The distribution of PAH-like UHC is derived from the broadband component of the spectra. Experience has shown that–for the light-load, non-sooting conditions explored here–this signal is best interpreted as an indicator of parent fuel compounds that have not undergone significant oxidation.

We have applied this improved diagnostic to examine the late-cycle distributions of UHC and CO within the cylinder, in order to identify the most important sources of engine-out emissions. Data obtained for an early-injection, highly dilute, operating condition at 50° after top dead center (aTDC) is shown in Figure 2. In the upper row of Figure 2, both measures of UHC provided by the deep-UV LIF diagnostic show that the main sources of UHC are found toward the center of the cylinder–near the injector–and in the squish volume. The PAH-like UHC is concentrated close to the injector, and likely arises from fuel which has dribbled from the injector nozzle. As distance from the nozzle increases, the presence of combustion intermediates, indicated by C_2, becomes more pronounced. Note that there is very little CO found in the near-nozzle region. In the presence of significant UHC, this indicates generally low temperatures and retarded progression of the combustion process.

In contrast, within the squish volume, copious amounts of CO are observed. Here, lean mixtures and heat losses to combustion chamber walls lead to slow oxidation. The squish volume is easily the dominant source of engine-out CO emissions, and–as discussed in our 2008 annual report–incomplete oxidation of CO is the most significant contribution to combustion inefficiency at this operating condition.

CO distributions predicted by numerical simulation are shown in the lower-right portion of Figure 2. Although CO can (dimly) be observed to be predicted within the squish volume, the dominant predicted source

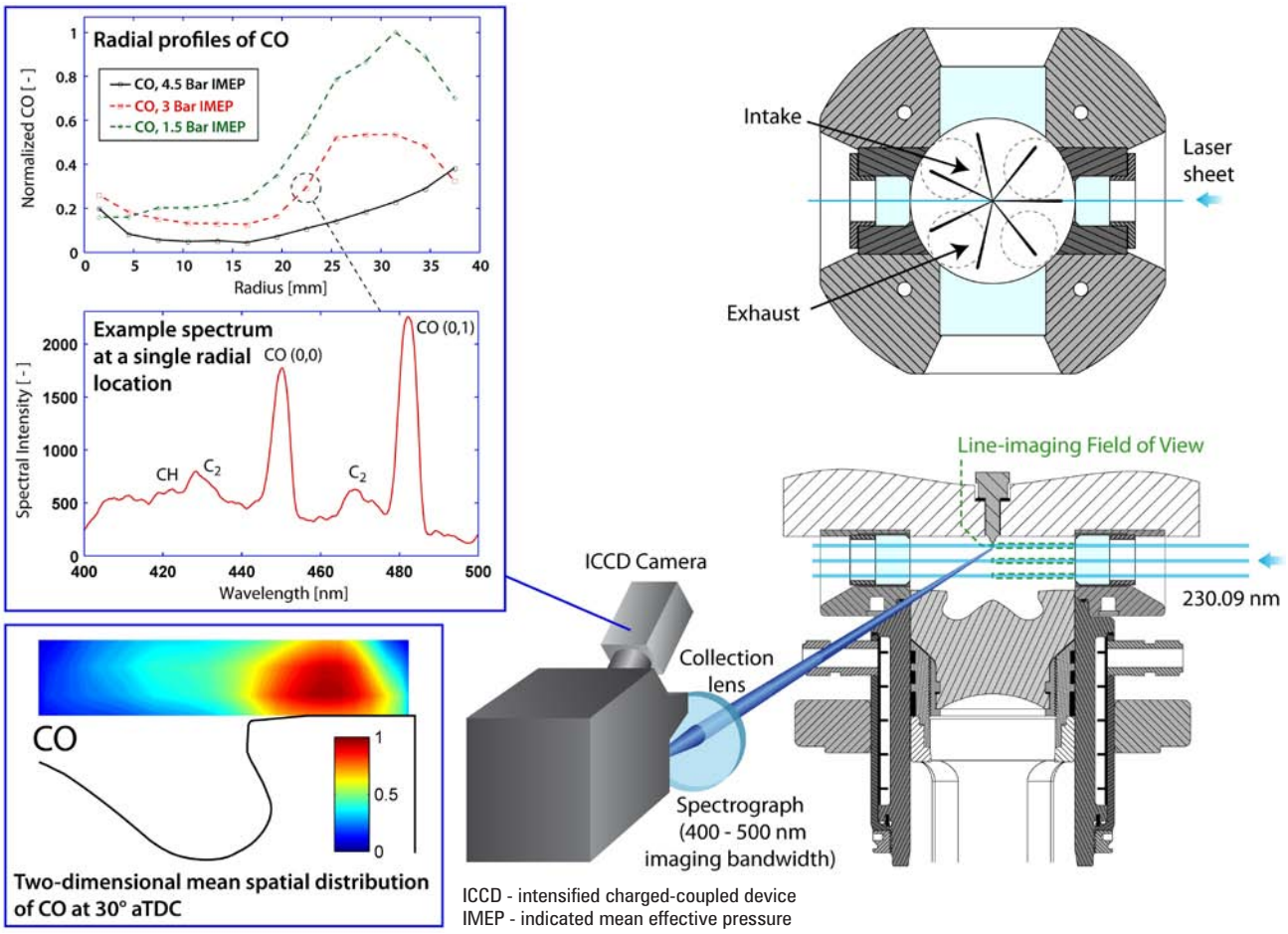

FIGURE 1. Schematic representation of the deep-UV LIF diagnostic. For each laser beam height, spectrally-resolved measurements allow radial profiles of each species to be measured. These radial profiles are subsequently combined into a mean, two-dimensional image.

is a plume of O_2-deficient mixture leaving the bowl. The experimentally determined CO distributions show no evidence of this plume–mixture leaving the bowl has lower measured CO levels than the surrounding fluid. Analysis of the photo-physics of the LIF process indicates that high temperatures in the mixture leaving the bowl could lead to ~30% signal loss. Nonetheless, this loss cannot explain the significant contrast between the measured and computed CO distributions. Moreover, the PAH-like UHC and C_2 distributions shown in the upper portion of the figure indicate that the flow leaving the bowl is free of UHC. The inevitable conclusion is that the numerical simulations have not accurately captured the fuel/air mixing processes, and that the mixture leaving the bowl is not so O_2-deficient as the simulations indicate.

Although the preceding results and discussion have clearly identified a need to improve the prediction of in-cylinder mixing processes, our research has also isolated an important flaw that can exist in reduced chemical kinetic mechanisms of hydrocarbon combustion. These mechanisms are often optimized to match the ignition characteristics of the fuel over a wide range of temperatures and densities. In the process, other aspects of the oxidation process may be compromised.

We have employed simulations of the combustion of a homogeneous mixture in an engine environment, for several full and reduced chemical kinetic mechanisms, to examine how the predicted yield of UHC and CO varies with equivalence ratio. Figure 3 presents the results obtained with three of these mechanisms. On each figure, the green and blue isopleths indicate the crank angles where the UHC and CO yield falls below 2% of the fuel energy for each ϕ. Also shown are the crank angles where the temperature exceeds the critical temperature required to achieve rapid UHC and CO oxidation, approximately 1200 K and 1500 K for UHC and CO, respectively.

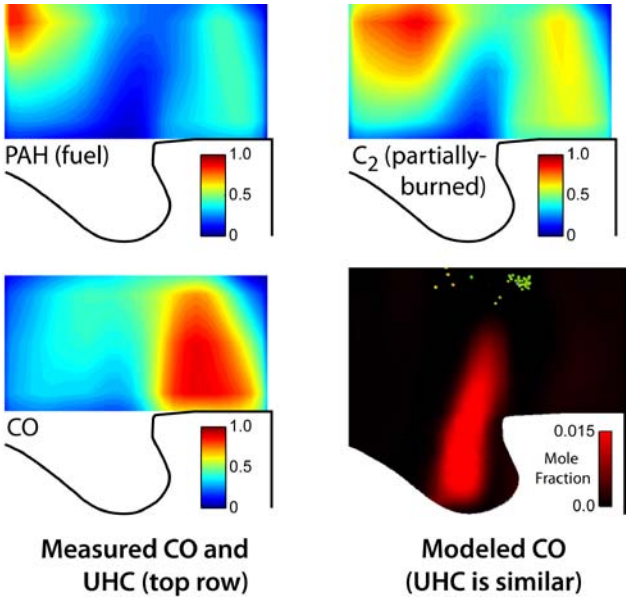

FIGURE 2. Measured in-cylinder spatial distributions of UHC and CO, and the corresponding CO distribution predicted via multi-dimensional simulation. The experiments clearly identify the squish volume and near-injector regions as the dominant sources of UHC and CO emissions. The predicted plume of CO leaving the bowl is not observed.

In the upper part of the figure, the results obtained with a detailed mechanism show that for $0.45 \lesssim \phi \lesssim 1.4$, the predicted UHC yield is low, while for $0.6 \lesssim \phi \lesssim 1.0$ the predicted CO yield is low. When the reduced kinetic mechanism represented by the middle portion of the figure is used, these ranges change to $0.5 \lesssim \phi \lesssim 1.1$ and $0.5 \lesssim \phi \lesssim 1.0$, respectively. The narrower range of equivalence ratios providing a low UHC yield will lead to higher predicted emissions levels when this reduced mechanism is employed in a multi-dimensional simulation. Conversely, CO emissions will be slightly under-predicted. However, only modest additional complexity in the reduced mechanism can reproduce the UHC and CO yields of the full mechanism, as is shown by the lower figure. When the latter, improved reduced mechanism is employed, the engine-out UHC emissions are significantly improved, as shown in Figure 4. The remaining discrepancy between the predictions and the measurements is likely due to inadequately capturing the mixing processes, as described above.

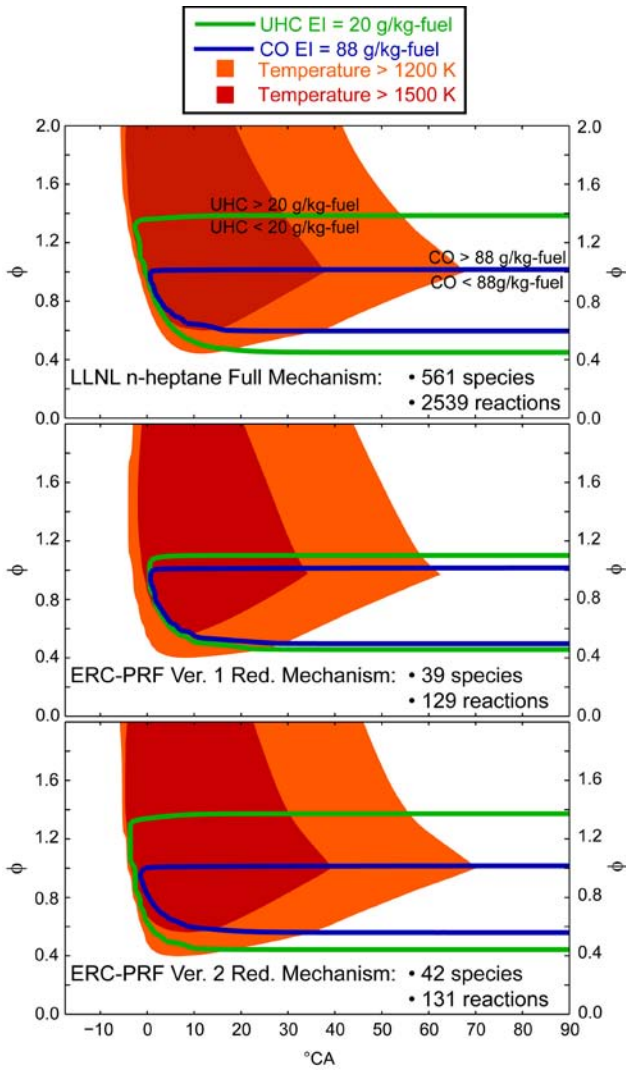

FIGURE 3. CO and UHC yield and gas temperature as a function of equivalence ratio and crank angle. Reduced mechanisms can result in a significant narrowing of the equivalence ratio band within which low UHC emissions are predicted. As shown in the bottom figure, this shortcoming can be remedied without adding significant complexity.

Conclusions

- A deep-UV LIF technique has been refined and extended to provide two-dimensional images of the in-cylinder distributions of CO, PAH-like UHC, and partial oxidation products.
- The technique has been applied to several operating conditions representative of different low-temperature combustion strategies, and has successfully identified the dominant sources of engine-out UHC and CO.
- Comparisons of the experimental data with the predictions of numerical models have identified discrepancies caused by inaccurate predictions of the fuel-air mixing processes.
- Fundamental studies of the performance of reduced chemical kinetic mechanisms in homogeneous engine environments have identified shortcomings in their predictions of CO and UHC yields. Improved reduced kinetic mechanisms have been developed which significantly improve the accuracy of the predicted emissions, without significant impact on computational cost.

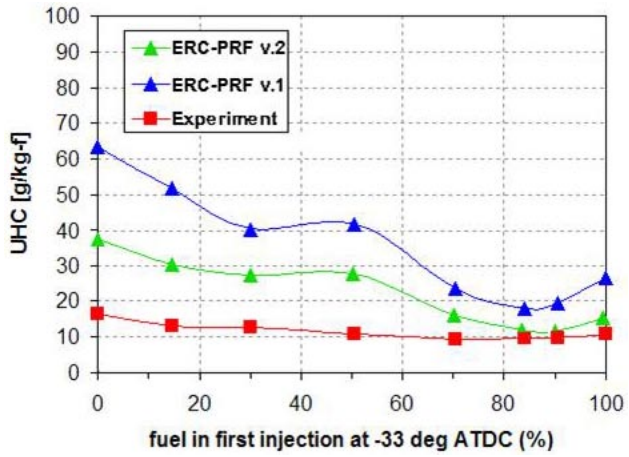

FIGURE 4. Multi-dimensional model predictions of engine-out UHC emissions obtained with the original and the improved reduced kinetic mechanism. The improved mechanism approximately halves the discrepancy between the predicted and the measured emissions.

References

1. "Laser-induced Fragmentation Fluorescence Detection of the Vinyl Radical and Acetylene," Osborn DL, Frank JH. *Chemical Physics Letters* 349: 43-50, 2001.

FY 2009 Publications/Presentations

1. "Investigation of UHC and CO Sources from Biodiesel Blends in a Light-Duty Diesel Engine Operating in a Partially Premixed Combustion Regime," Petersen BR, Ekoto IW, Miles PC. *Submitted to the 2010 SAE World Congress, Offer No.: 10PFL-0675.*

2. "Influence of Spray-Target and Squish Height on Sources of CO and UHC in a HSDI Diesel Engine During PPCI Low-Temperature Combustion," Aronsson U, Andersson Ö, Egnell R, Ekoto IW, Miles PC. *SAE International Fuels and Lubricants Meeting–SAE technical paper 2009-01-2810*, November 2–4, 2009, San Antonio, TX .

3. "The Impact of Squish Height and Spray Targeting on UHC and CO Emissions from Early-Injection (PCI-like) Low-Temperature Diesel Combustion," Aronsson U, Andersson Ö, Egnell R, Miles PC, Ekoto IW, Petersen BR. *DOE OFCVT AEC Working Group Meeting*, October 6–7, 2009, Southfield, MI.

4. "UHC and CO Emissions Sources from a Light-Duty Diesel Engine Undergoing Late-Injection Low-Temperature Combustion," Ekoto IW, Colban WF, Miles PC, Aronsson U, Andersson Ö, Park SW, Foster DE, Reitz RD. *ASME Internal Combustion Engine Division 2009 Fall Technical Conference–ICEF2009-14030*, September 27–30, 2009, Lucerne, Switzerland.

5. "UHC and CO Emissions Sources from a Light-Duty Diesel Engine Undergoing Dilution-Controlled Low-Temperature Combustion," Ekoto IW, Colban WF, Miles PC, Park SW, Foster DE, Reitz RD, Aronsson U, Andersson Ö. *9th International Conference on Engines and Vehicles – SAE 2009-24-0043*, September 13–18, 2009, Capri, Naples, Italy.

6. "Progress Towards Understanding Combustion Inefficiencies: In-Cylinder Sources of CO and UHC," Miles PC. *University of Wisconsin Engine Research Center Symposium : Reducing Fuel Consumption: Solutions and Prospects*, June 10–11, 2009, Madison, WI.

7. "Advanced Light-Duty Combustion Experiments and Light-Duty Combustion Modeling," Miles PC and Reitz, RD. *DOE Hydrogen Program and Vehicle Technologies Program Annual Merit Review and Peer Evaluation Meeting*, May 18–22, 2009, Arlington, VA.

8. "Examination of Initialization and Geometric Details on the Results of CFD Simulations of Diesel Engines," Bergin M, Musu E, Kokjohn S, Reitz RD. *ASME Internal Combustion Engine Division 2009 Spring Technical Conference–ICES2009-76053.* May 3–6, 2009, Milwaukee, WI.

9. "Sources of UHC Emissions from a Light-Duty Diesel Engine Operating in a Partially Premixed Combustion Regime," Ekoto IW, Colban WF, Miles PC, Park SW, Foster DE, Reitz RD. *SAE technical paper 2009-01-1446, accepted by SAE Int. J. Engines. Presented at the SAE World Congress,* April 20–23, 2009, Detroit, MI.

10. "Detailed Unburned Hydrocarbon Investigations in a Highly-Dilute Diesel Low Temperature Combustion Regime," Koci CP, Ra Y, Krieger R, Andrie M, Foster DE, Siewert RM, Durrett RP, Ekoto I, Miles PC. *SAE technical paper 2009-01-0928, accepted by SAE Int. J. Engines. Presented at the SAE World Congress,* April 20–23, 2009, Detroit, MI.

11. "UHC Emission Sources from a Light-Duty Diesel Engine Undergoing Dilution-Controlled Low-Temperature Combustion," Ekoto IW, Colban WF, Miles PC, Park SW, Reitz RD, Foster DE, Durrett RP. *DOE OFCVT AEC Working Group Meeting*, February 10–12, 2009, Livermore, CA.

12. "Experimental Assessment of a Non-Linear Turbulent Stress Relation in a Complex Reciprocating Engine Flow," Miles PC, RempelEwert BH, Reitz RD. *Exp. Fluids 47:451–461, 2009.*

13. "In-Cylinder PIV measurements in an Optical Light-Duty Diesel at LTC Conditions," Colban W, Ekoto I, Kim D, Miles PC. *Thermo-and Fluid-Dynamic Processes in Diesel Engines: THIESEL2008,* September 9–12, 2008, Valencia, Spain

14. "In-cylinder CO and UHC Imaging in a Light-Duty Diesel Engine during PPCI Low-Temperature Combustion," Kim D, Ekoto IW, Colban WF, Miles PC. *SAE Int. J. Fuels Lubr. 1:933-956, 2009. Also SAE technical paper2008-01-1602.*

15. "A Detailed Comparison of Emissions and Combustion Performance between Optical and Metal Single-Cylinder Diesel Engines at Low-Temperature Combustion Conditions," Colban WF, Kim D, Miles PC, Oh S, Opat R,

Krieger R, Foster D, Durrett, RP, Gonzalez MA. *SAE Int. J. Fuels Lubr. 1:505-519, 2009. Also SAE technical paper2008-01-1066.*

16. "The Impact of a Non-Linear Turbulent Stress Relationship on Simulations of Flow and Combustion in an HSDI Diesel Engine," Fife ME, Miles PC, Bergin MJ, Reitz RD, Torres DJ. *SAE Int. J. Engines. 1:991-1003, 2009. Also SAE technical paper2008-01-1363.*

Special Recognitions & Awards

1. Invited Speaker: *University of Wisconsin Engine Research Center Symposium : Reducing Fuel Consumption: Solutions and Prospects*, June 10–11, 2009, Madison, WI.

II.A.3 Heavy-Duty Low-Temperature and Diesel Combustion and Heavy-Duty Combustion Modeling

Mark P.B. Musculus
Combustion Research Facility
Sandia National Laboratories
P.O. Box 969, MS9053
Livermore, CA 94551-0969

DOE Technology Development Manager:
Gurpreet Singh

Objectives

The overall Office of Vehicle Technologies goal for this project is to develop fundamental understanding of advanced low-temperature combustion (LTC) technologies. The project includes diesel combustion research at Sandia National Laboratories (SNL) and combustion modeling at the University of Wisconsin (UW). The specific goals for Fiscal Year 2009 include:

- Extend diesel conceptual model to LTC (SNL).
- Understand multiple injection effects on LTC (SNL).
- Develop wall temperature diagnostic for studying liquid film dynamics (SNL).
- Improve computer modeling for LTC/diesel sprays and study piston geometry effects on LTC (UW+SNL).

Accomplishments

- Entrainment wave concept shown to explain many LTC phenomena, and is helping industrial partners to address practical engine issues as well as providing additional building blocks for conceptual model extension.
- Showed how post-injection combustion interacts with residual soot from the main injection to reduce engine-out soot.
- Demonstrated wall temperature diagnostic for studying liquid film dynamics.
- Improved computer models to reduce grid dependency so that they better agree with and supplement experiments.

Future Directions

Current results show that diesel jet interactions are critical for soot reductions with multiple injections:

- Use planar laser diagnostics (laser-induced incandescence, hydroxyl radical planar laser-induced fluorescence [OH PLIF]) to learn how soot formation dynamics can be controlled.
- Use planar-laser diagnostics (fuel tracer PLIF, formaldehyde PLIF) to understand mixing, ignition, and combustion dynamics of multiple injections.
- Understand how post-injection interactions with main-injection soot are affected by targeting: vary the injection spray angle and/or swirl.
- Use other injections schemes (split-main, pilot, three or more injections).

Continue to develop and refine conceptual model extension for LTC:

- Consolidate insights from multiple institutions and try to build a consensus on the chemical and mixing processes of LTC.

Introduction

Fuel concentration measurements in transient diesel jets reported in FY 2007 showed that fuel in the wake of the injection pulse mixes with ambient gases more rapidly than in a steady jet, potentially creating overly fuel-lean regions that do not burn to completion, causing unburned hydrocarbon emissions [1]. In FY 2008, a simple one-dimensional jet model was developed to analyze entrainment in diesel jets, and it predicted that a region of increased entrainment, termed the "entrainment wave," travels through the jet after the end of injection, increasing mixing by up to a factor of three [2]. This year, the entrainment wave concept is further applied to help explain soot formation and oxidation in diesel jets. These observations, together with an accumulation of measurements from previous fiscal years, are being gathered as the necessary building blocks for an extension of Sandia's diesel conceptual model [3] to LTC conditions.

Additionally, initial investigations of post-injections have provided insight into the in-cylinder mechanisms by which multiple fuel-injections during a single engine cycle can improve pollutant emissions tradeoffs. For example, de Ojeda et al. from Navistar [4] have demonstrated that adding a post injection helps extend the load limits of clean combustion (NOx level of 0.2 g/hp-hr and an after treatment-tolerant soot level) for loads ranging from 10 bar to 16.5 bar brake mean effective pressure in a medium-duty diesel engine with the use of an exhaust gas recirculation (EGR) rate of 44%. The improvement achieved in exhaust emission

performance was reported to be very sensitive to the delay from main injection and the fraction of fuel in the post-injection. Exhaust soot was reduced only with a post-injection dwell of more than 30 crank angle degrees (CAD), while the exhaust soot with close-coupled posts was the same as or higher than a single injection. Various and sometimes contradicting hypotheses have been offered in the literature to explain improvements in emission performance with post injections, and a comprehensive understanding of underlying in-cylinder mechanisms has not been established. One objective of this year's work is to use quantitative in-cylinder and exhaust soot measurements in a parametric study of post injections in an optical heavy-duty engine to provide a comprehensive picture of both (i) the effects of post injections on exhaust soot and (ii) the in-cylinder mechanisms responsible.

Approach

This project uses an optically-accessible, heavy-duty, direct-injection (DI) diesel engine (Figure 1). Windows provide imaging access to either (i) the piston bowl, through a flat piston-crown window, or (ii) the squish region above the piston bowl-wall, through a window in the cylinder head in place of one of the exhaust valves. The evolution and interaction of soot regions from both injections was visualized using high-speed imaging of soot luminosity, both in the piston bowl and in the squish regions. Figure 1 shows the setup of the 2-color optical diagnostic and high-speed camera for measurements in the piston bowl. Light emitted by glowing soot is captured by two photodiodes and imaged by an IDT-XS-4 high-speed digital camera as shown in Figure 1. The two photodiodes are equipped with band-pass filters to record light intensity in 10-nm-wide bands located about the center wavelengths (550 nm and 900 nm). For measurements in the squish region, the entire optical setup is moved to the upper viewport in Figure 1. In addition to the optical measurements, exhaust soot was also measured by filter-paper blackening using an AVL 415s variable sampling smoke meter. The engine is operated under EGR-diluted LTC conditions with 12.7% intake oxygen, corresponding to an EGR rate of about 55%, and using a range of main and post-injection timings.

As part of a continuing effort, improved computer models were developed for LTC/diesel sprays. The modeling work uses a version of the Los Alamos KIVA computer code that has been improved at UW. Instead of using full detailed chemistry, the model uses a reduced kinetic mechanism for n-heptane ignition and combustion so that solutions can be completed in a reasonable time [5], and gas-jet and vapor-particle sub-models have been added to reduce grid dependency for diesel sprays [6].

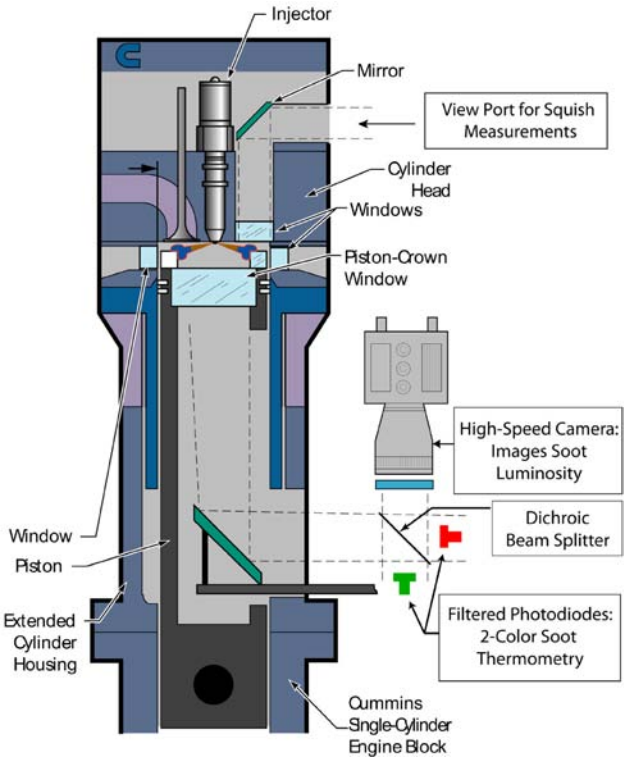

FIGURE 1. Schematic diagram of the optically accessible DI diesel engine and optical setup.

Results

Figure 2 shows images of soot luminosity for two different EGR-diluted LTC conditions, one with a short ignition delay (ID) on the left, and one with a long ID, on the right. The images were acquired through the piston-bowl window, 15 CAD after the start of injection (ASI), which is also 5 CAD after the end of injection (AEI). The dashed red lines show the nominal locations of the axes of the eight diesel sprays emanating from the centrally located fuel injector.

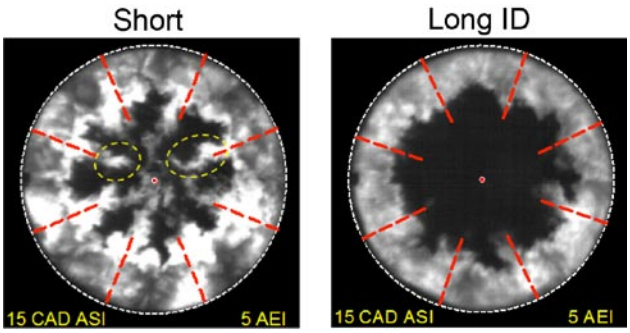

FIGURE 2. Images of LTC soot luminosity for short (left) and long (right) ID. The dashed red lines show the nominal spray axes.

For the condition with a short ID (left), the soot clouds in the diesel jets race back toward the injector after the end of injection, filling the center of the combustion chamber (center of image). After the end of injection, regions of soot in the center of the chamber rapidly oxidize, while soot near the outer boundaries remains late in the cycle. By contrast, for conditions with a long ID (right), the soot forms after the end of injection, near the outer boundaries of the combustion chamber, and it does not race back to the injector after the end of injection. The differing behavior of the soot clouds after the end of injection can be explained by the dynamics of the entrainment wave. For the short ID condition, combustion is active before the end of injection, so there is insufficient time for the entrainment wave to lean-out the near-injector mixtures before soot formation can occur. After soot is formed in the center of the combustion chamber, however, increased mixing from the entrainment wave rapidly oxidizes the soot near the injector. For the longer ID condition, the entrainment wave leans-out mixtures near the injector before combustion occurs, so that soot cannot form there. Instead, it can only form downstream, near the outer boundaries of the combustion chamber. These insights into the behavior of soot after the end of injection provide additional building blocks for a conceptual model extension for LTC conditions.

Figure 3 shows the exhaust filter smoke number (FSN) for EGR-diluted LTC conditions using a parametric sweep of the post-injection start of injection (SOI) at four different main-injection timings. The exhaust FSN for the main injection only are also shown for reference, as horizontal lines, color coded according to the legend. The data show that with constant main injection timing and quantity, adding a post-injection increases soot at small dwells between the main- and post-injection, but at larger dwells, the soot decreases.

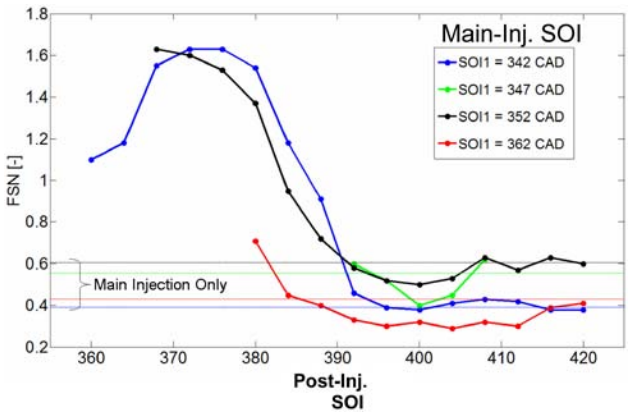

FIGURE 3. Variation of exhaust smoke as post injection timing is delayed for four main injection timings. Top dead center at compression corresponds to 360 CAD. The horizontal lines indicate the exhaust smoke for main injection only.

For early main-injections, the exhaust soot for the late post injections decreases at most to the level of the main injection only, but for later main injection conditions, the exhaust soot decreases below that of even the single main injection. These results provide clear evidence of interaction between post injections and late main injections – the post injection must affect residual soot from the main injection to reduce the exhaust soot emissions.

Figure 4 shows evidence of interaction between main and post injections, from soot luminosity images in the squish region above the piston for a main-injection only (top) or with a post injection (bottom). The images were acquired through the cylinder-head window (see Figure 1). In the images, only a portion of one of the eight jets is visible. The injector is to the left, outside of the field of view, as indicated by the straight dashed lines. The curved dashed lines show the contour of the piston bowl, with the squish region on the right. With a single main injection only (top), soot remains late in the cycle in the wake of the jet, distributed between squish and bowl regions. When a post-injection is added (bottom), the soot is pushed back into the squish region, where it oxidizes more quickly. Two-color soot thermometry measurements (not shown) confirm that

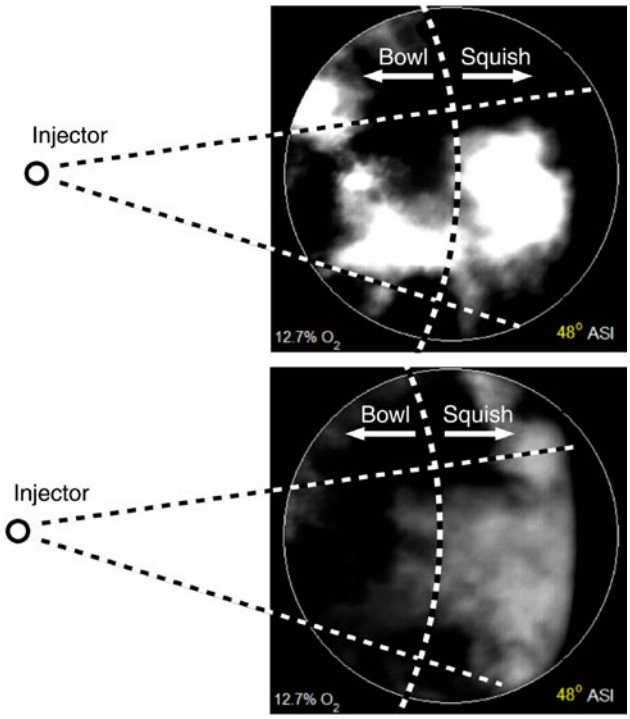

FIGURE 4. Soot luminosity images in the squish region above the piston for a main-injection only (top) and with a post injection (bottom) acquired through the cylinder head window (see Figure 1). A portion of one of the eight jets is visible and the injector is to the left, outside of the field of view, as indicated by the straight dashed lines. The curved dashed lines show the contour of the piston bowl, with the squish region on the right.

soot in the squish region is more rapidly oxidized when the post injection is added.

Such interactions favorable to soot oxidation only occur, however, when (i) the SOI of the post injection is sufficiently delayed that it produces no soot of its own, and (ii) soot from the main injection remains in the squish region, which means that the main-injection SOI must be relatively late. Figure 5 summarizes the interactions between post and main injections for conditions with either an early (top) or late (bottom) main-injection. For early main-injection conditions, most of the soot from the main injection is in the bowl (top left). A late post-injection creates very little soot of its own, but also does not interact with main-injection soot, so the main-injection soot is not reduced (top right). For late main-injection conditions, the soot is split between bowl and squish regions (bottom left). A late post-injection creates little soot of its own and also helps to oxidize soot in the squish region (bottom right).

Finally, Figure 6 shows a comparison of experimental images (top row) of OH fluorescence (green) and either formaldehyde (H_2CO) or polycyclic aromatic hydrocarbon (PAH) fluorescence (red), as labeled in the images, with model predictions (bottom row of images) of mass fractions (Y) of OH, formaldehyde, and acetylene (C_2H_2) soot precursor species. In the experimental images, the white dot indicates the location of the injector, and the white curved line shows the location of the piston bowl wall. The field of view for the model images is identical. For these late-injection LTC conditions, the recent

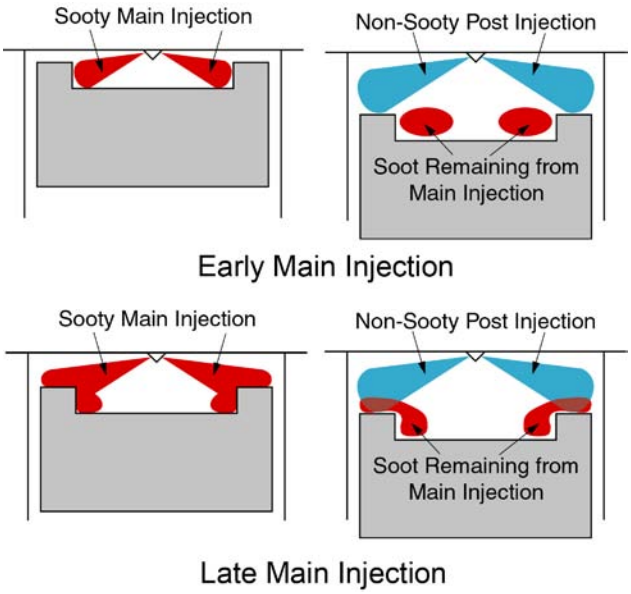

FIGURE 5. Illustration of the interactions between main and post injections with either an early (top) or a late (bottom) main injection.

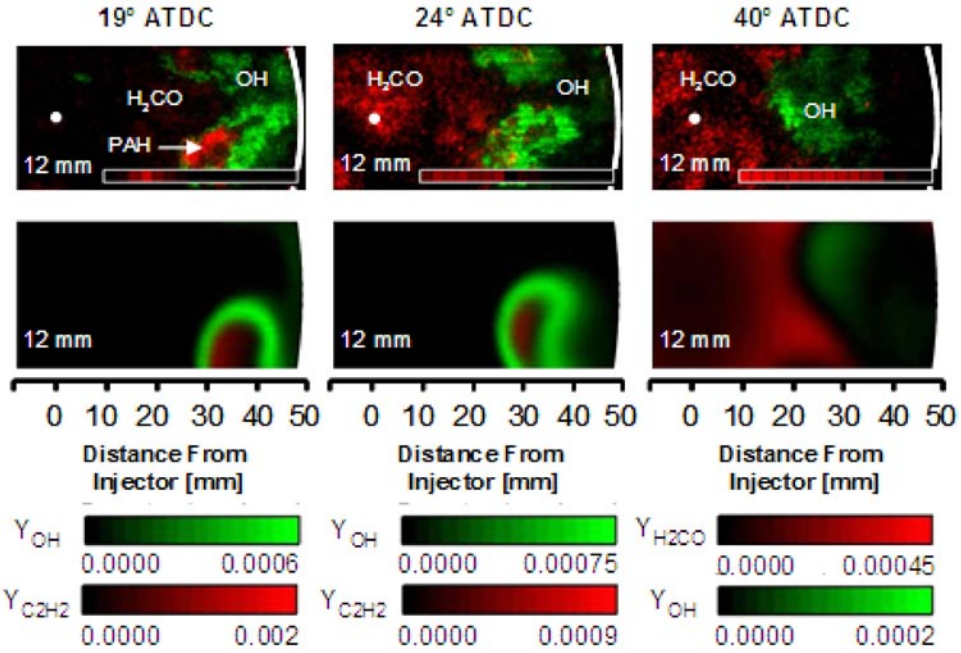

FIGURE 6. Comparison of experimental images (top row) of OH fluorescence (green) and either formaldehyde (H_2CO) or polycyclic aromatic hydrocarbon (PAH) fluorescence (red), as labeled in the images, with model predictions (bottom row of images) of mass fractions (Y) of OH, H_2CO, and C_2H_2 soot precursor species. In the experimental images, the white dot indicates the location of the injector, and the white curved line shows the location of the piston bowl wall. The field of view for the model images is identical.

model development efforts have improved model agreement with experimental measurements. The model predictions of acetylene soot precursor species agree well with measured PAH soot precursor species distributions. The location of OH distributions, which mark second-stage ignition and combustion of unburned fuel, also agree well, considering the cycle-to-cycle variation in the experiments. Model vapor-fuel distributions also agree well with experimental measurements (not shown). Both the models and the experiments show formaldehyde (H_2CO, red) remaining late in the cycle (right), which indicates unburned fuel. Furthermore, for these conditions, both models and experiments show smaller bowls help to direct hot combustion into over-lean regions to reduce unburned fuel.

Conclusions

The recent research efforts described in this report provide improved understanding of in-cylinder LTC spray, combustion, and pollutant-formation processes required by industry to build cleaner, more efficient, heavy-duty engines. Specific conclusions include:

- The entrainment wave concept explains many LTC phenomena, and is helping industrial partners to address practical engine issues. It also provides additional building blocks for an extension to LTC conditions of Sandia's conceptual model for conventional diesel combustion.
- If residual soot from the main injection remains in the squish region, which typically occurs for late main injections, then a late post injection may interact with and oxidize the squish region soot, thereby reducing exhaust soot emissions for LTC conditions.
- Improved computer models with reduced grid dependency agree with and supplement experimental measurements.

References

1. Musculus, M.P. B., "FY 2007 DOE FCVT Annual Report: Heavy-Duty Low-Temperature and Diesel Combustion Research (8748) and Heavy-Duty Combustion Modeling (12349)," 2007.

2. Musculus, M.P. B., "FY 2008 DOE VT Annual Report: Heavy-Duty Low-Temperature and Diesel Combustion Research (8748) and Heavy-Duty Combustion Modeling (12349)," 2008.

3. Dec, J.E., "A Conceptual Model of D.I. Diesel Combustion Based on Laser-Sheet Imaging," SAE Paper 970873, SAE Transactions, 106, No. 3, pp. 1319-1348, 1997.

4. Ojeda W., Zoldak P., Espinosa R., and Kumar R., "Development of a Fuel Injection Strategy for Partially Premixed Compression Ignition Combustion", SAE Paper 2009-01-1527, 2009.

5. Maroteaux, F. and Noel, L., "Development of a Reduced n-Heptane Mechanism for HCCI Combustion Modeling," Combustion and Flame 146, pp. 246-267, 2006.

6. "Reduction of Numerical Parameter Dependencies in Diesel Spray Models," N. Abani, A. Munnannur, R. Reitz, Journal of Engineering for Gas Turbines and Power 130 no. 3, 2008.

FY 2009 Publications/Presentations

1. "Effects of Piston Bowl Geometry on Mixture Development and Late-Injection Low-Temperature Combustion in a Heavy-Duty Diesel Engine," C. Genzale, R. Reitz, M. Musculus, SAE paper 2008-01-1330, SAE International Journal of Engines 1, pp. 913-937, 2008.

2. Book chapter for "Direct Injection Combustion Engines and Their Fuels for Automotive Applications in 21st Century," Woodhead Publishing of Cambridge, finalized for publication in 2009.

3. "Gradient Effects on Two-Color Soot Optical Pyrometry in a Heavy-Duty DI Diesel Engine," M. Musculus, S. Singh, and R. Reitz, Combustion and Flame 153, no. 1-2, pp. 216-227, 2008.

4. "Entrainment Waves in Diesel Jets," M. Musculus and K. Kattke, SAE paper 2009-01-1355, SAE International Journal of Engines 2, pp. 1170-1193, 2009.

5. "Mixing and Flame Structures Inferred from OH-PLIF for Conventional and Low-Temperature Diesel Engine Combustion," S, Singh, M. Musculus, R. Reitz, Combustion and Flame, 156, no. 10, pp. 1898-1908, 2009.

6. "Effect of Ignition Delay on In-Cylinder Soot Characteristics of a Heavy Duty Diesel Engine Operating at Low Temperature Conditions," M. Bobba, C. Genzale, M. Musculus, SAE paper 2009-01-0946, SAE International Journal of Engines 2, pp. 911-924, 2009.

7. "Influence of Diesel Injection Parameters on End-of-Injection Liquid Length Recession," S. Kook, L. Pickett, M. Musculus, SAE paper 2009-01-1356, SAE International Journal of Engines 2, 1194-1210, 2009.

8. "Liquid-Phase Diesel Spray Penetration during End-of-Injection Transient," S. Kook, L.M. Pickett, M.P.B. Musculus, K. Kattke and R.K. Gehmlich, COMODIA 2008, Japan.

9. "Reduction of Numerical Parameter Dependencies in Diesel Spray Models," N. Abani, A. Munnannur, R. Reitz, Journal of Engineering for Gas Turbines and Power 130 no. 3, 2008.

10. "Development of an Improved NOx Reaction Mechanism for Low Temperature Diesel Combustion Modeling," T. Yoshikawa, R. Reitz, SAE Paper 2008-01-2413, SAE International Journal of Engines 1, pp. 1105-1117, 2009.

11. "A Reduced Chemical Kinetic Model for IC Engine Combustion Simulations with Primary Reference Fuels," Y. Ra, R. Reitz, Combustion & Flame 155, pp. 713-738, 2008.

12. "A Vaporization Model for Discrete Multi-Component Fuel Sprays," Y. Ra, R. Reitz, Int. J. Multiphase Flow 35, 2009.

13. "Operating a Heavy Duty DICI Engine with Gasoline for Low Emissions," R. Hanson, D. Splitter, R. Reitz, SAE Paper 2009-01-1442, 2009.

14. "Numerical Simulation of Diesel and Gasoline-Fueled Compression Ignition Combustion with High Pressure Late Direct Injection," Y. Ra, J.-E. Yun, R. Reitz, Int. J. of Vehicle Design 50, No. 1-4, pp. 3-35, 2009.

15. "Numerical Parametric Study of Diesel Engine Operation with Gasoline," Y. Ra, J.E. Yun, R. Reitz, Comb. Sci. Tech. 181, pp.1-29, 2008.

II.A.4 Low-Temperature Diesel Combustion Cross-Cut Research

Lyle M. Pickett
MS 9053
Sandia National Laboratories
P.O. Box 969
Livermore, CA 94551-9053

DOE Technology Development Manager:
Gurpreet Singh

Objectives

- Develop high-speed imaging techniques to identify sources of unburned hydrocarbons (UHC) in low-temperature combustion (LTC) in diesel engines.
- Lead a multi-institution, international, research effort on diesel sprays, called the Engine Combustion Network (ECN).
- Develop models to predict liquid-phase penetration at early-injection conditions, providing pathways for prevention of liquid wall impingement.

Accomplishments

- Developed high-speed imaging tools that show the appearance of a cool-flame and the location of UHC after the end of injection and end of high-temperature combustion.
- Obtained a set of identical injectors, donated by Robert Bosch, LLC. Distributed injectors to participants of the ECN for research at specific injector and ambient conditions. Dataset will become a serious focal point for advanced experimental and model development, accelerating development of cleaner, more fuel efficient engines.
- Modeled and explained the dependency of ambient pressure, temperature, and fuel type on liquid penetration at early-injection conditions. Developed a model to predict injection durations needed to shorten liquid-phase penetration to be less than the quasi-steady liquid length.

Future Directions

- Develop a quantitative dataset of penetration, mixing, combustion, and soot formation for neat biodiesel and diesel.
- Quantify the extent of liquid penetration at problematic post-injection conditions, injections which are now used for diesel particulate filter regeneration.
- Perform direct measurements of mixing (equivalence ratio) at the time of the premixed burn in constant-injection-duration diesel fuel jets for various exhaust gas recirculation (EGR) levels. Mixing and combustion measurements will also be performed at the ECN working group conditions.
- Investigate jet-jet interaction effects on flame lift-off.

Introduction

LTC strategies have shown promise in reducing oxides of nitrogen (NOx) and particulate matter emissions, but they also may produce higher UHC and carbon monoxide (CO) emissions that can reduce combustion efficiency. In order to increase efficiency, while simultaneously keeping harmful emissions low, it is important to understand the sources of UHC and CO. We have studied the fundamental causes of UHC and CO formation in LTC with several phases of research over the past year, including (1) liquid spray penetration with potential for fuel liquid films and UHC, and (2) combustion transients after the end of injection that determine which regions of the spray burn effectively. We developed new high-speed diagnostics to measure these phenomena. Along with other work from our facility, these results provide data needed to accurately model LTC and develop optimized engines.

Approach

We used a constant-volume vessel for this research because of the ability to carefully control the charge-gas temperature and density within the chamber, as well as full optical access (100-mm access from multiple angles) for advanced diagnostics. Figure 1 shows the combustion vessel and several optical diagnostic setups. A common-rail diesel injector (single-hole) generates a spray that penetrates and autoignites at representative engine conditions. A more detailed description of the facility may be found in [1].

Mie-scattering and shadowgraph/schlieren images were simultaneously acquired using high-speed cameras shown in Figure 1. The shadowgraph/schlieren diagnostic identifies the boundary of the vapor phase of the spray, but in addition, it can show the cool flame, high-temperature ignition, and other temperature-sensitive diagnostics. The Mie-scatter diagnostic provides the liquid boundary of the spray. However, depending upon the filter and camera settings, the imaging setup can also measure high-temperature chemiluminescence or soot luminosity [2].

II.A.5 High Efficiency Clean Combustion in Light-Duty Multi-Cylinder Diesel Engine

Kukwon Cho, Robert M. Wagner (Primary Contact), C. Scott Sluder
Oak Ridge National Laboratory (ORNL)
2360 Cherahala Boulevard
Knoxville, TN 37932

DOE Technology Development Manager:
Gurpreet Singh

Objectives

- Expand operational range of high efficiency clean combustion (HECC) for conditions consistent with the Urban Dynamometer Drive Schedule as well as future down-sizing and down-speeding conditions.
- Improve the fundamental understanding of HECC from a thermodynamics perspective.
- Characterize the effect of the thermal boundary conditions of the engine on HECC stability, efficiency, and emissions.
- Support demonstration of DOE FreedomCAR emissions milestones for light-duty diesel engines.

Accomplishments

- Made significant modifications to the General Motors (GM) 1.9-L engine dynamometer cell including expanded ability to control the temperature of the exhaust gas recirculation (EGR), engine coolant, and engine oil systems.
- Characterized the effects of intake EGR/air mixture temperature and combustion chamber wall temperature on emissions, efficiency, and stability.
- Provided technical support in transitioning from the Mercedes-Benz (MB) 1.7-L engine to the GM 1.9-L engine for the emission controls activity at ORNL.
- Completed Fuels for Advanced Combustion Engines diesel fuels experiments/data analysis on GM 1.9-Liter engine to support fuel technology activity at ORNL.

Future Directions

- Explore the effect of thermal boundary conditions on HECC operation with expanded control of the thermal boundary conditions.
- Characterize efficiency/emissions potential of advanced gasoline-diesel combustion concepts on the GM 1.9-L engine.
- Continue to support efficiency and emission controls activities to ensure collaborative path toward Fiscal Year 2010 DOE FreedomCAR milestones.

Introduction

Advanced combustion modes such as premixed charge compression ignition (PCCI) have shown promise as potential paths for meeting 2010 and beyond efficiency and emissions goals. ORNL as well as others have shown success in achieving reduced emissions and acceptable efficiency using high charge dilution for a somewhat limited speed-load range. This activity builds on many years of HECC experience at ORNL, including the demonstration of HECC operation in a multi-cylinder engine, characterization of cylinder-to-cylinder stability issues, detailed speciation of hydrocarbons (HCs) in HECC modes, description of the effect of particulate matter (PM) precursors on engine-out emissions, and the demonstration of transitions to, from, and within HECC modes. The primary objective of this project is to investigate potential near-term technologies for expanding the usable speed-load range and to evaluate the potential benefits and limitations of these technologies for achieving HECC in light-duty diesel engines.

For further clarification, the term HECC was first introduced in the FreedomCAR Advanced Combustion and Emissions Control Tech Team and Diesel Cross-Cut Team in 2003. The intent was to convey the objectives of advanced combustion research in a fresh, all-encompassing name in a time when low-temperature combustion, PCCI, homogeneous charge compression ignition, modulated kinetics, and many more, but conveyed nothing about the advantages and were aligned with certain companies. DOE adopted HECC as the subject of a large request of proposals in 2004. ORNL adopted the term in 2004.

Approach

Among several HECC strategies, PCCI operation is the most compatible approach with near-term engine technologies. The injection timing in a PCCI approach remains as an effective control of ignition timing, unlike other HECC approaches. However, the variations in the thermochemical conditions in the cylinder can impose significant variations on the ignition delay, combustion stability, and resulting emissions. Hence, studying

the impact of those conditions can allow improved control of ignition timing through the adjustment of injection timing. Two parameters controlling thermal conditions in the cylinder, intake charge temperature and combustion chamber wall temperature, were considered for their effect on efficiency, emissions, and cyclic variations on the GM 1.9-Liter engine by using independent temperature control systems for the cooling loops of engine coolant, engine oil, and EGR coolant. The engine speed/load condition of 1,500 rpm, 2.6 bar brake mean effective pressure (BMEP), which is one of the representative modal conditions of light-duty diesel engine operation defined by an industry working group, was selected in this study.

Results

Two parameters affecting the in-cylinder thermal condition were investigated: (1) intake charge temperature and (2) combustion chamber wall temperature. The methodology used for controlling the intake charge temperature in this study is a feedback control system for the EGR cooling system. The modified engine system has a separate cooling loop for the EGR coolant, which can control both EGR coolant temperature level and EGR coolant flow rate independently from engine operating conditions. The heat rejection in the EGR cooler can be adjusted through EGR coolant temperature level as well as EGR coolant flow rate, thus controlling EGR cooler gas outlet temperature. The engine coolant temperature and engine oil temperature are controlled by individual feedback controllers which are able to adjust temperatures independent of engine operating conditions. This approach provides the ability to control the cylinder wall temperature through the effect of the cooling and lubrication fluid temperatures.

Three different levels of intake charge temperatures (82, 87, and 93°C) as well as engine coolant/oil temperatures (77, 87, and 97°C) were explored to investigate their effects on emissions, efficiency, and combustion stability of HECC operation. The test conditions investigated in this study are summarized in Table 1. The three intake charge temperatures were selected within the heat rejection capacity of the originally-equipped EGR cooler. The effects of combustion chamber wall temperatures on combustion stability of HECC operation were performed at three different coolant/oil temperatures levels.

The start of injection (SOI) timing sweep experiments were performed at each level of intake charge temperature and coolant/oil temperature. Figure 1 shows typical average heat release rate (HRR) traces for SOI timing sweeps with the normal intake charge temperature (87˚C). General trends that apply to SOI timing sweeps are as follows: the peak values of HRR were reduced and combustion phasing was retarded with SOI timing as shown in Figure 1. As expected, both NO_x and PM emissions decreased with retarded SOI timings, while brake specific fuel consumption (BSFC), carbon monoxide (CO) and HC emissions increased. These results are not shown here due to the concise nature of this report. The 1,000-cycle scatter plots of CA5 (crank angle of 5 degrees after

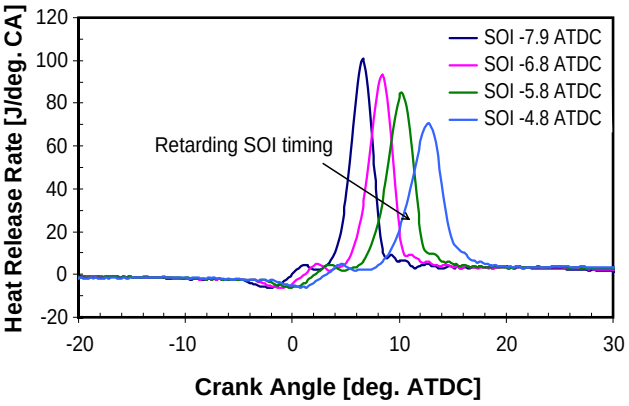

FIGURE 1. Average heat release rate traces for SOI timing sweeps at normal intake charge temperature.

TABLE 1. Summary of engine operating conditions

	Intake Charge Temperature			Combustion Chamber Wall Temperature		
Thermal Condition	**Low**	**Normal**	**High**	**Low**	**Normal**	**High**
Engine Speed [rpm]	1500			1500		
BMEP [bar]	2.6			2.6		
EGR Fraction [%]	35.1			35.8		
Air/Fuel Ratio	22.6			22.1		
Intake Oxygen Concentration [%]	16.5			16.3		
Intake Charge Temperature [°C]	*82.0*	*87.0*	*93.0*	89.0		
Coolant Temperature [°C]	85.5			*76.0*	*86.0*	*97.0*
Oil Temperature [°C]	86.7			*77.0*	*88.0*	*97.0*
Injection Timing [°ATDC]	Sweep			Sweep		
Injection Pressure [bar]	1200			1200		
Injection Event	Single Pulse			Single Pulse		

top dead center), which represents start of combustion (SOC) timing, at three different levels of coolant/oil temperatures are shown in Figure 2. Higher variability of the CA5 point was observed with retarded SOI timing at all coolant/oil temperature levels. As shown in Figure 2, the CA5 points were advanced with increased coolant/oil temperature levels, indicating shorter ignition delay. The cyclic dispersions of CA5 point at the same SOI timing are increased with lower coolant/oil temperatures.

To understand the effect of thermal conditions on PCCI combustion phenomena, the SOI timing was adjusted to maintain a constant CA50 point at approximately 9.0 to 9.5 degrees after top dead center (ATDC) for each temperature combination. Figure 3 (a) and (b) show NO_X, PM, CO, and HC emissions as well as BSFC for constant CA50 point conditions at three different levels of intake charge temperature and coolant/oil temperature, respectively. The CA50 points were maintained constant at approximately 9.0 degrees ATDC for varying intake charge temperature, and 9.4 degrees ATDC for varying coolant/oil temperatures. As shown in Figure 3, NO_X emissions do not show a strong sensitivity to variations of intake charge temperature or coolant/oil temperatures. PM emissions increase slightly with increasing intake charge temperature and coolant/oil temperatures. The variations of coolant/oil temperatures show a stronger sensitivity in PM emissions than the variations of intake charge temperature, but the levels of PM emissions are extremely low at all cases (< 0.10 filtered smoke number). The variations of coolant/oil temperatures also show more significant effects on CO and HC emissions than the variations of intake charge temperature. This could be explained in that varying either the intake charge temperatures or coolant/oil temperatures does not significantly affect the combustion temperature at the core region, thus the formation of NO_X is not affected significantly. However, since the formation of CO and HC emissions is closely related to the thickness of the flame quenching layer at the periphery of the combustion chamber, the thermal condition of the combustion chamber wall (variations of coolant/oil temperatures) shows more significant effects on CO and HC emissions than the intake charge thermal condition. The effect of intake charge temperature on BSFC does not show clear trends within the tested intake charge temperature ranges, but the highest BSFC is seen at the lowest coolant/oil temperature condition. The range of intake charge temperatures in this study does not seem to be wide enough to observe its impact on the combustion characteristics – as mentioned in the previous section, the intake charge temperatures selected in this study were based on the heat rejection capacity with the originally equipped EGR cooler. The standard deviation of CA5 and CA50 was less than 0.25 degrees for all cases.

The effect of intake charge temperature on the expansion of HECC operating range was further investigated by using an EGR cooler with a much higher heat rejection capacity than the originally-equipped one as reported at 2009 Annual Merit Review. As shown in Figure 4, the HECC operating range could be expanded by decreasing intake charge temperature with an EGR cooler of higher heat rejection capacity. At 1,500 rpm, HECC operation could be achieved up to 3.8 bar BMEP condition with decreased intake charge temperature of about 10˚C. The decreased intake charge temperature conditions exhibited a significant advantage in PM emissions. From the current study, the variations of combustion chamber wall temperature show more impact on CO and HC emissions of HECC operation than the variations of intake charge temperature. By combining the results of both investigations, robust HECC operation can be achieved and the range of HECC operation can be expanded by precisely controlling thermal conditions of both intake charge and

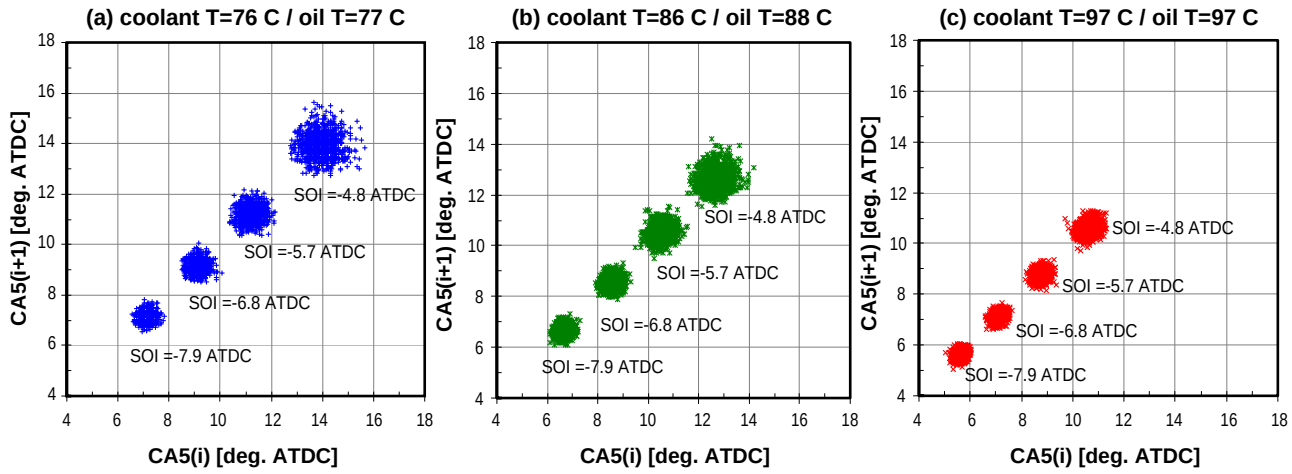

FIGURE 2. Scatter plots of CA5 points for SOI timing sweeps at different coolant/oil temperatures (1,000 cycles).

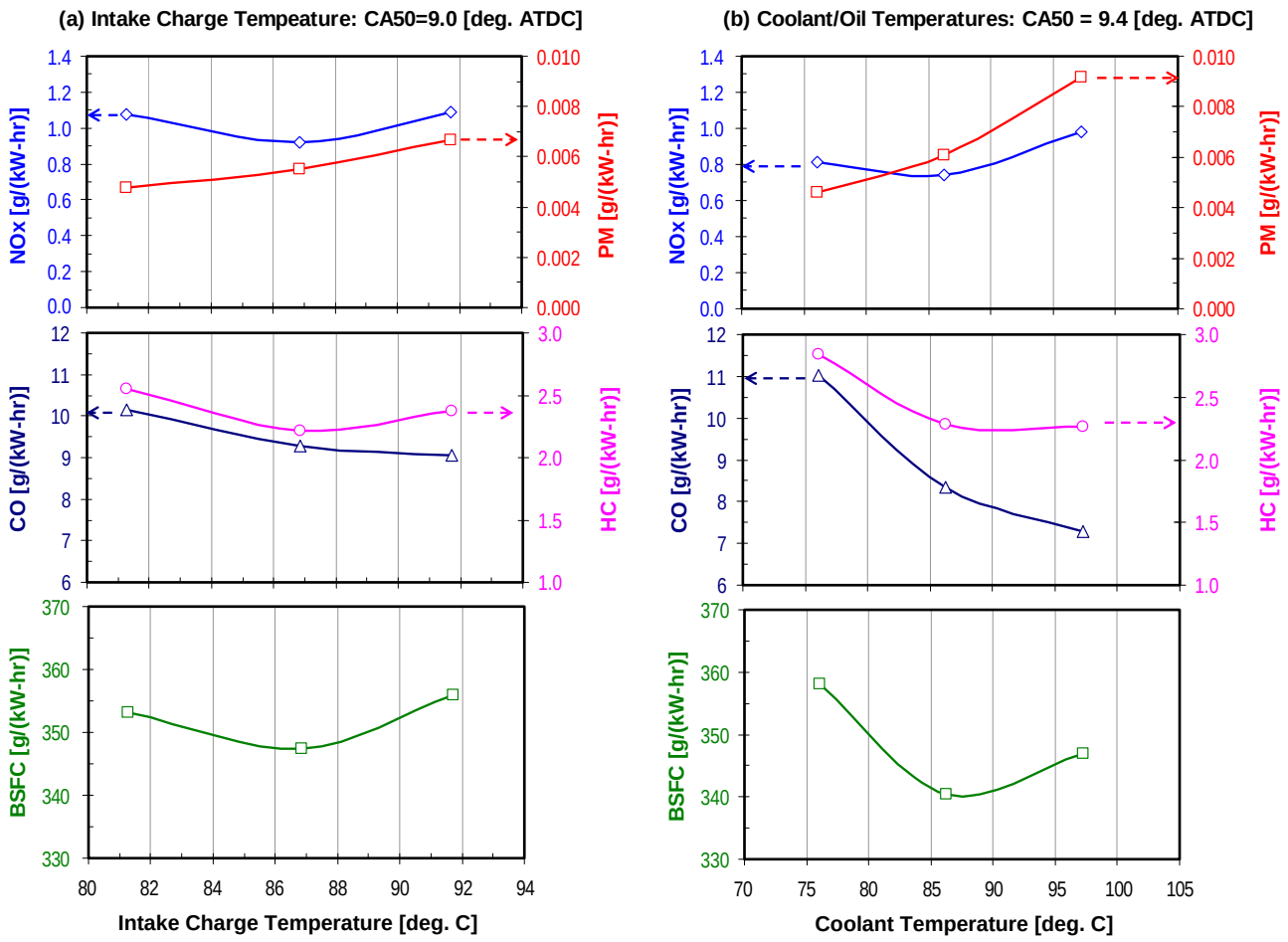

FIGURE 3. Comparisons of emissions and efficiency at constant CA50 conditions for (a) different intake charge temperatures, and (b) different coolant/oil temperatures.

combustion chamber wall without paying penalties in combustion stability or efficiency.

Conclusions

This activity has been successful at providing new insight into the implementation of advanced combustion operation on multi-cylinder engines and is an important component to demonstrating 2010 FreedomCAR efficiency and emissions milestones on light-duty diesel engines. Specific accomplishments are as follows:

- Substantial improvements in the engine dynamometer setup including expanded control of engine thermal boundary conditions and a second flexible control system for independent operation and control of all engine actuators and systems.
- Characterized the effect of intake charge temperature and combustion chamber wall temperature on emissions, efficiency, and cyclic dispersions on the GM engine:
  - A shorter ignition delay was observed with increasing intake charge temperature and combustion chamber wall temperature.
  - Both CO and HC emissions exhibit a strong sensitivity to the variations of combustion chamber wall temperature.
  - The HECC operating range was expanded with the extended intake charge temperature range enabled by a higher heat rejection capacity EGR cooler.
  - Robust HECC operation can be achieved and its operating range can be expanded by precisely controlling thermal conditions of both intake charge and combustion chamber wall without paying penalties in efficiency and emissions.
- Provided technical support in transitioning from the MB 1.7-L engine to the GM 1.9-L engine for the emission controls activity at ORNL.
- Completed Fuels for Advanced Combustion Engines diesel fuels experiments/data analysis on GM 1.9-L engine to support fuel technology activity at ORNL.

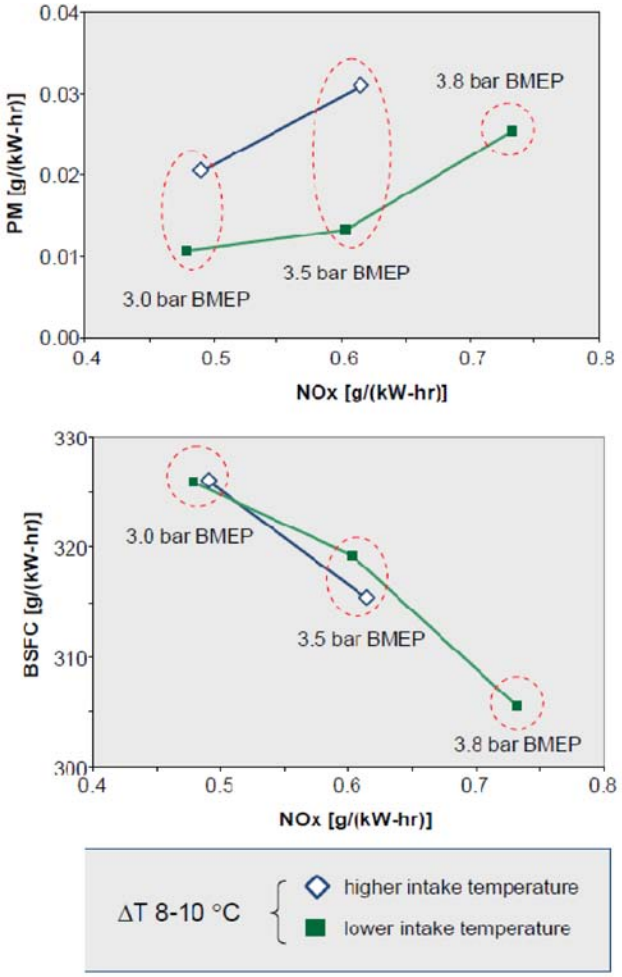

FIGURE 4. Intake charge temperature effects on expanding HECC operation range with a higher heat rejection EGR cooler.

FY 2009 Publications/Presentations

1. K. Cho, M. Han, C.S. Sluder, R.M. Wagner, "Experimental Investigation of the Effects of Fuel Characteristics on High Efficiency Clean Combustion in a Light-Duty Diesel Engine", SAE Paper 2009-01-2669 (San Antonio, TX, USA; November 2009).

2. K. Cho, R.M. Wagner, C.S. Sluder, K.D. Edwards, M. Han, "High Efficiency Clean Combustion Research at ORNL (multi-cylinder light-duty diesel engine)", Invited presentations at Korea Advanced Institute of Science and Technology (KAIST), Korea Institute of Machinery and Materials (KIMM), and Seoul National University (SNU) (Daejon & Seoul, South Korea; June 2009).

3. J.A. Massey, S.A. Eaton, R.M. Wagner, J.A. Drallmeier, "Contribution of combustion energy release to surface accelerations of an HCCI engine", 6th National Combustion Meeting of the Combustion Institute (Ann Arbor, MI, USA; May 2009).

4. R.M. Wagner, K. Cho, M. Han, C.S. Sluder, K.D. Edwards, "High Efficiency Clean Combustion in Multi-Cylinder Light-Duty Engines (ACE 17)", 2009 DOE Hydrogen Program and Vehicle Technologies Annual Merit Review (Arlington, VA, USA; May 2009).

5. R.M. Wagner, K. Cho, M. Han, C.S. Sluder, "Overview of engine efficiency activities at ORNL" and "Overview of High Efficiency Clean Combustion activities at ORNL", DOE Vehicle Technologies program mid-year review (Knoxville, TN, USA; October 2008).

6. M. Han, K. Cho, C.S. Sluder, R.M. Wagner, "Soybean and Coconut Biodiesel Fuel Effects on Combustion Characteristics in a Light-Duty Diesel Engine", SAE Paper 2008-01-2501 (Chicago, Il, USA; October 2008).

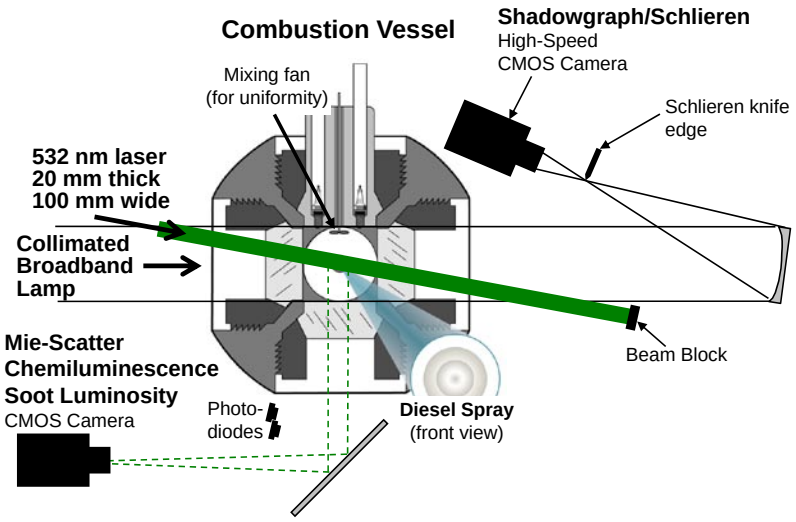

FIGURE 1. Combustion Vessel and High-Speed Imaging Setup

Results

Time-resolved information about the liquid and vapor penetration, and ignition is obtained by these combined high-speed diagnostics, as shown in Figure 2. The top of Figure 2 shows shadowgraph images of a non-reacting spray (0% O_2, left) and reacting spray at a LTC condition (12% O_2, right). The liquid boundary, obtained by simultaneous Mie-scatter imaging, is shown on the two vaporizing spray shadowgraph images as a solid blue line. Notice that shadowgraph images show a significant "background", which is caused by refractive index gradients that exist in the original ambient gases prior to injection. These features are caused by temperature gradients found in the ambient gases and in boundary layers at windows of the vessel. We will discuss alternative experimental setups and image corrections to remove this "background" below.

At the first time after the start of injection (ASI) is shown (514 μs), the liquid and vapor phases of the spray have already separated in the vaporizing sprays. Liquid penetrates to about 20 mm, but no further. (The extent of liquid penetration is a major issue for LTC, because of the likelihood of wall fuel films, unburned fuel, and increased UHC emissions. We have investigated the causes of this liquid penetration at early-injection conditions during this past year and summarized results in Ref. [3].) Meanwhile, the vapor boundary at the jet head initially penetrates to about the same distance for both non-reacting and reacting conditions.

Starting at about 700 μs ASI and continuing until 1,000 μs ASI, the head of the jet begins to change in the reacting jet. The original shadowgraph image shows the jet becoming more "transparent" at the head or edges of the reacting jet compared to the non-reacting jet. To illustrate, we have placed a dotted red line, showing the penetration distance of the non-reacting jet, at this same distance in the reacting jet for the 700 μs and 900 μs images. The head of the reacting jet appears to be missing. The "disappearance" of the jet's shadowgraph effect is caused by the first stages of ignition, or cool-flame activity, which break down the parent fuel molecule and also raise the temperature slightly, as illustrated at the bottom of Figure 2. These changes cause the refractive index of the jet to match the ambient more closely, thereby becoming more "transparent" in the original shadowgraph images. The same figure also shows why vapor

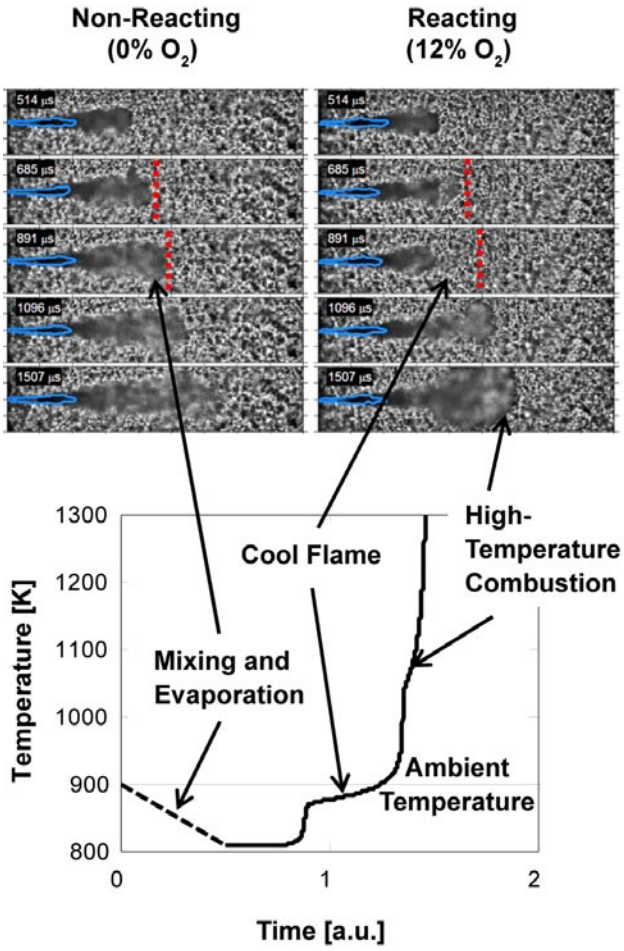

FIGURE 2. Non-reacting (top left, 900 K, 0% O_2) and reacting (top right, 900 K, 12% O_2) shadowgraph imaging time sequence. Liquid boundaries from Mie-scatter imaging are overlaid on vaporizing sprays with blue lines. Ambient density 22.8 kg/m^3. Injector conditions: 0.108 mm orifice, 110 MPa pressure, diesel fuel at 373 K, 3,000 μs injection duration. Bottom figure shows ignition stages of a fuel-air mixture in a perfectly-stirred reactor.

borders are identifiable in shadowgraph images–mixing and evaporation cools the vapor portions to form temperature gradients that are visible by schlieren/shadowgraph. During high-temperature ignition at about 1,000 μs ASI, the jet borders "re-appear" in the reacting shadowgraph images as high-temperature, low-density regions produce a very different refractive index gradient than that of the ambient gases. The reacting image at 1,500 μs also shows significant radial and axial expansion in what was formerly the "cool-flame" region.

The stages of ignition and high-temperature combustion are illustrated by examination of the jet axial penetration distances derived from the imaging, as shown in Figure 3. As suggested by the shadowgraph images, the initial penetration is the same for all sprays. However, by approximately 700 μs the head of the reacting jet "disappears" during cool-flame combustion, causing the calculated penetration distance to stay the same or even decrease. During ignition, the calculated penetration distance rises quickly back to the non-reacting and non-vaporizing value as high-temperature combustion reveals the jet. For reference, we also show the pressure rise and luminosity signal collected by two different photodiodes for the reacting jet condition. The photodiode with high sensitivity detects broadband high-temperature chemiluminescence as well as soot luminosity, if it forms later. The luminosity and pressure rise after about 1,000 μs ASI, which corresponds to the time of high-temperature ignition and area growth of the reacting sections of the jet. Figure 3 also shows that the liquid phase penetrates to only 20 mm, regardless if the spray is reacting and non-reacting.

The high-speed diagnostics shown above can also be applied to shorter injection events more typical of low-load LTC, as shown in Figure 4. In this case, we also turn off the mixing fan for the vessel, shown in Figure 1, to change the shadowgraph "background" caused by the ambient. Figure 4 shows that the ambient now has large-scale structure, rather than small-scale structure caused by more intense mixing from the fan. To more easily visualize the spray, we also apply a background correction at the right, where successive images are subtracted from one another [2]. After correction, the vapor region of the jet is less ambiguous. In addition, the camera used for Mie-scatter imaging was operated without any filters to collect both laser scatter from droplets as well as high-temperature (not cool-flame) chemiluminescence downstream. The upstream blue border line therefore represents liquid scatter, as before, but the downstream region also indicates high-temperature chemiluminescence boundaries.

Figure 4 shows that the liquid disappears shortly after 1,000 μs ASI, but there is no evidence of high-temperature ignition until approximately 2,000 μs ASI. Therefore, there is positive dwell between the end of injection (EOI) and the start of high-temperature combustion. This type of condition is quite typical for LTC combustion. The shadowgraph/chemiluminescence diagnostic shows that the high-temperature combustion occurs about 50 mm downstream of the injector. Despite clear evidence that fuel vapor exists upstream of 50 mm, the high-temperature combustion does not propagate upstream, even by 3,200 μs ASI. The combined imaging diagnostic therefore identifies the location of UHC, shown as dashed box region in Figure 4, resolved even for a single injection. The existence of UHC in the upstream region and high-

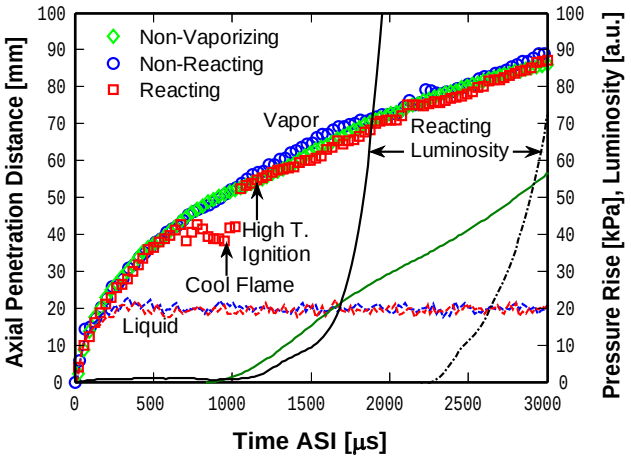

FIGURE 3. Axial penetration distances for the conditions of Figure 2. The vessel pressure rise and luminosity collected by two photodiodes is shown on the right axis for the reacting condition.

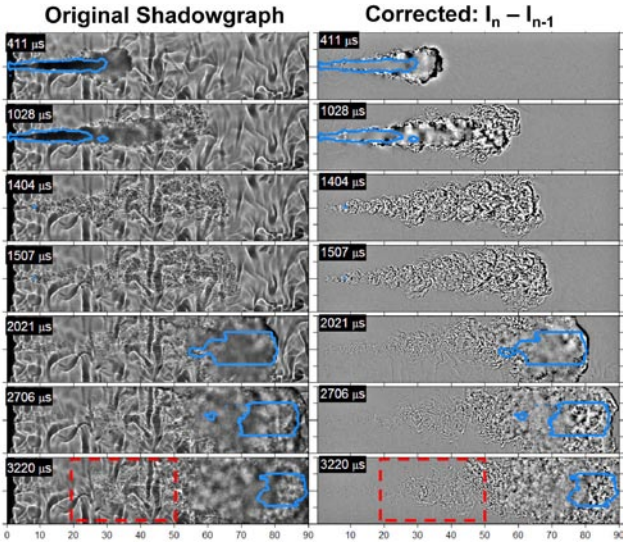

FIGURE 4. Reacting shadowgraph imaging, original (left) and corrected for background variation (right). Dashed boxed region shows UHC region after EOI. Ambient conditions: 900 K, 14.8 kg/m^3, 15% O_2. Injector conditions: 0.108 mm orifice, 110 MPa pressure, diesel fuel at 373 K, 1,050 μs injection duration.

temperature combustion downstream is consistent with earlier work from our laboratory at LTC conditions [4].

Given the success in using high-speed imaging to identify UHC sources, we applied the same diagnostics to a range of ambient and injector conditions, trying to understand what factors affect UHC existence near the injector region after the EOI. A contrasting result is given in Figure 5, a condition with (1) positive ignition dwell, (2) a larger nozzle size, (3) lower injection pressure, (4) higher ambient oxygen concentration, and (5) higher ambient temperature compared to that of Figure 4. All of these changes to conditions result in combustion that is more typical of conventional diesel than LTC. The imaging was once again performed with the fan turned off in order to make visualization of the spray easier. The near-injector region is shown at times relative to the end of injection, allowing observation of the timing and location of high-temperature combustion after the EOI.

The shadowgraph image sequence begins slightly before EOI, with the liquid and luminosity borders overlaid in blue. Because this condition has significant soot formation (and soot luminosity), it was not possible to operate the Mie-scatter camera without filters to simultaneously collect chemiluminescence, as in Figure 4. Instead, a 532-nm-centered bandpass filter (10 nm full width at half maximum) was used. Despite narrow filtering, a soot luminosity signal is present, forming a blue border downstream. The soot luminosity is also obvious in the shadowgraph imaging, appearing as brighter zones downstream. Before EOI the line-of-sight liquid and soot regions are merged together, but at EOI, when liquid begins to recede towards the injector, the two zones can be distinguished from each other as labeled on the figure.

The high-temperature combustion region is not immediately obvious in the shadowgraph as fuel vaporizes near the injector shortly after EOI. However, by about 220-280 μs after EOI, a shadowgraph zone with a sharp interface and smooth texture is evident, indicating a high-temperature combustion region. The high-temperature combustion zone is about 20 mm from the injector at this time, slightly upstream of the soot luminosity boundary. Figure 5 shows that the high-temperature zone rapidly advances towards the injector beginning at about 400 μs after EOI and by 500 μs after EOI it appears to move all of the way back to the injector. Since all identifiable regions of fuel vapor appear to transition to high-temperature combustion, minimal UHC is expected for this condition. This result is in contrast to that shown in Figure 4, where there was no significant propagation of reaction back towards the injector, leaving substantial regions of UHC.

Conclusions

The development of a simultaneous Mie-scatter, chemiluminescence, soot luminosity, and shadowgraph/schlieren high-speed imaging has shown to be a useful tool for interpretation of diesel combustion. In addition

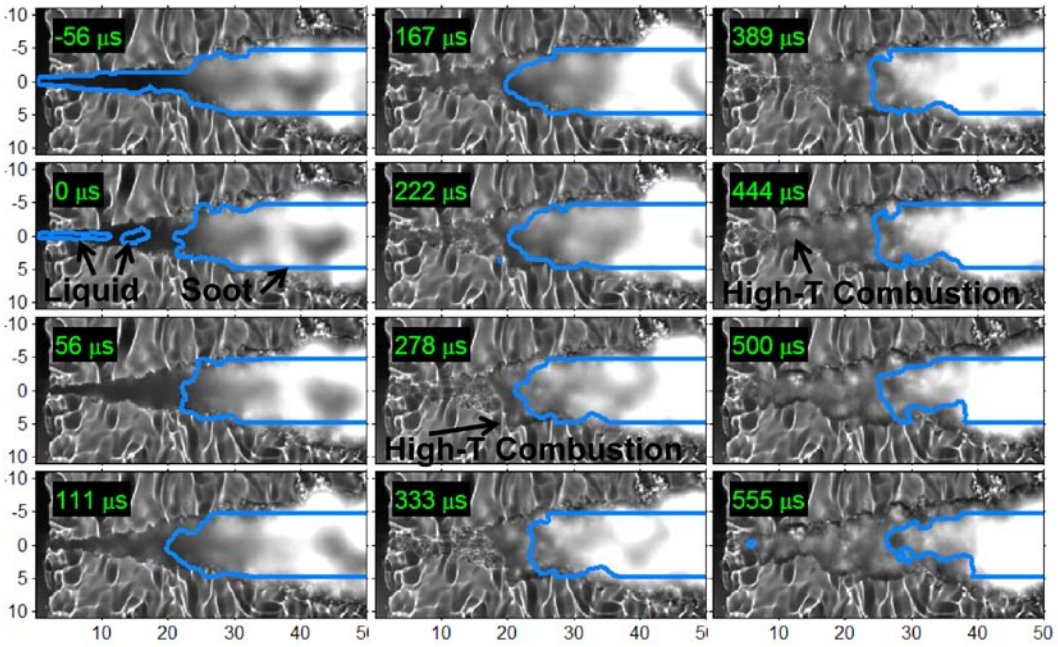

FIGURE 5. Reacting shadowgraph imaging (original) for the near injector region at time relative to the EOI. Ambient conditions: 1,000 K, 14.8 kg/m^3, 21% O_2. Injector conditions: 0.181 mm orifice, 76 MPa pressure, diesel fuel at 373 K, negative dwell conditions.

to liquid and vapor penetration, the technique detects cool-flame progression by a "disappearance" of the shadowgraph effect and high-temperature combustion by strong radial expansion and a smooth texture in the shadowgraph image. The contrast between high-temperature combustion regions, visible in the shadowgraph images downstream of the injector, and fuel vapor regions near the injector, allows identification of sources of UHC in a diesel spray. Results show that LTC conditions tend to leave significant regions of UHC near the injector, while high-temperature combustion propagates back to the injector for conventional diesel combustion.

References

1. Engine Combustion Network, http://www.ca.sandia.gov/ECN.

2. Pickett, L.M., Kook, S., and Williams, T.C., "Visualization of Diesel Spray Penetration, Cool-Flame, Ignition, High-Temperature Combustion, and Soot Formation Using High-Speed Imaging," SAE World Congress Paper 2009-01-0658, 2009.

3. Pickett, L.M., Kook, S., and Williams, T.C., "Transient Liquid Penetration of Early-Injection Diesel Sprays," SAE World Congress Paper 2009-01-0839, 2009.

4. Musculus, M.P.B, Lachaux, T., Pickett, L.M., and Idicheria, C.A. "End-of-Injection Over-Mixing and Unburned Hydrocarbon Emissions in Low-Temperature-Combustion Diesel Engines," SAE paper 2007-01-0907, 2007.

FY 2009 Publications/Presentations

1. Pickett, L.M., "Progress of the Engine Combustion Network," Directions in Engine Efficiency and Emissions Reduction Research Conference (DEER), Dearborn MI, Aug. 2009.

2. Kook., S., and Pickett, L.M., "Effect of Fuel Volatility and Ignition Quality on Combustion and Soot Formation at Fixed Premixing Conditions," SAE Powertrain, Fluids, and Lubricants Conference, SAE Paper 2009-01-2643, 2009.

3. Pickett, L.M., Kook, S., and Williams, T.C., "Visualization of Diesel Spray Penetration, Cool-Flame, Ignition, High-Temperature Combustion, and Soot Formation Using High-Speed Imaging," SAE World Congress Paper 2009-01-0658, 2009.

4. Kook, S., Pickett, L.M., Musculus, M.P.B., and Gehmlich, R. K., "Influence of Diesel Injection Parameters on End-of-Injection Liquid Length Recession," SAE World Congress Paper 2009-01-1356, 2009.

5. Pickett, L.M., Kook, S., and Williams, T.C., "Transient Liquid Penetration of Early-Injection Diesel Sprays," SAE World Congress Paper 2009-01-0839, 2009.

6. Abraham, J., Pickett, L.M., "Computed and Measured Fuel Vapor Distribution in a Full-Cone Spray at High Chamber Pressure and Temperature," 11th International Annual Conference on Liquid Atomization and Spray Systems, ICLASS 2009.

Special Recognitions & Awards/Patents Issued

1. SAE Excellence in Oral Presentation Award (2009 World Congress, Paper 2009-01-0658).

II.A.6 Large Eddy Simulation (LES) Applied to LTC/Diesel/Hydrogen Engine Combustion Research

Joseph C. Oefelein
Sandia National Laboratories
7011 East Avenue, Mail Stop 9051
Livermore, CA 94550

DOE Technology Development Manager:
Gurpreet Singh

Objectives

- Combine unique state-of-the-art simulation capability based on the LES technique with Advanced Engine Combustion research and development (R&D) activities.
- Perform companion simulations that directly complement optical engine (and supporting) experiments being conducted at the Combustion Research Facility (CRF).
- Focus initially on the optical hydrogen-fueled internal combustion (IC) engine experiment and systematically extend to low-temperature combustion (LTC) applications.

Accomplishments

- Completed development of improved high-pressure multiphase models for time-accurate treatment of direct-injection processes in diesel and LTC engines.
  - Initial emphasis on high-pressure hydrogen injectors, model validation using data from Petersen and Ghandhi (University of Wisconsin).
  - Direct applicability to liquid hydrocarbon injectors (collaboration with Musculus and Pickett, see www.ca.sandia.gov/ECN).
  - Performed detailed calculations of multi-orifice injectors using actual original equipment manufacturer (OEM) geometries and operating conditions.
- Continued to performed high-fidelity simulations of the optical hydrogen-fueled IC engine (H2ICE) in collaboration with Kaiser et al., systematically worked toward homogeneous charge compression ignition (HCCI) combustion in collaboration with Dec et al.
  - Validation through comparison of measured and modeled results.
  - Chemiluminescence imaging and particle image velocimetry (PIV).
  - Planar laser induced fluorescence (PLIF).
- Continued to improve performance and usability of Oefelein's massively-parallel LES solver ("RAPTOR") for IC engine related calculations as part of the DOE Office of Science innovative and novel computational impact on theory and experiment (INCITE) program.
  - Grand-challenge grant for central processing unit (CPU) time on DOE "capability-class" computers based on this projects objectives.
  - Multiyear award at National Center for Computational Sciences, Oak Ridge National Laboratory (ORNL, see www.nccs.gov). Thirty-million CPU hours in 2009 on the CRAY XT5 (i.e., 1.64-peta-flop system called Jaguar).

Future Directions

- Continue high-fidelity simulations of optical H2ICE.
  - Direct-injection with multi-orifice injectors shown here.
  - Validation through comparison of measured and modeled results.
    - Chemiluminescence imaging and PIV
    - PLIF
  - Joint analysis of data extracted from validated simulations.
    - Enhance basic understanding.
    - Improve engineering models.
- Systematically extend to HCCI engine experiments.
  - Perform detailed studies of low-temperature combustion processes.
  - Work toward treatment of complex hydrocarbon processes.
- Continue leveraging between DOE Office of Science and Energy Efficiency and Renewable Energy (i.e., bridge gap between basic and applied research).
  - Detailed validation and analysis of critical flow phenomena.
  - Access to high-performance leadership-class computers.

✧ ✧ ✧ ✧ ✧

Introduction

The objective of this research is to combine a unique high-fidelity simulation capability based on the LES

II.A.7 Computationally Efficient Modeling of High Efficiency Clean Combustion Engines

Daniel Flowers (Primary Contact), Salvador Aceves, Mark Havstad, Nick Killingsworth, Matt McNenly, Tom Piggott, Randy Hessel (University of Wisconsin-Madison)
Lawrence Livermore National Laboratory (LLNL)
7000 East Ave. L-792
Livermore, CA 94550

DOE Technology Development Manager: Gurpreet Singh

Subcontractor:
University of Wisconsin, Madison, WI

Objectives

- Obtain low-emissions, high-efficiency, high-load operation with homogeneous charge compression ignition (HCCI), premixed charge compression ignition (PCCI), and other low-temperature clean combustion regimes.
- Improve the numerics of chemical kinetics and fluid mechanics codes for faster execution on today's desktop or laptop computers.
- Provide analytical support for experimental projects within the Advanced Combustion in Engines program.

Accomplishments

- Demonstrated considerable (>200X) speedup in the execution of CHEMKIN multizone by replacing the default Gaussian elimination solver (DVODE) by an iterative solver developed at LLNL (DLSODPK) and an appropriate preconditioner.
- Demonstrated a new analysis tool for modeling of spark ignition (SI)-HCCI transition experiments conducted at Oak Ridge National Laboratory (ORNL).
- Accurately modeled partially premixed combustion in an optical engine (Steeper) with KIVA-multizone.

Future Directions

- Further accelerate CHEMKIN multizone execution: we are studying software and hardware implementations that will further reduce fluid mechanics and chemical kinetics calculations.
- Validate analysis tools under partially stratified conditions: we are working with engine researchers at Sandia Livermore (John Dec and Dick Steeper) to validate KIVA multi-zone code at partially stratified conditions.
- Demonstrate fast modeling of partially stratified combustion with an artificial neural network-based chemical kinetics model: we have previously demonstrated applicability of artificial neural networks for fast and accurate HCCI modeling. We see no limitations in using the same approach to model the more challenging problem of partially stratified combustion.

Introduction

Over the years, LLNL research has focused on the development of computational tools for engine analysis. LLNL's multizone model is the standard for HCCI and PCCI combustion, providing computational efficiency as well as high accuracy. However, as good as the multizone model is, it still requires months of running time on single processor computers when solving for PCCI problems in well resolved meshes (~100,000 elements) and detailed chemical kinetic mechanisms (hundreds of species). We are trying two approaches to reduce computational time: (1) improving the numerics of solving the rather large system of differential equations that results from multizone kinetics problems, and (2) testing new methodologies for fast HCCI/PCCI modeling such as artificial neural network-based chemical kinetic models and multiple reactor models for analysis of SI-HCCI transition experiments.

Approach

LLNL collaborates with other national laboratories, universities, and private industry by providing analytical support that complements the very high quality experimental work being conducted at institutions that participate in the DOE's Advanced Combustion in Engines program. Our research topics to date include homogeneous and partially stratified combustion, low-temperature direct-injected combustion, hydrogen engines, and SI-HCCI transition.

Results

Multizone chemical kinetics have demonstrated accuracy and computational efficiency in solving for homogeneous and partially stratified combustion. However, computational requirements still limit its applicability to large research institutions with access to massively parallel computers. We are developing fast solution algorithms that will democratize detailed engine computations enabling accurate HCCI/PCCI modeling on today's desktops and laptops.

The first step toward speeding up computations consists of a careful analysis of the computational effort required for solving a kinetic multizone problem. In this analysis we discovered that Jacobian generation and inversion takes 94% of the time (Figure 1) in a typical 20-zone run with 63 active chemical species and 152 quasi steady-state species [1]. The Jacobian matrix (Equation 1) takes the role of a multi-dimensional derivative guiding the iterations of the standard Newton-Raphson method toward a solution of a non-linear system, and its evaluation demands multiple expensive computations of chemical production rates for the different species.

$$\frac{\partial f_i}{\partial y_j} = \begin{pmatrix} \frac{\partial f_1}{\partial y_1} & \cdots & \frac{\partial f_1}{\partial y_N} \\ \vdots & \ddots & \vdots \\ \frac{\partial f_N}{\partial y_1} & \cdots & \frac{\partial f_N}{\partial y_N} \end{pmatrix} \quad \text{Equation 1}$$

Much progress toward reduced computational effort can be made by studying the structure of the Jacobian. Interactions between zones are typically small in CHEMKIN multizone problems, leading to block diagonal Jacobians (Figure 2), where blue represents regions of the Jacobian that contain high density of zeros. From Figure 2 it is apparent that the Gaussian elimination process used in the default CHEMKIN multizone solver (DVODE) is relatively inefficient because it spends much of its time operating in regions of the Jacobian where many terms are zero. Faster solutions can be achieved with an iterative solver that exploits the high density of zeros outside the main block diagonal.

We have demonstrated much improved numerical performance by replacing the standard integrator (DVODE) by an iterative solver developed at LLNL (DLSODPK) [2]. DLSODPK relies on an appropriate user-supplied preconditioner for fast solution of the system of nonlinear equations. Our research indicates that a reduced Jacobian that neglects all the terms that fall off the block diagonal (i.e., neglects all interactions between zones) is an appropriate preconditioner that substantially improves computational efficiency, speeding up calculations by a factor of 60 for a 20-zone problem and by a factor of 250 in a 40-zone problem. Larger improvements are expected as the number of zones grows. The new methodology solves large problems (40 zones and 63 active chemical species) within minutes (~10) on today's desktop or laptop computers.

It is important to note that use of DLSODPK does not neglect any terms in the equations or modify the physics of the problem. The preconditioner is a reduced Jacobian, but the full original system of equations is solved. Therefore, speedup is not obtained at the expense of accuracy. The two solvers (DVODE and DLSODPK) yield the same results for major species

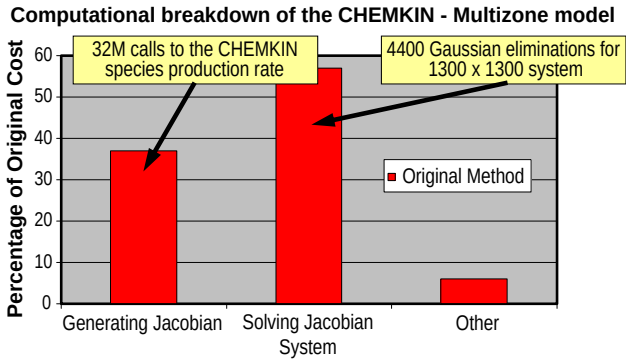

FIGURE 1. Computational cost breakdown of the CHEMKIN multizone model by function on a single processor and 20 zones. Generating and solving the Jacobian consumes 94% of the total computational time.

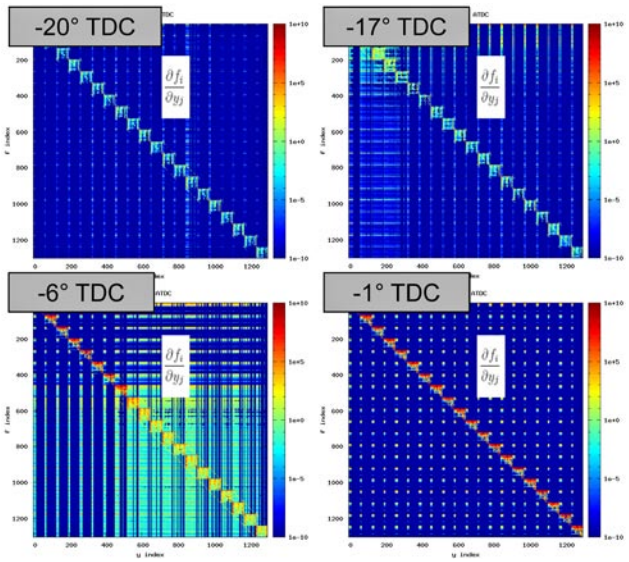

FIGURE 2. Jacobian matrix structure of the multizone model using 20 zones with a 63-species, reduced iso-octane mechanism at four crank angle positions: (a) -20° after top dead center (ATDC); (b) -17° ATDC; (c) -6° ATDC; and (d) -1° ATDC, for the SI-HCCI transition case described later in this report. The color scale indicates the magnitude of the Jacobian elements from 10^{10} to 10^{-10}.

concentrations to within six significant figures and radical species to within four significant figures.

Once we demonstrated the speed and accuracy of the new solver, we had an immediate application for it: SI-HCCI transition. This application demands analysis of ~100 consecutive engine cycles to study transient and chaotic behavior. A fast solver is therefore critical to enable comprehensive modeling within a reasonable time.

HCCI engines may not be able to deliver the full range of speed and load conditions. Thus, an important technical development needed to achieve widespread HCCI utilization is the ability to switch between HCCI and traditional propagating flame (e.g., SI) combustion as power and speed change. The development of combustion-mode switching requires that the fundamental nature of the transition be well understood, especially in the context of realistic engine conditions.

The goal of this task is developing a pragmatically detailed model capable of simulating the complex dynamic behavior observed during SI-HCCI transitions. Insight gained from this model into the mechanisms driving the inherent combustion instabilities can then be used to direct efforts to develop real-time diagnostics and controls for smoothing the SI-HCCI transition and stabilizing spark-assisted HCCI.

We have developed a CHEMKIN-based multizone model that simulates the expected combustion variations in a single-cylinder engine fueled with iso-octane as the engine transitions from SI combustion to HCCI combustion. The model includes a 63-species reaction mechanism [1] and mass and energy balances for the cylinder and the exhaust flow. We find that the model captures many of the important experimental trends (Figure 3) previously measured at ORNL [3], including stable SI combustion at low exhaust gas recirculation (EGR) (~0.10), transition to highly unstable combustion at intermediate EGR, and finally stable HCCI combustion at very high EGR (~0.75). Remaining differences between the predicted and experimental instability patterns indicate that there is further room for model improvement.

Finally, we have analyzed iso-octane PCCI combustion in an optical engine at Sandia Livermore (Steeper). We built a detailed 3-dimensional mesh (150,000 computational cells) that includes intake and exhaust ports and valves as well as the combustion chamber [4]. We model three consecutive cycles to make sure that gas exchange parameters converge from the initial estimates to steady-state values. The engine was run with considerable (150°) negative valve overlap (NVO), and 20% of the fuel is injected during NVO to enhance reactivity. The remaining fuel is injected during the intake event (270° before compression top dead center). The tool of analysis is LLNL's KIVA multizone.

Figure 4 shows that the numerical model is successful at capturing engine processes during NVO (compression, fuel injection and partial ignition), during the main cycle (main injection, compression and ignition), and during the exhaust process interrupted by valve closure. Small differences in peak cylinder pressure were attributed to exhaust port boundary conditions, and further improvements are expected as these are improved to better reflect real engine conditions.

In summary, KIVA multizone shows promise to deliver accurate predictions of partially stratified engine operation. Further validation and testing should improve the results and lead to a predictive modeling capability.

Conclusions

- We have greatly improved execution speed for CHEMKIN multizone by using an iterative solver with an appropriate preconditioner.
- Modeling of ORNL experiments demonstrates transition between stable SI operation at low EGR, chaotic SI-HCCI transition at intermediate EGR, and stable HCCI conditions at high EGR.
- KIVA multizone accurately predicts PCCI combustion in a glass engine running with considerable NVO and partial fuel injection during NVO.

References

1. Chen, J.-Y. and Tham, Y.F., "Speedy solution of quasi-steady-state species by combination of fixed-point iteration and matrix inversion," Combustion and Flame, Vol. **153**, pp. 634-646, 2008.

2. Brown, P.N. and Hindmarsh, A.C., "Reduced storage matrix methods in stiff ODE systems," Journal of Applied Mathematics and Computing, Vol. **31**, pp. 40-91, 1989.

3. Daw, C.S., Wagner, R.M., Edwards, K.D., Green, J.B. Jr., "Understanding the transition between conventional spark-ignited combustion and HCCI in a gasoline engine", Proceedings of the Combustion Institute, Vol. 31, pp. 2887-2894, 2007.

4. Hessel, R.P., Foster, D.E., Steeper, R.R., Aceves, S.M., Flowers, D.L., "Pathline Analysis of Full-cycle Four-stroke HCCI Engine Combustion Using CFD and Multi-Zone Modeling," SAE Paper 2008-01-0048, SAE Transactions, 2008.

FY 2009 Publications/Presentations

1. HCCI Engine Combustion Timing Control: Optimizing Gains and Fuel Consumption Via Extremum Seeking, N.J. Killingsworth, S.M. Aceves, D.L. Flowers,

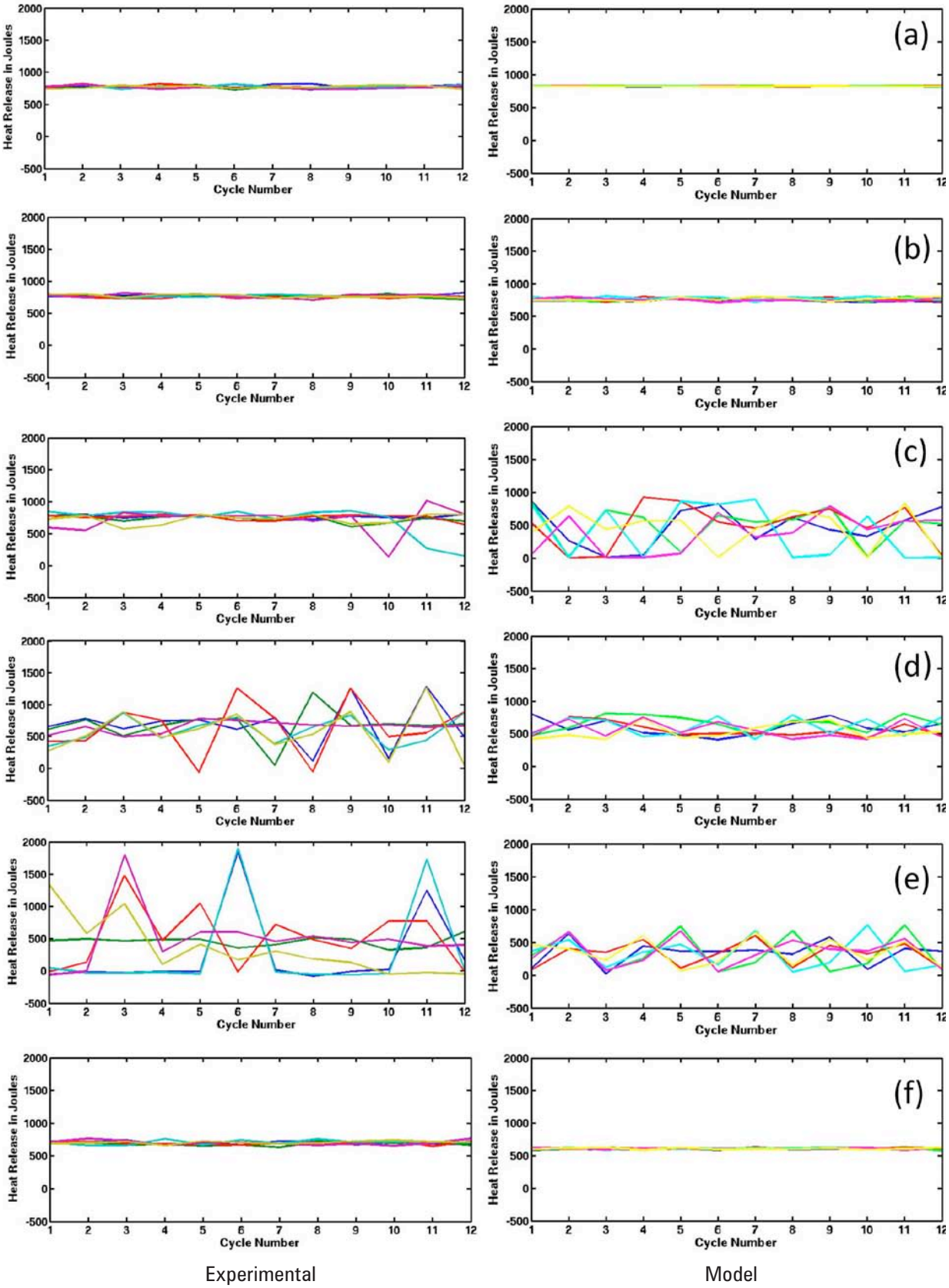

FIGURE 3. Selected time-series segments demonstrating typical combustion behavior during steady-state operation along the SI-HCCI transition pathway. Left column: experiments; right column: model. The different plots are for increasing levels of EGR: (a) 25%, (b) 37%, (c) 41%, (d) 45%, (e) 55%, (f) 75%.

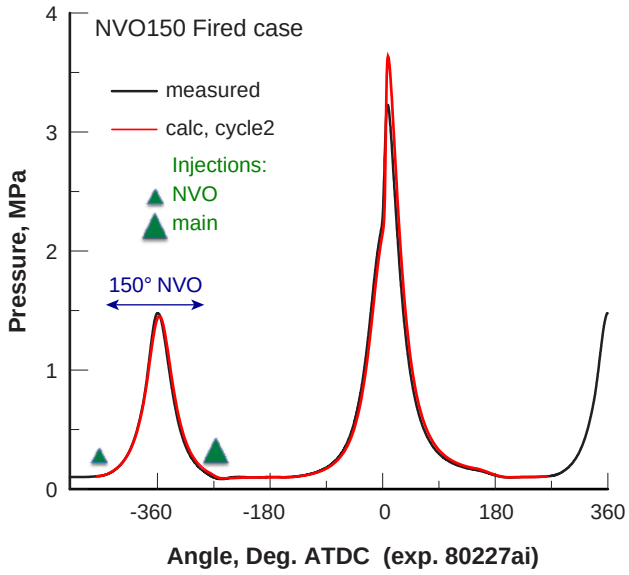

FIGURE 4. Comparison between experimental results (black) and numerical results (red) for the Sandia Livermore optimized engine operating with dual injection (NVO and main).

F. Espinosa-Loza, and M. Krstic, Accepted for publication, IEEE Transactions On Control Systems Technology, 2009.

2. Liquid penetration Length in Direct Diesel Fuel Injection, S. Martínez-Martínez, F.A. Sánchez-Cruz, J.M. Riesco-Ávila, A. Gallegos-Muñoz and S.M. Aceves, Applied Thermal Engineering, Vol. 28, pp. 1756-1762, 2008.

3. Pathline Analysis of Full-cycle Four-stroke HCCI Engine Combustion Using CFD and Multi-Zone Modeling, Randy P. Hessel, David E. Foster, Richard R. Steeper, Salvador M. Aceves, Daniel L. Flowers, SAE Paper 2008-01-0048, SAE Transactions, 2008.

4. Modeling Iso-octane HCCI using CFD with Multi-Zone Detailed Chemistry; Comparison to Detailed Speciation Data over a Range of Lean Equivalence Ratios, Randy P. Hessel, David E. Foster, Salvador M. Aceves, M. Lee Davisson, Francisco Espinosa-Loza, Daniel L. Flowers, William J. Pitz, John E. Dec, Magnus Sjöberg, Aristotelis Babajimopoulos, SAE Paper 2008-01-0047.

5. Demonstrating Optimum HCCI Combustion with Advanced Control Technology, Daniel Flowers, Nick Killingsworth, Francisco Espinoza-Loza, Joel Martinez-Frias, Salvador Aceves, Miroslav Krstic, Robert Dibble, SAE Paper 2009-01-1885, 2009.

6. Demonstrating direct use of wet ethanol in a homogeneous charge compression ignition (HCCI) engine, J. Hunter Mack, Salvador M. Aceves, Robert W. Dibble, Energy, Vol. 34, pp. 782-787, 2009.

7. Investigation of High Efficiency, Zero Emissions H2-O2-Ar Internal Combustion Engine, V. H. Rapp, Nick Killingsworth, Salvador Aceves, J.Y. Chen and Robert Dibble, Proceedings of the Australian Combustion Symposium, December 2–4, 2009, The University of Queensland, Australia.

Special Recognitions & Awards/Patents Issued

1. Salvador Aceves invited to serve as an opponent in Ph.D. exam, Chalmers University, Gothenburg, Sweden, September 2008.

2. Nick Killingsworth invited to deliver a seminar at the "Advanced Engine Control Symposium," Tianjin, China, November 2008.

technique with the Advanced Engine Combustion R&D activities at Sandia National Laboratories, CRF. The goal is to perform a series of benchmark simulations that identically match the geometry and operating conditions of select optical engine experiments. The investment in time and resources provides two significant benefits. After systematic validation of key processes using available experimental data, quantitative information can be extracted from the simulations that are not otherwise available. This information will provide 1) a detailed and complementary description of intricately coupled processes not measurable by experimental diagnostics, and 2) the information required for understanding and developing improved predictive models. The combination of detailed experiments, complementary simulations, and joint analysis of data will provide the basic science foundation required to systematically address the targeted research areas identified for clean and efficient combustion of 21st century transportation fuels and the development of new state-of-the-art IC engines.

Approach

In addition to providing a comprehensive multiscale modeling framework based on LES, we have established direct collaborations with two of the "flagship" experimental efforts at the CRF. A scientific foundation for advanced development of subgrid-scale (SGS) models for LES has been established in collaboration with Barlow et al. as a direct extension of the International Workshop on Measurement and Computation of Turbulent Nonpremixed Flames (i.e., the "TNF Workshop," www.ca.sandia.gov/TNF). Similarly, we have established collaborative research activities that focus on key optical engine experiments and the Engine Combustion Network (i.e., the ECN, as established by Pickett, www.ca.sandia.gov/ECN). The ECN has analogous objectives to those of the TNF workshop. The novelty of our approach is that it provides direct one-to-one correspondence between measured and modeled results at conditions unattainable using direct numerical simulation by providing detailed simulations that incorporate the fully coupled dynamic behavior of a given configuration in the full experimental or device-scale geometry without canonical approximations. Needs and milestones in three critical areas have been established as part of our long-term operating plan: 1) to continue a progression of LES studies focused on the CRF optically accessible H2ICE, 2) to establish a parallel task focused on HCCI engines, and 3) to perform a series of supporting studies focused on the development and validation of multiphase combustion models with emphasis placed on direct-injection processes.

Results

Direct injection (DI) has proven to be a promising option in diesel and LTC engines. In conventional diesel and HCCI applications, DI lowers soot and NO_x production and improves fuel economy. In H2ICEs, which are an alternative to fuel cells, DI provides the appropriate energy density required for high efficiency and low NO_x emissions. To realize the full benefit of DI, however, the effect of various injection parameters such as timing, duration, pressure, and dilution, must be investigated and optimized under a wide range of engine operating conditions. This year we completed development of a model framework for high-fidelity calculations of DI processes using the LES technique and an advanced property evaluation scheme.

Fundamental high-fidelity representations of DI processes in IC engines are an essential component toward the development a validated predictive modeling capability. However, detailed models are still lacking and few provide a rigorous description of transient processes that occur between the jets and the in-cylinder reacting flow environment as fuel is injected into an engine. As part of our research activities in 2009, we have performed one of the highest fidelity simulations of DI processes ever as a precursor to a full engine simulation (which is currently in progress as part of our 2009 INCITE grant). Figure 1 shows a representative result, which has been validated using experimental data from the University of Wisconsin. To the left are penetration measurements made experimentally compared to predicted results from LES. In the lower left is a corresponding shadowgraph image showing the transient structure of the turbulent jets. In the center is the corresponding LES calculation showing the complete computational domain (i.e., an actual OEM 3-orifice injector similar to that used in the optical engines at the CRF). To the right is an enlargement of one of the jets showing the turbulent structure in both the injector orifice and the ambient environment at an instant in time. The calculation was performed by gridding the entire injector, including the internal flow passages, sac, and needle valve actuator that controls the flow of fuel. A key issue in modeling flows at actual conditions is the fact that they produce extremely high Reynolds numbers. For the calculations performed here (as shown in Figure 1), the jet Reynolds number associated with each orifice of the 3-orifice injector is 720,000. The major objective of these calculations was to investigate issues related to transient combustion processes and to establish the appropriate resolution criteria and time-dependent boundary conditions. The coupled model is predictive in that the only adjustable parameters are the grid resolution (which we have now quantified) and boundary conditions (i.e., there are no tuned constants employed at any point in the calculation or SGS models).

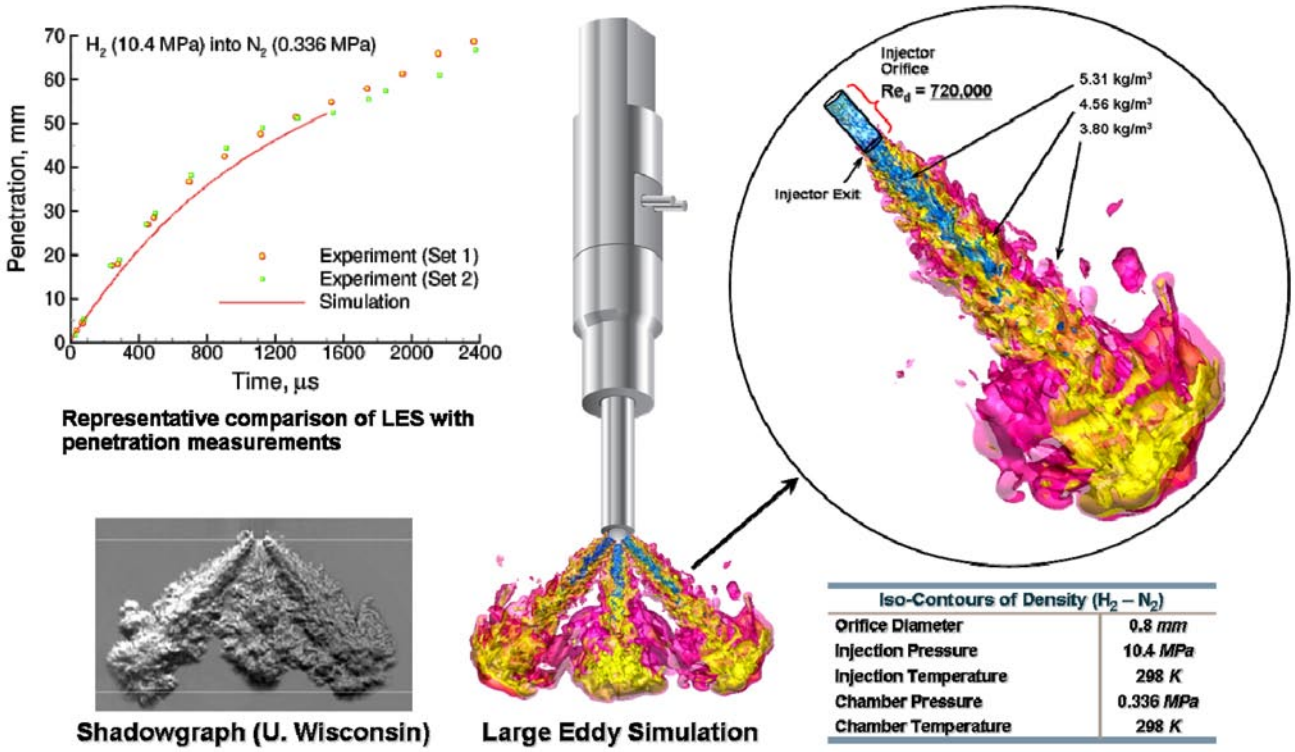

FIGURE 1. Representative result validated using experimental data from the University of Wisconsin. To the left are penetration measurements made experimentally compared to predicted results from LES. In the lower left is a corresponding shadowgraph image showing the transient structure of the turbulent jets that emanate from the injector. In the center is an instantaneous snapshot of the corresponding LES solution showing the complete computational domain (i.e., an actual OEM 3-orifice injector similar to that used in the optical engines at the CRF). To the right is an enlargement of one of the jets showing the turbulent structure in both the injector orifice and ambient environment at an instant in time.

To date there have been no calculations that represent the transient mixing dynamics behind the wake of actual injectors, at actual engine operating conditions, with this level of fidelity. The current calculations provide one of the first pictures of transient mixing and the effects of entrainment. Increased entrainment is induced by regions of low pressure behind the jet at the end of injection. It also propagates back during injection and dramatically affects the initial quasi-steady structure of the fuel jet. These effects are compounded by interactions between respective jet streams produced by the injector. The three jets associated with the injector in Figure 1, for example, interact with one another both during and after the injection pulse. In contrast to past work, results from the current calculations show precisely how the entrainment process evolves in time and how this affects the mixture state just prior to combustion. Events prior to combustion at this stage can be considered quantitative; once combustion is initiated the results are considered qualitative. From the quantitative perspective, results show at what point in the transient process the instantaneous field is near optimal for combustion. Such information is extremely relevant in the design of engines (both compression ignition and spark ignition). If mixing is to be optimized for various applications, understanding of the spatial and temporal evolution of the increased entrainment region after the deceleration phase at the end of injection is important. These results provide one of the first pictures of these processes. From the qualitative perspective, comparison of mixing rates shows that flames initially propagate at a much faster rate in certain regions of the flow, where mixing rates are slow, then become more diffuse in other regions of the flow, where mixing rates are high. The distribution of the turbulent mixing field changes rapidly over the duration of combustion, which has a profound effect on the flame dynamics and related emissions. The nature of these phenomena can be controlled by the way the injector is pulsed. The combination of LES calculations such as these and tight coupling with the companion experiments offers a new way to optimize advanced systems.

The calculations described above are a representative sample of a series being performed using Oefelein's RAPTOR code. RAPTOR is a massively parallel flow solver designed specifically for application of LES to turbulent, chemically reacting, multiphase flows. It solves the fully coupled conservation equations of mass, momentum, total-energy, and species for

a chemically reacting flow system (gas or liquid) in complex geometries. It also accounts for detailed chemistry, thermodynamics, and transport processes at the molecular level and uses detailed chemical mechanisms. The code is sophisticated in its ability to handle complex geometries and a generalized SGS model framework. It is capable of treating spray combustion processes and multiphase flows using a Lagrangian-Eulerian formulation. The numerical formulation treats the compressible form of the conservation equations, but can be evaluated in the incompressible limit. The theoretical framework handles both multi-component and mixture-averaged systems. The baseline formulation also employs a general treatment of the equation of state, thermodynamics, and transport properties that accommodates real gas or liquids with detailed chemistry and is not constrained to ideal gas applications. A key aspect of our research is to continue to apply RAPTOR in a way that makes these types of calculations more routine. As part of the DOE Advanced Scientific Computing Research Program Joule goal metric, we have recently demonstrated weak scaling with 100-percent efficiency on over 110,000 cores on the ORNL Cray XT5 system (Jaguar). This type of CPU power will in time provide a significantly new level of detail in the level of information available for the design and optimization of new engine concepts.

Conclusions

Calculations performed to date have provided a systematic path toward detailed simulations of in-cylinder processes. Future analysis will focus on multidimensional turbulence-chemistry interactions and related cycle-to-cycle variations in the actual engine geometry. The simulations will be coordinated with the experimental campaign at the CRF. In addition, we will begin to focus on high-pressure injection of liquid hydrocarbon fuels at thermodynamically near-critical and supercritical conditions. The multiphase injection dynamics associated with these conditions are common to state-of-the-art engines and dominate all subsequent modes of combustion. We will focus on the transient evolution of the injection process with different fuels to determine the mixture state and flow topology just prior to, and during, combustion. In addition, we will perform a series of simulations that identically match the hierarchy of direct injection experiments of Pickett (see www.ca.sandia.gov/ECN) using n-heptane as our initial fuel. This work will be complemented by extending our SGS model development efforts in combustion to high-pressure regimes in collaboration with Barlow et al. as an extension of the flames studies as part of the TNF workshop (www.ca.sandia.gov/TNF).

FY 2009 Publications/Presentations

1. B. Hu, M.P. Musculus, and J.C. Oefelein. Large eddy simulation of a transient gas jet with emphasis on entrainment. *SAE World Congress*, April 13–15 2010. Detroit, Michigan.

2. J.C. Oefelein and R. Sankaran. Large eddy simulation of turbulence-chemistry interactions in reacting flows: Experiences on the ORNL NCCS Cray-XT platforms (Jaguar). *Proceedings of the 21st International Conference on Parallel Computational Fluid Dynamics*, May 18–22 2009. Moffett Field, California.

3. J.C. Oefelein, J.H. Chen, and R. Sankaran. High-fidelity simulations for clean and efficient combustion of alternative fuels. *Journal of Physics*, **180**:1–5, 2009. DOI 10.1088/1742-6596/180/1/012033.

4. L. Lu, P.M. Najt, T.-W. Kuo, V. Sankaran, and J.C. Oefelein. A fully integrated linear eddy model and chemistry agglomeration model with detailed chemical kinetics for studying the effect of stratification on HCCI combustion. *Proceedings of the 6th Joint Meeting of the US Sections of the Combustion Institute*, Paper 13C2, May 17–20 2009. Ann Arbor, Michigan.

5. J.H. Frank, S.A. Kaiser, and J.C. Oefelein. Coupling imaging measurements and LES of dissipation structures in turbulent nonreacting jets and nonpremixed jet flames. *Proceedings of the 6th Joint Meeting of the US Sections of the Combustion Institute*, Paper 32D1, May 17–20 2009. Ann Arbor, Michigan.

6. J.H. Frank, S.A. Kaiser, and J.C. Oefelein. Coupling imaging diagnostics and large eddy simulation in turbulent nonreacting jets and nonpremixed jet flames. *Proceedings of the 4th European Combustion Meeting*, April 14-17 2009. Vienna, Austria.

7. V. Sankaran, T.G. Drozda, and J.C. Oefelein. A tabulated closure for turbulent nonpremixed combustion based on the linear eddy model. *Proceedings of the Combustion Institute*, **32**:1571–1578, 2009.

8. J.C. Oefelein. Toward high-fidelity simulations for clean and efficient combustion of alternative fuels. IFP *Workshop on Large Eddy Simulation for Internal Combustion Flows*, December 1–2 2008. Ruell-Malmaison, France.

9. T.G. Drozda, G.-H. Wang, V. Sankaran, J.R. Mayo, J.C. Oefelein, and R.S. Barlow. Scalar filtered mass density functions in non-premixed turbulent jet flames. *Combustion and Flame*, **155**:54–69, 2008.

10. P.K. Tucker, S. Menon, C.L. Merkle, J.C. Oefelein, and V. Yang. Validation of high-fidelity CFD simulations for rocket injector design. *44th AIAA/ASME/SAE/ASEE Joint Propulsion Conference and Exhibit*, Paper 2008-5526, July 21-23 2008. Hartford, Connecticut.

II.A.8 HCCI and Stratified-Charge CI Engine Combustion Research

John E. Dec
Sandia National Laboratories
MS 9053, P.O. Box 969
Livermore, CA 94551-0969

DOE Technology Development Manager:
Gurpreet Singh

Objectives

Project Objective:

- Provide the fundamental understanding (science-base) required to overcome the technical barriers to development of practical homogeneous charge compression ignition (HCCI) and HCCI-like engines by industry.

Fiscal Year 2009 Objectives:

- Determine the development of naturally occurring thermal stratification in an HCCI engine, using planar-imaging thermometry. Develop thermal-imaging diagnostic as part of this task.
- Evaluate the potential of intake boost for extending the high-load limit of HCCI by using exhaust gas recirculation (EGR) to control combustion-phasing advance – multi-year task.
  - FY 2009: Determine potential of boost with EGR for gasoline at a representative engine speed.
- Determine the performance of ethanol as a fuel for HCCI engines (cooperatively with M. Sjöberg of the Advanced SI-Engine Fuels Lab).
- Support chemical-kinetic and computational fluid dynamics (CFD) modeling work at Lawrence Livermore National Laboratory (LLNL) to help develop improved kinetic mechanisms for HCCI and to advance the understanding of in-cylinder processes through improved CFD capabilities.

Accomplishments

- Determined the evolution of naturally occurring thermal stratification in an HCCI engine, including the distribution of thermal inhomogeneities and their magnitude at a typical operating condition.
  - Developed a planar temperature-imaging diagnostic for HCCI engines.
- Showed that intake-pressure boosting has a strong potential for extending the high-load limit for gasoline-fueled HCCI, at a representative 1,200 rpm condition.
  - Achieved an indicated mean effective pressure, gross ($IMEP_g$) = 16.34 bar with no knocking and ultra-low oxides of nitrogen (NOx).
  - Demonstrated that EGR is effective for controlling boost-induced timing advance.
- Determined the behavior of ethanol as an HCCI fuel over a range of operating conditions. Work conducted cooperatively with M. Sjöberg of the Advanced SI-Engine Fuels Lab.
- Initiated a detailed exhaust-speciation analysis for the primary reference fuel blend (80% iso-octane and 20% n-heptane, PRF80) as a representative two-stage ignition fuel. Project conducted in cooperation with L. Davisson at LLNL.
- Supported chemical-kinetic and CFD modeling work at LLNL. Provided data and analysis for: 1) improving chemical-kinetic mechanisms, and 2) CFD modeling of fuel stratification to improve low-load combustion efficiency and emissions.

Future Directions

- Complete the investigation of intake boosting at a representative 1,200 rpm condition.
  - Conduct analysis to determine why highly retarded combustion timing could be achieved with very good stability when operating with intake boost.
- Expand the investigation of boosted HCCI to a wider range of operating conditions.
  - Determine the effects of engine speed on allowable boost-levels and fueling rate.
  - Investigate the effect of realistic turbocharger back pressures on boosted-HCCI performance.
- Investigate natural thermal stratification and its potential for extending the high-load limit of HCCI over a wider range of conditions.
  - Improve thermal-imaging diagnostic and optical setup for greater data throughput and improved accuracy.
  - Determine how thermal stratification is affected by various operating parameters.
  - Investigate methods of increasing the thermal stratification to allow higher loads.

- Collaborate with J. Oefelein *et al.* (Sandia) to apply large eddy simulation (LES) modeling to determine the main mechanisms producing thermal stratification, and how they might be enhanced.
- Conduct additional studies of the performance of ethanol over a wider range of operating parameters, including: EGR, load, and intake-boost (cooperatively with M. Sjöberg, Advanced SI-Fuels Lab).
- Continue to collaborate with LLNL on improving chemical-kinetic mechanisms and on combined CFD and kinetic modeling.

Introduction

HCCI engines have significant efficiency and emissions advantages over conventional spark-ignition and diesel engines, respectively. However, several technical barriers must be addressed before it is practical to implement HCCI combustion in production engines. One of the most important of these barriers is extending HCCI operation to higher loads, and two studies conducted during FY 2009 address this barrier. First, the development of naturally occurring thermal stratification of the charge in an HCCI engine has been mapped out using laser-sheet imaging. This understanding is important because the natural thermal stratification is critical for slowing HCCI combustion to allow high loads without knock. Second, the potential of intake-pressure boosting as a means of increasing the power output of HCCI engines has been investigated at a typical operating condition, and it was shown to allow loads close to those of turbocharged diesel engines, when applied with appropriate combustion-phasing control.

Two additional studies addressed the barriers of fuel effects and emissions of hydrocarbons (HC), Oxygenated hydrocarbons (OHC), and carbon monoxide (CO). Respectively, these studies included: 1) an investigation of ethanol as an HCCI fuel over a range of operating conditions, and 2) detailed exhaust speciation analysis of PRF80 as a representative two-stage ignition fuel over a range of fuel loads.

Approach

These studies were conducted in our dual-engine HCCI laboratory using a combination of experiments in both the all-metal and optically-accessible HCCI research engines. This facility allows operation over a wide range of conditions, and it can provide precise control of operating parameters such as combustion phasing, injection timing, intake temperature and pressure, and mass flow rates of supplied fuel and air. For the current studies, both engines were equipped with compression-ratio = 14 pistons. The facility is also setup to allow the use of cooled EGR. Additionally, the laboratory is equipped with a full emissions bench (HC, CO, CO_2, O_2, NO_X, and smoke), and a sample port on the exhaust runner of the metal engine allows collection of exhaust gases for detailed exhaust speciation.

The optically accessible engine was used for imaging the development of the thermal stratification, as shown schematically in Figure 1. This study first required the development of a planar temperature-imaging diagnostic. A tracer-based single-line planar laser induced fluorescence (PLIF) technique was selected for its good precision and simplicity. The principle of the technique relies on the temperature sensitivity of the PLIF signal of toluene, added as a 2% tracer in the fuel. Since thermal stratification develops prior to autoignition, all measurements were made for motored operation by replacing the intake air with nitrogen to prevent combustion which can lead to early tracer breakdown, adversely affecting the measurements. Operating with nitrogen also prevents oxygen quenching from substantially reducing the toluene fluorescence signal.

Intake-pressure boosting was investigated using the all-metal engine. The intake air was supplied by an air compressor and precisely metered by a sonic nozzle. For operation without EGR, air flow rates were adjusted to achieve the desired intake pressure. To compensate for the pressure-induced enhancement of autoignition and to provide the required combustion-phasing retard,

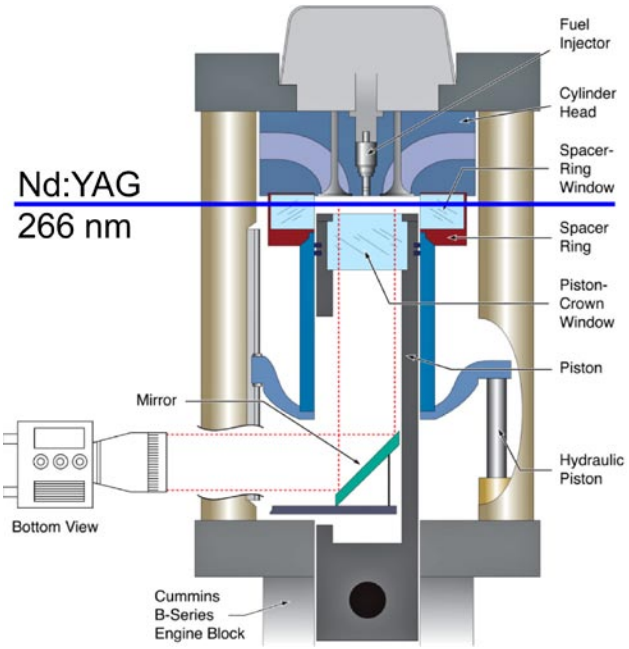

FIGURE 1. Schematic of the optically accessible HCCI engine showing the setup for planar temperature imaging. The line representing the laser corresponds to an edge-view of the horizontal laser sheet.

a combination of reduced intake temperature and cooled EGR was used. For operation with EGR, the intake-air flow was reduced, a valve on the EGR line was opened, and the exhaust back-pressure was adjusted by a throttle valve to produce enough EGR flow to reach the desired intake pressure with the reduced air flow. For this study, the intake charge was fully premixed using an electrically heated fuel vaporizer, and the engine was fueled with a research-grade 87-octane gasoline.

Studies of ethanol performance over a range of operating conditions were also conducted in the all-metal engine. In addition, the latest chemical-kinetic mechanism for ethanol was evaluated against the experimental data. For the detailed exhaust speciation analysis, samples were extracted from the exhaust-runner port of the metal engine and analyzed by two techniques in cooperation with an analytical-chemistry group at LLNL. Most species were measured with a gas chromatograph combined with a mass spectrometer, while light HC species were measured using a gas chromatograph combined with a flame ionization detector.

Results

Naturally occurring thermal stratification is critical for high-load HCCI operation because it causes the charge to autoignite sequentially, which decreases the heat release rate (HRR), reducing the propensity for engine knock. However, little is known about the development of this stratification or its distribution. Using the PLIF-based temperature diagnostic described above, the evolution of the thermal stratification of the bulk-gases was mapped from 305 to 390 degrees crank angle (°CA; 0°CA = top dead center [TDC]-intake and 360°CA = TDC-compression). As shown in Figure 1, a horizontal laser sheet entered the combustion chamber through one of the windows at the top of the cylinder wall, and images were acquired through the piston-crown window. The diagnostic was calibrated in situ by operating the engine over a range of intake temperatures [1]. This calibration and a series of other corrections allowed the raw PLIF images to be converted to quantitative temperature maps (T-maps), as shown in Figure 2. Since the objective is to determine the magnitude and distribution of the thermal inhomogeneities, all T-maps are presented as the temperature relative to the mean (ΔT).

Figure 3 shows a temporal sequence of T-maps from 305 to 380°CA. For these images, the laser-sheet elevation was adjusted with crank angle so that it remained at the mid-plane of the pancake combustion chamber to insure that the images are representative of the bulk-gases. Previous studies have shown that only thermal stratification of the bulk gases strongly affects the HRR, and therefore reduce the maximum pressure-rise rate (PRR) and engine knock [2]. As Figure 3

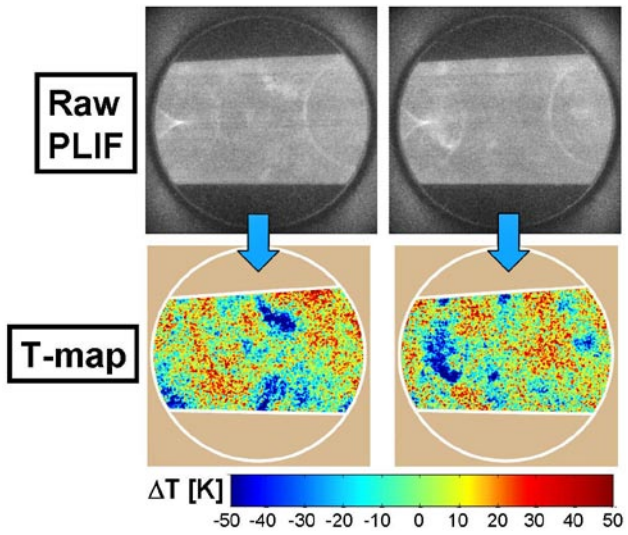

FIGURE 2. Conversion of raw toluene PLIF images to temperature maps.

shows, prior to about 330°CA, bulk-gas temperatures are nearly uniform. Thermal stratification then develops progressively in the latter part of the compressions stroke, reaching a maximum at TDC. Quantitative probability density function analysis of the images confirms that maximum thermal stratification occurs at TDC, and it shows that the magnitude of the measured stratification compares very well with the amount required to slow the HRR to the values measured for fired operation in the metal engine at a similar operating condition. In addition to these bulk-gas measurements, T-map images were acquired across the charge, from the mid-plane to the near-wall region, at two selected crank angles (330° and 360°CA). These images provide additional information on the temporal and spatial development of the thermal stratification. Also, temperature profiles derived from these images show that 95% of the temperature drop from the central bulk-gas to the wall occurs in the last 1–1.5 mm adjacent to the wall. A full presentation of these data and discussion of the results may be found in Ref. [1].

Intake-pressure boosting is widely used to increase the power output of internal combustion engines, and it the offers a means for increasing the power output of HCCI engines while still maintaining the dilute conditions required for low NOx. However, the application of boost to HCCI has been limited because it can be difficult to control knocking. In this work, the potential of intake boosting was investigated at a typical 1,200 rpm operating condition for intake pressures (P_{in}) from 100 kPa (naturally aspirated) up to P_{in} = 325 kPa absolute (highly boosted). For each P_{in}, the fueling was gradually increased from a moderately high-load up to the maximum load attainable at the knock/stability limit [3,4]. A combination of reduced intake temperature and

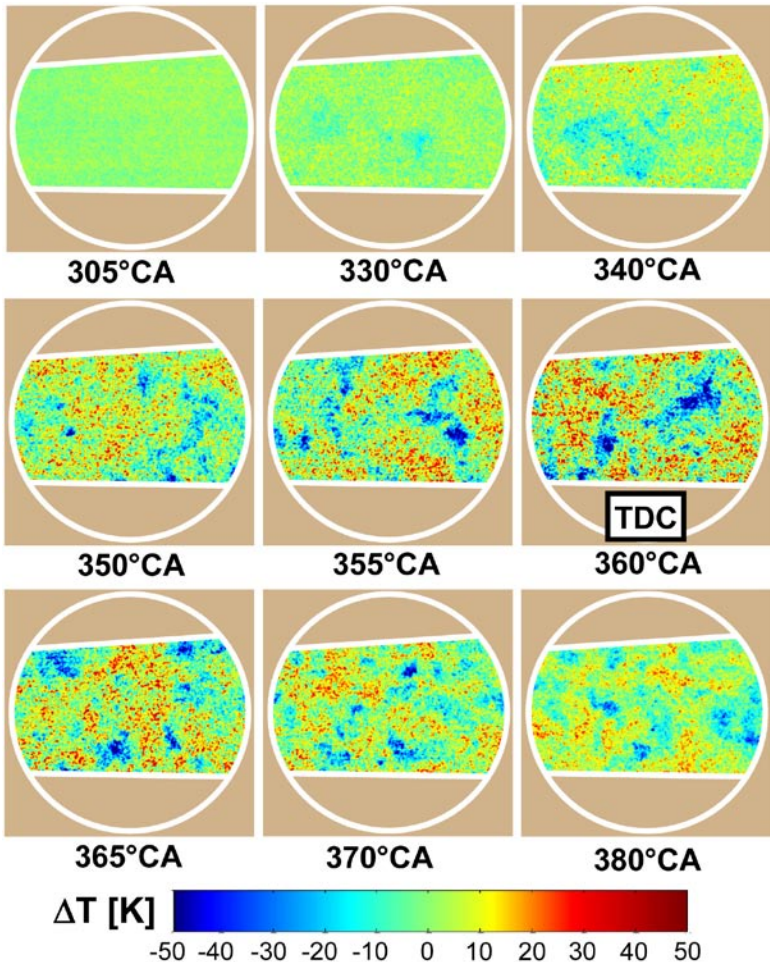

FIGURE 3. Temporal sequence of T-map images at the mid plane of the pancake combustion chamber. The white lines outline the limits of the laser sheet and the 70 mm diameter field of view through the piston-crown window.

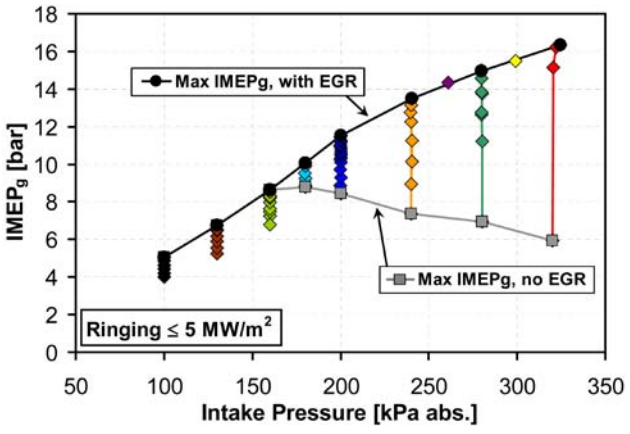

FIGURE 4. Maximum $IMEP_g$ at the knock/stability limit for various intake pressures, both with EGR and without.

cooled EGR was used to compensate for the pressure-induced enhancement of autoignition and to provide sufficient combustion-phasing retard to control knock [3]. In this work, knocking was quantified in terms of the ringing intensity [5], which was held ≤ 5 MW/m^2 so that there was no audible knocking or noticeable oscillations on the pressure trace.

As shown in Figure 4, the maximum attainable load increased progressively with boost from an $IMEP_g$ of about 5 bar for naturally aspirated conditions up to 16.34 bar for P_{in} = 325 kPa. For P_{in} = 100 kPa, an intake temperature (T_{in}) of 131°C was required to obtain autoignition with the desired combustion phasing. As boost was increased above 100 kPa, T_{in} was reduced both to compensate for the autoignition enhancement caused by the increased pressure and to provide the additional timing retard needed to prevent knocking. The latter is necessary because the pressure rise with combustion increases with boost due to the greater charge-mass in the cylinder, thereby increasing the PRR and knocking propensity. The process of reducing T_{in} with increased P_{in} was continued until T_{in} reached 60°C, which was taken to be the minimum T_{in} for this work because it is a typical out-of-intercooler temperature for diesel engines, and it is sufficiently warm to prevent condensation of water from EGR. Without further reduction of T_{in} and without EGR, the maximum load was limited as indicated by the "no-EGR" line in Figure 4, due to excessive ringing. For these conditions, the maximum attainable $IMEP_g$ is 8.8 bar at P_{in} = 180 kPa.

To reach higher loads, cooled EGR was added to further retard the combustion phasing [6], while T_{in} was held constant at 60°C. As Figure 4 shows, this allowed a substantial increase in load ($IMEP_g$). For the maximum load points at the various P_{in}, the ringing was kept ≤ 5 MW/m^2 (*i.e.* no knocking), and stability was very good with the coefficient of variation (COV) of the $IMEP_g$ < 1.5%, as shown in Figure 5a. Figure 5a also shows that the NOx emissions are extremely low (< 0.1 g/kg-fuel) at all boosted conditions, due to the low combustion temperatures. For the naturally aspirated condition, NOx was higher, but still comfortably below the U.S.-2010 emission standard for NOx (approximately 1 g/kg-fuel). Combustion and

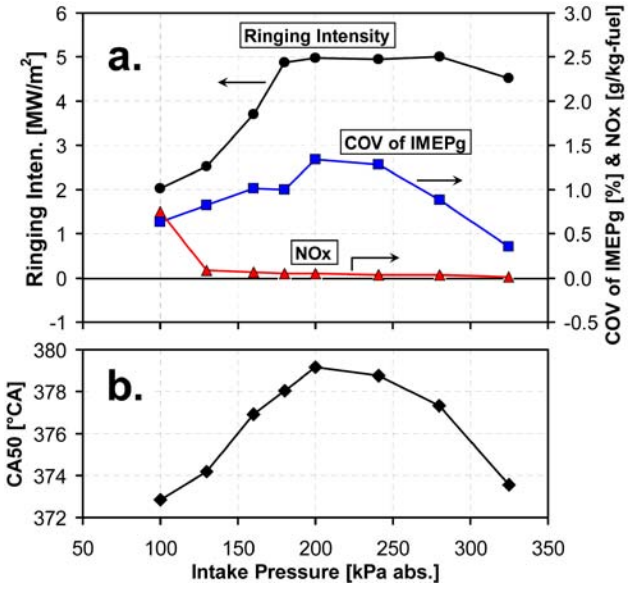

FIGURE 5. (a) Ringing intensity, COV of $IMEP_g$, NOx emissions, and (b) combustion phasing (CA50), for the maximum-load points in Figure 4.

indicated thermal efficiencies (not shown) are also good, ranging from 97 to 99% and from 42.5–47%, respectively. Central to achieving these results was the ability to retard combustion phasing (CA50) as late as 379° CA (19° after TDC) with good stability, as shown in Figure 5b. Note that less retard is necessary at the highest boost levels because the fuel/charge mass-ratio is reduced to accommodate the required high EGR levels. Further analysis is planned to determine why this highly retarded combustion phasing with low COV of $IMEP_g$ was possible under boosted conditions. Additional information may be found in Ref. [4].

Ethanol is an important renewable fuel, and it is widely used as a blending component in gasoline in concentrations up to 85%. Based on this, the characteristics of ethanol as an HCCI fuel have been evaluated over a range of operating conditions. This study showed that the autoignition requirements for ethanol are similar to gasoline for naturally aspirated operation at a moderately high load ($\phi = 0.38$). Changes in the required T_{in} with engine speed are also similar to those of gasoline for speeds ≥ 900 rpm. However, the enhancement of autoignition with intake boost is considerably less for ethanol than for gasoline. This latter finding is likely the result of ethanol being a true single-stage ignition fuel, unlike gasoline. As such, it shows a relatively low temperature-rise rate prior to the hot ignition point, and this rise rate is not enhanced with intake boost. Also, ethanol showed no low-temperature heat release at any condition. These characteristics could limit the allowable combustion-phasing retard, and therefore, the maximum loads that can be achieved without knock. On the other hand, these characteristics may offer advantages for controlling combustion phasing over the operating map, since the required T_{in} adjustments will be relatively small. Finally, comparison with the latest chemical-kinetic mechanism from the National University of Ireland – Galway, showed that the model performs fairly well, but lacks sufficient sensitivity to changes in P_{in}, T_{in}, and engine speed. A complete presentation of this investigation of ethanol may be found in Ref. [7].

HCCI engines can produce significant emissions of HC and OHC, particularly at low loads. Detailed speciation of these emissions is valuable for understanding the in-cylinder processes responsible for their formation, for supporting chemical-kinetic and CFD modeling, and for developing appropriate catalytic aftertreatment. Previous work has investigated the exhaust species for iso-octane as a representative single-stage ignition fuel [8]; however, little is known about how the exhaust species differ for two-stage ignition fuels. PRF80 was selected as a representative two-stage fuel, and detailed speciation measurements were made over a range of fueling rates, $0.08 \le \phi \le 0.32$. Analysis is not yet complete, but initial results indicate that unreacted fuel constitutes a much smaller fraction of the HC emissions compared to operating with neat iso-octane. The data also show that the *n*-heptane fraction of the fuel breaks down more readily than does the iso-octane fraction of the PRF80. Taken together, these findings indicate that the low-temperature ("cool-flame") reactions from the *n*-heptane produce substantial breakdown of the iso-octane, even when conditions are not favorable for complete combustion. Additional analysis and comparison of PRF80 data with iso-octane and gasoline results are planned.

Conclusions

- Planar T-map images show that thermal stratification of the bulk-gases develops progressively beginning about 330°CA and the maximum thermal stratification is reached at TDC (360°CA).
- The spatial distribution of thermal non-uniformities shows multiple, randomly distributed pockets of colder gases with a spatial scale of 5–11 mm. This distribution, and the finding that there is no consistent pattern from cycle to cycle, suggests a turbulent nature to the flow structures producing the stratification.
- The magnitudes of the thermal stratification and the cycle-to-cycle variation of the mean temperature match those required to achieve the observed performance of the fired metal engine at a similar operating condition.

- Intake-pressure boosting works very well for extending the high-load limit of gasoline-fueled HCCI at the 1,200 rpm operating condition studied.
  - A high load of 16.34 bar $IMEP_g$ was obtained with no ringing (*i.e.* no engine knock), very good stability, high efficiency, and ultra-low NOx.
  - Thus, well controlled, boosted HCCI has a strong potential for achieving high power levels, close to those of turbocharged diesel engines.
- The maximum attainable $IMEP_g$ increased almost linearly with boost up to $P_{in} = 200$ kPa, and above 200 kPa at a slightly lesser rate. However, the rate of increase was still substantial at the highest load, indicating that even higher loads could be achieved at greater boost levels.
- Ethanol works well as an HCCI fuel. Its autoignition requirements are similar to gasoline for naturally aspirated operation at a moderately high load ($\phi = 0.38$), but unlike gasoline, it maintains true single-stage ignition characteristics, with little enhancement of autoignition even under highly boosted conditions.
- Detailed exhaust speciation for PRF80, as a representative two-stage ignition fuel, shows that unreacted fuel is a much smaller fraction of the HC emissions than for single-stage fuels (iso-octane or gasoline).

References

1. Dec, J.E. and Hwang, W., "Characterizing the Development of Thermal Stratification in an HCCI Engine," SAE paper 2009-01-0650, 2009.

2. Dec, J.E., Hwang, W., and Sjöberg, M., "An Investigation of Thermal Stratification in HCCI Engines using Chemiluminescence Imaging," *SAE Transactions*, 115(3) pp. 759-776, paper 2006-01-1518, 2006.

3. Sjöberg, M., Dec, J.E., Babajimopoulos, A., and Assanis, D., "Comparing Enhanced Natural Thermal Stratification against Retarded Combustion Phasing for Smoothing of HCCI Heat-Release Rates," *SAE Transactions*, Vol. 113(3), pp. 1557-1575, SAE paper 2004-01-2994, 2004.

4. Dec, J.E. and Yang, Yi, "Boosted HCCI for High Power without Engine Knock and with Ultra-Low NOx emissions – using Conventional Gasoline," SAE paper offer no. 10PFL-0641, submitted to the 2010 SAE International Congress.

5. Eng, J.A., "Characterization of Pressure Waves in HCCI Combustion", SAE Paper 2002-01-2859, 2002.

6. Sjöberg, M., Dec, J.E., and Hwang, W., "Thermodynamic and Chemical Effects of EGR and Its Constituents on HCCI Autoignition," *SAE Transactions*, Vol. 116(3), SAE paper 2007-01-0207, 2007.

7. Sjöberg, M. and Dec, J.E., "Ethanol Autoignition Characteristics and HCCI Performance for Wide Ranges of Engine Speed, Load and Boost," SAE paper offer no. 10PFL-0176, submitted to the 2010 SAE International Congress.

8. Dec, J.E., Davisson, M.L., Leif, R.N., Sjöberg, M., and Hwang, W., "Detailed HCCI Exhaust Speciation and the Sources of Hydrocarbon and Oxygenated Hydrocarbon Emissions," SAE paper 2008-01-0053, 2008.

FY 2009 Publications/Presentations

1. Dec, J.E., "Advanced Compression-Ignition Engines – Understanding the In-Cylinder Processes," Invited Topical Review paper for the 32nd International Combustion Symposium, *Proceedings of the Combustion Institute*, Vol. 32, pp. 2727-2742, 2009.

2. Sjöberg, M., Dec, J.E., "Influence of Fuel Autoignition Reactivity on the High-Load Limits of HCCI Engines", *SAE Int. J. Engines* 1(1): 39-58, SAE paper 2008-01-0054, 2008.

3. Dec, J.E., Davisson, M.L., Leif, R.N., Sjöberg, M., Hwang, W., "Detailed HCCI Exhaust Speciation and the Sources of Hydrocarbon and Oxygenated Hydrocarbon Emissions," *SAE Int. J. of Fuels and Lubricants*, SAE paper 2008-01-0053, 2008.

4. Silke, E., Pitz, W.J., Westbrook, C.K., Sjöberg, M., and Dec, J. E., "Understanding the Chemical Effects of Increased Boost Pressure under HCCI Conditions," *SAE Int. J. of Fuels and Lubricants*, SAE paper 2008-01-0019, 2008.

5. Dec, J.E. and Hwang, W., "Analyzing Uncertainties for Improved Planar-Imaging Thermometry in an HCCI Engine," DOE Advanced Engine Combustion Working Group Meeting, February 2009.

6. Sjöberg, M. and Dec, J.E., "Influence of EGR-NOx on the High-Load Limits of HCCI Engines," Engine Combustion Processes – Current and Modern Techniques, 9th Congress, Germany, March 19–20, 2009.

7. Dec, J.E. and Hwang, W., "Characterizing the Development of Thermal Stratification in an HCCI Engine Using Planar-Imaging Thermometry," SAE paper 2009-01-0650, 2009 SAE International Congress, April 2009.

8. Sjöberg, M. and Dec, J.E., "Influence of EGR Quality and Unmixedness on the High-Load Limits of HCCI Engines," SAE paper 2009-01-0666, 2009 SAE International Congress, April 2009.

9. Dec, J.E., "Advanced Compression-Ignition Engines – Understanding the In-Cylinder Processes," invited seminar at Princeton University, April 2009.

10. Mehl, M., Pitz, W.J., Sjöberg, M., and Dec, J.E., "Detailed Kinetic Modeling of Low-Temperature Heat Release for PRF fuels in an HCCI Engine," SAE paper 2009-01-1806, 2009 SAE International Powertrain, Fuels and Lubricants Meeting, Florence Italy, June, 15–17, 2009.

11. Dec, J.E. and Yang, Y., "Boosted HCCI for High Power without Engine Knock, and with Ultra-Low NO_X Emissions using a Conventional Fuel," 15th DEER (Directions in Engine-Efficiency and Emissions Research) Conference, Dearborn, MI, August 2009.

12. Dec, J.E. and Yang, Y., "Boosted HCCI for High Power without Knock or NO_X – using Conventional Gasoline," DOE Advanced Engine Combustion Working Group Meeting, October 2009.

13. Dec, J.E., Sjöberg, M., and Hwang, W., "Isolating the Effects of EGR on HCCI Heat-Release Rates and NO_X Emissions," SAE paper 2009-01-2665, SAE Powertrains, Fuels, and Lubricants Meeting, San Antonio TX, November 2009.

14. Dec, J.E. and Yang, Y., "Boosted HCCI for High Power without Engine knock and with Ultra-Low NO_X Emissions – using Conventional Gasoline," SAE paper offer no. 10PFL-0641, submitted to the 2010 SAE International Congress, Detroit MI, April 2010.

15. Sjöberg, M. and Dec, J.E. "Ethanol Autoignition Characteristics and HCCI Performance for Wide Ranges of Engine Speed, Load and Boost," SAE paper offer no. 10PFL-0176, submitted to the 2010 SAE International Congress, Detroit MI, April 2010.

II.A.9 Automotive HCCI Combustion Research

Richard Steeper
Sandia National Laboratories, MS 9053
P.O. Box 969
Livermore, CA 94551-0969

DOE Technology Development Manager:
Gurpreet Singh

Objectives

This project comprises optical-engine investigations designed to enhance our understanding of in-cylinder processes in automotive-scale homogeneous charge compression ignition (HCCI) engines. Objectives for Fiscal Year 2009 include:

- Conduct experiments to characterize the negative valve overlap (NVO) strategy used to control and extend HCCI combustion. Specifically, quantify the thermal and chemical effects of NVO fueling.
- Continue the development of laser-based diagnostics, and conduct tests of the diagnostics in Sandia HCCI research engines.
- Continue the development and application of collaborative engine simulation and analysis tools for automotive HCCI combustion strategies.

Accomplishments

- Developed an algorithm for computing NVO cycle temperatures from experimental data. Validated the tool using planar laser induced fluorescence (PLIF) temperature measurements, GT-Power model estimates, and published iso-octane ignition data.
- Conducted engine experiments with and without NVO fueling to characterize low-load operation while varying main combustion phasing. Compared the two types of fueling using computed cycle temperatures in order to distinguish thermal and chemical effects of NVO fueling.
- Performed bench-top tests of a CO laser-absorption diagnostic for characterizing the extent of reactions during NVO reformation.
- Applied Stanford's two-wavelength PLIF diagnostic to capture cycle temperatures during fired NVO operation.
- Continued collaboration with the University of Wisconsin (UW) and Lawrence Livermore National Laboratory (LLNL) to develop modeling tools for automotive HCCI application.

Future Directions

- Apply infrared (IR) absorption and laser-induced fluorescence (LIF) optical diagnostics to characterize reforming reactions during the NVO period.
- Apply optical diagnostics to quantify piston wetting during NVO fuel injection to understand its effect on NVO- and main-combustion reactions.
- Validate the UW computational fluid dynamics (CFD) model of our automotive HCCI engine using optical and conventional measurements over a range of NVO operating conditions.
- Expand our tunable-diode-laser absorption diagnostic to permit in-cylinder measurement of H_2O, CO_2, and C_2H_2.

✧ ✧ ✧ ✧ ✧

Introduction

Major challenges to the implementation of HCCI combustion–including phasing control, operating-range extension, and emissions control–will require advanced charge-preparation strategies. Alternative strategies such as retarded injection and variable valve timing can be used to modify local charge composition and temperatures, thereby affecting, and possibly controlling, ignition phasing, rate of heat release, combustion efficiency, and engine-out emissions. This project is focused on understanding the in-cylinder processes characteristic of automotive HCCI engine combustion. Optical engine experiments employ in-cylinder diagnostics to quantify mixture preparation, ignition, combustion, and emission processes. Computational models help interpret the results and guide further research. The knowledge gained supports DOE's goal of facilitating the development of energy-efficient, low-emission engine combustion.

Approach

A variety of optical and mechanical diagnostics are applied to obtain information about HCCI in-cylinder processes. In-cylinder spray imaging allows assessment of spray evolution, penetration, and wall-wetting. LIF imaging produces fuel vapor and temperature distribution data, and statistics derived from the images quantify the state of mixing just prior to heat release. Chemiluminescence imaging provides information about combustion that can be related to the LIF fuel-distribution images. Finally, engine-out emission measurements help correlate mixture-preparation strategies with combustion/emission performance. Development of new diagnostics for in-

cylinder temperature measurements, a critical need for HCCI research, continues at Stanford University, with testing taking place in Sandia's optical engines. Work on a KIVA simulation of our automotive HCCI engine continues at UW and LLNL. Technical exchanges with manufacturers, national labs, and academia provide feedback and guidance for the research project.

Results

A current focus of our research is understanding the NVO strategy for HCCI combustion. In addition to trapping large amounts of residuals to control charge temperature and reaction rates, NVO operation also enables advanced fuel-injection strategies. Fuel can be injected during the NVO period to gain flexible and rapid control of main combustion phasing. Both the mass of NVO fuel injected and the timing of that injection (NVO SOI, or start of injection) can be easily adjusted, and many groups have demonstrated the resulting sensitive control of main CA10 (crank-angle location of 10% cumulative heat release during main combustion).

But our understanding of the process is incomplete: while thermal effects are straightforward (exothermic reactions during NVO elevating charge temperature), the nature and extent of chemical effects (NVO reforming reactions creating reactive species) are not. This year we conducted a series of experiments designed to separate the thermal and chemical effects of NVO fueling. Our approach was to compare conventional single-injection fueling (labeled *main-fuel tests*) with split-injection fueling in which a small fraction of the fuel is injected during NVO (labeled *NVO-fuel tests*). The idea was to compare cycle temperatures from a pair of experiments–one NVO-fuel and one main-fuel–that have the same CA10 phasing. If values of T_{IVC} (charge temperature at intake valve closing), for example, are similar for the pair of experiments, then we conclude that heat released during NVO fueling is simply compensated by a lower T_{INTAKE} required to achieve the same CA10. This we call a thermal effect. In contrast, if T_{IVC} values are dissimilar (and yet we still have the same CA10), we have reason to suspect that NVO reactions have changed the chemical composition. This is evidence of a chemical effect of NVO fueling on main combustion.

Cycle-Temperature Computation Algorithm

In order to make the comparisons described above, we developed an algorithm to accurately compute cycle temperatures based on measured cylinder pressures, mass flows, and a reference temperature. We were forced to develop our own tool since the obvious alternative, using a one-dimensional modeling tool such as GT-Power, excludes the possibility of heat release during NVO. Figure 1 illustrates key steps of the algorithm. Starting with a reference temperature measurement made in the exhaust port, we estimate an in-cylinder gas temperature near bottom dead center of exhaust. We use this temperature to model both the blowdown process following exhaust valve opening (EVO) plus the recompression process prior to exhaust valve closing (EVC) (including heat transfer) in order to compute T_{EVO} and T_{EVC}. These two temperatures allow us to calculate the fixed mass (and thereby, all temperatures) during the two closed portions of the cycle (NVO and main).

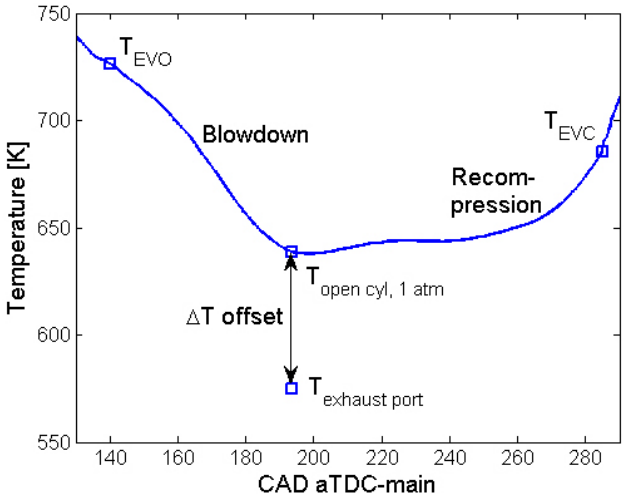

FIGURE 1. Initial steps of algorithm for computing cycle temperatures from measured cylinder pressures. Temperatures are shown for the open portion of the cycle between EVO and EVC.

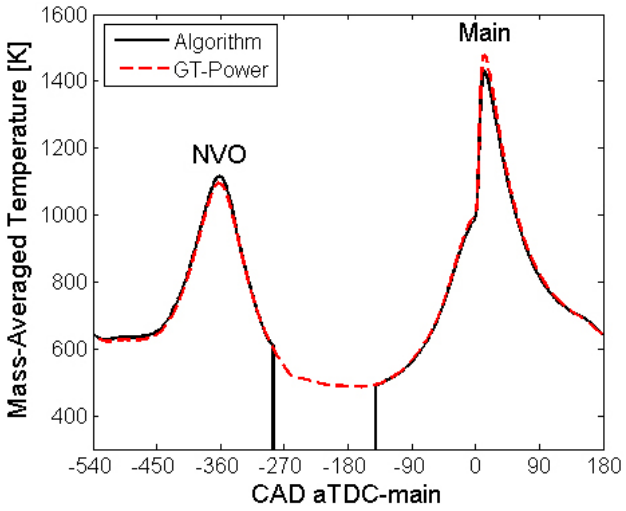

FIGURE 2. Computed (algorithm) and modeled (GT-Power) temperature traces for a typical low-load main-fuel experiment. The same comparison could not be made for an NVO-fuel test because of limitations of GT-Power. As in all report figures, the main fuel injection is 7.9 mg/cycle of iso-octane, and the symmetric (negative) valve overlap is 150 CAD.

Figure 2 demonstrates the success of the algorithm by comparing computed temperatures with those from GT-Power. Data are shown for a typical fired main-fuel experiment, and the close agreement provides confidence in our algorithm. There is a minor discrepancy in GT-Power's values at both top dead centers (TDCs) explained by the fact that it cannot account for the small quantity of unburned fuel in the experiment that is carried over to burn in the NVO period.

Two other analyses provided further validation of our temperature computations. First, we found favorable comparisons of our computed temperatures at ignition with published values for ignition temperatures of iso-octane at engine conditions. Second, we applied two-wavelength PLIF to make composition-temperature measurements during NVO operation. The PLIF diagnostic produces temperature images over a core region of our optical engine which we can integrate and compare with bulk mean temperatures computed by our algorithm. To illustrate, Figure 3 presents temperatures recorded at 24 CAD bTDC (crank angle degrees before top dead center) for tests covering a range of CA10. Both the PLIF data and the computed temperatures represent 50-cycle averages. The values and trends of the two measurements are very similar over this range of combustion phasing. The good agreement is tempered by an unexpected failure of core (PLIF) temperatures to exceed bulk (algorithm) temperatures (core temperatures should be higher since those measurements do not include colder boundary and crevice gases). However, results are consistent given our estimated PLIF temperature uncertainty of 4%.

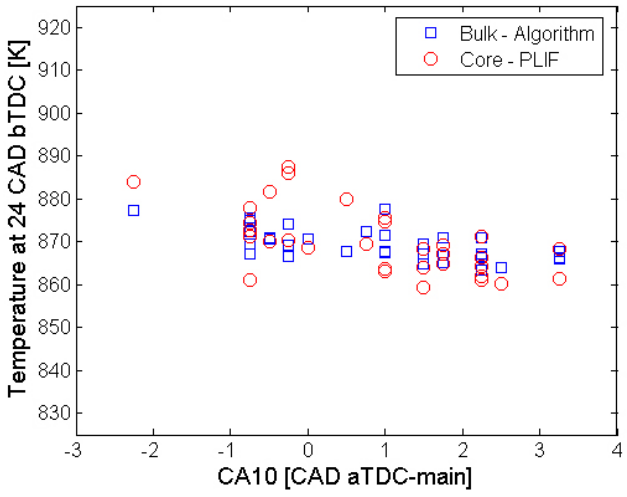

FIGURE 3. Comparison of computed bulk and PLIF core temperatures at 24 CAD bTDC of main combustion. The data represent NVO-fuel experiments in which either NVO fuel mass (0.9-1.4 mg/cycle) or NVO injection timing (100-15 CAD bTDC-NVO) is varied to adjust main-combustion CA10.

Thermal and Chemical Effects of NVO Fueling

We performed a large number of NVO-fuel and main-fuel experiments this year and applied our cycle-temperature computation tool to sort out effects of NVO fueling. An early, simple conclusion emerged: for cases in which most of the fuel injected during NVO burns promptly (i.e., during the NVO period), the effect on main combustion is predominantly thermal. In other words, heat released during NVO raises T_{IVO}, allowing a lower T_{INTAKE} to be used to achieve the same CA10. We found that high combustion efficiency during the NVO period is associated with early NVO injection timing. So for early-injection NVO fueling, there is a simple trade-off between NVO-fuel-mass injected and the amount of intake-charge heating required for a given main-combustion phasing.

Figure 4 illustrates trends associated with varying NVO injection timing. For early-injection NVO (earlier than 30 CAD bTDC), NVO combustion efficiency is relatively constant (not shown), while the T_{IVC} data (square symbols) climb steadily due to retarding of NVO heat release. The increasing T_{IVC} causes main CA10 to advance rapidly (circular symbols)–this is the

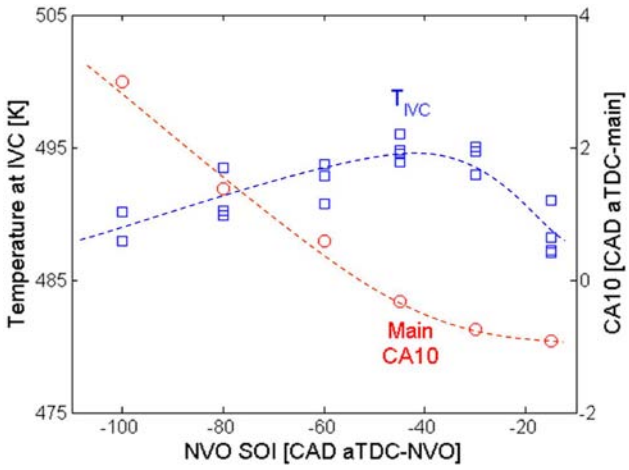

FIGURE 4. Calculated temperatures at IVC and associated main-combustion CA10 for an NVO injection-timing sweep with 1.2 mg/cycle of NVO fuel.

thermal effect discussed above. But injecting NVO fuel at 30 CAD bTDC or later causes a dramatic drop in the amount of heat released during NVO (not shown) which in turn causes the equally abrupt decline in T_{IVC} seen in Figure 4. Surprisingly though, main CA10 does not reverse its trend–despite much reduced IVC temperatures for late injection, CA10 continues to advance at a modest rate. This behavior suggests a *chemical effect* is associated with late-injection NVO fueling. Late NVO injection likely leads to piston wetting, and we hypothesize that resulting rich chemistry may produce reactive species during the NVO period that carry over and affect main combustion.

We have found further, strong evidence of chemical effects by comparing heat-release traces of late-injection NVO cases with main-fuel experiments. Cumulative apparent-heat-release traces from IVC to main ignition are plotted in Figure 5 for several typical experiments all with the same CA10. The main-fuel traces follow a downward curve that matches heat transfer losses estimated by the Woschni model (not shown). Early-injection NVO-fuel tests (not shown) follow this same curve. But the late-injection NVO-fuel cases in Figure 5 deviate dramatically around 60 CAD bTDC, showing clear evidence of early heat release well before main ignition.

For a wide range of late-injection NVO-fuel tests, we find consistent evidence of early main heat release. If we examine temperatures at IVC for example, they are consistently lower than main-fuel cases with the same CA10 phasing (bottom plot of Figure 6). But by the time of main ignition, the temperatures are indistinguishable (top plot of Figure 6), indicating that early exothermic reactions have raised temperatures during main compression for the NVO late-injection cases.

To enhance our understanding of NVO fueling, we have also conducted CHEMKIN simulations of the relevant iso-octane chemistry. Encouraging results show the same trends seen in Figures 5 and 6 but to a reduced degree. The CHEMKIN model identifies candidate species that may contribute to the chemical effects of NVO fueling. These modeling results, as well as the experimental and computational results discussed earlier in this report, are detailed in two publications submitted this year.

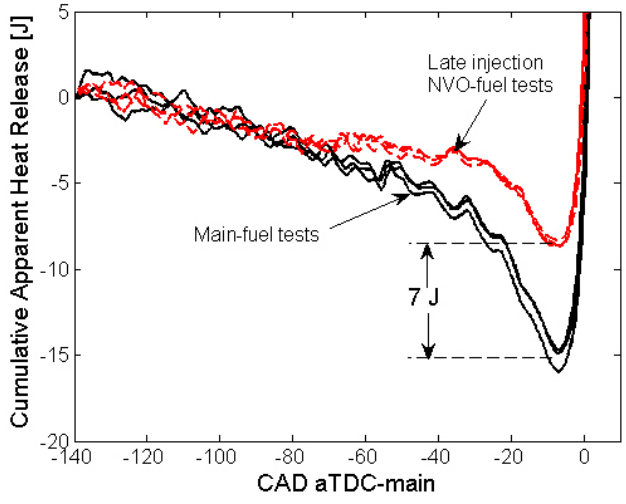

FIGURE 5. Cumulative apparent heat-release curves for main-fuel and late injection NVO-fuel cases. For the experiments shown, CA10 is constant at ~2 CAD after (a)TDC.

Other Activities

In support of our NVO engine project, we are actively developing diagnostics that can contribute to our understanding of HCCI combustion. This year we have continued our development of a CO-absorption diagnostic for measuring the products of NVO fueling. The diagnostic uses a tunable diode laser in a multi-pass configuration to capture spatially averaged, crank-angle-resolved measurements of in-cylinder CO concentration. We recently acquired a laser that operates farther into the infrared, potentially increasing sensitivity many fold. Bench tests of the new laser are currently underway.

The end of the year brought to a conclusion our project with Stanford University developing and applying the two-wavelength PLIF diagnostic described earlier. Results of the successful collaboration have been compiled in five publications. We plan to continue the application of LIF diagnostics in the coming year to assist in our characterization of the products of NVO fueling.

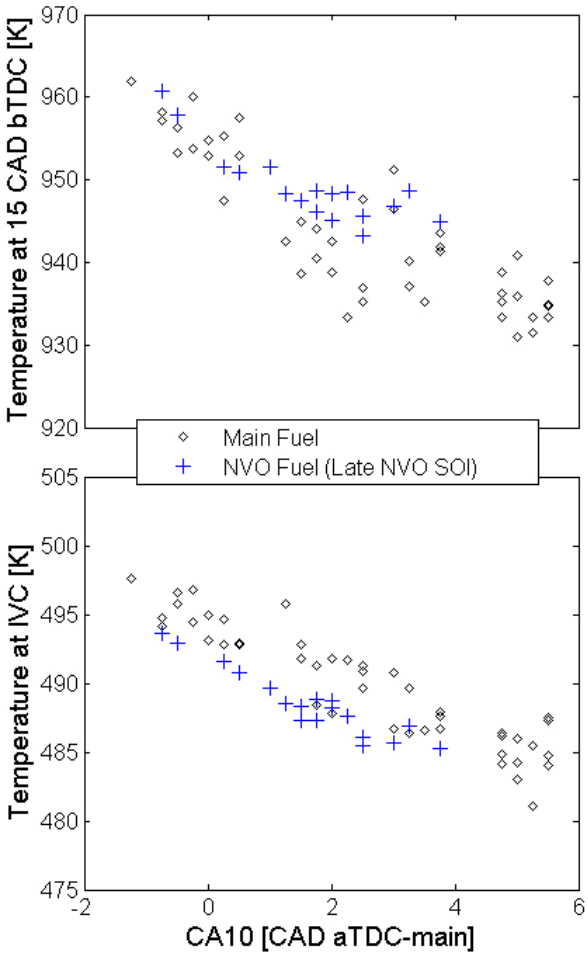

FIGURE 6. Computed temperatures at IVC (bottom) and at 15 CAD bTDC-main (top), comparing late-injection NVO-fuel and main-fuel tests. For the main-fuel tests, CA10 phasing is controlled using T_{INTAKE}, and for the NVO-fuel tests using NVO fuel mass.

CFD modeling of our automotive HCCI engine progressed this year in collaboration with LLNL (chemical kinetics modeling) and UW (KIVA implementation). Validation of motored and main-fuel operation against experimental data from our engine was successfully completed, and early tests of NVO fueling were begun.

Conclusions

- An algorithm for computing NVO cycle temperatures was developed. The tool has been tested for motored, main-fuel, and NVO-fuel experiments by comparing the results against temperature estimates from a GT-Power model, iso-octane ignition temperatures from the literature, and PLIF in-cylinder temperature measurements. Good agreement in all the comparisons gives confidence that the tool can provide the accuracy required for our analysis of NVO fueling experiments.
- A strategy comparing NVO-fuel experiments with main-fuel experiments was undertaken to sort out the thermal and chemical effects of NVO fueling. A range of main-combustion phasing was explored by varying intake temperature, NVO fuel fraction, and NVO fuel timing. The large database of experimental results was analyzed using our cycle-temperature algorithm.
- Fuel injected early during the NVO period combusts promptly, raising IVO and IVC temperatures, and advancing main combustion phasing. The effect of early-injection NVO fueling is mainly thermal.
- Fuel injected late in NVO (close to TDC) reacts only partially, leading to cooler IVC temperatures. But in spite of cooler IVC temperatures, main phasing remains advanced. Several consistent observations provide strong evidence that late-injection NVO fueling leads to significant early exothermic reactions during main compression.

FY 2009 Publications/Presentations

1. Steeper, R.R., "Automotive HCCI Combustion Research," DOE/OFCVT Advanced Engine Combustion and Fuels Program Annual Report, 2008.

2. Hessel, R.P., Foster, D.E., Aceves, S.M., Flowers, D.L., Pitz, W., and Steeper, R.R., "Pathline Analysis of Full-Cycle Four-Stroke HCCI Engine Combustion Using CFD and Multi-zone Modeling," SAE Int. J. Engines 1(1):27-38, 2008.

3. Fitzgerald, R.P., Steeper, R.R., and Snyder, J.A., "Effects of LIF Tracers on Combustion in a DI HCCI Engine," SAE Int. J. Fuels Lubr. 1(1):1491-1502, 2008.

4. Rothamer, D.A., Snyder, J., Hanson, R.K., and Steeper, R.R., "Two-Wavelength PLIF Diagnostic for Temperature and Composition," SAE Int. J. Fuels Lubr. 1(1):520-533, 2008.

5. Snyder, J.A., Hanson, R.K., Fitzgerald, R.P., and Steeper, R.R., "Dual-Wavelength PLIF Measurements of Temperature and Composition in an Optical HCCI Engine with Negative Valve Overlap," SAE Paper 2009-01-0661, 2009.

6. Rothamer, D. A., Snyder, J. A., Hanson, R. K., and Steeper, R. R., "Optimization of a Tracer-Based PLIF Diagnostic for Simultaneous Imaging of EGR and Temperature in IC Engines," Applied Physics B (Online First), 2009, doi:10.1007/s00340-009-3815-2.

7. Fitzgerald, R.P. and Steeper, R.R., "Thermal and Chemical Effects of NVO Fuel Injection on HCCI Combustion," submitted SAE Paper 10PFL-0536, 2010.

8. Fitzgerald, R.P., Steeper, R.R., Snyder, J.A., Hanson, R.K., and Hessel, R.P., "Determination of Bulk Cylinder Temperatures and Residual Gas Fraction for HCCI Negative Valve Overlap Operation," submitted SAE Paper 10PFL-0731, 2010.

9. Fitzgerald, R.P., "Effects of LIF Tracers on Combustion in a DI HCCI Engine," SAE Powertrains, Fuels, and Lubricants Meeting, Chicago, Oct. 7, 2008.

10. Snyder, J.A., "Dual-Wavelength PLIF Measurements in an NVO-HCCI Engine," DOE Advanced Engine Combustion Working Group Meeting, Sandia National Laboratories, Feb. 10, 2009.

11. Snyder, J.A., "Dual-Wavelength PLIF Measurements of Temperature and Composition in an Optical HCCI Engine with Negative Valve Overlap," SAE World Congress, Apr. 21, 2009.

12. Steeper, R.R., "Sandia Automotive HCCI Engine Research Project," DOE Vehicle Technologies Annual Merit Review, Arlington, VA, May 18, 2009.

Special Recognitions & Awards

1. 2009 Forest McFarland Award for outstanding contributions to SAE Engineering Meetings Board.

II.A.10 Achieving and Demonstrating Vehicle Technologies Engine Fuel Efficiency Goals

Robert M. Wagner (Primary Contact),
Thomas E. Briggs, Scott J. Curran,
Eric J. Nafziger, and K. Dean Edwards
Oak Ridge National Laboratory (ORNL)
2360 Cherahala Boulevard
Knoxville, TN 37932

DOE Technology Development Manager:
Gurpreet Singh

Objectives

- Demonstrate Fiscal Year 2009 DOE Vehicle Technologies milestone of 44% peak brake thermal efficiency (BTE) on a light-duty diesel engine.
- Design and build an Organic Rankine Cycle (ORC) and characterize the efficiency potential for the conversion of exhaust thermal energy to electrical power.
- Develop an ORC model for use with GT-Power to better understand potential and issues across a simulated light-duty drive cycle.

Accomplishments

- Demonstrated a peak BTE of 44.2% on a light-duty diesel engine through a combination of shaft power and electrical power generated from the exhaust heat of the engine.
- Developed a transient-capable ORC model for use with GT-Power cycle simulation software.
- Finalized a well-defined path to meeting FY 2010 efficiency and emissions milestones.

Future Directions

- Demonstrate a peak BTE of 45% on a light-duty diesel engine.
- Evaluate the potential of an ORC or other recovery technology for recovering exhaust energy under conditions consistent with road-load operation.
- Evaluate a prototype turbo-compounding system being developed and supplied to ORNL by VanDyne SuperTurbos.
- Perform vehicle systems level simulations with integrated transient-capable ORC model using GT-Drive and/or PSAT to estimate the potential benefits of and manage implementation issues associated with thermal energy recovery (TER) on light-duty vehicle applications.

Introduction

Modern light-duty diesel engines have peak BTEs in the range of 40-42% for high-load operation and lower efficiencies for part-load operation. The FreedomCAR roadmap has established efficiency and emissions goals for the next several years with a 45% peak efficiency being demonstrated in 2010, while meeting the Tier 2 Bin 5 emissions levels. The objective of this project is not to develop all the necessary technology to meet the efficiency and emissions goals but to serve as a focus for the integration of technologies into a multi-cylinder engine platform and to provide a means of identifying pathways for improved engine efficiency.

Approach

This activity makes use of knowledge discovery from internal ORNL activities, other national laboratories, universities, and industry. Internal activities include those focused on advanced combustion operation, aftertreatment, fuels, and unconventional approaches to improve combustion efficiency. This activity also makes use of technical contributions from external sources through regular interactions with the Advanced Engine Combustion working group administered by Sandia National Laboratories, the Cross-Cut Lean Exhaust Emissions Reduction Simulations working group administered by ORNL, and one-on-one interactions with industry teams such as Cummins Engines, Caterpillar, BorgWarner, VanDyne SuperTurbo, etc.

Substantial improvements in engine efficiency will require a reduction in thermal energy losses to the environment and a better understanding of thermodynamic loss mechanisms associated with the combustion process. With less than ½ of fuel energy converted to useful work in a modern engine, opportunity exists for significant advancements in engine efficiency. A fundamental thermodynamics perspective in combination with simulations and laboratory experiments is being used toward this purpose to provide guidance on developing and evaluating a path for meeting 2010 and intermediate milestones as well as longer term insight into the potential of future high efficiency engine-systems.

The following methodology is and has been used in this activity:

- Characterize current state-of-the-art light-duty engine technology. Note that this is a moving target as more advanced engines enter the market place.
- Improve fundamental understanding of internal combustion engine efficiency losses and opportunities.
- Identify and evaluate promising strategies to recover and/or reduce thermodynamic losses to the environment through engine-system simulations and experiments.
- Perform proof-of-principle demonstrations of selected concepts.

Technologies for improving efficiency and emissions in light-duty engines are being evaluated at ORNL on a General Motors (GM) 1.9-L common rail four-cylinder diesel engine. Earlier experiments were performed on a Mercedes-Benz 1.7-L common rail four-cylinder diesel engine. The engine platform was upgraded to reflect a change in the state-of-the-art in the market place. The GM engine is equipped with a microprocessor based dSpace control system which permits unconstrained access to engine hardware including the integration of custom control algorithms. This engine also has an electronic control unit (ECU) donated by GM which allows for the monitoring and manipulation of the base engine calibration.

Results

A peak BTE of 44.2% has been demonstrated on a light-duty diesel engine through a combination of engine shaft power and electrical power generated from the exhaust heat of the engine with an ORC. These accomplishments are interim milestones on the path to 2010 Vehicle Technologies milestones of 45% peak BTE and Tier 2 Bin 5 emissions. Advanced engine technologies identified and investigated in FY 2009 include TER, electrification of auxiliary components, advanced lubricants, and fuel properties. In addition, a flexible microprocessor-based control system was used for the re-optimization of engine parameters to make better use of these technologies. Peak BTE milestones and demonstration status are shown in Figure 1 for the past several years.

An ORC was developed and evaluated for the on-engine recovery of thermal exhaust energy. The system is a recuperated Rankine cycle with a three-stage boiler including a preheater, evaporator, and superheater as shown in the schematic in Figure 2. The system was designed to minimize refrigerant and exhaust restrictions to achieve maximum efficiency and minimum engine backpressure. Industrial grade components were

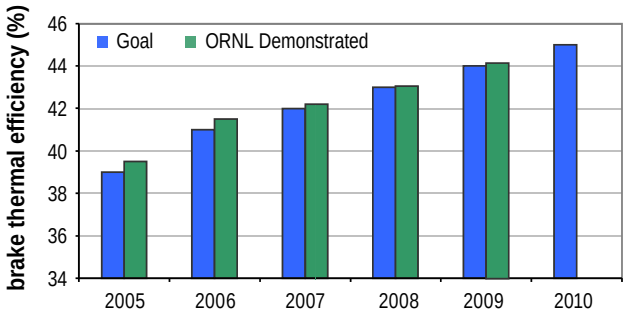

FIGURE 1. On path to demonstrating FY 2010 FreedomCAR engine and efficiency milestones including 45% peak BTE.

used whenever possible as packaging was not a design consideration since the system is only intended for laboratory evaluation. The most critical component to the ORC is the expander. After substantial research and discussions with suppliers and engine companies, an integrated turbine/generator system was chosen for the expander. The expander was developed by Barber-Nichols for use with R245fa working fluid and thermal conditions consistent with the GM 1.9-L peak efficiency point of 2,250 rpm, 18 bar brake mean effective pressure (BMEP). The working fluid was selected based on thermal performance but there are no substantial environmental concerns associated with this fluid. The ORC system is shown in Figure 3.

The ORC system was evaluated on-engine at the engine peak efficiency condition of 2,250 rpm and 18.0 bar BMEP. At this condition, the system was able to generate more than 2.9 kW of net electrical power from the exhaust heat, which corresponds to an 8% ORC efficiency. The 2.9 kW of net electrical power combined with a conservative peak BTE of 42.3% corresponds to a combined BTE of 44.2%. Combined power from the engine shaft and ORC are shown in Figure 4. Recall an engine-only peak BTE of 43.0% was demonstrated in FY 2008, further showing the potential of this approach to meet the FY 2010 BTE milestone. Note that the engine-out BTE of 42.3% was not simultaneous with ORC operation since all enabling technologies under investigation for this activity were not in place for these experiments. Experiments in FY 2010 will include all efficiency enabling technologies for a combined demonstration of BTE.

A system simulation and the design criteria indicate the ORC system is capable of generating more power than was achieved in these preliminary experiments. While 2.9 kW of net electrical power was used for meeting the milestone, a higher net electrical power of 3.4 kW was observed during the course of these experiments and the system design performance is estimated to be as high as 4.4 kW of net electrical power for the peak BTE exhaust conditions. Improvements

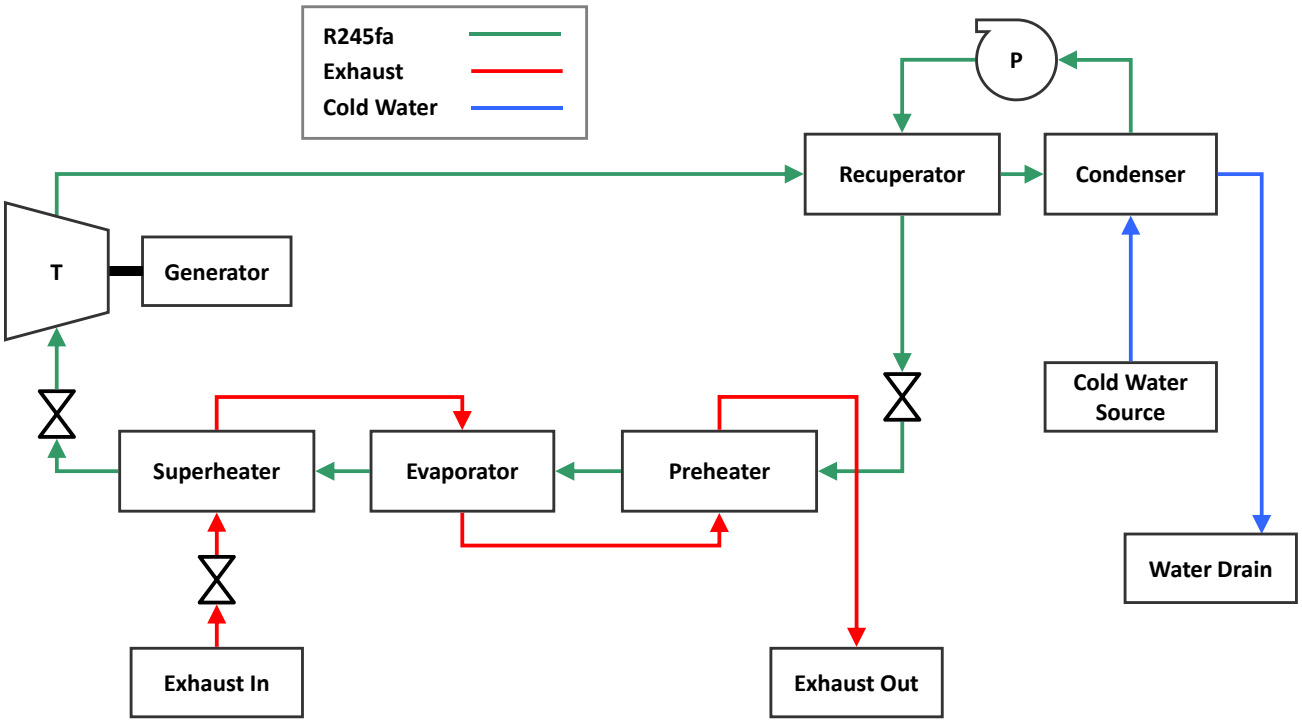

FIGURE 2. Schematic of Recuperative ORC

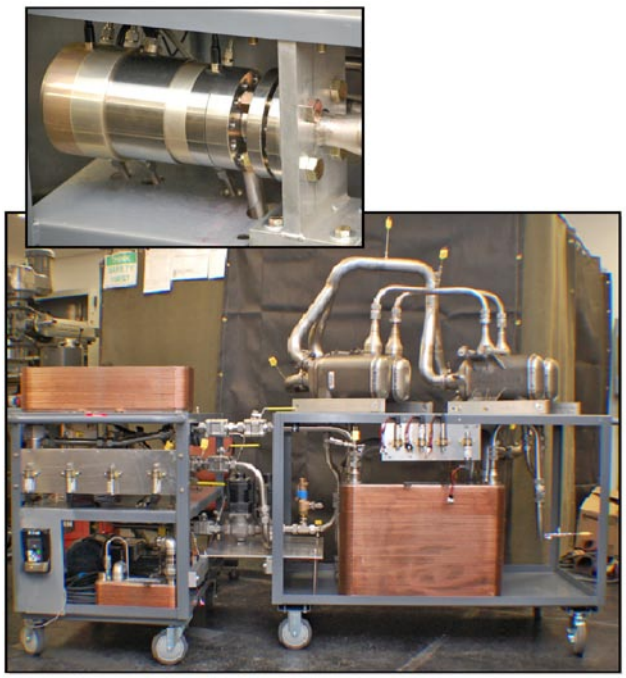

FIGURE 3. ORC and integrated turbine/generator expander before transferring the system to the engine laboratory.

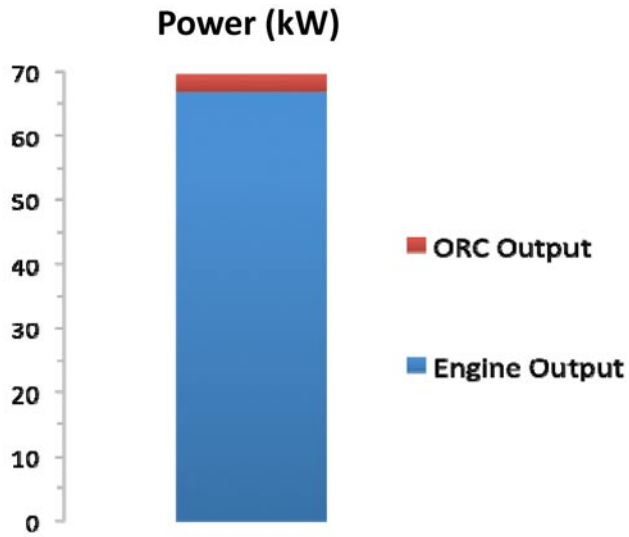

FIGURE 4. Combined power output of the engine and ORC at 2,250 rpm and 18.0 bar BMEP.

to the ORC system layout are in progress in an effort to achieve operation closer to the expected system design performance.

The ability of an ORC system to recover substantial thermal energy under conditions consistent with a light-duty drive cycle is unknown. Of particular concern is the low quality of exhaust and exhaust gas recirculation energy under these conditions as well as the transient nature of the light-duty drive cycle. The thermal time constants of the engine and the ORC are considerably

different and will most likely require the development/application of new technologies including thermal dampers and capacitors to better match the engine and ORC performance. An ORC model has been developed for use with GT-Drive to better understand the benefits and/or operational issues of an ORC for optimal efficiency. The preliminary model development is complete and will undergo evaluation with the latest version of GT-Drive (released in late September 2009) which includes improved modeling of air conditioning and waste heat recovery systems with support for two-phase working fluids including R245fa.

A TER technology better suited to the transient nature of the light-duty drive cycles is turbo-compounding. ORNL is informally collaborating with VanDyne SuperTurbo on an integrated supercharger/turbo-compound unit which is expected to have excellent transient response. ORNL is modeling the SuperTurbo system to guide prototype hardware development for the GM 1.9-L engine. VanDyne SuperTurbo intends to deliver a prototype unit to ORNL in FY 2010 for evaluation.

The path forward to the demonstration of FY 2010 efficiency and emissions milestones has been developed through extensive modeling, experiments, and interactions with the scientific community. The path will include a combination of the efficiency enabling technologies used this year as well as TER in combination with advanced combustion operation and the integration of appropriate aftertreatment systems. The advanced combustion and aftertreatment research is also being performed at ORNL and in close communication with this activity. Demonstration and verification of the milestones will be accomplished with on-engine experiments with a prototype TER system and vehicle system modeling with GT-Drive and/or PSAT.

Conclusions

This activity has shown progress toward the development, implementation, and demonstration of technologies for meeting and possibly exceeding Vehicle Technologies engine and efficiency milestones. Specific accomplishments are as follows:

- Demonstration of FY 2009 FreedomCAR milestone of 44% peak BTE on a light-duty diesel engine.
- Development and evaluation of an ORC through simulation and experiments on-engine.
- Thermal energy recovery being investigated on-engine and with transient-realistic models using GT-Drive. Modeling also allows for the evaluation of longer term technologies such as thermal dampers and capacitors.
- New insight into the thermodynamic availability of engine systems (*e.g.*, exhaust system, exhaust gas recirculation, etc.) across the speed/load operational range of a light-duty diesel engine and estimated potential fuel economy improvements over Federal Test Procedure drive cycle.
- Finalization of path forward to demonstration of FY 2010 efficiency and emissions milestones.

FY 2009 Publications/Presentations

1. T.E. Briggs, K. Cho, S. Curran, K. Edwards, E. Nafziger, R. Wagner, "A Waste Heat Recovery System for Light-Duty Diesel Engines", AEC Working Group Meeting (Detroit, MI; October 2009).

2. R.M. Wagner, T.E. Briggs, K.D. Edwards, R.L. Graves, "Progress on DOE Vehicle Technologies Light-Duty Diesel Engine Efficiency and Emissions Milestones", Poster Presentation, Direction in Engine-Efficiency and Emissions Research (DEER) Conference (Dearborn, MI; August 2009).

3. R.M. Wagner, T.E. Briggs, K.D. Edwards, R.L. Graves, "Development of a Waste Heat Recovery System for Light-Duty Diesel Engines", Poster Presentation, Direction in Engine-Efficiency and Emissions Research (DEER) Conference (Dearborn, MI; August 2009).

4. R.M. Wagner, T.E. Briggs, K.D. Edwards, "Achieving and Demonstrating Vehicle Technologies Engine Fuel Efficiency Mile-stones", 2009 DOE Hydrogen and Vehicle Technologies Merit Review (Washington, DC; May 2009).

5. *Invited.* R.M. Wagner, "Engine Fuel Efficiency Research at ORNL", Department of Mechanical Engineering, Missouri University of Science & Technology (Rolla, MO; April 2009).

6. R.M. Wagner, K. Cho, M. Han, C.S. Sluder, "Overview of engine efficiency activities at ORNL" and "Overview of High Efficiency Clean Combustion (HECC) activities at ORNL", DOE Vehicle Technologies program mid-year review (Knoxville, TN; October 2008).

7. R.M. Wagner, K.D. Edwards, Thomas E. Briggs, "Engine efficiency activities at ORNL", Meeting with Cummins (Columbus, IN; October 2008).

8. K.D. Edwards, R.M. Wagner, R.L. Graves, "Identification and evaluation of near- and long-term opportunities for efficiency improvement", AEC Working Group meeting (Auburn Hills, MI; September 2008).

II.A.11 KIVA-4 Development

David B. Carrington, David Torres
Los Alamos National Laboratory
P.O. Box 1663
Los Alamos, NM 87545

DOE Technology Development Manager:
Gurpreet Singh

Subcontractor:
Dr. Song-Charng Kong
Iowa State University, Ames, IA

Objectives

- Ready the KIVA-4 parallel version for release. To supply the engine modeling community an efficient internal combustion engine solver, including source code that they can modify or expand as needed.
- Create KIVA-4 modeling capability for piston-ring crevice and bowls with higher resolutions. This effort to help support, for example, homogeneous charge compression ignition (HCCI) modeling and Lawrence Livermore National Laboratory's (LLNL's) multi-zone method.
- Extend KIVA-4 capability to predict heat conduction in the combustion chamber via implementation of conjugate heat transfer modeling. This for more accurate prediction in wall film and its effects on combustion and emissions under, for example, premixed charge compression ignition (PCCI) conditions with strong fuel wall impingement.
- Create a cut-cell method with boundary-fitted cells for three-dimensional (3-D) grid generation. Having an in situ orthogonal 3-D generation capability would be most beneficial to users, particularly one which can utilizes computer aided design (CAD) rendered complex geometries. Grids to be generated in hours, in contrast to days or weeks for complex geometries.
- Extend KIVA-4 capability to use Cubit-generated unstructured grids. To have access to state-of-the-art grid generation capabilities at essentially no cost to U.S. citizens. Also, to have a platform generating unstructured grids to test various logic in KIVA-4 and for the *hp*-finite element method (FEM) version of KIVA now in development.
- Develop research code to investigate the advancement of speed, accuracy, robustness, and range of applicability of the KIVA combustion model and software to higher-order spatial accuracy with a minimal computational effort. Plan and research for changes to underlying discretization to utilize an *h-p* adaptive characteristic-based split (CBS) FEM.

Accomplishments

- KIVA-4 parallel version for release. Full version release in late fall with an alpha version now ready for release.
- Piston-ring crevice modeling in domains with piston rings on highly refined grids with bowls above the ring-walls and crevice regions are highly refined. This is working for two-dimensional (2-D) and 3-D sector and full 3-D grids and is included for the parallel KIVA-4 release. This work was performed in collaboration with Tom Piggot of LLNL.
- KIVA-4 capability has been extended to predict heat conduction in solids, that is, the combustion chamber.
- Cut-cell grid generation method for creating 3-D grids in hours, in contrast to days for complex geometries has been partially achieved.
- KIVA-4 now has support and capability to use Cubit-generated unstructured grids.
- Developed an *h*-adaptive CBS FEM for incompressible and compressible flows.

Future Directions

- Compare Sandia's diesel engine data with a large eddy simulation turbulence model in KIVA-4 on the complex diesel engine geometry in collaboration with Iowa State University.
- Continue cut-cell grid generation development to include more complex geometries and demonstration of solution on both a few general benchmarks and on a KIVA-engine test case. Continue the development of the moving grid system, and make use of more of the unstructured grid constructions in this process.
- Develop an *hp*-adaptive CBS FEM for multiphase incompressible and compressible flows and begin implementing this method to perform KIVA-type engine simulation, and also general reactive flow modeling common to any combustion type engine.

Introduction

Los Alamos National Laboratory (LANL) and its collaborators are facilitating engine modeling by improving accuracy of the modeling, providing for easier grid generation, and improving the robustness of the algorithms. We continue to improve the physical modeling methods, ease of gridding, altering and improving logic, subroutines and updating FORTRAN to latest standards as we proceed. We are developing and implementing new mathematical algorithms, those which represent the physics within an engine. We provide software that others may use directly or that they may alter with various models such as sophisticated chemical kinetics or different turbulent flow (turbulent closure modeling) and fuel injection models. We historically have provided a numerical platform for others to perform research on internal combustion and other types of engines and combustors.

Approach

Use of good engineering and computational practices for development of computational fluid dynamics (CFD) computer software to achieve the goals as outlined. Although this is a rather short statement, it encompasses a great many requirements including the following:

- Knowledge of turbulent multiphase fluid dynamics with combustion.
- Knowledge of and skill in implementing numerical methods for CFD on moving grids.
- Good software management and writing practice.
- Adequate documentation.
- Use of good guidelines.
- Reliance on collaborations, research, management, and experience to find and pursue fruitful paths.

Results

A newer version of KIVA-4 is ready for distribution, one which utilizes many computers and a message-passing interface known as MPI [1]. That is, the new software uses many computer processors to simulate an engine. These processors can be distributed on various machines or be local to a single machine. This distribution of the engine domain or geometry and accompanying discretization of the equations for mass, momentum and energy transport allows for a greater domain resolution to be solved in parallel, resulting in solutions in a shorter period of time. Solution of a slanted valve hemi-head on four processors is shown in Figure 1.

Support of HCCI engines and diesel engines in general is being provided by KIVA-4. In this vein LANL is providing capability to LNLL for use in their multi-zone HCCI calculations. It is believed or has been shown, that a source for pollutants and soot is found in the ring crevice portion of the piston/cylinder system. We have modified KIVA-4 to support geometries with piston-ring crevices as well as various standard piston bowl geometries. Shown in Figure 2 are two engine simulations which run on 3-D geometries, a sector region and a full piston region. Also, 2-D grids are supported in KIVA-4 for this type of geometry.

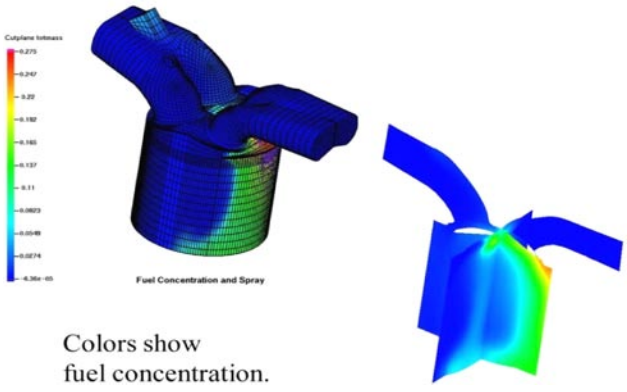

FIGURE 1. Parallel Solution of a 4-valve (slanted) Engine with Hemi-Head on Four Processors

Better modeling has been achieved for combustion by providing for wall temperature variation and heat flux. Combustion is very sensitive to in-cylinder mixture which, in turn, is sensitive to wall temperature and heat flux. Our collaborator Dr. Kong and his students at Iowa State University have implemented a conjugate heat transfer model into KIVA-4 to predict non-uniform wall temperature distribution. Additionally, combustion utilizing direct fuel injection often uses very early injection timing that can result in strong spray/wall impingement. The Iowa State University group has also implemented a new wall-film wetting mechanism developed at LANL. This combined with the calculation of heat flux and wall temperature of the combustion chamber/cylinder will improve the accuracy of combustion simulations, as it provides a better model to account for the details of the physical processes in the system. Validation of model versus an analytic solution is show in Figure 3a, with KIVA-4 producing the exact solution to conduction heat transfer. In Figure 3b, changes in piston surface temperature from the solution of conjugate heat transfer is shown. A non-uniform surface temperature is shown from impingement of fuel jet onto the piston's flat surface.

Providing for easier grid generation is currently being accomplished along two avenues. We have been developing code for KIVA-4 which will allow for grids generated by the Cubit software developed by Sandia National Laboratories and their collaborators. The grids produced are in a Genesis II-type format. Software is available to convert from the Genesis II

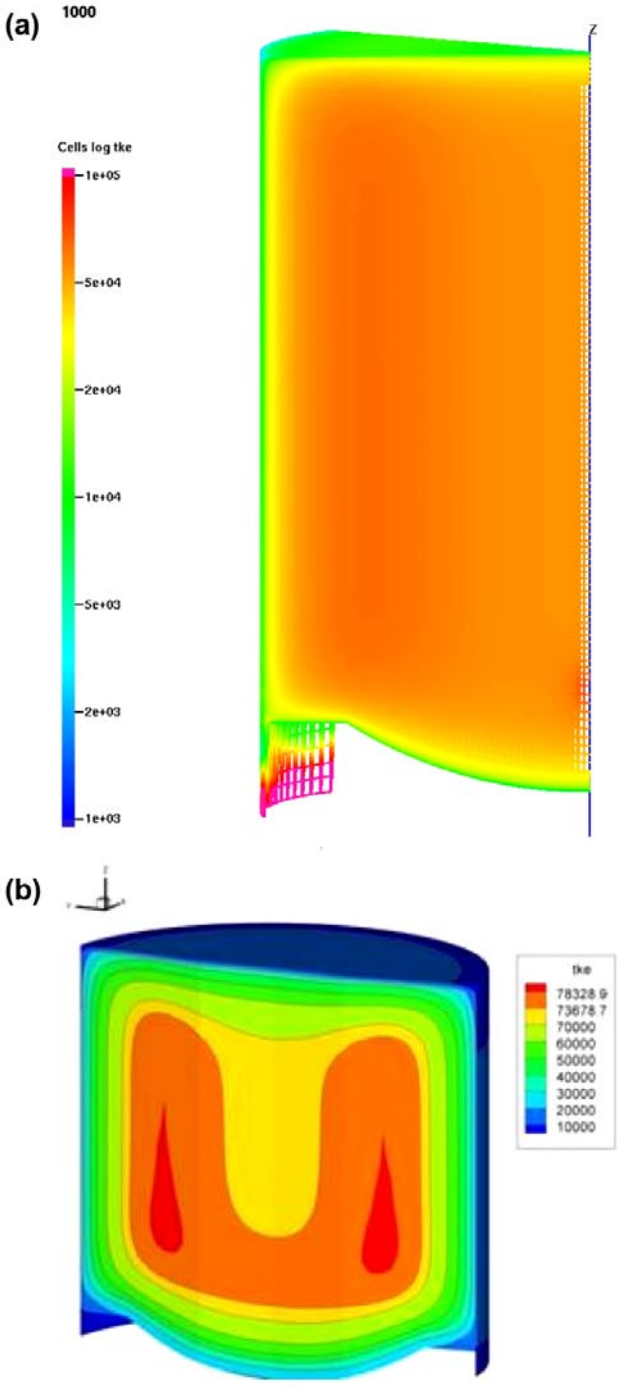

FIGURE 2. a) 3-D Sector and b) Full Piston Grids (b) for HCCI Simulations (High resolution in boundary and crevice regions.)

format to KIVA-4, called Cubit2Kiva (Los Alamos identifier LA-CC-09-048). The unstructured hexahedral grids generated by this state-of-the-art grid generation software are testing the KIVA-4 unstructured grid discretization system in new ways, particularly algorithms used to simulate moving parts in an engine. By flexing KIVA-4's logic we are better able to improve the robustness of the moving parts algorithms. In

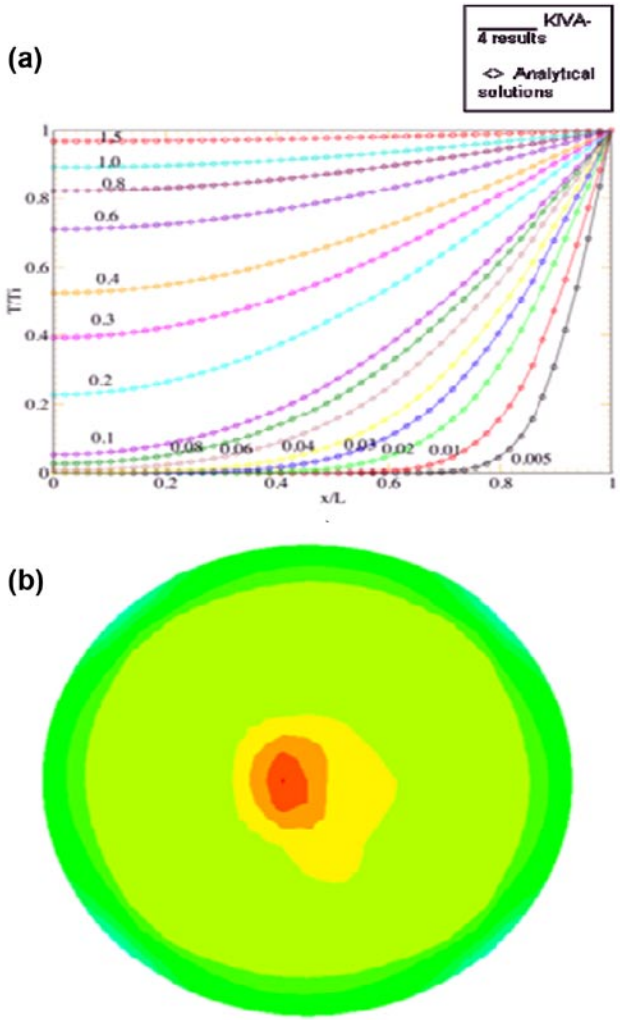

FIGURE 3. a) Validation experiment in slab geometry, KIVA-4 conduction vs. analytic; b) Non-uniform surface temperature resulting from a single fuel jet impingement on a flat piston as predicted by conjugate heat transfer modeling in KIVA-4.

Figure 4, a simple piston with a deep bowl is depicted with a Cubit unstructured grid. In this vein LANL has provided capability to LNLL for use in their multi-zone HCCI calculations. We are working to achieve more robust moving parts algorithms and provide modeling capability for all engine configurations. The Cubit grids will also support work on new algorithm developments, particularly the CBS *hp*-adaptive FEM scheme now being developed.

A new cut-cell grid generation technique is being implemented for KIVA-4. The method utilizes elements at the boundary which are currently in the KIVA-4 repertoire, particularly hexahedral, tetrahedral and prisms, to form the cells at the boundary. The domain is formed by overlaying the engine cylinder to be modeled with an orthogonal hexahedral grid extending beyond the boundaries of the domain. Then by using a stereo-

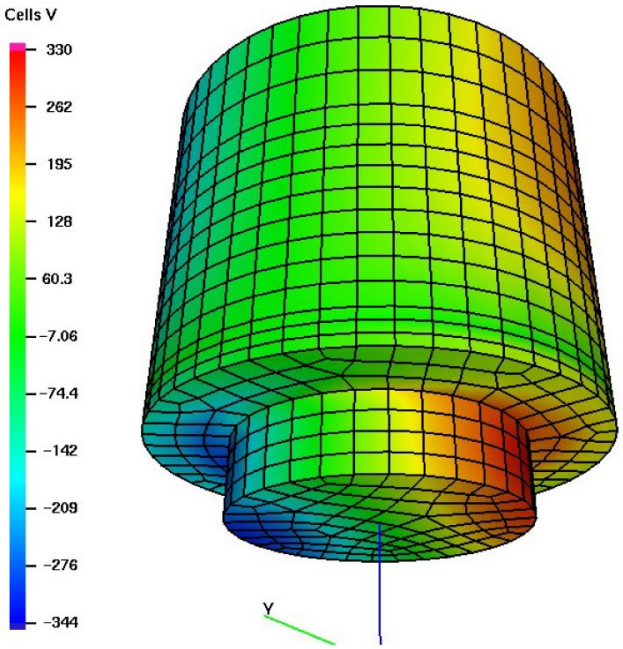

FIGURE 4. Cubit Unstructured Grid for a Simple Piston with a Deep Bowl used in a KIVA-4 Simulation

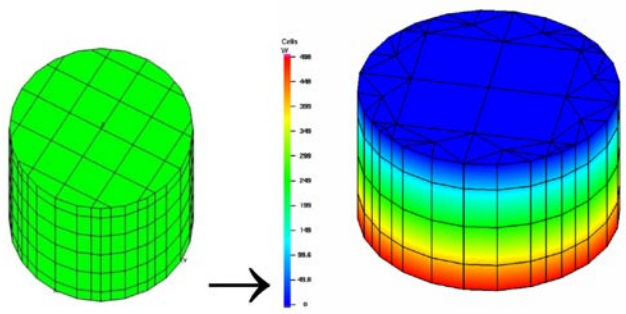

FIGURE 5. Cut-Cell methodology rendering a grid with polygonal boundary elements as developed from an STL file then adjusted to a KIVA-4 grid, a boundary-fitted Cartesian grid.

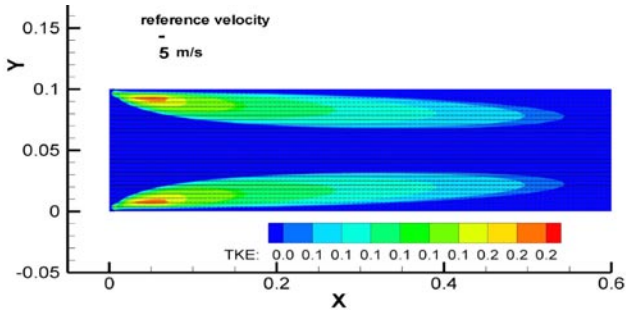

FIGURE 6. CBS FEM Modeling 2-D Turbulent Duct Flow using a k-*w* Two-Equation Closure

lithographic (STL) CAD rendering of the engine, a faceted depiction, the orthogonal grid is "cut" at the domain's boundary. Boundary cells are generated that are generally polyhedral at this point. These are further dissected to form hexahedral, tetrahedral and prisms. This system therefore is called a boundary-fitted Cartesian grid utilizing a cut-cell methodology as is shown in Figure 5.

Geometric resolution is paramount to accuracy as are the general algorithms and their equations used to represent physical processes occurring in engines. Resolution ushers in a need for greater computational power and a need for parallel processing. But, solving the resolved problem alone with more computing power isn't the only path which needs pursuing to achieve a desired accuracy. There are limits to parallel efficiency on complex engine domains, particularly those with moving parts. It is generally better to have algorithms which are more accurate at a given resolution and also provide for higher resolution and accuracy only where and when it is required in the time evolving simulation process.

Looking to the future and addressing the needs of internal combustion engine research and development, we recently began researching a CBS FEM as developed by Zienkiewicz and Codina [2]. This construction is a variational form, more specifically, a Galerkin-type FEM that utilizes conservative momentum and energy transport and precise Petrov-Galerkin stabilization. The algorithm is known as a projection method; a method now having great popularity in the finite element community. This method, combined with higher order polynomial approximation for model dependent physical variables (*p*-adaptive) along with grid enrichment (locally higher grid resolution – *h*-adaptive) and Arbitrary Lagrangian-Eulerian will provide for highly accurate and robust solutions in the next generation of KIVA, particularly on complex domains. We are beginning to develop this CBS algorithm for KIVA-hpFE from our *hp*-adaptive FEM research code and formulating the process for implementing into the KIVA-4 code structure [3-7]. Results from the algorithm simulating a 2-D turbulent duct flow are shown in Figure 6.

Conclusions

The following conclusions are drawn from the work described.

1. A KIVA-4 parallel version is nearly ready for release. This to supply the engine modeling community an efficient internal combustion engine solver and source code. Full version release in late fall with a beta version ready for release now. This is a great step forward in the ability of KIVA-4 and the KIVA project in general, providing for more rapid

simulations on today's platforms, from smaller mini-super computers, small Linux systems, to the world's fastest computer.

2. Piston-ring crevice modeling in domains with piston rings or piston ring crevices on grids with bowls above the ring has been achieved requiring modifications to the piston snapping and grid rezoning algorithms. Walls and crevice regions are highly refined in the grids for these configurations, this for 2-D and 3-D grids (sector and full piston) and is included for the parallel KIVA-4 release. This effort is to help support, for example, HCCI modeling and use of LLNL's the multi-zone method. The parallel version of this should greatly help the engine simulation communities' efforts to resolve even more details of the internal combustion engine and physical processes therein.
3. Extending KIVA-4 capability to predict heat conduction in solids, that is, in the combustion chamber, has been achieved. This to provide more accurate prediction of wall film wetting and subsequent evaporation. For example, to provide more accurate wall heat flux effects on combustion and emissions under PCCI engine conditions injected with fuel having wall impingement.
4. Development of a cut-cell grid generation method for creating 3-D grids in hours is making progress toward grid generation capability of a complete engine cylinder system.
5. Cubit-generated grids for KIVA-4 is being supported and was helpful in developing item 2 above and will help support efforts in item 6 below. This exercise points to needed improvements in the mesh movement and unstructured grid constructions.
6. Development of an *h*-adaptive CBS FEM for incompressible and compressible flows has been achieved. This method is a new solution algorithm for advancing the speed, accuracy, robustness, and range of applicability of the KIVA combustion model and software to higher-order spatial accuracy with a minimal computational effort. The results to date are promising.

References

1. David Torres, Yuanhong Li and Song-Charng Kong, *Partitioning Strategies for Parallel KIVA-4 Engine Simulations*, Computers and Fluids, 2009.

2. Zienkiewicz O.C. and Codina, R., (1995) "A general algorithm for compressible and incompressible flow, Part I, The split characteristic based scheme," International Journal of Numerical Methods in Fluids, Vol. 20, pp. 869– 885.

3. Carrington, D.B., (2009) "A characteristic-based split hp-adaptive finite element method for combustion modeling in KIVA-hpFE," Los Alamos National Laboratory, report. LA-UR-09- 06527, Los Alamos, NM.

4. Carrington, D.B., (2007) "An h-adaptive *k-w* finite element model for turbulent thermal flow," Los Alamos National Laboratory, report. LA-UR-06-8432, Los Alamos, NM.

5. Carrington, D.B, and Pepper, D.W., (2007) "An h-adaptive *k-w* finite element model for turbulent thermal flow," *14th International Conference on Finite Elements in Flow Problems*, IACM & USACM, Santa Fe, NM, Los Alamos National Laboratory LA-UR-07-1761.

6. Wang, X., Carrington, D.B., Pepper, D.W., (2009) "An adaptive FEM model for unsteady turbulent convective flow over a backward-facing step," Journal of Computational Thermal Sciences, accepted (being published), Begell House Inc.

7. Wang, X. and Pepper, D.W. [2007], Application of an *hp*-adaptive FEM for Solving Thermal Flow Problems, *AIAA Journal of Thermophysics and Heat Transfer,* Vol.21, No.1, pp. 190 – 198.

FY 2009 Publications/Presentations

1. David Torres, Yuanhong Li and Song-Charng Kong, *Partitioning Strategies for Parallel KIVA-4 Engine Simulations*, Computers and Fluids, 2009.

2. Wang, X, Carrington, D.B., Pepper, D.W., *An Adaptive FEM Model for Unsteady Turbulent Convective Flow Over a Backward-Facing Step*, Journal of Computational Thermal Sciences, Begell House Inc., vol. 1, no. 2, pp. 121-135, 2009.

3. David Carrington and Dave Torres, *KIVA Modeling to Support Diesel Combustion Research*, 2009 Merit Review, Arlington, VA, May. 2009, Los Alamos Scientific Report, LA-UR-09-01740.

4. David Carrington and Dave Torres, *T-3 Combustion Modeling and KIVA for FY 2009*, *AEC/HCCI Working Group Meeting*, Livermore, CA, Feb. 2009, Los Alamos Scientific Report, LA-UR-09-00553.

5. Xue,Q., S.C. Kong, D.J. Torres, Z. Xu and J. Yi, *DISI Spray Modeling using Local Mesh Refinement*, SAE 2008-01-0967.

6. Fife, M., P. Miles, M. Bergin, R. Reitz and D.J. Torres, The Impact of a Non-Linear Turbulent Stress Relationship on Simulations of Flow and Combustion in an HSDI Diesel Engine, SAE 2008-01-1363.

II.A.12 Chemical Kinetic Models for HCCI and Diesel Combustion

William J. Pitz (Primary Contact),
Charles K. Westbrook, Marco Mehl
Lawrence Livermore National Laboratory (LLNL)
P.O. Box 808, L-372
Livermore, CA 94551

DOE Technology Development Manager:
Gurpreet Singh

Objectives

- Develop detailed chemical kinetic models for fuel components used in surrogate fuels for diesel and homogeneous charge compression ignition (HCCI) engines.
- Develop surrogate fuel models to represent real fuels and model low-temperature combustion strategies in HCCI and diesel engines that lead to low emissions and high efficiency.
- Characterize the role of fuel composition on low-temperature combustion modes of advanced combustion engines.

Accomplishments

- Developed for the first time, a low and high temperature mechanism for 2,2,4,4,6,8,8-heptamethylnonane, a primary reference fuel for diesel, and a component to represent iso-alkanes in diesel fuel.
- Developed improved detailed chemical kinetic models for components and surrogates for gasoline fuels that will more accurately simulate combustion under HCCI conditions.

Future Directions

- Development of a high and low temperature mechanism for selected higher molecular weight iso-alkanes, an important chemical class in diesel fuel.
- Development of a high and low temperature mechanism for a high molecular weight alkyl-benzene, to represent aromatics in diesel fuel.
- Development of an improved mechanism for toluene and benzene.
- Development of efficient software to create reduced mechanisms for use in multidimensional engine simulation codes.
- Write a review paper that has recommendations for future research directions on diesel surrogate fuels for Progress in Energy and Combustion Sciences.

Introduction

Hydrocarbon fuels for advanced combustion engines consist of complex mixtures of hundreds of different components. These components can be grouped into a number of chemically distinct classes, consisting of n-alkanes, iso-alkanes, cycloalkanes, alkenes, oxygenates, and aromatics. Biodiesel contains its own unique chemical class called methyl esters. The fractional amounts of these chemical classes are quite different in gasoline, diesel fuel, oil-sand derived fuels and bio-derived fuels, which contributes to the very different combustion characteristics of each of these types of combustion systems.

Approach

To support large-scale computer simulations of each kind of engine, it is necessary to provide reliable chemical kinetic models for each of these chemical classes in fuels. However, few specific hydrocarbon components of some of these fuel classes have been modeled. For example, models for benzene and toluene have been developed, although models for few if any larger aromatic compounds such as naphthalene or styrene currently exist. Similarly, detailed models for small iso-alkanes such as iso-octane have been developed, but detailed models do not yet exist for the much larger versions such as heptamethylnonane, characteristic of diesel fuels. Biodiesel is composed of large methyl esters, but few detailed chemical kinetic models of these components have been developed. Current approaches to this problem are to construct a detailed model, containing one or more representatives of each class of components to serve as a surrogate mixture. In order for such a surrogate mixture model to be useful, each component must have a well-tested detailed kinetic model that can be included. This high-level approach can create realistic surrogates for gasoline or diesel fuel that reproduce experimental behavior of the practical real fuels. Detailed kinetic models for surrogate fuels can then be simplified as needed for inclusion in multidimensional computational fluid dynamics (CFD) models or used in full detail for purely kinetic modeling.

Results

There is a need to extend chemical kinetic models to address iso-alkanes because they are recommended as surrogate components for diesel fuel and one particular recommended component is 2,2,4,4,6,8,8-heptamethylnonane (iso-cetane) [1]. Heptamethylnonane is one of the primary reference fuels used to rate the ignition properties of diesel fuel. It can be used to represent the iso-alkane chemical class which comprises about 12-25% of diesel fuel in North American [1]. This year, the LLNL chemical kinetics team developed a chemical kinetic model for heptamethylnonane and published it in one of the most recognized combustion journals, Combustion and Flame [2]. This model allows the simulation of both low and high temperature chemistry of heptamethylnonane. The inclusion of low temperature chemistry in the model is important for simulation of new modes of combustion in engines such as HCCI and premixed charge compression ignition (PCCI). The task of developing the mechanism with 1,114 species and 4,468 reactions was very ambitious. Figure 1 shows an example of the mechanism validation by comparison of computed results with experimentally measured results for ignition delays in a high pressure shock tube [2]. It is important to properly predict ignition delay times to ensure accurate prediction of ignition phasing in a diesel engine. The pressures considered of 10 and 40 atm and the temperatures of 870 to 1,300 K are very relevant to conditions in a diesel engine. The agreement between the predicted and measured ignition delay times is quite good. Figure 2 shows a comparison of predictions of the ignition delay times of heptamethylnonane (HMN) with fuels that we have previously modeled. In the low temperature combustion region of 700 to 900 K, the HMN model predicts ignition delay times in between that of iso-octane and a number of large n-alkanes. This intermediate behavior is due to the presence of three CH_2 groups in HMN that can interact at low temperatures through alkylperoxy isomerizations that lead to chain branching. In comparison, iso-octane has one CH_2 group with no other CH_2 group to interact with. Consequently, its reactivity at low temperature is inhibited. At high temperatures above 900 K, all the large alkanes have similar ignition delay times.

We have made considerable progress in Fiscal Year 2009 in developing improved chemical kinetic models for gasoline components and surrogate fuels. Probably the most relevant components to include in surrogate fuel models for gasoline are n-heptane, iso-octane and toluene. N-heptane and iso-octane are the primary reference fuels for gasoline and can be used to represent the n-alkane and iso-alkane chemical groups in gasoline [3]. Toluene is present in concentrations up to 30% in gasoline and can be used to represent the aromatic chemical class in gasoline [3]. Over the last year, we have made considerable progress in improving the chemical kinetic models for n-heptane, iso-octane, toluene and their mixtures, the latter which can be used as a surrogate fuel to represent gasoline. We have improved our n-heptane and iso-octane chemical kinetic models so that they are more accurate over the very wide range of pressure and temperature encountered in an internal combustion (IC) engine. Figure 3 shows that computed ignition delay times from the improved model compare very well with experimentally measured ones for n-heptane over a wide range of pressures of 3-50 atm and temperatures from 700-1,200 K.

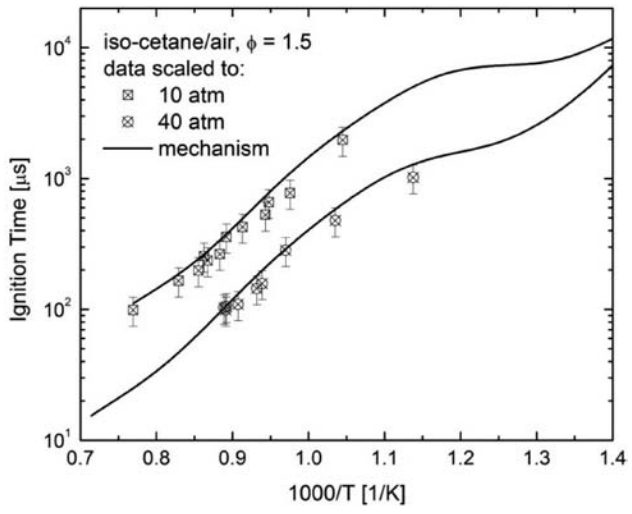

FIGURE 1. Predictions of the newly developed heptamethylnonane (iso-cetane) model (curves) compared to experimental measurements (symbols) in a high-pressure shock tube [2]. (Fuel/air mixtures, equivalence ratio of 1.5)

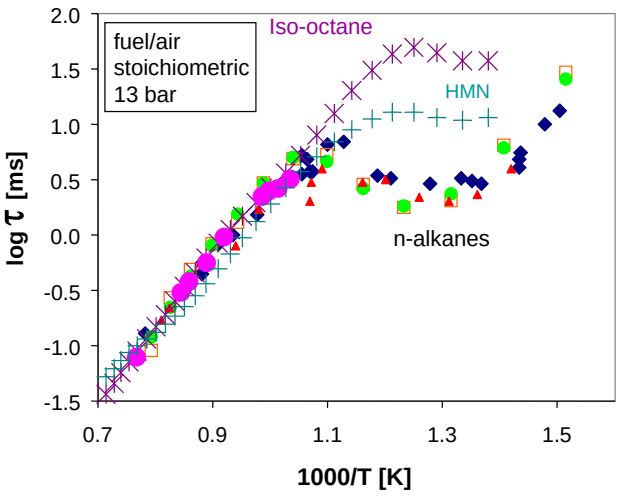

FIGURE 2. Computed and experimental ignition delay times for stoichiometric mixtures of heptamethylnonane, iso-octane and large n-alkanes in air at 13 bar pressure over the low and high temperature range. (+ Predicted HMN, * Predicted iso-octane)

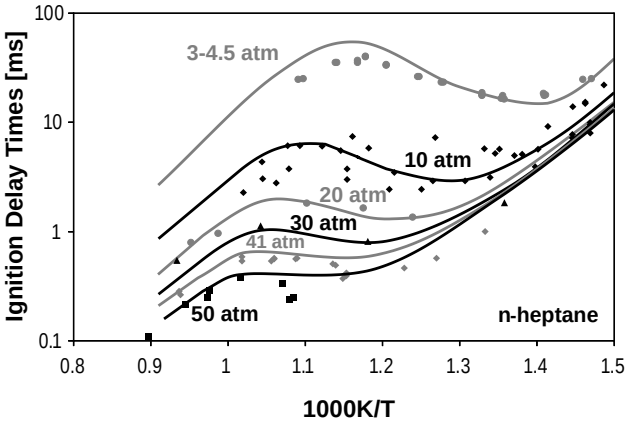

FIGURE 3. Computed and measured ignition delay times for stoichiometric mixtures of n-heptane over a range of pressures and temperatures including the low temperature combustion region.

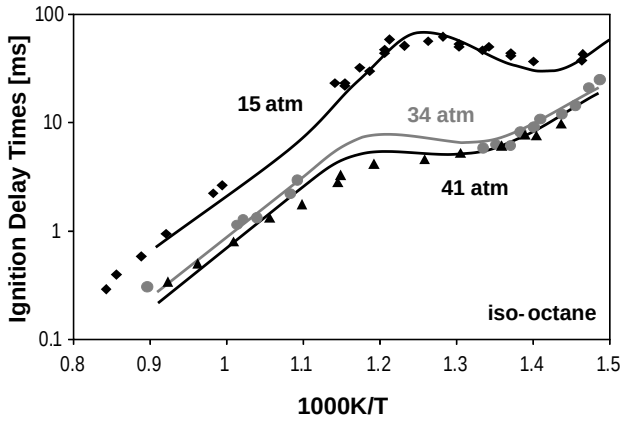

FIGURE 4. Computed and measured ignition delay times for stoichiometric mixtures of iso-octane over a range of pressures and temperatures including the low temperature combustion region.

Similarly for iso-octane, Figure 4 shows that computed ignition delay times compare well with experimentally measured ones over a wide range of pressures including 15-41 atm and temperatures including 700-1,200 K. The development of an improved model for toluene has been very challenging due to the complexity of its chemistry and the lack of information regarding reaction pathways and their associated rate constants, but we have been able to make considerable improvements in the model's predictive capabilities in FY 2009. Figure 5 shows an example of the improved behavior of our toluene model at 12 and 50 atm and over a temperature range of 1,000-1,200 K. The model predictions compare very well with experimental measurements [4] and the predictions are quite improved compared with those of currently available models for toluene.

It is important to validate mixtures of components as well as pure components to verify that the chemical kinetic model properly accounts for fuel component interactions. We tested binary and tertiary mixtures of our component models and compared computed ignition delay times to experimentally measured times in rapid compression machines (RCMs) [5]. RCMs simulate conditions of temperature and pressure attained in IC engines. These binary mixtures considered included n-heptane/toluene, iso-octane/toluene, iso-octane/1-hexene, and toluene/1-hexene. The predicted ignition delay times of these binary mixtures compared well with experimental measurements in an RCM [5]. Finally, we compared the predictions of a surrogate model for gasoline that contained 1-hexene, iso-octane and toluene to measurements of the ignition delay in an RCM. The end-of-compression pressures were about 13 atm and the temperatures ranged from 650 to 850 K which covers the region of low temperature combustion. As shown in Figure 6, the gasoline surrogate model performs quite well compared to the experimental data.

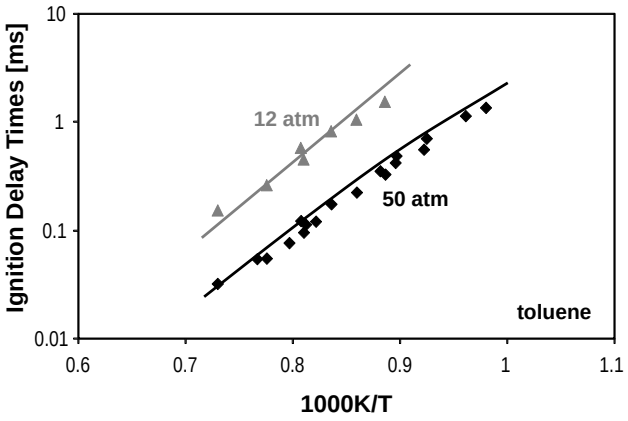

FIGURE 5. Computed and experimental [4] ignition delay times for stoichiometric mixtures of toluene over a range of pressures and temperatures relevant to internal combustion engines.

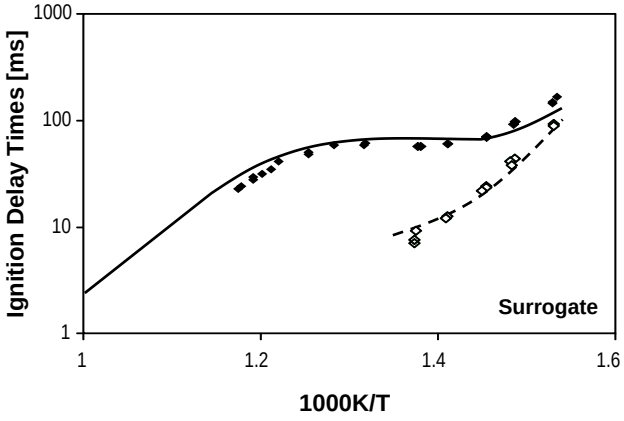

FIGURE 6. Computed and experimental [5] ignition delay times in a rapid compression machine for a stoichiometric mixture of n-heptane, iso-octane and toluene (47%, 35%, and 18%, respectively) over a range of temperatures and pressures near 13 atm.

Conclusions

- For the first time, a chemical kinetic model for 2,2,4,4,6,8,8-heptamethylnonane, a primary reference fuel for diesel, was developed and validated for low and high temperature chemistry regimes. This model is available to represent iso-alkanes in diesel fuel [6].
- The predictive capabilities of detailed chemical kinetic mechanisms for critical components in gasoline (n-heptane, iso-octane and toluene) were improved at conditions found in IC engines.
- Chemical kinetic models for binary and tertiary mixtures of gasoline components were tested and compared well to experimental data in rapid compression machines.

Acknowledgements

This work performed under the auspices of the U.S. Department of Energy by Lawrence Livermore National Laboratory under Contract DE-AC52-07NA27344.

References

1. J.T. Farrell, N.P. Cernansky, F.L. Dryer, D.G. Friend, C.A. Hergart, C.K. Law, R. McDavid, C.J. Mueller and H. Pitsch, "Development of an experimental database and kinetic models for surrogate diesel fuels," *SAE Paper 2007-01-0201, 2007 SAE World Congress*, Detroit, MI, 2007.

2. M.A. Oehlschlaeger, J. Steinberg, C.K. Westbrook and W.J. Pitz, "The autoignition of iso-cetane at high to moderate temperatures and elevated pressures: Shock tube experiments and kinetic modeling," *Combust. Flame* 156 (11) (2009) 2165-2172.

3. W.J. Pitz, N.P. Cernansky, F.L. Dryer, F. Egolfopoulos, J.T. Farrell, D.G. Friend and H. Pitsch, "Development of an Experimental Database and Kinetic Models for Surrogate Gasoline Fuels," *SAE 2007 Transactions Journal of Passenger Cars - Mechanical Systems, SAE Paper 2007-01-0175*, 2007.

4. H.-P.S. Shen, J. Vanderover and M.A. Oehlschlaeger, "A shock tube study of the auto-ignition of toluene/air mixtures at high pressures," *Proc. Combust. Inst.* 32 (1) (2009) 165-172.

5. G. Vanhove, G. Petit and R. Minetti, "Experimental study of the kinetic interactions in the low-temperature autoignition of hydrocarbon binary mixtures and a surrogate fuel," *Combust. Flame* 145 (3) (2006) 521-532.

6. W.J. Pitz, C.K. Westbrook, H.J. Curran, M. Mehl, O. Herbinet and E.J. Silke, "LLNL Chemical Kinetic Mechanisms," https://www-pls.llnl.gov/?url=science_and_technology-chemistry-combustion, 2009.

FY 2009 Publications/Presentations

1. M.A. Oehlschlaeger, J. Steinberg, C.K. Westbrook and W.J. Pitz, "The autoignition of iso-cetane at high to moderate temperatures and elevated pressures: Shock tube experiments and kinetic modeling," *Combust. Flame* 156 (11) (2009) 2165-2172.

2. C.K. Westbrook, W.J. Pitz, O. Herbinet, H.J. Curran and E.J. Silke, "A Detailed Chemical Kinetic Reaction Mechanism for n-Alkane Hydrocarbons from n-Octane to n-Hexadecane," *Combust. Flame* 156 (1) (2009) 181-199.

3. Y. Sakai, A. Miyoshi, M. Koshi and W.J. Pitz, "A kinetic modeling study on the oxidation of primary reference fuel-toluene mixtures including cross reactions between aromatics and aliphatics," *Proc. Combust. Inst.* 32 (2009) 411-418.

4. M. Mehl, W.J. Pitz, M. Sjöberg and J. E. Dec, "Detailed kinetic modeling of low-temperature heat release for PRF fuels in an HCCI engine," *SAE 2009 International Powertrains, Fuels and Lubricants Meeting, SAE Paper No. 2009-01-1806*, Florence, Italy, 2009.

5. O. Herbinet, W.J. Pitz and C.K. Westbrook, "Detailed chemical kinetic mechanism for the oxidation of biodiesel fuels blend surrogate," *Combust. Flame* (2009) In press.

6. M. Mehl, G. Vanhove, W.J. Pitz and E. Ranzi, "Oxidation and combustion of the n-hexene isomers: a wide range kinetic modeling study," *Combust. Flame* 155 (2008) 756–772.

7. C.K. Westbrook, W.J. Pitz, M. Mehl and H.J. Curran, "Detailed chemical kinetic models for large n-alkanes and iso-alkanes found in conventional and F-T diesel fuels," *U.S. National Combustion Meeting*, Ann Arbor, MI, 2009.

8. M. Mehl, A. Frassoldati, R. Fietzek, T. Faravelli, W.J. Pitz and E. Ranzi, "Chemical kinetic study of the oxidation of toluene and related cyclic compounds," *Fall Technical Meeting of the Western States Section of the Combustion Institute*, Irvine, CA, 2009.

9. M. Mehl, H.J. Curran, W.J. Pitz and C.K. Westbrook, "Detailed Kinetic Modeling of Gasoline Surrogate Mixtures," *U.S. National Combustion Meeting*, Ann Arbor, MI, 2009.

10. M. Mehl, H.J. Curran, W.J. Pitz and C.K. Westbrook, "Chemical kinetic modeling of component mixtures relevant to gasoline," *4th European Combustion Meeting*, Vienna, Austria, 2009.

11. A. Frassoldati, M. Mehl, R. Fietzek, T. Faravelli, W.J. Pitz and E. Ranzi, "Kinetic Modeling of Toluene Oxidation for Surrogate Fuel Applications," *Italian Section of the Combustion Institute Combustion Colloquia*, Naples, Italy, 2009.

12. C.K. Westbrook, W.J. Pitz, H.-H. Carstensen and A.M. Dean, "Development of Detailed Kinetic Models for Fischer-Tropsch Fuels," *237th ACS National Meeting & Exposition*, Salt Lake City, Utah, 2009.

13. W.J. Pitz, C.K. Westbrook, M. Mehl, O. Herbinet, H.J. Curran and E.J. Silke, "LLNL Chemical Kinetics Modeling Group," *Journal of the Combustion Society of Japan* 50 (154) (2008) 331-336.

Special Recognitions & Awards/Patents Issued

1. SCIENCEWATCH© identified Charles Westbrook and William Pitz as in the top 25 most cited authors in the area of energy and fuels for the period of 1998 to 2008.

2. William Pitz received an award as co-author on the best paper of the year from the Japanese Combustion Society. The paper is "A Kinetic Modeling Study on the Oxidation of Primary Reference Fuel-Toluene Mixtures Including Cross Reactions between Aromatics and Aliphatics", Y. Sakai, A. Miyoshi, M. Koshi, W.J. Pitz, Proceedings of the Combustion Institute, 2009.

II.A.13 Hydrogen Free-Piston Engine

Peter Van Blarigan
Sandia National Laboratories
P.O. Box 969, MS 9661
Livermore, CA 94551-0969

DOE Technology Development Manager:
Gurpreet Singh

Objectives

- Study the effects of continuous operation (i.e. gas exchange) on indicated thermal efficiency and emissions at high compression ratios (~20-40:1) utilizing homogeneous charge compression ignition (HCCI) combustion in an opposed free-piston linear alternator engine.
- Concept validation of passively coupling the opposed free pistons via independent linear alternators connected to a common load to maintain piston synchronization.
- Proof of principle of electronic variable compression ratio control by means of mechanical control of bounce chamber air control (BCAC) rebound devices.

Accomplishments

- Fabricated and assembled the major components needed for the research prototype, including engine combustion chamber, intake and exhaust manifolds, pistons, magnets, linear alternators, and other associated hardware.
- Analyzed the research experiment for stability of piston coupling via prototype resistive load circuit with Mathematica-based model.
- Purchased and installed 1,000 psi air compressor and associated hardware to serve as air supply for BCAC system.
- Designed and fabricated piston lock-and-release mechanism intended to lock pistons in place for starting and release pistons simultaneously to ensure piston synchronization on first stroke.

Future Directions

- Complete assembly of research prototype engine, BCAC system, and piston lock-and-release mechanism as well as associated support and data acquisition hardware.
- Initially run the engine under air injection motoring mode only to test the stabilizing capability of the linear alternator coupling.
- Perform combustion experiments and measure indicated thermal efficiency at various compression ratios and equivalence ratios with both conventional and alternative fuels: hydrogen, natural gas, ethanol, biofuels, propane, gasoline, other renewables.

Introduction

As fuel efficiency of the typical American automobile becomes more important due to hydrocarbon fuel cost and availability issues, powertrain improvements will require smaller output engines combined with hybrid technologies to improve efficiency. In particular, the plug-in hybrid concept will require an electrical generator of approximately 30 kW output. Unfortunately, current crankshaft spark-ignition internal combustion engines with optimized power outputs of 30 kW have thermal efficiencies of less than 32%.

The free-piston generator of this project has a projected fuel-to-electricity conversion efficiency of 50% at 30 kW output. The project has progressed by conducting idealized combustion experiments, designing and procuring the linear alternators required for control and power conversion, and conducting computational fluid dynamics design of the inlet/exhaust processes. The design has evolved into a dynamically balanced configuration suitable for seamless incorporation into an automotive application or distributed auxiliary power unit. The ultimate goal is to combine the developed components into a research prototype for demonstration of performance. Figure 1 shows the improvement based on single-cycle experiments.

Approach

By investigating the parameters unique to free-piston generators (linear alternator, opposed-piston coupling, uniflow port scavenging) as separate entities, each piece can be used at its optimum design point. More importantly, upon assembly of a research prototype for performance demonstration (the goal of this project), understanding of the pieces in the device will allow proper contribution of each component to the combined performance of the assembly.

Last year, the opposed-piston research prototype was designed and orders made for fabrication. This year, activity has been focused on the assembly of fabricated

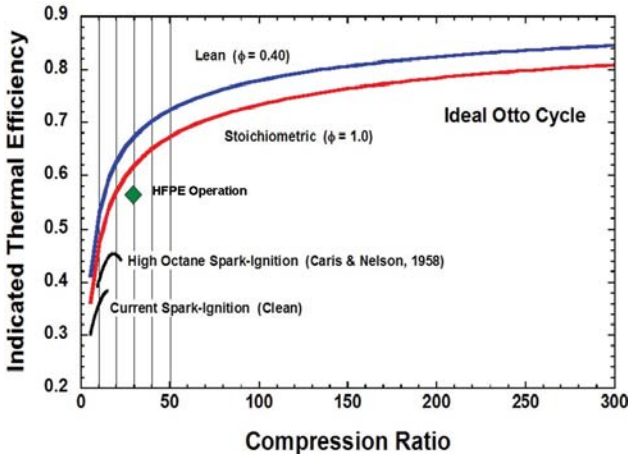

FIGURE 1. Indicated Efficiency as a Function of Compression Ratio (Expected hydrogen free-piston engine operation shown by diamond.)

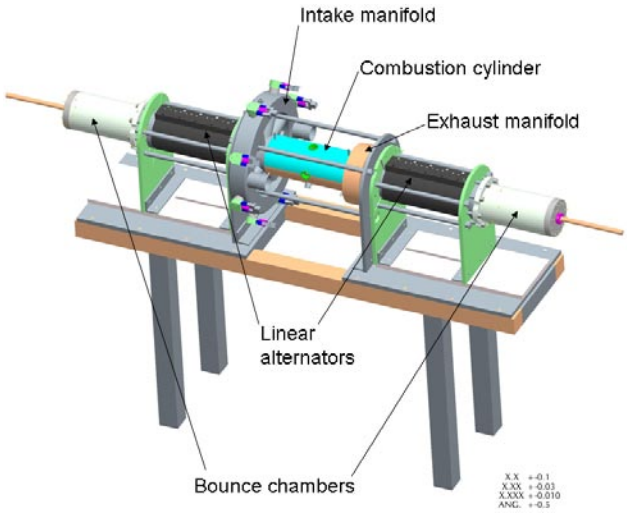

FIGURE 2. The HFPE Research Prototype Computer-Aided Design Model

parts as they are received and the installation of associated support hardware in the test cell. In addition, the equipment needed to supply the 1,000 psi air for the BCAC system was purchased and installed. A piston lock-and-release mechanism was designed for starting purposes. Also, a new phase of collaboration with General Motors (GM) and the University of Michigan on a more detailed simulation of the Sandia research prototype in a ground-up hybrid vehicle model began in May.

Results

The majority of our efforts this year have been concentrated on assembling fabricated parts as they are received and preparing necessary support systems in the test cell. Figure 2 shows the computer-aided design model of the hydrogen free-piston engine (HFPE). Figure 3 shows the major components of the HFPE that have been assembled to date. They include the central combustion chamber, the intake manifold and fuel injectors (on right side), the exhaust manifold (on left side), the dual linear alternators, the pistons, the load resistors, the lubrication system, and associated connections and support systems. Not shown in the figure is a two-stage regenerative blower capable of providing intake air at 175 cfm and 10 psi in order to simulate supercharging, essential for a two-stroke engine. Also not visible in the figure are the rare-earth NdFeB-bonded magnets, which were manufactured and magnetized at separate facilities. The fuel injectors currently installed are compatible with gaseous fuels such as hydrogen, natural gas, and liquefied petroleum gas. They can be easily swapped with liquid fuel-compatible injectors in order to test fuels such as ethanol and other renewables.

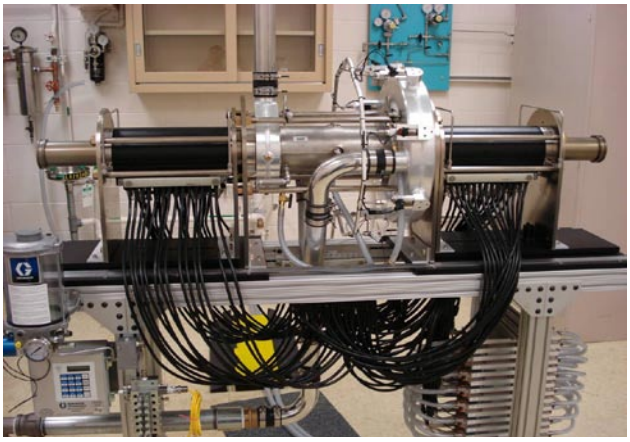

FIGURE 3. The Sandia HFPE Research Prototype

As part of the experimental design process it was realized that the capability to start the piston oscillation and bring the motoring engine to the desired compression ratio before fuel is introduced would be an important capability. We began investigating various concepts to introduce extra gas into the bounce chambers when the pistons are near their full outward travel position (maximum combustion chamber volume) and a method for venting the extra gas when the pistons are near the full inward travel position (minimum combustion chamber volume). In this way the energy to drive the pistons inward can be provided and controlled. We investigated using both helium and air as the working fluid in the bounce chamber, and it was ultimately decided to go with air to avoid the cost of acquiring and handling helium. The high-pressure air (up to 1,000 psi) is introduced through a piston-actuated valve in the bounce chamber cylinder head and vented into a plenum that surrounds the venting ports in the

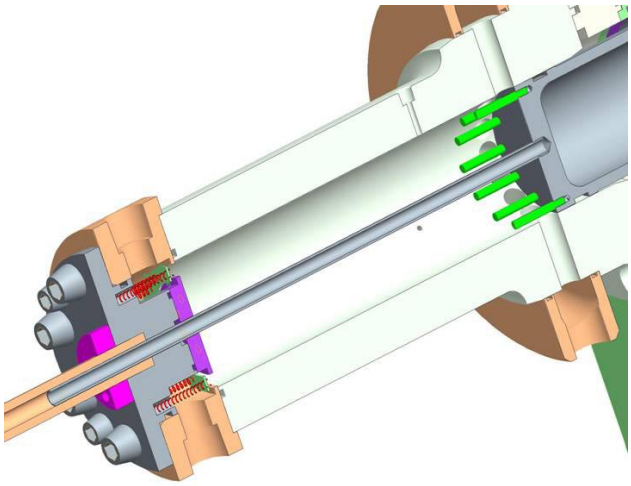

FIGURE 4. Overview of BCAC system, showing Piston-Actuated Injection Valve to the Left and Vent Ports to the Right

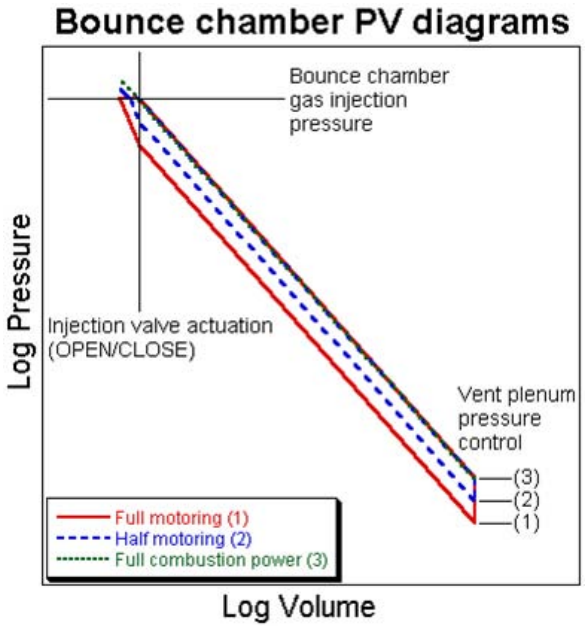

FIGURE 5. BCAC Pressure-Volume Diagrams for Various Operating Modes

bounce chamber cylinder walls. Figure 4 shows the configuration of the BCAC.

Figure 5 shows the pressure-volume diagrams for BCAC operation under three modes. Full motoring mode occurs when no fuel is injected on the combustion side and all power comes from injected air into the bounce chamber. Full combustion power mode means all power comes from engine combustion; no air is injected into the bounce chamber, which acts like a sealed air spring. Half motoring mode is a 50/50 power combination of fuel combustion and bounce chamber air injection. The various compression lines represent different starting pressures for the air in the bounce chamber at the start of the bounce chamber compression stroke (denoted by 1, 2, and 3). This pressure can be determined by controlling the vent plenum pressure. Air injection is by means of a piston-actuated valve that opens and closes at the same point. This valve controls the supply of controlled, high-pressure air (up to 1,000 psi). This ensures the same amount of air is present in the bounce chamber during expansion across all modes of operation. Thus, the quantity of air added to the bounce chamber is controlled by the pressure of the bounce chamber exhaust plenum. By raising the plenum pressure sufficiently, no extra air will be admitted to the bounce chamber, requiring all of the alternator power output and losses to be provided by combustion. A feedback control system can therefore utilize the piston displacement diagnostic to control the plenum pressure as the fuel rate is changed, resulting in a constant compression ratio under all fueling conditions. In addition, during full combustion power mode, control of the vent plenum pressure in the bounce chamber will allow the bounce chamber air to get "topped-off" after every cycle and replenish any air that may have escaped around the bounce chamber piston seals.

The second benefit of the BCAC system is the ability to simulate compression ratio control via load change. In a practical application of the HFPE, the effective compression ratio of the engine can be determined by controlling the electrical load of the linear alternators. An increase in the effective compression ratio of the engine will provide more energy output that can be used to satisfy the increased electrical load (assuming identical fuel type and equivalence ratio). Since the HFPE prototype will have a fixed resistive load without computer control, it's necessary to control the compression ratio with the bounce chambers. The BCAC system allows this flexibility by simultaneously controlling both the injection and vent pressures of the bounce chamber air. When an increase in compression ratio is desired, both the BCAC injection and vent pressures are increased. Figure 6 illustrates this during full motoring in going from a compression ratio of 20 to 40. This boosting method increases the oscillation frequency of the pistons from 23 Hz at 20:1 compression ratio to 28 Hz at 40:1. This allows for increased electrical energy generation by the linear alternators, while at the same time maintaining nearly identical piston travel and BCAC injection valve displacements, critical for proper operation of the BCAC system. In addition, if the linear alternators are unable to absorb all the power produced by combustion, the BCAC system can be configured to operate as an air compressor, pumping air from the low-pressure vent manifold to the

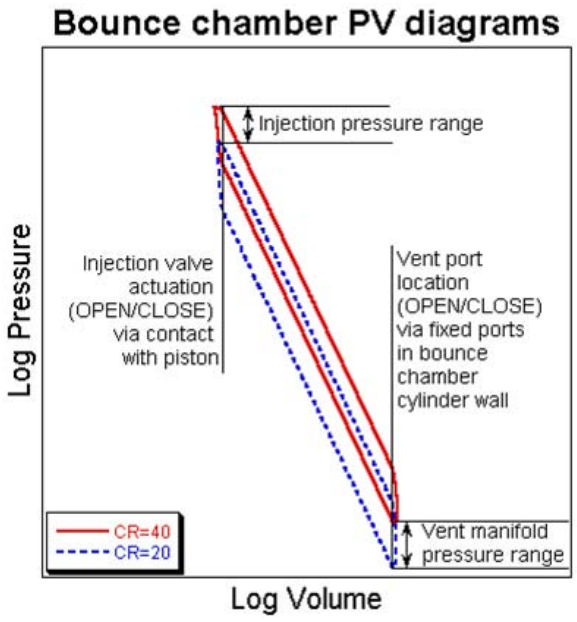

FIGURE 6. BCAC Pressure-Volume Diagrams for Compression Ratio Control

high-pressure injection manifold, thereby serving as an additional load device.

In simulations of the BCAC system, the first stroke was started with both pistons locked at their respective outer ends (bounce chambers fully compressed). The bounce chambers were set to the appropriate pressure (the injection pressure corresponding to the desired compression ratio). The pistons were then released and the high-pressure air in the bounce chambers forced the pistons to compress the air in the combustion chamber to the desired compression ratio. Initially it was hoped that on the HFPE prototype the pistons would not have to be locked and that the bounce chamber and injection valve volumes would be sufficiently small to quickly fill with high-pressure air. However, computational fluid dynamics simulations of the filling process showed inadequate fill times. Thus, a piston lock-and-release mechanism was designed to lock the pistons in place. This mechanism features a cylindrical pin designed to latch into a plate attached to the crown of the bounce chamber pistons and lock the pistons in place. A spring-loaded puller inside of the cylindrical pin is what releases the pin from the piston. This spring-loaded puller is held in place by another transversely-mounted pin, which is removed manually to release the tension on the spring. The current design of the entire piston lock-and-release mechanism will be undergoing a series of experimental tests in a full-scale model in order to optimize cylindrical pin and latch plate strength, contact angles between the pin and plate, as well as spring design.

The opposed-piston configuration was chosen for two main reasons: inherent mechanical balance of overall engine and the opportunity to utilize a central combustion chamber with highly efficient uniflow scavenging via intake and exhaust ports. However, opposed-piston synchronization is critical to sustaining balance and gas exchange, as well as combustion and mechanical durability. Ronald Moses, a consultant, has been modeling opposed-piston synchronization stability for various loads. His model is written in Mathematica and includes a full simulation of piston dynamics, linear alternator electromagnetics, and electrical load circuitry. It also includes simplified gas exchange, energy input, and friction. The model was used to analyze the stability of the HFPE prototype load circuit, which is designed to minimize internal resistive heating of the stator assemblies and reduce required cooling. The analysis has shown that the simple resistive load circuit is effective in maintaining piston synchronization. Future stability modeling efforts will investigate the effect of the BCAC system on piston synchronization and possible active control of the BCAC system as a viable backup approach should passive coupling fail.

In addition to the modeling at Sandia, General Motors is funding work at the University of Michigan to assess the Sandia HFPE potential for improving vehicle fuel economy and emissions as well as stability and compression ratio control. The model will be built in a MATLAB/Simulink framework and feature a zero-dimensional thermodynamic model (including combustion kinetics, scavenging, heat transfer, and friction), a linear alternator model (using various linear alternator and load circuitry designs), a dynamic force balance model, and a BCAC model (to simulate start-up and motoring). The model will be validated by the experimental data of the Sandia HFPE and then be used to explore other conditions beyond the experimental test matrix, such as different fuels and intake conditions.

Conclusions

- HFPE research prototype fabrication and assembly nearly complete.
- Stability modeling of prototype load circuit shows adequate power output and piston synchronization.
- BCAC concept developed to achieve desired resonant piston motion for starting and to test linear alternator coupling before combustion is initiated.
- BCAC will also provide proof-of-concept of variable compression ratio via load control as well as serve as additional load if needed.
- Piston lock-and-release mechanism design complete. Subsystem hardware testing on full-scale component model about to commence.
- Collaboration with GM and University of Michigan on modeling of the Sandia prototype engine and various alternator designs is ongoing.
- Project on track to start and conclude experimental tests in Fiscal Year 2010.

FY 2009 Publications/Presentations

1. Aichlmayr, H.T., Van Blarigan, P. **Modeling and Experimental Characterization of a Permanent Magnet Linear Alternator for Free-Piston Engine Applications** *ASME Energy Sustainability Conference* San Francisco CA, July 19–23 2009.

II.A.14 Optimization of Direct Injection Hydrogen Combustion Engine Performance, Efficiency and Emissions

Thomas Wallner
Argonne National Laboratory
9700 S. Cass Avenue
Argonne, IL 60439

DOE Technology Development Manager:
Gurpreet Singh

Objectives

- Meet the engine efficiency and emissions goals set for hydrogen internal combustion engines by applying advanced mixture formation and combustion techniques.
- Gain understanding of mixture formation and combustion phenomena in hydrogen engines as a basis for goal-oriented optimization steps.
- Evaluate the effectiveness of combining advanced injection strategies with in-cylinder emissions reduction measures.

Accomplishments

- Employing a multiple injection strategy allows maintaining the same engine efficiency as achieved with single injection while reducing oxides of nitrogen (NOx) emissions by as much as 85%.
- Evaluated the potential of exhaust gas recirculation (EGR) for NOx emissions reduction and found that an emissions reduction of up to 70% is feasible with an efficiency loss of approximately 1%.
- Tests using a single-hole nozzle injector showed that in general injection towards the spark plug is beneficial for engine efficiency but results in higher NOx emissions.
- Integrated three-dimensional (3-D) computational fluid dynamics (CFD) simulation in the analysis and optimization process in close coordination with the optical experiments performed at Sandia National Laboratories.

Future Directions

- Upgrade research engine to optimized bore-stroke ratio.
- Expand efficient operating regime to higher speeds using Piezo-driven injectors.
- Continue developing improved injector nozzle designs for specific operation conditions (injector location, injection strategy) supported by optical engine results (Sandia National Laboratories) and 3-D CFD simulation.
- Combine optimized mixture formation strategies with in-cylinder NOx emissions reduction measures.

Introduction

Hydrogen is widely considered an excellent alternative fuel and deemed one of the most promising energy carriers for a future transportation scenario [1]. During the past several decades extensive research of hydrogen as a fuel for use in internal combustion engines has been performed. The U.S. Department of Energy has set challenging targets for the performance and emissions behavior of hydrogen combustion engine vehicles including a peak brake thermal efficiency of 45%, NOx emissions as low as 0.07 g/mile and a power density comparable to gasoline engines [2]. Hydrogen direct injection was found to be a preferable mixture formation concept mainly due to the increased power density and the potential of reducing NOx emissions compared to port injection [3].

Approach

Argonne National Laboratory's Engines and Emissions Group operates a single-cylinder hydrogen engine employing high-pressure direct injection. The research engine is set up for running real-world test conditions including turbocharging and supercharging as well as external EGR in combination with direct injection. Test programs and standardized mapping points are developed in close collaboration with Ford Motor Company and Sandia National Laboratories. Since high-pressure direct injection requires the use of advanced injection equipment for hydrogen capable of operating safely and reliably at pressures in excess of 100 bar that are not commercially available, a lease contract for high-pressure prototype injectors has been established with Westport Power Inc.

Results

Understanding of Basic Mixture Formation Characteristics

A simple injector nozzle with a single injection hole was designed with the injector mounted in a central location adjacent to the spark plug. The injection hole

is located under an angle of 50° to the injector axis. The single-hole design was purposely chosen to simplify the setup and guarantee a single injection jet avoiding any jet-to-jet interaction inside the combustion chamber [4]. Various injection directions were investigated as part of this study. An injection angle ϕ was defined to distinguish between injection directions with ϕ=0° referring to the injection directions towards the spark plug. Injection directions of 0, 45, 90, 180, 270 and 315° were investigated.

In order to fully investigate each configuration a sweep of start of injection (SOI) was performed for each injection direction. This sweep was started out with early injection shortly after intake valve closing (SOI=140 degrees crankangle [°CA] before top dead center [BTDC]) and SOI was retarded with a step width of 20°CA until the end of injection coincided with spark timing or stable combustion could not been maintained. Combustion is generally considered stable if the coefficient of variation of indicated mean effective pressure does not exceed a certain threshold. It was observed that retarding the SOI for certain configurations resulted in misfires and incomplete combustion events with unburned hydrogen exceeding 20,000 ppm.

At low engine loads the injection duration is short and late injection timings (SOI=20°CA BTDC) can be realized. However, as can be seen in Figure 1, these late injection cases cannot be realized for all injection angles. The dots indicating tested operating points clearly show that the late injection case with SOI=20°CA BTDC could only be run with injection towards the spark plug. The reason for the limitations in start of injection is likely due to the stratification resulting from late injection. Given that the overall air/fuel ratio for this particular operating point is very lean (Φ~0.25) an unfavorable stratification could result in zones with air/fuel ratio less than the lower flammability limit (Φ~0.1) in the vicinity of the spark plug. Only an injection towards the spark plug with very late SOI ensures that there is sufficient hydrogen in the spark plug area to create an ignitable mixture. The strong effect of stratification can also be seen when analyzing the NOx emissions data for this particular load point (Figure 1). Due to the extremely lean overall air/fuel ratio the NOx emissions are generally remarkably low

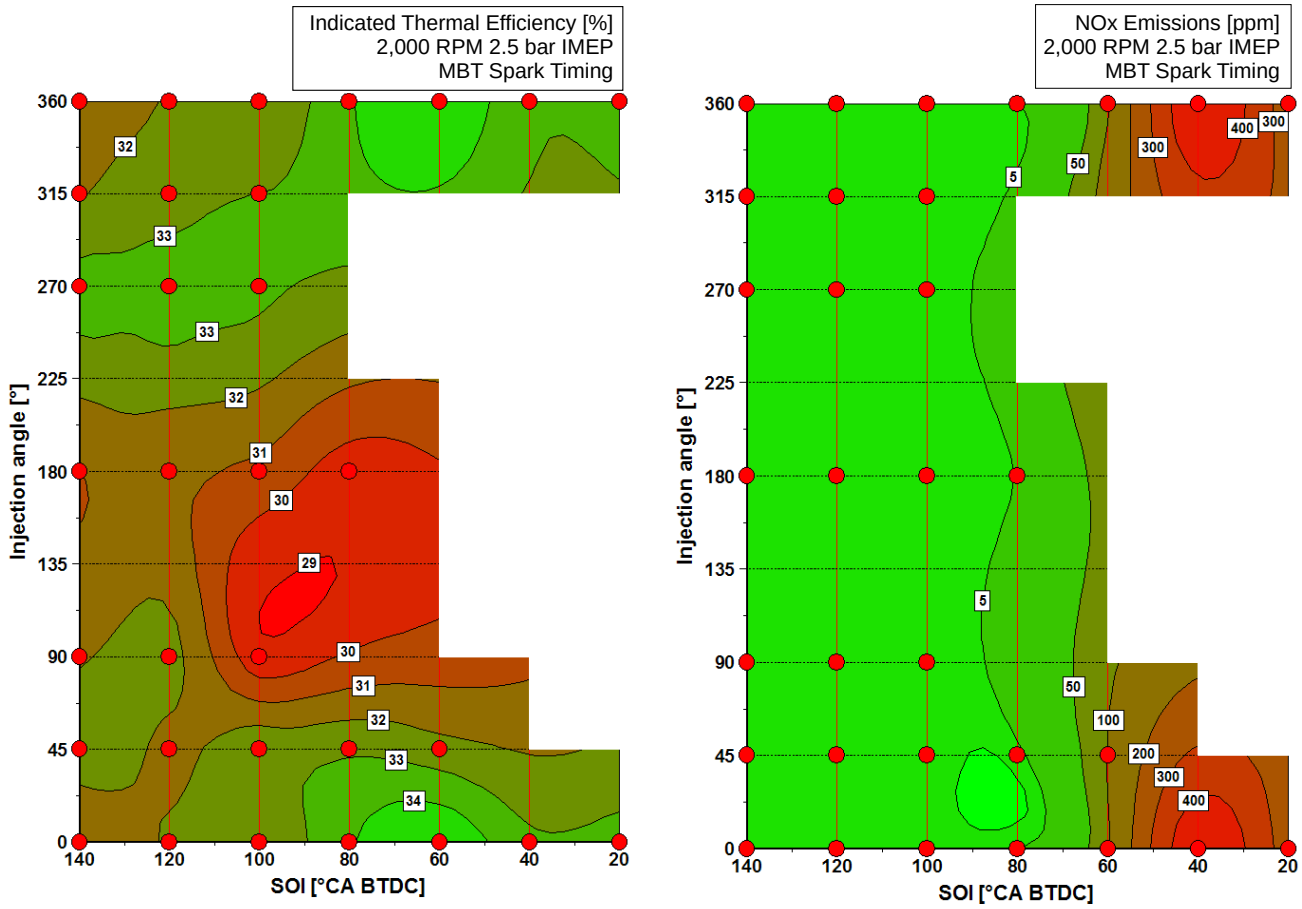

FIGURE 1. Indicated efficiencies (left) and NOx emissions (right) as a function of SOI and injection angle for low load (2.5 bar IMEP).

with levels of 5 ppm or less for all cases with relatively early injection (SOI=80°CA BTDC or earlier). However, further retarding the SOI, which was only possible with injection towards the spark plug, resulted in a dramatic increase in NOx emissions. This is due to the fact that a late SOI with injection angle towards the spark plug results in mixture stratification effects with local zones that have a much richer air/fuel ratio than the very lean overall air/fuel ratio. As can be seen from Figure 1 optimization of injection angle and SOI can result in a dramatic increase in engine efficiency without a penalty in NOx emissions. As an example an injection away from the spark plug (ϕ=180°) with an SOI of 80°CA BTDC yields an indicated thermal efficiency of 30% at an emissions level of 5 ppm. Changing the injection angle to ϕ=0° (injection towards the spark plug) at the same start of injection results in an engine efficiency of 34% at an identical NOx emissions level.

Figure 2 shows the mixture at spark timing in two orthogonal sections resulting from 3D-CFD simulation. For the early injection timing in Figure 2a, at the time of spark an ignitable mixture is located in a broad region around the spark plug with a local equivalence ratio Φ of about 0.4. This suggests that the resulting mixture can burn reliably as observed from engine testing (Figure 1). Even though a large amount of hydrogen is still located far from the spark location, in most of the combustion chamber an ignitable mixture (Φ 0.1) is present. Early injection provides enough time for some mixture homogenization. For injection towards the spark plug along the pent roof (ϕ=0°) stable operation could be maintained for late injection (SOI=40°CA, Figure 1). The corresponding simulation results, visualized in Figure 2b, again show an ignitable mixture present near the spark plug ($\Phi\approx$0.2). However, as opposed to early injection, this is directly due to the injector aiming towards the spark plug. The bulk of the fuel has already passed the spark plug, but the wake of the jet still contains enough fuel to ignite, with the flame kernel then presumably growing towards richer mixtures, where the most of the heat release and NOx formation will take place.

Figure 2c shows simulation results for injection towards the intake valves (ϕ=90°). Again the jet wake can be distinguished clearly, but the fuel remaining in the wake is too far away from the spark plug. Simulation results are shown here for timings close to top dead center (TDC) only, but in performance testing the engine could not be run stably with any reasonable spark timing. This is consistent with the near-nozzle regions of a jet leaning rapidly after end of injection due to enhanced entrainment [5], leaving not enough fuel behind to convect or diffuse to the spark plug if it is not located directly in the jet wake.

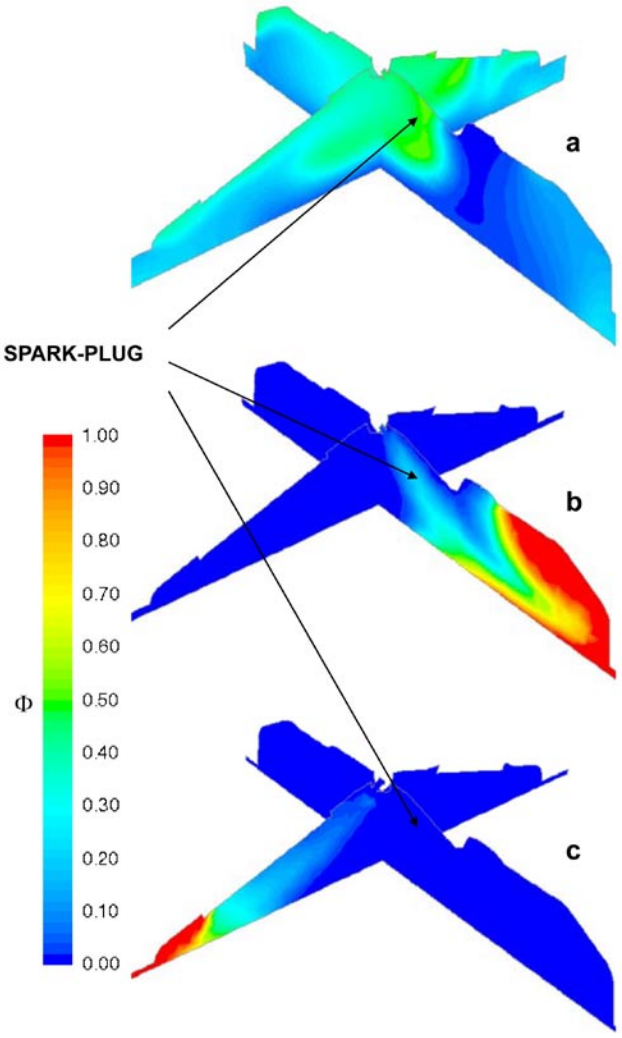

FIGURE 2. Simulated equivalence ratio (Φ) at maximum brake torque (MBT) spark timing for:
a) Injection angle of 0° and SOI = -140°CA (MBT=-23°CA);
b) Injection angle of 0° and SOI = -40°CA (MBT=-8°CA);
c) Injection angle of 90° and SOI = -40°CA (MBT=TDC)

NOx Emissions Reduction at Constant Engine Efficiency using Multiple Injection Strategy

In order to prove the emissions reduction potential with multiple injections the load area relevant for this study was limited to medium and high engine loads where conventional port injection and direct-injection strategies struggle to meet stringent emissions regulation. Multiple injection strategies are compared to a single injection strategy which is used as a baseline to quantify efficiency and emissions effects. In addition to varying the fraction of hydrogen injected during the first and second pulse the SOI of the second injection pulse was varied as well to allow identification of an optimum configuration.

The trade-off between indicated thermal efficiency and NOx emissions for the medium load case (6 bar indicated mean effective pressure [IMEP]) at 1,000 RPM is summarized in Figure 3. The graph shows the results for all injection directions and all investigated injection strategies. This includes single injection only as well as ratios of primary to secondary injection of 80, 70 and 60% as well as 50% for selected injection directions. A general trend of reduced emissions with decreased engine efficiency can be observed – however, certain combinations of multiple injections allowed a significant reduction in NOx emissions with a simultaneous increase in engine efficiency.

Plotting indicated efficiencies as a function of injection direction and ratio of primary versus secondary injection allows identifying promising injection strategies (Figure 4). The achievable efficiencies range from 27% to approximately 31%. The lowest efficiency results from multiple injections towards the intake valve (ϕ=45°) and intake quenching zone (ϕ=90°) at larger proportions of fuel injected during the second pulse (60%). Similarly low efficiencies are achieved when using multiple injections towards the exhaust valve (ϕ=315°) or exhaust quenching zone (ϕ=270°). The highest efficiencies result from multiple injections towards the spark plug with 70% of the fuel injected during the first injection pulse. For the same ratio of primary to secondary injection the highest efficiency is achieved with injection towards the spark plug (ϕ=0° and ϕ=360°, respectively) followed by injection away from the spark plug (ϕ=180°). Injection towards the valves and quenching zones both on the intake and exhaust side results in reduced engine efficiency. Further analysis of the pressure traces and heat release rates revealed that there were only slight differences in the combustion duration and peak heat release rates which would not explain the differences in efficiency. However, the injection direction also influences the location of the diffusion flame resulting from the second injection pulse. One could hypothesize that an injection towards the spark plug and consequently right into the center of the combustion chamber will result in reduced wall heat losses compared to an injection away from the spark plug. The resulting diffusion flame might even burn closer to the combustion chamber walls for injection directions towards the valves and quenching zones resulting in a further increase in wall heat losses and consequently lower indicated thermal efficiencies.

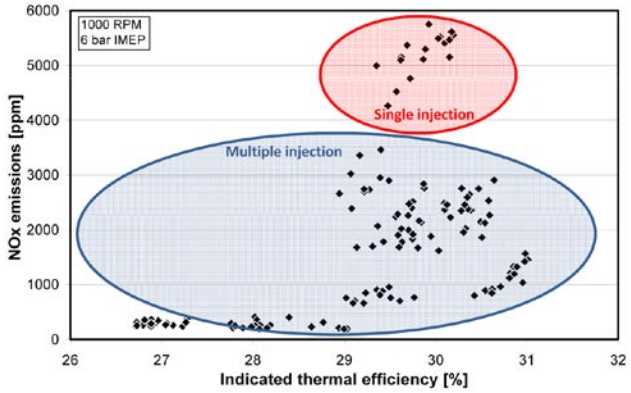

FIGURE 3. Trade-off between indicated efficiency and NOx emissions with single and multiple injection strategies for various injection directions.

Aside from significant impact on engine efficiency and combustion characteristics the injection strategy also dramatically influences the emissions behavior. There is a strong correlation of NOx emissions and global air/fuel ratio. For direct injection strategies and in particular for stratified injection or multiple injection operation the local air/fuel ratios determine the overall emissions signature. Figure 4 summarizes the effect of ratio of primary to secondary injection and injection angle on NOx emissions for an engine speed of 1,000 RPM and medium engine load (6 bar IMEP). The start of the second injection as well as the spark timing was set to achieve maximum brake torque. It is apparent from this graph that the ratio of primary to secondary injection has a strong influence on the engine-out emissions. Compared to the influence of the injection ratio the injection directions show only a minor impact on NOx emissions with advantages of injection directions towards the valves and quenching zones both on the intake and exhaust side compared to injection towards or away from the spark plug. The more dominant impact of the ratio of primary versus secondary injection can be explained by using the global NOx characteristics and applying them to localized zones.

Early direct injection (100% ratio of primary to secondary injection) results in a fairly homogeneous mixture at the end of the compression stroke. The global air/fuel ratio for this particular load point is around Φ~0.75 resulting in very high NOx emission in excess of 5,000 ppm for the 100% ratio case. Applying a multiple injection strategy obviously reduces the NOx emissions with improvement being closely related to the split ratio of the injections.

Overall a multiple injection strategy with an advantageous split of primary versus secondary injection allows avoiding the NOx critical air/fuel ratio regimes by locally forming rich and lean mixtures.

NOx Emissions Reduction using Exhaust Gas Recirculation

Experiments with external EGR were performed at various loads at an engine speed of 2,000 RPM, which is representative for typical automotive applications. Operating points of 4 bar IMEP as a typical medium load point and 8 bar IMEP as a typical high load point were investigated. A 13-hole injector in central location

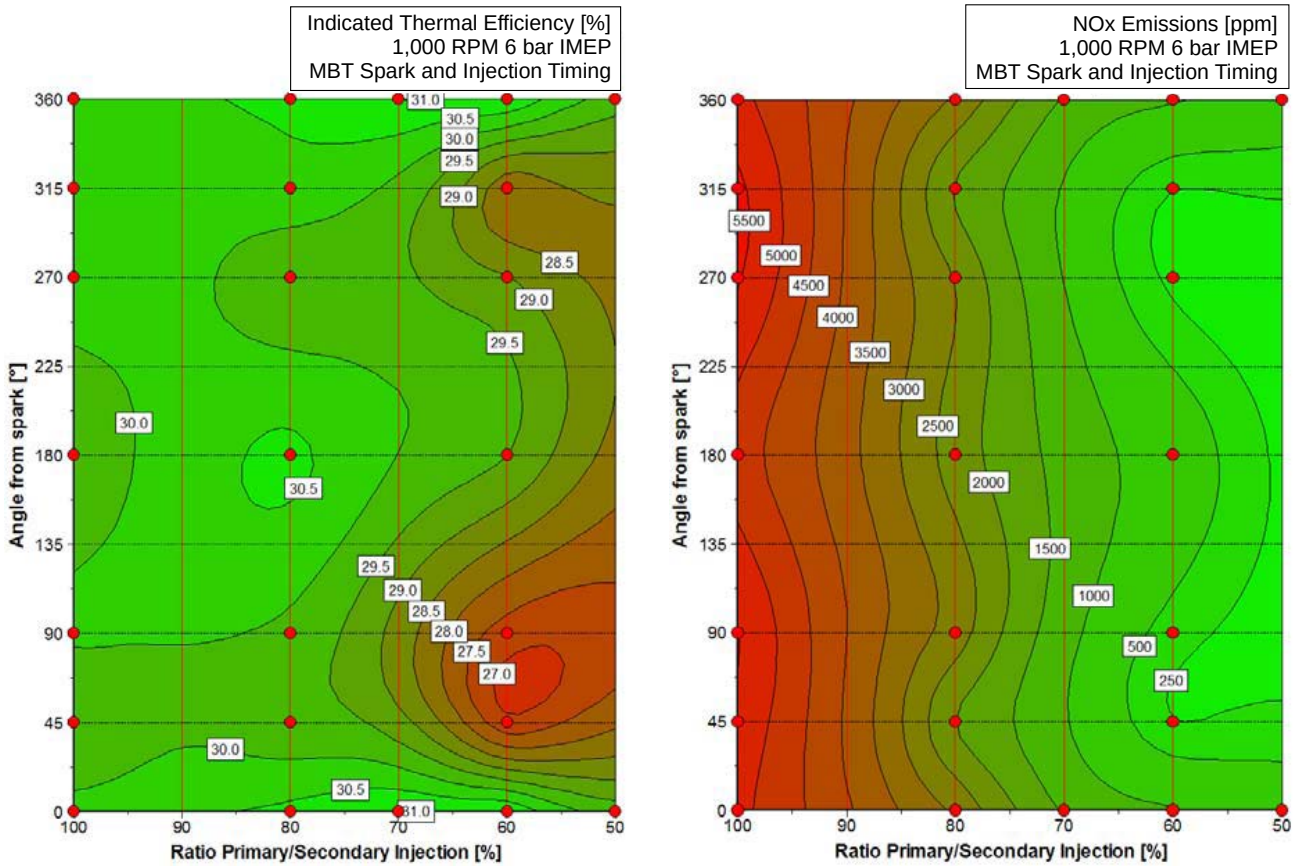

FIGURE 4. Indicated efficiencies (left) and NOx emissions (right) as a function of injection direction and ratio between primary and secondary injection.

was used for these tests, the injection timing was held constant at 80°CA BTDC for the high load point and 20°CA BTDC for the medium load point. Tests were run for both, uncooled as well as cooled EGR and their effectiveness for NOx emissions reduction and engine efficiency impact were compared to water injection. All results were collected running the engine at wide-open-throttle (WOT) conditions with the load adjusted by changing the amount of hydrogen injected.

Figure 5 shows the cylinder pressure traces and heat release rates for several EGR levels at the high load point of 8 bar IMEP. With increased EGR rate the combustion duration increases while the peak heat release rate decreases. This might be counterintuitive at first since the overall relative air/fuel ratio for the higher EGR cases is much richer than without EGR suggesting higher flame speeds. However, the presence of exhaust gas as an inert constituent reduces the speed of the combustion process.

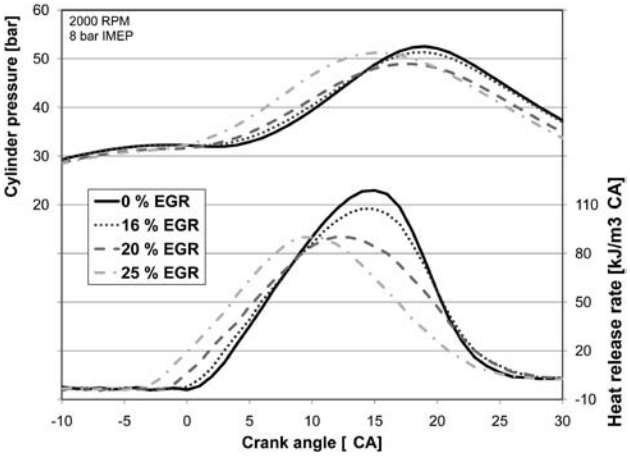

FIGURE 5. Influence of EGR on pressure traces and heat release rates at high engine load.

The effectiveness of EGR can be evaluated by comparing the NOx emissions reduction potential versus the related loss in indicated thermal efficiency to water injection as an alternative measure for in-cylinder emissions reduction. Figure 6 compares the results of this EGR study to water injection experiments previously performed on this research engine [6]. Because the results are from different injection configurations and injection strategies the emissions reduction measures are compared on a relative basis. At the medium engine load a NOx emissions reduction of up to 40% compared to the base case could be achieved with water injection

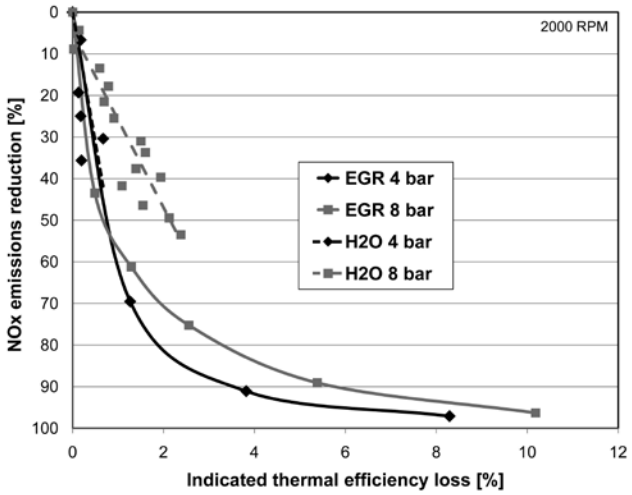

FIGURE 6. Comparison of EGR versus water injection in terms of NOx emissions reduction potential and related efficiency loss for medium and high engine load.

at a respective loss in indicated thermal efficiency below 1%. These reductions were achieved at moderate amounts of water injection and similar results could be achieved with EGR. At the high engine load of 8 bar IMEP EGR proves itself to be even more effective than water injection. A NOx emissions reduction of 50% with water injection resulted in a loss in indicated thermal efficiency of around 2% whereas a NOx emissions reduction in excess of 60% could be achieved with EGR at a respective efficiency loss of slightly more than 1%.

EGR cooling did not show any significant advantages in engine efficiency or NOx emissions reduction compared to the uncooled case but is expected to add additional complexity to the EGR setup and might also cause complications due to condensation.

Conclusions

- Especially at low engine load injection towards the spark plug also results in the widest range of injection timings that can be operated at stable conditions allowing very late injection resulting in significant efficiency improvements compared to other strategies; however, an optimization solely based on engine efficiencies might result in configuration with dramatically increased NOx emissions.
- 3-D CFD simulation is employed as an additional tool to gain further insight into the mixture formation processes of hydrogen internal combustion engines.
- It is possible to maintain the same engine efficiency as achieved with single injection by employing multiple injection strategies while reducing NOx emissions by as much as 85%.
- Employing EGR provides significant reductions in NOx emissions in excess of 90% relative to operation without EGR can be achieved at medium as well as high engine load; however, the recirculation of exhaust gas also resulted in a loss in indicated thermal efficiency of up to 10% with high EGR rates relative to the base case without EGR.
- A NOx emissions reduction of 50% with water injection resulted in a loss in indicated thermal efficiency of around 2% whereas a NOx emissions reduction in excess of 60% could be achieved with EGR at a respective efficiency loss of slightly more than 1%.

References

1. Wimmer, A., Wallner, T., Ringler, J., Gerbig, F. 'H2-Direct Injection – A Highly Promising Combustion Concept.' SAE Paper 2005-01-0108. SAE World Congress. 2005.

2. U.S. Department of Energy, FreedomCAR and Fuel Technical Partnership Technical Goals, Washington, D.C., 2002.

3. Ringler, J., Gerbig, F., Eichlseder, H., Wallner, T. 'Insights into the Development of a Hydrogen Combustion Process with Internal Mixture Formation.' 6th International Symposium on Combustion Diagnostics. Baden-Baden. Germany. 2004.

4. Kovac, K., Wimmer, A., Hallmannsegger, M., Obieglo, A., Mixture formation and combustion in a hydrogen engine – A challenge for the numerical simulation, Proceedings Motorische Verbrennung – aktuelle Probleme und moderne Lösungsansätze, 2005.

5. M.P.B. Musculus, K. Kattke, Entrainment Waves in Diesel Jets, SAE Paper 2009-01-1355 (2009).

6. Nande, A., Wallner, T., Naber, J. "Influence of Water Injection on Performance and Emissions of a Direct-Injection Hydrogen Research Engine." SAE International Powertrains, Fuels and Lubricants Meeting, Chicago/IL, 2008.

FY 2009 Publications/Presentations

1. Wallner, T.: 'Opportunities and risks for hydrogen internal combustion engines in the United States.' Der Arbeitsprozess der Verbrennungskraftmaschine. Graz / Austria. 2009

2. Wallner, T.; Scarcelli, R.; Lohse-Busch, H.; Wozny, B.; Miers, S.: 'Safety Considerations for Hydrogen Test Cells.' 3rd International Conference on Hydrogen Safety (ICHS3). Ajaccio/France. 2009

3. Scarcelli, R.; Wallner, T.; Salazar, V.; Kaiser, S.: 'Modeling and Experiments on Mixture Formation in a Hydrogen Direct-Injection Research Engine.' 9th International Conference on Engines and Vehicles (ICE2009). Capri/ Italy. 2009

4. Wallner, T.; Nande, A.; Scarcelli, R.: 'Evaluation of exhaust gas recirculation (EGR) in combination with direct injection (DI) on a Hydrogen Research Engine.' World Hydrogen Technology Convention. New Delhi/India. 2009

5. Wallner, T.; Scarcelli, R.; Nande, A.; Naber, J.: 'Assessment of Multiple Injection Strategies in a Direct Injection Hydrogen Research Engine.' 2009 SAE International Powertrains, Fuels and Lubricants Congress. Florence/Italy. 2009

6. Wallner, T.; Nande, A.; Naber, J.: 'Study of Basic Injection Configurations using a Direct-Injection Hydrogen Research Engine.' SAE World Congress. Detroit / MI. 2009

7. Salazar, V.; Kaiser, S.; Nande, A.; Wallner, T.: 'The influence of injector position and geometry on mixture preparation in a DI hydrogen engine.' 9th International Congress 'Engine Combustion Process - Current Problems and Modern Technologies'. Munich/Germany. 2009

II.A.15 Advanced Hydrogen-Fueled ICE Research

Sebastian A. Kaiser
Sandia National Laboratories
P.O. Box 969, MS 9053
Livermore, CA 94551

DOE Technology Development Manager:
Gurpreet Singh

Objectives

The hydrogen internal combustion engine (H_2ICE) project aims to provide the science base for the development of high-efficiency hydrogen-fueled vehicle engines. The technical focus is on direct-injection strategies, using laser-based in-cylinder measurements closely tied to numerical simulations, which are performed by both Sandia-internal and external collaborators. Knowledge transfer to industry and academia is accomplished by publications, collaborations, and dedicated working-group meetings.

Specifically, at this point the goals of the project are to:

- Quantify the influence of injection strategies on pre-combustion in-cylinder mixing of fuel and air.
- Complement metal-engine research and development at Ford and single-cylinder engine research at Argonne National Laboratory (ANL).
- Provide data for and help in development of large eddy simulation (LES) as well as industrially applicable computational fluid dynamics (CFD) modeling.
- Investigate influence of charge stratification on the combustion event and nitric oxide formation.

Accomplishments

- Assembled extensive image database on fuel/air mixing in a direct-injection hydrogen engine (DI-H_2ICE).
- Investigated a broad range of injection strategies and injector-nozzle geometries with realistic injection pressures.
- Used optical fuel-distribution measurements to validate an industrially applicable CFD simulation of mixture formation in DI-H_2ICEs (calculations at ANL).
- Assembled accurate solid model of engine head to enhance the value of the optical measurements as a reference database for simulation validation.
- Substantially improved inter-laboratory coordination of research activities with ANL to increase synergies.

Future Directions

- Complete database on hydrogen/air mixture preparation with in-cylinder velocity measurements for selected injection strategies.
- Install new engine head, supplied by Ford, featuring central or side injection and central ignition.
- Supplement quantitative laser-based techniques with qualitative high-speed Schlieren measurements to understand temporal development mixture formation.
- Use planar laser-induced fluorescence of hydroxyl radicals (OH-PLIF) to investigate combustion with multiple injections per cycle.
- May publish optical data and boundary conditions on the Web via Sandia-led "Engine Combustion Network" [1], an interactive database.

Introduction

H_2ICE development efforts are focused to achieve an advanced hydrogen engine with peak break thermal efficiency greater than 45%, near-zero emissions, and a power density that exceeds gasoline engines. Such advanced engines can be part of a powertrain with efficiency similar to systems based on fuel cells [2]. With respect to these efforts, the DI-H_2ICE is one of the most attractive options [3]. With DI, the power density can be approximately 115% that of the identical engine operated on gasoline. In addition, the problems of pre-ignition associated with port-fuel-injection can be mitigated. Lastly, in-cylinder injection offers multiple degrees of freedom available for controlling emissions and optimizing engine performance and efficiency.

The challenge with DI-H_2ICE operation is that in-cylinder injection affords only a short time for hydrogen-air mixing, especially when start of injection (SOI) is retarded with respect to intake-valve closure (IVC) to reduce the compression work of the engine and to mitigate preignition. Since mixture distribution at the onset of combustion is critical to engine performance, efficiency, and emissions, a fundamental understanding of the in-cylinder mixture formation processes is necessary to optimize DI-H_2ICE operation. At the same time, predictive simulation tools need to be developed to be able to optimize injection and combustion strategies.

Correct prediction of mixture formation before the onset of combustion is of great importance for any engine simulation. Quantitative imaging of this process in Sandia's optically accessible H_2ICE can therefore provide a benchmark test for advanced and industrially applicable computations.

Approach

The engine in Sandia's H_2ICE laboratory is a fully optically accessible, passenger-car sized single-cylinder engine with spark ignition and direct high-pressure injection of gaseous hydrogen. Previously, a fluorescence technique had been improved to fit the requirements of hydrogen fuel (Publication 1, SAE paper 2009-01-1534). This fiscal year, that quantitative imaging technique was used to make extensive measurements of the fuel injection and subsequent mixture formation. The objective was to increase both physical understanding as well as to establish a reference database for concurrent and future development of simulation tools for H_2ICEs. A broad array of injector nozzles, injector locations, injection timings, and fuel pressures was tested. The chosen operating point, with a global equivalence-ratio of 0.25 at 1,500 rpm is a low-load point where efficiency can greatly profit from suitable mixture stratification. The nozzle geometries investigated included both multi-hole designs, which are likely to be used in production engines, as well as a single-hole nozzle, which proved to be very valuable in initial simulation validation.

Imaging of the fuel distribution was performed in the motored engine between the SOI and an estimated "spark" timing. For the latter, the spark timing for maximum brake-torque in ANL's fired thermodynamic engine was taken as an estimate of when mixture formation should be viewed as completed in the motored optical engine. For most injector configurations, the fuel dispersion during the compression stroke is highly three-dimensional. Therefore, images in two orthogonal sets of planes were acquired, yielding a complete picture of mixture formation. As an example, Figure 1 shows measurements for one particular data set arranged in their positions and orientations with respect to the engine geometry. During and shortly after the injection, measurements in a vertical plane intersecting the injector's axis capture most of the relevant details. Late in the compression stroke, with the geometry of the remaining cylinder volume now more "pancake-like", most of the information can be captured by an array of horizontal planes. In between, both sets of planes are necessary to understand the convection and dispersion of the fuel cloud.

In a separate project, researchers at Sandia (principal investigator J. Oefelein) are developing an LES as a detailed, high-fidelity model of in-cylinder processes. The optically accessible hydrogen engine

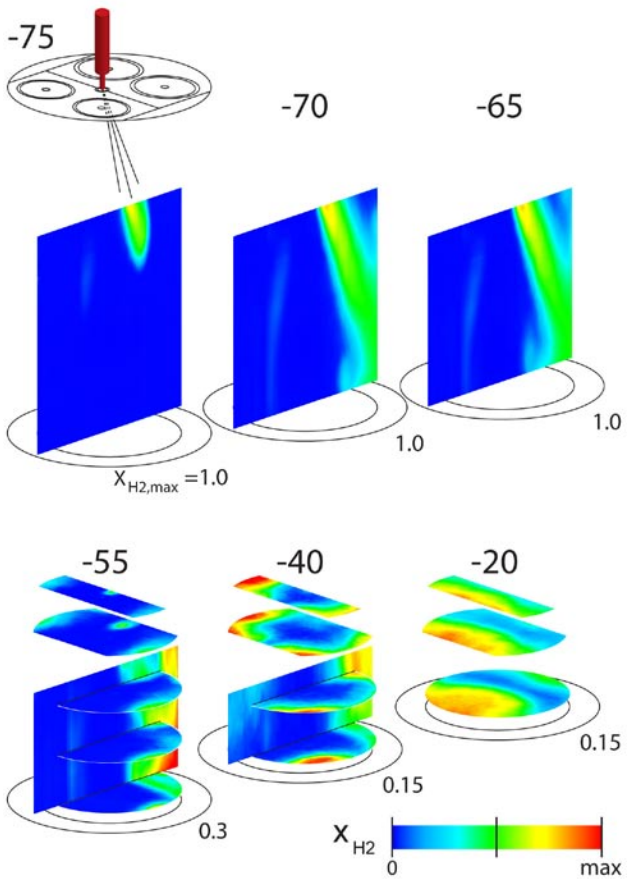

FIGURE 1. Time series of mean fuel mole-fraction x_{H2} in two orthogonal sets of planes for injection from a single-hole injector with SOI = -80° crank angle (CA). The crank angle of the measurement is indicated above each image assembly. The color scale varies as indicated below the images. The vertical dimension has been stretched by about a factor of three to better visualize the stacked horizontal planes. Piston top and engine-head geometry are shown schematically. Note that the valves are not in a flat configuration in the actual engine, but in the pent-roof geometry typical for spark-ignition engines.

is one of the first test cases for this model. Data from the current study are being used to validate the simulation. Through validation, this simulation will ideally complement optical experiments in providing detailed physical understanding of in-cylinder processes. However, what is also needed is a tool to perform cruder, but computationally less expensive simulations that industry can apply to optimize the combustion strategy. Such a simulation is being developed at ANL (principal investigator T. Wallner) using the commercially available CFD code FLUENT™. Our group closely works with ANL to validate this simulation, and in turn to use computational results to augment the investigations in the optical engine. This collaboration is within the continuing work of the H_2ICE working group, led by ANL, Ford, and Sandia.

Results

Detailed results on the temporal evolution of the in-cylinder fuel concentration, as measured by planar laser-induced fluorescence of acetone as a tracer for hydrogen fuel, can be found in Publication 3, SAE paper 2009-01-2682. As an example of the observed phenomena, Figure 2 shows the mixture formation process for an asymmetric 5-hole injector, mounted in side position, with the holes pointing upwards as shown in the accompanying sketch of the nozzle pattern.

Three different injection timings were used: the earliest timing possible after IVC (SOI = -140°CA), intermediate timing (SOI = -80°CA), and the latest timing for which stable operation was possible in ANL's all-metal engine (SOI = -40°CA). For the earliest injection timing, with low cylinder pressure at the time of injection, the fuel quickly penetrates the cylinder. In the remainder of the compression stroke, the fuel cloud convects back towards the injector through extensive jet/wall interaction. Despite the long time for mixture formation, significant stratification, mostly in the horizontal direction, remains at the end of the compression stroke. The intermediate injection timing also results in jet/wall interaction, but there is not enough time for the fuel cloud to complete its tumble-like circumferential motion through the cylinder volume all the way back to the injector. The optical measurements imply that this injector configuration could perform well with late injection, since for SOI = -40°CA the fuel is concentrated near the centrally located spark plug, away from the cylinder walls.

For this injector, the image sets taken during injection (earliest measurements for each injection timing) show strong asymmetry of the emerging jet pattern. This is not due to imperfections in the nozzle holes. Rather, inspection of single-shot images (not shown) shows that there are large shot-to-shot fluctuations of the distribution of fuel between the jets. It appears that there is partial jet merging, influenced by large-scale turbulent fluctuations in the jet periphery, resulting in cycle-to-cycle variations of the fuel distribution. Measurements using a 6-hole injector with a slightly greater angle between jets (45° versus 35° for the 5-hole) showed no jet merging, while in imaging of the jets emerging from a 13-hole injector with a narrower angle (30°) total collapse of all 13 jets into one is visible (see Publication 3, SAE paper 2009-01-2682 for images). Thus the spacing and angle between the holes in the 5-hole injector may represent the limiting case for jet merging under the currently investigated conditions.

A feature that was also observed with other injector configurations can be seen in Figure 2: for early injection, remarkably little fuel remains near the injector after the injection event is over. This "leaning" of the

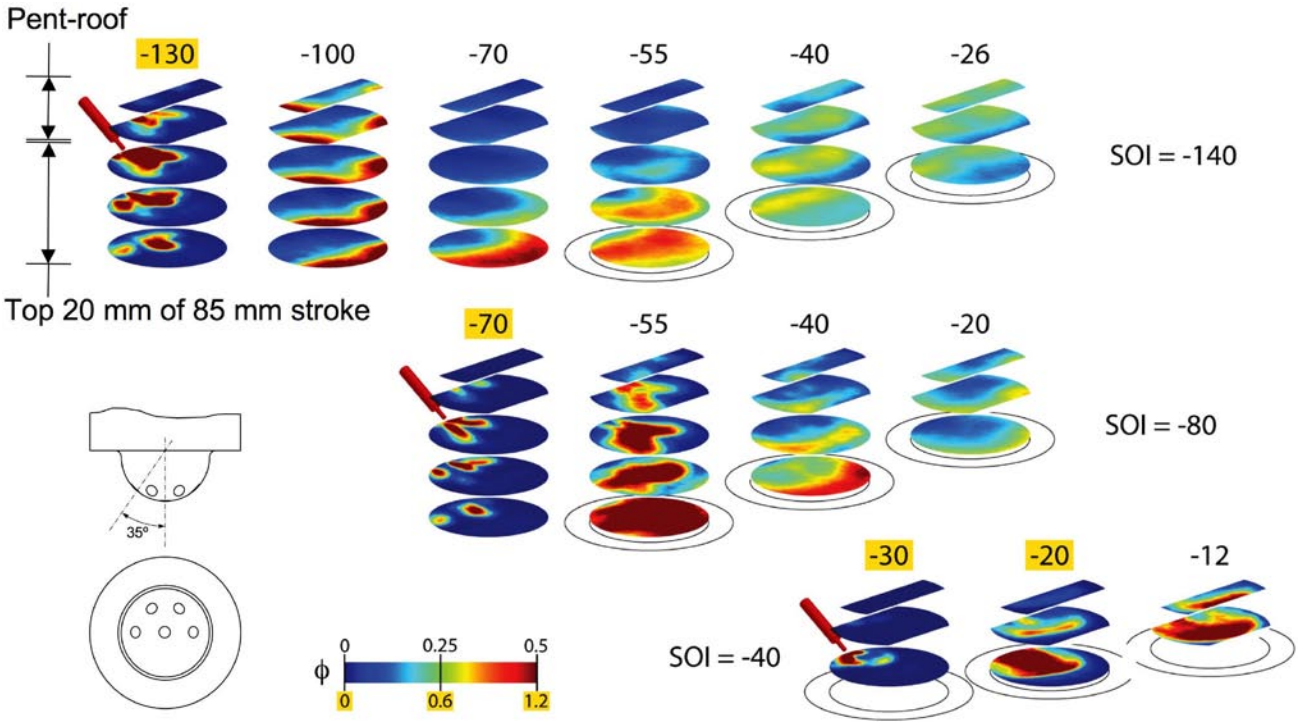

FIGURE 2. Mean equivalence-ratio fields for injection from the asymmetric 5-hole injector with the holes pointing upwards, mounted in side position. In the cylinder bore, the central 65 mm of the 92 mm bore are visible. Injection pressure 100 bar, intake pressure 1 bar, 1,500 rpm. The equivalent homogeneous, global equivalence ratio is 0.25.

near-nozzle region is quite generic in transient jets, and it has also been observed in the gas phase of diesel jets [4]. Musculus [5] uses a simple model to explain the associated enhanced entrainment of ambient bulk gas. An important implication of this is that when the injector is mounted near the spark plug (as with central injection) the fuel will have to be re-directed towards the spark, which will limit how late injection can be timed.

For all injector configurations, the intermediate injection timing, SOI = -80°CA, is an interesting case in that the fuel jets interact with the walls and themselves much more than for later injection, yet the final mixture is much more inhomogeneous than it is for earlier injection. Thus, one would expect large differences in the final mixture stratification between different configurations. Figure 3, top, directly compares the fuel distributions at the time of "spark" for different multi-hole-injector configurations. Surprisingly, the fuel distributions for all five configurations are quite similar. All feature a very lean zone in the center, with equivalence ratios of 0.1 and less, and conversely most of the fuel is concentrated towards the side walls of the combustion chamber, with peak equivalence ratios of 0.3 to 0.45. Much fuel may even be outside of the field of view. Also, in all configurations horizontal inhomogeneity dominates vertical stratification, i.e., in each image set all planes are similar. From a practical point of view all five spatial distributions are unfavorable, since fuel is located next to the wall and would burn with high heat and crevice losses. Figure 3, bottom, plots the combustion stability as a function of SOI for the 6-hole injector in side position. Performance testing at Sandia and ANL does not match perfectly, yet, consistent with the above result, it shows that intermediate injection timings result in less stable operation than both early and late injection. No effort was made here to optimize the piston-top surface to redirect the jets in a favorable way, as for example in many wall-guided gasoline DI systems. Nevertheless, it can be seen that only for very late injection the fuel can be expected to actually be anywhere near the injector at the time of spark.

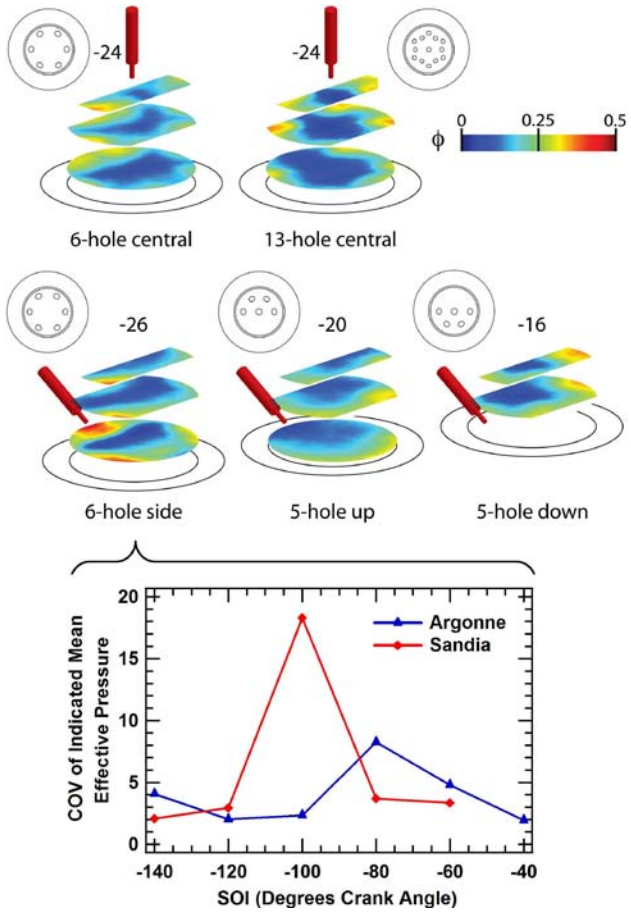

FIGURE 3. Top: Fuel distribution towards the end of the compression stroke for five different injector configurations with intermediately retarded injection (SOI = -80°CA). Images were taken at maximum break-torque spark timing (crank angle indicated above each image stack) as determined in the fired metal engine at ANL. Bottom: Coefficient of variation (COV) for the 6-hole injector in side location as a function of injection timing. Measurements in Sandia's optical engine and ANL's metal engine are shown. Operating conditions as for Figure 2.

As introduced above, an industrially applicable CFD simulation of DI operation of a hydrogen-engine is being developed at ANL so that future optimization of injection and combustion strategies can be accelerated. An initial comparison for a single-hole injector in one particular configuration is presented in Publication 3, SAE paper 2009-24-0083. To summarize the results, the fuel penetration is captured qualitatively correct for late and intermediate injection timings, but the fuel dispersion is underestimated. This results in a pre-spark mixture that is more stratified than what is observed experimentally. Part of this discrepancy seems to result from mesh dependence of the simulation in near-wall regions. Also, the jet-induced turbulence may not be predicted correctly. To investigate both aspects more closely, fuel imaging in the vertical plane during and shortly after injection was performed. For the chosen single-hole injector in central location, this phase of the mixture formation has intense jet/wall interaction, in addition to the highly turbulent hydrogen jet. Imaging from the side with a vertical laser sheet yields a field of view that includes both the cylinder wall and the piston top, where the jet impinges.

Figure 4 shows a comparison of the ensemble-averaged fuel mole-fraction as measured in the optical engine compared to the prediction by the FLUENT™ calculation. The simulation employed a commonly used variation of the k-ε turbulence model on about 1.1 million grid points, without a sub-model for the supersonic fuel jet. Simulation and experiment agree qualitatively, and for the most part quantitatively as well. The simulation can capture such fine details as

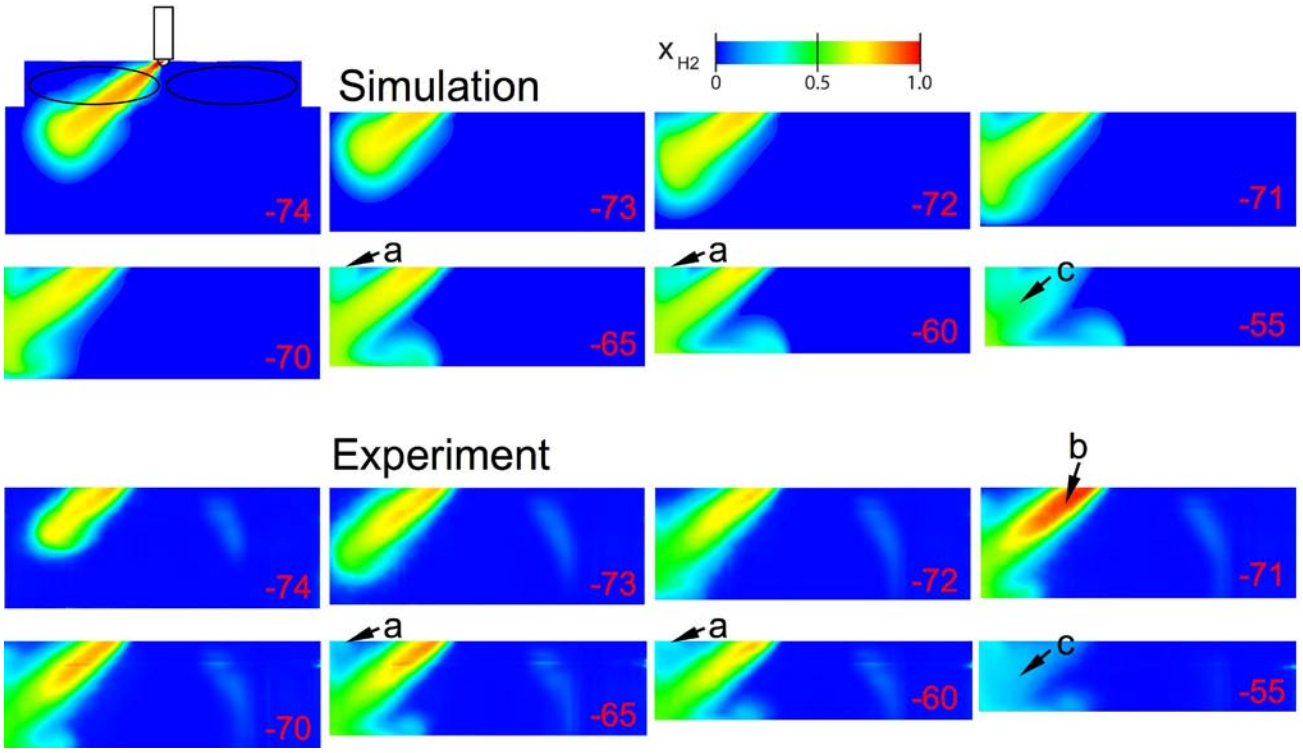

FIGURE 4. Experimental/numerical comparison of the mean fuel mole-fraction fields for injection from a single-hole injector for SOI = -80°CA. The field of view spans the whole width of the cylinder bore and the height from piston top to just below the fire deck, but not the pent-roof combustion chamber. Features designated by arrows and letters are referred to in the text. Operating conditions as for Figure 2.

the small zone of fuel-recirculation caused by the "lip" where the square end of the pent-roof overhangs the round cylinder bore (marked by arrows and the letter "a" in Figure 4). However, there are also obvious discrepancies. During part of the injection event, simulation and experiment show considerably different fuel mole-fractions in the central part of the jet (marked "b"). This is due to details in the photophysical behavior of the fluorescent fuel tracer, acetone, that cannot be accounted for properly in the experimental data reduction. However, in subsequent measurements changes in the experimental procedure have been successful in removing this inaccuracy at the slight expense of measurement precision. More concerning is the discrepancy in the fuel concentration near the nozzle after the end of injection (EOI), marked "c". The rapid transients in the near-nozzle region after EOI have been shown to be sensitive to the details of the rate-of-injection transients at EOI [5]. This may imply simulation inaccuracies in the rate transients of the fuel delivery or in the fluid dynamics of the enhanced entrainment that follows EOI. Accurate prediction of the mixture composition in the near-nozzle region is expected to be important when injection and spark are in close spatial and temporal proximity. Therefore future work will include using experiments in the optical engine, including in-cylinder velocity measurements, to help improve simulation fidelity in this region. Finally it should be stressed that this paragraph does not nearly capture all of the CFD development (which is not done in our group), but rather is just intended to provide a snapshot of the current status of its interaction with our optical-engine work.

Conclusions

- An extensive database on fuel/air mixing in a direct-injection hydrogen-fueled engine has been assembled and is being used for physical understanding and simulation validation.
- For all injector configurations and all but the latest injection timings, extensive jet/wall interaction determines the details of pre-spark fuel distribution.
- The momentum from the injection dominates the in-cylinder convection. Drastic increase in intake-induced tumble flow can change this somewhat for early injection timings (not discussed in text above).
- For intermediate injection timings, all injector configurations investigated yield an unfavorable pre-spark stratification. Improvements may include using a shaped piston top.
- Depending on the jet divergence-angle in multi-hole nozzles, jet merging may not occur at all, may

yield complete merging, or may cause injection-to-injection instabilities.

- Initial comparisons of optical results to CFD performed at ANL show that end-of-injection transients need improved treatment in the simulation.

References

1. Engine Combustion Network, https://share.sandia.gov/ecn/, Editor: Picket L.M., 2009.

2. Rousseau A., Wallner T., Pagerit S., Lohse-Busch H., Prospects on Fuel Economy Improvements for Hydrogen Powered Vehicles, SAE paper 2008-01-2378, 2008.

3. White C.M., Steeper R.R., Lutz A.E., The Hydrogen-fueled Internal Combustion Engine: A Technical Review, Int. J Hydrogen Energy 31:1292-1305, 2006.

4. Genzale C.L., Reitz R.D., Musculus M.P.B., Effects of Piston Bowl Geometry on Mixture Development and Late Injection Low Temperature Combustion in a Heavy-Duty Diesel Engine, SAE Paper 2008-01-1330, 2008.

5. Musculus M.P.B., Kattke K., Entrainment Waves in Diesel Jets, SAE Paper 2009-01-1355, 2009.

FY 2009 Publications/Presentations

1. Salazar V.M., Kaiser S.A., Halter F., Optimizing Precision and Accuracy of Quantitative PLIF of Acetone as a Tracer for Hydrogen Fuel, SAE paper 2009-01-1534.

2. Scarcelli R., Wallner T., Salazar V.M., Kaiser S.A., Modeling and Experiments on Mixture Formation in a Hydrogen Direct-Injection Engine, SAE paper 2009-24-0083.

3. Salazar V.M., Kaiser S.A., An Optical Study of Mixture Preparation in a Hydrogen-fueled Engine with Direct Injection Using Different Nozzle Designs, SAE paper 2009-01-2682.

4. Kaiser S.A., Salazar V.M., White C.M., The Influence of Injector Position and Geometry on Mixture Preparation in a DI Hydrogen Engine, presented at the AEC working group meeting, Livermore, CA, Feb. 2009.

5. Siebers D.L, Kaiser S.A., Status of the H_2ICE Collaborative Task, presented at the Spring Meeting of the IEA's Implementing Agreement for Energy Conservation and Emissions Reduction in Combustion, Paris, March 2009.

6. Kaiser S.A., Salazar V.M., Update on Sandia Optical Hydrogen-Engine Research, presented at the Ford/National Labs H_2ICE Meeting at ANL, Argonne, IL, March 2009.

7. Kaiser S.A., Salazar V.M., Wallner T., Nande A.M., The Influence of Injector Position and Geometry on Mixture Preparation in a DI hydrogen Engine, presented at the 9th Congress on Engine Combustion, Munich, Germany, March 2009.

8. Salazar V.M., Kaiser S.A., Halter F., Optimizing Precision and Accuracy of Quantitative PLIF of Acetone as a Tracer for Hydrogen Fuel, presented at the 5th Int'l. Workshop on Optical Diagnostics for Engine Comb. Research, Erlangen, Germany, March 2009.

9. Kaiser S.A., Sandia Hydrogen-Fueled Engine, presented at the DOE / Office of Vehicle Technology Annual Review, Washington, D.C., May 2009.

10. Salazar V.M., Kaiser S.A., Wallner T., Direct-injection Strategies for a Hydrogen-fueled Engine Evaluated in a Thermodynamic and an Optical Engine, presented at the 6th US National Combustion Meeting, Ann Arbor, MI, May 2009.

11. Kaiser S.A, Salazar V.M, Scarcelli R., Wallner T., Direct-Injection Strategies for a Hydrogen-fueled Engine: An optical and numerical investigation, presented at the Task Leaders Meeting of the IEA's Implementing Agreement for Energy Conservation and Emissions Reduction in Combustion, Lake Louise, AB, Canada, September 2009.

II.A.16 Advanced Diesel Engine Technology Development for High Efficiency, Clean Combustion

Donald Stanton
Cummins Inc.
1900 McKinley Ave.
Columbus, IN 47201

DOE Technology Development Manager:
Roland Gravel

NETL Project Manager: Carl Maronde

Subcontractors:
- Oak Ridge National Laboratory, Oak Ridge, TN
- BP Global Fuels Technology, Warrenville, IL

Objectives

- To design and develop advanced engine architectures capable of achieving U.S. Environmental Protection Agency (EPA) 2010 emission regulations while improving the brake thermal efficiency by 10% compared to current production engines.
- To design and develop components and subsystems (fuel systems, air handling, controls, etc.) to enable construction and development of multi-cylinder engines.
- To perform an assessment of the commercial viability of the newly developed engine technology.
- To specify fuel properties conducive to improvements in emissions, reliability, and fuel efficiency for engines using high efficiency clean combustion (HECC) technologies. To demonstrate a viable approach to reduce petroleum imports by at least 5% via renewable fuel sources. To demonstrate the technology is compatible with B20 (biodiesel).
- To further improve the brake thermal efficiency of the engine as integrated into the vehicle. To demonstrate robustness and commercial viability of the HECC engine technology as integrated into the vehicle.

Accomplishments

Heavy-Duty – 15L ISX Engine

- Can meet the 10% fuel efficiency improvement target using no oxides of nitrogen (NOx) aftertreatment while meeting U.S. EPA 2010 emission standards for Class 8 commercial vehicles.
- Achieving greater than 15% improvement in efficiency compared to the project target of 10% using the HECC-developed technology with selective catalytic reduction (SCR) NOx aftertreatment while meeting U.S. EPA 2010 emission standards for Class 6, 7, and 8 commercial vehicles.
- Fuel savings of 690 million gallons of oil per year for Class 8 trucks and fuel savings of 215 million gallons of oil per year for Class 6 and 7 trucks can be achieved based on the efficiency improvements demonstrated.
- Additional fuel consumption improvements of 3-4% can be achieved through better integration of the engine with the transmission and vehicle systems (down-speeding the engine, transmission shift pattern, axle ratio, etc.).
- 40-60% reduction in particulate matter (PM) emissions with a new combustion system design (piston, fuel injector configuration, intake air swirl level, etc.) along with down-speed engine operation.
- Completed vehicle drivability assessment with dowspeed engine operation.
- The design and commercialization assessment of a new generation of Cummins XPI high-pressure common rail fuel system has been completed (greater injection capability, cavitation mitigation, improved fuel tolerancing, and lower parasitics).
- Finalized the choice for the diesel particulate filter (DPF) to achieve reduced back pressure, linearity between soot loading and pressure drop, improved hysterisis, and high temperature stability.
- Reduced the precious metal content of the diesel oxidation catalyst (DOC).
- Supplier assessments for all the engine technologies have been completed. All key engine components will be supplied by Cummins Component Business Units.

Light-Duty 6.7L ISB Engine

- U.S. EPA 2010 Tier 2 Bin 8 steady-state and transient NOx emissions compliance have been achieved without NOx aftertreatment for the 6.7L ISB engine used in the light-duty truck market while exceeding the 10% improvement in brake thermal efficiency project target. Drive cycle efficiency improvements range from 13% to 18%.
- Analysis and design of additional subsystem technology for the 6.7L ISB have been completed to enable an additional 4% improvement in brake

thermal efficiency (enabling technologies include variable valve actuation, combustion system optimization, and fuel injection equipment).
- Design completed for a novel variable valve actuation system with emphasis on improving the production viability.

Fuels Technology Exploration

- HECC engine technology developed as part of this project has been shown to be robust for fuel economy and emissions with variations in diesel fuel properties representative of commercially available fuels in the marketplace. Confirmed aftertreatment system performance is robust against diesel fuel property variations.
- The development of virtual and real fuel sensing technology is required to maximize the fuel economy benefit associated with HECC technology when using renewable fuels such as biodiesel.
- The fuel economy benefits associated with HECC engine technology developed can not be maintained when using biofuels at constant NOx emissions. However, a reduction of 20% to 40% in PM can be achieved with the use of biofuels.
- Three new fuel virtual sensors have been developed for biofuel content.

Future Directions

- Complete the structural analysis of the final combustion system for the 15L ISX engine.
- Complete the commercial viability assessment of HECC technologies for the 15L ISX and the 6.7L ISB engines.
- Complete vehicle packaging studies for the engine and aftertreatment components.
- Confirm transient fuel consumption improvements over a variety of vehicle duty cycles using a combination of test cell and software analysis.
- Finalize the development of the SCR dosing system controls strategy to maximize engine efficiency.
- Optimize the cost of the ammonia slip catalyst (ASC) and reduce the size of the SCR system catalyst.
- Optimize the DOC formulation that thrifts the precious metal content.
- Development of on-board diagnostics (OBD) associated with the implementation of the new HECC subsystem technology to achieve proper functioning during in-use operation.
- Project close out in 2010.

Introduction

Cummins Inc. is engaged in developing and demonstrating advanced diesel engine technologies to significantly improve engine thermal efficiency while meeting U.S. EPA 2010 emissions. The essence of this effort is focused on HECC in the form of low-temperature, highly-premixed combustion in combination with lifted flame diffusion controlled combustion. Reduced equivalence ratio, premix charge in combination with high exhaust gas recirculation (EGR) dilution has resulted in low engine-out emission levels while maintaining high expansion ratios for excellent thermal efficiency. The various embodiments of this technology require developments in component technologies such as fuel injection equipment, air handling, EGR cooling, combustion, and controls. Cummins is committed to demonstrate commercially-viable solutions which meet these goals. Recent efforts have focused on integration of the engine technology with aftertreatment systems to maximize fuel efficiency improvements.

In addition to the engine technologies, Cummins is evaluating the impact of diesel fuel variation on the thermal efficiency, emissions, and combustion robustness of HECC technology. Biofuels are also being evaluated as part of the fuels study to determine if the thermal efficiency improvements and emissions compliance can be maintained.

Approach

Cummins' approach to these project objectives continues to emphasize an analysis-led design process in nearly all aspects of the research. An emphasis is placed on modeling and simulation results to lead the way to feasible solutions.

Three areas of emphasis that lead to substantial improvements in engine thermal efficiency are the maximization of the engine closed cycle efficiency, the reduction of open cycle losses and engine parasitics, and the integration of HECC engine technology with aftertreatment. Engine system solutions to address the three areas of emphasis include air handling schemes, control system approaches, EGR cooling strategies, fuel system equipment, and aftertreatment design. Based on analysis and engine testing, subsystem component technologies are identified for further development. Cummins is uniquely positioned to develop the required component technologies via the Cummins Component Business unit. A variety of laboratory tests are conducted to verify performance and to tune system functions. Model predictions are verified and refined as necessary. Often, different portions of the system are pre-tested independently to quantify their behavior, and the data are analyzed in a model-based simulation before combined hardware testing is conducted.

Concurrent to laboratory testing and tuning, vehicle system performance is planned and obtained. Once satisfactory test cell system performance is verified, the vehicle demonstration is conducted.

Data, experience, and information gained throughout the research exercise will be applied wherever possible to the final commercial products. Cummins intends to continue to hone its technical skill and ability through this research while providing satisfactory results for our customers. Cummins continues to follow this cost-effective, analysis-led approach both in research agreements with the Department of Energy as well as in its commercial product development. Cummins feels this common approach to research effectively shares risks and results.

Results

The U.S. EPA 2010 emissions standard poses a significant challenge for developing clean diesel powertrains that are affordable. Along with exhaust emissions, an emphasis on heavy-duty vehicle fuel efficiency is being driven by increased energy costs as well as the potential regulation of greenhouse gases. An important element of the success of meeting emissions while significantly improving efficiency is leveraging Cummins component technologies such as fuel injection equipment, aftertreatment, turbomahcinery, electronic controls, and combustion systems. Innovation in component technology coupled with system integration is enabling Cummins to move forward with the development of high-efficiency, clean diesel products with a long-term goal of reaching a 55% peak brake thermal efficiency for the engine plus aftertreatment system.

The Cummins global product strategy for diesel powertrain systems is to create engine architectures that allow system calibration to achieve a wide range of system-out NOx compliance to meet the diversity of future worldwide exhaust emissions standards. A variety of engine architectures is being explored by Cummins to meet U.S. EPA 2010 NOx emission standard based on two primary strategies to control NOx: cooled EGR (no NOx aftertreatment) and SCR. An in-cylinder solution for NOx control based on cooled EGR can be achieved with advancements in component technology thus eliminating the need for NOx aftertreatment. The current in-cylinder architecture can achieve compliance with the 2010 NOx regulation along with PM compliance with the use of a diesel particulate filter. Cummins has demonstrated the ability to reach U.S. EPA 2010 emissions levels without the use of NOx aftertreatment. However, obtaining robust PM emissions and low fuel consumption has been the primary focus during 2009. Significant progress has been made to lower the PM levels with less variation. This has been accomplished through downspeeding the engine to allow more time for soot oxidation along with a redesign of the combustion system. Measurements have indicated that a 40% to 60% reduction in PM levels has been obtained. This allows Cummins to meet the 10% fuel consumption reduction target while meeting the U.S. EPA 2010 emission standard without NOx aftertreatment. Variable valve actuation provides additional PM robustness, but involves substantial technology development to meet the durability demands of the heavy-duty trucking market. Vehicle heat rejection at higher engine ratings remains an issue for the in-cylinder NOx control architecture.

Much of the enabling technology for in-cylinder NOx control can also be used to provide significant fuel economy improvements for the variety of SCR-related architectures. However, there still remains a greater than 7% fuel economy benefit associated with the SCR architectures compared to the in-cylinder NOx control architecture using the same component technology. Additional engine performance capability can be achieved in the form of increased power density for an SCR engine architecture assuming the vehicle application can accommodate a larger catalyst size. The larger catalyst poses challenges for vehicle packaging, thermal management of the catalyst bed temperature, and cost. Therefore, there exists a complex system integration and optimization task to select the right SCR catalyst size for a given power density that can involve also the choice of engine displacement for a given application. Analysis and engine testing at Cummins indicate that the SCR engine architecture is better suited for engine downsizing compared to an in-cylinder solution. The power density of the in-cylinder NOx control architecture is limited by peak cylinder pressure due to the high rate of charge flow. Work completed in 2009 indicates that the aftertreatment size can be reduced compared to SCR systems that will be launched in 2010. This is attributed in part to the HECC engine technologies that provide a system that is robust to engine-out emissions variation. In addition, the HECC engine can achieve a wide range of engine-out emissions that provide robustness.

Conclusions

During Fiscal Year 2009, all milestones and deliverables have been met for the Cummins HECC project. Accomplishments include:

Heavy-Duty – 15L ISX Engine

- Can meet the 10% fuel efficiency improvement target using no NOx aftertreatment while meeting U.S. EPA 2010 emission standards for Class 8 commercial vehicles.
- Achieving greater than 15% improvement in efficiency compared to the project target of 10% using the HECC-developed technology with SCR

NOx aftertreatment while meeting U.S. EPA 2010 emission standards for Class 6, 7, and 8 commercial vehicles.

- Fuel savings of 690 million gallons of oil per year for Class 8 trucks and fuel savings of 215 million gallons of oil per year for Class 6 and 7 trucks can be achieved based on the efficiency improvements demonstrated.
- Additional fuel consumption improvements of 3-4% can be achieved through better integration of the engine with the transmission and vehicle systems (downspeeding the engine, transmission shift pattern, axle ratio, etc.).
- 40-60% reduction in particulate matter emissions with a new combustion system design (piston, fuel injector configuration, intake air swirl level, etc.) along with downspeed engine operation.
- Completed vehicle drivability assessment with dowspeed engine operation.
- The design and commercialization assessment of a new generation of Cummins XPI high-pressure common rail fuel system has been completed (greater injection capability, cavitation mitigation, improved fuel tolerancing, and lower parasitics).
- Finalized the choice for the DPF to achieve reduced back pressure, linearity between soot loading and pressure drop, improved hysterisis, and high temperature stability.
- Reduced the precious metal content of the DOC.
- Supplier assessments for all the engine technologies have been completed. All key engine components will be supplied by Cummins Component Business Units.

Light-Duty 6.7L ISB Engine

- U.S. EPA 2010 Tier 2 Bin 8 steady-state and transient NOx emissions compliance have been achieved without NOx aftertreatment for the 6.7L ISB engine used in the light-duty truck market while exceeding the 10% improvement in brake thermal efficiency project target. Drive cycle efficiency improvements range from 13% to 18%.
- Analysis and design of additional subsystem technology for the 6.7L ISB have been completed to enable an additional 4% improvement in brake thermal efficiency (enabling technologies include variable valve actuation, combustion system optimization, and fuel injection equipment).
- Design completed for a novel variable valve actuation system with emphasis on improving production viability.

Fuels Technology Exploration

- HECC engine technology developed as part of this project has been shown to be robust for fuel economy and emissions with variations in diesel fuel properties representative of commercially-available fuels in the marketplace. Confirmed aftertreatment system performance robust against diesel fuel property variations.
- The development of virtual and real fuel sensing technology is required to maximize the fuel economy benefit associated with HECC technology when using renewable fuel sources such as biodiesel.
- The fuel economy benefits associated with HECC engine technology can not be maintained when using biofuels at constant NOx emissions. However, a reduction of 20% to 40% in PM can be achieved with the use of biofuels.
- Three new fuel virtual sensors have been developed for biofuel content.

II.A.17 High Efficiency Clean Combustion (HECC) Advanced Combustion Report

Scott Fiveland
Caterpillar, Inc.
P.O. Box 1875
Peoria, IL 61656-1875

DOE Technology Development Manager:
Roland Gravel

NETL Project Manager: Carl Maronde

Subcontractors:
- ExxonMobil, Paulsboro, NJ
- Sandia National Laboratories (SNL), Livermore, CA
- Oak Ridge National Laboratory (ORNL), Oak Ridge, TN
- ENSYS, Madison, WI

Objectives

- Identify and develop technologies to enable low-temperature, high-efficiency combustion.
- Define technologies necessary to achieve a 10% reduction in fuel consumption while meeting Environmental Protection Agency 2010 on-highway and Tier 4 non-road emissions requirements.

Accomplishments

- Identified an interaction between combusting sprays of 10-hole and 14-hole injector nozzles that affects flame lift-off length and may partially explain high soot emissions from such nozzles at high engine loads.
- Completed testing of premixed charge compression ignition (PCCI) combustion using gasoline and diesel fuel blends. The fuel blend did not significantly increase the PCCI operating range, but did show smoke emissions reduction across the entire operating range.
- Completed a well-to-wheels (WTW) energy audit for three heavy-duty diesel engine applications and four combustion system/fuel configurations.

Future Directions

- Identify an air system configuration that delivers the exhaust gas recirculation (EGR) needed for PCCI combustion and meets the engine performance requirements.
- Develop an alternative fueling strategy to extend the thermodynamic advantages of PCCI to full load.

Introduction

Improving fuel efficiency while meeting future emissions levels in the diesel on-road and off-road environments is an extremely difficult challenge but is necessary to maintain the level of customer value demanded by the end users of compression ignition engines. Caterpillar® is currently engaged with several partners to address this challenge using advanced low-temperature combustion regimes enabled by advanced fuel system technologies and advanced engine design concepts. Advanced combustion regimes can provide a direct improvement in thermodynamic efficiency, as well as an indirect benefit in the form of lower particulate emissions, which in turn, require less fuel consumption for diesel particulate filter regeneration.

Premixed, compression ignition combustion, such as homogeneous charge compression ignition (HCCI) or PCCI can increase thermodynamic efficiency, through shorter combustion duration, and lower soot emissions. While full-load operation of diesel PCCI has been demonstrated, the actions necessary to achieve that objective negated the efficiency benefits of the premixed combustion. Past efforts in this project have shown that the high efficiency benefits of diesel premixed combustion are practically limited to load range below about 7 bar brake mean effective pressure (BMEP). Unfortunately, the optimal engine recipe to maximize the efficiency benefit from PCCI tends to be detrimental to the efficiency and performance of the engine at full load. The current focus of the project is to develop a diffusion combustion solution that is more compatible with part-load application of PCCI, and to explore alternative fuel strategies that allow the operating range and efficiency benefit of PCCI combustion to be extended to full load.

Approach

This project provides a fundamental understanding of the in-cylinder fuel/air mixing and combustion process, including the impact of fuel properties, through the use of single-cylinder engine testing, advanced optical diagnostics and computational fluid dynamics. We are actively developing high-efficiency, clean-combustion enabling technologies such as fuel injection technologies, controls strategies, heat

rejection reduction technologies and advanced engine concepts. The integration of enabling technologies and advanced combustion recipes is performed using engine system simulation tools and validated through multi-cylinder engine testing. Successful completion of this project will provide Caterpillar® and DOE with a clear understanding of the technology hurdles that must be overcome to increase the thermal efficiency and reduce emissions on future compression ignition engines.

Results

Sandia Optical Engine Experiments: Activities at SNL during Fiscal Year 2009 focused on updating the fuel system of the Sandia Compression-Ignition Optical Research Engine to enable utilization of a current production Caterpillar CR350 common rail fuel injector. This activity was undertaken to further enable combustion experiments with higher injection pressures, such as an investigation of "lifted flame" combustion.

Low-Temperature Combustion Development: The concept of enhancing air-entrainment prior to the lift-off length in diesel fuel jet combustion has the potential to dramatically reduce soot emissions. When used in conjunction with EGR, both NOx and smoke could potentially be kept at low levels to minimize the use of diesel exhaust aftertreatment with good thermal efficiency. This concept extends from the work at SNL where diesel fuel jets burning with conventional diffusion flame structure were shown to exhibit little or no smoke formation when mixing is enhanced prior to the location where combustion begins (termed the lift-off length) [1]. This is accomplished by manipulating the lift-off and mixing parameters (such as increasing injection pressure, decreasing injector hole diameter, and lowering ambient temperature) so that enough air is entrained into the jet to cause combustion to occur only in regions that the equivalence ratio is less than 2, where soot formation is avoided. The current project focuses on making this type of combustion feasible in a high-load engine operating condition.

Previous experiments in the project successfully demonstrated low NOx, low soot combustion at 50% load by utilizing the lifted flame concept. To extend the load range, the number of fuel injector orifices had to be increased to supply the necessary fuel injection rate. As the number of injector orifices was increased, the smoke emissions significantly increased. During FY 2009, a series of experiments were undertaken to determine the cause of the smoke increase. The impact of the number of injector orifices on flame lift-off was measured in a high-temperature pressure vessel facility under steady conditions

The initial round of tests revealed a significant transient effect on the lift-off length as measured by CH chemiluminescense at 430 nm. A comparison of the flame lift-off for a 6- and 10-hole injector nozzle at the same test conditions can be seen in Figure 1. While the lift-off length in both cases is nearly equal at the beginning of combustion, the lift-off length regresses toward the nozzle in the case of the 10-hole nozzle while remaining relatively constant in the case of the 6-hole nozzle. These results may indicate an increasing interaction between the combusting sprays as the spacing between sprays decreases, which may, in part, explain the higher smoke emissions. Additional testing in the high-temperature pressure vessel is planned, as well as flame lift-off measurements in the Sandia optical engine.

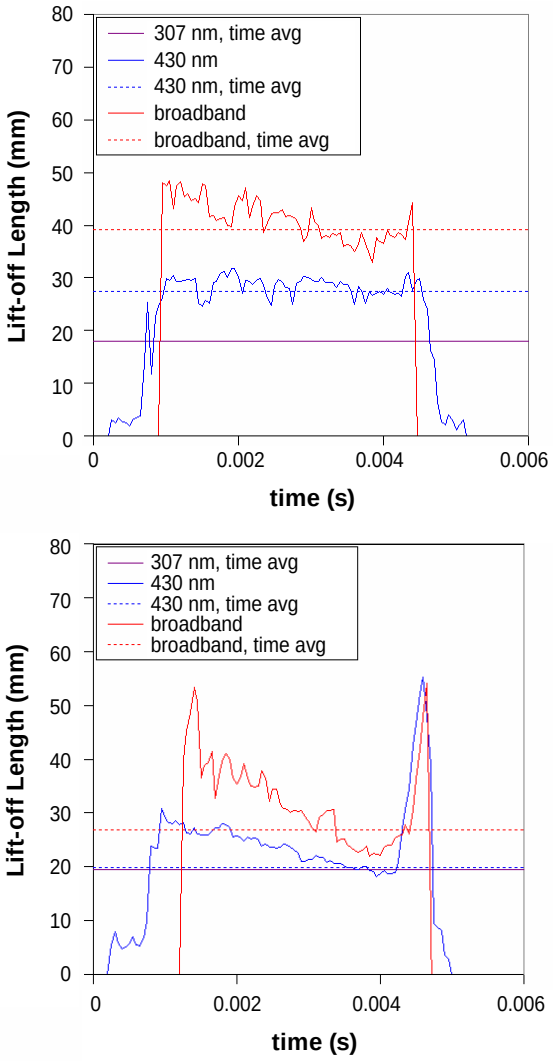

FIGURE 1. Time dependence of the measured lift-off length for three different wavelengths imaged in this study for the 6-hole micron nozzle (top) and the 10-hole micron nozzle (bottom) at 850 K, 100 bar and 300 MPa injection pressure.

Fuel Property Effects Investigation: One avenue to extend the load range of PCCI combustion is through the use of a fuel with more desirable ignition characteristics and higher volatility. Since no commercially available fuel is ideal across the entire engine operating range, the combustion characteristics fuel blends of gasoline and diesel fuel were investigated. In addition, fuel system concepts were studied to determine if a system that direct injected a blend of gasoline and diesel fuel was feasible.

During FY 2008, a gasoline and diesel fuel blend with a derived cetane number of 26 was tested and compared to diesel fuel. At low loads, the fuel blend exhibited increased ignition delay, as expected, and produced slight improvement in efficiency and reduction in smoke emissions. At half load and above, the ignition delay of the fuel blend did not differ significantly from that of diesel fuel. The fuel blend did not increase thermodynamic efficiency at higher loads, it did result in lower smoke emissions by up to 50% at 2010 NOx levels as shown in Figure 2. While smoke emissions were reduced and efficiency was slightly improved at low loads, the fuel blend tested did not significantly increase the load range of PCCI combustion.

Well-to-Wheels Analysis: To identify opportunities for improving thermal efficiency it is imperative to perform a complete energy audit on various (on-highway and off-highway) applications, which enables the understanding of energy flow through the system. The efficiency improvements are possible both by improved component efficiencies and by improved system integration. The analysis was divided into two discreet sections: A well-to-tank (WTT) analysis and a tank-to-wheels (TTW) analysis were performed.

The TTW energy audit was performed on three different applications, namely an off-highway hauling machine application, an off-highway cyclic machine application and an on-highway truck application, all of them powered by a Caterpillar® heavy-duty engine. For each of these applications, four different sources of energy supply are considered. Those were: diffusion combustion-based (conventional) heavy-duty diesel engine; an engine based on PCCI combustion using a low cetane fuel; lean-burn heavy-duty natural gas engine; and a stoichiometric gasoline combustion-based heavy-duty engine. The diesel-based diffusion combustion was defined as the baseline case and the other three concepts of power generation were evaluated with the assumption that the engine was run in the exact manner as in the baseline diesel case, i.e. the PCCI, natural gas and gasoline cases had the same engine speed/load to compare TTW efficiencies for each case. The analysis was done using a combination of engine data, application field data and Caterpillar® proprietary cycle simulation tools.

A WTT comparison was also completed on the fuels of interest from the applications selected, including diesel, low-cetane fuel, gasoline and natural gas. This comparison examined the processes involved in producing, transporting, manufacturing and distributing these fuels, with the intention of including all steps from extraction of the energy carrier to refueling of the vehicles. This was undertaken so that when combined with the TTW analysis, a view of the overall efficiency potential across the fuel/engine systems of interest could be obtained. Ultimately, this view across the combined WTW analysis enables one to take into account energy/efficiency differences in both the production and consumption of the fuels. This understanding across the fuel/engine systems can allow informed selection of routes to gain efficiency in both the vehicle and fueling pathways to provide overall best paths to improved future efficiency.

2nd Law Analysis: During FY 2009, ORNL worked with Caterpillar® in characterizing potential strategies for reducing thermodynamic losses and improving thermodynamic availability of the exhaust gases. A thermodynamic availability analysis package has been developed by ORNL, allowing examination of results from Caterpillar®'s in-house engine simulation software. Simulations with this model are used to evaluate potential means for reducing irreversibilities and determine what effect that reduction will have on the distribution of available energy. Validation of the model is complete and the model is now being used to investigate the potential efficiency improvement technology options like reducing heat transfer through exhaust runners or reducing heat loss across the engine by raising the coolant temperature. Both technologies resulted in increased availability in the exhaust stream which could potentially be recovered by waste recovery systems.

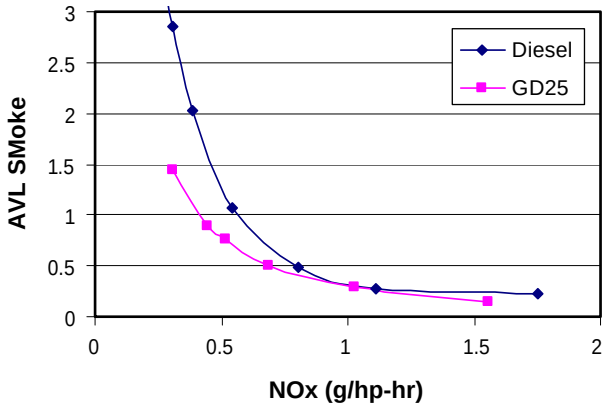

FIGURE 2. Comparison of the smoke-NOx tradeoff curve between diesel and the gasoline/diesel fuel blend with 26 derived cetane number at 1,200 rpm and 11 bar BMEP. EGR rate was 40%.

Conclusions

- Initial measurements of flame lift-off length of multi-plume combusting sprays showed a regression toward the nozzle as the number of injector orifices increased, which may indicate an interaction between sprays that becomes more significant as spacing between jets decreases.
- Testing of a gasoline and diesel fuel blend showed a reduction of smoke emissions compared to diesel fuel. However, the fuel blend did not significantly increase the PCCI operating range.
- A well-to-wheels analysis of three applications utilizing a heavy-duty diesel engine was completed.
- A thermodynamic analysis tool was coupled to engine simulation software to allow investigation of potential heat loss reduction to increase thermal efficiency. An engine model was created and validated against experimental test data.

References

1. Picket and Siebers, Combust. Flame 138:114-135.

FY 2009 Publications/Presentations

1. Scott Fiveland, "Development of Enabling Technologies for High Efficiency, Low Emissions Homogeneous Charge Compression Ignition (HCCI) Engines", US DOE Program Merit Review, May 18, 2009.

2. Chris Gehrke and Sangsuk Lee, "Development of Advanced Combustions Technologies for Increased Thermal Efficiency", 2009 DEER Conference, August 3, 2009.

II.A.18 Low-Temperature Combustion Demonstrator for High Efficiency Clean Combustion

William de Ojeda, PhD, PE
Navistar, Inc.
10400 W. North Avenue
Melrose Park, IL 60160

DOE Technology Development Manager:
Ken Howden

NETL Project Manager: Samuel Taylor

Subcontractors:
- Lawrence Livermore National Laboratory
- Continental
- BorgWarner
- Mahle
- ConocoPhillips
- University of California, Berkeley
- Ricardo

Objectives

- Demonstrate low-temperature combustion (LTC) in a multi-cylinder engine with a power density of 12.6 bar brake mean effective pressure (BMEP).
- Demonstrate engine operation over transient emission cycles.
- Achieve NOx U.S. 2010 engine-out emissions without aftertreatment.
- Achieve 10% fuel efficiency improvement over conventional combustion.

Accomplishments

- Engine testing on the Navistar 6.4L V8 engine demonstrated the application of LTC by use of exhaust gas recirculation (EGR), charge temperature control and the use of a multiple injection strategy. Engine testing yielded engine NOx levels below 0.2 g/bhp-hr and soot levels manageable by a diesel particular filter. Overall, tests demonstrated a gain in the engine break thermal efficiency of up to 5% with respect to the base.
- Further improvements in the engine efficiency were sought by the installation of a variable valve actuation (VVA) system. The VVA system was validated in a dedicated test rig, accumulating over 400 hours of testing before engine installation. The fuel injection and VVA controls were integrated into the electronic control unit (ECU) with the previously developed cylinder pressure feedback system.
- VVA proved capable to extend the LTC regime with extraordinary results over soot reduction and improved engine thermal efficiency. For operating loads up to 5 bar BMEP, at engine-out 0.2 gNOx/bhp-hr, soot was reduced to levels below 0.01 g/bhp-hr. The engine brake specific fuel consumption (BSFC) was reduced by nearly 5%. Tests were run up to 8 bar. The higher load results will be presented at a later date.

Future Directions

- VVA demonstrated its effectiveness to adjust in-cylinder charge-air bulk properties. The dramatic reduction of soot at very low engine-out NOx correlated with a fundamental understanding of the combustion process, flame temperatures and local equivalence ratios associated with NOx formation, and for soot formation and oxidation. The ongoing experimental work will continue with the support of modeling. Previous KIVA simulations captured the combustion process, matching experimental pressure and heat release traces. The simulations gave good correlations with experimental data in single- and multiple-injection conditions. This tool should be used to further optimize combustion boundary conditions provided by VVA to extend the operation of LTC.
- The impact of the VVA hardware goes beyond the in-cylinder combustion development. Testing indicated the VVA system provides a unique tool to accurately adjust air during transients. VVA further provides an accurate control over exhaust temperatures and significantly improves the effectiveness of the diesel particulate filter.
- The engine which previously ran through the federal transient heavy-duty cycle will be re-run with the VVA hardware. The project scope, which includes the development of a prototype ECU to handle in-cylinder combustion diagnostics and feedback, will be expanded to use valve timing control.

Introduction

The mechanism of LTC has been documented in the pioneering work of reference [1]. LTC suppresses soot by lowering the combustion temperature. At low flame temperatures, the reactions forming soot particles from polycyclic aromatic hydrocarbons are inhibited

even at air-fuel ratios approaching near stoichiometric conditions. Furthermore, when in-cylinder temperatures are limited to 2,000 K, the NOx formation reactions are also prevented.

Homogeneous charge compression ignition (HCCI) relies on fuel introduced early in the compression stroke to yield lean, well-premixed conditions. Under HCCI, the mixture autoignites at multiple points in the combustion chamber which results in low flame temperatures. The homogenous conditions, however, are difficult to attain with the characteristically low volatile-high Cetane number diesel fuel. The ignition timing is sensitive to the resulting mixture (temperature and composition) and combustion is extremely rapid [2].

LTC relies on the use of high EGR rates and low intake manifold temperatures rather than the lean and homogenous characteristics of HCCI. The high EGR LTC approach yields a more controllable combustion as fuel injection timing and ignition are still relatively close coupled. The heavy EGR however can result in poor combustion efficiencies [3]. As load increases the high rates of EGR require large boost. Limits in boost will translate to large increases in soot levels.

The present work combined LTC at part loads with a partially premixed charge compression ignition (PCCI) combustion [4] strategy. Like LTC, PCCI relied on EGR. A fuel injection strategy promoted early fuel mixing with multiple pilots. Work demonstrated NOx below 0.2 g/bhp-hr and an after-treatment tolerant soot level can be obtained with this concept up to a load of 16.5 bar BMEP.

The work was extended to include a VVA system, with control over the intake valve closing (IVC) timing. The focus of the work was to extend the operation of the LTC regime.

Approach

- Phase I (completed) consisted of applied research, determining engine boundary conditions, and combustion system design.
- Phase II (completed) consisted of exploratory development, engine hardware and control system procurement, and controls software development.
- Phase III (completed) consisted of steady-state engine testing, optimization of combustion hardware and fueling strategy, and further controls system development.
- Phase IV (in progress) consists of transient testing. This phase is also to demonstrate the capabilities of the VVA version of the engine.

Results

Engine Layout with VVA. The VVA consisted of a loss motion electro-hydraulic device designed to cause early closure of the intake valves during the induction stroke. The installation is illustrated in Figure 1 and its functioning in Figure 2.

Effects of IVC. Data is reported at 4.3 bar BMEP and 2,050 rpm. Figure 3 shows reduced temperatures at top dead center (TDC) as valve duration is reduced; peak bulk combustion temperatures climbed higher than baseline. Decreasing the pressure and temperature at the start of combustion promoted the low-temperature reaction (LTR) of diesel fuel. As IVC was advanced, the LTR energy released and the separation from the high-temperature reaction increased.

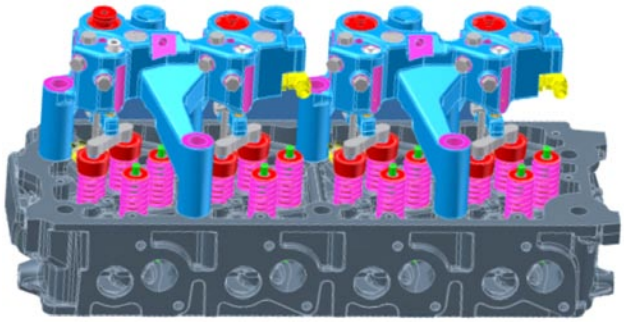

FIGURE 1. VVA System on Cylinder Head

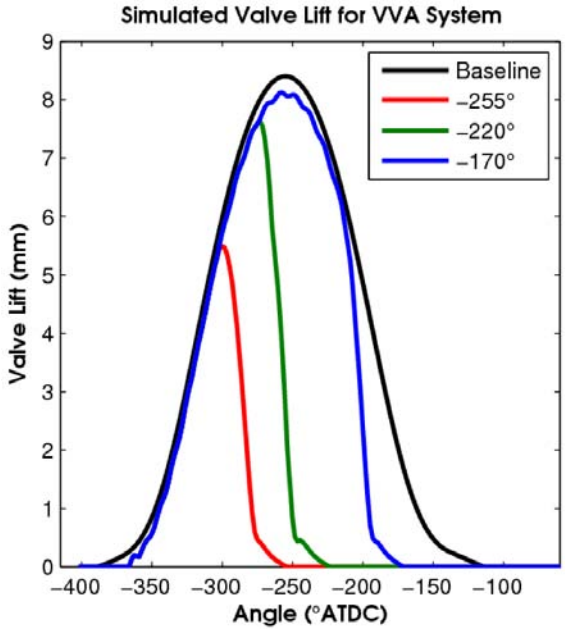

FIGURE 2. Valve Lift Profiles

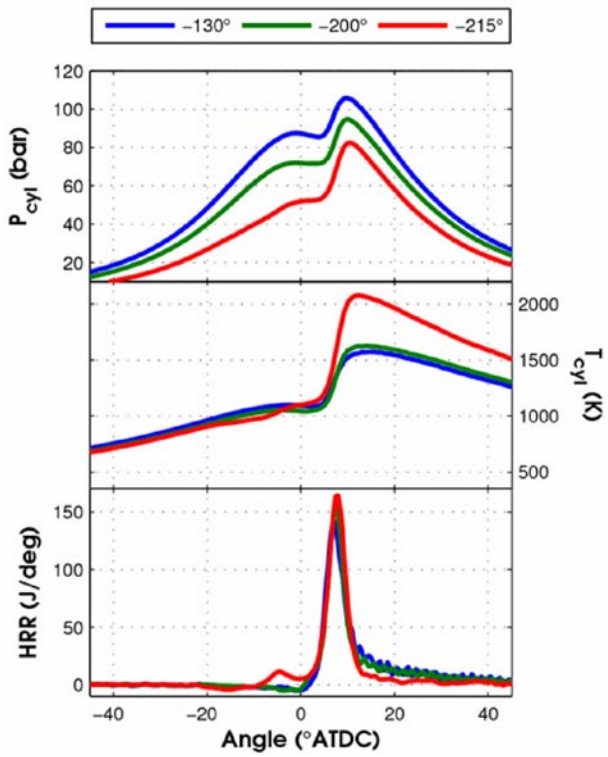

FIGURE 3. (a) Pressure, (b) Temperature, and (c) Heat Release Rate (HRR)

Ignition Delay and Soot. Advanced IVC increased ignition delay. The effects are seen in the soot emissions of Figure 4. The long ignition delays increased the amount of fuel in the premixed burn, seen earlier in Figure 3, leading to a dramatic soot decrease. IVC yielded an operation region with 0.01 g/bhp-hr soot and 0.2 gNOx/bhp-hr (2010 standards).

Fuel Economy. High air/fuel ratios, late combustion, and low intake temperatures are used to limit soot – conditions that can result in poor fuel efficiency due to higher engine back pressures, poor combustion phasing, or large heat rejection. The VVA system provides a tool to help manage these conditions by providing other means to increase ignition delay. Figure 5 shows that by increasing max in-cylinder temperatures and keeping carbon monoxide emissions low, BSFC and soot emissions can be simultaneously reduced.

Conclusions

- At a constant 0.2 g/bhp-hr NOx, advanced IVC drastically reduced soot emissions. At 5 bar BMEP, above 90% soot reduction led to engine-out 0.01 g/bhp-hr results while simultaneously lowering fuel consumption by 5%.
- IVC led to high combustion bulk temperatures contributing to further soot oxidation.

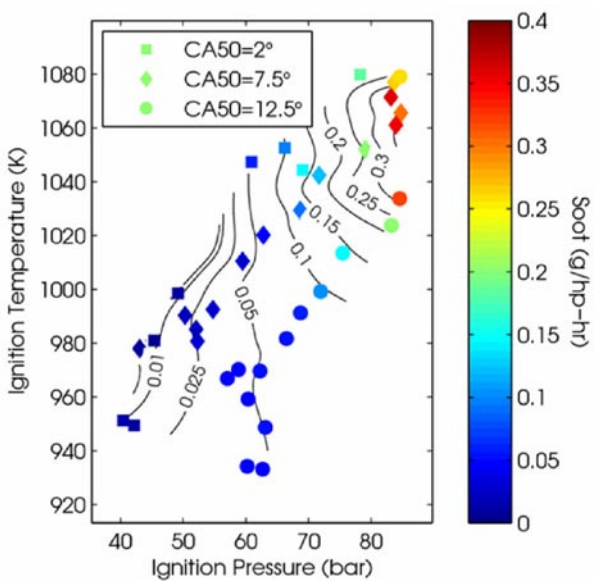

FIGURE 4. Soot as a Function of Ignition Pressure And Temperature CA50 - crank angle for 50% heat release

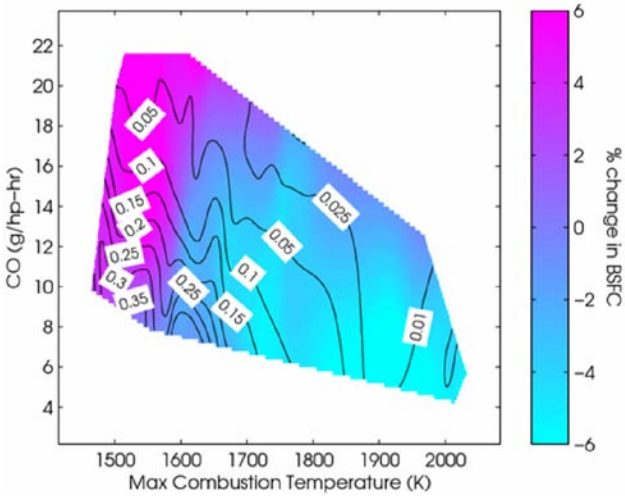

FIGURE 5. BSFC and Soot as a Function of CO and Temperatures

- Improved thermal efficiencies were caused by lower ignition temperatures and pressures that enabled long ignition delays, increasing the amount of fuel in the premixed flame and reducing the magnitude of the diffusion flame that follows. IVC also enabled a reduction in differential pressure across the engine.

References

1. Epsey C., and Dec J.E., "Diesel Engine Combustion Studies in a Newly Designed Optical-Access Engine Using High-Speed Visualization and 2-D Laser Imaging", SAE 930971.

2. Hasegawa, R., Yanagihara, H., "HCCI combustion in a DI Diesel Engine," SAE 2003-01-0745.

3. Musculus, M., Lachaux, T., Ticket, L.M., "End-of-Injection over-mixing and unburned hydrocarbon emissions in Low-Temperature-Combustion Diesel Engines," SAE 2007-01-0907.

4. Weiskirch C., and Mueller E., "Advanced in Diesel Engine Combustion: Split Combustion", SAE Paper No. 2007-01-0178.

FY 2009 Publications/Presentations

1. William de Ojeda, Daniel Cornelius, Raj Kumar, "Effect of Variable Valve Timing on Diesel Combustion Characteristics", submitted to the 2010 SAE World Congress, Detroit.

2. William de Ojeda, Daniel Cornelius, Raj Kumar, Phil Zoldak, Raul Espinosa, "Development of a Fuel Injection Strategy for Partially Premixed Compression Ignition Combustion", SAE 2009-01-1527 SAE World Congress, Detroit.

3. de Ojeda, W., Zoldak, P., Espinosa, R., Kumar, R., Cornelius, D., "Multicylinder Diesel Engine Design for LTC operation", Diesel Engine Development, DEER 2009, Dearborn, Michigan.

II.A.19 Stretch Efficiency – Exploiting New Combustion Regimes

C. Stuart Daw (Primary Contact), Josh A. Pihl, V. Kalyana Chakravarthy, James C. Conklin, Ronald L. Graves
Oak Ridge National Laboratory (ORNL)
NTRC Site
2360 Cherahala Blvd.
Knoxville, TN 37932

DOE Technology Development Manager:
Gurpreet Singh

Objectives

- Analyze and define specific pathways to improve the energy conversion efficiency of internal combustion engines from nominally 40% to as high as 60%, with emphasis on opportunities afforded by new approaches to combustion.
- Establish proof of principle of pathways to stretch efficiency.

Accomplishments

- Conducted detailed thermodynamic analysis of the theoretical efficiency benefits of thermochemical exhaust heat recuperation in an idealized internal combustion engine.
- Submitted manuscript on thermodynamic analysis of thermochemical recuperation.
- Designed, procured, and began assembly of components for regenerative air preheating with thermochemical recuperation (RAPTR) experiment.

Future Directions

- Complete construction of RAPTR bench-top constant volume combustor.
- Experimentally demonstrate low-irreversibility combustion in the RAPTR bench-top apparatus.
- Analyze data from RAPTR experiments to determine efficiency implications and appropriate ways to model exergy losses under different operating modes.
- Continue exploring better ways for recuperating exhaust heat and utilizing compound cycles for extracting work.
- Continue exercising engine and combustion models to identify combustion modifications that would mitigate exergy losses.

Introduction

In conventional internal combustion engines, the largest efficiency losses (approximately 20-25% of the available fuel energy) occur in the combustion process itself. These losses are due to the generation of thermodynamic entropy by unrestrained chemical reactions. However, it is theoretically possible to carry out combustion reactions in a more restrained way (closer to equilibrium) that produces less entropy and preserves more of the original fuel energy for work. The goal of this project is to identify and demonstrate strategies that enable combustion under conditions closer to chemical equilibrium and thereby increase the overall efficiency of the combustion process.

Approach

Our approach to improving internal combustion engine efficiency is to understand the losses in current engines and then develop ways to mitigate them. Previous analytical studies of the exergy losses in current engines conducted in collaboration with Professors Jerald Caton (Texas A&M University) and David Foster (University of Wisconsin) identified the irreversibility of the combustion step as the largest single contributor to fuel exergy loss. Our current efforts are focused on development, analysis, and experimental evaluation of novel approaches to combustion that can reduce this inherent irreversibility. A common theme of all the novel approaches being considered is that they attempt to create conditions under which the combustion reactions occur closer to a state of chemical equilibrium.

The first novel combustion approach being investigated combines two fundamental concepts to achieve reaction conditions closer to equilibrium:

- counterflow preheating of the inlet fuel and air with exhaust, and
- catalytic steam reforming of the fuel as it is preheated.

Counterflow preheating brings the air and fuel feeds closer to the temperature of the combustion process in as reversible a manner as possible, minimizing the entropy generation due to internal heat transfer. Catalytic steam reforming converts thermal energy recuperated from the exhaust into chemical energy in the fuel reformate. In essence, exhaust heat is used to upgrade the fuel to species with a higher heating value (H_2 and CO). These two concepts are specific implementations of more general concepts that emerged

from our previous analytical and literature investigations referred to as CPER [1] and thermochemical recuperation (TCR) [2].

We are currently focused on quantifying and demonstrating the potential efficiency benefits of these two approaches through a combination of thermodynamic analysis and experimental evaluation. Much of our efforts for Fiscal Year 2009 centered on a detailed thermodynamic analysis of the theoretical potential of thermochemical recuperation applied to an idealized internal combustion engine. A schematic of the system analyzed is shown in Figure 1. It consisted of:

- a frictionless adiabatic piston engine operating at steady-state over an ideal Atkinson cycle,
- a fuel vaporizer that utilizes residual exhaust heat to convert the fuel (and water) feed from liquid to gas phase,
- a catalytic steam reformer integrated with an exhaust gas heat exchanger, and
- an intercooler that cools the reformer product gases to their boiling point.

We conducted detailed 1st and 2nd law analyses on this system to quantify the piston work output and exergy flows as a function of degree of reforming for three fuels: methanol, ethanol, and isooctane.

In parallel with these thermodynamic analyses, we have continued working on the RAPTR experiment. We completed the system design, procured the components, and are in the process of assembling the device. Once construction is complete, we will use the RAPTR combustor to experimentally evaluate some of the theoretical concepts we have analyzed over the past year.

Results

To better understand the potential impact of TCR, it is first helpful to consider the example differences among fuels when they are fed directly to our ideal engine without any reforming, summarized in Table 1.

TABLE 1. Summary of thermodynamic differences among selected engine fuels fed to an ideal engine.

	X*	$\Delta X_m/X$	$\Delta X_c/X$	W*
H_2	1.00	0.0219	0.1162	1.00
CO	1.12	0.0198	0.0887	1.07
H_2/CO	1.04	0.0214	0.1070	1.02
Methanol	1.01	0.0108	0.1990	0.971
Ethanol	0.957	0.0070	0.2019	0.924
n-Heptane	0.917	0.0027	0.2005	0.892
Isooctane	0.920	0.0024	0.2031	0.893

The first column of Table 1 (X^*) compares the relative chemical exergy of stoichiometrically equivalent amounts of several common engine fuels (in a gaseous state) at ambient conditions. By stoichiometrically equivalent, we mean the amount of fuel which would be fully consumed when burned with a fixed amount of air. The exergy value listed for each fuel is normalized to that of H_2 to facilitate comparisons. The second and third columns of Table 1 list the fraction of the original exergy in each fuel that would be destroyed by fuel-air mixing ($\Delta X_m/X$) and combustion irreversibility ($\Delta X_c/X$), respectively. We see here that the fraction of exergy destroyed by air-fuel mixing is relatively low for all fuels (typically less than 2%). The irreversibility losses for combustion (column four) are much larger, and H_2 and

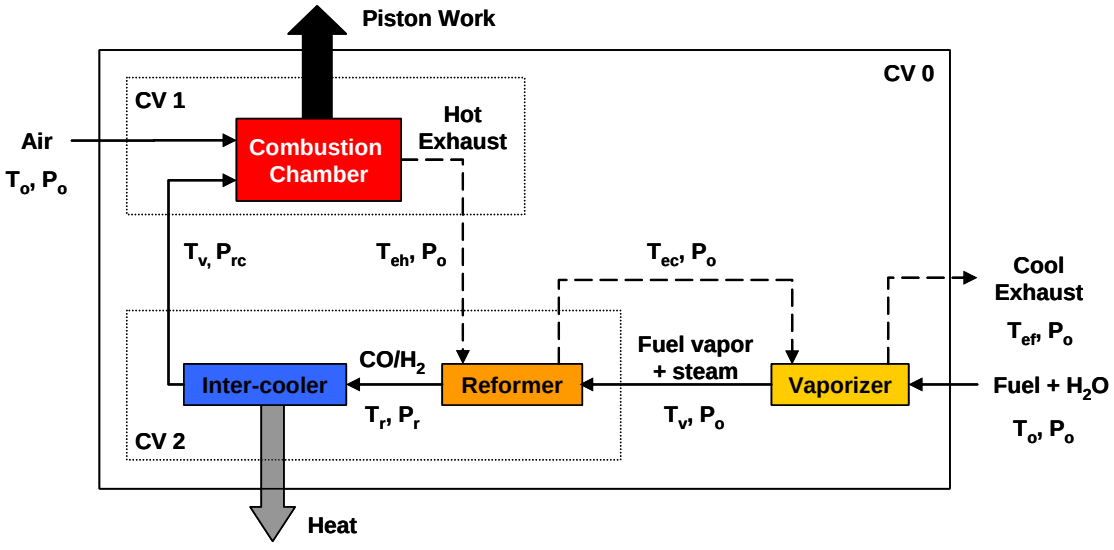

FIGURE 1. Schematic of Conceptual Ideal Piston Engine Utilized for TCR Study

CO clearly stand out from the other fuels in having the lowest losses. The reduced combustion irreversibility for CO and H_2 can be explained by the reduction in the total number of gas molecules that occurs during combustion of these fuels, which lowers the entropy of the products. Combustion entropy is also generated by heat transfer between the reactant and product molecules, so the overall entropy change for H_2 and CO combustion is still positive, but the net entropy increase is smaller than it would otherwise be. For all the other fuels, the total number of molecules increases with combustion and the final entropy is accordingly higher. Relative work output from the ideal engine for each fuel is listed in the fifth column (W^*). Both CO and H_2 generate significantly more work compared to the other fuels. This difference is due to both the high inherent exergy contents and the lower combustion irreversibility for these fuels. That is, less of their initial exergy is destroyed by combustion, so more is left to convert to work.

Figure 2 shows the impact of TCR on methanol, ethanol, and isooctane (the latter two blended with stoichiometric quantities of water) combustion in our idealized engine. Figure 2(a) shows that the decomposition of methanol to H_2 and CO occurs at a relatively low temperature (400-500 K), while the complete reformation of hydrous ethanol requires a temperature of about 800 K and full steam reformation of isooctane is only approached when the reformer exit temperature exceeds 900 K. The higher operating temperatures require increasing fractions of the post-expansion exhaust enthalpy to drive the reformer, as illustrated in Figure 2(b). These increases in exhaust energy recuperation result in more piston work. Figure 2(c) shows that complete reformation of methanol increases the net expansion work by more than 5% of the original fuel exergy, while ethanol TCR increases the normalized work output by 9%. For isooctane, TCR boosts work output by over 11% to achieve nearly 70% overall engine efficiency. Effectively, this improvement amounts to about half of the losses associated with combustion irreversibility. Even accounting for typical inefficiencies in real engines, this is substantial.

To better explain the efficiency trends with increasing reformation and between the three fuels, we have plotted the peak combustion temperatures and pressures for TCR of methanol, ethanol, and isooctane in Figure 3. Increased fuel reforming generates higher peak combustion temperatures and pressures. These higher temperatures and pressures are due to the higher enthalpy of combustion and lower combustion irreversibility (see Table 1) of the reformate (H_2 and CO) mixtures relative to the original fuel molecules. Since the combustion process is assumed to be adiabatic, all of the increased exergy in the combustion products can be converted to piston work in the subsequent expansion step. In short, in the absence of heat loss effects, TCR

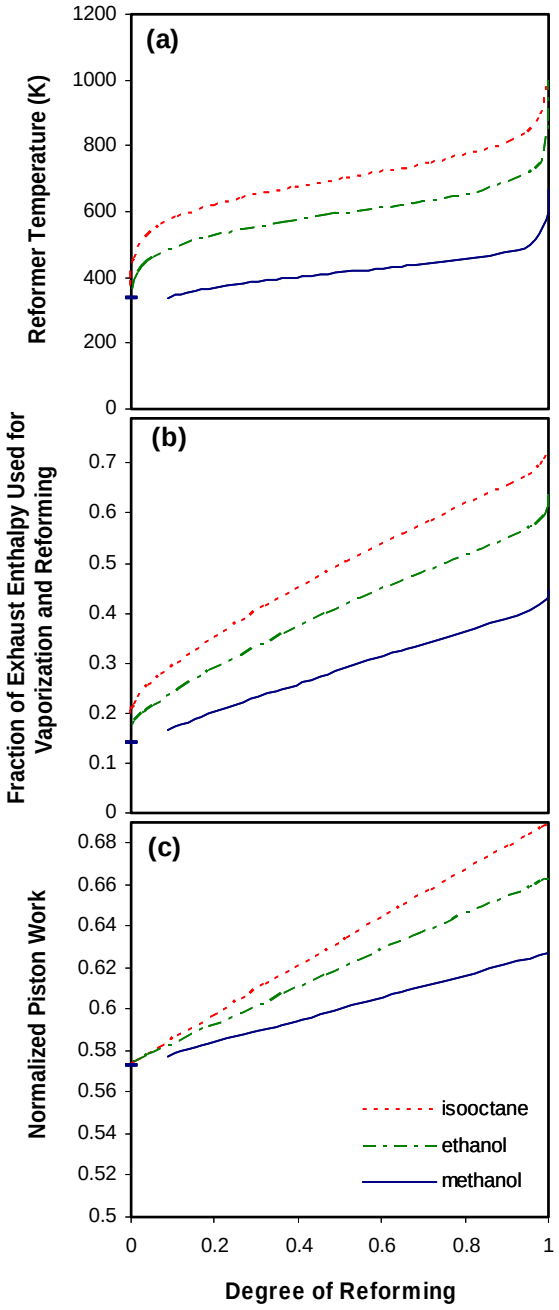

FIGURE 2. (a) Reformer temperature, (b) exhaust enthalpy used for vaporization and reforming, and (c) normalized work output for constant-volume TCR of isooctane (---), ethanol (-·-), and methanol (—).

effectively uses waste exhaust heat to upgrade the hydrocarbon fuel to reformate, which burns with higher heat release and lower irreversibility.

To further explore the effects of TCR, we have plotted the distributions of exergy destruction and conversion within the components of the idealized TCR combustion engine in Figure 4. The plot contains

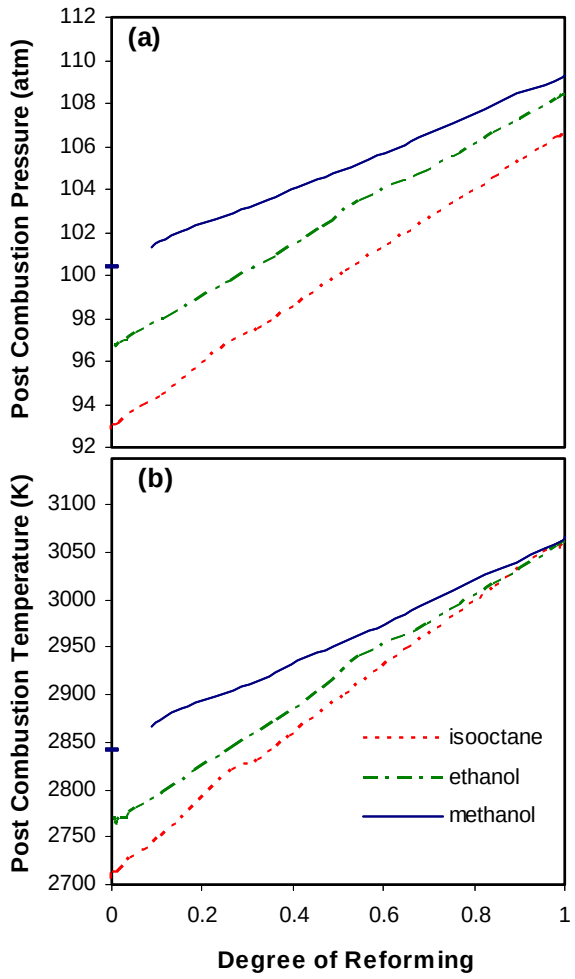

FIGURE 3. (a) Reformer temperature, (b) exhaust enthalpy used for vaporization and reforming, and (c) normalized work output for constant-volume TCR of isooctane (---), ethanol (-•-), and methanol (—).

exergy distributions for all three fuels for two cases: no reforming and roughly 95% reformer conversion. Introducing TCR has several impacts on the overall exergy balance. First, there are two new sources of exergy destruction due to entropy generation in the reformer and heat released from the intercooler. Second, the mixing entropy increases with reformate and air compared to fuel and air. Third, the combustion irreversibility decreases as the fuel is converted to H_2 and CO in the reformer. Fourth, since exhaust heat is used to drive the endothermic reforming reactions, less exergy is lost to the exhaust. The benefits of reduced combustion irreversibility and exhaust exergy outweigh the losses due to the reformer and reformate/air mixing, resulting in higher normalized work output with TCR.

Conclusions

Our initial thermodynamic investigation of TCR indicates that it could result in substantial boosts in internal combustion engine efficiency (as measured in terms of single-stage work output) for a range of fuels. For an ideal stoichiometric engine fueled with methanol, TCR can increase the estimated ideal engine efficiency by about 5% of the original fuel exergy. For ethanol and isooctane the estimated efficiency increases for constant volume reforming are 9% and 11% of the original fuel exergies, respectively. The efficiency improvements from TCR are due to lower exhaust exergy losses and reduced combustion irreversibility with the reformed fuels, but are offset to some extent by entropy generation in the reformer and heat released from the intercooler.

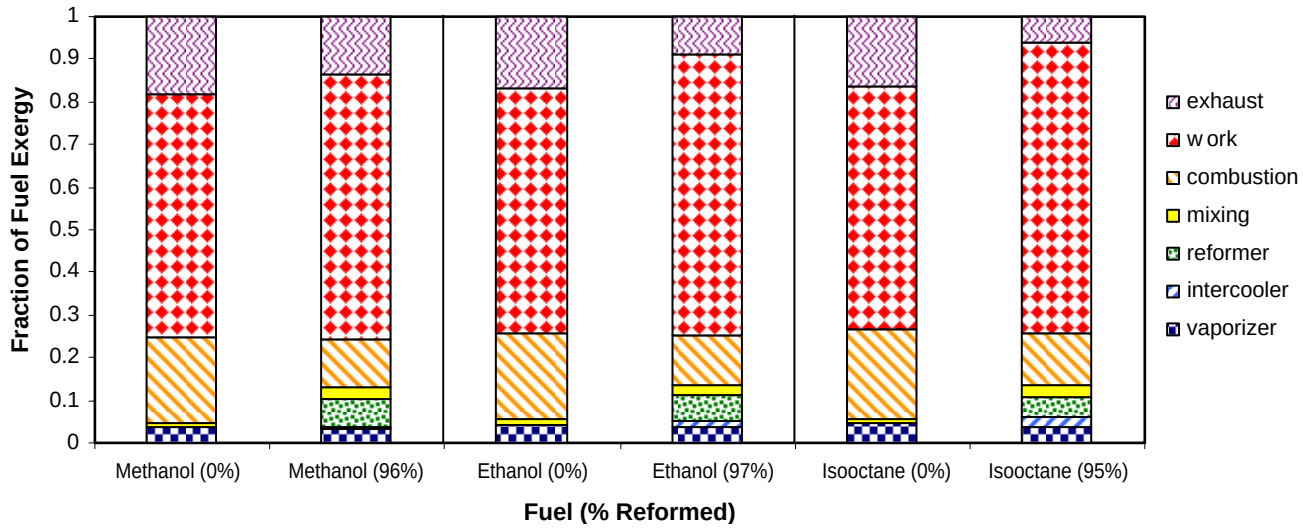

FIGURE 4. Distribution of exergy destruction/conversion for the idealized combustion engine with TCR for each of the three fuels at low and high degrees of reforming.

References

1. C.S. Daw, K. Chakravarthy, J.C. Conklin and R.L. Graves, "Minimizing destruction of thermodynamic availability in hydrogen combustion," International Journal of Hydrogen Energy, 31, 728, 2006.

2. Thermochemical Fuel Reformer Development Project: Higher Efficiency and Lower Emissions for Reciprocating Engines Used in Distributed Generation Applications. EPRI, Palo Alto, CA, California Energy Commission, Sacramento, CA: 2006. 1012774.

FY 2009 Publications/Presentations

1. C. Stuart Daw, Josh A. Pihl, V. Kalyana Chakravarthy, James C. Conklin, Ronald L. Graves, "Stretch Efficiency for Combustion Engines: Exploiting New Combustion Regimes," 2009 DOE Vehicle Technologies Program Merit Review, May 20, 2009.

2. V. Kalyana Chakravarthy, C. Stuart Daw, Josh A. Pihl, James C. Conklin, "A Study of the Theoretical Potential of Thermochemical Exhaust Heat Recuperation in Internal Combustion," submitted to Energy & Fuels, September 2009.

II.A.20 Advancements in Engine Combustion Systems to Enable High-Efficiency Clean Combustion for Heavy-Duty Engines

Houshun Zhang (Primary Contact), Yury Kalish
Detroit Diesel Corporation
13400 Outer Drive, West
Detroit, MI 48239-4001

DOE Technology Development Manager:
Roland Gravel

NETL Project Manager: Carl Maronde

Objectives

Explore advancements in engine combustion systems to enable high-efficiency clean combustion (HECC) techniques to improve thermal efficiency and minimize cylinder-out emissions.

Accomplishments

- Experimentally validated analytical approach to optimize pre-mixed charge compression ignition (PCCI) combustion and utilized it to direct experiments, achieving up to 5% thermal efficiency improvement while maintaining the same emission levels as the baseline engine.
- Experimentally demonstrated transient control methodology to achieve up to 2.5% thermal efficiency improvement over a transient cycle compared to the baseline engine with simultaneous significant reduction in engine-out NO_x.
- Experimentally explored piston bowl shapes for optimal emissions and combustion, including one design that resulted in significant reduction in soot with minimum brake specific fuel consumption (BSFC) penalty.
- Investigated turbocharger system impact on engine performance and emissions experimentally demonstrating up to 1.5% thermal efficiency improvement over a wide range of speeds and loads.
- Quantified the performance of a variable injection nozzle on multiple flow benches and identified the technical barriers moving forward.
- Developed and validated model-based control modules for multiple-input and multiple-output control of injection timing, injection pressure, pilot injection timing, and exhaust gas recirculation (EGR) in an off-line computational environment.

Future Directions

- Continue evaluation of advanced combustion concepts with advanced fuel injection systems.
- Continue development of closed-loop real-time combustion control using novel in-cylinder sensors.
- Consolidate fuel injection strategy and multiple combustion modes to maximize thermal efficiency while maintaining or reducing engine-out emissions compared to baseline.
- Continue transient combustion and control development using next generation model-based control technology.
- Integrate optimized sub-components and optimized combustion strategy into a system targeting 10% thermal efficiency improvement.

Introduction

Detroit Diesel is conducting a cooperative agreement project with DOE with a focus on HECC development for heavy-duty truck engines. This project consists of three major tasks – (1) advanced concept development, (2) subsystem development, and (3) system integration. The primary objective of the project is to explore advancements in engine combustion systems using HECC techniques to improve thermal efficiency while minimizing cylinder-out emissions. Throughout the project, an integrated analytical/experimental approach has been applied to identify and validate the most promising engine system technologies and component enhancements. This annual report summarizes the progress and key findings achieved during this reporting period.

Approach

The fuel injection system and next generation model-based control are identified as two of the most important enabling technologies in achieving the thermal efficiency goal of the project. Two primary fuel injection systems under consideration are shown in Figure 1. They are the Delphi E3 and Bosch ACRS fuel injection systems, each offering its own unique features. A total engine system development approach must be used to fully utilize these two fuel injection systems in conjunction with many other subcomponents and technologies such as EGR, turbocharging, and combustion chamber optimization. In the past decades,

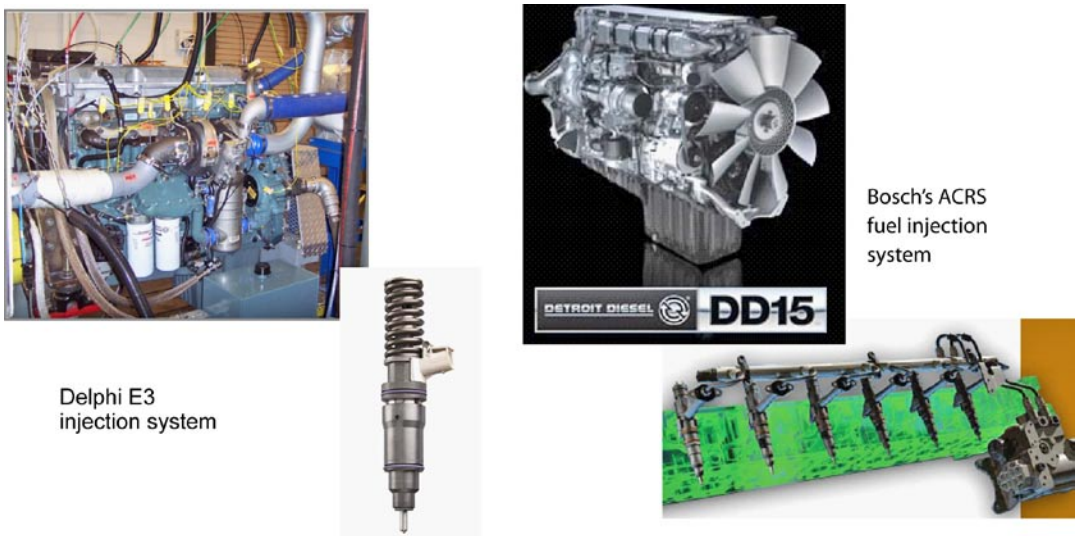

FIGURE 1. Advanced Fuel Injection Systems

while working on both internally-funded and DOE-funded projects, Detroit Diesel has developed a proven methodology of combining experimental and analytical tools to facilitate integrated engine, aftertreatment and vehicle development. Advanced analytical tools are used to carry out systematic simulation and design not only of individual components, but also of an integrated engine system with a focus on key operating modes selected from typical vehicle operation. These optimized individual components, as well as a complete system, are then validated experimentally through steady-state and transient engine tests. After careful calibration optimization in a transient engine test cell, the engine system is installed in a vehicle to undergo a comprehensive validation. The test results are then used to validate and update the analytical models as necessary, starting the next loop of development. This iterative process continues until optimal system is obtained. Throughout this process, model-based control plays a key role in enabling efficient integration of the various subsystems by ensuring optimal performance of each system within the total engine package. This system approach results in a shortened development cycle and substantial NO_X-PM trade-off and fuel economy improvement for both engine and vehicle.

Results

The validated analytical approach has been extensively used to provide valuable design direction and to guide experiments. Figures 2 and 3 show examples of how analytical tools can directly benefit the project. Simulation provided boundary conditions including EGR rate, intake and exhaust pressures and temperatures, and injection parameters, which allowed the experimental work to quickly identify the key control parameters to achieve the optimal results. Figures 2 and 3 show the trade-off of NO_X versus BSFC, and NO_X versus soot. Over 5% BSFC improvement was obtained while maintaining the same emission levels. Table 1 shows that experiments produced almost the same results as early combustion simulations predicted for PCCI combustion optimization.

Development of next generation control has also produced significant results during this reporting period. Instantaneous and integrated emissions and fuel consumption targets were established to allow the real-time optimizer to track engine operation across any operating cycle. The use of 'inverse targets' of desired NO_X, PM and fuel efficiency for given engine output speeds and torques was investigated. This task was initially performed off-line with subsequent on-line validation. A real-time optimizer was developed and exercised to allow on-line real time optimization

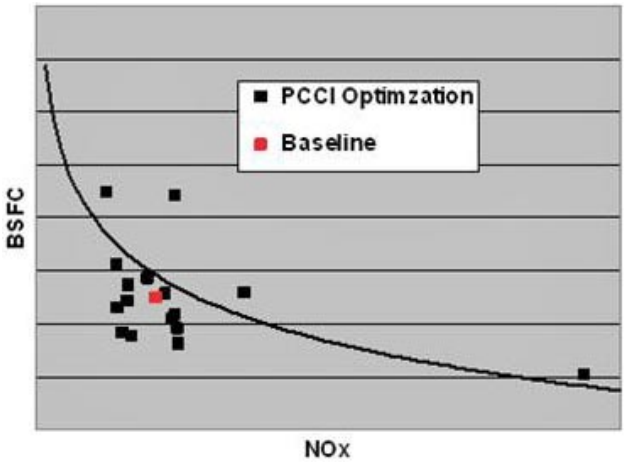

FIGURE 2. BSFC and NO_X Trade-Off (PCCI Testing with Help of Combustion Analyses)

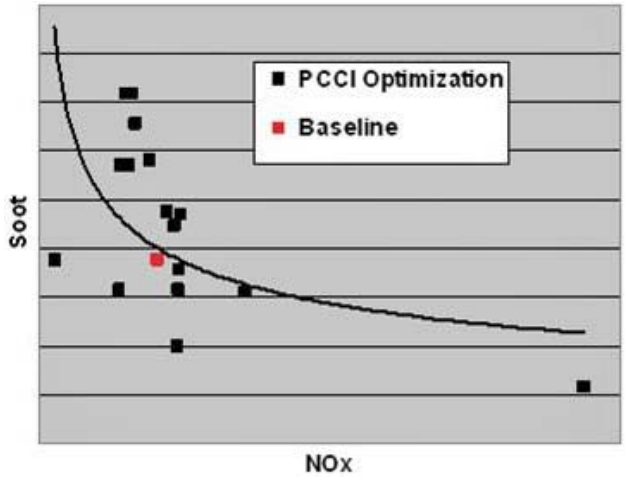

FIGURE 3. Soot and NO_x Trade-Off (PCCI Testing with Help of Combustion Analyses)

TABLE 1. Experimental Validation of Analytical Results

	SOI	AFR	EGR	Boost	NOx	SFC	% gain
	deg		%	bar	g/kgf	g/kW-h	
Simulation	-6.85	25.5	37	1.7	3.2	233.3	
	-10	25.2	45	1.5	3.7	208.1	**10.8**
Experiment	-6.85	24.9	37	1.4	1.9	240.6	
	-10	21.5	44	1.3	2.1	217.9	**9.4**

of fuel efficiency. The ability of the optimization scheme to steer the engine control in real-time has been demonstrated, resulting in a series of engine control schemes for low NO_x, low PM or optimized fuel efficiency. Direct outcomes of the implementation of this model-based control into an engine control unit are shown in Figures 4 and 5. Figure 4 shows that over 2.0% fuel economy improvement is obtained with significant engine-out NO_x emissions reduction compared to the baseline. Figure 5 represents the transient trace of NO_x over an FTP cycle and shows that the NO_x reduction occurs across the entire operating range.

In addition to fuel injection and control development, we recognize the importance of optimizing other combustion components and the air system. This includes evaluation of different piston bowl shapes to better match fuel injection system and evaluation of different turbocharger configurations. Figure 6 shows an example of piston bowl shape optimization, demonstrating PM reduction for most operating points with substantial improvement at light loads, over 60% in some cases. This improvement, however, occurred at the expense of slight deterioration in fuel economy. This set of results indicates the direction for further optimization of piston bowl shape with the focus on fuel economy improvement.

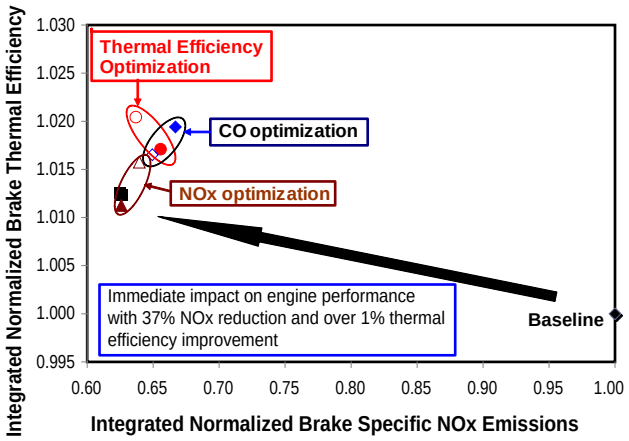

FIGURE 4. Controller Optimization over Transient Cycle

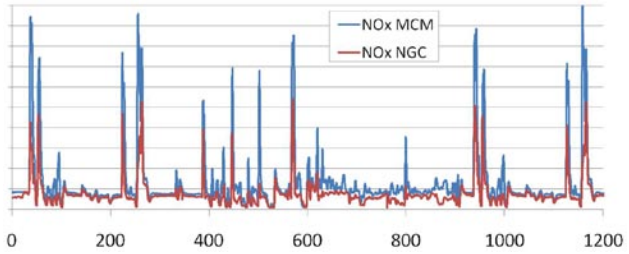

FIGURE 5. Comparison of Federal Test Procedure NO_x Emissions for Baseline Control and Next Generation Controller (NGC)

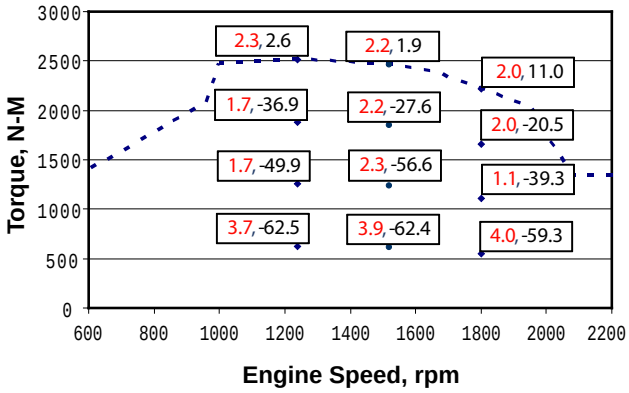

FIGURE 6. Piston Optimization [%BSFC (Red), %Smoke (Black) – Positive numbers indicate increase]

In order to reduce pumping loss and provide more effective EGR flow to improve combustion, investigation of different turbocharger housings and flow entry geometries was conducted. The impact on engine performance and emissions was evaluated, and demonstrated up to 1.5% thermal efficiency improvement with some design features.

Conclusions

The key accomplishments of this heavy-duty truck engine development project in this reporting period are summarized as follows:

- Experimentally demonstrated up to 5% thermal efficiency improvement through PCCI combustion optimization on a multi-cylinder engine by using analytical simulations to drive experimental investigations.
- Experimentally demonstrated transient control methodology on a transient cycle to achieve up to 2.5% thermal efficiency improvement compared to the baseline engine with simultaneous significant engine-out NO_x reduction.
- Experimentally demonstrated combustion chamber features for optimal emissions and combustion including a piston design with significant soot reduction, and identified a path to piston designs with potential thermal efficiency improvements.

FY 2009 Publications/Presentations

1. Christopher Atkinson, Marc Allain, Yury Kalish, and Houshun Zhang, "Model-Based Control of Diesel Engines for Fuel Efficiency Optimization", SAE Paper 2009-01-0727.

2. Deyang Hou, Houshun Zhang, Yury Kalish, Chia-fon F. Lee, and Way Lee Cheng, "Adaptive PCCI Using Micro-Variable Circular-Orifice (MVCO) Fuel Injector – Key Enabling Technologies for High Efficiency Ultra Clean Diesel Engines." SAE paper 2009-01-2508.

3. Hai-Wen Ge, Yu Shi, Rolf D. Reitz , David D. Wickman, Guangsheng Zhu, Houshun Zhang, and Yury Kalish, "Heavy-Duty Diesel Combustion Optimization Using Multi-Objective Genetic Algorithm and Multi-Dimensional Modeling." SAE Paper 2009-01-0716.

4. Houshun Zhang, Yury Kalish, Marc Allain, and Guangsheng Zhu, "High Efficiency Clean Combustion for Heavy-Duty Engine," 15th Annual Directions in Engine-Efficiency and Emissions Research (DEER) Conference, Dearborn, MI (Aug 3–6, 2009).

5. Marc Allain, Alexander Kropp, Yury Kalish, Houshun Zhang, and Chris Atkinson, "Demonstrating and Validating a Next Generation, Model-Based Controller for Fuel-Efficient, Low Emissions Diesel Engines," 15th Annual Directions in Engine-Efficiency and Emissions Research (DEER) Conference, Dearborn, MI (Aug 3–6, 2009).

6. Rakesh Aneja, Yury Kalish, and David Kayes, "Integrated Powertrain and Vehicle Technologies for Fuel Efficiency Improvement and CO_2 Reduction," 15th Annual Directions in Engine-Efficiency and Emissions Research (DEER) Conference, Dearborn, MI (Aug 3–6, 2009).

II.A.21 Development of High Efficiency Clean Combustion Engine Designs for Spark-Ignition and Compression-Ignition Internal Combustion Engines

Part I - Spark-Ignition Internal Combustion Engines

Kenneth J. Patton
General Motors (GM)
Powertrain Advanced Engineering
Mailcode 483-710-270
895 Joslyn Ave.
Pontiac, MI 48340

DOE Technology Development Manager:
Ken Howden

NETL Program Manager: Carl Maronde

Objectives

- Develop and demonstrate engine designs which enable homogeneous charge compression ignition (HCCI) combustion systems.
- Use analysis, design, prototype builds, and testing of prototype builds to confirm capability and performance of individual components, subsystems, and complete engine systems.
- Develop and demonstrate an "enabling" engine which uses a lower-risk variable valvetrain system to enable HCCI operation in an effort to express a production-feasible hardware solution.
- Develop and demonstrate a fully-flexible engine which uses a higher-risk, but more capable, variable valvetrain system to explore the benefits of HCCI operation.
- Reduce technical risk and cost of all components and systems by defining component and subsystem requirements, evaluating alternative technologies, working with supply base, identifying areas for improvement and simplification, and executing hardware solutions.

Accomplishments

- Enabling engines have been demonstrated on a dynamometer and in a vehicle. Functionality of engines and vehicle was as expected. While some specific challenges remain, the demonstration properties have been highly successful in meeting the stated objectives.
- One continuing specific challenge is the durability and robustness of production-feasible and cost-effective in-cylinder pressure sensing subsystems. This project continues to evaluate alternative technologies and supplier solutions in efforts to identify acceptable solutions. Major progress has been made in developing good requirements for cylinder pressure sensing subsystems. Some progress has been made in encouraging the supply base.
- One continuing specific challenge for the enabling engine is the robustness of mode-switching from spark-ignition (SI)-to-HCCI and HCCI-to-SI regimes. Demonstration of hardware which enables good switching has been completed, and execution of capable/robust/responsive engine controls is an ongoing development project which will extend beyond the scope of this project.
- One continuing specific challenge is the noise and vibration performance of the engine in HCCI mode and during mode-switching. This is important in terms of customer acceptance of HCCI. Demonstration hardware has been shown to be sufficiently capable, and the tradeoff between fuel economy improvement and noise/vibration performance has been explored. Ongoing development which will extend beyond the scope of this project will continue to focus on maximizing the fuel economy benefit while meeting noise performance requirements.
- Fuel efficiency improvements demonstrated by the enabling engine have been as expected. Overall vehicle fuel economy benefits are highly dependent on the engine speed/load and on the amount of time spent in HCCI mode, so many challenges remain in extracting HCCI fuel economy benefits in the real world and on fuel economy driving cycles.
- The fully-flexible multi-cylinder engine design, procurement, and build has been completed.
- Spin-rig testing of the fully-flexible multi-cylinder engine design has been carried out, both as a checkout for hardware/software functionality, and as a diagnostic tool to improve performance and robustness of the valve motion control algorithms. Significantly more time on the spin rig than was planned was required to achieve good robustness, and as the year ends it appears that robust valve motion control is becoming a reality.
- More spin-rig work is required to ensure adequate protections for certain valve event commands; this is extending the amount of time that the engine runs on the spin rig (as opposed to firing on the dynamometer, which is a higher-risk task).

- Heavy use of analytical tools has enabled execution of a valve actuator design which stays true to the prototype actuator concepts which were executed earlier in the project. This is a significant advance in electro-hydraulic valve actuation technology.
- The demonstrated prototype actuator functionality can deliver the expected capabilities in the multi-cylinder engine.
- One specific challenge for the fully-flexible actuation system is its performance under the wide variety of ambient temperature and pressure conditions expected in normal vehicles. The demonstration hardware will be capable of quantifying this performance, and will be an important source of data to be used for developing more complete subsystem requirements for production fully-flexible engines.
- One specific challenge for the fully-flexible actuation system is its noise and vibration performance. Both the prototype hardware already demonstrated, and the upcoming multi-cylinder hardware, will be important contributors to the identification of specific noise source in the fully-flexible actuation system.

Future Directions

- Close out the remaining tasks (primarily generation of performance data) on the already-demonstrated enabling engine hardware.
- Continue to use the enabling engine as the test bed for production-style cylinder pressure sensing subsystems.
- Demonstrate the fully-flexible engine.

Approach

- Using analysis, design tools, prototype subsystem builds, multi-cylinder engine builds, and vehicle builds, demonstrate enabling and fully-flexible engine systems which run HCCI combustion systems.
- Focus on the engine design and base engine hardware portions of the HCCI solution for this project, but use other necessary GM efforts outside this project to contribute combustion system operating strategy and powertrain control system development and execution.

Results

In the zone of HCCI operation, fuel efficiency benefits of as low as 8% and as high as 20% have been measured. Outside the zone of HCCI operation, of course, the measured benefits are essentially zero since they are normal SI mode. Real-world and on-cycle fuel economy benefits will be highly dependent on the speed/load operation of the engine and the amount of time the vehicle can spend in HCCI mode. Base engine hardware capability for the enabling engine is sufficient to enable HCCI operation.

Conclusions

This project is continuing to be a successful demonstration of gasoline engine designs which enable HCCI combustion systems. The gasoline engine hardware designed and demonstrated so far have been key contributors to GM's overall efforts to understand, develop, and demonstrate HCCI vehicle solutions. Next steps in the project are being pursued as planned.

Part II - Compression-Ignition Internal Combustion Engines

Manuel A. Gonzalez D. (Primary Contact), Joshua Bedford, and Russell Durrett
General Motors
895 Joslyn Ave.
Pontiac, MI 48340

DOE Technology Development Manager: Ken Howden

NETL Program Manager: Carl Maronde

Objectives

- Design and implement simple variable value actuation (VVA) mechanism solutions including advanced charging components in a multi-cylinder engine combined with aftertreatment technology for reaching beyond Tier 2 Bin 5 tailpipe emission targets.
- Explore the trade-offs and synergies of VVA with an advanced charging system and calibration on the multi-cylinder engine.
- Quantify the benefits and limitations of using VVA to reduce engine-out pollutant emissions and improve fuel economy at Tier 2 Bin 5 engine-out NOx emission levels using a single-cylinder engine with a fully flexible valve actuation (FFVA) system.
- Explore the operating conditions where the strategies can be applied, and identify the potential merit of simple VVA mechanisms for future engine system implementations.

- Design a FFVA system for single-cylinder engines in support of wider understanding of the technology and for multi-cylinder engine development.

Accomplishments

- Assessed the kinematic and dynamic requirements for a two-step mechanism for generating diesel engine exhaust valve re-opening events.
- Assessed the brake thermal efficiency and emission benefits of internal exhaust gas recirculation (IEGR) for engine performance at key operating points in the warm-up phase of the Federal Test Procedure (FTP) driving cycle.
- Assessed the benefits and limitations of IEGR for controlling exhaust temperatures.
- Design and implementation of a two-stage turbocharging system for charging requirements of VVA in a multi-cylinder diesel engine.
- Design and implementation under motoring conditions of a concentric camshaft mechanism for variable effective compression ratio in a multi-cylinder diesel engine.
- Design of fully flexible VVA system for independent control of each valve in a single-cylinder engine with packaging in a base multi-cylinder engine head.

Future Directions

- Experimental testing of a concentric camshaft mechanism for variable effective compression ratio in a multi-cylinder diesel engine.
- Review of VVA profiles for functionalities at key conditions of engines in driving cycles.
- Design of purpose-built mechanisms for specific functionalities on cold- and hot-engine operation.
- Further understanding of the synergy of intake and exhaust camshaft valve actuation mechanisms on steady-state and transient engine in-cylinder conditions.
- Validate emissions and fuel efficiency benefits with single-cylinder and multi-cylinder engine development.
- Further development of systems for VVA maximizing functional design, packaging and manufacturing considerations for potential applications.

Approach

- VVA in a multi-cylinder work was performed based on modeling and single-cylinder engine assessment.
- Valve actuation mechanisms and charging requirements for selected valve events have been reviewed, designed and implemented in a multi-cylinder diesel engine (Figure 1).
- Comprehensive studies of the benefits of IEGR on diesel fuel economy and emissions have been conducted for achieving Tier 2 Bin 5 NOx emission levels combined with aftertreatment systems. The design and implementation of these simple VVA systems in the multi-cylinder are under current development.

Results

- IEGR has been applied up to 2,000 rpm, 47% part load on the engine operating map with an exhaust valve rebreathing event.
- Estimated 50% reduction in unburned hydrocarbons emissions during the first 200 sec of the FTP cycle, also with up to 34% reduction in carbon monoxide emissions based on weighted emission factors (Figure 2).
- It is feasible to increase the conversion efficiency of the diesel oxidation catalyst (DOC) at idle by increasing engine-out temperatures with IEGR.
- Engine-out smoke can increase up to around 1.0 filter smoke number however this can be controlled by injection strategy.
- The coefficient of variation of indicated mean effective pressure can be reduced up to 40% with IEGR.
- The fuel consumption increases with IEGR up to 3.6% at specific part-load keypoints. However, during the 200 sec warm-up phase, overall brake specific fuel consumption (BSFC) increases 1.3%. A higher engine-out exhaust temperature of up to 40°C can be achieved. Energy utilization for having higher exhaust temperatures is compensated by using between 35 and 97% less external EGR with

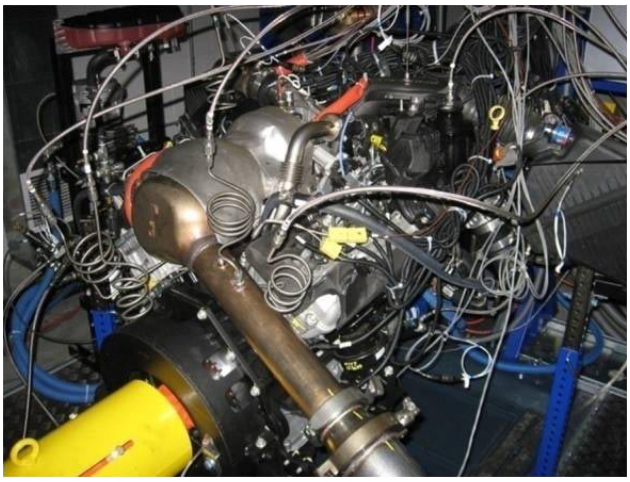

FIGURE 1. Multi-Cylinder Diesel Engine Installed in a Test Cell for Variable Valve Actuation Testing

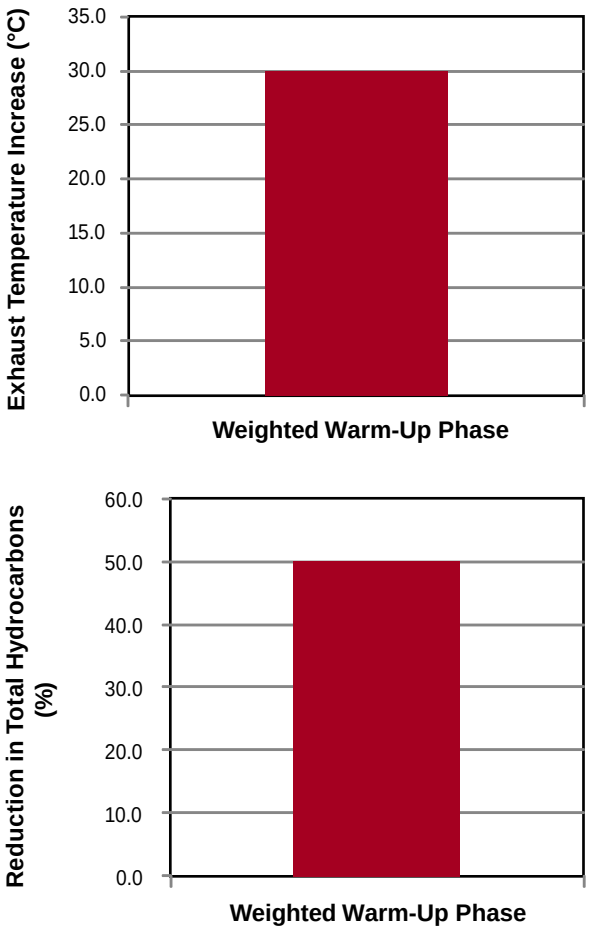

FIGURE 2. Benefits of IEGR in a Multi-Cylinder Diesel Engine (Weighted results on keypoints for the first 200 sec of the FTP cycle.)

reduced pumping losses at constant NOx emissions for specific valve lift profiles.

- Generating a matching of the exhaust temperatures increases at 800 rpm, the corresponding BSFC for IEGR is 8% lower than the BSFC required using main injection with retarded timing, but also having 50% lower emissions of hydrocarbons. IEGR is a promising effective technique for exhaust gas temperature management.
- At 800 rpm, there is an increase of up to 40°C in the temperature at the turbine inlet which compounds with the higher conversion in the DOC resulting in up to 60°C increase at in DOC outlet temperature for improved downstream aftertreatment efficiency.
- There are moderate differences in engine performance when comparing the location of the IEGR actuating valve in the combustion chamber relative to the position of the tangential or helical intake ports. In those cases studied, this is mostly due to differences in the calibration approach used.
- The exhaust rebreathing flow affecting the overall in-cylinder flow structure for mixing might be a meaningful factor determining exhaust emissions when high amounts of exhaust rebreathing mass are used. This is a subject for further study at variable air-fuel ratio capabilities and decoupling air flow dynamics from specifc air-fuel ratio effects when higher temperatures and mass rates of the rebreathing charge are applied.

Conclusions

- Specific mechanisms and charging requirements have been characterized for VVA in a diesel engine for providing increasing degrees of freedom for system optimization. Encouraging results have been observed using VVA in a diesel engine.
- By adopting IEGR, engine-out emissions can be reduced; energy utilization required for warm-up during cold-start can be further optimized; combustion stability can be enhanced at part loads and combustion noise and smoke can be further controlled when combined with tailored injection strategies.
- A new design of a fully-flexible VVA system for a single-cylinder engine has been completed.
- This project is continuing to be a successful demonstration of diesel engine designs for improved powertrain performance. The work performed is a key contributor to determine the technology merit of VVA for new diesel engines.

Patents Issued

1. Manuel Angel Gonzalez Delgado; Rober J. Moran; Sameer Bhargava; Ronald Jay Pierik, “Engine including valve lift assembly for internal EGR control” U.S. and international patent application.

II.A.22 Light Duty Efficient Clean Combustion

Donald Stanton
Cummins Inc.
1900 McKinley Ave.
Columbus, IN 47201

DOE Technology Development Manager:
Roland Gravel

NETL Project Manager: Carl Maronde

Objectives

- Improve light-duty vehicle (5,000 lb. test weight) fuel efficiency over the Federal Test Procedure (FTP) city drive cycle by 10.5% over today's state-of-the-art diesel engine.
- Develop and design an advanced combustion system that synergistically meets Tier 2 Bin 5 oxides of nitrogen (NOx) and particulate matter (PM) emissions standards while demonstrating efficiency improvements.
- Maintain power density comparable to that of current conventional engines for the applicable vehicle class.
- Evaluate different diesel fuel properties and ensure combustion system compatibility with commercially-available biofuels.

Accomplishments

- Can achieve 0.08 g/mi NOx on the FTP-75 emissions certification cycle without NOx aftertreatment while improving the fuel efficiency by 4.5% relative to the 10.5% target.
- Can achieve 0.07 g/mi NOx on the FTP-75 emissions certification cycle with selective catalytic reduction (SCR) NOx aftertreatment while improving the fuel efficiency by 9.1% relative to the 10.5% target.
- Completed the design and testing of a sequential 2-stage turbocharger to provide power density, minimize pressure drop, and deliver the targeted air/fuel and exhaust gas recirculation (EGR) rates.
- The design and testing of a combustion system (piston, fuel injector configuration, and intake swirl level) to extend the early pre-mixed charged, compression ignition (PCCI) combustion regime was completed.
- Integration of a piezo fuel system with steady-state calibration to demonstrate the ability to reduce PM emissions while meeting the noise, vibration, and harshness (NVH) requirements for light-duty vehicle application.
- Created and procured a novel variable valve actuation (VVA) design to provide intake and exhaust valve manipulation.
- Steady-state testing completed using a full authority VVA system to demonstrate the potential fuel efficiency improvement and combustion stability associated with low-temperature combustion (LTC).
- Closed-loop combustion controls implemented.
- Extended project to include SCR NOx aftertreatment architecture to meet the need for supplemental FTP2 (SFTP2) emissions certification.
- Selected an SCR NOx aftertreatment design for engine integration based on validated system modeling.

Future Directions

Phase 1 has been focused heavily on applied research as directed through the analysis-led-design initiative. During Phase 2, Advanced Development, the emphasis on simulation will be reduced and experimental development and validation will become the primary focus. During 2010, we expect to:

- Perform multi-cylinder engine testing using the Phase 2 hardware (revised 2-stage sequential turbo, piezo fuel system, high-capacity EGR, controls, and aftertreatment).
- Develop a detailed engine calibration using the Phase 2 technology to meet FTP75 and SFTP2 emissions certification.
- Incorporate a new SCR system design with full engine and aftertreatment calibration.
- Continue VVA testing and design refinement.
- Explore technology to enhance aftertreatment thermal management.
- Transient assessment of fuel efficiency improvements using test cell and software analysis procedure.
- Test biofuel blends to demonstrate compatibility.
- Assess suppliers of critical components for technology and commercial readiness to ensure the technologies required for the planned architecture will be available for production.

Introduction

Light-duty vehicles account for over 60% of all transportation energy consumption in the United States. Reducing petroleum fuel use and greenhouse gas emissions will require limiting the fuel consumed in light-duty vehicle engines. Today nearly all light-duty vehicles in the United States are powered by gasoline engines. Diesel engines have significant efficiency benefits over gasoline engines, and there are opportunities to further improve the diesel combustion system. If 30% of the light truck fleet in the United States were to transition to diesel engines, fuel consumption would be reduced by approximately 90 million barrels of oil per year. When fully implemented, developments proposed in this project will enable a 10.5% efficiency improvement, increasing potential fuel savings to 119 million barrels per year. The fuel savings associated with this project would reduce greenhouse gas emissions by eliminating the production of 11 million metric tons of CO_2 per year.

Cummins will develop and demonstrate combustion technologies for diesel engines that realize 10.5% efficiency improvements while meeting U.S. EPA Light-Duty Emissions Standards (Tier 2, Bin 5) in a robust and cost-effective manner. The work integrates the areas of LTC, air handling, advanced fuel systems, and closed-loop controls to support high efficiency, low emission combustion concepts. Multiple steps are planned in the development process including analysis led design, concept integration, advanced system development and demonstration.

Approach

The project strategy is focused on the expansion of LTC to meet project objectives. LTC will result in very low engine-out emissions while achieving high efficiency. Two modes will be evaluated to expand the LTC region: smokeless rich combustion and early PCCI. Cummins believes these two modes offer the most opportunity for efficiency improvements while maintaining extremely low engine-out emissions.

As the engine transitions to higher speed and load operation, the combustion mode will transition to lifted-flame diffusion-controlled combustion. Lifted-flame diffusion-controlled combustion occurs when the diffusion flame is positioned further downstream of the liquid diesel fuel compared to conventional diffusion controlled diesel combustion. Anchoring the diffusion flame further downstream allows more air to be entrained into the combustion plume, resulting in lower equivalence ratios in the region of first stage reactions. The overall consequence is lower soot formation as the engine transitions from lower load PCCI combustion to high-load engine performance.

Although the details are not yet finalized, the potential SFTP2 regulation proposes to mandate tailpipe-out emissions levels over the aggressive US06 drive cycle that are similar in magnitude to the levels required for the light load FTP75 urban drive cycle. This represents a significant risk for an in-cylinder NOx solution since the US06 drive cycle produces significant high-load, high-speed engine operation. As a result, both in-cylinder and advanced SCR solutions are being considered.

Results

The first phase of the project, Applied Research, has been focused primarily on analysis-led-design. Combustion models have been used to analyze and optimize the combustion recipe. Engine cycle simulation models have been used to evaluate VVA, air handling and EGR components and to investigate preliminary architecture options. Controls algorithms and software have been developed and tested in the software simulation environment. Based on this work, preliminary engine architectures have been developed for both in-cylinder and advanced SCR solutions.

The preliminary architectures are designed to improve fuel efficiency by focusing on four main areas; closed-cycle efficiency improvements, air handling/EGR systems, advanced controls, and aftertreatment. The major contributors to closed-cycle efficiency improvements include expansion of LTC, combustion system optimization, enhanced EGR cooling, and VVA. Air handling and EGR system improvements include high-efficiency two-stage variable-geometry turbocharger (VGT), advanced low pressure drop EGR cooling systems, and VVA. Controls efforts are focused on closed-loop combustion control and model-based air handling controls. Both paths also include a reduction in fuel economy penalties associated with the diesel particulate filter (DPF) via reduced regeneration frequency and pressure drop.

Based on the analysis and engine data, an estimate of fuel efficiency improvements for the preliminary architectures has been developed. The estimated fuel efficiency improvements for the in-cylinder solution are shown in Table 1. The efficiency improvements shown are relative to the current baseline engine which is equipped with an LNT NOx aftertreatment system.

As shown in Table 1, the estimated fuel efficiency improvement for an in-cylinder NOx emissions solution is 11.5%, which exceeds the project goal of 10.5%. However, the most significant risk associated with an in-cylinder solution is that it will not be capable of meeting the emissions requirements required by the potential SFTP2 regulation. Hence, a high-efficiency SCR NOx aftertreatment solution is also being investigated. The estimated efficiency improvement for the SCR

TABLE 1. Estimated improvements in fuel efficiency for an in-cylinder NOx emissions solution relative to an architecture employing an LNT NOx aftertreatment system.

Category	Major Technologies	Fuel Efficiency Improvement
Closed-Cycle	Expand LTC Optimize combustion system Enhanced EGR cooling VVA	3%
Air Handling/EGR	High-efficiency two-stage VGT Low pressure drop EGR VVA	2%
Controls	Closed-loop combustion control Model-based air handling controls	1.5%
Aftertreatment	Elimination of LNT Reduced DPF regeneration	5%
Total		**11.5%**

architecture, relative to the baseline LNT architecture, is similar to the in-cylinder solution. However, since the SCR solution enables high engine-out NOx over much of the drive cycle, closed-cycle efficiency improvement is expected to be slightly greater. Due to urea consumption and thermal management, efficiency improvements associated with aftertreatment are expected to be slightly less than the in-cylinder solution. During the next phase of the project, Advanced Development, efficiency improvements with be validated and optimized experimentally. A final architecture decision will be made based on the results of these experiments.

Conclusions

During 2009, all project milestones and deliverables were completed. All subsystem technologies (fuel system, turbomachinery, combustion system, aftertreatment, etc.) were integrated on a multi-cylinder engine. A summary of the achievements are listed based on limited engine testing and analysis:

- Can achieve 0.08 g/mi NOx on the FTP75 emissions certification cycle without NOx aftertreatment while improving the fuel efficiency by 4.5% relative to the 10.5% target.
- Can achieve 0.07 g/mi NOx on the FTP75 emissions certification cycle with SCR NOx aftertreatment while improving the fuel efficiency by 9.1% relative to the 10.5% target.
- Completed the design and testing of a sequential 2-stage turbocharger to provide power density, minimize pressure drop, and deliver the targeted air/fuel and EGR rates.
- Completed the design and testing of a combustion system (piston, fuel injector configuration, and intake swirl level) to extend the early PCCI combustion regime.
- Integration of a piezo fuel system with steady-state calibration to demonstrate the ability to reduce PM emissions while meeting the NVH requirements for the light-duty vehicle application.
- Created and procured a novel VVA design to provide intake and exhaust valve manipulation.
- Steady-state testing completed using a full authority VVA system to demonstrate the potential fuel efficiency improvement and combustion stability associated with LTC.
- Closed-loop combustion controls implemented.
- Extended project to include SCR NOx aftertreatment architecture to meet the need for SFTP2 emissions certification.
- Selected an SCR NOx aftertreatment design for engine integration based on validated system modeling.

FY 2009 Publications/Presentations

1. 2009 DEER Conference Presentation – "Technology Development for Light Duty High Efficient Diesel Engines", presented by Donald Stanton, 5th August, 2009.

II.A.23 Advanced Boost System Development for Diesel HCCI Application

Harold Sun
Ford Motor Company
2101 Village Road
Dearborn, MI 48214

DOE Technology Development Manager:
Ken Howden

NETL Project Manager: William Cary Smith

Subcontractors:
- Wayne State University, Detroit, MI
- ConceptsNREC, White River Junction, VT

Objectives

The overall objective is to support industry efforts of clean and efficient diesel engine development for passenger and commercial applications. More specifically:

- ConceptsNREC objectives: leads boost system design, optimization, computer-aided engineering (CAE) stress analysis and fabrication of prototypes as well as flow bench test; provides turbocharger maps for various turbo technologies to support system level simulation/integration.
- Wayne State University objectives: leads computational fluid dynamics (CFD) analysis and analytical validation of various turbocharger concepts designed by ConceptsNREC.
- Ford Motor Company objectives: leads system integration, cascade system requirement, boost system development design target, validation and demonstration of fuel economy improvement of light-duty diesel engine performance on engine test bench.

Accomplishments

Task 2 – Aerodynamic design, CFD validation and structure analysis of the turbocharger were completed. However, based on the findings from flow bench test, further design changes were made on compressor and CFD validation, CAE structure analyses for high/low cycle fatigue durability compliance as well as flow bench test were repeated on two compressor impellers, five different compressor diffusers and three different casing treatment designs. Supported by flow bench data, the latest compressor and turbine design is expected to achieve design targets in terms of compressor and turbine efficiencies.

Task 4 –Prototype fabrication and flow bench validation of the advanced boost systems was partially pulled up to validate some of the design concepts and analyses.

- Aerodynamic design, and CFD and structure analysis of the mixed flow turbine was completed. A total of 12 compressor design iterations were made for optimal performance.
- A Honeywell GT35 turbocharger was modified with a mixed flow turbine that fits into the existing variable nozzle turbine structure. Six design iterations of turbine have been carried out to make sure the turbine meets our design target and structure, and that low/high cycle fatigue testing meets the design guidelines. The fabrication and flow bench test validation on two compressor wheels (including seven different diffuser configurations and three casing treatment options) and one mixed flow turbine wheel have been completed. The test data were used to guide the final design iteration of the compressor and turbine.
- The flow bench data indicated that some of the technologies used for compressor performance enhancement did not achieve the desired design targets: a) an ultra-low solidity diffuser vane improves low-end compressor efficiency but it narrows the flow range; b) CFD analyses did not identify any significant benefit for variable inlet guide vanes. Surprisingly, an optimized casing treatment showed improved compressor efficiency with wide operation range, when matched with an optimized compressor impeller. As a result, a vaneless compressor with optimal casing treatment and impeller was adopted as the final compressor configuration.
- The mixed flow turbine demonstrated the anticipated efficiency improvement at the low speed ratio area, along with 4% improvement in flow capacity with the similar inertia of a conventional radial flow turbine.
- During 2009, two invention disclosures were filed, two journal papers were published, and three presentations were made at the SAE Congress and DEER conferences.

Future Directions

- Fabricate the final version of the compressor and turbine based on the prior flow bench test data and prior design iterations and CAE/CFD analyses.
- Migrate the same technologies to a small turbocharger design/optimization to support light-duty diesel applications.

Introduction

Diesel homogeneous charge compression ignition (HCCI) and low-temperature combustion (LTC) have been recognized as effective approaches to dramatically reduce diesel emissions. However, high levels of exhaust gas recirculation (EGR) are needed to achieve homogeneous or partially homogeneous modes, which often drive the compressor and turbine into less efficient or even unstable operational areas.

To support industry efforts of clean and efficient internal combustion engine development for passenger and commercial applications, this project will focus on complete and optimal system solutions to address boost system challenges, such as efficiency degradation and compressor surge, etc., in diesel combustion/emission control system development, and to enable commercialization of advanced diesel combustion technologies, such as HCCI/LTC.

Approach

There are several boosting concepts that have been seen in the literature and will potentially be helpful to extend the operation range with decent efficiency. They are primarily single-stage turbochargers so that they are cost-effective, have small package space, and small thermal inertia while providing enough EGR that is required by advanced combustion concepts such as HCCI/LTC.

This project will particularly focus on the following:

- Compressor variable inlet guiding vane (VIGV): by varying the air rotational flow direction at compressor inlet to have a better alignment with compressor blades, the compressor can work at a smaller mass flow without surge or stall.
- Similarly, an optimized casing treatment on the compressor housing can also re-align the re-circulated air flow to extend the surge margin.
- Variable geometry compressor: an optimized airfoil diffuser can push the surge line to a lower flow rate on the compressor map, often at the expense of efficiency in the off-peak operation range and possibly reduce full flow capacity. A variable vane at compressor diffuser areas can maintain high compressor efficiency at a wide range of operation.
- Dual sequential compressor volute/outlet: a bifurcated volute that has dual outlets and can be opened sequentially to match air exit velocity to compressor vane geometry. This is an alternative design concept that is simpler, more economical and potentially more durable than a variable geometry compressor since it has only one moving part: the switching valve.
- The mixed flow turbine is an attractive option to improve efficiency on the turbine side. Current turbine efficiency at light load and low speed is substantially lower than its peak efficiency. The target of this study will focus on high turbine efficiency at a lower speed ratio to improve EGR pumping capacity and vehicle fuel economy on customer driving cycles.

The above technologies have been fully investigated with well-validated numerical simulation methods. Some of them have been investigated via flow bench testing. The variable diffuser vane compressor was eliminated based on flow bench testing due to larger than expected operation range constraints; the VIGV technology was considered non-compatible with our optimized impeller geometry; the dual sequential compressor volute has merit in efficiency and operation range enhancement based on numerical study. However, this technology is difficult to implement in small turbochargers due to package space constraints.

Results

- Figure 1 shows the fabricated parts of two compressor wheels and the mixed flow turbine wheel.
- Figure 2 is the turbocharger assembly. The fabricated compressor wheel and turbine wheel were installed on a Honeywell GT35 donor turbocharger. Best compressor performance was obtained with guide vanes inside the casing treatment. A diffuser with from five to 11 vanes as well as a vaneless diffuser was numerically analyzed and tested on a flow bench.
- The compressor efficiency with a vaneless diffuser and impeller #2, casing treatment option C, as compared with those that are currently in production, is shown in Figure 3. Apparently the newly developed compressor demonstrated an

FIGURE 1. Mixed Flow Turbine Wheel and Compressor

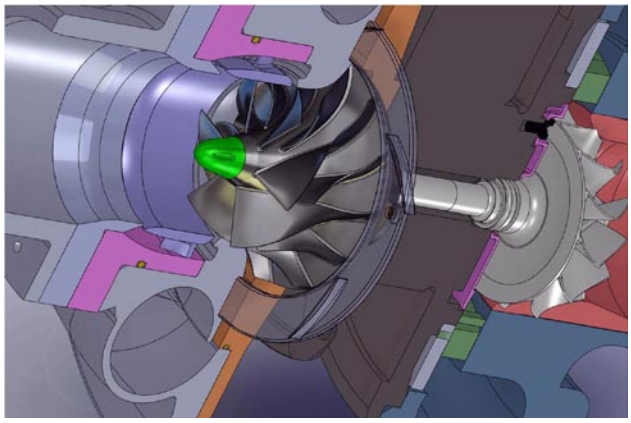

FIGURE 2. Turbocharger Assembly

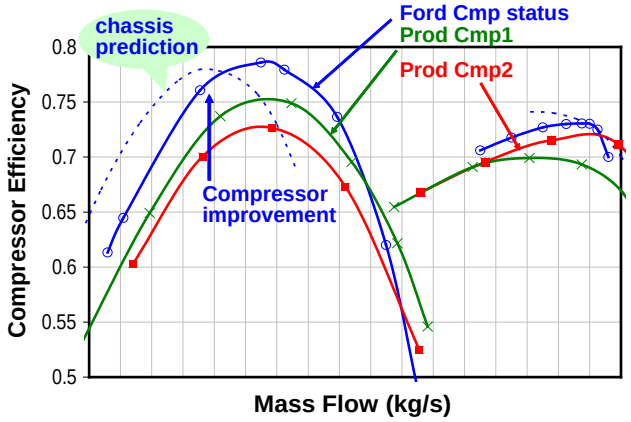

FIGURE 3. Compressor Efficiency, CFD vs. Flow Bench Test at 70,000 RPM

efficiency advantage of 10-12% at low mass flow area. Further improvements have been identified and incorporated in the final version of the compressor design.

- The mixed flow turbine also demonstrated efficiency improvement at low speed ratios where the future high EGR diluted engine will be operated frequently (Figure 4). However, there exist substantial uncertainties during the cold turbine test, e.g. heat transfer loss, tip clearance loss and bearing friction loss, etc., which has to be quantified in the future flow bench tests.

Conclusions

The first round of design, analysis and flow bench tests have demonstrated efficiency improvement on both compressor and turbine, especially at low compressor mass flow and low turbine speed ratio areas where most customer driving cycle operation will be done. The test data also identified areas for further improvement.

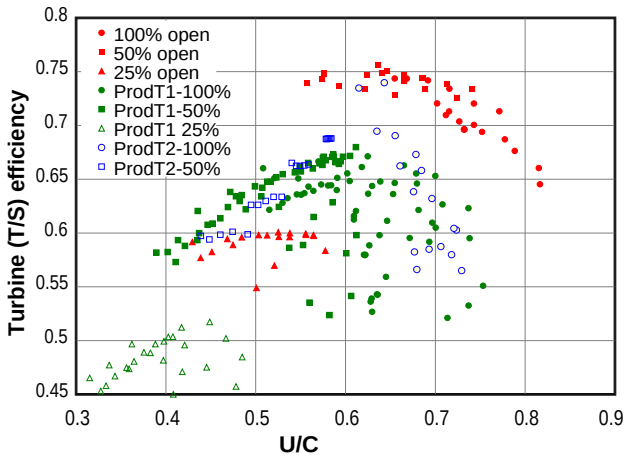

FIGURE 4. Flow Bench Test of Mixed Flow Turbine vs. Production Turbine Performance

The test data guided design optimization for better efficiency and wider flow range. The final design and analyses of the compressor and turbine will be completed in the near future. The strategy will focus on compressor impeller improvement and casing treatment optimization, rather than variable compressor inlet guide vane and variable diffuser vane as previously suggested. The next steps will include: fabrication of the redesigned compressor and turbine wheel, using fewer moving parts in the compressor to achieve wider operation range with efficiency improvement, and flow bench test validation.

FY 2009 Publications/Presentations

1. DEER 2009 conference, August 3–6, 2009.

2. SAE 2009-01-0985, "Numerical Investigation of Advanced Compressor Technologies to Meet Future Diesel Emission Regulations."

3. SAE 2009-01-0936, "Numerical Study of Ultra Low Solidity Airfoil Diffuser in an Automotive Turbocharger Compressor."

4. "Numerical investigation of the influence of variable diffuser vane angles on the performance of a centrifugal compressor", J. Automobile Engineering, Vol. 233.

5. "Numerical simulation of air flow through turbocharger compressors with dual volute design", Applied Energy, Vol. 86, 2009.

6. "Challenges and opportunities in turbocharger technology for future diesel LTC", Global Powertrain Congress, Nov. 4-5, 2009.

Patents Issued

1. Improve compressor surge margin with active casing treatment (pending).

II.A.24 Light Duty Combustion Visualization

Stephen Ciatti (Primary Contact),
Swaminathan Subramanian
Argonne National Laboratory
9700 S. Cass Ave.
Bldg. 362
Argonne, IL 60439

DOE Technology Development Manager:
Gurpreet Singh

Subcontractor:
University of Illinois at Chicago, Chicago, IL

Objectives

- Utilize in-cylinder combustion imaging to expand the operational limits of low-temperature combustion in a production automotive engine.
- Optimize the use of low-cetane fuels and engine compression ratio to meet the DOE goals of 45% brake thermal efficiency (BTE), super ultra low emissions vehicle engine-out emissions and high power density.
- Quantify the advanced control strategies required to accomplish these goals.

Accomplishments

- The General Motors (GM) 1.9-L turbodiesel engine has successfully been operated using the open architecture engine controller made by Drivven. The entire stock speed/load map was replicated using this separate engine controller.
- The ability of the controller to automatically adjust engine operating parameters, called "Next Cycle" (NC) control to maintain crank angle (CA)50 at a set location, cylinder by cylinder, was accomplished. Exhaust gas recirculation (EGR) settings from 0% to 40% were operated, as well as neat biodiesel and ultra-low sulfur diesel fuel. The engine was able to "self-optimize" each cylinder independently regardless of EGR setting or fuel.
- Low cetane fuels, such as iso-paraffinic kerosene and naptha-type gasoline fuels were acquired from BP and the U.S. Air Force.
- Compression ratio piston crowns ranging from 14:1 through 16:1 were manufactured by GM and shipped to Argonne.

Future Directions

- Evaluate the operation of the engine using NC control using stock piston crowns (17.5:1) and iso-paraffinic kerosene fuel and naptha-type fuel.
- Analyze the performance and emissions signature obtained by operating these fuels, especially NO_X emissions and brake specific fuel consumption.
- Conduct additional experiments using lower compression ratio piston crowns.

Introduction

Current diesel and spark ignition engines each suffer from inherent difficulties regarding efficiency or emissions. Spark ignition engines are limited in efficiency due to throttling losses and knock-limited compression ratio reduction. Diesel engines have inherent soot/NO_X challenges. Advanced combustion seeks to address these challenges by creating a combustion system that does not need a throttle to control power output, yet does not create soot/NO_X challenges at the same time.

Approach

The intent of this project is to utilize low-cetane fuels to create a combustion system that relies on premixed, but not well-mixed, fuel/air mixtures to control power output and emissions. Some stratification is needed to control power output, but premixing is also needed to avoid soot/NO_X. With large amounts of EGR (50% or greater) combined with fuel that is more difficult to auto-ignite than diesel, the fuel can be injected into the combustion chamber and allowed to pre-mix before ignition occurs.

Making this type of combustion system function requires special engine controller capability as well as the ability to adjust injection parameters on the fly, cylinder by cylinder. The open architecture controller allows the engine to be operated at a variety of conditions, allowing for some degree of self-optimization.

Results

The 1.9-L GM diesel engine has been successfully operated using NC control. The effect of NC control under high EGR conditions can be seen in Figures 1 and 2. In Figure 1, the engine was operated on the stock

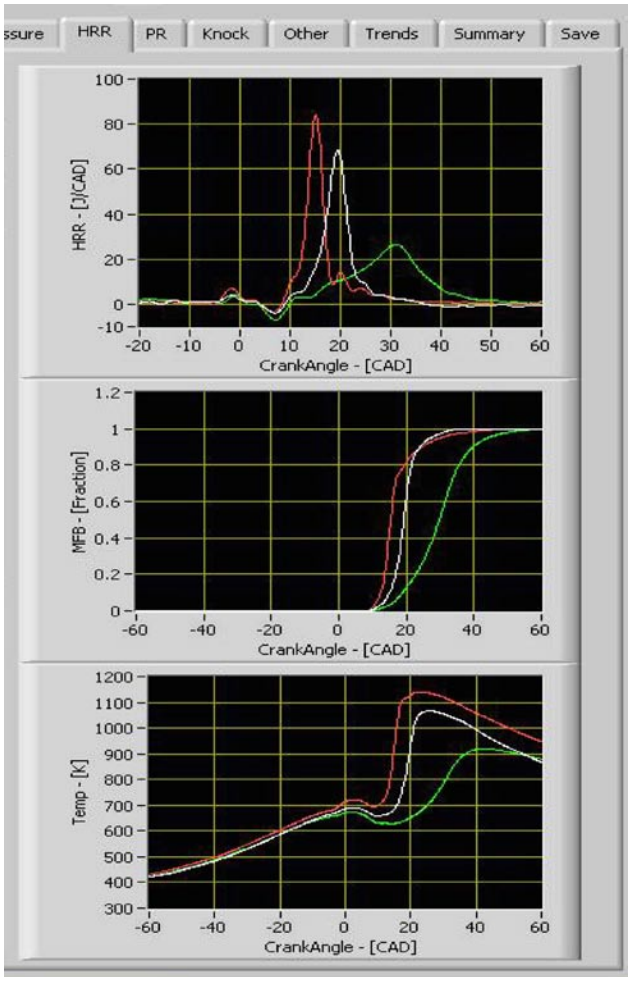

FIGURE 1. Engine Operated with Stock Fuel Maps

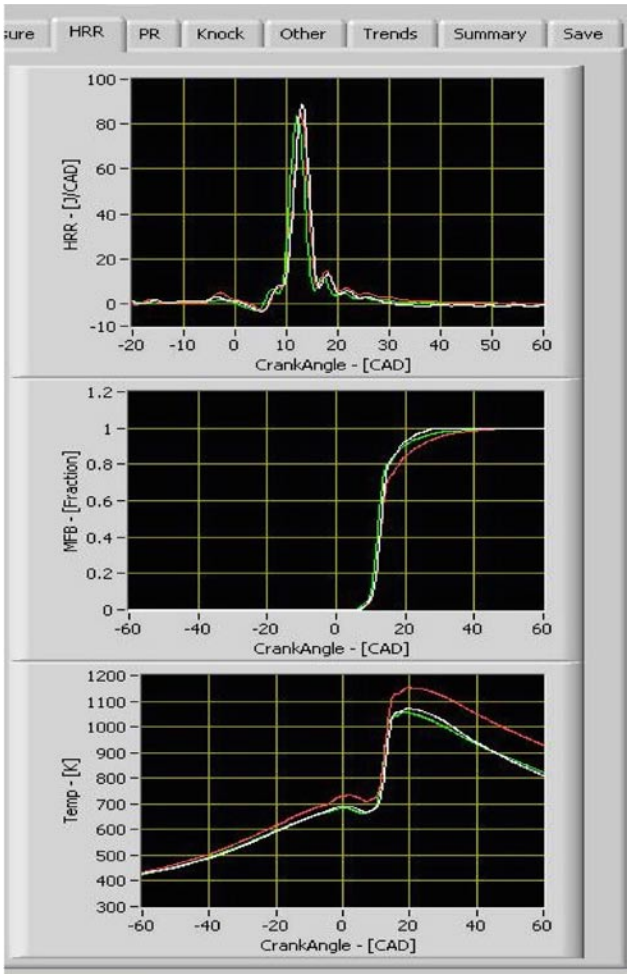

FIGURE 2. Engine Operated with NC Control for each Cylinder

engine map. In Figure 2, NC control was utilized to make each cylinder consistent. In the case of Figure 2, the engine controller was able to self-optimize each cylinder's injection timing to provide tremendous consistency of operation. Since this is a production engine, the EGR cylinder-to-cylinder distribution is not even. As a result, cylinder 3 in particular tends to ingest much more EGR than the other cylinders. NC control can account for this challenge and mitigate the negative consequences. It is anticipated that this strategy will also work well for low-temperature combustion operation, since EGR distribution will likely be rather uneven and at very high levels.

Conclusions

- The open engine controller is capable of responding quickly enough to provide NC control within 1-2 engine operating cycles to change injection parameters on the fly.
- Use of NC control allows for low-temperature combustion operation and optimization, as well as self-optimization for EGR and alternative fuel operation.

FY 2009 Publications/Presentations

1. Monthly teleconference with General Motors regarding progress.

2. Annual Merit review presentation in May 2009.

II.A.25 Spark-Assisted HCCI Combustion

K. Dean Edwards,
Robert M. Wagner (Primary Contact),
C. Stuart Daw, Charles E.A. Finney
Oak Ridge National Laboratory (ORNL)
2360 Cherahala Boulevard
Knoxville, TN 37932

Keith Confer (Primary Contact),
Matthew Foster
Delphi Automotive Systems
Auburn Hills, MI 48326

DOE Technology Development Manager:
Gurpreet Singh

Objectives

- Demonstrate a practical application of homogeneous charge compression ignition (HCCI) in a production-level, light-duty gasoline engine.
- Develop engine-system model for real-time diagnostics and control.

Accomplishments

- Demonstrated spark ignition (SI), spark-assisted (SA)-HCCI, and HCCI on a multi-cylinder production engine at the Delphi research facility in Rochester, NY.
- Characterized cyclic and cylinder dispersion of SA-HCCI based on data from the multi-cylinder engine.
- Continued collaboration with Lawrence Livermore National Laboratory (LLNL) in related activity to better understand the role of kinetics on SA-HCCI and fundamental mechanisms leading to the development of combustion instabilities.
- ORNL issued a patent on HCCI combustion mode transition control concepts (US 7,431,011).

Future Directions

- Continue hardware evaluation and integration of valve mechanism for controlling intake/exhaust valve lift and timing.
- Calibration of the SA-HCCI model with data from the single- and multi-cylinder engines.
- Implement and evaluate control strategy for multi-mode operation on the multi-cylinder HCCI engine which is now located at the Delphi research facility in Auburn Hills, Michigan.

Introduction

An improvement in the fuel efficiency of gasoline engines is necessary to realize a significant reduction in U.S. energy usage. HCCI in internal combustion engines is of considerable interest because of the potential reductions in flame temperature and oxides of nitrogen (NO_X) emissions as well as potential fuel-economy improvements resulting from un-throttled operation, faster heat release, and reduced heat-transfer losses. However, for many transportation applications, HCCI may not be possible or practical under the full range of speed and load conditions. Thus, the most important technical developments needed to achieve wide-spread HCCI utilization are expansion of the operational range and the ability to switch between HCCI and traditional propagating flame (e.g., SI) combustion as power and speed change. Several recent studies have begun to address the control issues but have not focused on the fundamental nature of the transition dynamics associated with switching from SI to HCCI combustion. The development of both combustion-mode switching and stabilization technologies requires that the fundamental nature of the transition be well understood, especially in the context of realistic engine conditions.

Delphi Automotive Systems and ORNL have established a Cooperative Research and Development Agreement (CRADA) on the control of advanced mixed-mode combustion for gasoline engines. ORNL has extensive experience in the analysis, interpretation, and control of dynamic engine phenomena, and Delphi has extensive knowledge and experience in powertrain components and subsystems. The partnership of these knowledge bases is critical to overcoming the critical barriers associated with the realistic implementation of HCCI and enabling clean, efficient operation in the next generation of transportation engines.

Approach

Significant progress in expanding the usefulness of advanced combustion modes of operation in gasoline engines will require an improved understanding of the potential of control methods to stabilize the transition between SI and HCCI combustion modes as well as to stabilize intermediate hybrid (mixed-combustion) modes which exhibit characteristics and benefits of SI and HCCI combustion. This improved understanding will be used to develop control strategies for improved utilization of hybrid combustion modes as well as for the development of physical models which will be useful

for linking global combustion characteristics with fuel chemistry.

A single-cylinder research engine was used in the preliminary phase of this activity to improve the fundamental understanding of SI-HCCI combustion dynamics. The engine was a 0.5-L single-cylinder AVL research engine with an 11.34:1 compression ratio. To achieve the transition from SI to HCCI combustion, this engine was fitted with a full-authority hydraulic variable valve actuation system which allowed high levels of exhaust gas to be retained in the cylinder through manipulation of the intake and exhaust valve events. All of these experiments were performed at stoichiometric fueling conditions and a range of speeds and loads.

The current phase of this activity is being performed using a multi-cylinder research engine developed by Delphi Automotive Systems and installed at the Delphi facilities in Auburn Hills, Michigan. Specific tasks for the multi-cylinder effort include:

- Development and baseline of engine/management systems. The research platform under development is a 2.2-L four-cylinder engine equipped with direct-injection fuel delivery, production-realistic flexible valve train components, and an advanced high-speed controller.
- Mechanistic and physical modeling and control-algorithm development for improved understanding of physics governing mixed-mode operation and for real-time, multi-cylinder prediction and control.
- Conventional SI, HCCI, and SA-HCCI steady-state experiments to explore the operational range and potential benefits of mixed-mode operation.
- HCCI and SI transient experiments which will include maneuvering within the HCCI envelope as well as mode switching between SI, mixed-mode, and HCCI operation.

Results

In our research, the transition between conventional SI and HCCI operation is achieved with high levels of exhaust gas retained in the cylinder through manipulation of the intake and exhaust valve events. Unfortunately, this results in a strong coupling between successive cycles with small variations in the thermal and chemical composition of the retained exhaust gas leading to large variations in the combustion process. Recent results from our research have shown that, due to this highly variable combustion, the SI-HCCI mode transition is very unstable with high torque variations, high unburned hydrocarbon emissions, and potential for engine stalling.

At lower exhaust gas recirculation (EGR) levels, communication between cycles is limited and dilution levels are too low to have significant impact on flame speed. As a result, combustion is stable and dominated by SI. At high EGR levels, dilution is too high to support a propagating flame and combustion is dominated by HCCI. Despite the greater opportunity for communication between cycles, combustion is stable with little cycle-to-cycle variability. At intermediate EGR levels, behavior becomes much more complex as SI and HCCI compete with one another, even occurring together during the same cycle. Combustion mode switches between SI, HCCI, and SA-HCCI from one cycle to the next as conditions within the cylinder dictate. Complex, recurring patterns of behavior are observed as combustion becomes stabilized or destabilized due to small changes in the temperature and composition of the residual gases. SA-HCCI combustion will often become stable for several consecutive cycles when SI and HCCI are in relative proportions. However, conditions will eventually develop which favor one mode over the other. This destabilizes the system resulting in rapid combustion mode switching (often following recurring patterns) until the system can again reach equilibrium. There are conditions where steady-state operation is difficult because dilution is too high to support SI combustion but not high enough to support full transition to HCCI. Misfire becomes more prevalent cooling the engine and often leading to engine stall.

SA-HCCI produces NO_x emissions similar to HCCI but with lower pressure rise rates making it a promising approach for operating at higher loads than can be achieved with pure HCCI. However, a better understanding of the fundamental causes of the combustion instabilities is needed in order to develop better controls to further stabilize combustion.

A SA-HCCI model was developed based on this conceptual understanding of the combustion dynamics. The purpose of this modeling effort is to ultimately have a low-order model to support real-time diagnostics and control of the engine at the electronic control unit level. The approach is to couple simple sub-models for SI and HCCI as illustrated in Figure 1. While this model was initially discussed in the 2008 annual report, model development has continued throughout the current fiscal year. The model makes use of a diluent-limited flame propagation model and a temperature-driven residual combustion model to simulate the complex interactions of flame propagation and compression ignition for SA-HCCI operation. Data collected from the multi-cylinder engine will be used to calibrate the model and ultimately as a foundation for the development of control algorithms. ORNL is also working closely with a modeling team at LLNL to better understand the role of kinetics in the use of SA-HCCI for expanding the operational range of HCCI-like combustion modes as well as in the development of combustion instabilities. This is a leveraged effort which is expected to improve

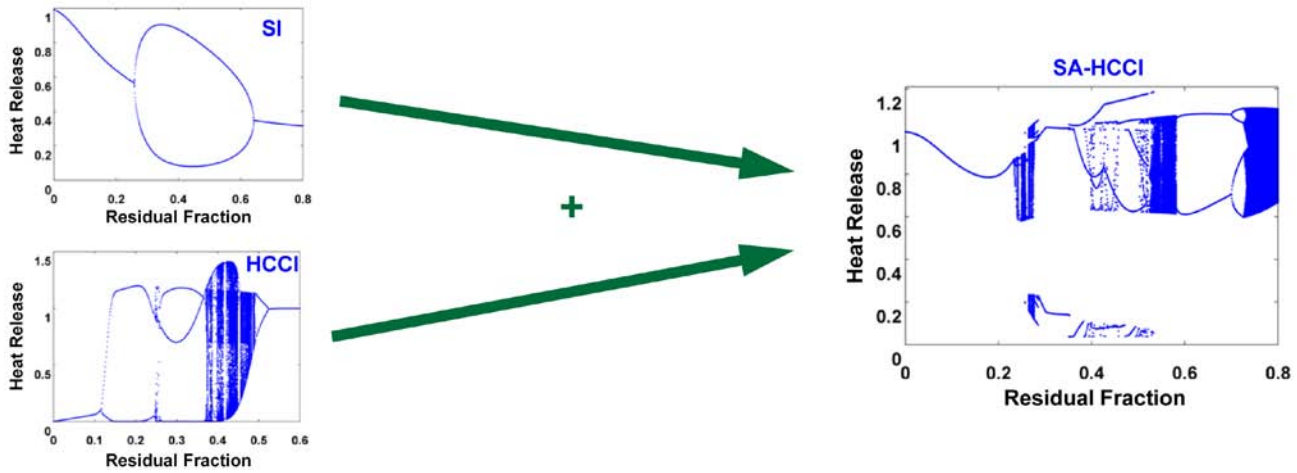

FIGURE 1. SA-HCCI model couples simple SI and HCCI models with appropriate rules for switching between the two as conditions dictate.

our fundamental understanding of the cycle-to-cycle dynamics and ultimately our approach to more robust operation through adaptive controls.

After initial development and evaluation at the Delphi Technical Center in Rochester, New York, the multi-cylinder engine (Figure 2) has been relocated to the new facilities in Auburn Hills, Michigan. A 4-cylinder, 2.2-L engine with direct injection was chosen as the base platform for this effort. Modifications to the engine include the addition of new fuel injectors with improved injection control and cam phasers with 80° of authority. A two-step valve-lift mechanism developed by Delphi will also be added to allow operation in the two combustion modes. The mechanism (shown schematically in Figure 3) includes two cam profiles: a high-lift profile for SI operation and a low-lift profile for HCCI operation. A GT-Power model of the engine has been developed for initial evaluation of the design requirements (such as valve phasing and lift profiles) needed to achieve a wide operating range for SI and HCCI. The initial designs have been fabricated and are being evaluated on-engine to further refine the final design. In addition to the stock 10-mm lift-cams used to baseline the engine in SI operation, three low-lift fixed cams are being evaluated to determine which provides the widest range of HCCI operation. A variety of injection strategies (including injecting some portion of the fuel during recompression) are also being evaluated.

SI, HCCI, and SA-HCCI operation has been successfully demonstrated on the multi-cylinder engine. The stock cams with 10-mm lift profiles were used to baseline engine operation in SI mode. HCCI and SA-HCCI operation have been achieved over a limited operating range using cam profiles with 6-mm of valve lift. Figure 4 shows the range of operation that has been explored for each combustion mode. HCCI operation (with and without SA) is limited by a number of factors

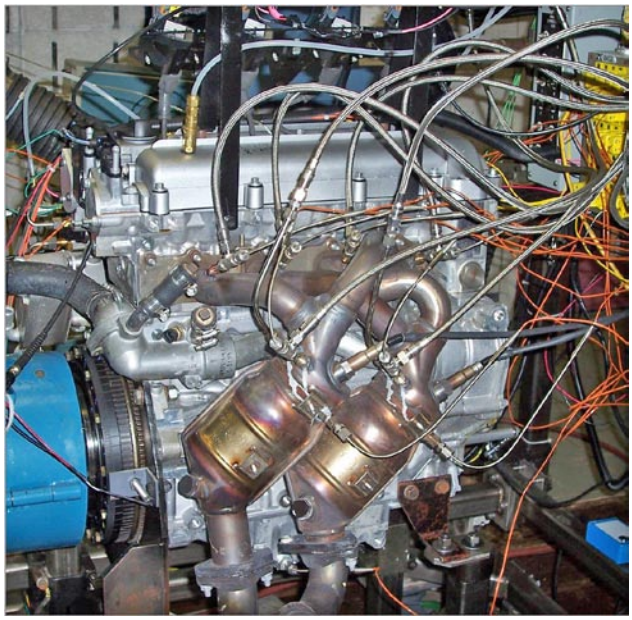

FIGURE 2. Multi-Cylinder Engine Installation at Delphi Technical Center in Rochester, New York

including combustion instability and high pressure rise rates at low speed and load. The low-lift intake cams restrict valve flow and, at high engine speeds, there is insufficient time to complete gas exchange. At high loads, in addition to high pressure rise rates, HCCI operation fails to provide a benefit to fuel efficiency or NO_x emissions with the 6-mm-lift cam design. Evaluation of cam designs with maximum lifts of 5.6 and 4 mm and shorter duration is currently underway. These lower-lift cam designs are expected to increase the percentage of trapped residual and further increase the range of operation for HCCI and SA-HCCI.

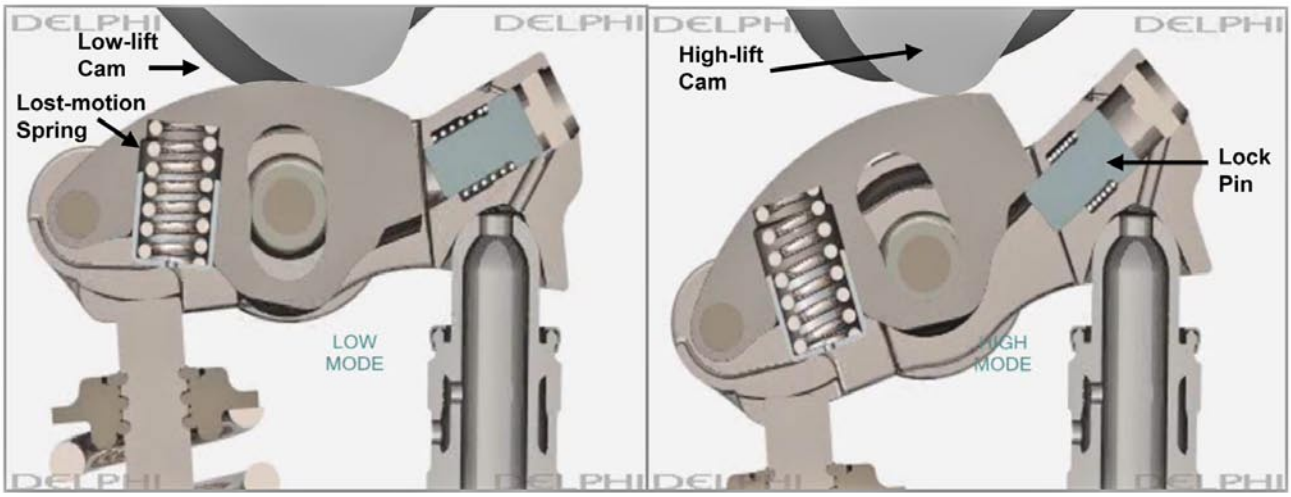

FIGURE 3. Schematic of Delphi Two-Step Valve-Lift Mechanism [1]

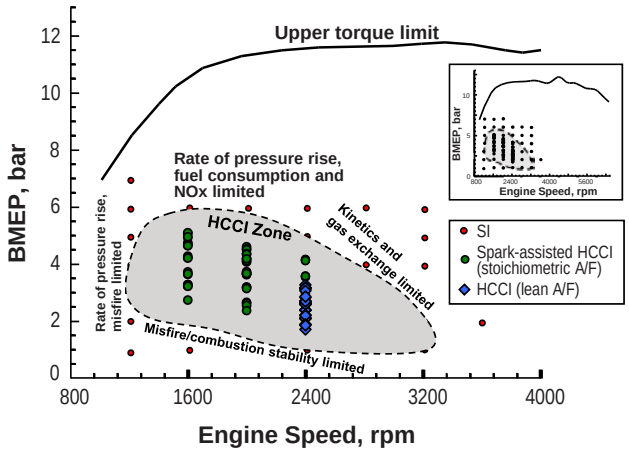

FIGURE 4. Operating limits explored to date with the multi-cylinder engine using 10-mm-lift (SI) and 6-mm-lift (HCCI) cam designs.

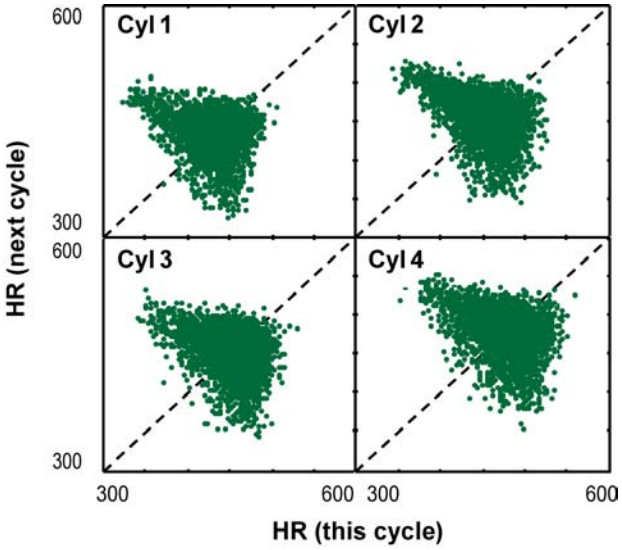

FIGURE 5. First-return maps of cycle-integrated heat release during unstable SA-HCCI operation.

Analysis of data collected during SA-HCCI operation along the unstable boundary shows that the behavior of the multi-cylinder engine has a strong deterministic component, implying appropriate control strategies could possibly reduce combustion variability and expand the HCCI operating window. At these conditions, first-return maps of cycle-integrated heat release (such as those in Figure 5) indicate the presence of both deterministic and stochastic elements in the combustion behavior. The triangular patterns seen in the maps indicate an underlying functionality between current and past performance. (Purely stochastic combustion variations would produce a random distribution of points.) The behavior seen here is reminiscent of that observed in highly diluted SI combustion with ultra-lean operation or high external EGR. Based on our past experience with controlling lean-limit combustion [2,3], it seems likely that appropriate control strategies could successfully reduce combustion variability and extend the HCCI operating range. Additional analysis shows that cylinder cross-talk (which could complicate control) is limited at these conditions.

Conclusions

The multi-cylinder engine platform for this study is now operational and providing new data in support of expanding the operational range of HCCI-like combustion. These data in combination with modeling are expected to continue to provide new insight into engine control strategies as well as advance the fundamental understanding of cyclic and cylinder

dispersion issues commonly associated with these types of combustion processes. This CRADA ends in FY 2010 and discussions are underway to establish a new CRADA which will build upon these results and experimental setups.

References

1. N. Hendriksma, T. Kunz, C Greene (2007) "Design and development of a 2-step rocker arm." SAE 2007-01-1285.

2. L.I. Davis, Jr., L.A. Feldkamp, J.W. Hoard, F. Yuan, F.T. Connolly, C.S. Daw, J.B. Green, Jr. (2001) "Controlling cyclic combustion variations in lean-fueled spark-ignition engines." SAE 2001-01-0257.

3. K.D. Edwards, R.M. Wagner (2004) "Application of adaptive control to reduce cyclic dispersion near the lean limit in a small-scale, natural gas genset." *Proceedings of the ICEF 2004*. ICEF 2004-855.

FY 2009 Publications/Presentations

1. C.E.A. Finney, C.S. Daw, K.D. Edwards, R.M. Wagner (2009) "A simple model for exploring the cyclic dynamics of spark-assisted HCCI". 6th US National Combustion Meeting (17-20 May 2009; Ann Arbor, MI, USA).

2. K.D. Edwards, R.M. Wagner, C.S. Daw, C.E.A. Finney, K. Confer, M. Foster (2009) "Ignition control for HCCI". US DOE Office of Vehicle Technologies 2009 Annual Merit Review (20 May 2009; Crystal City, VA, USA).

Special Recognitions & Awards/Patents Issued

1. US Patent 7,431,011. "A method for diagnosing and controlling combustion instabilities in internal combustion engines operating in or transitioning to homogeneous charge compression ignition modes".

II.B.1 CLEERS Aftertreatment Modeling and Analysis

Maruthi Devarakonda, Do Heui Kim,
Ja Hun Kwak, John Lee, Chuck Peden,
Mark Stewart, Janos Szanyi, Russell Tonkyn,
Diana Tran, Alla Zelenyuk,
Darrell Herling (Primary Contact)
Institute for Interfacial Catalysis
Pacific Northwest National Laboratory
P.O. Box 999, MSIN: K2-03
Richland, WA 99352

DOE Technology Development Manager:
Ken Howden

Objectives

- Lead and contribute to the Cross-Cut Lean Exhaust Emissions Reduction Simulations (CLEERS) activities:
  - Provide project updates to the industry sub-team, solicit feedback, and adjust work scope accordingly.
  - Lead technical discussions, invite distinguished speakers, and maintain an open dialogue on diesel particulate filter (DPF), selective catalytic reduction (SCR), and lean-NO_X trap (LNT) modeling issues.
- Develop improved modeling capabilities for diesel particulate filtration through first-principles simulations and fundamental experiments.
- Develop kinetic models for the Fe-zeolite urea-SCR catalyst, including the inhibition models to understand and quantify the impact of H_2O and hydrocarbons on NO_X conversion.
- Develop a fundamental understanding of NO_X adsorber technology operation with primary focus on chemical reaction mechanisms correlated with catalyst material characterization.

Accomplishments

- Participated in monthly CLEERS teleconferences and coordinated the calls focused on DPF and SCR technologies.
- Processed multiple three-dimensional (3-D) digital maps of pore structures obtained from micro X-ray scans of commercial cordierite and silicon carbide DPF substrates.
- Used digital DPF pore structures to study resolution and sample size necessary for representative predictions.
- Developed and validated the Fe-zeolite urea-SCR catalyst model based on steady-state bench reactor tests. Validated NH_3 storage, NH_3 oxidation and standard SCR kinetic models using the thermal transient micro-reactor tests.
- Measured the inhibition effect of H_2O and toluene on NO oxidation over Fe-zeolite catalyst through steady-state and thermal-transient reactor tests, and developed kinetics-based and neural networks-based inhibition models to describe the experimental observations.
- Demonstrated that the common catalyst metal, Pt, is dispersed on the γ-alumina support surface by anchoring to penta-coordinated Al sites using ultra-high field nuclear magnetic resonance (NMR) spectroscopy coupled with ultra-high resolution transmission electron microscopy (TEM).
- Performed computational studies of the adsorption of NO_X on a variety of alkaline earth oxide surfaces to compare with our experimental results, including calculations of NO_X adsorption on supported BaO surfaces as a function of the BaO particle size.
- Fourteen publications and 19 public presentations (eight of these were invited) have resulted from this work during the past fiscal year.
- Co-organized special sessions on diesel emission control for the 21st meeting of the North American Catalysis Society.

Future Directions

- Conduct fundamental filtration experiments with samples of commercial filter substrates using lab-generated soot and simple aerosols.
- Validate discrete particle filtration project by comparison to theoretical unit collector models.
- Further examine the hydrocarbon poisoning of SCR catalysts using engine-out hydrocarbon and fuel-component hydrocarbon species, and incorporate the inhibition model into the Fe-zeolite SCR model.
- Examine the SCR catalyst deactivation through reactor testing and spectroscopic analysis, and develop a model to describe the performance degradation behavior.
- Investigate the hydrolysis of HNCO over an Fe-zeolite SCR catalyst.
- Examine the interaction between LNT and SCR catalysts in the integrated LNT-SCR system through reactor testing and modeling.
- Develop a new model to describe the NO_X reduction performance of SCR/DPF technology.

- Continue studies of CO_2 and H_2O effects on BaO morphology changes and NO_X storage properties.
- Detailed characterization (e.g., Fourier transform infrared [FTIR], TEM) of the active sites (especially with respect to deactivation) and material properties of promoter species (such as ceria).

Introduction

CLEERS is a research and development focus project of the Diesel Cross-Cut Team. The overall objective is to promote the development of improved computational tools for simulating realistic full-system performance of lean-burn engines and their associated emissions control systems. Three fundamental research projects are sponsored at Pacific Northwest National Laboratory through CLEERS, focusing on the three most prominent technologies for diesel exhaust after-treatment:

- Diesel Particulate Filters (DPF)
- Selective Catalytic Reduction (SCR)
- Lean NO_X Traps (LNT)

Resources are shared between the three efforts in order to actively respond to current industrial needs. In Fiscal Year 2009, more emphasis was placed on the SCR and LNT activities because of urgent application issues associated with these technologies.

Among the pollutants present in lean engine exhaust, the combination of dry carbon (soot), unburned fuel and lubricant oil are often called particulate matter (PM), and can be removed by a filter (DPF). Carbon monoxide (CO) and hydrocarbons (HC) can be easily removed by an oxidation catalyst because of the excess oxygen in the exhaust. However, such an oxidizing exhaust condition makes the removal of NO_X a major challenge. Most of research in the lean-NO_X reduction area has been thus far focused on two different catalyst technologies: LNT that can store NO_X under lean conditions and reduce NO_X under rich conditions, and SCR that can selectively remove NO_X with ammonia.

Among the catalysts for SCR technology, base metal exchanged zeolite catalysts (e.g., Cu- and Fe-zeolite) are being considered for vehicle applications because of their high NOx reduction efficiency over a wide temperature range [1]. However, the NO_X reduction efficiency at low temperatures continues to be a major challenge, because unburned HC and H_2O are known to inhibit NO_X reduction performance. Moreover, the advanced combustion technologies that are being developed to lower NO_X emissions often produce more HC emissions at low exhaust temperatures. Thus, we have conducted laboratory reactor testing using Fe-zeolite catalyst, and developed a kinetic model to study the impact of H_2O and hydrocarbon inhibition on NO_X reduction to help improve the NO_X reduction performance at low temperatures.

The NO_X adsorber catalyst (a.k.a. LNT) is based on the ability of certain oxides, such as alkaline and alkaline earth oxide materials, to store NO_X under lean conditions and release it during rich (excess reductant) engine operation cycles. Among the catalysts developed to date [2], the most extensively studied catalyst system continues to be based on barium oxide (BaO) supported on a high surface area alumina (Al_2O_3) material [3]. Our project is aimed at developing a fundamental understanding of the operation of the LNT technology especially with respect to the optimum materials used in LNTs. As noted in the Accomplishments section, we have made progress in a number of areas. For the purposes of this report, we briefly highlight progress in two areas: studies of i) the synthesis of γ-alumina supported Pt catalysts that led to the identification of anchoring sites for Pt; and ii) the relative effectiveness of alkaline earth oxides for NO_X uptake.

Approach

For the Fe-zeolite SCR model development, a steady-state reactor model was first developed using flow-reactor experiments. Various reactor tests were conducted to probe the NO_X reduction mechanism and kinetics using a monolith catalyst core. The model was coded as a C language S-function, and the simulation was conducted in Matlab/Simulink. Steady-state surface isotherm tests were also conducted to generate the Langmuir isotherms, from which the rate parameters for NH_3 adsorption-desorption were determined [4].

To better understand the inhibition of H_2O and hydrocarbons on NO_X reduction, we investigated the impact of H_2O concentrations on NO oxidation, which has been identified as one of the major reaction steps. Based on the adsorption tests, a H_2O storage model was developed to predict the inhibition effect of H_2O on NO oxidation [5]. A neural network model was also developed for improved accuracy at high temperatures. For hydrocarbon inhibition study, toluene was selected as an aromatic fuel-component hydrocarbon species, and its impact on NO oxidation reaction was examined under steady-state and thermal-transient conditions [6].

LNT performance is evaluated in a fixed bed reactor operated under continuous lean-rich cycling. Rapid lean-rich switching is enabled just prior to the elevated temperature zone (furnace) where the LNT materials are contained in quartz tubing. For a typical baseline performance testing, the sample is heated to a reaction temperature in flowing He, the feed switched to a 'lean-NO_X' mixture containing oxygen and NO, as well as CO_2 and/or H_2O. After an extended period

(15 minutes or more), multiple rich/lean cycles of 1 and 4 minute duration, respectively, are run and NO_X removal performance is assessed after at least three of these are completed. In the LNT technology, the state of the system is constantly changing so the performance depends on when it is measured. Therefore, we obtain NO_X removal efficiencies as "lean conversion (4 minutes)", which measures NO_X removal efficiencies for the first 4 minutes of the lean-period.

The LNT catalysts were prepared by the incipient wetness method, using an aqueous alkaline earth nitrate solution and a γ-alumina support (200 m^2/g,). These catalysts are dried at 125°C and then 'activated' via a calcination at 500°C in flowing dry air for 2 h. State-of-the-art techniques such as solid-state NMR [7], X-ray diffraction, X-ray photoelectron spectroscopy, TEM/energy dispersive spectroscopy, FTIR, Brunauer-Emmett-Teller/pore size distribution, and temperature programmed desorption/reaction (TPD/TPRx), available at PNNL and at the Oak Ridge Laboratory High Temperature Materials Laboratory (ORNL-HTML), were utilized to probe the changes in physicochemical properties of the catalyst samples.

DPF modeling activities focused on the continued refinement and validation of first-principles tools for simulation of filtration phenomena at the scale of individual pores and particles. Digital geometries obtained from commercial silicon carbide and cordierite filter substrates were used in 3-D lattice-Boltzmann flow field simulations (Figure 1) to study the required resolution and sample size necessary for representative predictions of filter back-pressure.

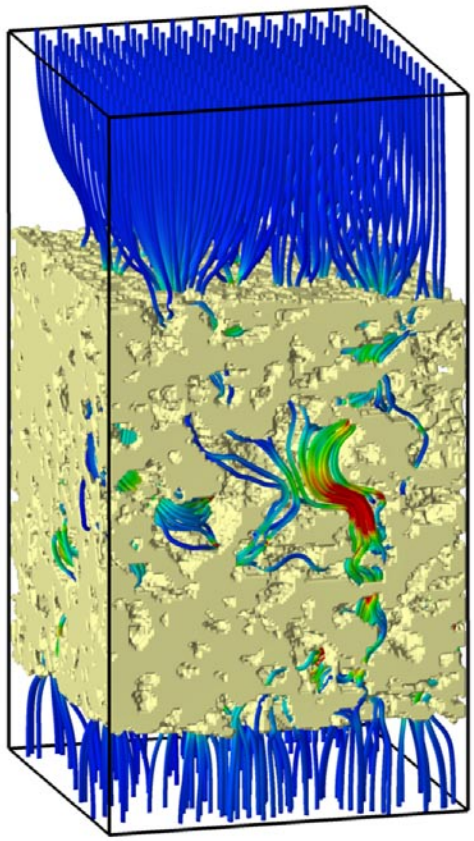

FIGURE 1. Three-dimensional flow field simulation through reconstructed cordierite filter wall.

Results

1. SCR

Steady-state NH_3 storage measurements were conducted and the amount of stored NH_3 was estimated from the mass balance calculations. During the adsorption tests, an empty SCR catalyst was exposed to the inlet feed gas, which included NH_3, CO_2, H_2O and balance He. Once the outlet NH_3 concentrations reached steady-state, NH_3 was removed from the feed and the weakly adsorbed NH_3 was allowed to desorb from the catalyst. The temperature was then increased to 550°C at a 10°C/minute, and remained at 550°C until NH_3 desorbed completely.

Kinetic rate equations for NH_3 adsorption and desorption were then used to define a Langmuir isotherm, and the slope and y-intercept of the isotherm were used to determine some of the rate parameters, as shown in Figure 2. A single site has been assumed for the NH_3 storage model.

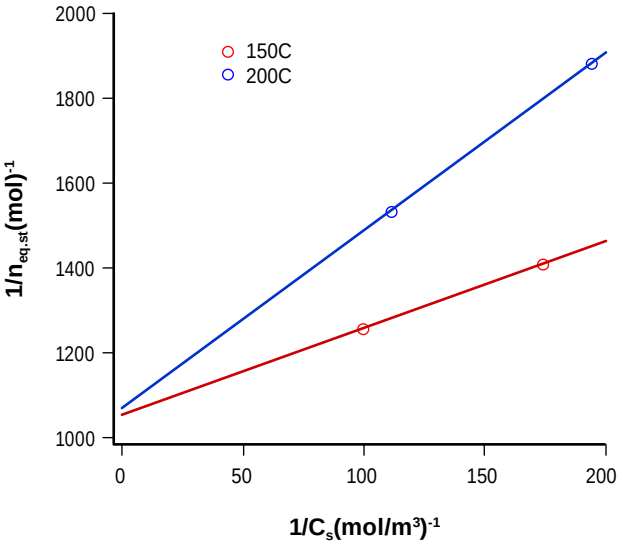

FIGURE 2. Langmuir isotherms generated from steady state NH_3 adsorption tests. NH_3 of 200 ppm and 350 ppm is injected at 150°C and 200°C respectively.

The rate parameters obtained were then used in a one-dimensional (1-D) SCR catalyst model, which simulates the gas phase and surface phase concentrations of NH_3 along the axial length of an Fe-zeolite catalyst. More details about the model can be found in [4]. Parameter identification for all the reactions were done using Matlab's Optimization toolbox. The model was updated by incorporating the kinetics of NH_3 oxidation, NO oxidation and various SCR reactions.

The kinetic sub-models of the transient SCR model were validated against the experimental data obtained using a thermal transient micro-reactor system. The details of the micro-reactor and the thermal control scheme are described in [8]. The current 1-D transient SCR model contains the kinetic models for NH_3 storage, NH_3 oxidation and standard SCR reactions. The rate parameters obtained from the steady-state tests were used without tuning. As shown in Figure 3, a good agreement was obtained between the model prediction and the experimental data.

As shown in Figure 4, NO oxidation was severely inhibited even at a very low H_2O concentration level. To investigate H_2O inhibition of NO oxidation, a kinetic model was developed to describe the adsorption and desorption of H_2O, which was then incorporate into the 1-D Fe-zeolite SCR model. The adsorption was assumed to be non-activated, while desorption activation energy depended on the H_2O coverage.

Once the adsorption model was validated, the inhibition model was developed. In the inhibition model, the rates of NO oxidation and NO_2 dissociation were defined as a function of equilibrium constant and H_2O storage in the catalyst as described in the following equations. Model parameters were tuned using the H_2O adsorption measurement at 260°C, and the model was then validated against measurement at different temperatures.

$$r_{f,oxi} = \frac{A_{f,oxi} e^{\frac{-E_{f,oxi}}{RT}} c_{NO} \sqrt{c_{o_2}}}{\left(1 + K \frac{\theta_{H_2O}}{1-\theta_{H_2O}}\right)}$$

$$r_{b,oxi} = \frac{A_{b,oxi} e^{\frac{-E_{b,oxi}}{RT}} c_{NO_2}}{\left(1 + K \frac{\theta_{H_2O}}{1-\theta_{H_2O}}\right)}$$

Among various HC species found in the exhaust, toluene was selected as the representative aromatic fuel-component HC. The impact of toluene on NO oxidation was examined through step temperature tests and periodic ramp temperature tests in the presence and absence of H_2O [6,9]. After one temperature ramp cycle (down and up) with NO and O_2 only, the cycle was repeated with H_2O and/or toluene. As shown in Figure 5, significant reduction in NO oxidation was observed in the presence of H_2O and/or toluene at below 450°C. Interestingly, a very small amount of toluene (25 ppm) showed nearly as much effect as 1.6% H_2O. Thermal transient micro-reactor tests using powder catalysts are currently being conducted for the model development and validation.

2. LNT

In many heterogeneous catalysts, the interaction of metal particles with their oxide support can alter the electronic properties of the metal, and can play a critical role in determining particle morphology and maintaining dispersion. We used a combination of

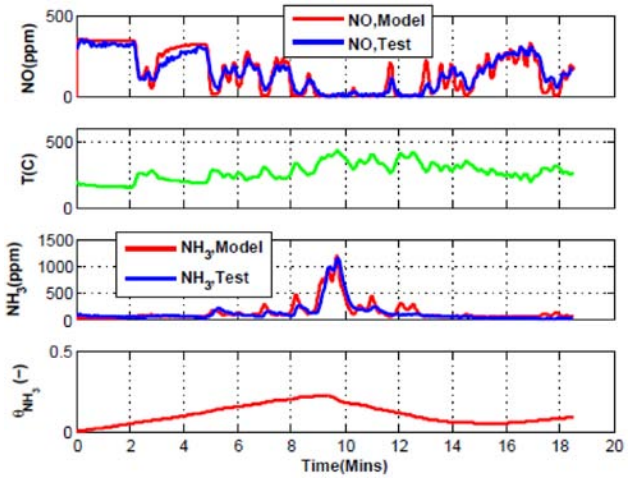

FIGURE 3. Standard SCR kinetic model validation on a thermal transient micro-reactor. Feed gas: 350 ppm NO_x, 350 ppm NH_3, 14% O_2, 5% CO_2, 2.5-5% H_2O and the balance N_2.

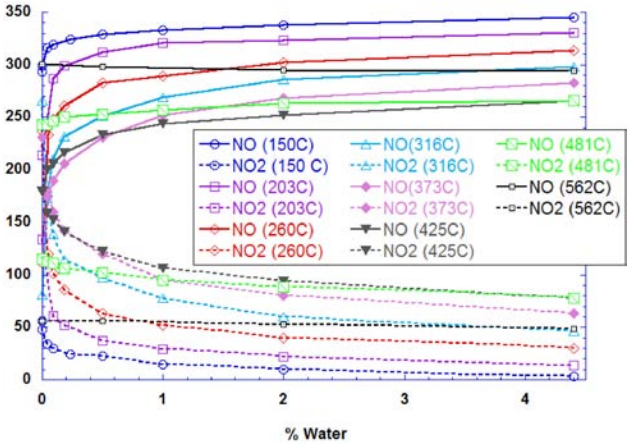

FIGURE 4. Effect of H_2O on NO oxidation as a function of temperature and H_2O concentration. Feed gas: NO of 350 ppm, 14% O_2, 5% CO_2.

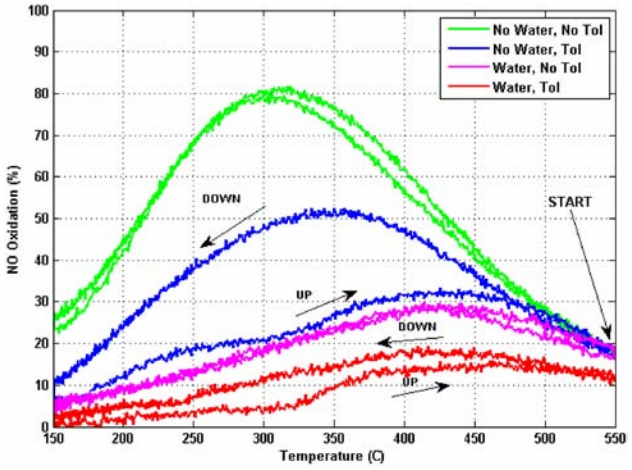

FIGURE 5. NO oxidation performance during toluene inhibition with and without H_2O in the stream as a function of gas temperature. The arrows indicate the direction of temperature ramps.

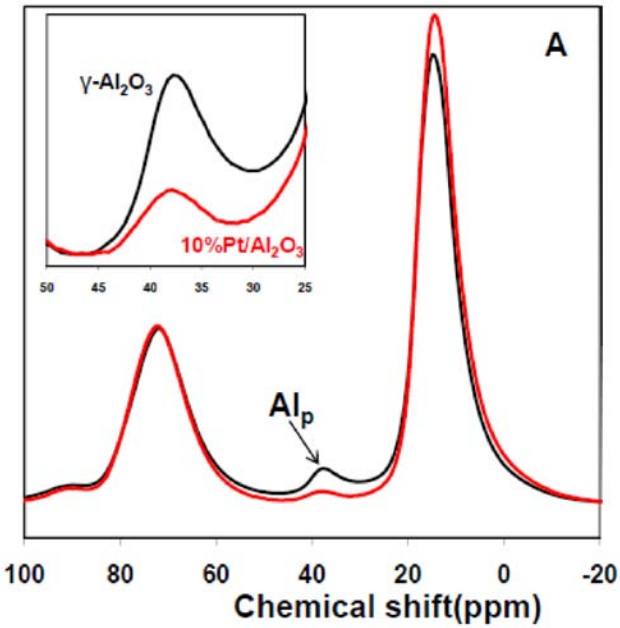

FIGURE 6. ^{27}Al MAS-NMR spectra of γ-Al_2O_3 (black) and 10 wt% Pt/γ-Al_2O_3 (red) (both samples were calcined at 573 K prior to NMR measurements).

ultrahigh magnetic field, solid-state magic angle spinning nuclear magnetic resonance (MAS-NMR) spectroscopy and high-angle annular dark-field scanning transmission electron microscopy, coupled with density functional theory calculations, to reveal the nature of anchoring sites of a catalytically active phase of platinum on the surface of a γ-Al_2O_3 catalyst support material [10]. The results obtained show that coordinatively unsaturated penta-coordinate Al^{3+} (Al^{3+}_{penta}) centers, present on the (100) facets of the γ-Al_2O_3 surface, are anchoring Pt. At low loadings, the active catalytic phase is atomically dispersed on the support surface (Pt/ Al^{3+}_{penta}=1), whereas two-dimensional (2-D) Pt rafts form at higher coverages.

High resolution ^{27}Al solid state MAS-NMR spectra collected at ultra-high magnetic fields for the γ-Al_2O_3 support and 10 wt% Pt/γ-Al_2O_3 samples after annealing at 573 K are displayed in Figure 6. The spectrum of the metal-free oxide support exhibits three peaks centered at 13, 35, and 70 ppm chemical shifts (referenced to 1 M aqueous $Al(NO_3)_3$). The two characteristic ^{27}Al NMR features of γ-Al_2O_3 at 13 and 70 ppm represent Al^{3+} ions in octahedral (Al^{3+}_{octa}) and tetrahedral (Al^{3+}_{tetra}) coordination, respectively. The NMR peak at 35 ppm chemical shift has been assigned to Al^{3+} ions in pentahedral coordination (Al^{3+}_{penta}) [11]. These penta-coordinate sites are created on the γ-Al_2O_3 surface by dehydration and dehydroxylation at elevated temperatures (here at 573 K) [11]. Loading Pt onto the γ-Al_2O_3 support and calcining the catalyst material at 573 K results in a substantial decrease in the number of Al^{3+}_{penta} sites as evidence by the large drop in the intensity of the 35 ppm NMR peak. Concomitantly, the intensity of the 13 ppm NMR feature increases with the loading of Pt onto γ-Al_2O_3, which suggests the conversion of the Al^{3+}_{penta} sites into Al^{3+}_{octa} (coordinative saturation; the total number of Al^{3+} ions remains constant). These results strongly suggest that Pt atoms bind to the Al^{3+}_{penta} sites on the γ-Al_2O_3 surface through oxygen bridges, thereby coordinatively saturating these sites (penta- to octahedral conversion).

Quantitative analysis of an extensive number of similar NMR experiments suggest that, at loadings of 1 wt% Pt or lower, each occupied Al^{3+}_{penta} site interacts with exactly one Pt atom, meaning that all Pt must be atomically dispersed. In order to substantiate our claim of single-atom Pt dispersion at loadings ≤1 wt%, we collected high angle annular dark field scanning transmission electron microscopy (HAADF STEM) images at the ORNL-HTML for the 1 wt% Pt/γ-Al_2O_3 sample calcined at 573 K. The HAADF STEM image shown in Figure 7 demonstrates the almost perfect atomic dispersion of Pt on the γ-Al_2O_3 surface at 1 wt% loading.

We performed density functional theory (DFT) calculations in order to obtain specific information about (a) the energetics of the interaction of PtO particles with the surface of γ-Al_2O_3, and (b) the likely stable structures of the experimentally (HAADF STEM) observed single atoms at low Pt coverages and 2-D PtO rafts at higher coverages. Figure 8 displays a schematic representation of the stable surface structure that highlights the specific interactions between Pt and the Al^{3+}_{penta} sites on the γ-Al_2O_3surface.

In this past year, we also investigated the formation of “surface” and “bulk” nitrates on a series of alkaline

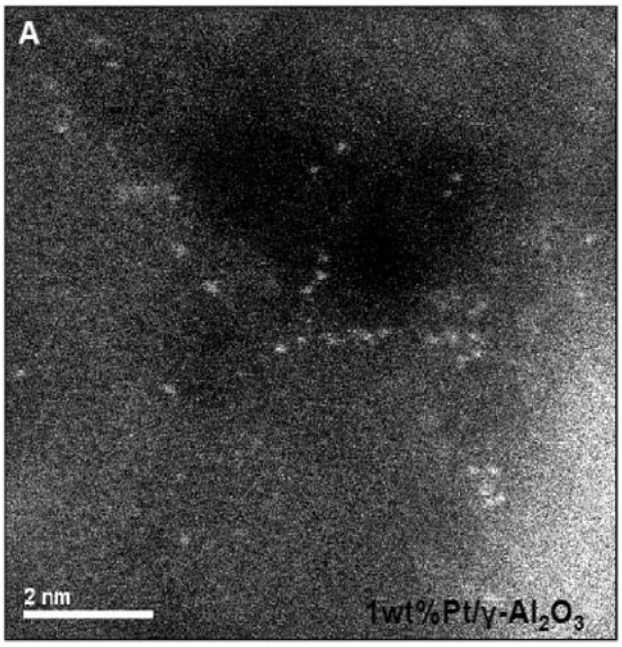

FIGURE 7. High resolution STEM images of 1 wt% Pt/γ-Al_2O_3.

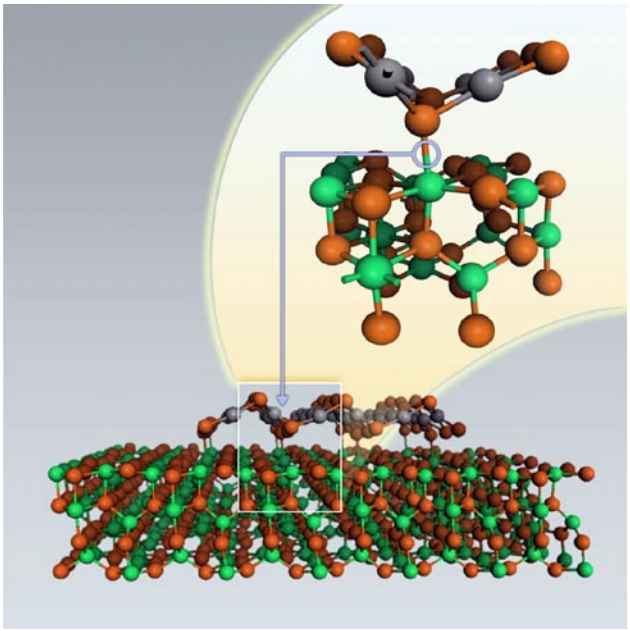

FIGURE 8. Optimized PtO overlayer structures on the γ-Al_2O_3(100) surface.

earth oxides (AEOs), $AE(NO_3)_2$ using first-principles DFT calculations to compare with our experimental observations that determined the relative performance of these various NO_x storage materials [12]. Calculated vibrational frequencies of the surface and bulk nitrates based on our proposed structural models are in good agreement with experimental measurements of AEO/γ-Al_2O_3 materials after prolonged NO_2 exposure (Figure 9). This indicates that experimentally observed "surface" nitrates are most likely formed with isolated two dimensional (including monomeric) AEO clusters on the γ-Al_2O_3 substrate, while the "bulk" nitrates are formed on exposed (including [001]) surfaces (and likely in the bulk as well) of large three dimensional AEO particles supported on the γ-Al_2O_3 substrate. Also in line with the experiments, our calculations show that the low and high frequency components of the vibrations for both surface and bulk nitrates are systematically red shifted with the increasing basicity and cationic size of the AEOs.

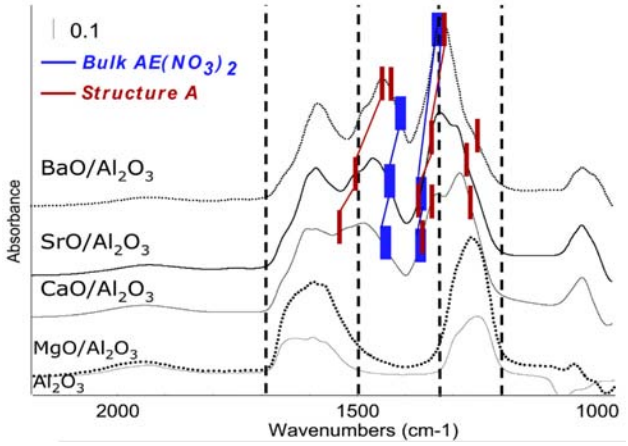

FIGURE 9. Comparison of calculated and experimental vibrational frequencies for "bulk" nitrates. The blue bars represent calculated frequencies of cubic bulk $AE(NO_3)_2$. The dark red bars represent calculated frequencies of "bulk" model nitrates.

3. DPF

DPF modeling activities focused on the continued refinement and validation of first-principles tools for simulation of filtration phenomena at the scale of individual pores and particles. DPF flow simulations with varying spatial resolution indicated that better convergence could be obtained when a relaxation parameter of less than 1.0 was used in the Lattice-Boltzmann method. In any case, cell sizes of roughly 3 microns or less appear to be necessary for permeability predictions within 25% of the converged value. Simulations with cell sizes of 1.6 microns gave permeability estimates within 1.5% of the converged value with a relaxation parameter of 0.625. Simulations with varying domain extents indicated that a representative equivalent volume for silicon carbide substrates may be much smaller than for cordierite substrates. This stems from the more uniform, more inter-connected structure in the sintered SiC media compared to cordierite. For the SiC filter examined,

representative results could be obtained from filter wall surface areas as small as 400 microns on a side, while the cordierite filter examined could require an area larger than 800 microns on a side in order to be representative.

Conclusions

- A kinetic model for a Fe-zeolite SCR catalyst based on Langmuir isotherms has been developed to describe various reaction pathways. Kinetic parameters were obtained from steady-state reactor tests, and validated against thermal-transient reactor tests.
- The effects of toluene (aromatic fuel-component HC) and H_2O on NO oxidation have been examined over a Fe-zeolite catalyst, and kinetic models have been developed to describe the inhibition behavior.
- Previously proposed "surface" and "bulk" nitrates formed on AEO/γ-Al_2O_3 catalysts from NO_2 exposures were elucidated at the atomic level for the first time, with excellent agreement between calculated vibrational frequencies based on the proposed molecular structure models and experimental FTIR measurements of AEOs/γ-Al_2O_3 catalysts after prolonged NO_2 exposure. Based on these results, we conclude that the previously assigned "surface" nitrates are a consequence of NO_X adsorption on 'submonolayer' AEO structures on the γ-Al_2O_3 surface whereas "bulk" nitrates form from NO_X adsorption on (and in) supported AEO particles.
- Pentacoordinate Al^{3+} ions have been identified as the anchoring of catalytically active phases (Pt) to the γ-Al_2O_3 support surface on the basis of results from ultra-high magnetic field ^{27}Al MAS-NMR measurements. At low (≤1 wt%) Pt loadings, Pt is atomically dispersed on the support surface (Pt/Al^{3+}_{penta}=1). When the loading of Pt exceeds the number of Al^{3+}_{penta} sites, 2D PtO rafts form as evidenced by HA-ADF STEM measurements. DFT calculations provide further confirmation for the energetic feasibility of the formation of these 2-D rafts as well as for their energetically most stable overlayer structure.
- Micro-scale DPF simulations using the lattice Boltzmann method gave better permeability predictions at lower spatial resolutions when a relaxation parameter less than 1.0 was used.
- Cell sizes of roughly 3 microns or less may be required for adequate resolution of the complex flow fields through common DPF micro-structures.
- Representative predictions may be obtained from much smaller domains in micro-scale simulations of sintered filter media such as silicon carbide, while larger domains are necessary for cordierite.

References

1. G. Cavataio, J. Girard, J. Patterson, C. Montreuil, Y. Cheng and C. Lambert, DOE Cross-cut Lean Exhaust Emissions Reduction Simulations (*CLEERS*) Workshop, www.cleers.org, May 2007.

2. (a) Miyoshi, N.; Matsumoto, S.; Katoh, K.; Tanaka, T.; Harada, J.; Takahashi, N.; Yokota, K.; Sugiura, M.; Kasahara, K. SAE Paper 950809, 1995; (b) Miyoshi, N.; Matsumoto, S. *Sci. Technol. Catal.* 1998, 245.

3. Epling, W. S.; Campbell, L. E.; Yezerets, A.; Currier, N.W.; Parks, J. E. *Catal. Rev.–Sci. Eng.* 2004, 46, 163.

4. M. Devarakonda, R. Tonkyn and J. Male, *Chemical Engineering Journal* (Review).

5. M. Devarakonda, R. Tonkyn and D. Herling, *Chemical Engineering Science*, (Review).

6. R. Tonkyn, D. Tran, M. Devarakonda, and D. Herling, *Applied Catalysis B: Environmental*, (Review).

7. Kwak J.H.; Hu, J.Z.; Kim, D.H.; Szanyi, J.; Peden, C.H.F. *J. Catal.* 2007, 251, 189-194.

8. D. Tran, R. Tonkyn, M. Devarakonda, N. Anheier, D. Hopkins and D. Herling, (In Preparation).

9. M. Devarakonda, R. Tonkyn and D. Herling, *SAE World Congress*, April 2010.

10. Kwak, J.H.; Hu, J.; Mei, D.; Yi, C.-W.; Kim, D.H.; Peden, C.H.F.; Allard, L.; Szanyi, J. *Science* 2009, 325, 1670.

11. (a) Chen, F.R.; Davis, J. G.; Fripiat, J.J. *J. Catal*. 1992, 133, 263; (b) Kwak, J.H.; Hu, J.Z.; Kim, D.H.; Szanyi, J.; Peden, C.H.F. *J. Catal.* 2007, 251, 189.

12. (a) Mei, D.; Ge, Q.; Kwak, J.H.; Kim, D.H.; Verrier, C.; Szanyi, J.; Peden, C.H.F. *Phys. Chem. Chem. Phys.* 2009, 11, 3380; (b) Verrier, C.; Kwak, J.H.; Kim, D.H.; Peden C.H.F.; Szanyi, J. *Catal. Today* 2008, 136, 121.

FY 2009 Presentations

Invited

1. M. Devarakonda., "Micro-reactor Modeling and Investigation of HNCO as a Reactant for NO_x Control", CTI forum for NO_x Reduction, Southfield, MI., December 2008.

2. J. Male., "Opportunity NO_x – Catalytic NO_x Aftertreatment", Snow Symposium, University of Oregon, February 2009.

3. M. Devarakonda., "Energy Efficient Emission Control – A Need for Optimality", Mechanical, Industrial and Manufacturing Engineering Department, University of Toledo, Toledo, OH., September 2009.

4. Peden, CHF. "Fundamental Studies of Catalytic NOx Vehicle Emission Control." Invited Presentations made by Chuck Peden at the following locations:

- Politechnico di Milano, Milan, Italy, May 2009.
- Annual DOE/EE/OVT Peer Review, May 2009.

5. Peden, CHF. "The Use of Ultrahigh Field NMR Spectroscopy to Study the Surface Structure and Catalytic Properties of Poorly Crystalline γ–Al_2O_3." Invited Presentations made by Chuck Peden at the following locations:

- Annual Meeting of the American Institute of Chemical Engineers, Philadelphia, PA, November 2008.
- 6th World Conference on Catalysis by Acids and Bases, Genoa, Italy, May 2009.

6. Kim, DH. "NOx abatement catalyst: an essential enabler for clean and fuel-efficient transportation." Department seminar at the School of Mechanical and Materials Engineering, Pullman, WA, April 2009.

Contributed

1. M.L. Stewart, "Continuing Development of Micro-Scale Simulation Methods for DPFs." Presented by Mark L. Stewart at 12th CLEERS Workshop, Dearborn, MI in April 2009.

2. M. Devarakonda, R. Tonkyn, D. Tran, J. Male and D. Herling, "Bench Reactor Studies and Reactor Modeling for NO_x Control in Diesel Engines Using NH_3", Presented by M. Devarakonda at the 12th CLEERS Workshop, Dearborn, MI in April 2009.

3. D. Tran, M. Devarakonda, R. Tonkyn and D. Herling, "Modeling and Experimental Investigation of Fe-zeolite Urea-SCR Catalysts for NO_x Aftertreatment", Presented by D. Tran at 21st North American Catalysis Society Meeting (NAM), San Fransisco, CA, June 2009 (Poster).

4. R. Tonkyn, M. Devarakonda, D. Tran and D. Herling, "Modeling and Experimental Studies of HNCO as a Reactant for NO_x Control", Presented by R. Tonkyn at 21st North American Catalysis Society Meeting (NAM), San Fransisco, CA, June 2009.

5. M. Devarakonda, R. Tonkyn, D. Tran and D. Herling, "Hydrocarbon Inhibition and HC Storage Modeling in Fe-zeolite Catalysts for HD Diesel Engines", Presented by M. Devarakonda at Directions in Engine-Efficiency and Emissions Research Conference (DEER), Dearborn, MI, August 2009.

6. Kwak JH, D Mei, CW Yi, DH Kim, CHF Peden, LF Allard, and J Szanyi. "Specific role of alumina surfaces for BaO anchoring and nitrate formations in BaO/γ-Al_2O_3 NOx Storage Materials." Presented by Ja Hun Kwak at the 21st North American Catalysis Society Meeting, San Francisco, CA, June 2009.

7. Verrier CM, JH Kwak, DH Kim, C Cao, CHF Peden, G Clet, and J Szanyi. "The Effect of CO_2 on NOx Storage/Reduction Catalysts." Presentation by Janos Szanyi at the 21st North American Catalysis Society Meeting, San Francisco, CA. June 2009.

8. Mei D, Q Ge, JH Kwak, DH Kim, CM Verrier, J Szanyi, and CHF Peden. "Density functional theory study of surface and bulk nitrates of γ-Al_2O_3 supported alkaline earth oxides." Presented by Donghai Mei at the 21st North American Catalysis Society Meeting, San Francisco, CA. June 2009.

9. Cao C, JH Kwak, DH Kim, CHF Peden, and J Szanyi. "In Situ FTIR and TPD Studies on the Interaction of NOx with CeO_2." Presented by Chundi Cao at the 21st North American Catalysis Meeting (NAM), San Francisco, CA, June 2009.

10. Peden CHF. "Fundamental Studies of NOx Adsorber Materials at PNNL." Presented by Chuck Peden at the 11th DOE CLEERS Workshop, Dearborn, MI, May 2009.

11. DH Kim, JH Kwak, X Wang, J Szanyi, JC Hanson, and CHF Peden. "Various Roles of Water in the Regeneration Processes over the Pt-BaO/Al_2O_3 Lean NOx Trap Catalysts." Presented by Do Heui Kim at the Annual Meeting of the American Institute of Chemical Engineers, Philadelphia, PA, November 2008.

FY 2009 Publications

1. M. Devarakonda, R. Tonkyn and J. Male, "Modeling of a Fe-zeolite Urea-SCR Catalyst Based on Langmuir Isotherms", Chemical Engineering Journal (Review).

2. M. Devarakonda, R. Tonkyn and D. Herling, "Experimental and Modeling Studies of H_2O Inhibition of NO_x Oxidation on a Fe-zeolite Urea-SCR Catalyst", Chemical Engineering Science (Review).

3. R. Tonkyn, D. Tran, M. Devarakonda, and D. Herling, "Steady State and Thermal Transient Investigation of NO Oxidation on a Fe-zeolite Urea-SCR Catalyst", Applied Catalysis B: Environmental, (Review).

4. D. Tran, R. Tonkyn, M. Devarakonda, N. Anheier, D. Hopkins and D. Herling, "Transient Thermal Effects of Water and Hydrocarbons on NO_x Conversion Performance of a Fe-zeolite Urea-SCR Catalyst", (In Preparation).

5. M. Devarakonda, R. Tonkyn and D. Herling, "Hydrocarbon Effect on a Fe-zeolite Urea-SCR Catalyst: An Experimental and Modeling Study", SAE World Congress, 2010-01-0103, April 2010.

6. J. Yang, M. Stewart, G.D. Maupin, D.R. Herling, and A. Zelenyuk, "Single Wall Diesel Particulate Filter (DPF) Filtration Efficiency Studies Using Laboratory Generated Particles." Chemical Engineering Science 64(8):1625-1634.

7. Kim, D.H.; Kwak, J.H.; Szanyi, J.; Wang, X.Q.; Peden, C.; Howden, K. "Fundamental Studies of NOx Adsorber Materials." Combustion and Emission Control for Advanced CIDI Engines, FY2008 Progress Report, pp. 145-151.

8. Mei, D.; Ge, Q.; Kwak, J.H.; Kim, D.H.; Szanyi, J.; Peden, C.H.F. "Adsorption and Formation of BaO Overlayers on γ-Al_2O_3 Surfaces." *Journal of Physical Chemistry C* **112** (2008) 18050-18060.

9. Kwak, J.H.; Mei, D.; Yi, C.-W.; Kim, D.H.; Peden, C.H.F.; Allard, L.; Szanyi, J. "Understanding the nature of surface nitrates in BaO/gamma-Al_2O_3 NOx storage materials: A combined experimental and theoretical study" *Journal of Catalysis* **261** (2009) 17-22.

10. Mei, D.; Ge, Q.; Kwak, J.H.; Kim, D.H.; Verrier, C.; Szanyi, J.; Peden, C.H.F. "Characterization of Surface and Bulk Nitrates of γ-Al_2O_3–Supported Alkaline Earth Oxides using Density Functional Theory." *Physical Chemistry Chemical Physics* **11** (2009) 3380-3389.

11. Mei, D.; Ge, Q.; Szanyi, J.; Peden, C.H.F. "A First-Principles Analysis of NO_x Adsorption on Anhydrous γ-Al_2O_3 Surfaces." *Journal of Physical Chemistry C*, **113** (2009) 7779-7789.

12. She X.; Flytzani-Stephanopoulos, M.; Wang, C.M.; Wang, Y.; Peden, C.H.F. 2009. "SO_2-induced stability of Ag-alumina catalysts in the SCR of NO with methane." *Applied Catalysis. B, Environmental* **88** (2009) 98-105.

13. Kwak, J.H.; Hu, J.; Mei, D.; Yi, C.-W.; Kim, D.H.; Peden, C.H.F.; Allard, L.; Szanyi, J. "Coordinatively Unsaturated Al^{+3} Centers as Binding Sites for Active Catalyst Phases: Strong Interactions Between Pt and γ-Al_2O_3 Surfaces." Science **325** (2009) 1670-1673.

14. Mei, D.; Szanyi, J.; Kwak, J.H.; Peden, C.H.F. "Catalyst Size and Morphology Effects on the Interaction of NO_2 with BaO/γ-Al_2O_3 Materials." Catalysis Today (2010) submitted for publication.

II.B.2 Enhanced High Temperature Performance of NOx Storage/Reduction (NSR) Materials

Do Heui Kim, George Muntean, Chuck Peden (Primary Contact)
Institute for Interfacial Catalysis
Pacific Northwest National Laboratory (PNNL)
P.O. Box 999, MS K8-93
Richland, WA 99354

DOE Technology Development Manager:
Ken Howden

Cooperative Research and Development Agreement (CRADA) Partners:
- Neal Currier, Randy Stafford, Alex Yezerets - Cummins Inc.
- Hai-Ying Chen, Howard Hess - Johnson Matthey

Objectives

Identify approaches to significantly improve the high temperature performance and stability of lean-NOx trap (LNT) technology via a pursuit of a more fundamental understanding of:

- the various roles for the precious metals;
- the mechanisms for these various roles;
- the effects of high temperatures on precious metal performance in their various roles;
- mechanisms for higher temperature NOx storage performance for modified and/or alternative storage materials;
- the interactions between the precious metals and the storage materials in both optimum NOx storage performance and long-term stability; and
- the sulfur adsorption and regeneration mechanisms for modified and/or alternative storage materials.

Accomplishments

- Two major thrusts this year:
  - Promotional Effect of CO_2 on Desulfation Processes for Pre-Sulfated Pt-BaO/Al_2O_3 LNT Catalysts
    - A combination of various techniques shows that the presence of CO_2 promotes the removal of sulfur species, especially at temperatures below 500°C, with a corresponding suppression of BaS phase formation, thus resulting in a lower amount of residual sulfur on the sample after desulfation.
  - Effect of Sulfation Levels on the Desulfation Behavior of Pre-Sulfated Pt-BaO/Al_2O_3 LNT Catalyst
    - In the previous work, we reported [1] superior intrinsic NOx uptake of Pt-BaO/CeO_2 samples compared to Pt-BaO/Al_2O_3 over the entire temperature range studied, and that the ceria-supported sample showed superior sulfur resistance after equivalent exposures to SO_2.
    - By using the various characterization tools, we found that the sulfur species on the Pt-BaO/CeO_2 sample are less likely to be removed as H_2S and have more tendency to stay on the material, thus demonstrating the significant dependence of support on the desulfation behavior of LNT materials.
- Three public presentations and four manuscripts have been cleared for release by CRADA partners.

Future Directions

- Complete studies of sulfur-loading levels on the desulfation behavior of model BaO-based LNT materials to develop a fundamental understanding of these effects.
- Determine the effects of H_2O and CO_2 on the desulfation of ceria-supported BaO LNT materials.
- Compare behavior of ceria-supported and ceria-doped, alumina supported BaO LNT materials.
- Initiate studies to determine performance limitations, sulfur sensitivity and desulfation behavior of candidate alternative support materials that provide improved high temperature performance.

Introduction

The NOx adsorber (also known as a LNT) technology is based upon the concept of storing NOx as nitrates over storage components, typically barium species, during a lean-burn operation cycle and then reducing the stored nitrates to N_2 during fuel-rich conditions over a precious metal catalyst [2]. This technology has been recognized as one of the most promising approaches for meeting stringent NOx emission standards for diesel vehicles within the Environmental Protection Agency's 2007/2010 mandated limits. However, in looking forward to 2012

and beyond with expected more stringent regulations, the continued viability of the NSR technology for controlling NOx emissions from lean-burn engines such as diesels will require at least two specific, significant and inter-related improvements. First, it is important to reduce system costs by, for example, minimizing the precious metal content while maintaining, even improving, performance and long-term stability. A second critical need for future NSR systems will be significantly improved higher temperature performance and stability. Furthermore, these critically needed improvements will contribute significantly to minimizing the impacts to fuel economy of incorporating the NSR technology on lean-burn vehicles. To meet both of these objectives, NSR formulation changes will be necessary. Importantly, such material changes will require, at a minimum an improved fundamental understanding of the following things:

- the various roles for the precious metals;
- the mechanisms for these various roles;
- the effects of high temperatures on the precious metal performance in their various roles;
- mechanisms for higher temperature NO_x storage performance for modified and/or alternative storage materials;
- the interactions between the precious metals and the storage materials in both optimum NO_x storage performance and long term stability; and
- the sulfur adsorption and regeneration mechanisms for modified and/or alternative storage materials.

The objective of this CRADA project is to develop a fundamental understanding of candidate next generation NSR materials for NOx after-treatment for light-duty lean-burn (including diesel) engines. The project will focus on characterizing and understanding the six issues described just above. Model catalysts and more fully formulated catalysts will both be studied.

Approach

In a microcatalytic reactor system, LNT performance is evaluated in a fixed bed reactor operated under continuous lean-rich cycling. Rapid lean-rich switching is enabled just prior to the elevated temperature zone (furnace) where the LNT materials are contained in quartz tubing. After removing water, the effluent of the reactor can be analyzed by mass spectrometry and by a chemiluminescent NOx analyzer. For a typical baseline performance testing, the sample is heated to a reaction temperature in flowing He, the feed switched to a 'lean-NOx' mixture containing oxygen and NO, as well as CO_2 and/or H_2O. After an extended period (15 minutes or more), multiple rich/lean cycles of 1- and 4-minute duration, respectively, are run and NOx removal performance is assessed after at least three of these are completed. In the LNT technology, the state of the system is constantly changing so that performance depends on when it is measured. Therefore, we obtain NOx removal efficiencies as "lean conversion (30 minutes)", which measures NOx removal efficiencies for the first 30 minutes of the lean-period. In addition, material treatments such as SO_2 aging, and post mortem catalyst characterizations were conducted in the same test stand without exposing the catalyst sample to air. We have established a reaction protocol, which evaluates the performance of samples after various thermal aging and sulfation condition. In this way, we could identify optimum de-sulfation treatments to rejuvenate catalyst activities.

State-of-the-art catalyst characterization techniques such as X-ray diffraction (XRD), X-ray photoelectron spectroscopy (XPS), transmission electron spectroscopy (TEM)/energy dispersive spectroscopy (EDS), Brunauer-Emmett-Teller/pore size distribution, and temperature programmed desorption/reaction (TPD/TPRX) were utilized to probe the changes in physicochemical properties of the catalyst samples under deactivating conditions; *e.g.*, thermal aging and SO_2 treatment. Specifically, H_2 TPRX, in situ sulfur K-edge X-ray absorption near edge spectroscopy (XANES) and time-resolved X-ray diffraction (TR-XRD) methods were used extensively to quantify the levels, speciation and phase of sulfur on the model adsorber material (Pt-BaO/Al_2O_3 and Pt-BaO/CeO_2) as a function of desulfation process.

Results

Promotional Effect of CO_2 on Desulfation Processes for Pre-Sulfated Pt-BaO/Al_2O_3 LNT Catalysts

A combination of H_2 TPRX, TR-XRD and XPS analysis has been used to investigate the effects of CO_2 on the desulfation of pre-sulfated Pt-BaO/Al_2O_3 samples [3]. The H_2 TPRX in Figure 1 demonstrates that the presence of CO_2 promotes the removal of sulfur species, especially at temperatures below 500°C for both Pt-BaO(8)/Al_2O_3 and Pt-BaO(20)/Al_2O_3 catalysts. To understand the effect of CO_2 on these phase changes as a function of temperature during desulfation, we measured XRD patterns in an in situ reactor while increasing the temperature in the presence of H_2 and CO_2, conditions that are very similar to those used in the H_2 TPRX experiments with CO_2. Figure 2a shows the TR-XRD data obtained during desulfation with H_2 in the presence of CO_2 for a sulfated Pt-BaO(20)/Al_2O_3 sample. Although a BaS phase, indicated by an XRD peak at 2θ of 16.8°, is seen to form at the expense of $BaSO_4$ (XRD peak at 24.8°) during the desulfation, the temperature where this phase change begins is ~650°C (Figure 2b), significantly higher than 550°C observed for the case of CO_2-free desulfation [1]. Such a result implies that

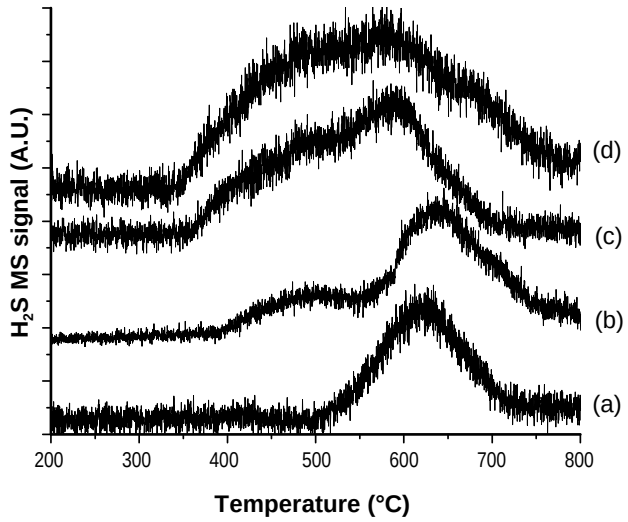

FIGURE 1. H_2 TRPX spectra of Pt-BaO(20)/Al_2O_3 and Pt-BaO(8)/Al_2O_3 in the absence of CO_2 (a and c) and in the presence of CO_2 (b and d).

CO_2 suppresses the formation of BaS crystallites for the Pt-BaO(20)/Al_2O_3 sample to some extent, as evidenced by the temperature shift by 100°C, while promoting the additional desorption of sulfur containing gases at lower temperature below 550°C, in the form of H_2S. It can be summarized that CO_2 promotes sulfur removal by increasing the temperature at which BaS crystallites are formed by 100°C for the Pt-BaO(20)/Al_2O_3 sample, thus resulting in a lower amount of residual sulfur on the sample after desulfation.

Characteristics of Desulfation Behavior for Pre-Sulfated Pt-BaO/CeO_2 LNT Catalysts: the Role of the CeO_2 Support

Recently, we reported [4] superior intrinsic NOx uptake of Pt-BaO/CeO_2 samples compared to Pt-BaO/Al_2O_3 over the entire temperature range studied, and that the ceria-supported sample showed superior sulfur resistance after equivalent exposures to SO_2. Indeed, the ceria-supported catalyst exhibited a remarkably high resistance to Pt sintering during high temperature reductive desulfation, which can be explained by a strong Pt-ceria interaction [5]. A central question from these recent studies is to account for these improved properties, especially those observed during sulfur uptake and removal processes.

The desulfation of pre-sulfated Pt-BaO/CeO_2 LNT catalysts was investigated by H_2 TPRX, in situ TR-XRD, and in situ S K-edge XANES techniques [6]. Compared with Pt-BaO/Al_2O_3 materials, a reductive treatment in H_2 for the CeO_2-supported sample up to 800°C removes, at most, only a very small amount of sulfur species. As shown in Figure 3, the results of in situ TR-XRD measurements demonstrate that the quantity of a BaS

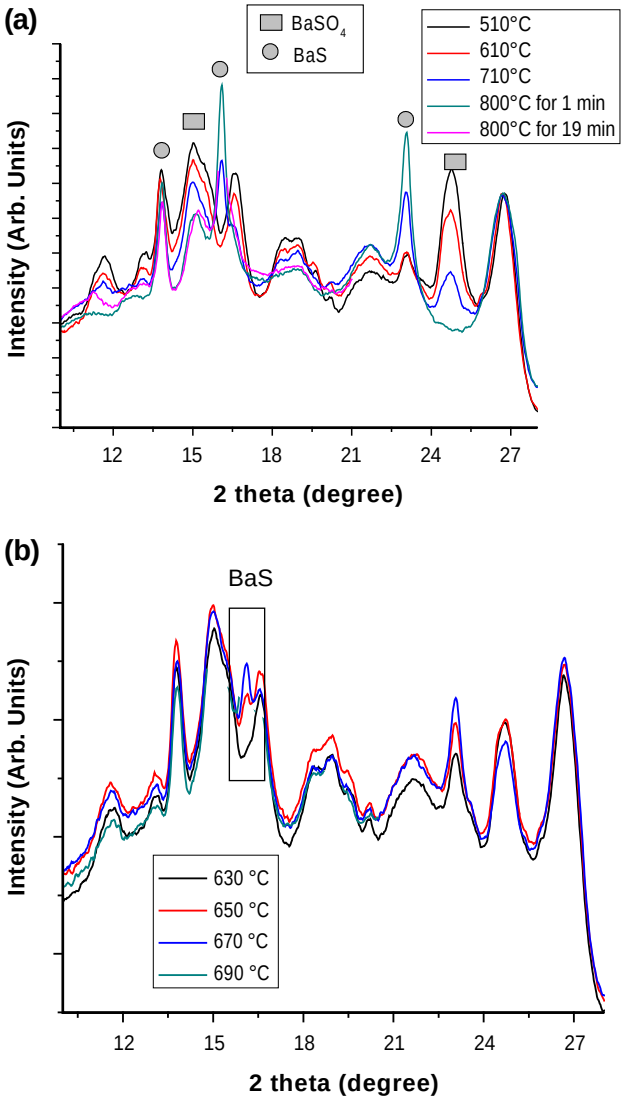

FIGURE 2. TR-XRD diffractograms of pre-sulfated Pt-BaO(20)/Al_2O_3 obtained during the temperature ramping in the presence of both H_2 and CO_2. Figure 2(a) and 2(b) plot the XRD data for temperature ranges of 510–800°C and 630–690°C, respectively.

phase formed on Pt-BaO/CeO_2 is much smaller than that on Pt-BaO/Al_2O_3, implying that the formation of BaS crystallites, which occurs during the reduction from sulfate (SO_4^{2-}) to sulfide (S^{2-}), is significantly suppressed in the CeO_2-supported catalyst. As the desulfation temperature increases under reducing conditions (in H_2), in situ S XANES spectra show that, compared with alumina-supported samples, the reduction temperature for sulfates (S^{6+}) decreases by about 150 K, as demonstrated in Figure 4. Concomitantly, the formation of sulfur species with lower oxidation states (S^{2-} - S^{4+}) is enhanced. The absolute intensities of S XANES spectra before and after desulfation are very similar, implying that the amount of sulfur-containing species removed during the reductive treatment is negligible, in agreement

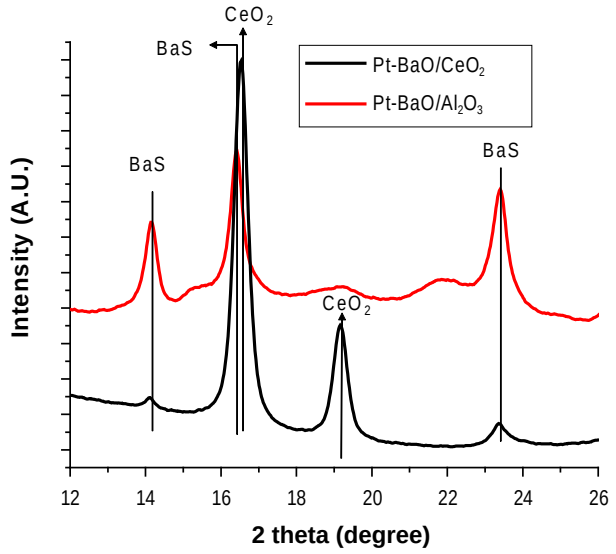

FIGURE 3. XRD patterns for Pt-BaO/CeO_2 and Pt-BaO/Al_2O_3 after reduction in H_2 up to 800°C.

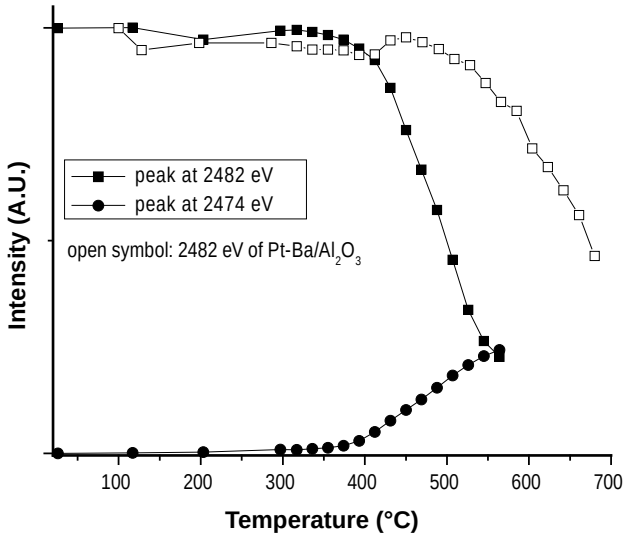

FIGURE 4. Intensities of the peaks at 2,482 eV (solid squares) and 2,474 eV (solid circles) for sulfated Pt-BaO/CeO_2 during reduction in H_2 from room temperature to 550ºC. For comparison, the intensities of the peak at 2,482 eV for sulfated Pt-BaO/Al_2O_3 is displayed with the open square symbols.

with the results of H_2 TPRX. These results suggest that H_2S produced by the reduction of $BaSO_4$ is readily re-adsorbed on the ceria support to form ceria-sulfur complexes (e.g. Ce_2O_2S). The high affinity of ceria for H_2S, combined with the ease of reducibility of the ceria support material gives rise to various oxidation states of sulfur after high temperature H_2 treatments. Thus, the results of this study clearly show that the ceria support strongly affects the overall desulfation mechanism.

Conclusions

PNNL and its CRADA partners from Cummins Inc. and Johnson Matthey have initiated a new CRADA project aimed at improving the higher temperature performance and stability of LNT technology. Results obtained this year demonstrate that the presence of CO_2 promoted the desulfation steps by inhibiting the formation of BaS phase. By using in situ characterization techniques, we can figure out that the sulfur species formed on Pt-BaO/CeO_2 sample is less likely to be removed and has more tendency to stay in the catalyst, even after desulfation up to 800ºC. This result implies that the desulfation mechanism totally depends on the support material. In overall, these approaches are expected to give invaluable information to overcome the critical stability issues in LNT catalysts.

References

1. D.H. Kim, J. Szanyi, J.H. Kwak, T. Szailer, J. Hanson, C.M. Wang, C.H.F. Peden, Journal of Physical Chemistry B, 2006, 110, 10441.

2. Epling, W.S.; Campbell, L.E.; Yezerets, A.; Currier, N.W.; Parks, J.E. Catalysis. Review.–Science and Engingeering 2004, 46, 163.

3. Kim, D.H.; Kwak, J.H.; Szanyi, J.; Wang, X.; Engelhard; M.H.; Peden, C.H.F. Topics in Catalysis, 52 (2009) 1719.

4. Kwak, J.H.; Kim, D.H.; Szayni, J.; Peden, C.H.F. Applied Catalysis B-Environmental 2008, 84, 545.

5. Nagai, Y.; Hirabayashi, T.; Dohmae, K.; Takagi, N.; Minami, T.; Shinjoh, H.; Matsumoto, S. Journal of Catalysis 2006, 242, 103.

6. Kim, D.H.; Kwak, J.H.; Szanyi, J.; Wang, X.; Li; G.; Hanson, J.C.; Peden, C.H.F. Journal of Physical Chemistry C, in press.

FY 2009 Publications/Presentations

1. Do Heui Kim, J.H. Kwak, J. Szanyi, X. Wang, M.H. Engelhard and C.H.F. Peden, "Promotional effect of CO_2 on the desulfation processes for pre-sulfated Pt-BaO/Al_2O_3 lean NOx trap catalysts", Topics in Catalysis, 52 (2009) 1719. DOI (10.1007/s11244-009-9328-8).

2. Do Heui Kim, J. Szanyi, J.H. Kwak, X. Wang, J.C. Hanson, M. Engelhard and C.H.F. Peden, "Effects of sulfation level on the desulfation behavior of pre-sulfated Pt-BaO/Al_2O_3 lean NOx trap catalysts: a combined H_2 TPRX, *in-situ* sulfur K-edge XANES, XPS and TR-XRD study", Journal of Physical Chemistry C, 113 (2009) 7336.

3. Do Heui Kim, Ja Hun Kwak, Janos Szanyi, , Xianqin Wang, Guosheng Li, Jonathan C. Hanson, Charles H.F. Peden, "Characteristics of Desulfation Behavior for Pre-Sulfated Pt-BaO/CeO_2 Lean NOx Trap Catalysts: The Role of the CeO_2 Support", J Phys. Chem. C, accepted.

4. D.H. Kim, X.Q. Wang, G.G. Muntean, C.H.F. Peden, K. Howden, R.J. Stafford, J.H. Stang, A. Yezerets, W.S. Epling, N. Currier, H.Y. Chen and H. Hess, "Mechanisms of Sulfur Poisoning of NOx Adsorber Materials" in *Combustion and Emission Control for Advanced CIDI Engines: 2008 Annual Progress Report*.

5. D. H. Kim, X. Wang, G.G. Muntean, C.H.F. Peden, N. Currier, B. Epling, R. Stafford, J. Stang, A. Yezerets, H.-Y. Chen, and H. Hess, "Mechanisms of Sulfur Poisoning of NOx Adsorber Materials", presentation at the DOE Combustion and Emission Control Review, Washinton, D.C., May, 2009.

6. D.H. Kim, J.H. Kwak, J. Szanyi, Xianqin Wang, M.H. Engelhard, C.H.F. Peden, "Promotional effect of CO_2 on desulfation processes for pre-sulfated Pt-BaO/Al_2O_3 lean NOx trap catalysts", 8th International Congress on Automotive Pollution Control (CAPOC), Brussels, Belgium, 2009, April..

7. D.H. Kim, J.H. Kwak, J. Szanyi, Xianqin Wang, J. Hanson, William Epling, C.H.F. Peden, "Various roles of water in the deactivation of Pt/BaO/Al_2O_3 Lean NOx Trap Catalysts", 2008 AIChE annual meeting, Philadelphia, PA, 2008 November.

II.B.3 Characterizing Lean-NOx Trap Regeneration and Desulfation

James Parks (Primary Contact),
Vitaly Prikhodko
Oak Ridge National Laboratory (ORNL)
2360 Cherahala Boulevard
Knoxville, TN 37932

DOE Technology Development Manager:
Ken Howden

Objectives

- Establish relationships between exhaust species and various lean-NOx trap (LNT) regeneration strategies.
- Characterize effectiveness of in-cylinder regeneration strategies.
- Develop stronger link between bench- and full-scale system evaluations.
- Provide data through Cross-Cut Lean Exhaust Emissions Reduction Simulations (CLEERS) to improve models. Use models to guide engine research.

Accomplishments

- The temporal profiles of reductant emissions during LNT regeneration have been measured with in-line ultraviolet adsorption spectroscopy; NH_3 release occurs after the initial NOx release as observed in bench flow reactor studies [1].
- The quantity of NH_3 formation as a function of rich duration of the LNT regeneration event has been measured, and furthermore, the NOx reduction gained by using the NH_3 on the downstream selective catalytic reduction (SCR) catalyst has been characterized.
- NOx reduction efficiencies of 90% from the LNT alone have been increased to >98% from the LNT+SCR combination for equivalent fuel penalty.

Future Directions

- Evaluate the performance of the LNT+SCR approach at higher space velocities (reduced catalyst size and cost).
- Conduct experiments relative to lean gasoline engine applications of LNTs.

Introduction

As part of the Department of Energy's strategy to reduce imported petroleum and enhance energy security, the Office of Vehicle Technologies has been researching enabling technologies for more efficient diesel engines. NOx emissions from diesel engines are very problematic and the U.S. Environmental Protection Agency (EPA) emissions regulations require ~90% reduction in NOx from light- and heavy-duty diesel engines over the 2004 to 2010 timeframe. One active research and development focus for lean-burn NOx control is in the area of LNT catalysts. LNT catalysts adsorb NOx very efficiently in the form of a nitrate during lean operation, but must be regenerated periodically by way of a momentary exposure to a fuel-rich environment. This rich excursion causes the NOx to desorb and then be converted by precious metal catalysts to harmless N_2. The momentary fuel-rich environment in the exhaust occurs 2-4 seconds for every 30-90 seconds of normal lean operation (depending on operating conditions). The rich exhaust can be created by injecting excess fuel into the cylinder or exhaust, throttling the intake air, increasing the amount of exhaust gas recirculation (EGR), or through some combination of these strategies. The controls methodology for LNTs is very complex, and there is limited understanding of the how all of the competing factors can be optimized.

While LNTs are effective at adsorbing NOx, they also have a high affinity for sulfur. As such, sulfur from the fuel and possibly engine lubricant (as SO_2) can adsorb to NOx adsorbent sites (as sulfates). Similar to NOx regeneration, sulfur removal (desulfation) also requires rich operation, but for several minutes, at much higher temperatures. Desulfation intervals are much longer, on the order of hundreds or thousands of miles, but the conditions are more difficult to achieve and are potentially harmful to the catalyst. Nonetheless, desulfation must be accomplished periodically to maintain effective NOx performance. There is much to be learned with regard to balancing all the factors in managing LNT NOx control performance, durability, and sulfur tolerance.

The objective of this project is to understand the complex chemistry that occurs during the regeneration processes for LNTs through experiments conducted on a full-size engine-LNT catalyst system; supplemental research in a more controlled experiment is also conducted on a bench flow reactor for comparison. Different strategies for introducing the excess fuel for regeneration can produce a wide variety of hydrocarbon and other species. Specific regeneration strategies were developed for this project by operating the engine with net rich air-to-fuel ratios; such "in-cylinder" techniques

utilize throttling to reduce air flow and extra fuel injection pulses during the combustion event to increase fueling. A primary focus of this work is to examine the effectiveness of various regeneration strategies in light of the species formed and the LNT formulation since the combined chemistry of the exhaust produced by the regeneration strategy and the chemistry of the LNT catalyst dictate performance.

Approach

A light-duty diesel engine is operated on a motoring dynamometer, and LNT catalysts are studied with regeneration strategies that utilize extra fuel injected into the cylinders. A 1.7-L 4-cylinder Mercedes-Benz common rail engine was used for the results presented here; however, a new 1.9-L 4-cylinder General Motors diesel engine has been installed for ongoing and future use in this project. Both engines are equipped with an electronic engine control system that provides bypass of the original equipment controller for stand-alone control of the engine. The controllers are capable of monitoring and controlling all the electronically-controlled parameters associated with the engine (i.e., fuel injection timing/duration/number of injections, fuel rail pressure, turbo wastegate, electronic throttle, and electronic EGR). The experimental setup allows for full exhaust species characterization throughout the catalyst system. This includes the measurement of key reductants such as H_2, CO, and hydrocarbons as well as NOx and potential nitrogen-based by-products such as NH_3 at various locations within the catalyst system. A full set of analyzers is applied to sample the various species; analysis techniques include: chemiluminescence for NOx, Fourier transform infrared spectroscopy for NH_3, magnetic sector mass spectrometry for H_2, non-dispersive infrared analysis for CO, and flame ionization detector analysis for hydrocarbons.

In Fiscal Year 2009, the LNT technology was combined with a downstream SCR catalyst to form a LNT+SCR system. The combination of these catalysts has been pursued by automotive companies. In the LNT+SCR approach, NH_3 that is formed during regeneration of the LNT is used by the downstream SCR catalyst to reduce NOx. The potential advantages of this approach are: lower precious metal quantities can be used (since the SCR catalyst does not contain precious metals) and no onboard storage of NH_3 is required. In addition to the analytical capabilities described above, in-line ultraviolet (UV) adsorption spectroscopy was implemented in the exhaust system to analyze NH_3 release by the LNT and use by the SCR catalyst.

Results

The exhaust system for this study was composed of a diesel oxidation catalyst (DOC), diesel particulate filter (DPF), LNT, and SCR catalyst in order from the engine to tailpipe. Figure 1 shows a picture of the system attached to the light-duty diesel engine; a schematic of the catalyst system is also shown. Text in the picture shows the in-line UV spectroscopy tools that were used for analysis of rapidly changing NH_3 concentration in the exhaust. The UV technique was used to measure NH_3 immediately downstream of the LNT catalyst as well as downstream of the SCR catalyst.

Figure 2 shows data from the LNT+SCR system and the intricate relationship between the two catalysts. LNT regeneration began at approximately 60 seconds and continued every 30 seconds until a time of 660 seconds. Prior to LNT regeneration, the engine-out and tailpipe NOx levels were the same (~500 ppm). As LNT regeneration commenced, the LNT-out NOx level dropped rapidly; furthermore, the SCR-out NOx level was even lower than the LNT-out level suggesting an immediate contribution from the SCR catalyst to

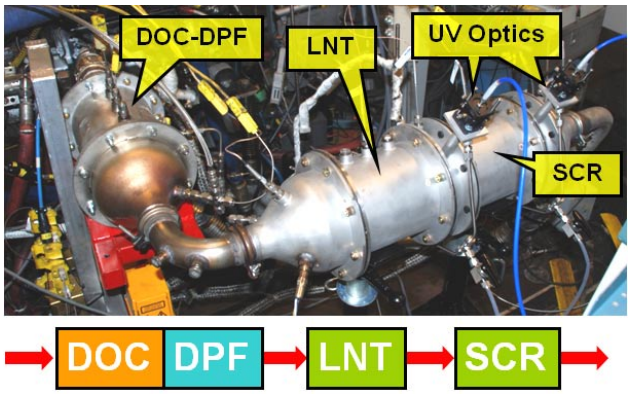

FIGURE 1. Picture and schematic of the LNT+SCR catalyst system on the light-duty diesel engine.

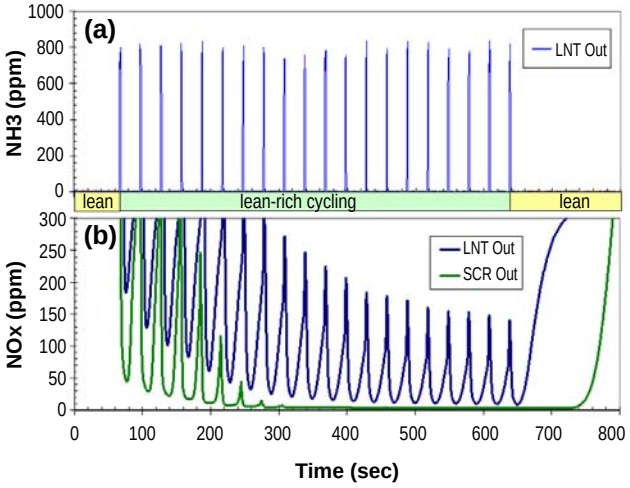

FIGURE 2. NH_3 at the LNT-out position (a) and NOx at the LNT-out and SCR-out positions (b) as a function of time.

the overall NOx reduction efficiency of the system. As observed in the LNT-out NH_3 data, NH_3 was formed immediately with the first regeneration event of the LNT. A peak of NH_3 emission from the LNT is observed with every LNT regeneration event, and the magnitude of the NH_3 peak is similar. As the LNT regenerates, LNT-out NOx levels continue to drop until a steady-state condition occurs with approximately 50 ppm average NOx. NOx variations due to the cyclic nature of the LNT catalyst are observed in the LNT-out data and are typical of the technology. In contrast, the SCR-out NOx levels are relatively steady and furthermore are reduced to <5 ppm (or about one order of magnitude from the LNT-out levels). Thus, the overall system is reducing NOx via two mechanisms: NOx storage and reduction by the LNT and NOx reduction via the SCR reaction with NH_3 produced by the upstream LNT. The combined catalyst approach yields extremely low tailpipe NOx levels despite high engine-out NOx (no EGR used for the Figure 2 data). Another important aspect of the data in Figure 2 occurs after the LNT regeneration stops. Although LNT-out NOx levels rise fairly soon as expected, the SCR-out NOx levels continue to remain low for approximately 100 seconds. This effect is due to NH_3 that has been stored on the SCR catalyst from previous LNT regeneration events. This detail is important since the stored NH_3 can enable continued NOx reduction when LNT regeneration is not feasible or preferred.

The details of NH_3 release from the LNT are critical to understanding and optimizing the LNT+SCR system. It is known from bench flow reactor studies with simulated exhaust that NH_3 release from the LNT increases with increasing reductant supply and increasing NOx storage on the LNT [1]. The in-line UV spectroscopy technique employed in this study confirmed the bench reactor findings with respect to the details of NH_3 release. Figure 3 shows the NH_3 release from the LNT for LNT regeneration event rich durations from 1 to 5 seconds. With 1 second duration, no NH_3 is released by the LNT, and only small amounts of NH_3 are observed with 2 second duration. However, for 3 to 5 seconds of duration, a large amount of NH_3 is formed. The NH_3 release also coincides with reductant breakthough as observed in bench studies. Thus, "over-regeneration" of the LNT leads to the most NH_3 production for the SCR catalyst.

The production and utilization of NH_3 by the system and the resulting NOx reduction efficiency are summarized in Figure 4. Figure 4 shows the NOx reduction efficiency attained by the LNT, the SCR (relative to engine-out NOx), and combined LNT+SCR. The data is a function of the rich duration for a 30 second lean-rich period. As the rich duration increases, the LNT NOx reduction efficiency increases as expected. As the rich duration reaches 4 to 5 seconds, little NOx reduction performance is gained by the LNT

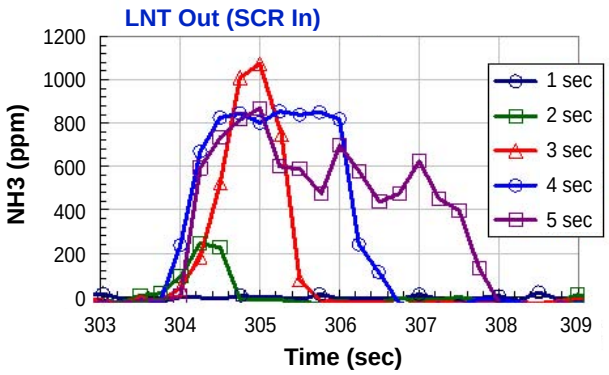

FIGURE 3. NH_3 vs. time at the LNT-out position as a function of the rich duration of the LNT regeneration event.

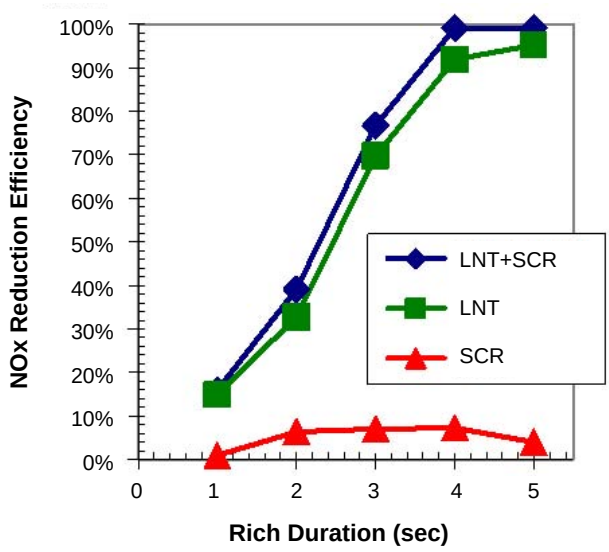

FIGURE 4. NOx reduction efficiency of the LNT and SCR components as well as the combined LNT+SCR NOx reduction efficiency as a function of the rich duration of the LNT regeneration.

as complete regeneration occurs and NOx capacity limitations are reached. The contribution from the SCR catalyst is relatively small as the upstream LNT takes care of most of the NOx. Importantly, the NOx contribution by the SCR catalyst peaks around 3 seconds rich duration and is limited at rich durations above and below 3 seconds. Reasons for these limitations are expressed by Figure 5 which shows NOx and NH_3 in the system. Figure 5a shows that at low rich durations, a large amount of NOx slips past the LNT to the SCR but little NH_3 is released by the LNT for the SCR reaction. At higher rich durations, a large amount of NH_3 is released by the LNT, but lower amounts of NOx are present. Thus, the SCR reaction is limited by insufficient NH_3 at low rich durations and insufficient NOx at high rich durations. The highest SCR contribution occurs at the 3-second midpoint where an

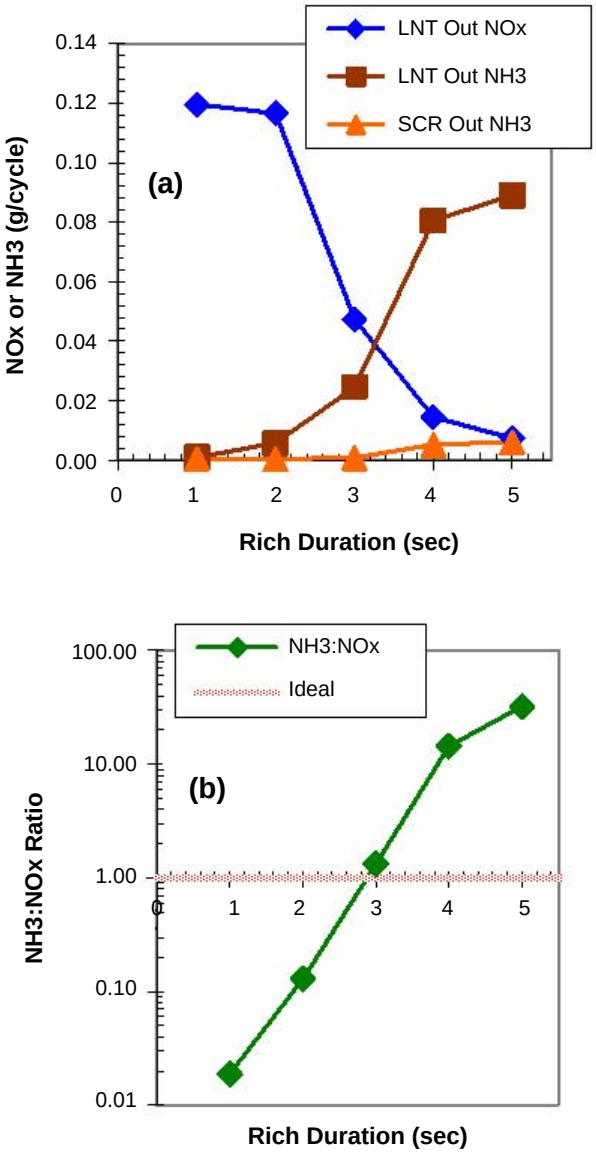

FIGURE 5. Amounts of NOx and NH_3 in the system as a function of the LNT regeneration rich duration (a) and the resulting NH_3:NOx ratio for the SCR reaction (b).

NH_3:NOx ratio of 1 occurs which is optimal for the SCR reaction (see Figure 5b).

Conclusions

- The temporal profiles of reductant emissions during LNT regeneration have been measured with in-line UV adsorption spectroscopy; NH_3 release occurs after the initial NOx release as observed in bench flow reactor studies [1].
- The quantity of NH_3 formation as a function of rich duration of the LNT regeneration event has been measured, and furthermore, the NOx reduction gained by using the NH_3 on the downstream SCR catalyst has been characterized.
- NOx reduction efficiencies of 90% from the LNT alone have been increased to >98% from the LNT+SCR combination for equivalent fuel penalty.
- The highest contribution from the SCR component of the system occurs at a NH_3:NOx ratio of 1 and is at a midpoint between limitations due to insufficient NH_3 production by and low NOx slip from the LNT catalyst.

References

1. Castoldi, L., Nova, I., Lietti, L., and Forzatti, P., *Catalysis Today* **96**, pp.43-52 (2004).

FY 2009 Publications/Presentations

1. Jim Parks and Vitaly Prikhodko, "Ammonia Production and Utilization in a Hybrid LNT+SCR System", *SAE Technical Paper Series* 2009-01-2739 (2009) [*accepted for publication in November 2009*].

2. Jim Parks, Vitaly Prikhodko, Bill Partridge, and Jae-Soon Choi, "Reductant Utilization in a LNT + SCR System", *2009 Directions in Engine-Efficiency and Emissions Research Conference (DEER)*, August 3-6, 2009 (2009).

3. Jim Parks, Vitaly Prikhodko, John Storey, Teresa Barone, Sam Lewis, Mike Kass, and Shean Huff, "Emissions from Premixed Charge Compression Ignition (PCCI) Combustion and Affect on Emission Control Devices", *21st North American Meeting of the North American Catalysis Society 2009 conference*, June 7-12, 2009 (2009).

4. Vitaly Prikhodko and Jim Parks, "Effect of Regeneration Strategy on LNT-SCR Hybrid System Performance", *12th DOE Crosscut Workshop on Lean Emissions Reduction Simulation*, April 28-30, 2009 (2009).

5. Jim Parks, Shean Huff, Mike Kass, Brian West, Todd Toops, and Vitaly Prikhodko, "Lean NOx Trap Catalysis: Exhaust Chemistry Related to Advanced Diesel Engines", *SAE Light-Duty Diesel Emissions Control Symposium*, Ypsilanti, MI, November 3-5, 2008.

II.B.4 Development of Chemical Kinetics Models for Lean NOx Traps

Richard S. Larson
Sandia National Laboratories
MS 9409, P.O. Box 969
Livermore, CA 94551-0969

DOE Technology Development Manager:
Kenneth Howden

Collaborators:
V. Kalyana Chakravarthy, Josh A. Pihl, Jae-Soon Choi, and C. Stuart Daw (Oak Ridge National Laboratory, Knoxville, TN)

Objectives

- Identify a set of elementary (microkinetic) surface reactions that can account for the observed behavior of a lean-NOx trap (LNT) during a complete storage/regeneration cycle.
- Optimize the kinetic parameters associated with these reactions by matching model predictions with laboratory reactor data.
- Extend the mechanism to include reactions involving sulfur-containing species, with the aim of describing both catalyst degradation during normal operation and catalyst restoration during high-temperature desulfation.
- Use the validated reaction mechanism to suggest improvements in the usage of existing LNT materials and to help in the development of a new generation of catalysts.

Accomplishments

- Modified our previously developed mechanism for chemistry on the precious metal sites, and re-optimized the corresponding kinetic parameters (as detailed in the following), in response to the realization that transient effects and NOx storage were not always negligible during the comprehensive set of steady flow temperature sweep experiments.
- Made further refinements to our previously developed mechanism for chemistry on the NOx and oxygen storage sites, combined this with the modified precious metal mechanism, and performed a global optimization of the kinetic parameters in the overall mechanism by fitting simultaneously data for all of the steady flow and long cycle experiments.
- Streamlined our thermodynamically consistent mechanism for sulfation and desulfation, and used the standard optimization methodology to fit semi-quantitatively some published data for gas production during high-temperature desulfation.

Future Directions

- Account for the role of hydrocarbons and partial oxidation products as alternate reductant species during normal catalyst regeneration.
- Enhance the transient plug flow reactor code with a complete energy balance equation, and use this to simulate more conventional short storage/regeneration cycles, in which temperature excursions cannot be neglected or easily measured.
- Use the validated reaction mechanisms to investigate coupling between an LNT and other devices in the aftertreatment train.

Introduction

The increasingly strict constraints being placed on emissions from diesel and other lean-burn engines require the development of a new generation of aftertreatment technologies. LNTs represent one option for achieving the stated targets with regard to NOx emissions. In an LNT, NOx produced during normal lean engine operation is trapped and stored via adsorption on high-capacity catalytic sites, and periodically this stored NOx is released and reduced to harmless N_2 on precious metal sites by imposing rich conditions for a short time. While this qualitative description is widely accepted, a detailed quantitative understanding of the underlying chemistry is not yet available. Such knowledge is needed in order to use the LNT concept to best advantage, so it is the principal goal of this project to develop an elementary reaction mechanism that describes both phases of LNT operation.

A complicating factor in the use of LNTs is that sulfur-containing contaminants in the fuel can lead to degradation in the catalyst performance over time, so periodic desulfation episodes are needed in addition to the ordinary regeneration (deNOx) excursions. Thus, a truly comprehensive mechanism must include reactions of sulfur-containing species alongside those describing storage, release, and reduction of NOx.

Clearly, a kinetics model with the ability to simulate all phases of LNT operation must account for the chemistry occurring on several kinds of catalytic sites: the metal oxide sites used to store NOx, additional oxide sites used (sometimes) for oxygen storage, and the

precious metal sites involved primarily in the reduction of released NOx. While it is tempting to associate each of these kinds of sites with a particular part of the LNT cycle, it must be remembered that the desorption of NOx from the storage sites is an integral part of the regeneration process, while oxidation of NO on the precious metal sites is thought to be a key part of the storage phase. Nevertheless, it is possible to design experiments that isolate (to a large extent) a particular subset of the chemistry, and this has been used to facilitate model development in this project. Thus, work in previous years led first to a tentative mechanism for the precious metal sites alone, and the basic mechanism was then completed by appending reactions for the storage sites. As will be explained below, more recently it became necessary to refine the mechanism in order to account for modest deficiencies in the original assumptions. In any case, the addition of sulfation/desulfation reactions involving all kinds of sites is fairly straightforward if one assumes that the roles of nitrogen- and sulfur-containing species are analogous.

Approach

Our basic approach to mechanism development is to assemble a candidate set of elementary reactions, often with poorly known kinetic parameters, and then to optimize the parameters by fitting the results of reactor simulations to bench-scale experimental data provided by our collaborators at Oak Ridge National Laboratory. This process requires two principal pieces of supporting software: a reactor code to simulate flow through a single monolith channel using the proposed reaction mechanism (expressed in Chemkin format), and an optimization code to carry out the fitting process on a massively parallel machine. For the simulation of both storage/regeneration and sulfation/desulfation cycles, we have used a specially developed transient Chemkin-based plug flow code, and for the optimization we have adopted the Sandia APPSPACK code [1], which is ideally suited to this application.

As mentioned above, a tentative mechanism for the chemistry occurring on the precious metal sites was constructed and validated in previous years [2]. Our original intention was to incorporate this essentially without modification into the complete mechanism, thus minimizing the number of parameters to be determined on the basis of time-consuming transient simulations. However, it eventually became clear that this approach would lead to noticeable and avoidable errors, so the decision was made to treat the precious metal parameters once again as adjustable. A comprehensive LNT mechanism was then constructed by adding a set of candidate reactions for the storage sites, and the entire set of kinetic parameters was estimated by fitting simultaneously the experimental data (specifically, the exit gas concentrations) for not only a set of three long storage/regeneration cycles [3], but also the complete set of steady flow temperature sweeps used previously [2].

In any mechanism development effort, a significant issue that must be addressed during the optimization process is that not all of the parameters can be varied independently if thermodynamic consistency is to be maintained. Thus, a number of well-defined relationships among the various parameters must be enforced; this reduces the size of the optimization problem, but it greatly increases the programming complexity. In addition, all of the activation energies, whether varied independently or computed from thermodynamic constraints, are required for physical reasons to be non-negative. Fortunately, the resulting inequality constraints are easily handled by APPSPACK.

A further complication in simulating LNT cycles is the issue of mass-transfer resistance within both the gas-phase boundary layer and the catalyst washcoat. A full treatment of these phenomena would result in a transient two-dimensional reactor model, which would be computationally prohibitive in light of the large number of simulations needed for parameter optimization. As an alternative, we have formulated and implemented a one-dimensional lumped-parameter description of mass transfer. Ultimately, however, we have found that the inclusion of a mass transfer resistance does not significantly improve the quality of the data fits. Because of this, and in light of the crudeness of this submodel, we have elected to abandon it and to pursue a purely kinetic description of LNT behavior.

Results

As noted above, we have found it advisable to modify both the structure (slightly) and the kinetic parameters of the precious metal mechanism from those previously presented [2]. The original work involved simulating a large set of steady flow temperature sweep experiments under the assumptions that (a) there was no significant NOx storage, so that a precious metal mechanism alone would suffice, and (b) the temperature ramps were slow enough that a steady-state reactor code could be used. While these assumptions were largely valid, we have now concluded that they did lead to some noticeable errors. An example of this is provided by a comparison of Figures 1 and 2. The former shows the results of a particular simulation (involving a feed mixture with NO_2 and H_2 in a 1:10 ratio) using a steady-state code and the precious metal mechanism alone, while the latter shows results for the same case using a fully transient code and the complete LNT mechanism. While the two plots agree very well qualitatively, there is an obvious shift in the temperature range over which NO_2 is replaced by NH_3 as the dominant (nontrivial) species in the exit gas. Because of deviations like this, it was concluded that adherence to the original precious

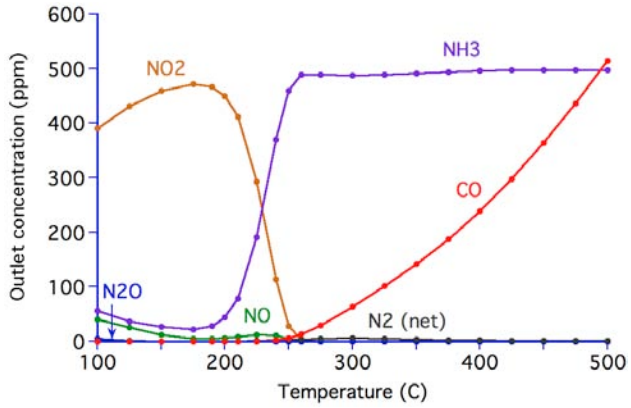

FIGURE 1. Simulated outlet concentrations for temperature sweep with 1:10 NO_2/H_2 using steady-state code and precious metal mechanism.

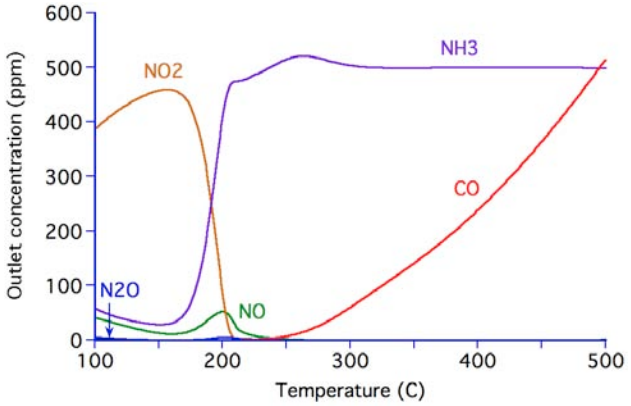

FIGURE 2. Simulated outlet concentrations for temperature sweep with 1:10 NO_2/H_2 using transient code and full mechanism.

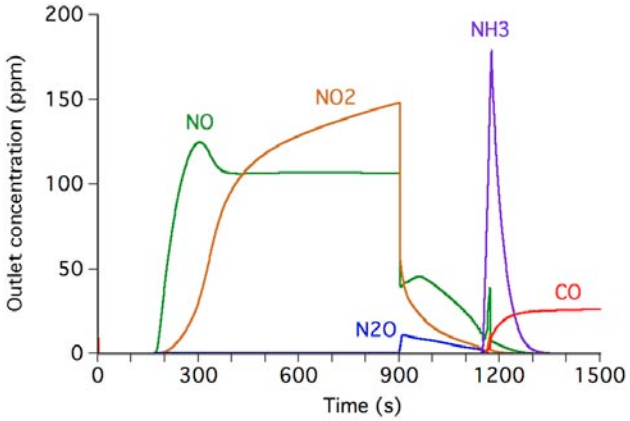

FIGURE 3. Simulated outlet concentrations for the benchmark long storage/regeneration cycle at 300°C.

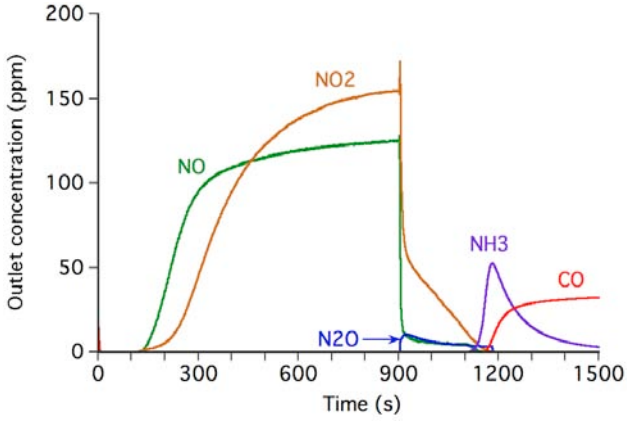

FIGURE 4. Experimental outlet concentrations for the benchmark long storage/regeneration cycle at 300°C [3].

metal mechanism could compromise the ability to fit transient data for full storage/regeneration cycles. Thus, as noted previously, the precious metal parameters were once again allowed to vary and were re-optimized simultaneously with those of the storage phases.

During the year, the submechanism describing chemistry on the baria (NOx storage) sites underwent significant revision with respect to not only the kinetic parameters, but also the reaction set itself. First of all, adsorbed oxygen was removed from the list of surface species, forcing initial NOx storage to take place via displacement of surface carbonates and hydroxides. Perhaps more significant was the addition of a set of spillover reactions describing direct reduction of nitrates and direct oxidation of nitrites by species on the precious metal sites. This was done to account for the fact that the kinetic behavior of a baria site seems to depend on its proximity to the precious metal phase. Even with these additions, however, the final storage mechanism was quite small, consisting of just five reactions involving only the baria sites, six spillover reactions, and one reaction describing oxygen storage on ceria.

Reassuringly, the improved fidelity of the temperature sweep simulations (with respect to both the reactor code and the mechanism) led to a noticeable improvement in the overall fit to the corresponding data. Ironically, however, this did not allow the long storage/regeneration cycles to be simulated with much greater accuracy, as was the original motivation. Figure 3 shows the simulation results for our benchmark cycle at a nominal temperature of 300°C, while the corresponding experimental results are shown in Figure 4. The agreement is quite acceptable overall, but there are some noticeable discrepancies, most obviously in the size and duration of the ammonia peak (although the timing is reproduced very accurately). The situation here contrasts sharply with that at 200°C (not shown), where the amount of ammonia is predicted very well, while the amount of N_2O is not. It is also worth noting in Figure 3 that the total amount of NOx slip between the onset

of regeneration and the first appearance of ammonia is simulated fairly well, even though the relative amounts of the two NOx species are not. In any case, exhaustive efforts have convinced us that the current modeling framework is probably not capable of eliminating the last discrepancies between the simulations and the data; a major overhaul, such as the inclusion of different classes of storage sites (as has been done in other studies) or a sophisticated mass transfer model, would probably be necessary, although it would inevitably require a large increase in computational effort.

In keeping with the stepwise approach to mechanism development, a submechanism describing sulfation and desulfation phenomena was constructed by appending sulfur-specific reactions to the finalized mechanism for normal LNT operation and then optimizing the new parameters (to the extent possible). From the rather large set of candidate reactions originally proposed, it was found that a surprisingly small number was sufficient to reproduce acceptably the limited experimental data available. Specifically, the mechanism as finally adopted included:

(a) adsorptions of the gas-phase molecules SO_2, SO_3, and H_2S on precious metal sites;
(b) stepwise surface decompositions of the adsorbed molecules;
(c) reduction of adsorbed SO_3 by adsorbed H or CO;
(d) storage of SO_3 on baria sites (in the form of sulfate) via displacement of carbonates and nitrates; and
(e) storage of SO_3 on ceria sites via direct reaction with stored oxygen.

To exercise the mechanism, a sulfation episode was first simulated by repeating the 300°C storage/regeneration cycle described above with 10 ppm of SO_2 added to the lean-phase feed. This was followed by a desulfation regime following the procedure described in [4], specifically temperature-programmed reduction to about 670°C under an atmosphere containing 0.1% H_2. The relative amounts of H_2S and SO_2 evolved in the simulation as a function of temperature were compared to the experimental values and thereby used to adjust the kinetic parameters. The computed results were also checked for consistency with certain qualitative behaviors, such as the absence of sulfur-containing species in the exit gas during normal regeneration (and storage), the concentration of stored sulfates at the front end of the reactor, and the completeness of desulfation at the end of the temperature ramp and subsequent high-temperature soak.

Figure 5 shows computed results for the desulfation regime using the (tentatively) optimized kinetic parameters, while Figure 6 shows the corresponding experimental data (with concentrations in arbitrary units). It can be seen that the simulation of H_2S production is quite good, whereas the predicted peak

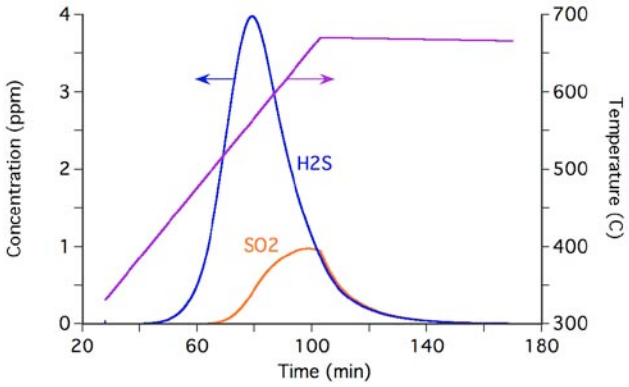

FIGURE 5. Simulated outlet concentrations for desulfation via temperature-programmed reduction under 0.1% H_2.

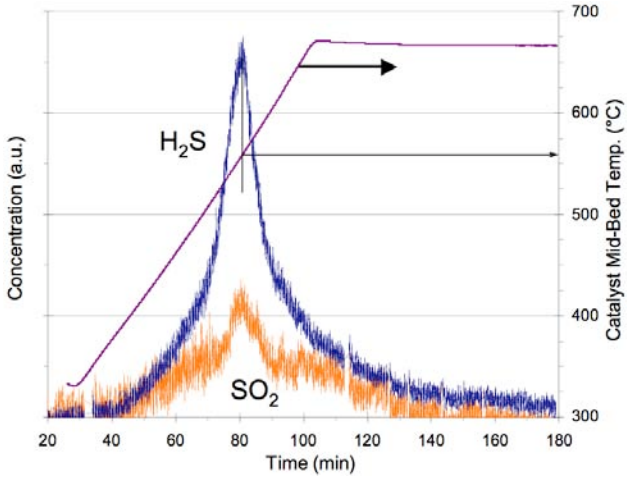

FIGURE 6. Experimental outlet concentrations for desulfation via temperature-programmed reduction under 0.1% H_2 [4].

of SO_2 production is at too high a temperature, even though the total amount evolved seems to be accounted for reasonably well. It is possible that some of the reactions not included in the final mechanism, such as oxidations of surface H_2S fragments, could help to overcome the remaining discrepancies.

Conclusions

- Contrary to previous assumptions, transient effects and NOx storage cannot necessarily be neglected in simulating the steady flow temperature sweep experiments originally used to construct the precious metal mechanism.
- The behavior of an LNT during both steady flow temperature sweeps and long storage/regeneration cycles can be simulated quite well with a single elementary reaction mechanism and without including any mass transfer resistance, provided that a transient reactor code is used in all cases.

- A very simple sulfation/desulfation mechanism can account for both irreversible sulfate storage at normal cycle temperatures and the observed evolution of product gases during high-temperature desulfation in the presence of hydrogen.

References

1. J.D. Griffin, T.G. Kolda, and R.M. Lewis, Sandia National Laboratories Report SAND2006-4621, 2006.

2. R.S. Larson, J.A. Pihl, V.K. Chakravarthy, T.J. Toops, and C.S. Daw, *Catal. Today* **136**, 104 (2008).

3. J.A. Pihl, M.S. Thesis, University of Wisconsin–Madison, 2005.

4. J.-S. Choi, W.P. Partridge, and C.S. Daw, *Appl. Catal. B* **77**, 145 (2007).

FY 2009 Publications/Presentations

1. R.S. Larson, "Microkinetic Modeling of Lean NOx Trap Storage and Regeneration," Advanced Engine Combustion Working Group Meeting, Livermore, California, February 11, 2009.

2. R.S. Larson, J.A. Pihl, V.K. Chakravarthy, J.-S. Choi, and C.S. Daw, "Microkinetic Modeling of Lean NOx Trap Storage/Regeneration and Sulfation/Desulfation," Twelfth CLEERS Workshop, Dearborn, Michigan, April 30, 2009.

3. R.S. Larson, "Benchmark Reaction Mechanisms and Kinetics for Lean NOx Traps," DOE Vehicle Technologies Program Annual Merit Review, Arlington, Virginia, May 19, 2009.

4. W.P. Partridge, J.-S. Choi, J.A. Pihl, T.J. Toops, N.A. Ottinger, J.E. Parks, V.K. Chakravarthy, R.S. Larson, C.S. Daw, A. Yezerets, and N.W. Currier, "Elucidating Lean NO_X Trap Regeneration and Degradation Chemistry: Insights from Intra-Catalyst Spatiotemporally Resolved Measurements," 21st North American Meeting of the North American Catalysis Society, San Francisco, California, June 7–12, 2009.

5. R.S. Larson, V.K. Chakravarthy, J.A. Pihl, and C.S. Daw, "Microkinetic Modeling of Lean NOx Trap Storage and Regeneration," journal paper in preparation (2009).

II.B.5 NOx Abatement Research and Development CRADA with Navistar, Inc.

Josh A. Pihl (Primary Contact), Todd J. Toops
Oak Ridge National Laboratory
2360 Cherahala Blvd.
Knoxville, TN 37932

CRADA Partner:
Vadim Strots, Brad Adelman, Ed Derybowski
Navistar, Inc.

DOE Technology Development Manager:
Ken Howden

Objectives

- Explore leading edge engine and emissions control technology.
- Enable compliance with emissions regulations while maintaining or improving overall engine efficiency.
- Develop a transient evaluation protocol for urea selective catalytic reduction (SCR) catalysts that provides data for control model parameter estimation and validation.
- Exercise the protocol on fresh and aged catalysts.
- Fully analyze the resulting data sets to yield insights on catalyst surface chemistry and aging effects.

Accomplishments

- Refined protocol to simplify inlet gas composition transitions and add steady-state operating points.
- Executed protocol on fresh and engine-aged samples.
- Transferred data to Michigan Technological University (MTU) for use in model calibration and validation.
- Identified mechanisms by which aging impacts catalyst performance.

Future Directions

- Optimize transient evaluation protocol to identify a minimal set of sufficient steps and operating conditions required for model calibration and validation.
- Transfer protocol to the Cross-Cut Lean Exhaust Emissions Reduction Simulations (CLEERS) SCR focus group as a starting point for development of a standard CLEERS transient SCR protocol.
- Measure soot oxidation kinetics of engine-generated soot loaded in miniature diesel particulate filter (DPF) samples for use in a DPF regeneration control model.

Introduction

Governments around the world are implementing increasingly stringent emissions standards for both light-duty and heavy-duty vehicles. The legislated reductions in particulate matter (PM) and oxides of nitrogen (NOx) are particularly challenging for lean-burn engines (such as diesels) which are unable to use the three-way catalysts developed for stoichiometric gasoline vehicles. The U.S. DOE has identified high-efficiency, lean-burn engines as a promising strategy for reducing petroleum consumption. However, the engine modifications and/or aftertreatment technologies (such as DPFs, lean-NOx traps [LNTs], and urea-SCR systems) required to meet emissions regulations can result in increased fuel consumption. Meeting emissions standards while also maintaining or improving the high efficiency of lean-burn engines requires simultaneous optimization of both engine and aftertreatment operating strategies. Development of these strategies is complicated by the presence of storage functions in all three of the aftertreatment technologies mentioned above: DPFs store soot, LNTs store NOx, and SCR catalysts store NH_3. The presence of storage precludes the use of steady-state operating maps typically used in engine calibration and requires consideration of stored species in control models and operating strategies. The current focus of this Cooperative Research and Development Agreement (CRADA) is to assist our industrial partner in the development of such control models. These efforts will help our partner bring to market high-efficiency engine systems that are compliant with emissions regulations. The protocols and insights into aftertreatment device operation developed from this project should also be more broadly useful to the engine aftertreatment research and development community as a whole.

Approach

Our efforts under this CRADA for Fiscal Year 2009 have focused on urea-SCR systems. During FY 2008 ORNL and Navistar developed a transient evaluation protocol that measures the NH_3 storage capacity and reaction kinetics of key processes occurring over a urea-SCR catalyst. This year we have further refined the transient evaluation protocol based on feedback from our partners at MTU. ORNL used an automated bench-scale flow reactor to exercise the revised protocol

on core samples cut from fresh and engine-aged SCR catalysts provided by Navistar. The data from the protocol experiments have been transferred to MTU for use in development, calibration, and validation of a urea-SCR control model. ORNL fully analyzed the protocol data to draw conclusions about the surface chemistry of urea-SCR catalysts and the mechanisms by which aging reduces catalyst performance.

Results

The revised protocol includes steps to measure the following catalyst properties:

- NH_3 storage capacity by three independent techniques:
  - Uptake during adsorption
  - Release during isothermal and temperature programmed desorptions
  - Reduction of NOx by stored NH_3
- Steady-state SCR kinetics with varying reactant compositions:
  - NH_3/NO: 0.8, 0.9, 1.0, 1.1, 1.2
  - NO_2/NOx: 0.0, 0.25, 0.5, 0.7, 1.0
- NH_3 oxidation kinetics
- NO oxidation kinetics

The protocol was run over a range of temperatures (150-550°C), gas hourly space velocities (GHSV; 60,000, 90,000, and 120,000 hr^{-1}), and reactant concentrations (150, 300, and 450 ppm NOx). Results from selected portions of the protocol are shown in Figures 1-4.

Figures 1 and 2 are examples of the types of steady-state data that can be extracted from the protocol runs. Figure 1 shows the NOx conversion activity of the catalyst as a function of temperature for three NO_2/NOx ratios (0.0, 0.5, and 1.0) over a fresh catalyst. As expected for a zeolite-based SCR catalyst, 1:1 mixtures of NO and NO_2 yield much higher SCR reaction rates than NO or NO_2 alone. For this particular formulation, NO_2 is more reactive than NO, particularly at the lowest and highest temperatures. Figure 2 summarizes NOx conversion as a function of NH_3/NO ratio and temperature. At 300°C and below, the NOx conversion decreases with increasing NH_3 dose. This behavior indicates that NH_3 inhibits the NO SCR reaction at low temperatures. Above 300°C, the trend reverses, and NOx conversion improves with increasing NH_3 concentration.

In addition to the steady-state data typically collected for evaluation of SCR catalysts, the test protocol includes transient steps that generate additional insights into the catalyst surface chemistry. Figure 3 shows the NH_3 released from the catalyst during the temperature programmed desorption (TPD) at the end of the protocol run. For adsorption temperatures above 300°C, all of the NH_3 is released during the isothermal desorption step prior to the TPD. For adsorption

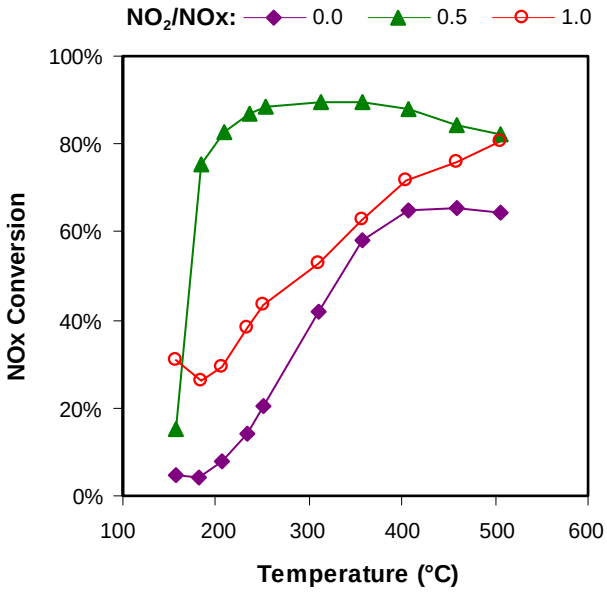

FIGURE 1. SCR NOx conversion as a function of temperature for NO_2/NOx ratios of 0.0, 0.5, and 1.0. Data collected with a fresh catalyst sample operated at a GHSV of 120,000 hr^{-1} under 300 ppm NO, stoichiometric quantities of NOx (300 ppm NO, 150 ppm NO + 150 ppm NO_2, and 225 ppm NO_2, respectively), 10% O_2, 5% H_2O, and 5% CO_2.

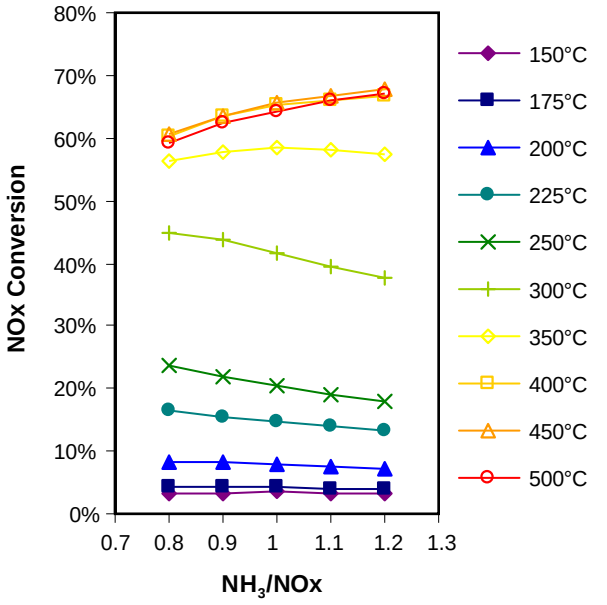

FIGURE 2. SCR NOx conversion as a function of NH_3/NOx ratio at various operating temperatures. Data collected with a fresh catalyst sample operated at a GHSV of 120,000 hr^{-1} under 300 ppm NO, 10% O_2, 5% H_2O, and 5% CO_2.

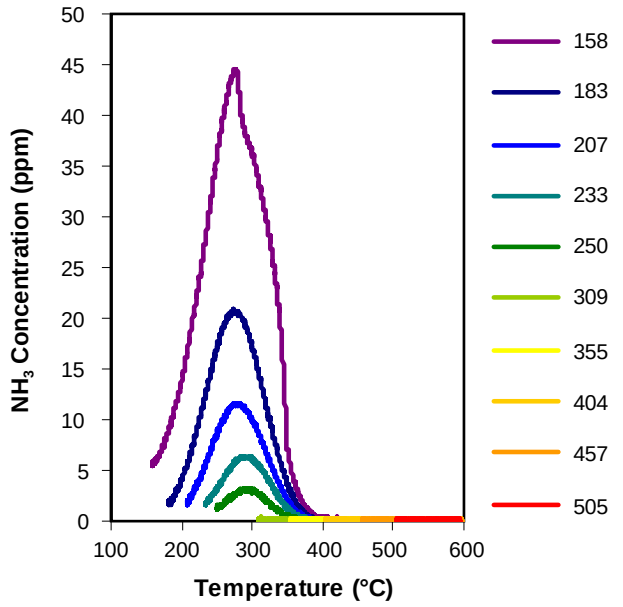

FIGURE 3. Concentration of NH_3 released as a function of temperature during the TPD portion of the protocol. Data collected with a fresh catalyst sample operated at a GHSV of 120,000 hr^{-1} under 300 ppm NO, 10% O_2, 5% H_2O, and 5% CO_2.

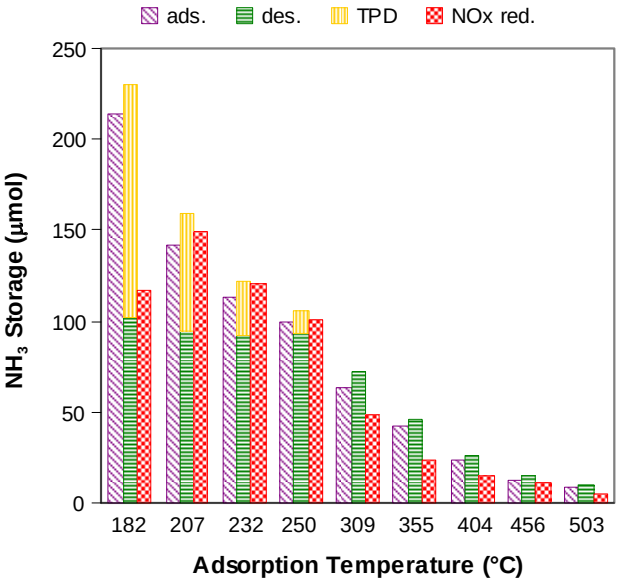

FIGURE 4. Catalyst NH_3 storage capacity as a function of adsorption temperature as measured by uptake during adsorption (ads.), release during isothermal desorption (des.) and temperature programmed desorption (TPD), and NOx converted by stored NH_3 after removing NH_3 from the feed gas (NOx red.).

temperatures below 300°C, the amount of NH_3 desorbed during the TPD increases with decreasing adsorption temperature. For all but one of the TPD runs, there is a single NH_3 desorption feature centered at approximately 300°C. At 150°C there is a second low temperature NH_3 desorption, likely due to formation of ammonium nitrates on the catalyst surface.

The protocol includes several transient steps that provide independent measures of NH_3 storage capacity under various operating conditions. These include adsorption under inert conditions, isothermal and TPD, and reactivity of NO with stored NH_3 after the NH_3 feed is shut off. Integrating the NH_3 stored, released, or reacted during each of these steps yields the capacities summarized in Figure 4. The integrals from the two desorption steps are shown as stacked bars to indicate the total NH_3 desorbed. This plot yields two noteworthy insights. First, with the exception of the lowest temperature run, the three storage capacities are fairly consistent across the three measurement techniques. Based on this observation, we conclude that a measurement of NH_3 storage capacity can be achieved through any of the three techniques. The exception to this conclusion is for temperatures below 200°C, where the slow SCR kinetics limit the NOx reacted with stored NH_3. At these low temperatures, the appropriate measure of NH_3 storage capacity will depend on the application of the measurement.

The other interesting insight from Figure 4 comes from a comparison of the NH_3 desorbed during the isothermal and TPD steps. The trends for these two desorption steps are consistent with the presence of two different NH_3 storage sites on the catalyst surface. The first site, associated with the isothermal desorptions, is in equilibrium with the gas phase: the stored NH_3 desorbs as soon as NH_3 is removed from the feed gas. This site appears to be saturated at temperatures below 300°C. At higher temperatures, the amount of NH_3 stored on this site decreases with increasing temperature, but there is still some storage remaining even at 500°C. The second site, associated with the TPD releases, only stores NH_3 at temperatures below 300°C. The amount stored increases with decreasing temperature. The NH_3 stored at this site is not released until the catalyst temperature is increased (or it reacts with NOx), and the peak desorption occurs at around 300°C. Comparing these results with the NH_3 inhibition results shown in Figure 2, it appears that NH_3 stored at this second site inhibits SCR reaction rates, and this site is therefore critical for SCR reactions.

In addition to generating insights on SCR reaction rates and surface chemistry, the protocol data is being used by our partners at MTU for development of a urea-SCR model with sufficient accuracy and computational efficiency to be used in model-based urea control system design. They are using selected segments of the test protocol to isolate global kinetic parameters by using optimization routines to minimize the difference between measured and simulated concentration profiles. The results of one such parameter identification process are shown in Figure 5 for NH_3 uptake and oxidation.

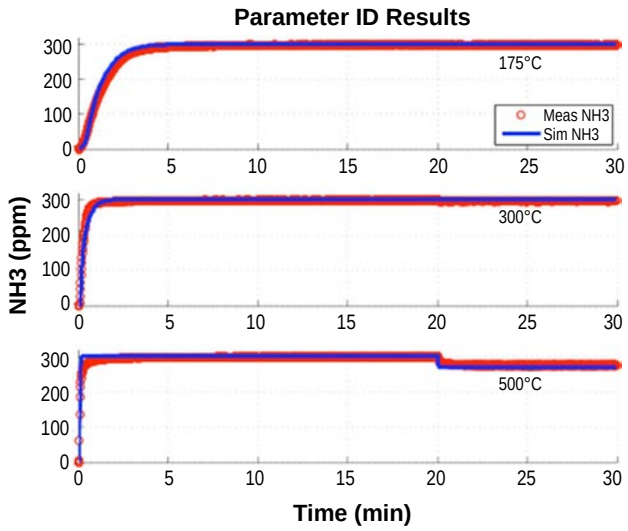

FIGURE 5. Comparison between measured and simulated NH_3 concentration profiles during the NH_3 adsorption and oxidation steps of the transient SCR catalyst evaluation protocol run at 175, 300, and 500°C and a GHSV of 90,000 hr^{-1}.

We also ran the experimental protocol on engine-aged catalyst samples to see how the measured reaction kinetics and storage capacities vary with catalyst aging. Core samples were cut from the front face and back face of the first SCR brick from the exhaust system of an engine that was run on a dynamometer. Figure 6 shows results from selected portions of the protocol (NO SCR and NH_3 oxidation) for these two aged samples. The data reveal two separate aging mechanisms that impacted catalyst performance. At low temperatures, both catalysts suffered a roughly equivalent drop in both NO and NH_3 conversion (Figures 6a and 6b). This is likely due to hydrothermal aging, which results in lower active catalyst surface area (due to washcoat sintering, zeolite dealumination, and/or loss of exchanged metal cations from the zeolite structure). The second aging mechanism is evidenced by a further drop in NOx conversion along with an increase in NH_3 conversion for the front face core sample (compared to the rear face) under SCR conditions at high temperatures. Figure 6c reveals why the high temperature performance of the front face core drops so much: the NH_3 oxidation rate has increased by over an order of magnitude. The most plausible explanation for such a large increase in NH_3 oxidation is deposition of precious metals volatilized from the upstream diesel oxidation catalyst (DOC) onto the front face of the SCR catalyst [1].

Conclusions

We refined the urea-SCR transient evaluation protocol developed during FY 2008 and ran it on fresh and aged catalyst samples. The protocol enabled measurements of reaction rates and NH_3 storage capacities over a wide range of operating conditions. It also yielded insights into the surface chemistry occurring on the SCR catalyst, including NH_3 inhibition of SCR reactions and the presence of two apparent NH_3 storage sites. MTU is using the protocol data to identify parameters for their urea SCR model, which they are developing for model-based urea control system design. The protocol data also highlighted two different degradation mechanisms occurring in engine-aged samples: hydrothermal aging and deposition of precious metals volatilized from an upstream DOC.

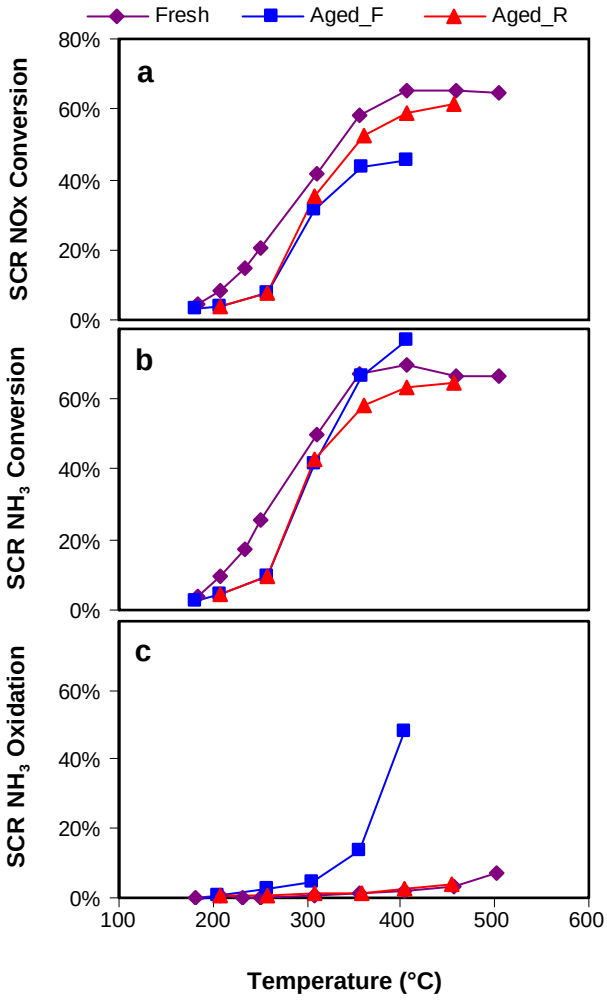

FIGURE 6. (a) SCR NOx conversion, (b) SCR NH_3 conversion, and (c) NH_3 oxidation conversion as a function of temperature for fresh (Fresh), front face of aged brick (Aged_F), and rear face of aged brick (Aged_R) SCR catalyst core samples.

References

1. H.-W. Jen, J.W. Girard, G. Cavataio, M.J. Jagner, "Detection, Origin and Effect of Ultra-Low Platinum

Contamination on Diesel-SCR Catalysts," SAE Technical Paper 2008-01-2488 (2008).

FY 2009 Publications/Presentations

1. J.A. Pihl, T.J. Toops, V.O. Strots, E.M. Derybowski, "Development and Implementation of Experimental Protocol for Steady-State and Transient SCR Kinetics," 12th DOE Crosscut Workshop on Lean Emissions Reduction Simulation Workshop, Dearborn, MI, April 28, 2009.

2. J.A Pihl, T.J. Toops, V.O. Strots, E.M. Derybowski, "NOx Abatement Research and Development – CRADA with Naistar Incorporated," 2009 DOE Vehicle Technologies Merit Review, Arlington, VA, May 21, 2009.

3. J.A. Pihl, T.J. Toops, V.O Strots, S.B. DeLand, G.G. Parker, J.H. Johnson, "Development & Implementation of Experimental Protocol for Steady-State and Transient SCR Kinetics," abstract accepted by 2009 American Institute of Chemical Engineers Annual Meeting, Nashville, TN, to be presented November 12, 2009.

II.B.6 Fundamental Sulfation/Desulfation Studies of Lean NOx Traps, DOE Pre-Competitive Catalyst Research

Todd J. Toops (Primary Contact),
Nathan Ottinger and Josh A. Pihl
Oak Ridge National Laboratory (ORNL)
2360 Cherahala Blvd.
Knoxville, TN 37932

DOE Technology Development Manager:
Ken Howden

Objectives

- Provide a better understanding of the fundamental deactivation mechanisms that result during desulfation of lean-NOx traps (LNT).
- Investigate methods for improving performance and/or durability of LNTs.

Approach

- Conduct pre-competitive LNT research.
- Study deactivation and regeneration mechanisms fundamentally.
- Coordinate efforts with other projects to maximize knowledge findings.
- Investigate materials changes that can improve NOx reduction performance and/or desulfation behavior.

Accomplishments

- Confirmed the improvement in performance and desulfation properties with 5% mol Ca introduction into the BaO storage phase of an LNT catalyst:
  - Improvement is due to a synergistic effect as Ca-only catalyst results in higher desulfation temperatures.
- Determined sulfur stability and desulfation characteristics of individual components of a commercial LNT catalyst.
- Presented results at 12th Cross-Cut Lean Exhaust Emissions Reduction Simulations (CLEERS) Workshop, 21st North American Catalysis Society Meeting, and 2009 DOE Vehicle Technologies Merit Review.
- Prepared paper for submission to Applied Catalysis B.

Future Directions

- Determine the stability of the Ca in the Ba lattice to understand if the observed performance improvements withstand aging.
- Confirm key material impact from Ca insertion and work with modelers at the ORNL Center for Nanophase Materials Science (CNMS) to understand how the improvement is occurring:
  - Use modeling results to identify other dopants and appropriate concentrations to investigate.

✧ ✧ ✧ ✧ ✧

Introduction

Increasingly stringent emissions regulations have necessitated the introduction of new catalytic emissions control devices for vehicles with lean-burn engines. While lean-burn engines are typically more fuel efficient than their stoichiometrically operated counterparts, emissions control catalysts can incur a "fuel penalty." For example, LNT catalysts require periodic operation under fuel-rich conditions, increasing vehicle fuel consumption. The key to deployment of lean-burn engine technology lies in optimizing the aftertreatment system such that emissions regulations are met without substantially reducing fuel economy. This project pursues two paths to achieve this goal for LNT technologies. The first path focuses on establishing a fundamental understanding of the underlying LNT chemistry to improve the accuracy of computer simulations used to design, develop, and control LNT aftertreatment systems. This includes identifying the roles of the catalytic phases of commercial-intent LNTs, elucidating reaction pathways, and determining the fate of sulfur in the catalyst. This effort is closely tied to the CLEERS kinetics activities and serves as guidance for the research undertaken in that project.

The second path, which is more in line with the exploratory role of this project, is aimed at making modifications to the LNT catalyst with the goal of either improving the performance or lowering the required desulfation temperature. This effort is possible due to collaboration with ORNL's CNMS, a DOE-Basic Energy Sciences national user facility. CNMS synthesizes the LNT catalysts to our specification and fully characterizes the samples. We then evaluate the LNTs under typical operating conditions, and work to correlate performance changes to material properties. In taking this multi-pronged approach to studying LNT fundamentals, we are able to make the biggest impact in the most areas.

Approach

Our approach to understanding LNT fundamentals utilizes the unique capabilities and expertise developed in previous years of this project, i.e. the differential microreactor and the barrel-ellipse diffuse reflectance infrared fourier transform spectroscopy (DRIFTS) reactor. The microreactor is operated to minimize heat and mass transfer effects, enabling analysis of the underlying LNT reactions. The microreactor is capable of running a suite of catalyst characterization experiments, including surface area measurements through physisorption and chemisorption, quantification of reaction kinetics, characterization of catalyst performance under realistic operating conditions, and measurement of surface species stability through temperature programmed reactions. It was designed for relatively quick and easy sample loading, so several catalysts can be studied in a short period of time. In addition to the measurement of the reaction kinetics, it is important to understand the catalyst surface chemistry. The DRIFTS reactor enables these measurements at elevated temperatures and using simulated engine exhaust, including H_2O and CO_2. The ability to make these measurements under realistic conditions offers the ability to identify "real-world" reaction intermediates and thus confirm mechanistic models or suggest new reaction pathways.

TABLE 1. Catalyst properties for the initial LNT substitution effort using Ca, K, or La as the dopant.

Catalyst	Pt (wt %)	Ba (mol %)	Dopant (mol %)	Surface Area (m^2/g)
Pt/Al_2O_3	1.5%	-	-	133
Ba-only	1.1%	20%	0%	77
Ca+Ba	1.1%	19%	1%	79
K+Ba	1.1%	19%	1%	78
La+Ba	1.1%	19%	1%	80

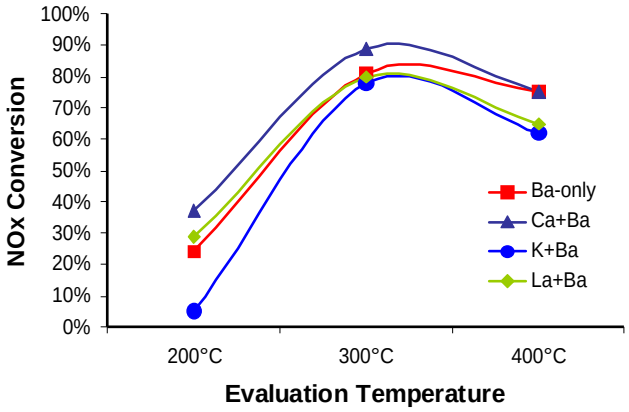

FIGURE 1. NOx performance for the initial LNT substitution effort using Ca, K, or La as the dopant.

Results

Impact of Dopants on a Ba LNT Storage Material

The goal of this portion of the project is to understand how storage material dopants affect LNT performance and desulfation. Last year a series of experiments was presented on LNT-dopant work; however, some concerns arose regarding the sulfation and desulfation efforts, so the experiments were repeated with sulfur on each of the samples. The base LNT catalyst was $Pt/Ba/Al_2O_3$, and through aqueous techniques, 5% mol of the Ba was substituted with Ca, K, or La. The specific final catalyst compositions and Brunauer-Emmett-Teller surface areas are listed in Table 1. The Ca-doped material showed a significant increase in performance at 200 and 300°C, while also maintaining high conversion at 400°C as shown in Figure 1. Conversely, both the K- and La-doped LNT catalysts showed moderate decreases in performance at 200 and 400°C, while matching the Ba-only performance at 300°C. Following the performance measurements, the samples were then sulfated to 5.5 mg S/g_{cat} and desulfated to 1,000°C. Figure 2a shows that the LNTs all had similar bimodal desulfation behavior, but there are significant differences in the stability of the sulfur released for the different LNTs. Separating the sulfur removed into low temperature ($T_{release} < 650$°C) and high temperature ($T_{release} > 650$°C), it is clear that the Ca+Ba LNT contains the highest quantity of low-temperature sulfur, as shown in Figure 2b. Conversely, the K+Ba sample contains the highest quantity of high-temperature sites. These results confirm the general trends observed last year. The lower stability of sulfur on the Ca+Ba sample could translate to a reduced fuel penalty and better catalyst durability due to the lower temperatures and/or shorter times required for desulfation.

As a follow up to these promising results, a series of Ca+Ba LNTs was prepared and studied: 5% Ca+Ba, 10% Ca+Ba, 20% Ca+Ba and Ca-only. The specific final catalyst compositions are listed in Table 2. Figure 3 shows that the performance for the Ca-based samples continues to show moderate increases in performance compared to the Ba-only sample; most interesting of these improvements is the ~20% increase in NOx conversion at 400°C for the Ca-only sample. An improvement in high temperature performance typically indicates that the storage sites are more stable on this catalyst, and, as shown in Figure 4, the sulfation/desulfation experiments confirm this conclusion. The Ca-only sample has the highest amount of sulfur released in the high-temperature region. Based purely on the Ca-only and Ba-only results, it would be expected

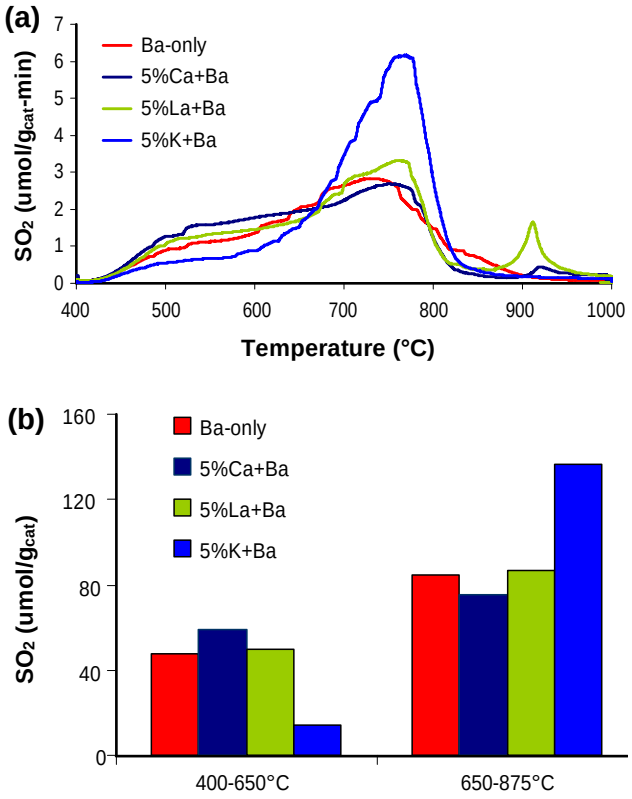

FIGURE 2. (a) Desulfation profile following sulfation at 400°C for the initial LNT substitution effort using Ca, K, or La as the dopant. (b) Integration of the desulfation profile for the given temperature window.

TABLE 2. Catalyst properties for the LNT substitution effort using varying levels of Ca as the dopant.

NSR Catalyst	Pt (wt%)	Ba (mol%)	Ca (mol%)
Pt/Al_2O_3	1.5%	-	-
Ba-only	1.1%	20%	0%
5%Ca+Ba	1.1%	19%	1%
10%Ca+Ba	1.1%	18%	2%
20%Ca+Ba	1.1%	16%	4%
Ca-only	1.1%	0%	20%

that the 5% Ca+Ba sample would have slightly higher sulfur stability than the Ba-only sample; yet, the 5% Ca+Ba continues to have the most low-temperature sulfur storage and best low-temperature performance. These contrasting results illustrate that a synergistic effect of Ca+Ba occurs in these samples. Materials characterization to understand physical properties that lead to the change in chemical behavior is ongoing.

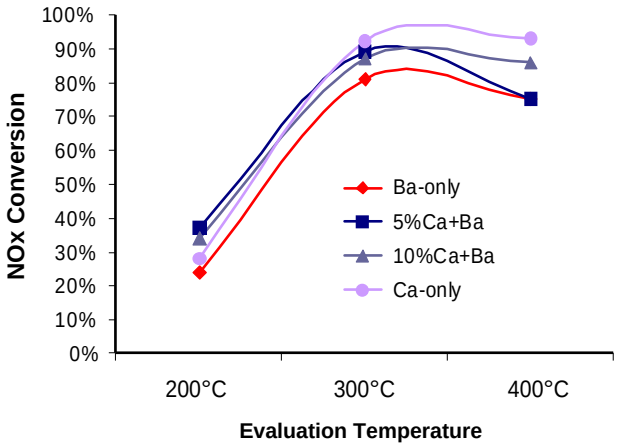

FIGURE 3. NOx performance for the LNT substitution effort using varying levels of Ca as the dopant.

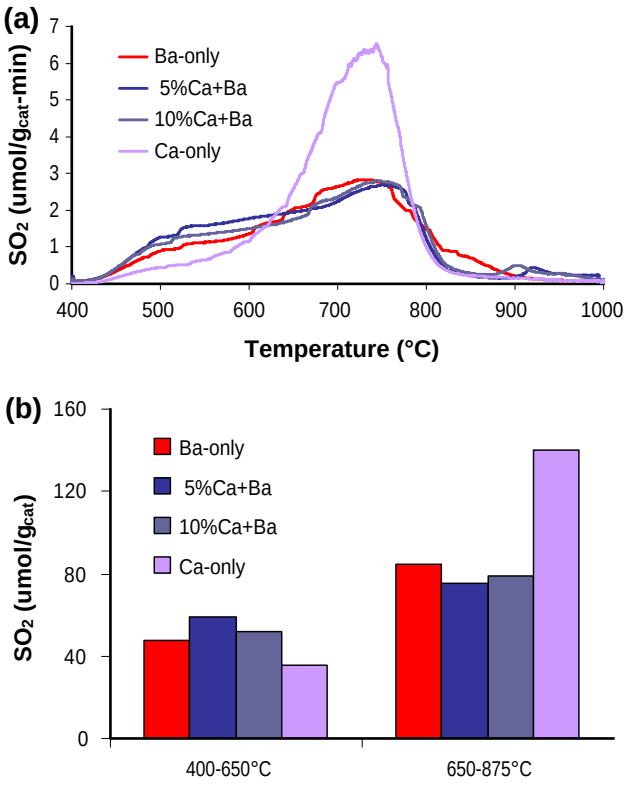

FIGURE 4. (a) Desulfation profile following sulfation at 400°C for the LNT substitution effort using varying levels of Ca as the dopant. (b) Integration of the desulfation profile for the given temperature window.

Sulfation/Desulfation Behavior of LNT Components

Significant effort was also put forth this year to understand the functionality of the individual components that are found in a commercially available LNT. Using both the micro-reactor and DRIFTS instrument, the NOx and SOx stability was studied on the following combinations of components found in a commercially-available Umicore LNT (the CLEERS reference catalyst): Pt/Al_2O_3, $Pt/Ba/Al_2O_3$, $Pt/MgAl_2O_4$, Pt/CeO_2-ZrO_2, and $Pt/Ba/CeO_2$-ZrO_2. The desulfation profiles, following a 400°C sulfation procedure, are shown in Figure 5. Interestingly, Pt/Al_2O_3 which is generally thought of having the least stable sulfates, has significant low-temperature and high-temperature sulfur release–it is still releasing sulfur at 750°C. This broad range of sulfur release illustrates the inherent heterogeneity that exists on the surface of the γ-Al_2O_3 support. The lowest temperature of peak sulfur release occurs on Pt/CeO_2-ZrO_2, from which all of the sulfur is released below 650°C. Through detailed materials characterization it has been shown that both of these components are used to support the Ba-storage phase in this Umicore LNT catalyst [1-2]. In comparing the behavior of these more complex Pt/Ba/support systems (see Figure 5), it is very interesting to see that the use of CeO_2-ZrO_2 as a support lowers the de-sulfation temperature of Ba by 100°C compared to using the Al_2O_3 support. It is uncertain of the exact nature of this benefit, but it is clear there is a significant support interaction occurring that in turn affects the sulfur stability. DRIFTS NOx storage and sulfation experiments confirm the results of the micro-reactor work.

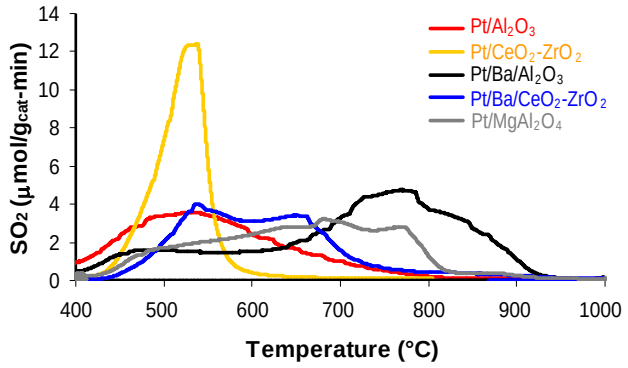

FIGURE 5. Pt/Al_2O_3, Pt/Ceria-Zirconia, $Pt/Ba/Al_2O_3$, Pt/Ba/Ceria-Zirconia, and $Pt/MgAl_2O_4$ desulfation profiles following sulfation at 400°C.

Conclusions

- Introducing Ca benefits both the NOx performance and desulfation behavior of a model Ba-based LNT, and of the four concentrations studied, a 5 mol% Ca substitution showed the best performance and desulfation benefit.
- Through analysis of individual components in the CLEERS LNT reference catalyst, the relative stability of sulfur was found to increase in the following order:
  - Pt/Al_2O_3<Pt/CeO_2-ZrO_2<$Pt/Ba/CeO_2$-ZrO_2< $Pt/MgAl_2O_4$<$Pt/Ba/Al_2O_3$

References

1. J.-S. Choi, C.S. Daw, T.J. Toops, J.A. Pihl, W.P. Partridge, C.E.A. Finney, V. Prikhodko, M.J. Lance, N.A. Ottinger, and V.K. Chakravarthy, 2009 DOE Vehicle Technologies Program Annual Merit Review, Arlington, Virginia, May 18–22, 2009.

2. J.-S. Choi, W.P. Partridge, N.A. Ottinger, J.A. Pihl, T.J. Toops, C. Stuart Daw, 21st North American Catalysis Society Meeting, San Francisco, CA, June 7–12, 2009.

FY 2009 Publications/Presentations

1. J.-S. Choi, W.P. Partridge, N.A. Ottinger, J.A. Pihl, T.J. Toops, M. Lance, C. Finney, C. Stuart Daw, "Stepwise Desulfation and its Impact on LNT Performance - Study of CLEERS Reference Catalyst", 12th Cross-Cut Lean Exhaust Emissions Reduction Simulations (CLEERS) Workshop, Dearborn, MI, April 28–30, 2009.

2. J.-S. Choi, C.S. Daw, T.J. Toops, J.A. Pihl, W.P. Partridge, C.E.A. Finney, V. Prikhodko, M.J. Lance, N.A. Ottinger, and V.K. Chakravarthy, "CLEERS coordination and development of catalyst process kinetic data", presented at the 2009 DOE Vehicle Technologies Program Annual Merit Review, Arlington, Virginia, May 18–22, 2009.

3. J.-S. Choi, W.P. Partridge, N.A. Ottinger, J.A. Pihl, T.J. Toops, C. Stuart Daw, "Impact of Stepwise Desulfation on the Performance of a Ba-Based Commercial Lean NOx Trap Catalyst", 21st North American Catalysis Society Meeting, San Francisco, CA, June 7–12, 2009.

4. T.J. Toops, C.N. Liang, J.A. Pihl, N.A. Ottinger, "Impact of Dopants in Ba-Based NOx Storage Reduction (NSR) Catalysts on Sulfation, Desulfation, and Performance", 21st North American Catalysis Society Meeting, San Francisco, CA, June 7–12, 2009.

II.B.7 NO_X Control and Measurement Technology for Heavy-Duty Diesel Engines

Bill Partridge[1] (Primary Contact), Neal Currier[2], Ray Shute[2], Jae-Soon Choi[1], Jim Parks[1], Mike Cunningham[2], Alex Yezerets[2], Mike Ruth[2]
[1]Oak Ridge National Laboratory (ORNL)
[2]Cummins Inc.
2360 Cherahala Blvd.
Knoxville, TN 37932

DOE Technology Development Manager:
Ken Howden

Objectives

- Improve diesel engine-catalyst system efficiency through better combustion uniformity, engine calibrations and catalyst control.
- Work with industrial partner to develop full-scale engine-catalyst systems to meet efficiency and emissions goals.

Accomplishments

- Licensed Cooperative Research and Development Agreement (CRADA)-developed Fuel-in-Oil tool for rapid, on-engine measurements of oil dilution by fuel to Da Vinci Emissions Services, Ltd.
- Developed instrument for detecting cylinder-to-cylinder combustion variations within a single engine cycle through direct, on-engine measurements in undiluted exhaust.
- Applied combustion variation diagnostic to engine measurements at Cummins engine plant in Columbus, IN.
- Characterized nature of how sulfur degrades water-gas shift (WGS) reaction during lean-NO_X trap (LNT) regeneration, and the relationship between sulfur degradation of WGS, NO_X storage and reduction (NSR) and oxygen storage capacity (OSC) catalyst functions; this detailed information enables advanced catalyst control strategies to improve system cost, fuel economy and durability.
- One archival publication.
- Eight presentations.
- Two patents submitted.
- One CRADA-developed technology licensed.

Future Directions

- Quantify engine combustion non-uniformities and develop mitigation strategies.
- Enable development of self-diagnosing smart catalyst systems through:
  - Detailed characterization of the spatiotemporal relationship between natural and indicator chemical functions and catalyst properties throughout the catalyst operation and ageing.
  - Develop methods for in situ, on-engine-system assessment of catalyst state.

Introduction

A combination of improved technologies for engine and aftertreatment control of NO_X and particulate emissions are required to efficiently meet 2013 emission regulations. These include advanced combustion and associated engine hardware and controls, improved catalyst systems, and overall system management improvements. There are specific needs in terms of reducing cylinder-to-cylinder and cycle-to-cycle combustion variations, and continuous catalyst-state monitoring. For instance, combustion variations mandate system-calibration tradeoffs which move operation away from optimum efficiency points. Combustion variations are amplified at high exhaust gas recirculation (EGR) conditions which are expected in advanced engine systems. Advanced efficiency engine systems require understanding and reducing combustion variations. Conventional catalyst-control strategies, some of which are based on degraded end-of-life catalyst performance, execute desulfation events too frequently and for too long. Improved efficiency, durability and cost can be achieved through advanced control methodologies based on continuous catalyst-state monitoring; these advanced control methods reduce the fuel penalty associated with catalyst maintenance (e.g., desulfation, regeneration) and extend the lifetime of the catalyst by triggering maintenance events only when and for as long as required as indicated by real-time catalyst-state monitoring, as opposed to being preprogrammed. Continuous catalyst-state monitoring also provides a solution for 2013 regulations which require identification of the specific component function (e.g., oxidation) responsible in the event that a component's (e.g., NO_X catalyst) performance falls outside the regulatory window. These engine, combustion and catalysis advances require development and application

of enhanced diagnostic tools to realize these technology improvements.

Approach

Developing and applying minimally invasive advanced diagnostic tools to resolve spatial and temporal variations within operating engines and catalysts has been central to the historical successes of this CRADA partnership, and continues to be a key element of the project approach. These include small capillary and optical-fiber based technologies which are able to resolve spatiotemporal variations without changing the measurement environment or requiring significant hardware modifications for applications. Integral to this work are coating technologies to create localized fiber and capillary transducers to detect variations; e.g., species, temperature, pH, etc. The approach relies heavily on optical and mass-spectrometry, but also includes other techniques such as electrical impedance spectroscopy. Diagnostics are developed and demonstrated on bench reactors and engine systems (as appropriate) at ORNL prior to field application at Cummins. In some cases discrete-sensor technology is a stepping stone and may be further developed and integrated in system components; e.g., to create self-diagnosing smart catalyst systems.

Diagnostics are applied at ORNL and Cummins to study the nature and origins of performance variations. In combustion studies, this may be manifested in cylinder-to-cylinder CO_2 variations due to non-uniform fueling, air and/or EGR charge, fuel spray, component tolerance stacking, or other variations. Detailed measurements can be used to identify and evaluate corrective measures; e.g., hardware and control changes. In catalyst studies, this may be spatial and temporal variations unique to each catalyst function (e.g., NSR, OSC, WGS) during operation and how these vary with ageing (e.g., sulfation). This detailed information is applied to understand how catalysts function and degrade, develop device and system models, and develop advanced control strategies.

Results

Combustion Uniformity

Cylinder-to-cylinder H_2O variations within a single engine cycle were measured in the exhaust manifold of a turbocharged diesel engine. This was based on development and application of a diagnostic using near-infra-red (NIR) spectroscopy and a unique rapid-scanning NIR optical-fiber-ring laser. The Rapid Scanning NIR (RSNIR) laser is a simpler version of the Fourier Domain Mode Locked (FDML) laser [1], that allows the NIR spectrum to be scanned from 1,330 to 1,380 nm in 0.3 ms (3kHz); for faster applications the FDML source enables ca. 80 kHz spectral scanning. These measurements provide insights into high-frequency engine variations in much greater detail than previously possible. The measurements are being used to study the origins of these variations. This work demonstrates the capability of the RSNIR instrument to resolve fast exhaust variations in engine performance; this same temporal resolution will be possible for FSNIR instruments in other spectral ranges to detect other exhaust species (e.g., CO_2). Development and applications of these instruments will enable greater engine combustion uniformity and in turn engine control closer to optimum performance to achieve greater fuel economy and lower emissions.

Catalyst Chemistry Measurements and Insights

The detailed nature of sulfation-related degradation on LNT-catalyst WGS reaction was investigated. Exhaust oxygen readily displaces S (sulfur) from Pt (platinum) sites to the surrounding catalyst, and mobile surface S can migrate back to Pt sites during extended oxygen-free operation. However, on realistic LNT lean-rich cycling timescales (e.g., 60-s lean, 5-s rich), there is not sufficient time for mobile surface S to poison Pt sites. Thus, exhaust oxygen mitigates sulfur degradation of WGS by preventing S contamination of platinum sites. Nevertheless, a drastic WGS degradation occurs with sulfation; thus there appears to be some other route primarily responsible for WGS sulfur degradation. DRIFTS measurements indicate that degradation does not appear to be due to S impacting the Pt electronic structure and in turn Pt-CO affinity; at least not at the 325°C analysis temperature. Microreactor analysis of sulfated-model-catalyst sample sections, shows that WGS degradation is nonlinear with S loading, and that degradation appears to approach a non-zero asymptote at high S loadings. The metal-support (and/or NO_X storage component) interface appears to be uniquely relevant to WGS activity, and thus WGS degradation is most sensitive to S loading at this interface. However, it is currently unclear whether initial sulfation occurs preferentially at this interface, or if sulfation is more uniformly distributed across the catalyst surface and that WGS simply uniquely sensitive to sulfation of the metal-support interface.

Separate work has shown that under lean conditions NO_X is initially stored preferentially around the perimeter of the Pt sites, while S is stored relatively uniformly across the catalyst and not correlated with the Pt site distribution [2,3]. However during rich conditions it appears that gas-phase S (not mobile surface S) forms an S layer over the Pt sites, and this S is subsequently oxidized and stored in close proximity to the Pt-site perimeter when lean conditions resume [2]. This and our WGS experimental results suggest that higher-concentration sulfur islands grow

around the catalyst metal sites. The general picture is randomly distributed S throughout the catalyst field, and higher density S islands around the Pt; these islands may be caused by S oxidation during lean conditions (and subsequent Ba sulfate formation likely near the Pt perimeter), and formation and oxidation of Pt-S layers during lean-rich cycling. Such a model is similar to the conceptual model of WGS degradation from carbon formation proposed by Goguet et al. [4]. WGS is unlikely to be sensitive to S deposition in the washcoat field remote to Pt, which is consistent with our measurement of a non-zero WGS activity asymptote at high S loading. Nevertheless, the high sensitivity of WGS to initial sulfation, indicates this earliest S is changing the metal-support interface. Because of this, WGS is a good indicator of the actual S deposition front. In contrast to the WGS performance, NSR is insensitive to the initial S deposition; i.e., even with sulfation NO is oxidized at the Pt sites and is able to access S-free Ba (barium) sites in the washcoat field beyond the sulfated metal-support interface via spillover and/or desorption into the gas phase and readsorption.

Thus, the nature and detailed routes for S degradation of the LNT catalyst's NSR and WGS functions are different. Figure 1 shows a global conceptual model for S degradation of NSR [5], OSC, and WGS, and emphasizes how each catalyst function has differing spatial distribution with progressing sulfation. Clarifying the nature of LNT WGS sulfation as provided by this work enables better catalyst system design and control for improved emissions and efficiency.

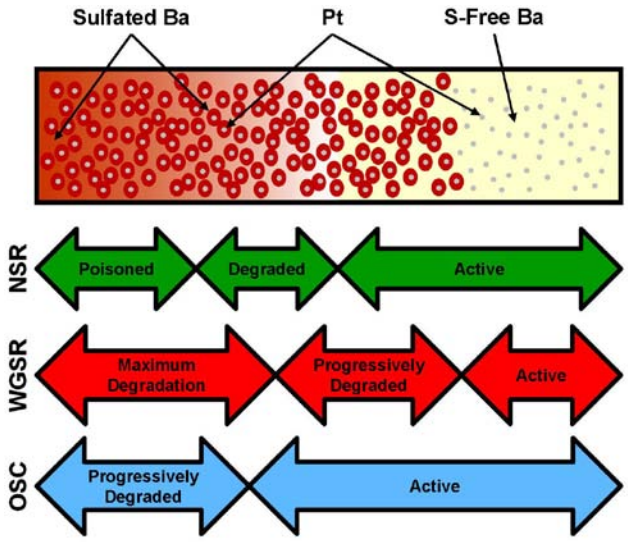

FIGURE 1. Global conceptual model showing distributed sulfation of LNT functions NSR, WGS and OSC. WGS indicates the leading edge of LNT sulfation, and the WGS sulfation front leads the NSR and OSC sulfation fronts. The sulfur impact is different for each LNT chemical function.

WGS is integral to Cummins' patented on-board diagnostic strategy for catalyst-state assessment and control; e.g., for determining when and for how long to desulfate. In WGS, exhaust CO and H_2O react over the catalyst to create H_2 and CO_2. Standard universal exhaust gas oxygen (UEGO) sensors have a cross sensitivity to H_2 in addition to their primary target O_2 response. By understanding the H_2 cross sensitivity, the catalyst WGS activity can be deduced from the UEGO signals. Furthermore, by understanding how the various catalyst functions (NSR, OSC, WGS, etc.) vary with operation and ageing (e.g., sulfation), the catalyst state can be continuously monitored via the UEGO sensor variations. In this way, advanced catalyst control methodologies can be developed to achieve improved fuel economy, cost and durability.

Conclusions

- Licensing of CRADA-developed oil-dilution tool to Da Vinci Emissions Services, Ltd. will further broaden benefit of the CRADA to industry.
- RSNIR diagnostic resolves cylinder-specific combustion variations and can be used to develop more uniform engine systems for improved efficiency and emissions.
- LNT WGS function is uniquely sensitive to sulfation, and provides a very sensitive indication of the leading edge of catalyst sulfation.
- LNT WGS sulfation front leads the NSR sulfation front, and can be used along with UEGO H_2 cross sensitivity to develop advanced control strategies for improved fuel economy, cost and durability.

References

1. Kranendonk, Parks, Prikhodko & Partridge, Society of Automotive Engineers paper 2009-01-0239, 2009.

2. Fridell, Persson, Olsson, Westerberg, Amberntsson & Skoglundh, Topics in Catal., V16/17, 133, 2001.

3. Sakamoto, Okumura, Kizaki, Matsunaga, Takahashi & Shinjoh, J. of Catal. V238, 361, 2006.

4. Goguet, Meunier, Tibiletti, Breen & Burch, J. Phys. Chem. B, V108, 20240, 2004.

5. Choi, Partridge, Daw, Appl. Catal. B: Environmental, V77, 145, 2007.

FY 2009 Publications/Presentations

Papers

1. William P. Partridge and Jae Soon Choi, "NH_3 formation and utilization in regeneration of $Pt/Ba/Al_2O_3$ NO_X storage-reduction catalyst with H_2," Applied Catalysis B: Environmental **91** (2009) 144-151.

Presentations

1. Jim Parks, Bill Partridge and Vitaly Prikhodko "An Optical Backscatter Sensor for Particulate Matter Measurement," presented at the SAE 2009 World Conference in Detroit, MI on April 20–23, 2009.

2. Laura A. Kranendonk, James E. Parks II, Vitaly Prikhodko and William Partridge "High Speed H_2O Concentration Measurements Using Absorption Spectroscopy to Monitor Exhaust Gas," presented at the SAE 2009 World Conference in Detroit, MI on April 20–23, 2009.

3. Bill Partridge, Jae-Soon Choi, Josh Pihl, Todd Toops, Nathan Ottinger, Jim Parks, Alex Yezerets , Neal Currier, "Understanding the Distributed Intra-Catalyst Impact of Sulfation on Water Gas Shift in a Lean NO_X Trap Catalyst," 12th DOE Crosscut Workshop on Lean Emissions Reduction Simulation, University of Michigan, Dearborn, Michigan, April 30th, 2009.

4. Jae-Soon Choi, Bill Partridge, Nathan Ottinger, Josh Pihl, Todd Toops, Michael Lance, Charles Finney, Stuart Daw, "Stepwise Desulfation & its Impact on LNT Performance; Study of CLEERS Reference Catalyst," 12th DOE Crosscut Workshop on Lean Emissions Reduction Simulation, University of Michigan, Dearborn, Michigan, April 30th, 2009.

5. W.P. Partridge, J.-S. Choi, J.E. Parks, T.J. Toops, J.A. Pihl, N.A. Ottinger, N. Currier, A. Yezerets, M. Cunningham, M. Ruth, "Cummins/ORNL FEERC CRADA: NO_X Control & Measurement Technology for Heavy Duty Diesel Engines," 2009 DOE Vehicle Technologies Program Annual Merit Review, Arlington, Virginia, May 21, 2009.

6. Jae Soon Choi, Bill Partridge, Nathan Ottinger, Josh Pihl, Todd Toops, Stuart Daw, "Impact of Stepwise Desulfation on the Performance of a Ba-Based Commercial Lean NO_X Trap Catalyst," North American Catalysis Society, 21st North American Meeting, San Francisco, California, June 9, 2009.

7. Bill Partridge, Jae Soon Choi, Jim Parks, Josh Pihl, Todd Toops, Nathan Ottinger, Alex Yezerets, Neal Currier, "Elucidating Lean NO_X Trap Catalyst Regeneration & Degradation Chemistry: Insights from Intra-Catalyst, Spatiotemporally Resolved Measurements," Keynote Lecture, Catalysis for Environmental Protection topical area, North American Catalysis Society, 21st North American Meeting, San Francisco, California, June 9, 2009. ***Invited***

8. Bill Partridge, Jae-Soon Choi, Jim Parks, Sam Lewis, Neal Currier, Mike Ruth, Robert Smith, George Muntean, John Stang, Alex Yezerets, "Measuring Transient Chemistry Distributions Inside Automotive Catalyst & Engine Systems," General Electric Global Research Center's Symposium on Emissions and After Treatment, Niskayuna, New York, September 17, 2009. ***Invited***

Special Recognitions & Awards/Patents Issued

Awards

The CRADA-developed SpaciMS received the 2009 National Award for Excellence in Technology Transfer presented annually by the Federal Laboratory Consortium for Technology Transfer (FLC). The award recognizes laboratory employees who have accomplished outstanding work in the process of transferring a technology developed by a federal laboratory to the commercial marketplace.

Licensed Technologies

The CRADA-developed Fuel-in-Oil Diagnostic (US Appl. No.: 12/137,964, "Laser Induced fluorescence fiber optic probe measurement of oil dilution by fuel," ORNL Ref. No.: 1940.0, Filed 6/13/2008) was licensed by UT-Battelle (ORNL Contractor) to Da Vinci Emissions Services, Ltd. (www.davinci-limited.com) on 10-13-2009.

Patents Submitted

1. US Appl. No.: 12/326,223; L.C. Maxey, W.P. Partridge, S.A. Lewis, J.E. Parks "Optically Stimulated Differential Impedance Spectroscopy," ORNL Ref. No.: 1861.0, Filed 12/2/2008.

2. US Appl. No.: 12491781; J.E. Parks, W.P. Partridge "Optical Backscatter Probe for Sensing Particulate in a Combustion Gas Stream," ORNL Ref. No.: 2130.0, Filed June 25, 2009.

II.B.8 Efficient Emissions Control for Multi-Mode Lean DI Engines

James Parks (Primary Contact), Kukwon Cho, Vitaly Prikhodko
Oak Ridge National Laboratory (ORNL)
2360 Cherahala Boulevard
Knoxville, TN 37932

DOE Technology Development Manager:
Ken Howden

Objectives

- Assess the relative merits of meeting emission regulations via catalytic aftertreatment or advanced combustion for diesel engines capable of operating in multiple combustion modes ("multi-mode" engines).
- Determine the fuel efficiency of combinations of catalytic aftertreatment and advanced combustion modes.
- Characterize exhaust chemistry from advanced combustion and the resulting evolution of chemistry in catalysts for emissions control to improve the understanding of advanced engine and aftertreatment systems.

Accomplishments

- Demonstrated reducing the fuel penalty from 4.2% to 3.1% for regeneration of a diesel particulate filter (DPF) by incorporating advanced combustion modes with lower particulate emissions in a multi-mode strategy.
- Characterized a multi-walled carbon nanotube hydrocarbon selective catalytic reduction (HC-SCR) catalyst for lean NOx control (with University of Kentucky).

Future Directions

- Investigate synergies between SCR and advanced combustion (high efficiency clean combustion, HECC).
- Study the potential of on-board diagnostics for reducing the fuel penalty of DPFs.

Introduction

New combustion regimes are being investigated as a means to increase the efficiency of, and to reduce the emissions from, diesel engines. The reduction of emissions during combustion is beneficial to the fuel efficiency of the system as a whole (engine plus emissions control system or "aftertreatment"). Specifically, lower engine-out NOx emissions can remove some burden from post-combustion emissions controls, and can thereby reduce the fuel penalty associated with NOx reduction. Although new combustion techniques have been developed that offer advantages for both engine fuel efficiency and emissions, often the techniques are not attainable over the entire range of load and speed required for market acceptance. Thus, engines designed to implement the new combustion techniques often operate in a "multi-mode" fashion where, at certain loads, the engine is operated with advanced combustion techniques and, at other loads, the engine is operated with more traditional diesel combustion. While modern control systems enable switching between the multiple modes of operation, the optimization of the system for fuel efficiency and emissions becomes more complex. One particular challenge is optimizing the size, cost, and complexity of the emissions control system. This project is aimed at understanding the complex issues of efficiency and emissions management for multi-mode engines with advanced emission control systems. Characterization of combustion exhaust chemistry and catalytic control are conducted to assist industry in the design of multi-mode engine and emission control systems.

Approach

This research has been conducted at ORNL in conjunction with ongoing engine studies. Two related projects at ORNL ("Measurement and Characterization of LNTs," and "Exploring Advanced Combustion Regimes for Efficiency and Emissions" in the Advanced Combustion Engines Program) are being leveraged with this activity. Experiments were performed on a Mercedes-Benz 4-cylinder, 1.7-liter diesel engine that has been significantly upgraded with advanced technologies (variable geometry turbocharger, high throughput exhaust gas recirculation [EGR], multi-injection control, etc.) to enable advanced combustion studies. The engine is operated on an engine dynamometer in ORNL's facility. A second more modern General Motors 1.9-liter 4-cylinder diesel engine has been installed at the same location for experiments to be conducted next year. All experiments were conducted at steady-state load and speed conditions which were chosen and weighted for

estimating Federal Test Procedure (FTP) drive cycle emissions based on industry guidance. Low-temperature combustion (LTC) is a relatively new combustion mode that enables an order of magnitude reduction in NOx and particulate matter (PM) emissions through high levels of EGR. HECC is a new evolution of LTC that achieves extremely low NOx and PM emissions while maintaining low brake specific fuel consumption (BSFC); HECC has comparable fuel efficiency to traditional modes [1]. HECC achieves good efficiency and emissions by coupling high levels of EGR with advanced injection timing and higher fuel injection pressures. Although NOx and PM emissions are reduced in HECC, carbon monoxide (CO) and hydrocarbon emissions increase. Formaldehyde emissions increase as well; formaldehyde is classified as a Mobile Source Air Toxic by the Environmental Protection Agency. Thus, while the emissions control system does not need to reduce NOx and PM significantly during HECC, higher CO and hydrocarbon emission control is needed. Experiments were conducted to understand the synergies between HECC combustion and advanced aftertreatment (specifically a catalyzed DPF) and focused on comparing fuel efficiencies of the combined engine and emissions control system for conventional combustion (manufacturer set level of EGR) and HECC. The lean-NOx trap (LNT) used for the study was provided by a member of the Manufacturers of Emission Control Association and has been used in other studies at ORNL.

Results

The light-duty diesel engine was operated with conventional and HECC combustion modes. Conventional combustion is simply the manufacturer or "stock" type of combustion. HECC combustion is attained by advancing fuel injection timing, increasing EGR rate, and increasing fuel injection pressure. A dramatic drop in PM and NOx emissions is achieved with HECC vs. conventional combustion. In this study, the engine was operated with a diesel oxidation catalyst (DOC), DPF, and a LNT catalyst, and the focus of the project was the DPF catalyst. Extra fuel is required to heat the DPF catalyst to temperatures of approximately 600ºC for the purpose of oxidizing (burning) the PM (or soot) that has accumulated on the DPF during engine operation; this operation is known as "desoot". Since desoot entails a fuel penalty due to the extra fuel required, the system fuel efficiency is compromised. The intent of this study was to understand the benefits of lower PM from HECC on reducing the fuel penalty for desoot operations.

The frequency of the desoot operation greatly affects the fuel penalty. Furthermore, the frequency of desoot operation is primarily a function of the amount of PM trapped by the DPF. The amount of PM on the DPF is monitored via a backpressure sensor in the exhaust system. As the amount of PM on the DPF increases, the backpressure from the clogged DPF rises. Initiation of the DPF desoot process is controlled based on the backpressure. Figure 1 shows the rise in backpressure from the DPF as a function of time for conventional and HECC combustion; the engine load and speed are 2.0 bar and 1,500 rpm. The larger amount of PM emitted from conventional combustion causes the backpressure to rise at a faster rate in comparison to the HECC case. There are some other interesting features of the data as well related to the LNT catalyst which is also part of the system. Periodic spikes occur in the data where LNT regeneration events were conducted. LNT regeneration requires rich exhaust conditions, and these conditions are obtained by throttling the engine and adding extra fuel in the engine cylinders. Such operation typically increases PM emissions and reduces exhaust flow rate. Since conventional combustion has higher NOx emissions than HECC, the LNT regeneration must occur more frequently, and as expected the spikes from LNT regeneration in the conventional data are more frequent than for the HECC data. Furthermore, more frequent LNT regeneration events lead to higher engine-out emissions which, in addition to the base higher PM emissions, further increases the PM emissions from conventional combustion.

Figure 2 shows the backpressure rise rates determined from data collected as shown in Figure 1 for both conventional and HECC modes at various engine load and speed combinations. The checkered pattern indicates data without LNT regeneration. As apparent from the solid bar data which includes LNT regeneration, the LNT regeneration events add significant PM to the DPF. Thus, the benefits of HECC with respect to PM emissions are two-fold: direct lower engine-out PM emissions from HECC and indirect

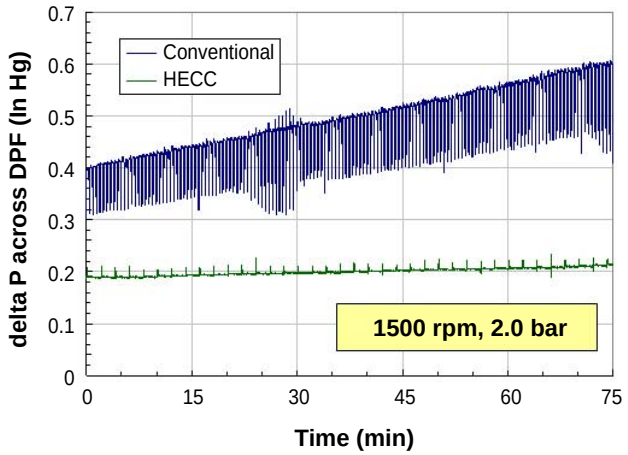

FIGURE 1. Rise in backpressure across the DPF due to varying PM emission rates from conventional (manufacturer) and HECC combustion.

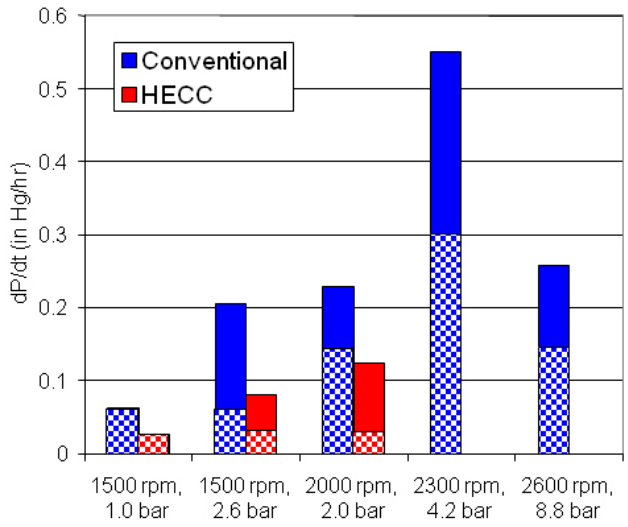

FIGURE 2. Backpressure rise rate across the DPF from conventional and HECC combustion for various speed and load conditions. The checkered pattern indicates data without LNT regeneration.

lower engine-out emissions from HECC due to lower NOx emissions from HECC which result in less frequent LNT regeneration. At the light to medium loads where HECC is achieved, DPF backpressure rise rates are reduced by 40-60%. The highest DPF backpressure rise rate is observed for the 2,300 rpm and 4.2 bar point associated with moderate acceleration. At the highest load point of 2,600 rpm and 8.8 bar, temperatures in the DPF increased to a point where PM oxidation began to occur thus reducing the overall backpressure rise rate for this steady-state experiment.

A compilation of the data from Figure 2 was formed based on weightings for the various load and speed points to simulate the effect of PM emissions on system fuel efficiency over FTP-type driving conditions. In this calculation, lower weightings are given to the higher loads which are not experienced as frequently. The results from the calculation are shown in Figure 3. Here the compilation which includes both conventional and HECC combustion modes is called "multi-mode", and the compilation of all conventional operation is called "conventional". The multi-mode case gives an overall lower backpressure rise rate due to the lower PM emissions from HECC. This leads to less frequent desoot operations and lower fuel penalty for multi-mode as compared with conventional. Finally, the combined fuel use of the engine and aftertreatment system is summarized in the plot of BSFC. Although fuel use during HECC operation is slightly higher than conventional fuel consumption by the engine, the lower fuel penalty for DPF regeneration from HECC gives lower overall fuel consumption for the multimode case as compared with conventional combustion.

Conclusions

- Advanced combustion modes such as HECC have lower PM emissions and can greatly reduce the frequency of desoot operations of the DPF which leads to lower fuel consumption from the desoot process.
- The lower NOx emissions from HECC also help to reduce PM emissions and desoot fuel penalty for the case when LNT aftertreatment is used since the frequency of the PM-rich LNT regeneration is also reduced by HECC.
- On a system fuel consumption basis, the lower fuel penalty from desoot operation with HECC better enables HECC to compete with conventional combustion on a system fuel consumption basis.

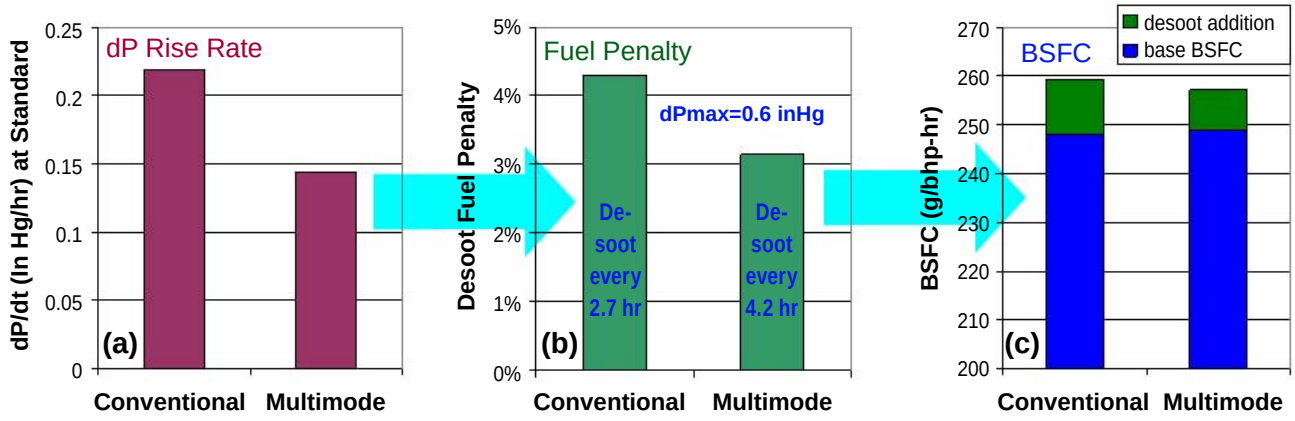

FIGURE 3. Backpressure rise rate (a) determines the fuel penalty (b) for DPF regeneration based on the required desoot frequency (shown in text), and the fuel penalty affects the overall engine system fuel efficiency (c) expressed as BSFC. The multi-mode case includes both conventional and HECC combustion modes and gives a lower backpressure rise rate which leads to a lower fuel penalty and overall lower system BSFC as compared with conventional combustion only.

References

1. C. Scott Sluder and Robert M. Wagner, "An Estimate of Diesel High-Efficiency Clean Combustion Impacts on FTP-75 Aftertreatment Requirements", *SAE Technical Paper Series* 2006-01-3311 (2006).

FY 2009 Publications/Presentations

1. Vitaly Y. Prikhodko and James E. Parks, "Implications of Low Particulate Matter Emissions on System Fuel Efficiency for High Efficiency Clean Combustion", *SAE Technical Paper Series* 2009-01-2709 (2009) [*accepted for publication in November 2009*].

2. Vitaly Prikhodko and Jim Parks, "Impact of Lower PM from Multimode Operation on Fuel Penalty from DPF Regeneration", *2009 Directions in Engine-Efficiency and Emissions Research Conference (DEER)*, August 3–6, 2009 (2009).

3. Jim Parks, Vitaly Prikhodko, John Storey, Teresa Barone, Sam Lewis, Mike Kass, and Shean Huff, "Emissions from Premixed Charge Compression Ignition (PCCI) Combustion and Affect on Emission Control Devices", *21st North American Meeting of the North American Catalysis Society 2009 conference*, June 7–12, 2009 (2009).

4. Jim Parks, Shean Huff, Mike Kass, Brian West, Todd Toops, and Vitaly Prikhodko, "Lean NOx Trap Catalysis: Exhaust Chemistry Related to Advanced Diesel Engines", *SAE Light-Duty Diesel Emissions Control Symposium*, Ypsilanti, MI, November 3–5, 2008.

5. E. Santillan-Jimenez, M. Crocker, J.E. Parks II, C. Salinas Martinez de Lecea, "Carbon nanotube supported metal catalysts for NOx reduction using hydrocarbon reductants", 5th International Conference on Environmental Catalysis, Belfast, Ireland, August 31 – September 3, 2008.

Special Recognitions & Awards/Patents Issued

1. Patent Issued: Graves, Ronald L., West, Brian H., Huff, Shean P., Parks, II, James E., "Advanced engine management of individual cylinders for control of exhaust species", US Patent 7,469,693 (December 30, 2008).

II.B.9 Cross-Cut Lean Exhaust Emission Reduction Simulation (CLEERS): Administrative Support

Stuart Daw
Oak Ridge National Laboratory (ORNL)
National Transportation Research Center
2360 Cherahala Boulevard
Knoxville, TN 37932-6472

DOE Technology Development Manager:
Ken Howden

Key ORNL personnel involved in this activity are Stuart Daw, Vitaly Prikhodko, and Charles Finney.

Objectives

Coordinate the CLEERS activity for the Diesel Cross-Cut Team to accomplish the following:

- Promote development of improved computational tools for simulating realistic full-system performance of lean-burn engines and associated emissions controls.
- Promote development of performance models for emissions control components such as exhaust manifolds, catalytic reactors, and sensors.
- Provide consistent framework for sharing information about emissions control technologies.
- Help identify emissions control research and development (R&D) needs and priorities.

Accomplishments

- Continued co-leading the CLEERS Planning Committee and facilitation of the selective catalytic reduction (SCR), lean-NOx trap (LNT), and diesel particulate filter (DPF) Focus Group telecoms with strong domestic and international participation.
- Continued co-leading the LNT Focus Group and refinement of the standard LNT materials protocol.
- Analyzed identified key R&D priorities from the 2007 and 2008 CLEERS surveys and the current DOE national lab projects to identify potential gaps in current emissions control R&D portfolio.
- Provided regular update reports to DOE Diesel Cross-Cut Team.
- Organized 12th CLEERS workshop at University of Michigan, Dearborn on April 28-30, 2009.
- Maintained CLEERS Web site (www.cleers.org) including functionalities, security, and data to facilitate web meetings and serve focus group interactions.

Future Directions

- Continue co-leading CLEERS planning committee.
- Continue co-leading the LNT Focus Group and support the DPF and SCR Focus Groups as needed.
- Continue providing standard reference LNT materials, data, and kinetic modeling results for Focus Group evaluation.
- Organize and conduct the 2010 CLEERS workshop in the spring of 2010.
- Continue expanding basic data and model exchange between CLEERS and other Office of Vehicle Technologies (OVT) projects.
- Continue maintenance and expansion of CLEERS Web site.
- Continue providing regular update reports to the DOE Diesel Cross-Cut team.

Introduction

Improved catalytic emissions controls will be essential for utilizing high efficiency lean-burn engines without jeopardizing the attainment of much stricter U.S. Environmental Protection Agency emission standards that will take effect in 2010 and beyond. Simulation and modeling are recognized by the DOE Diesel Cross-Cut Team as essential capabilities needed to achieve this goal. In response to this need, the CLEERS activity was initiated to promote improved computational tools and data for simulating realistic full-system performance of lean-burn engines and the associated emissions control systems. Specific activities supported under CLEERS include:

- Public workshops on emissions control topics.
- Collaborative interactions among Cross-Cut Team members, emissions control suppliers, universities, and national labs under organized topical focus groups.
- Development of experimental data, analytical procedures, and computational tools for understanding performance and durability of catalytic materials.
- Establishment of consistent frameworks for sharing information about emissions control technologies.

- Recommendations to DOE and the DOE Cross-Cut Team regarding the most critical emissions control R&D needs and priorities.

ORNL is involved in two separate DOE-funded tasks supporting CLEERS:

- Overall administrative support; and
- Joint development of benchmark LNT kinetics with Sandia National Laboratories and Pacific Northwest National Laboratory (PNNL).

Approach

In the administrative task, ORNL coordinates the CLEERS Planning Committee, the CLEERS focus groups, CLEERS public workshops, and the CLEERS Web site (http://www.cleers.org). The specific activities involved include:

- Coordination of the CLEERS Planning Committee and the LNT Focus Group.
- Organization of the annual CLEERS public workshops.
- Maintenance of the CLEERS Web site.
- Preparation and presentation of status reports to the Cross-Cut Team.
- Response to requests and inquiries about CLEERS from the public.

Results

The 12th CLEERS workshop was held April 28–30, 2009 at the Dearborn campus of the University of Michigan. More than 90 foreign and domestic attendees from equipment suppliers, engine and vehicle manufacturers, universities, software vendors, and consultants were present to hear and discuss 34 contributed and three invited presentations on experimental measurements and simulations of lean exhaust aftertreatment control systems. As in the past, the meeting was structured around lean-NOx and particulate emissions control technologies. This year there was also a special emphasis on the relationship between modeling and simulation and on-board diagnostics (OBD). Details of the technical program and presentations are available on the Web site (http://www.cleers.org) under the 12th workshop heading. Important observations from this workshop included:

- Feedback from CLEERS (e.g., the CLEERS survey results) is clearly influencing the directions of research at universities and national labs.
- Recent results with dual-stage hydrocarbon (HC)-SCR NOx control suggest HC-SCR performance may now be competitive with urea-SCR.
- Direct application of micro-kinetics for catalytic exhaust aftertreatment still has major technical barriers to overcome to be practical.
- Emission control models are now sufficiently mature that combined and full systems simulations of technology options (e.g., gasoline versus diesel hybrids) are now becoming much more reliable.
- OBD discussion has led to recognition of some important new factors which should be considered in planning CLEERS related projects.

The workshop OBD discussion was highlighted by an afternoon panel session in which four industry OBD experts (including Alex Yezerets from Cummins, John van Gilder from General Motors, Mark Allain from Daimler, and Michiel van Niewstadt from Ford) discussed their individual perspectives and answered questions from the audience. Highlights from this discussion included the following points:

- Aftertreatment devices need to be designed for OBD, not OBD designed for aftertreatment devices.
- Pressure sensors are not a long term solution for DPF OBD.
- DPFs will have to be redesigned for OBD but the nature of this redesign is still unclear.
- LNT oxygen storage can be used for OBD similar to the approach used in three-way catalyst systems.
- There is considerable doubt about the adequacy of ammonia sensors for OBD.
- Modeling of emissions component failure modes should be an explicit R&D activity.
- For OBD, sensor robustness is more important than sensor accuracy.

Beyond the workshop, the LNT, SCR, and DPF Focus Groups have continued monthly technical topic phone/Web meetings throughout the year. Typical attendance has been 15-25 participants, with considerable international participation. This forum has turned out to be especially useful in keeping the U.S. members updated on recent developments in Europe.

As follow-on to the CLEERS R&D priority surveys conducted in 2007 and 2008, the CLEERS Planning Committee also compared the current 2009 R&D activities among the CLEERS community with the highest priority emissions control modeling and analysis needs identified by the surveys. The purpose of this exercise was to identify possible 'gaps' in current portfolio of R&D activities (both industrial- and government-funded) and develop proposed recommendations for new or adjusted R&D activities to the Crosscut Team and DOE. While the committee's access to industry activities was necessarily limited, it appears the emissions control-related projects being

supported by OVT align well with identified needs. One specific R&D area where the committee recommended that additional resources should be considered is in OBD/sensor-related improvements. This includes development of both improved sensor hardware and basic information about device chemistry and operation that would allow more effective use of existing sensors. A prominent example of the latter is the OBD diagnostic protocol developed for LNT aging by Cummins. In developing this protocol, Cummins relied heavily on basic studies of LNT chemistry and function carried out at PNNL and ORNL.

Also as a result of the above investigation of possibilities for improving the mix of CLEERS related R&D activities, the Planning Committee has recommended increasing the emphasis on experimental measurement and modeling of urea-SCR NOx control catalysts during the coming fiscal year. In addition, the committee feels that simulation of integrated vehicle systems (including hybrid vehicles) and multi-component devices (e.g., SCR-DPF) should receive increased emphasis.

Conclusions

CLEERS continues to provide a very effective forum for researchers in industry, national labs, universities, and supplier companies to share the most current non-proprietary information regarding the measurement, modeling, and performance simulation of lean exhaust emissions control technologies. The success of CLEERS is most noticeable in the broad participation in the public workshops and technical focus meetings and the large number of visits to the CLEERS Web site. Through the interactive feedback obtained from surveys of the CLEERS community, the CLEERS Planning Committee has been able to effectively advise the DOE and the DOE Diesel Cross-Cut Team about how to maximize the use of R&D resources to address the highest priority emissions control modeling and simulation needs of the industry. The positive feedback we have received from the CLEERS collaborators seems to confirm that CLEERS has been effective at improving the collaborations among the DOE labs, universities, and industry partners.

FY 2009 Publications/Presentations

1. 12th CLEERS Workshop presentations at http://www.cleers.org.

2. "CLEERS Coordination and Development of Catalyst Process Kinetic Data," J.-S. Choi et al., 2009 DOE Hydrogen Program and Vehicle Technologies Annual Merit Review, Crystal City, May 18-22, 2009.

II.B.10 Cross-Cut Lean Exhaust Emission Reduction Simulation (CLEERS): Joint Development of Benchmark Kinetics

Stuart Daw (Primary Contact),
Jae-Soon Choi, Josh Pihl, Bill Partridge,
Todd Toops, Charles Finney, Michael Lance,
Kalyana Chakravarthy
Oak Ridge National Laboratory (ORNL)
2360 Cherahala Boulevard
Knoxville, TN 37932-1563

DOE Technology Development Manager:
Ken Howden

Objectives

Coordinate ORNL's collaboration with Pacific Northwest National Laboratory (PNNL), and Sandia National Laboratories (SNL) in the development of kinetics information needed for aftertreatment component simulation through the following:

- Provide benchmark laboratory measurements of oxides of nitrogen (NOx) reduction chemistry and reaction rates in lean-NOx traps (LNTs) and selective catalytic reduction (SCR) catalysts under realistic operating conditions.
- Correlate laboratory measurements of LNT and SCR catalysts with test-stand/vehicle studies.
- Develop and validate global chemistry and (loworder) models for LNT and SCR kinetics.

Accomplishments

- Determined types, spatial distribution, stability and performance impact of sulfur on a commercial LNT through the following:
  - Specialized LNT sample analyses using scanning electron microscopy and electron probe microanalysis.
  - Characterization of sulfated model LNT components with temperature-programmed reduction (TPR) and diffuse reflectance infrared fourier transform spectroscopy (DRIFTS) and comparison with a commercial LNT.
  - Reactor evaluation of the impact of stepwise desulfation on specific LNT functions and global performance.
- Continued refinement of detailed LNT cycling model in collaboration with SNL.
- Refined a conceptual model of LNT sulfation and desulfation based on the primary mechanisms and processes identified.
- Implemented a low-order version of the LNT cycling model including sulfation and desulfation in conventional and hybrid vehicle systems simulations.
- Used surface spectroscopy to probe the mechanism by which hydrocarbons impact the NOx reduction performance of an Fe zeolite urea SCR catalyst.

Future Directions

- Understand the detailed structures and mechanistic implications of the different LNT sulfur species identified in Fiscal Year 2009.
- Broaden the understanding of LNT NH_3 chemistry by evaluating performance as a function of the nature of reductant (H_2, CO, HCs).
- Perform detailed identification of surface spectral features of CLEERS reference urea SCR catalyst under relevant operating conditions to refine mechanistic understanding of HC fouling.

✧ ✧ ✧ ✧ ✧

Introduction

Improved catalytic emissions controls will be essential for utilizing high-efficiency lean-burn engines without jeopardizing the attainment of much stricter U.S. Environmental Protection Agency emission standards scheduled to take effect in 2010. Simulation and modeling are recognized by the DOE Diesel Cross-Cut Team as essential capabilities needed to achieve this goal. In response to this need, the CLEERS activity was initiated to promote improved computational tools and data for simulating realistic full-system performance of lean-burn engines and the associated emissions control systems.

ORNL is involved in two separate DOE-funded tasks supporting CLEERS:

- Overall administrative support; and
- Joint development of benchmark LNT kinetics with SNL and PNNL.

Approach

In the benchmark kinetics task (covered by this report), ORNL is collaborating with SNL and PNNL to produce kinetic information for LNT and urea-SCR aftertreatment devices, both as individual and system integrated components. The results of this work are discussed with the LNT, Diesel Particulate Filter, and SCR Focus groups prior to publication to provide technical review and guidance to the labs. Specific activities involved include:

- Regular direct interactions among ORNL, PNNL, and SNL.
- Experimental measurements of LNT chemistry and reaction rates using laboratory reactors and prototype devices installed on engine test stands and vehicles.
- Analysis and reconciliation of experimental data from different sources with predictions from computer simulations.
- Publications in journals and presentations in public meetings and on the Web site.

Results

The major focus of experimental LNT research this year has been to identify roles that different sulfur types play in overall LNT performance. The fuel-sulfur-induced performance degradation is an importance technical barrier particularly for lean gasoline operation as illustrated by a recent CLEERS Industry Priority Survey [1]. Fuel sulfur can alter the function of multiple LNT components simultaneously, leading to complex trends in performance degradation. Periodic high temperature rich purges are required to remove accumulated sulfur and regain LNT performance, but such "desulfation" consumes extra fuel and can accelerate thermal aging. Development of LNTs with enhanced sulfur tolerance and fuel efficiency will require improved understanding of underlying sulfur chemistry in fully formulated LNT catalysts under realistic driving conditions.

Over the last two years, ORNL developed a conceptual sulfation model for the CLEERS reference catalyst (a commercial Ba-based LNT designed for gasoline direction injection application) with sulfation [2,3]. This model links changes in spatiotemporal reactions (e.g., NOx storage-reduction, oxygen storage-reduction, reductant consumption) and global performance (e.g., NOx conversion, NH_3 selectivity). Detailed in situ reactor analyses reveal that sulfur poisons the NOx-storage-reduction function along the catalyst axis in a plug-like manner. In contrast, sulfur deactivates oxygen-storage much less aggressively, leading to a more dispersed deactivation front. These findings have been used to explain increased NH_3 production with sulfation [3].

This fiscal year, we characterized sulfation of the CLEERS reference LNT catalyst with a range of techniques. The catalyst was sulfated in a bench flow reactor and the washcoat composition, structure and sulfur distribution were analyzed with various specialized techniques such as high-resolution electron probe microanalysis, microscopy, and TPR. Significant washcoat components of catalytic relevant were found to be present mainly as four distinct domains (Figure 1):

- Mg/Al mixed oxide with Pt, Ce
- Al oxide with Rh, Pd
- Ce/Zr mixed oxide with Pt, Pd, Ba (high Ba content)
- Ce/Zr mixed oxide with Pt, Pd, Ba (low Ba content)

Sulfur was present in the form of sulfates whose content was the highest in the LNT front and decreased along the axis. Barium exhibited the highest sulfur affinity leading to a plug-like axial progression of its sulfation. Sulfation of Al, Mg/Al, and Ce/Zr oxides was less complete and involved a more axially dispersed front. Nonetheless, sulfur storage on these oxides was significant thereby delaying the axial progression of the Ba sulfate front. These characterization results are consistent with performance trends published earlier [2,3], and refine our understanding of sulfation mechanisms as depicted in Figure 2.

To further elucidate the various sulfur species roles, we performed stepwise desulfation of the CLEERS LNT catalyst and intermittently evaluated its NOx control performance. Results are summarized in Figure 3. In the first low-temperature step (T_{max}= 492°C), 46% of the sulfur was removed with negligible impact on NOx storage capacity (determined by 15-min lean exposure). In contrast, in short cycling (60/5-s lean/rich) the catalyst exhibited decreased NOx conversion and

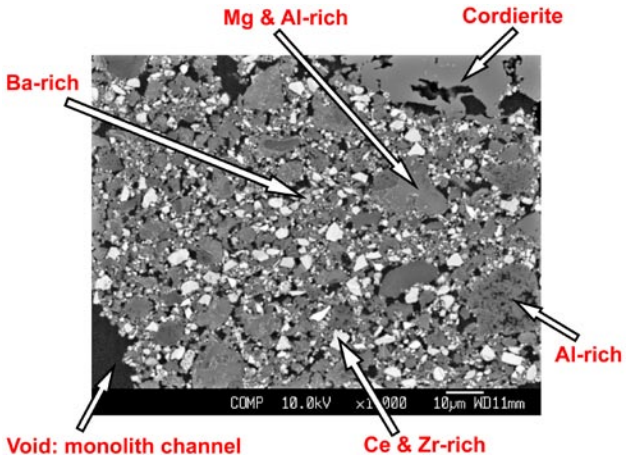

FIGURE 1. Backscattered electron image of the CLEERS reference LNT in a sulfated state; a washcoat cross-section (i.e., in the thickness plane) in a corner of a flow channel is shown.

increased NH_3 selectivity. This observation indicates that a large amount of S is associated with Al, Mg/Al, and/or Ce/Zr oxides and it implies that incomplete desulfation can actually worsen catalyst performance by "secondary" poisoning of relevant sites (e.g., Ba) by S from less stable sites. Higher temperature desulfation in the 2nd and 3rd steps removed an additional 26% of the sulfur, with a major recovery of short cycling NOx performance. The final desulfation step (at 690°C) removed the remaining 28% of the sulfur and significantly increased total NOx storage capacity. The above results confirm that LNTs form various types of sulfates that have different effects on LNT functions and global performance depending on how the device is cycled.

ORNL has been collaborating with SNL to take into account the experimental sulfation findings in LNT modeling. In addition, we have continued to address remaining questions about the details of the dominant reaction steps during both fast and slow cycling. Comparisons of model predictions with experiment indicate that the controlling steps are different between slow and fast cycling, implying that at least two different types of NOx storage sites have to be included in a comprehensive model. It also appears that solid-phase diffusion in the washcoat is an important factor for realistic LNTs. A lower-order version of the fast-cycling model (with appropriate kinetics for the 'fast' NOx storage sites and a correlation for sulfation effects) has been implemented in the PSAT simulation software developed and maintained by Argonne National Laboratory. Simulations using this LNT model for conventional and hybrid passenger vehicles indicate that about half of the fuel efficiency benefit of diesel engines (accounting for differences in energy density between gasoline and diesel fuel) are lost when NOx control with LNTs is taken into account.

For urea-SCR research, we continued our collaborative work with PNNL to elucidate the mechanisms by which hydrocarbons impact the CLEERS reference Fe zeolite urea SCR catalyst. Our counterparts at PNNL conducted flow reactor experiments to characterize the performance impact of various hydrocarbon species, while ORNL focused on in situ DRIFTS experiments to identify the species on the catalyst surface under relevant operating conditions. Figure 4 shows the DRIFT spectra collected during experiments conducted at 200°C. Spectrum (1), collected under NH_3, O_2, H_2O, and CO_2, illustrates the substantial NH_3 storage capacity of the catalyst. Spectrum (2),

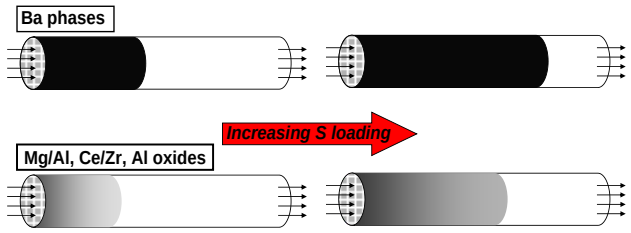

FIGURE 2. Conceptual depiction of the axial progression of sulfation for different LNT components. Darker color indicates higher degree of sulfation for a given component.

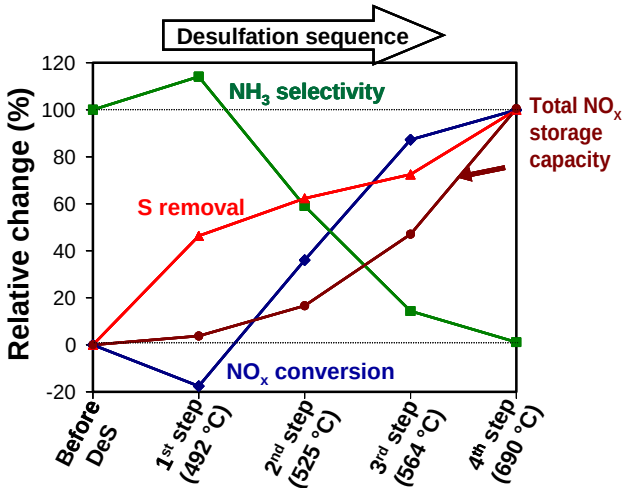

FIGURE 3. Impact of stepwise desulfation on LNT performance: relative changes in total NOx storage capacity, NOx conversion, and NH_3 selectivity as a function of total sulfur removed.

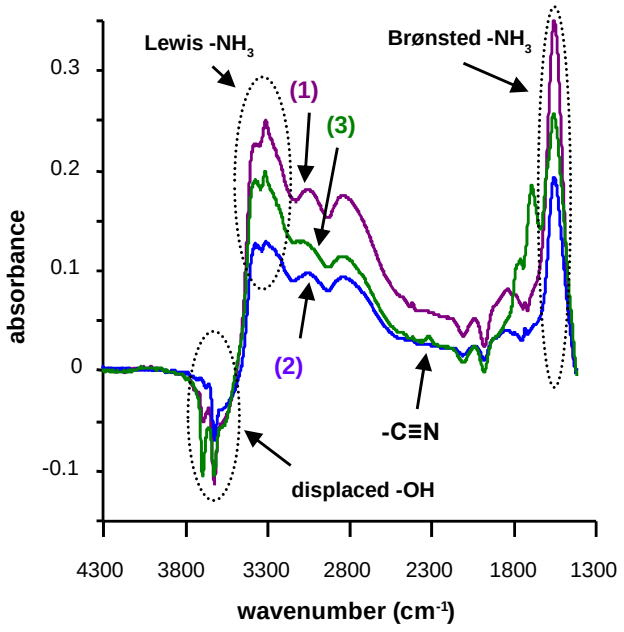

FIGURE 4. DRIFT spectra of the CLEERS reference Fe zeolite urea SCR catalyst at 200°C under (1) 350 ppm NH_3, 14% O_2, 4.5% H_2O, 5% CO_2, (2) 350 ppm NO, 350 ppm NH_3, 14% O_2, 4.5% H_2O, 5% CO_2, and (3) 50 ppm toluene, 350 ppm NO, 350 ppm NH_3, 14% O_2, 4.5% H_2O, 5% CO_2. (background spectrum: 14% O_2, 4.5% H_2O, 5% CO_2)

which also included NO in the gas mixture, shows a reduction in NH_3 on the catalyst surface due to its consumption by the NO SCR reaction. In Spectrum (3), toluene was introduced, generating adsorbed hydrocarbon species (1,600-1,800 cm^{-1}). There is also a new peak characteristic of compounds that contain a C≡N bond at 2,250 cm^{-1}, providing evidence that toluene is reacting on the catalyst surface. Fe zeolites are known to catalyze the ammoxidation reaction, so the C≡N feature in the spectrum could be due to a nitrile compound such as benzonitrile. Introduction of toluene also increased the amount of NH_3 on the catalyst surface, leading us to conclude that toluene does not impact catalyst performance by blocking NH_3 adsorption. Instead, toluene (or its decomposition products) appears to be poisoning active sites critical for the SCR reaction. This reduces the rate of NH_3 consumption, resulting in more NH_3 on the surface.

Conclusions

- Detailed spatio-temporal measurements of the CLEERS LNT reference catalyst have confirmed that multiple sulfur compounds form during sulfation. These compounds form and decompose at different rates and have distinct roles in altering LNT performance, implying that LNT formulation needs to be coordinated with the lean-rich cycling and desulfation strategies.
- Hydrocarbon poisoning of the CLEERS reference SCR catalyst appears to occur by blocking active sites critical for one or more surface reaction steps in the SCR reaction rather than by blocking ammonia adsorption.
- Questions remain about the detailed reaction steps needed to successfully model both short and long-cycle LNT behavior with a single set of reaction parameters. Results continue to indicate that intra-solid diffusion still needs to be a critical part of any successful model.
- Simplified kinetic models are now being successfully used to simulate vehicle systems with LNT lean NOx controls.

References

1. "CLEERS Research Prioritization: Analysis of Focus Areas" (2007), www.cleers.org.

2. J.-S. Choi, W.P. Partridge, and C.S. Daw, "Sulfur impact on NOx storage, oxygen storage and ammonia breakthrough during cyclic lean/rich operation of a commercial lean NOx trap", Applied Catalysis B: Environmental 77 (2007) 145-156.

3. J.-S. Choi, W.P. Partridge, J.A. Pihl, and C.S. Daw, "Sulfur and temperature effects on the spatial distribution of reactions inside a lean NOx trap and resulting changes in global performance", Catalysis Today 136 (2008) 173-182.

FY 2009 Publications/Presentations

1. W.P. Partridge and J.-S. Choi, "NH3 formation and utilization in regeneration of Pt/Ba/Al2O3 NOx storage-reduction catalyst with H2", *Applied Catalysis B: Environmental* 91 (2009) 144-151.

2. V.Y. Prikhodko, K. Nguyen, J.-S. Choi, and C.S. Daw, "Axial length effects on lean NOx trap performance", *Applied Catalysis B: Environmental* 92 (2009) 9-16.

3. J.A. Zandhuis, C.E.A. Finney, T.J. Toops, C.S. Daw, and T.J. Fox, "Nondestructive X-ray inspection of thermal damage, soot and ash distributions in diesel particulate filters", SAE Technical Paper 2009-01-0289 (2009).

4. W.P. Partridge, J.-S. Choi, J.A. Pihl, T.J. Toops, N.A. Ottinger, A. Yezerets, and N.W. Currier, "Elucidating Lean NOx Trap Catalyst Regeneration & Degradation Chemistry: Insights from Intra-Catalyst, Spatiotemporally Resolved Measurements", keynote lecture at the 21st North American Catalysis Society Meeting (NAM), San Francisco, California, June 7–12, 2009.

5. J.-S. Choi, W.P. Partridge, N.A. Ottinger, J.A. Pihl, T.J. Toops, and C.S. Daw, "Impact of stepwise desulfation on the performance of a Ba-based commercial lean NOx trap catalyst", presented at the 21st North American Catalysis Society Meeting (NAM), San Francisco, California, June 7–12, 2009.

6. J.-S. Choi, M.J. Lance, C.E.A. Finney, L.R. Walker, and C.S. Daw, "Quantification of elemental spatial correlations in commercial automotive catalysts", presented at the 21st North American Catalysis Society Meeting (NAM), San Francisco, California, June 7–12, 2009.

7. J.A. Pihl, T.J. Toops, C.S. Daw, R.G. Tonkyn, J.L. Male, D.R. Herling, "Mechanisms of hydrocarbon poisoning of a urea-SCR Catalyst", presented at the 21st North American Catalysis Society Meeting (NAM), San Francisco, California, June 7–12, 2009.

8. J.-S. Choi, C.S. Daw, T.J. Toops, J.A. Pihl, W.P. Partridge, C.E.A. Finney, V. Prikhodko, M.J. Lance, N.A. Ottinger, and V.K. Chakravarthy, "CLEERS coordination and development of catalyst process kinetic data", presented at the 2009 DOE Vehicle Technologies Program Annual Merit Review, Arlington, Virginia, May 18–22, 2009.

9. J.-S. Choi, W.P. Partridge, J.A. Pihl, T.J. Toops, N.A. Ottinger, and C.S. Daw, "Stepwise desulfation and its impact on LNT performance – Study of CLEERS reference catalyst", presented at the 12th DOE Crosscut Workshop on Lean Emissions Reduction Simulation, Dearborn, Michigan, April 28–30, 2009.

10. Richard S. Larson, V. Kalyana Chakravarthy, Josh A. Pihl, Jae-Soon Choi, C. Stuart Daw, "Microkinetic modeling of lean NOx trap storage/regeneration and sulfation/desulfation", presented at the 12th DOE Crosscut Workshop on Lean Emissions Reduction Simulation, Dearborn, Michigan, April 28–30, 2009.

11. V. Kalyana Chakravarthy, Zhiming Gao, and C. Stuart Daw, "After-treatment modeling for hybrid vehicles using PSAT," presented at the 12th DOE Crosscut Workshop on Lean Emissions Reduction Simulation, Dearborn, Michigan, April 28–30, 2009.

Special Recognitions & Awards/Patents Issued

1. Invited topical keynote talk by W.P. Partridge at the 21st North American Catalysis Society Meeting (NAM), San Francisco, California, June 7–12, 2009.

1. Invited topical talk by W.P. Partridge at the GE Emissions Aftertreatment Symposium, GE Global Research Laboratories, September 17, 2009.

II.B.11 Development of Advanced Diesel Particulate Filtration Systems

Kyeong Lee (Primary Contact) and Seung Yang
Argonne National Laboratory
9700 S. Cass Ave.
Argonne, IL 60564

DOE Technology Development Manager:
Ken Howden

Objectives

- Evaluate pressure drops across the diesel particulate filter (DPF) membrane during particulate matter (PM) filtration processes.
- Develop technologies to reduce pressure drops across the DPF membrane.
- Measure the thermo-physico-chemical properties of diesel PM emissions for future numerical calculations.

Accomplishments

- Analyzed the detailed filtration characteristics and pressure drop behaviors of modified DPF membranes.
- Visualized filtration processes in DPF membranes.
- Proposed a mechanism of soot cake formation.
- Measured the oxidation rate, heat release, amount of soluble organic compounds (SOCs), and specific heats of diesel particulate emissions.

Introduction

Since the U.S. Environmental Protection Agency instituted stringent particulate matter emission standards for heavy-duty engines, the development of advanced DPF systems has been an urgent task for the diesel industry. Because the efficient control of soot deposits in DPFs involves the detailed characterization of important properties related to soot formation [1-2], researchers have performed soot oxidation experiments to measure oxidation rates, heat release, and the amount of SOCs and ash. The researchers also modified the geometry of DPF membrane channels by shifting the front plug position for the purpose of increasing filtration areas and tested pressure drop characteristics in comparison with those of conventional DPF membranes.

Results

For soot loading, a DPF testing system was connected to the exhaust pipe of a General Motors light-duty diesel engine right after the exhaust manifold. The DPF testing system mainly consisted of a flow reactor where a lab-scaled DPF membrane was installed, a high-resolution imaging system with a stereomicroscope, a data acquisition system, and pressure/flow sensors. The 2-inch diameter by 6-inch long cordierite membranes were bisected in the length direction to visualize the filtration processes through a glass window in the flow reactor. Microscopic video images were recorded during the entire filtration period.

The geometry of the membrane channels were modified by changing the front plug (or outgoing-flow channel plug) position in three different ways: ¼, ½, and ¾ positions of the entire membrane length from the DPF inlet surface. Each modified membrane is called ¼ plug position (1/4PP) membrane, ½ plug position (1/2PP) membrane, and ¾ plug position (3/4PP) membrane, respectively. These membranes were tested to evaluate the effects of plug position shift on pressure drop, compared with the conventional DPF membrane.

Figure 1 shows the effects of front plug position shift on pressure drop in clean DPF membranes as a function of air flow rate, in comparison with those in a conventional DPF. The pressure drop significantly increased with increase of flow rate and also with increase of the plug position shift.

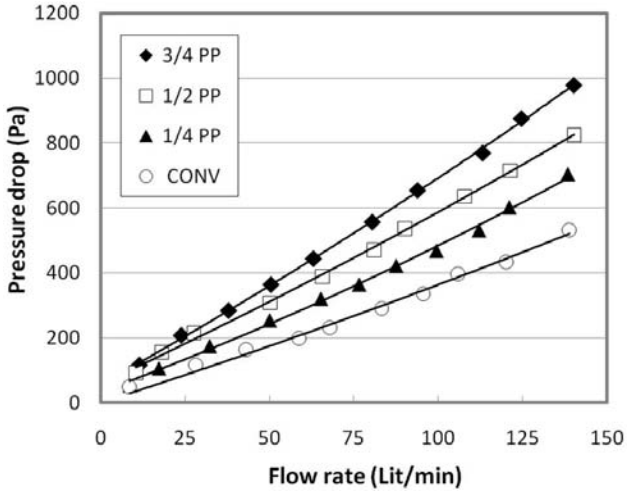

FIGURE 1. Effects of Plug Position Shift on Pressure Drop in Clean DPFs at Various Flow Rates

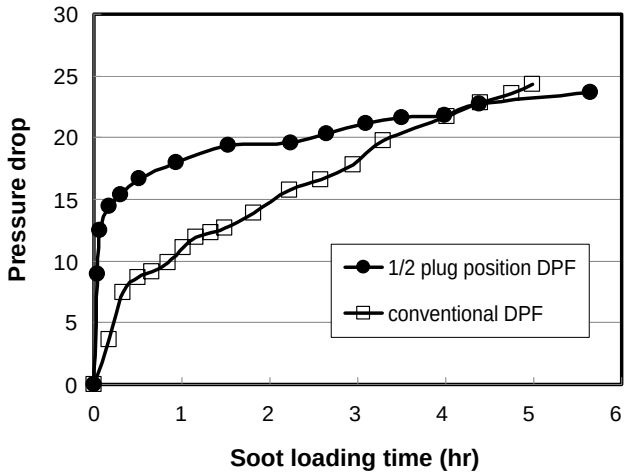

FIGURE 2. Effects of Soot Loading on Pressure Drop

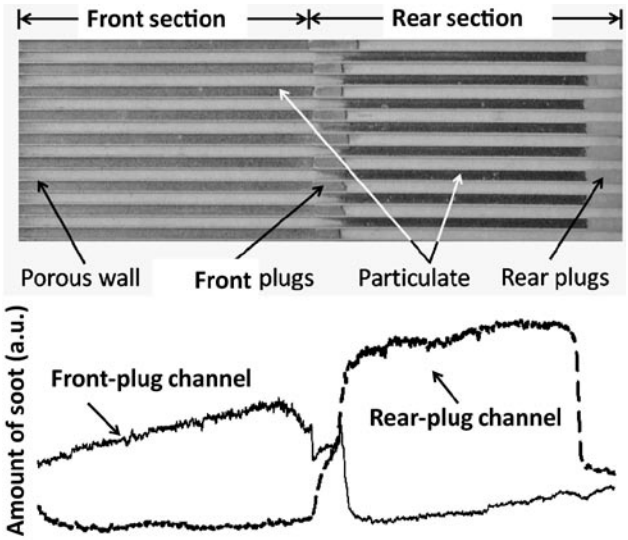

FIGURE 3. Image of Soot Loading and its Soot Loading Profiles (1/2PP Membrane)

Figure 2 shows the effects of soot loading on the pressure drop both in the modified 1/2PP DPF membrane and conventional DPF membrane. At the very initial period of soot loading in the 1/2PP DPF membrane, the pressure drop increased at a significantly higher degree than did that in the conventional one, and then gradually increased with soot loading, displaying a much lower increase rate than that in the conventional DPF membrane. Four hours after soot loading, the level of pressure drop became almost the same between the two membranes and then finally the pressure drop in the conventional membrane exceeded that in the modified one. Similar behaviors appeared in a previous study performed with an inlet-membrane DPF [3], where a thin layer formed on the surface of incoming flow channel contained tiny pores.

High-resolution video images, recorded in real time during the filtration experiment, revealed the detailed characteristics of filtration processes. Figure 3 shows a still image of soot loading in the 1/2PP DPF membrane and its soot loading profiles along the channels in terms of grey level. As shown in the photo, more particulates were collected in the rear section of membrane, while the front section of modified channels does a certain level of soot filtration. The soot loading is quite evenly distributed both in the front and rear sections. The amount of soot loading along the channels was evaluated by averaging the longitudinal profiles of grey levels along all the channels (8). As evident in the profile, the amount of soot loading started to significantly increase near the end of front section, where plugs are located. The maximum soot loading was measured at the end of rear section, while the minimum soot loading was measured at the entrance of front section.

Figure 4 shows the detailed images of the soot cake in membrane channels. The incoming flow channels are completely dark, where soot particles were filtered. As expected, however, the outgoing flow channels are quite clean, the surface of which displays the exits of numerous pores. A few pores appeared to be dark, while a majority of others are still clean. This observation implies that a majority of pores are filled with soot particles only in the middle of their passages. These pores should be complex in the shape of passages.

Figure 5 shows the heat release measured by a thermogravimetric analyzer (TGA) during the oxidation of diesel particulates. The experiments revealed that the PM samples consistently contained about 20 wt% of SOCs and displayed a maximum oxidation rate of 1.2 wt%/min. Also the residual ashes remained after the completion of oxidation at an average portion of 7.4 wt%±0.32. The average heat release turned out to be approximately 14.6 kJ/g.

The specific heat of diesel soot was measured as a function of temperature by using a differential scanning calorimeter, as shown in Figure 6. The result showed

$$\text{Heat release (kJ/g)} = \left[\int_{t_1}^{t_2} \frac{dH}{dt}\,dt\right] \cdot \left(\frac{1}{M_0 - M_r}\right)$$

dH/dt: Heat flow rate (mW)
t: Time (s)
Mo: Initial mass (mg)
Mr: Residual mass (mg)

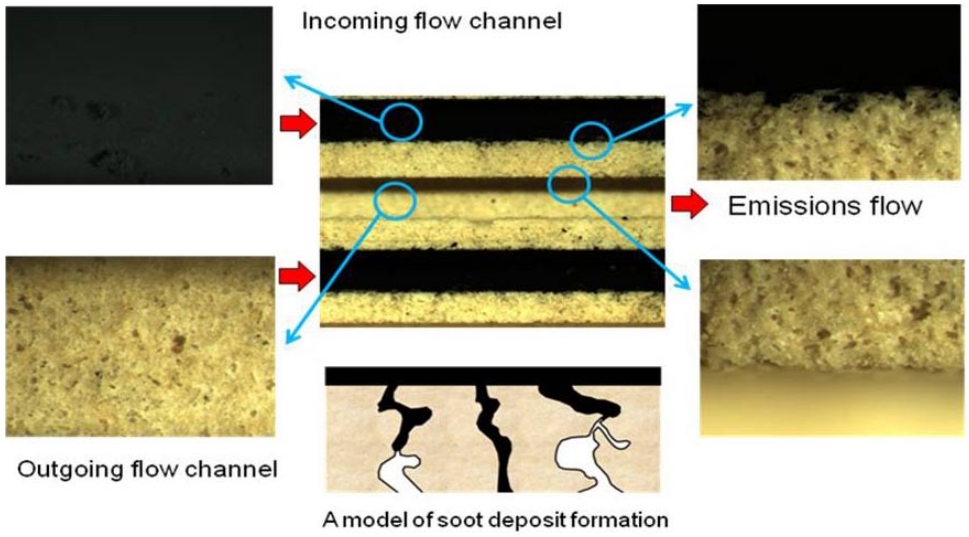

FIGURE 4. Suggested Model of Soot Cake Formation

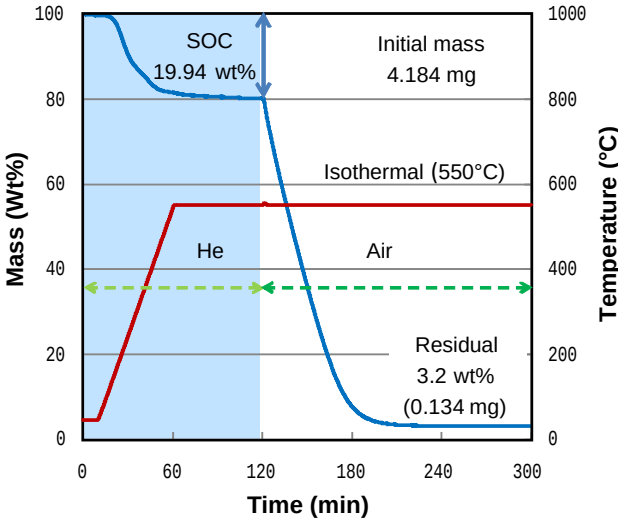

FIGURE 5. Heat Release Measured During Diesel PM Oxidation

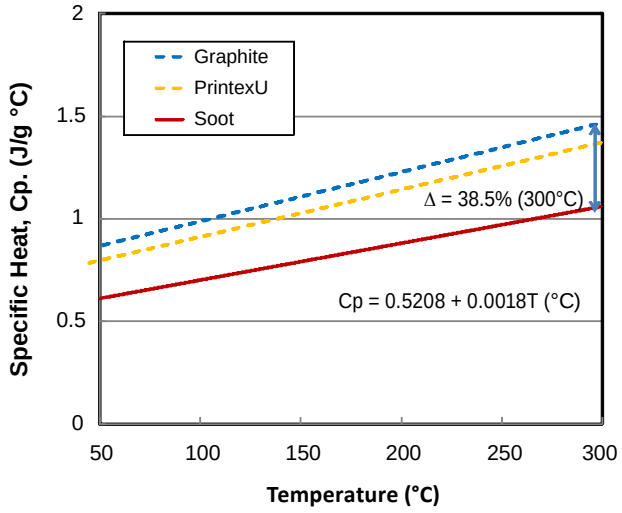

FIGURE 6. Specific Heats Measured as a Function of Temperature

that the specific heat of diesel soot was significantly different from those of soot artifacts, suggesting that researchers use the accurate values measured in this work.

Future Directions

- Evaluate filtration efficiencies for conventional/modified membranes at various engine operating conditions.
- Measure soot oxidation rates and heat release as a function of engine operating condition and SOF concentration.
- Evaluate regeneration efficiencies in conventional membranes at various engine conditions.
- Analyze gaseous emissions at the DPF exit during regeneration.

Conclusions

- The pressure drop in a modified DPF membrane increased as the front plug position was shifted to the membrane exit, mainly due to the increase of wall-through losses, while the frictional losses and inertial losses were not significant in magnitude. The optimum position of plug shift was determined by examining parametric relations between permeability and plug position.

- The microscopic soot imaging revealed a soot formation mechanism in a DPF membrane.
- The TGA experiments successfully evaluated the oxidation rates of diesel PM and amount of SOCs and ashes contained in the PM samples.
- The DSC experiments were successfully conducted to measure the specific heat of diesel PM as a function of temperature, showing the significantly different magnitude than those of diesel soot artifacts.

References

1. Lee, K.O., Zhu, J., Effects of Exhaust System Components on Particulate Morphology in a Light- Duty Diesel Engine, presented at SAE World Congress, 2005-01-0184, 2005.

2. Karin, P., Cui, L., Rubio, P., Tsuruta, T., Hanamura, K., Microscopic Visualization of PM Trapping and Regeneration in Micro-Structural Pores of a DPF Wall, presented at SAE World Congress, 2009-01-1476, 2009.

3. Furuta, Y., Mizutani, T., Miyairi, Y., Yuki, K., Kurachi, H., Study on Next Generation Diesel Particulate Filter, presented at SAE World Congress, 2009-01-0292, 2009.

II.B.12 Diesel Soot Filter Characterization and Modeling for Advanced Substrates

Thomas Gallant (Primary Contact),
Mark Stewart, Do Heui Kim, Gary Maupin
Pacific Northwest National Laboratory (PNNL)
P.O. Box 999
Richland, WA 99352

DOE Technology Development Manager:
Ken Howden

Objectives

- Adapt the micro-modeling capabilities developed by the Cross-Cut Lean Exhaust Emissions Reduction Simulations Program to investigate substrate characteristics and spatial location of catalyzed washcoats on backpressure, soot regeneration and lean-oxides of nitrogen (NOx) trap (LNT) function.
- Incorporate simplified LNT kinetics into the PNNL micro-model and exercise the model to answer key questions regarding Dow's acicular ceramic material (ACM) substrate attributes.

Accomplishments

- Identified and incorporated LNT kinetics into a one-dimensional (1-D) wall-flow micro-model.
- Conducted a multi-channel reactor experiment to determine the 'flow-through' versus 'wall flow' performance.
- Conducted single-channel reactor experiments to document NOx uptake of Dow's LNT washcoat.
- Investigated the effect of soot loading on NOx uptake.

Future Directions

No additional work is planned for this project beyond March 2010.

Introduction

PNNL, in collaboration with Dow Automotive, has been able to utilize advanced micro-modeling techniques, i.e., lattice Boltzmann, to optimize a catalyzed ACM for maximum soot loading on a diesel particulate filter. To meet future particulate matter (PM) and NOx emissions, such as light-duty diesel applications which are sensitive to size and weight limitations, the incorporation of the PM and NOx reduction function into one wall flow substrate is desirable. The major drawback with current 'wall-flow' substrate technologies is the backpressure requirement, which limits the washcoat loading for the NOx adsorption function. The ACM open structure allows for high soot loading without significant backpressure build-up; therefore, high washcoat loading for a NOx adsorber function with minimal backpressure is also possible with ACM.

However, the interaction of the PM and NOx washcoat functions can have either a synergistic or detrimental effect on the contiguous or integrated washcoat functions. Modeling the fundamental chemistry and physics of these gas-solid phase interactions will establish the design criteria for optimal washcoat distribution. Dow Chemical has a patent application on several concepts which utilize the unique ACM substrate structure and the ability to distribute the catalytic functions. The substrate and catalytic options are numerous and therefore, too expensive and time consuming to produce catalyzed materials and conduct laboratory performance tests. With the successful validation of the micro-model for a specific LNT function, the optimal spatial distribution of the various catalyst functions can be optimized for fuel efficiency and emissions. PNNL's micro-modeling and single-channel validation testing will allow Dow Automotive to make informed decisions and minimize process research and development to optimize the material for specific light-duty engine applications.

Approach

This investigation will follow the process of identifying and combining LNT kinetics into PNNL's existing micro-modeling capabilities developed for Dow's ACM substrate and then, exercise the micro-model to answer key questions regarding the potential advantages of the substrate to incorporate unique washcoats. In addition to micro-modeling, reactor experiments with LNT wash-coated single channels will be utilized to investigate key questions not amenable to micro-modeling or to aid in the validation of the micro-model. Once the micro-model has been validated with experimental results, the micro-model will be used explore other concepts identified by Dow's patent application US 2006/0193757 A1.

The work has been focused on a list of key questions, relating to a LNT concept identified in Dow's patent application, which can be answered by the micro-modeling or single-channel reactor studies. The key questions include:

- Is there an advantage of an additional oxidation catalyst upstream versus uniformly dispersed?
- What is the performance difference between "flow-through' versus 'wall-flow' conversion?
- What is the impact on adsorption of NOx on passive soot oxidation rates?
- Does reduction of NO_2 to NO by soot oxidation inhibit rates of NOx adsorption in subsequent catalyst?
- Is the oxidation of reductants by upstream precious metal catalysts a significant barrier to NOx reduction during rich phases?

Results

LNT Kinetics

The first task was to identify a kinetic model that was relatively simple but provided an adequate representation of LNT NOx adsorption kinetics. The intent was to use this model with either a simple 1-D 'wall-flow' model or possibly incorporate into the existing micro-model. After reviewing 16 recently published papers, the model described in a conference paper by Kromer, et al., and then elaborated upon by Cao, et al. [1] provided the best balance for this work. The model included both fast and slow sites for disproportionation reaction, as well as sites for direct NO adsorption. Although a few parameters, e.g., a pre-exponential term for NO oxidation, were not explicitly included in the papers, reasonable estimates were incorporated with little effect on the results. After a few iterations of adjusting parameters to match results in the Cao paper, a satisfactory kinetic model was developed that agreed reasonably well with the data in the Cao paper.

Reactor Experiments: NOx Uptake

To determine performance differences of a 'flow-through' (unplugged channels) and 'wall-flow' (plugged channels), a single-channel reactor experiment was designed to quantitatively measure NOx uptake for each concept. This experiment required a four-channel mini-brick cut from a 10-channel catalyzed mini-brick supplied by Dow. The mini-brick was uniformly coated with a LNT washcoat. Alternating channels were plugged and then removed to make a comparison on the same set of channels. The results, Figure 1, showed no significant difference in NOx uptake performance which supported the value of a 'wall-flow' concept using ACM.

The next step was to determine the effect of soot on NOx uptake. A single channel which had previously been characterized in the reactor for NOx uptake was loaded with actual engine-derived soot from the exhaust of a diesel Jetta. The NOx uptake experiments were repeated and then, the remaining soot was removed by oxidation at 500°C, 600°C and 700°C. The results of these experiments are being evaluated but it appears that soot had a significant effect on NOx uptake. It still needs to be determined if this reduction in NOx uptake was due to NO_2 beginning to be converted to NO from soot oxidation and/or from a thermal excursion which sintered the precious metal catalyst.

1-D 'Wall-Flow' Modeling

The initial assumptions for the LNT micro-modeling included a 30K/hr space velocity and at conditions described in the Cao paper [1]. The micro-modeling cases for answering the key questions are outlined in Figure 2. The results from the micro-modeling have shown that:

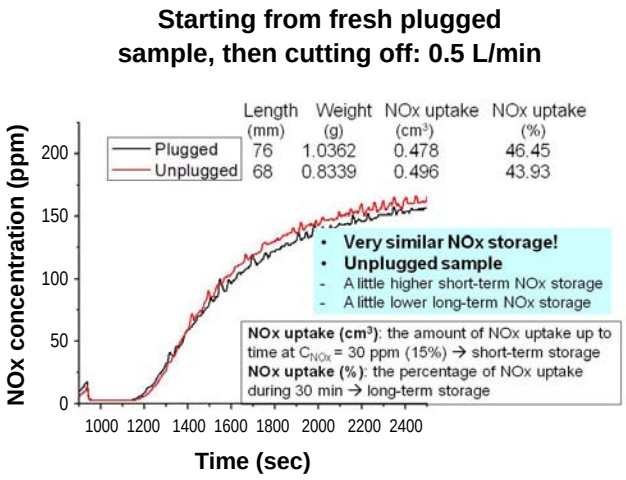

FIGURE 1. 'Flow-Through' versus 'Wall-Flow' NOx Uptake Performance

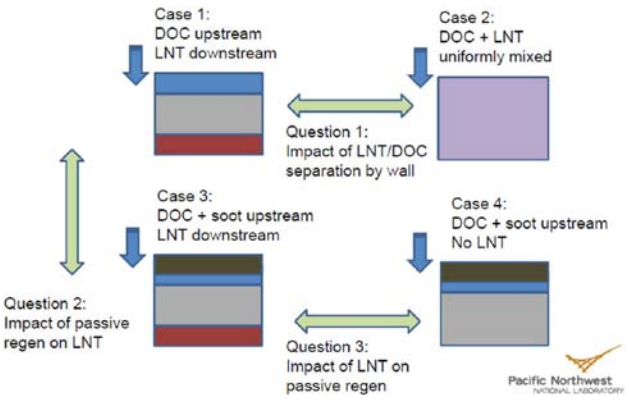

FIGURE 2. 1-D Micro-Modeling Cases

- Question 1: Separating the LNT and diesel oxidation catalyst (DOC) by a wall thickness has a very slight benefit for NOx removal. The transport in the wall direction is diffusion dominated and the wall resistance is low enough such that no strong concentration gradients were produced.
- Question 2: The LNT has a very small effect on passive regeneration, whereby, the LNT catalyst absorbs NO_2 but also produces NO_2 from NO.
- Question 3: Passive regeneration has a negative impact on NOx removal, whereby, soot oxidation by NO_2, i.e., converting NO_2 to NO, results in a significant reduction in NOx adsorption.

Conclusions

1-D micro-modeling, combined with single-channel reactor experiments, has answered some key questions regarding NOx uptake performance of a wall flow concept and catalyst distribution. However, the results of the 1-D micro-modeling should be validated by single-channel reactor experiments, prior to investigating other catalyst distribution concepts.

References

1. Cao, L., et al., *Kinetic Modeling of NOx Storage/Reduction on Pt/BaO/Al2O3 Monolith Catalysts.* Industrial & Engineering Chemistry Research, 2008, **47**(23), 9006-9017.

FY 2009 Publications/Presentations

1. Diesel Soot Filter Characterization and Modeling for Advanced Substrates, 2009 DOE Hydrogen Program and Vehicle Technologies Annual Merit Review and Peer Evaluation Meeting, May 18–22.

II.B.13 Degradation Mechanisms of Urea Selective Catalytic Reduction Technology

Do Heui Kim, Chuck Peden (Primary Contact)
Institute for Interfacial Catalysis
Pacific Northwest National Laboratory (PNNL)
P.O. Box 999, MS K8-93
Richland, WA 99354

DOE Technology Development Manager:
Ken Howden

CRADA Partners:
Se H. Oh, Chang H. Kim, Steven J. Schmieg
General Motors (GM)

Objectives

- Develop an understanding of the deactivation mechanisms of and interactions between the diesel oxidation catalyst (DOC) and the urea selective catalytic reduction (SCR) catalyst used in light-duty diesel aftertreatment systems.
- Understand the difference between actual field aging and aging under laboratory conditions, information essential in developing a rapid assessment tool for emission control technology development.
- Determine the role of the various aging factors impacting long-term performance of these catalyst systems, in order to provide information about what operating conditions should be avoided to minimize catalyst deactivation.

Accomplishments

- Cooperative Research and Development Agreement (CRADA) signed and project initiated in January, 2009.
- Two major thrusts this year:
  - Several state-of-the-art characterization tools were found to be useful for investigating degradation mechanisms of the "development" DOC and SCR catalysts. In particular, to date we have used:
    - Transmission electron spectroscopy/X-ray diffraction (TEM/XRD): structural and catalytic phase/morphology information
    - X-ray photoelectron spectroscopy (XPS): chemical state of active catalytic phases
  - Based on a correlation of performance measurements (GM) and characterization results (PNNL) obtained to date, the following are indicated as the primary reasons for deactivation:
    - DOC catalyst: sintering of active metal (Pt/Pd) particles.
    - SCR catalyst: structure destruction of zeolite and agglomeration of ion-exchanged metal species.
  - One public presentation.

Future Directions

- Revise the initial laboratory aging protocol.
  - Based on the evaluation of the first round of DOC and SCR catalysts, current laboratory aging protocols will be revised and tested.
- Continued evaluation of the most effective characterization tools in order to provide additional crucial information about materials changes in the active catalytic phases.
  - Several additional state-of-the-art characterization techniques will be applied to link between the structural changes and the deactivation of catalyst materials.
  - In situ X-ray absorption near-edge spectroscopy, electron paramagnetic resonance and ^{27}Al nuclear magnetic resonance (NMR)
  - H_2 temperature-programmed reduction and NO temperature programmed desorption

Introduction

Diesel engines can offer substantially higher fuel efficiency, good driving performance characteristics, and reduced carbon dioxide (CO_2) emissions compared to stoichiometric gasoline or gasoline-electric hybrid engines. For these reasons along with favorable taxation policies, diesel-powered passenger vehicles have been gaining popularity in Europe in recent years. Despite the increasing public demand for higher fuel economy and reduced dependency on imported oil, however, meeting the stringent emission standards with affordable methods has been a major challenge for the wide application of these fuel-efficient engines in the U.S. market. The selective catalytic reduction of NOx by urea (urea-SCR) is one of the most promising technologies for NOx emission control for diesel engine exhausts. Compared to the competing lean-

NOx reduction technologies such as the NOx adsorber technology (a.k.a. lean-NOx trap), urea-SCR offers a number of advantages, including excellent NOx reduction efficiency over a wide temperature range and overall lower system cost, etc. Therefore, urea-SCR technology is being considered by automotive manufacturers as the most reasonable path to meet the emission standards for 2010 and beyond diesel vehicles. To ensure successful NOx emission control, a DOC and a urea-SCR catalyst with high activity and durability are critical for the emission control system. Because the use of this technology for mobile applications is new, the lack of experience makes it especially challenging to satisfy the durability requirements. Of particular concern is being able to realistically simulate the actual field aging of diesel aftertreatment catalysts under laboratory conditions, which is necessary both as a rapid assessment tool for verifying improved performance and certifiability of new catalyst formulations. In addition, it is imperative to understand deactivation mechanisms to develop improved catalyst materials.

GM and PNNL are investigating fresh, laboratory- and engine-aged DOC and SCR catalysts in this CRADA project that began in January, 2009. These studies are intended to lead to a better understanding of various aging factors that impact the long-term performance of catalysts used in the urea-SCR technology, and improve the correlation between laboratory and engine aging in order to reduce development time and cost. Investigations of DOC catalysts will include oxidation of hydrocarbons and NO, and SCR catalysts for low-temperature NOx conversion activity, ammonia slip at low temperatures and ammonia oxidation at high temperatures.

Approach

This project is focusing on the characterization of catalyst materials used in the urea-SCR technology with special attention to the materials' sensitivity to conditions of laboratory (e.g., oven and laboratory reactor) and engine (e.g., engine dynamometer) aging protocols. In particular, a primary area of emphasis will be on establishing the relevance of rapid laboratory catalyst aging protocols with the specific aging phenomena observed in realistic engine operating conditions. This information will aid the development of improved catalyst formulations and the optimal integration of new catalyst formulations into GM's aftertreatment systems. More importantly, the information will also aid in understanding how catalyst degradation occurs in the field, and developing ways to improve the durability of catalyst materials.

GM has been providing both fresh and aged catalyst materials used in the urea-SCR technology and making experimental measurements of changes in the catalytic performance of these materials before and after the aging. PNNL has been utilizing state-of-the-art analytical techniques to investigate the surface and bulk properties of these catalysts as well as the changes in these properties induced by the aging process. In particular, catalyst characterization techniques such as XRD, XPS, TEM/energy dispersive X-ray (EDS), Brunauer-Emmett-Teller/pore size distribution, and ^{27}Al solid state NMR are being utilized to probe the changes in physicochemical properties of the DOC and SCR catalyst samples under deactivating conditions; e.g., hydrothermal aging at various temperatures. This work is being performed on a group of model and development catalysts. By developing a good understanding of performance degradation mechanisms during the catalyst aging, PNNL and GM expect to be able to provide a framework for developing robust urea-SCR aftertreatment systems, a better definition of the operational window for current materials, and perhaps also suggesting formulation changes that have potential to demonstrate improved performance and long-term durability.

Results

Physicochemical Investigation of the Degradation Mechanism for DOC Catalysts

A commercial DOC, consisting of noble metal deposited on an alumina-based support, was thermally aged at different temperatures. In particular, an "aged C" sample was aged at higher temperature than "aged A" (the same catalyst formulation). These aged samples were tested with NO and hydrocarbon oxidation reactions to determine deactivation of the catalyst. As shown in Figure 1, there is a significant decrease in activity for NO (Figure 1a) and hydrocarbon oxidation (Figure 1b). For example, the light-off temperature for hydrocarbon oxidation shifted to higher temperatures by ~70ºC, demonstrating significant degradation of the oxidation function. The particles in the aged samples were investigated with TEM/EDS analysis. As illustrated in Figure 2a, the mildly aged sample (aged A) contains the platinum group metal (PGM) particles ranging from 2 to 6 nm in size. On the other hand, the particles in the more severely aged sample (aged C) grow significantly to sizes of 100 nm or more (see Figure 2b), consistent with XRD results. Therefore, the active surface area of PGM has decreased drastically as a result of the thermal aging process, causing the deactivation of NO and hydrocarbon oxidation. In order to quantify the changes in PGM particle size as a function of treating time, we performed a time-resolved XRD experiment for a fresh DOC catalyst under aging conditions at 900°C. Figure 3 clearly shows that the PGM particles grow rapidly within the first 5 hrs of exposure time, followed by a gradual increase in the size as the aging continues, similar to behavior we have observed in previous studies [1]. This result implies that even short time

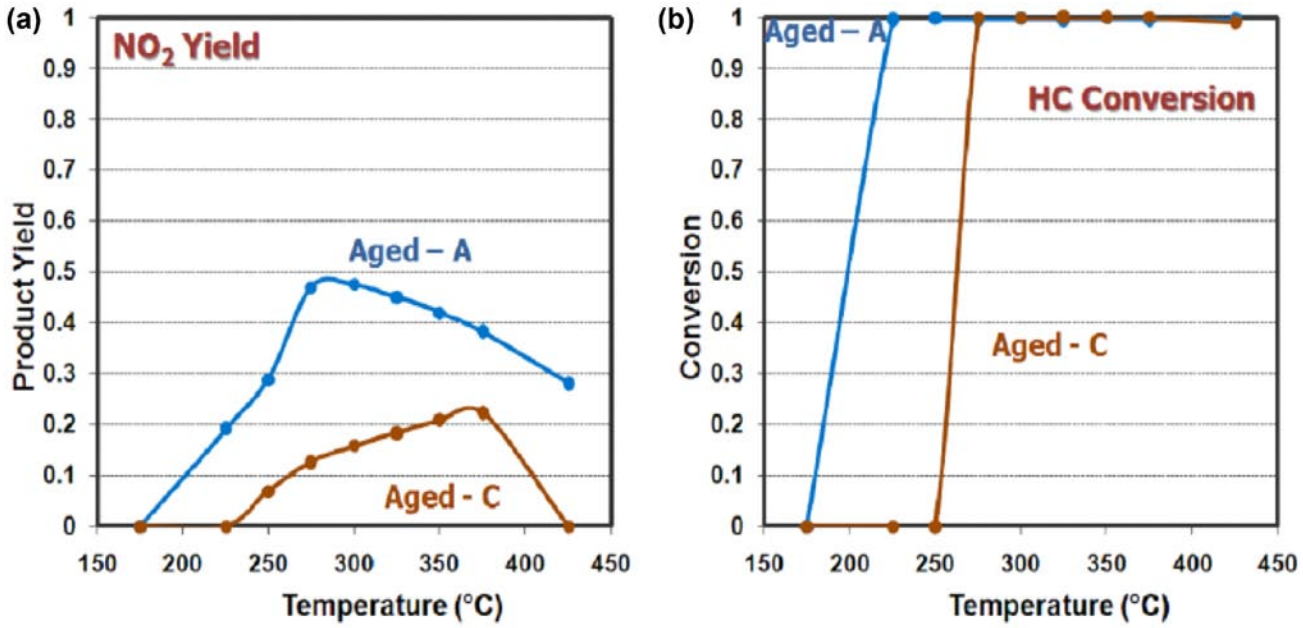

FIGURE 1. Changes in activity over aged A and aged C samples for NO oxidation (a) and hydrocarbon (C_3H_6) oxidation (b).

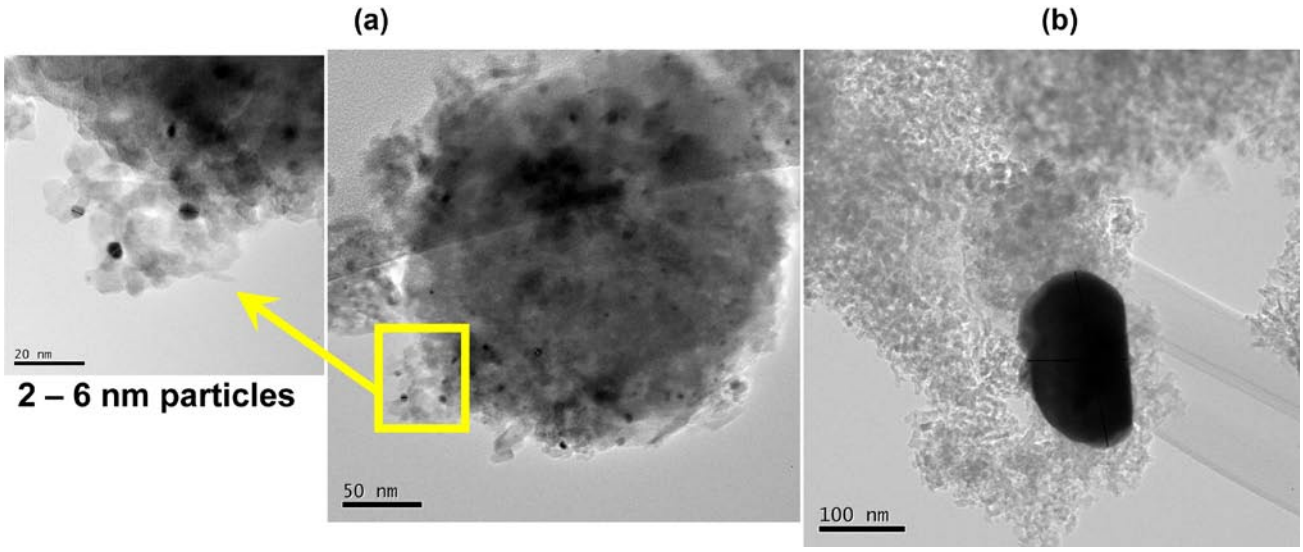

FIGURE 2. TEM Pictures of Aged A (a) and Aged C Samples (b)

exposures of a DOC catalyst to high temperatures during operation can be detrimental and thus should be taken into consideration in developing durable DOCs. More detailed research on the behavior of PGM resulting from the thermal aging is still in progress.

Physicochemical Investigation of the Degradation Mechanism for SCR Catalysts

A commercial SCR catalyst (metal loaded zeolite) was thermally aged in a laboratory oven. Figure 4 shows GM-measured changes in the NOx conversion as a function of aging time at constant temperature, where activity is shown to decrease slowly up to the aging time of 24 hr. However, there is a drastic decrease in NOx conversion from 24 hr to 48 hr, and almost no activity was observed after aging for 48 hr, implying complete deactivation of the catalyst. We investigated the heavily aged sample by using scanning electron microscopy (SEM) and TEM. An SEM picture in Figure 5a clearly demonstrates that zeolite morphology becomes inhomogeneous, consistent with a collapse of the zeolite structure, as also confirmed by XRD measurements. In addition, agglomeration of metal

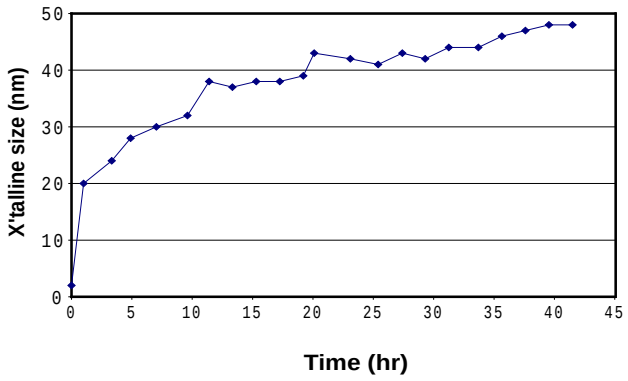

FIGURE 3. Changes in PGM particle size with aging time at 900°C, which are obtained by analyzing time-resolved XRD patterns.

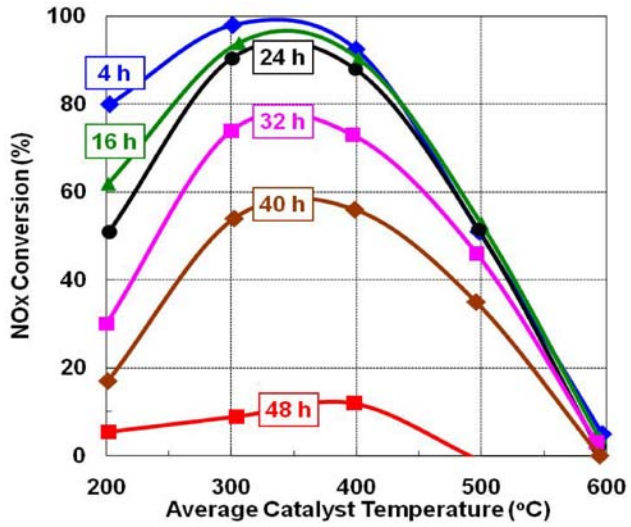

FIGURE 4. Changes in NOx Conversion over Aged Urea-SCR Catalysts as a Function of Aging Time

clusters are clearly seen in the TEM micrograph (in the circle) of Figure 5b, arising from the thermal aging process. This process is expected to have a negative effect on the catalytic activity due to significantly lower amounts of the active sites and greater consumption of the reductants (NH_3) by oxidation with O_2. Therefore, it can be summarized that the destruction of zeolite structure and the agglomeration of metal active site are indicated as the primary reasons for severe SCR catalyst deactivation, which is in good agreement with previous studies [2]. Currently, in order to obtain a quantitative relationship between activity and catalyst changes during the hydrothermal aging as a function of time and temperature, detailed catalyst characterization experiments focusing on molecular level active phase changes are underway.

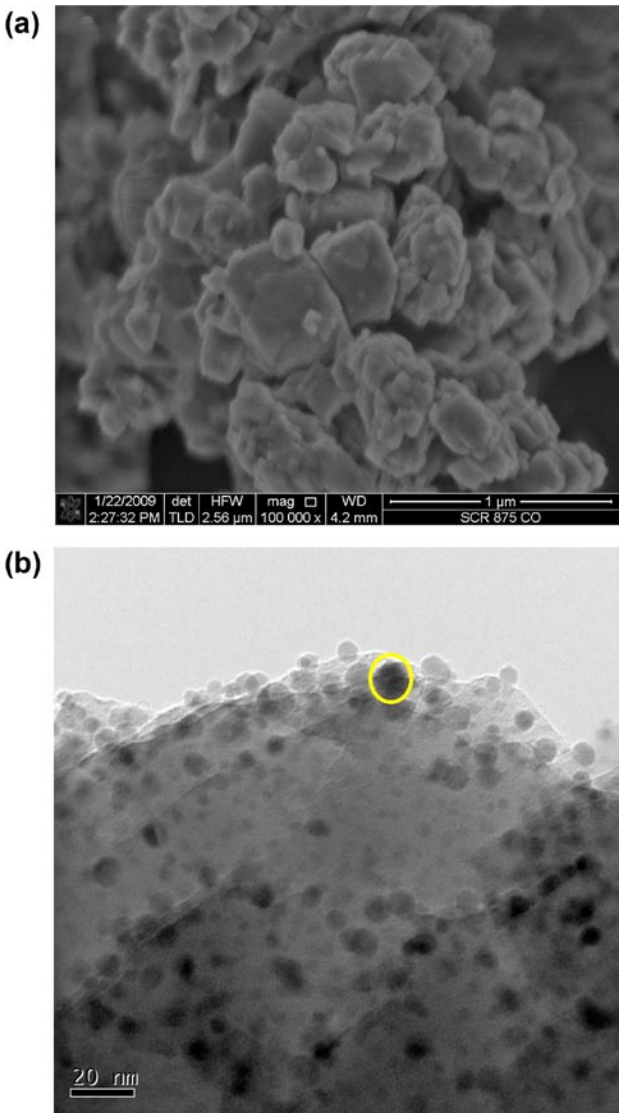

FIGURE 5. SEM (a) and TEM (b) Micrographs of a Heavily Aged Urea-SCR Catalyst

Conclusions

PNNL and GM are carrying out a project to study the mechanisms of deactivation of SCR and DOC materials arising from thermal aging. Results demonstrate that the growth of PGM in DOC catalyst is a primary cause of deactivation. For the case of the urea-SCR catalyst, both the collapse of zeolite structure and the growth of active metal particles are observed for a heavily aged sample and attributed to the main reason for the activity loss. We are currently pursuing a molecular-level understanding of the deactivation mechanisms related to the activity degradation by using a number of state-of-the-art catalyst characterization techniques.

References

1. D.H. Kim, Y.-H. Chin, G. Muntean, A. Yezerets, N. Currier, W. Epling, H.-Y. Chen, H. Hess and C.H.F. Peden, Industrial and Engineering Chemistry Research, 45 (2006) 4415.

2. J.Y. Yan, G.-D. Lei, W.M.H. Sachtler and H.H. Kung, J. Catalysis, 161 (1996) 43.

FY 2009 Publications/Presentations

1. D.H. Kim, C.H.F. Peden, Chang H. Kim, Steven J. Schmieg, and Se H. Oh, "Degradation Mechanisms of Urea Selective Catalytic Reduction Technology", presentation at the DOE Combustion and Emission Control Review, Washington, D.C., May, 2009.

II.B.14 Low-Temperature Oxidation Catalyst Development Supporting Homogeneous Charge Compression Ignition (HCCI) Development

Ken Rappe (Primary Contact), Liyu Li, Jonathan Male, Yu Su, Jamie Holladay
Pacific Northwest National Laboratory (PNNL)
Energy and Efficiency Science and Technology Division
P.O. Box 999 MS K6-28
Richland, WA 99354

DOE Technology Development Manager:
Ken Howden

Objectives

- Develop a novel oxidation catalyst applicable for the HCCI engine platform.
- Demonstrate carbon monoxide (CO) light-off via 50% oxidation at less than 150°C.
- Demonstrate CO oxidation via 99% oxidation at higher temperatures.
- Demonstrate hydrocarbon (HC) oxidation via 90% oxidation at 175°C and higher.
- Demonstrate HC light-off via 50% oxidation at less than 150°C.

Accomplishments

- Developed a novel oxidation catalyst platform based on the CeO_2 system with Pr inserted into the CeO_2 matrix.
- Demonstrated the basis behind the improved material performance via improved system reduction-oxidation (redox) capacity.
- Demonstrated the ability to oxidize CO at temperatures well less than 100°C.
- Demonstrated the ability to oxidize HC surrogates at lower temperatures.
- Demonstrated the ability to improve propane (HC surrogate) oxidation activity via novel catalyst pretreatment.
- Demonstrated the ability to assist in facilitating the HCCI engine platform via novel oxidation catalysis via CO oxidation and HC oxidation at lower temperatures.

Future Directions

- No additional work is planned under the effort.
- Significant control challenges currently face the HCCI engine development platform. Once rectified, a novel after-treatment oxidation catalysis platform such as this system needs to be demonstrated on an HCCI-configured engine over a range of transient and steady-state conditions to demonstrate both activity and durability.

Introduction

The diesel engine is currently the primary engine employed in the long- and short-haul commercial trucking industry. The attractive nature of the diesel engine primarily lies in attractive wear characteristics, high mileage, and ability to deliver power efficiently under high-load conditions.

HCCI is a combustion strategy that has gained a lot of interest recently in alleviating the significant NO_x and particulate emissions that burden the technology. However, HCCI results in elevated levels of products of incomplete combustion, including CO and various hydrocarbon species.

HCCI combustion poses inherent challenges to conventional low-temperature oxidation catalysis. The lower burn characteristics result in lower engine exhaust temperature profiles than is seen with conventional diesel engines. These lower exhaust temperatures are often below the light-off temperatures for conventional oxidation catalysts currently employed in after-treatment systems. Thus, this is the focus of the current body of work.

Approach

- Screen active work in novel oxidation catalysis development.
- Test representative samples of current systems under investigation to determine area for investigation.
- Develop novel oxidation catalyst platform based upon results in the aforementioned screening effort.
- Develop structure-activity relationships for the system under investigation.

Results

Road-mapping efforts identified areas under current study in the literature holding potential for improved low-temperature CO and HC catalytic oxidation. An extensive catalyst formulation and screening effort was undertaken consisting of quickly testing representative samples of the various systems identified in the literature

review. The purpose of the screening effort was to identify systems that showed promise and warranted further investigation for low temperature CO and hydrocarbon catalysis.

Results of the screening efforts demonstrated that the systems holding the most promise and warranting further interrogation included the CeO_2 systems (Pt and Pd) and the multi-component Pt systems that included CeO_2 (excluding the $Ce_{0.7}Sn_{0.3}O_2$ system). For this reason, CeO_2 systems were examined further in the project.

2%Pd/CeO_2 was employed as the focus of the CeO_2–system study. These investigations included investigating the effect of the Pd source as well as effect of the CeO_2 source. Remarkable improvements were made in the lower temperature activity of the Pd/CeO_2 system (CO and C_3H_6), whereas little improvement was made with higher temperature activity (C_3H_8 and CH_4). For this reason, the next phase of the effort focused on improving the higher temperature activity of the system (i.e. improving the C_3H_8 and CH_4 activity).

In an attempt to improve the high-temperature activity of the system, Pr was employed via blending into the CeO_2 matrix. The motivation behind this lies with the knowledge that insertion of transition metals (e.g. Pr, Tb) into the CeO_2 matrix has previously demonstrated improved low-temperature redox capacity [1,2].

Figure 1 shows the CO, C_3H_6, C_3H_8 and CH_4 results [at 240 L/(g-hr)] of eight catalysts prepared with varying amounts of Pr inserted into the CeO_2 matrix (from 0% to 100%). The CO and C_3H_6 activity of the system decreased steadily with increasing amounts of Pr blended into the CeO_2 matrix. This effect, however, was fairly subtle with up to 10% PrO_2 blended into the CeO_2 matrix. In comparison, the C_3H_8 and CH_4 activity peaked at 10-20% PrO_2. A 0.1:0.9 molar ratio of Pr:Ce blended into the CeO_2 support matrix was identified as optimum for improved C_3H_8 and CH_4 activity.

Figure 2 shows the Brunauer-Emmett-Teller (BET) results for the 2%Pd/$Ce_XPr_{1-X}O_2$ system, representing the same eight catalysts as discussed in the activity results above. Results shown include total surface area (m^2/g), average pore size (nm), and pore volume (cm^3). The results show a small effect of increasing amounts of Pr on the total surface area of the system up to 20% blended into the CeO_2 matrix. Past 20%, a significant loss in surface area is seen with the system. Similarly, the BET results in Figure 2 show a small effect of small amounts of Pr (up to 20% Pr) on the average pore size of the system. Additionally, similar to the surface area, a significant increase in the average pore size is seen with Pr levels greater than 20%. The pore volume of the system, in contrast to the surface area and average pore size of the system, reaches a maximum at 10% Pr and decreases with Pr loadings less than or greater than this.

Figure 3 shows the pore size distribution results for the 2%Pd/$Ce_XPr_{1-X}O_2$ system. Figure 4 shows the results for 0%, 10%, and 20%, 30%, 50%, and 100% Pr, with 0% Pr shown for reference. The results show that up to 20% Pr has little effect on the pore size distribution of the system. There does appear to be a slight decrease in the pore size maxima, and Pr does appear to bring in larger pores asymmetrically, but both of these effects are quite subtle. In contrast, the results show that Pr amounts greater that 20% in the CeO_2 matrix has a drastic effect on the pore size distribution. The result is a significant decrease in the maxima (eliminating the maxima altogether) and drastic broadening of the distribution to larger pores asymmetrically. In comparison to 20% Pr and lower, it appears that significant structure change occurs when greater than 20% Pr is blended into the system. It is not evident yet what this structure change is

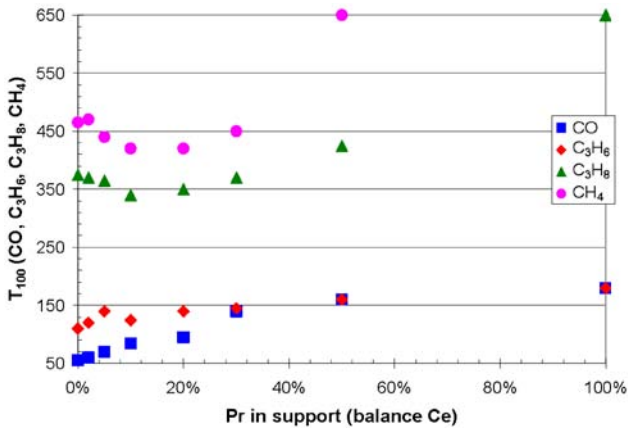

FIGURE 1. Summary of T_{100} temperatures at 240 L/(g-hr) space velocity for CO, C_3H_6, C_3H_8, and CH_4 on 2%Pd/$Ce_XPr_{1-X}O_2$ where X = 1, 0.98, 0.95, 0.9, 0.8, 0.7, 0.5, and 0.

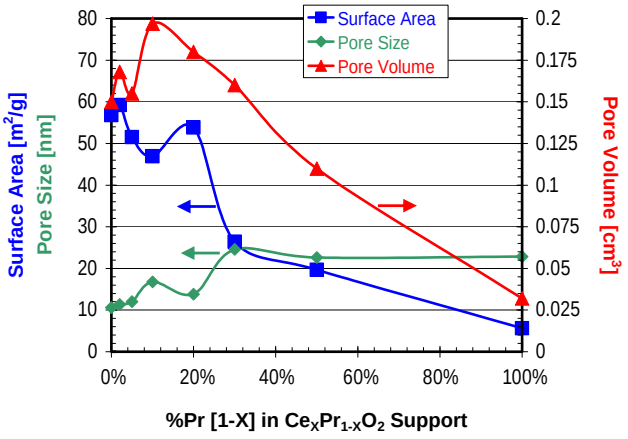

FIGURE 2. Summary of BET results presented as total surface area, average pore size, and total pore volume for 2%Pd/$Ce_XPr_{1-X}O_2$ where X = 1, 0.98, 0.95, 0.9, 0.8, 0.7, 0.5, and 0.

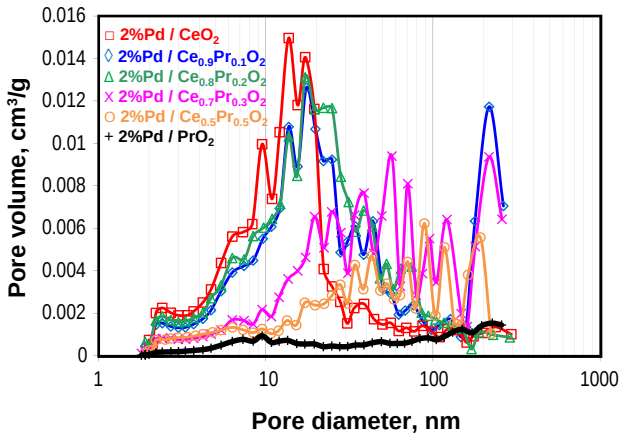

FIGURE 3. Pore size distribution summary for 2%Pd/$Ce_XPr_{1-X}O_2$ where X = 1, 0.9, 0.8, 0.7, 0.5 and 0.

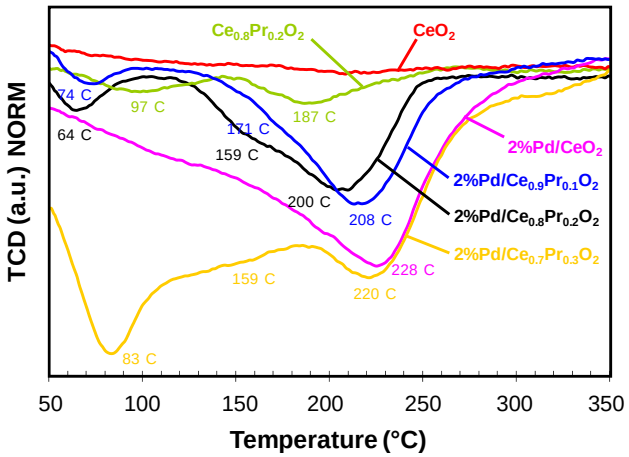

FIGURE 4. Results of TPO studies on CeO_2 and $Ce_{0.8}Pr_{0.2}O_2$ supports, 2%Pd/$Ce_{0.7}Pr_{0.3}O_2$ catalyst, 2%Pd/$Ce_{0.8}Pr_{0.2}O_2$ catalyst, 2%Pd/ $Ce_{0.9}Pr_{0.1}O_2$ catalyst, and 2%Pd/CeO_2 catalyst, presented as normalized thermal conductivity detector (TCD) response versus temperature.

a result of (new phase, structure collapse, etc.), but it is definite and significant.

The X-ray diffraction (XRD) measurement results for the 2%Pd/$Ce_XPr_{1-X}O_2$ system show that Pr blends into the CeO_2 matrix as PrO_2 up through 50% Pr. However, in the absence of CeO_2 in the matrix, Pr naturally forms $PrO_{1.83}$. This is important, as an atom that naturally forms a 1:1.83 ratio oxide, now present in an oxide matrix at a 1:2 oxide ratio, would definitely have improved redox capacity. Thus, we see evidence as to the reason behind the improved oxidation performance for the CeO_2 system with small amounts of Pr blended into the oxide matrix. However, we would also expect to see a weakening of the structure. The cubic structure cell parameter for the system shows the crystal cell structure swell slightly but definitely with 10% Pr blended into the system, and swell even greater with 20% Pr blended into the system. Then, the mixed oxide with greater than 20% Pr present in the system (i.e. 30% and 50% Pr) shows the crystal structure shrink back down in size. It is important to keep in mind that the Pr is present as PrO_2 in the structure. Only with pure PrO_2, which forms Pr_6O_{11}, do we see a significant change in the structure.

The results from Figures 1 through 3 suggest that significant and drastic changes are occurring to the Ce/Pr mixed oxide structure between 80% Ce/20% Pr and 70% Ce/30% Pr. The changes that occur to the 70% Ce/30% Pr catalyst versus the 80% Ce/20% Pr catalyst suggest that the stress the PrO_2 puts on the CeO_2 matrix becomes too great. It is obvious from the characterization results that the structure suffers significant collapse. Thus, with the $Ce_XPr_{1-X}O_2$ system, there is obviously a trade-off between improved redox capacity and crystal structure stability.

Figure 4 shows the temperature programmed oxidation (TPO) results for the 2%Pd/$Ce_XPr_{1-X}O_2$ system. Comparison of the CeO_2 and $Ce_{0.8}Pr_{0.2}O_2$ results show Pr oxidation features at 97° and 187°C, likely corresponding to surface- and bulk-Pr species. Comparison of the CeO_2 and 2%Pd/CeO_2 results show a very large and broad Pd oxidation feature at 228°C. Comparing this information with the results from 2%Pd/$Ce_{0.8}Pr_{0.2}O_2$, and 2%Pd/$Ce_{0.9}Pr_{0.1}O_2$ shows effects to both the Pd and the Pr oxidation features. The Pd oxidation feature decreases in temperature from 228°C to 208°C and 200°C with 10% and 20% Pr blended into the CeO_2 matrix, respectively. This indicates improved oxidation capacity present between the Pd metal and the support with the presence of Pr. Similarly, the surface- and bulk-Pr oxidation features at 97°C and 187°C decrease in temperature to 74°C and 171°C at 10% Pr, and to 64°C and 159°C at 20% Pr. The improved oxidation capacity of both the Pd metal as well as the surface- and bulk-Pr species clearly suggest an increased synergistic effect of Pr blended into the CeO_2 matrix.

Figure 5 shows the H_2 chemisorption results for the 2%Pd/$Ce_XPr_{1-X}O_2$ system, presented as both milliliters (mL) of H_2 chemisorbed per gram (g) of Pd metal as well as theoretical metal dispersion. The synergistic effect of the presence of Pr in the matrix is again evident from the H_2 chemisorption studies, an effect which is lost at >20% Pr blended into the system. Results show >100% effective metal dispersion at 90% Ce/10% Pr and 80% Ce/20% Pr, an effect which can be attributed to the well known H_2 spill-over effect [3]. Again, these results indicate improved interaction between the Pd metal and the support with the presence of Pr. This suggests an improved system with optimal metal–support interaction.

The results demonstrate that the improved propane and methane activity results can be attributed to the

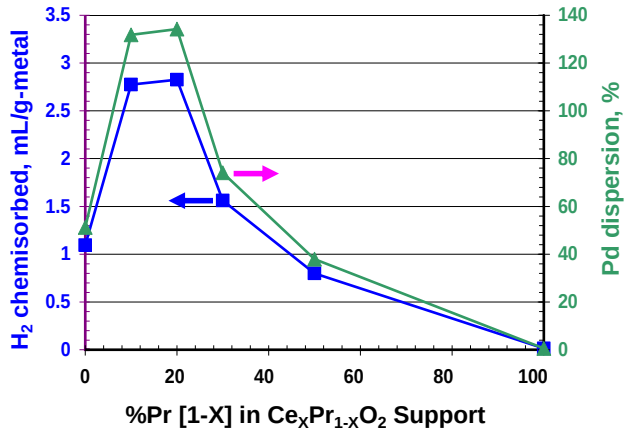

FIGURE 5. Summary of H_2 chemisorption studies, presented as mL H_2 chemisorbed (0°C, 1 atm) per gram of metal, and effective percentage palladium metal dispersion, for 2%Pd/$Ce_XPr_{1-X}O_2$ where X = 1, 0.9, 0.8, 0.7, 0.5, and 0.

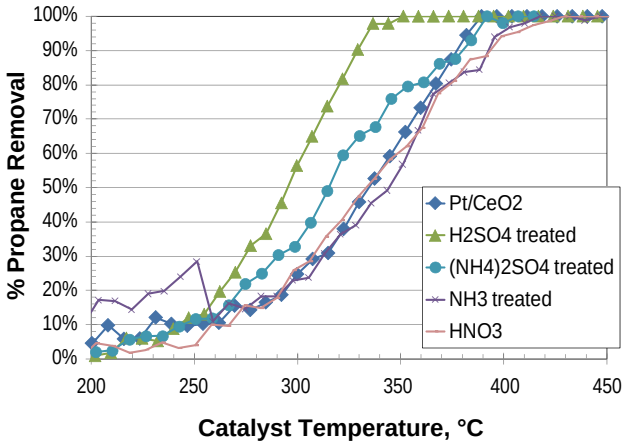

FIGURE 6. Effect of pretreatment on the propane activity of the 2%Pt/$Ce_{0.9}Pr_{0.1}O_2$ catalyst.

improved redox capacity of the catalytic system via the stable insertion of Pr into the CeO_2 matrix. When present in stable proportions, Pr allows more effective oxygen transport between the metal and the support. The key here appears to be the ability to insert Pr and maintain the structural properties of the support system. The decreased CO and C_3H_6 activity of the system is likely attributed to the slight reduction in surface area of the system. These results suggest that a method which allows larger amounts of Pr inserted into the CeO_2 matrix while maintaining a stable oxide matrix would prove valuable, and could lead to further improvement of propane and methane activity.

The 2%Pt/$Ce_{0.9}Pr_{0.1}O_2$ system was employed for investigating the effect of different pretreatments on the propane catalytic activity of the system. The four pretreatments employed were H_2SO_4, HNO_3, NH_3 and $(NH_4)_2SO_4$. Figure 6 shows the catalytic activity results for the four pretreated samples as well the original untreated sample. NH_3 and HNO_3 pretreatment had very little effect on the propane activity of the system. However, H_2SO_4 and $(NH_4)_2SO_4$ pretreatment significantly improved the propane activity of the system, with the H_2SO_4 pretreated sample having the greatest activity.

Conclusions

HCCI is presented as a "high-efficiency clean combustion technology" because of its ability to significantly minimize NO_X and PM engine emissions, which have historically posed the greatest barrier(s) to the diesel engine in the U.S. marketplace. In the efforts discussed above, PNNL has demonstrated (via novel oxidation catalyst development) the ability to mitigate the inherent and unique engine emission challenges that currently face HCCI combustion strategies, helping to facilitate its applicability and ultimate implementation. Engine testing performed at Caterpillar shows that this can be accomplished with less platinum group metal requirements versus comparable supplier catalysts, helping to achieve engine cost requirements in addition to emission target requirements.

References

1. Ferrer, V, A Moronta, J Sanchez, R Solano, S Bernal, D Finol. *Cat. Today*. **2005**, 107-8, 487-492.

2. Logan, AD, and M Shelef. *J. Mat. Res.* **1994**, 9 (2), 468-475.

3. Gatica, JM, RT Baker, P Fornasiero, S Bernal, J Kaspar. *J. Phys. Chem*. B. **2001**, 105 (6), 1191-1199.

FY 2009 Publications/Presentations

1. "Low Temperature Hydrocarbon/CO Oxidation Catalysis in Support of HCCI Emission Control," poster presentation given at the 2009 U.S. DOE Hydrogen Program and Vehicle Technologies Program Annual Merit Review, Washington, D.C.

Special Recognitions & Awards/Patents Issued

1. Pacific Northwest National Laboratory has submitted an invention disclosure report, titled, "Low Temperature Oxidation Catalyst for Homogeneous Charge Compression Ignition Emission Reduction."

II.C.1 Exhaust Energy Recovery

Christopher R. Nelson
Cummins Inc.
1900 McKinley Ave.
Columbus, IN 47203

DOE Technology Development Manager:
Roland Gravel

NETL Project Manager: Carl Maronde

Objectives

- Improve engine fuel efficiency by 10% through the recovery of waste heat energy.
- Reduce the need for additional cooling capacity in Class 8 trucks.
- Provide conditioning (cooling) for combustion charge air.

Accomplishments

- Successfully operated the engine and energy recovery system in a performance test cell. This was the first Cummins on-engine, R245fa-based, organic rankine cycle (ORC) energy recovery system. Successfully demonstrated the system's predicted 8% fuel economy benefit from exhaust gas recirculation (EGR) and exhaust gas energy recovery.
- Met the program goal of 10% fuel efficiency improvement through the recovery of waste heat energy when combined with the benefit of electric engine parasitics.
- Demonstrated a system which mitigates the need for increased cooling capacity in Class 8 trucks.
- Demonstrated a system which provides conditioning of combustion charge air.
- Demonstrated effective controls to operate the energy recovery system through all engine operating conditions.
- Refined the energy recovery system components and subsystems to minimize cost, complexity, and improve performance.
- Established and executed a second-generation system for test in the coming year.

Future Directions

Continued effort is planned in the pursuit of an effective and efficient ORC waste heat recovery (WHR) system. Activities to date have successfully demonstrated the predicted fuel efficiency benefit of this concept. Future work is focused on enhancing performance and refining system architecture to be integrated into Cummins' future products. During 2010, we expect to:

- Proceed with second-generation system hardware testing and demonstration. Second-generation hardware incorporates production-intent design features.
- Demonstrate additional fuel economy benefit from also recovering heat from compressed fresh charge air.

This cost-shared project will be concluded at the end of March, 2010.

The ORC WHR concept introduces a significant number of new and different technologies into the engine systems which Cummins Inc. has traditionally pursued. Successful system integration for practical implementation will continue to require that subsystem architectures be carefully reviewed for their effect on the overall engine, driveline, and vehicle.

Introduction

With the advent of low-NOx combustion techniques using cooled EGR, engine heat rejection increased, driving cooling package size 'in vehicle' to its limit. A means to mitigate this increased heat rejection is desired to avoid increasing the size of vehicle cooling packages. A solution which serves this purpose while also providing operating efficiency benefits would be ideal. Application of an ORC to an engine's waste heat streams which already require cooling offers this ideal solution.

The ORC is essentially a 'steam power plant' thermodynamic cycle wherein a working fluid (akin to water) is heated to boiling and superheated (heated beyond boiling). Thereafter, the superheated fluid is passed through an expansion device where it releases its energy to create mechanical power. When an ORC is applied to an engine's waste heat streams, the additional power it generates is added to the engine's performance for the same amount of fuel burned, improving economy and reducing emissions (CO_2 reduction). Using the ORC to extract useful energy reduces the amount of heat which must be rejected and minimizes cooling package size.

In the current work, heat energy is recovered from the engine's EGR stream and compressed, fresh charge air stream. Conversion of that heat to power relieves

the engine's cooling system of a significant amount of load. As the heat rejection system must be designed to discard heat at maximum performance conditions, it is over-designed for off-peak operation. During off-peak operation, the excess capacity is utilized by recovering additional energy from the main exhaust gas stream. In this manner, the heat rejection system is more fully utilized and maximizes the benefit of the energy recovery system.

Approach

Cummins' approach to the program objectives emphasizes analysis-led-design in nearly all aspects of the research. An emphasis is placed on modeling and simulation results to lead the way to feasible solutions.

With the advent of cooled EGR-based combustion technology, the need to provide an effective cooling system for combustion charge conditioning has become vital. The additional cooling required for EGR and fresh charge air to thereby achieve low intake manifold temperatures (to support clean combustion) has driven an increase in vehicle cooling system performance. An ORC extracting heat energy from the engine's EGR and charge air streams reduces the heat load on the engine system cooling package and simultaneously provides extra power for the engine system.

The first-generation recovery system utilized a turbine-type ORC expander directly coupled to a high speed electric generator. High-voltage, high frequency power from the generator was appropriately conditioned to drive a flywheel-integrated motor-generator (FMG) to thereby supplement engine brake power. The presence of a high-voltage (340 VDC) power system on-engine allowed inclusion of previously demonstrated fuel economy benefits (an additional 2%) from electric parasitics (such as electrically driven water pump, air compressor, air conditioning compressor, power steering pump, etc.).

Second-generation system design seeks to reduce cost and complexity. The ORC turbine-expander will be coupled to the engine's crankshaft through a speed-reducing gearbox, eliminating the cost and complexity of the high-speed electric generator, the power conditioning hardware, and the FMG. This mechanical implementation of the ORC concept will avoid electric power conversion losses and slightly improve ORC efficiency.

Results

During the year, testing of first-generation hardware was completed which demonstrated predicted performance. Working from this experience, a second-generation system was devised to reduce system cost/complexity and improve robustness/durability.

Hardware Test Results

Figures 1 presents the first-generation system hardware performance results when recovering energy from both EGR and engine exhaust gas.

As shown in Figure 1, first-generation, ORC-based energy recovery hardware applied to a 2010-based Cummins ISX heavy-duty diesel engine provided a 7.4% fuel efficiency improvement across the Heavy Duty Corporate Composite (HDCC) operating cycle. The ISX engine used in this portion of the study did not require NOx reducing aftertreatment to meet 2010-intent emissions performance and a high rate of EGR was available for energy recovery.

The demonstrated benefit was slightly below 8% as predicted through model-based analysis. This was due to greater than anticipated flow restrictions within the ORC system plumbing and additional parasitic losses (windage) in the system's generator. It is reasonable to assume that refined engineering development of first-generation hardware would eliminate these losses and allow the system to achieve its predicted performance. The above results include consideration of a system condenser which is appropriately sized for a 2007 model year, Class 8 truck-tractor. Also, as first-generation system architecture included a high-voltage electric power system, an additional 2% fuel efficiency benefit from the use of electrically-driven engine parasitics can be included in the results to achieve the program's 10% fuel efficiency improvement target.

Second-Generation System Design and Development

Moving forward from test experience, a second-generation system was developed which significantly reduced the potential production cost of the ORC-based energy recovery system. The high-speed electric generator, power conditioning electronics, and flywheel-integrated motor-generator were replaced by a gearbox which couples the ORC expander-turbine to the engine's crankshaft. Anticipated power transmission parasitic losses through this arrangement are expected to be less than those experienced with the electrically-based system.

A significant amount of work occurred during the year to prove out concepts which will insure robust system operation in-vehicle. Configuration of the system's condenser and feedpump were found to be critical during testing to insure continuous system performance through all operating conditions. Several arrangements were devised, modeled, and tested on-bench. In several instances, experimentation led modeling as transient simulation models of ORC systems were not widely available.

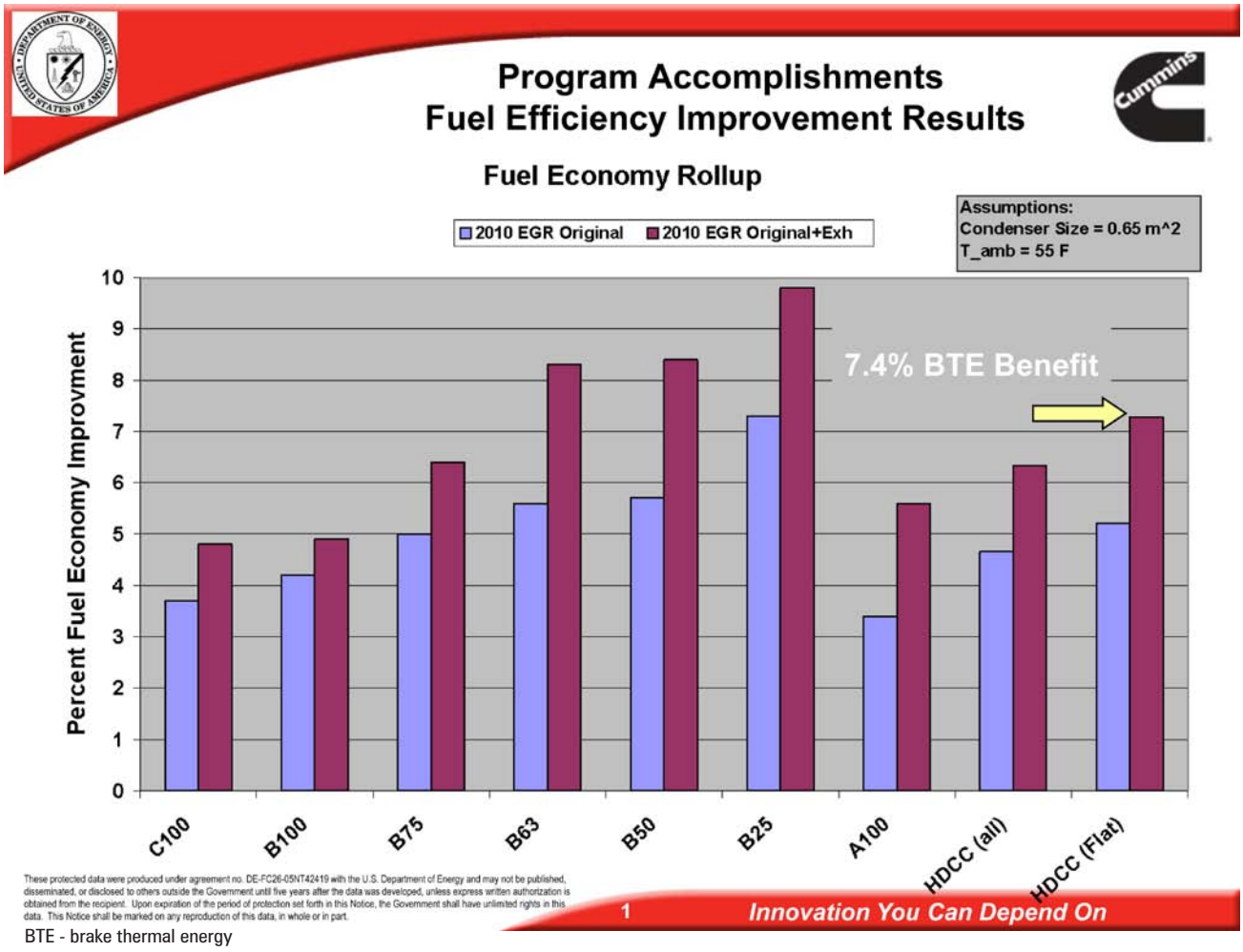

FIGURE 1. Performance of the First-Generation Cummins ISX-Based ORC Energy Recovery System

Conclusions

A tremendous amount of progress has been achieved by this project. It has successfully demonstrated the potential of ORC-based energy recovery when applied to on-highway, heavy-duty diesel engines. The fuel economy potential and emissions reduction potential of this technique have been recognized.

- The program's 10% efficiency improvement goal has been demonstrated. Model-based performance predictions were met and validated.
- Hardware testing provided a solid foundation to proceed towards next-generation hardware. First-generation hardware effectively demonstrated the practicality of an on-engine, ORC-based, energy recovery system.
- Robust system controls were developed and demonstrated. These will be further refined and applied to the next generation system hardware.

FY 2009 Publications/Presentations

1. 2009 DEER Conference Presentation – "Exhaust Energy Recovery", presented by Christopher R. Nelson, August, 2009.

II.C.2 An Engine System Approach to Exhaust Waste Heat Recovery

Rich Kruiswyk
Caterpillar Inc.
P.O. Box 1875
Mossville, IL 61552-1875

DOE Technology Development Manager:
John Fairbanks

NETL Project Manager: Carl Maronde

Subcontractors:
- Alipro, Peoria, IL
- ConceptsNREC, Oxon, UK
- eServ, Peoria, IL
- Turbo Solutions, Norwich, VT
- Barber-Nichols Inc., Arvada, CO

Objectives

Overall Objective:

- Develop a new air management and exhaust energy recovery system that will demonstrate a 10% improvement in overall thermal efficiency with no emissions increase.
- Demonstrate the resulting system and the efficiency benefits on a laboratory engine.

Phase III Objective:

- Demonstration of significant progress (+5-10%) in thermal efficiency improvement via testing and analysis of prototype components. This will include an on-engine system demonstration of prototype hardware.

Accomplishments

- Demonstrated a production-viable version of a novel nozzled/divided turbine stage on a turbocharger gas stand. An improvement of approximately 6% in turbine efficiency was demonstrated relative to the baseline production turbine stage.
- Demonstrated a second-generation mixed-flow turbine design on a turbocharger gas stand. An improvement in turbine efficiency of 6-8% over the first-generation design was demonstrated. An improvement in turbine efficiency of approximately 2% was demonstrated relative to the baseline production turbine stage.
- Demonstrated a high efficiency, highly backswept compressor stage on a turbocharger gas stand. An improvement of 1-1.5% in compressor efficiency was demonstrated relative to the baseline production compressor stage.
- Completed detailed design and procurement for high efficiency compressor and turbine stages for the low-pressure stage of the series turbocharged demo engine. Gas stand testing will happen in the fourth quarter of 2009.
- Developed and implemented a new test methodology which enables the testing of turbocompound power turbines on the gas stand rather than on-engine. The new test method facilitates the measurement of detailed aerodynamic and rotordynamic performance of the power turbine. This new test method is now being used for the evaluation of alternate power turbine bearing systems with the goal of identifying an optimum system.

Future Directions

The Phase III objective is to demonstrate significant progress toward the goal of a 10% improvement in thermal efficiency using prototype components. There will be two elements to this demonstration:

- An on-engine demonstration of a 5 to 7% improvement in thermal efficiency using advanced turbocharger technologies, intercooling, insulated exhaust ports, and mechanical turbocompound.
- Parallel developments of technologies for future integration into the system solution, including the mixed flow turbine and electric turbocompound.

Introduction

On today's heavy-duty diesel engines approximately 25% of the fuel energy leaves the exhaust stack as waste heat. Consequently, recovering energy from the diesel engine exhaust should pay significant dividends in improving diesel engine fuel efficiency. In this project Caterpillar is developing practical and production-viable solutions for improving waste heat recovery from heavy-duty diesel engines, with a goal of demonstrating a 10% improvement in thermal efficiency over today's production engines. Emphasis is placed on developing and incorporating cutting edge technologies that meet demanding cost, packaging, and drivability requirements, and that are compatible with anticipated future aftertreatment needs. Technologies under investigation include high-efficiency turbochargers, turbogenerators,

advanced bearing systems, and effective engine insulating components.

Approach

Achieving a 10% improvement in engine thermal efficiency via improved waste heat recovery is a very challenging goal. The Caterpillar team determined that achieving this goal with a practical and production-viable solution would require a system approach. This means developing technologies that will reduce all forms of exhaust energy loss, including: blowdown losses, aero machinery losses, fluid frictional losses, losses due to pulsating exhaust flow, heat transfer losses, and losses of energy out the exhaust stack. The team makes use of Caterpillar's advanced engine simulation and test capabilities to determine the performance targets of the individual components in the system. Detailed component design, analysis, and testing are then used to verify that these performance targets can be met. Consultation with outside technical experts is used to help push the envelope of component capabilities.

Results

The Caterpillar recipe for achieving a 10% improvement in engine thermal efficiency breaks down as follows: +4% from implementation of turbocompound to recover stack waste heat, +3.7% from improving turbocharger efficiencies, +1.3% from intercooling the series turbocharging system, +0.5% from insulating the engine exhaust ports, and +0.5% from reducing exhaust piping flow losses. In addition, investigation of methods to recover waste heat from high-pressure loop exhaust gas recirculation (EGR) streams is underway. Progress in these areas is reported in the following:

Turbocompound Development: A high efficiency bearing system has been designed for a mechanical turbocompound power turbine unit. Changes to the bearing design and transmission gearing were incorporated to improve the power turbine rotordynamic behavior and to eliminate failure modes observed on the previous generation design. A new test methodology has been developed that enables the testing of the power turbine on a turbocharger gas stand for detailed rotordynamic and aerodynamic evaluation. Measurements of several bearing system alternatives are currently underway.

High Efficiency Turbomachinery: A novel high-efficiency turbine with a nozzled/divided turbine housing was tested that demonstrated turbine efficiency improvements of 5-6% over today's current production high-pressure turbine stage (see Figure 1). This demonstration utilized a second-generation design believed to be suitable for volume production. On-engine investigations of this technology are currently underway.

A second-generation mixed-flow turbine stage has been designed, procured, and tested on the Caterpillar gas stand. The peak turbine efficiency was approximately 2% higher than the current production turbine stage, with an efficiency characteristic better suited for on-engine exhaust pulse energy utilization (see Figure 2). An on-engine demonstration is planned for fourth quarter of 2009.

A high-efficiency, highly-backswept compressor stage has been designed, procured, and tested on the Caterpillar gas stand. The peak compressor efficiency was approximately 1-1.5% higher than the current production compressor stage, short of the target of a 2-3% improvement. Detailed analysis of the results is underway to determine the pathway to further improvements.

Waste Heat Recovery from High Pressure Loop EGR Streams: Future low-emissions engine solutions,

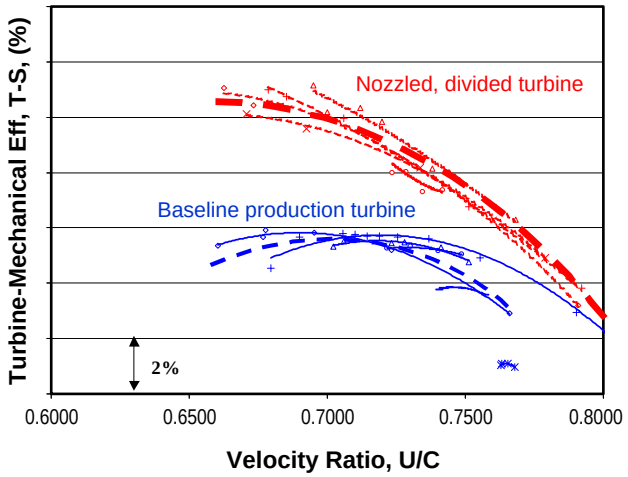

FIGURE 1. Gas Stand Result – Radial Nozzled Turbine Stage

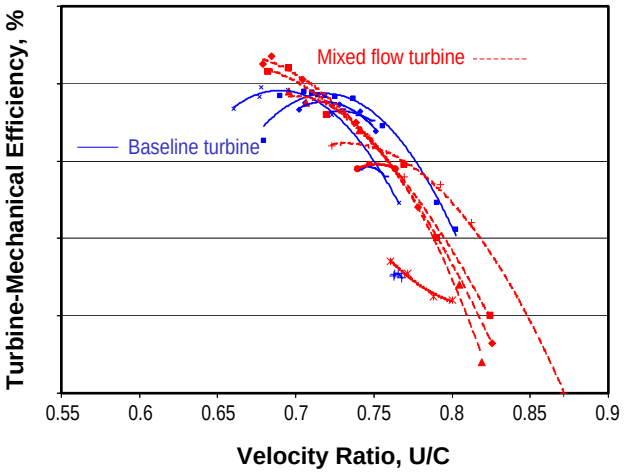

FIGURE 2. Gas Stand Result – Mixed Flow Turbine Stage

such as certain high-efficiency clean combustion solutions, may benefit from the inclusion of a high-pressure loop EGR stream. In-depth analysis on the benefits of turbocompound as an efficient high-pressure loop EGR driver are ongoing – preliminary results indicate that the use of turbocompound as an EGR driver can offer significant efficiency benefits relative to methods commonly used in production today, such as variable geometry turbines, backpressure valves, and asymmetric turbines.

Conclusions

The results of components tests, component design and analysis, and engine simulation has resulted in high confidence that the project goal of a 10% improvement in engine thermal efficiency can be achieved. A predicted system-level benefit of 8.0% is solidly based on a combination of:

- Components for which performance has been demonstrated via bench tests of prototype hardware.
- Components for which performance has been predicted from design/analysis tools. In these cases confidence is bolstered by the similarity of these components to prototypes that have been demonstrated in hardware as part of prior research programs.

Additional technologies are under investigation and show promise for further improvements, thus leading to the conclusion that the 10% target can be met.

FY 2009 Publications/Presentations

1. Presented on 21 May 09 at the U.S. DOE Merit Review, Washington, D.C.

2. Presented on 5 Aug 2009 at the U.S. DOE Diesel Engine-Efficiency and Emissions Research (DEER) conference, Dearborn, MI.

II.C.3 Very High Fuel Economy, Heavy-Duty, Narrow-Speed Truck Engine Utilizing Truck Engine Utilizing Biofuels and Hybrid Vehicle Technologies

Chun Tai (Primary Contact), Hyungsuk Kang
Volvo Powertrain North America
13302 Pennsylvania Avenue
Hagerstown, MD 21742

DOE Technology Development Manager:
Roland Gravel

NETL Project Manager: Samuel Taylor

Subcontractors:
- AVL North America, Plymouth, MI
- Ricardo North America, Belleville, MI and Burr Ridge, IL
- Southwest Research Institute® (SwRI®), San Antonio, TX
- Volvo Powertrain, Goteborg, Sweden
- Volvo Technology AB, Goteborg, Sweden

Objectives

- Develop a highly efficient engine system, including mild hybridization, to reduce carbon dioxide (CO_2) emissions from a long haul truck by >10%, in comparison to current production technology, while meeting U.S. 2010 emission levels.
- Develop an engine platform that is capable and tolerant of biodiesel specifications.
- Develop multi-fuel vehicles and drivetrains that are compatible with the long-term use of combinations of fossil and bio-based diesel fuels.

Accomplishments

- Simulation has shown that a narrow speed band turbocompound engine can achieve a 5 gm/kW-hr fuel consumption reduction over a typical European long haul cycle.
- Ultra-high injection pressures ranging from 1,300 – 5,000 bar were investigated in a Volvo D12 (12 L) engine and by the use of computational fluid dynamics (CFD) analysis. It was found that higher injection pressures were effective in reducing soot but produced an increase in NOx emissions.
- Combustion system development to improve the specification for a narrow-speed turbocompound engine was carried out in a single-cylinder D13 (13 L) engine, supplemented and guided by CFD calculations. Different hardware configurations involving the number of nozzles, flow rate, spray angle, cam rate and compression ratio were investigated. The optimal configuration produced a 0.6% reduction in brake specific total fuel consumption, BSTC, (which includes penalty for urea consumption) compared to the U.S. 2010 baseline.
- A Volvo D13 engine was modified and tested at SwRI® to run at stoichiometric conditions with a three-way catalyst (TWC). The feasible load range was limited to 25% - 50% of full load due to the thermal limits of exhaust system components. The diesel particulate filter (DPF) operates satisfactorily during stoichiometric operation, although appropriate regeneration strategies need to be developed. The TWC is effective in reducing NOx emissions to low levels. Relative to a conventional lean diesel baseline, fuel consumption is high due to throttled and rich operation.
- Basic layouts of different waste heat recovery (WHR) power transmissions have been developed and theoretical analyses are ongoing. An electric turbocompound engine is being tested and optimized for best fuel economy. The engine and an integrated starter-alternator-motor have been functionally linked and control strategies have been developed. A complete powertrain has been built and is being tested.
- Single-cylinder engine tests of the combustion properties of pure Swedish Environmental Class 1 (EC1) diesel fuel (<10 ppm sulfur, by weight) have established a baseline for studying the effects of blending of fatty acid methyl ester (FAME) biofuels into diesel fuel. A variety of blends of FAME biofuels in EC1 diesel and 100% biofuel have been tested. Blending FAME biofuels into diesel fuel reduces soot emissions, with increasing fractions of FAME fuel resulting in decreased levels of soot.

Future Directions

- Phase 2: Development of engine/transmission hardware/software design specifications and preparation for prototype procurement.
- Phase 3: Engine/transmission hardware/ software development, testing and verification of components.
- Phase 4: System assembly and vehicle verifications on bio-fuels.

Introduction

This project, referred to as the Bilateral Program, is a cost-shared effort being conducted by the Volvo Powertrain North America division of Mack Trucks, Inc. (a unit of Volvo AB) and Volvo AB of Sweden. It is jointly funded by the U.S. Department of Energy and the Swedish Energy Agency. The overarching goals are the reduction of petroleum consumption and a reduction in both regulated emissions (hydrocarbons [HC], carbon monoxide [CO], oxides of nitrogen [NOx] and particulate matter [PM]) as well as greenhouse gases (GHG), mainly CO_2, from heavy-duty diesel engines in the truck fleet. To that end, an extensive set of technologies is being studied and developed which can be implemented and integrated as a system into heady-duty vehicles. The major areas of focus include the development of a very high efficiency powertrain system, including an optimized narrow-speed turbocompound engine, an automated powershift transmission and mild hybridization, as shown in Figure 1. An additional area of focus is the adaptation of the diesel engine for the use of biofuels, primarily FAME fuels, and blends of FAME biofuels with conventional petroleum-based diesel fuel.

Approach

The effort directed at developing a highly efficient powertrain system includes fundamental combustion investigations such as the effect of diesel injection pressure and rate shaping to be implemented in an engine designed to operate within a narrow speed range, allowing further optimization of fuel efficiency and emission control. As part of this work, operation of the engine at or near stoichiometry ($\lambda \sim 1$) with the use of a TWC has been quantified. In addition to the development of the reciprocator itself, exhaust WHR is being utilized to further improve net engine output efficiency. Two different WHR concepts have been investigated – capturing exhaust energy through a turbine located in the hot exhaust stream (turbocompound) and the use of a Rankine bottoming cycle, based on exhaust energy, to power a turbine. Both WHR systems can produce energy in either mechanical form or, using a conversion device, in electrical form for storage. Hybrid components and features are included in the powertrain concept allowing for engine shutdown at idle and the recovery of inertial energy of the vehicle during deceleration. Finally, a fully automated powershift transmission is being developed so that the engine can be more effectively operated under optimal conditions and, also, to reduce the losses in the driveline between the engine output and the production of tractive force at the tire-road interface. Figure 2 shows the targeted contributions to energy efficiency improvement from the various technologies which are incorporated.

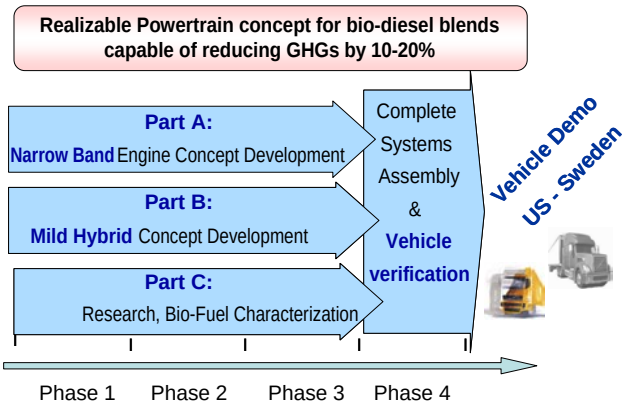

FIGURE 1. Bilateral Program Elements and Workflow

Although a variety of fuels have been evaluated, the biofuel research has concentrated on the testing of FAME fuels, both pure and in blends with a standardized EC1 fuel, containing less than 10 ppm sulfur (by weight). Systematic single-cylinder tests have been carried out to determine thermal efficiency, combustion characteristics, regulated and unregulated emissions as well as the trade-off between brake specific NOx and soot and between brake specific fuel consumption (BSFC) and brake specific NOx. These test were conducted in parallel with injection simulation and combustion CFD calculations but were limited in their usefulness by the absence of available detailed chemical kinetic mechanisms that could adequately differentiate between the various fuels. In addition to the basic combustion work, particulate particle size distributions have been measured, and, using specialized test equipment, the effects of biodiesel fuels and blends on the type of soot, the rate of soot combustion and the fraction ash formation were studied in order to assess the effect of these fuels on DPF function and regeneration.

Results

Simulated Reduction in Fuel Consumption for Narrow-Speed Turbocompound Engine

Figure 3 shows the results of simulation of a narrow-speed turbocompound engine operating on a long haul European cycle (LM13). A reduction of 5 gm/kW-hr can be achieved due to the effects of optimal operation of the engine in a narrow band of lower speed and capturing exhaust energy using a power turbine, i.e., turbocompound. The reduction in fuel consumption accounts for the urea required to reduce NOx in a selective catalytic reduction catalyst.

Ultra-High Pressure Fuel Injection

The effect of ultra-high injection pressure on diesel ignition and flame propagation has been investigated in a Volvo D12 engine at 1,500 rpm and 50% load.

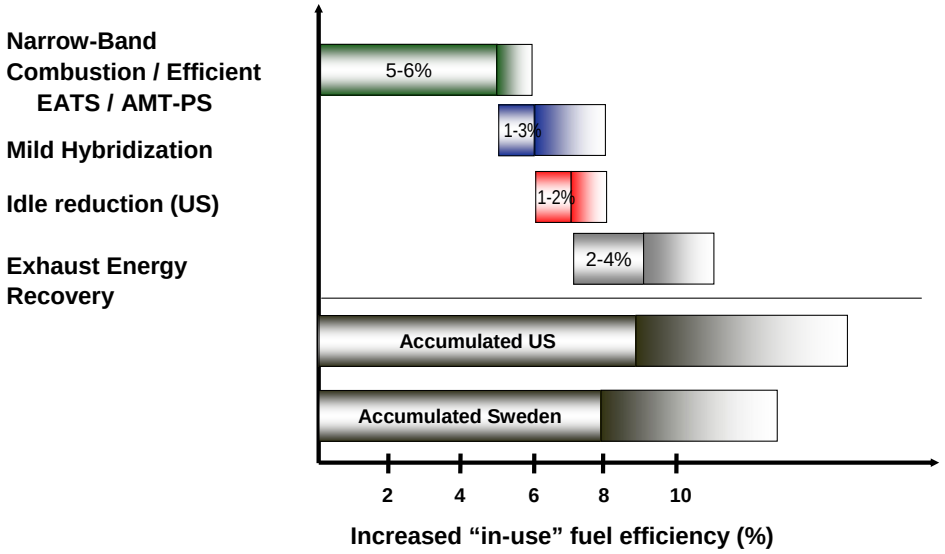

EATS - Engine aftertreatment system; AMT-PS - Automatic-manual transmission – powershift

FIGURE 2. Targets for improvements to energy efficiency from technologies employed in the project.

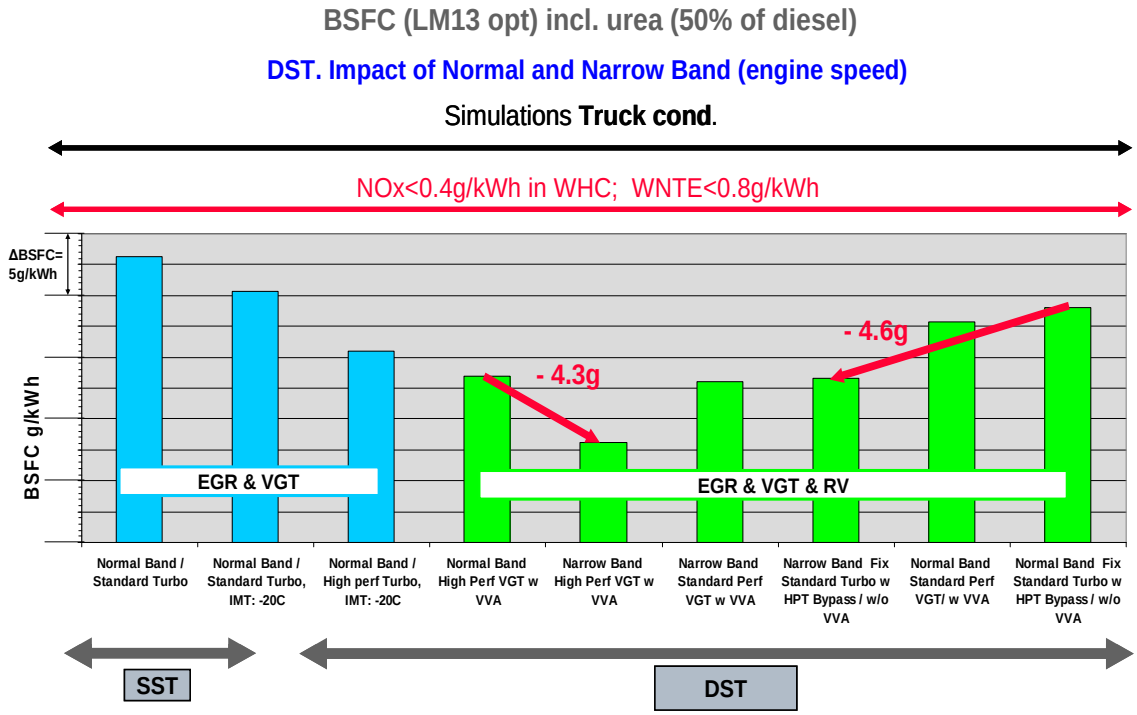

WHC - World harmonized cycle; WNTE - Within not-to-exceed limit; EGR – Exhaust gas recirculation; VGT – Variable geometry turbocharger; RV – Reed Valve; SST – Single-stage turbo; DST – Dual-stage turbo; IMT – Inlet manifold temperature; VVA – Variable valve actuation; HPT – High performance turbo

FIGURE 3. Simulated reduction in fuel consumption for turbocompound narrow-speed engine over the European long haul cycle (LM13).

The data acquisition system sampled time-averaged signals of raw emissions, fuel consumption, pressures, temperatures and flows of air, fuel, oil and cooling water. Fast transient signals such as injection and cylinder pressure were sampled by an AVL data acquisition system. From these sampled data, the accumulated heat release was calculated. The emissions of NOx, HC, CO, and CO_2 were measured using standard instrumentation

and soot was measured by a smoke meter. Commercial European diesel fuel was used in the experiments.

Additional CFD simulations were performed using the KIVA-3V code, with a Kelvin-Helmholtz/Rayleigh-Taylor spray breakup model and a diesel surrogate mechanism involving 83 species and 445 reactions. A range of higher injection pressure levels were projected and the injection rates were estimated for the current study. Three different rate shapes of injection were projected and investigated as well. Computations demonstrate that high-pressure injection strongly affects engine ignition and combustion. An increase in injection pressure leads to reduced ignition delay time, higher in-cylinder pressure peak, advanced combustion phasing, and faster flame propagation.

It was found that the specific soot level was reduced whereas the specific NOx levels tended to increase as injection pressure was increased.

Turbocompound, Narrow-Speed Combustion System Development

Combustion development was carried out in a single-cylinder D13 (13 L) engine. The system-out emission levels correspond to U.S. 2010 standards. Two loads at an engine speed at a cruise speed were tested. Variations in nozzle specification (number of holes, spray angle, flowrate), cam rate, and compression ratio were studied.

The tests were performed in conjunction with an on-line gas exchange model to give conditions for the charge gas and exhaust manifold. In this way, the single-cylinder combustion system results can be made applicable to the multi-cylinder engine. The gas exchange model also provided the turbocompound torque contribution for calculation of a relevant multi-cylinder BSFC. The experimental tests were supported and guided by extensive CFD analysis, which aided in the interpretation of the results.

The results for the tested hardware were modeled for the purpose of optimization. The best hardware configuration was found to BSTC gain of 0.6% compared to baseline (U.S. 2010 specification).

Stoichiometric Operation with TWC

SwRI® was contracted to investigate the stoichiometric operation of a Volvo D13 diesel engine, including exhaust and cylinder head temperature characterization and TWC feasibility study. A unique, lower flow turbocharger had to be designed and fabricated for stoichiometric engine operation. Engine performance was tested at nine points. Emissions data (gaseous, smoke number and PM) were acquired with and without the TWC installed.

The major results were as follows:

- Under stoichiometric conditions with no exhaust gas recirculation, the engine can only run 25-50% load (relative to standard diesel operation) due to exhaust component temperature limitations.
- For the loads tested, the cylinder head temperature measurements show reasonable values and cylinder-to-cylinder thermal balance is acceptable.
- The DPF functions satisfactorily during stoichiometric diesel operation, even with inlet smoke numbers in the 5-7 filter smoke number range. The DPF showed at least 50% NOx reduction rate over the range of stoichiometric operating conditions tested as a result of the presence of CO, a reducing agent.
- The DPF performs well in removing PM, but regeneration requires that the engine run leaner than the stoichiometric point in order to gain enough O_2 to support regeneration. New DPF regeneration strategies will need to be developed for the stoichiometric diesel approach to avoid thermal runaway.
- Tailpipe HC emissions are low.

Figure 4 shows the NOx level at five different speed/load points, measured at engine-out, DPF-out and TWC-out locations.

Biodiesel Fuels

Testing of the combustion properties of pure EC1 diesel fuel was carried out to establish a relevant baseline for the study of the effects of blending FAME biofuels into diesel fuel. The following fuels have been tested over a wide range of speeds and loads:

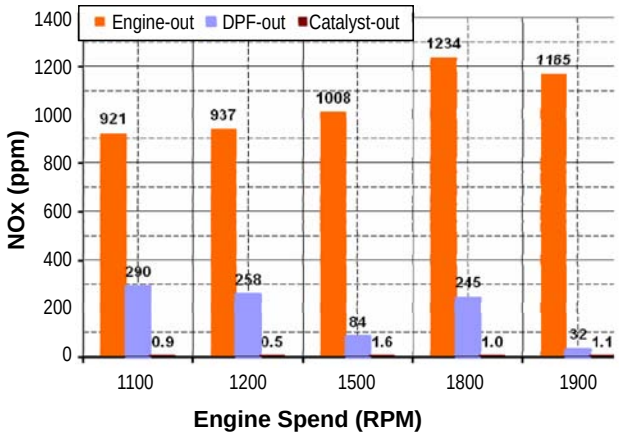

FIGURE 4. Engine-out, DPF-out and TWC-out NOx emissions. (Note that TWC-out emission levels are not visible on chart due to low values but are labeled.)

- Pure EC1 diesel (B0)
- 15% FAME in 85% EC1 diesel (B15)
- 30% FAME in 70% EC1 diesel (B30)
- Pure FAME (B100)

Emissions, fuel efficiency and particle size distributions were obtained.

Blending of FAME biofuel into diesel has a very positive effect on soot emissions. Increased fractions of FAME fuels blended into EC1 decrease soot to a larger extent. This can be seen in Figure 5 in the brake specific soot vs. brake specific NOx tradeoffs for various fuels, including standard diesel fuels, FAME fuels and proprietary biofuels tested.

Information relevant to the regeneration and function of the DPF has also been obtained. The rate of combustion, the heat of combustion and the ash fraction were determined for each type of soot. From the temperature-programmed oxidation experiments, the rate of combustion was found to be as follows: B30>B15>Volvo standard diesel (VSD10, <10 ppm sulfur, by weight). B30 had almost the double amount of ash content as compared to the other two types of soot. The heat of reaction was similar for the soot from all three types of fuel.

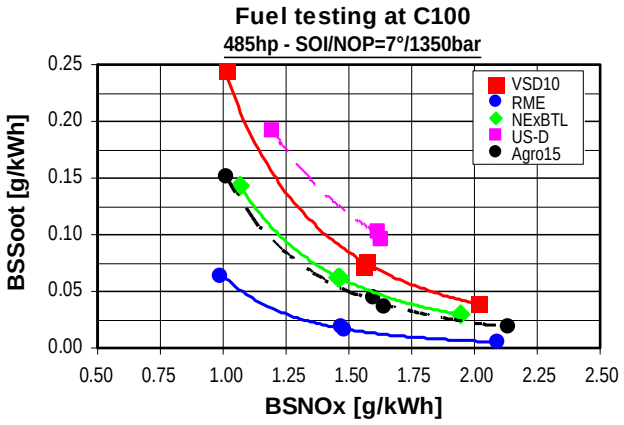

C100 - 100% load point at C-speed (as defined in the federal emissions regulation protocol); SOI - Start of injection; NOP - Nozzle opening pressure; VSD10 - Volvo standard diesel (<10 ppm sulfur, by weight); RME – Rapeseed methyl ester; NExBTL - A patented Neste Oil (Finland) biodiesel fuel produced by a vegetable oil refining process; US-D – U.S. diesel fuel; Agro15 - The name of a fuel consisting of 85% Swedish Environmental Class 1 Diesel (having low aromatic content), 10% heavy alcohols (with an average of 6 carbon atoms) made from bio source and 5% rapeseed methyl ester

FIGURE 5. Brake specific soot (BSSoot) vs. brake specific NOx (BSNOx) for various diesel, biodiesel and biodiesel fuel blends.

Conclusions

- A narrow-speed turbocompound engine has been simulated and shows a reduction in fuel consumption of 5 g/kW-hr over a typical European long haul cycle.
- Ultra-high injection pressure produces lower soot emissions but higher NOx emissions.
- Optimization of the combustion system for a turbocompound, narrow-speed engine yields a small but measurable improvement in the fuel consumption characteristics of the engine.
- Diesel operation at stoichiometry can, in principle, simplify the emission control system required for U.S. 2010 emission standards but significant issues concerning exhaust system component temperatures, DPF regeneration strategy and higher fuel consumption present formidable barriers.
- The use of FAME and other similar biofuel blends in diesel fuel is feasible from a combustion standpoint and produces lower soot emissions at comparable efficiency and NOx emissions.

FY 2009 Publications/Presentations

1. DOE Quarterly report, Q3-2008
2. DOE Quarterly report, Q4-2008
3. DOE Quarterly report, Q1-2009
4. DOE Quarterly report, Q2-2009
5. DOE Merit Review, May 21, 2009

II.C.4 Advanced Start of Combustion Sensor – Phase II: Pre-Production Prototyping

Chad Smutzer (Primary Contact) and
Dr. Robert Wilson
TIAX LLC
15 Acorn Park
Cambridge, MA 02140

DOE Technology Development Manager:
Roland Gravel

NETL Project Officer: Samuel Taylor

Subcontractor:
Wayne State University, Detroit, MI

Objectives

- Develop an accelerometer-based start of combustion (SOC) sensor which provides adequate SOC event capture to control a homogeneous charge compression ignition (HCCI) engine in a feedback loop.
- Ensure that the developed sensor system will meet cost, durability, and software efficiency (speed) targets.
- The Phase II objective is to have a pre-production prototype.

Accomplishments

- Three engines of same model line/different serial number have been installed and tested to verify engine-to-engine repeatability of the SOC sensor system (a potential drawback of accelerometer-based systems), including two dynamometer setups and one vehicle setup.
- An initial real-time version of the SOC algorithm has been developed to optimize the algorithm for accuracy and processing speed.
- Data over the operating range of interest (the expected HCCI engine operating envelope of low to medium speed, low to medium load) has been recorded.
- Twenty-two original equipment manufacturers (OEMs) and Tier 1 suppliers were contacted to push this technology out into the marketplace, ten of which have requested further information.

Future Directions

- Further project progress depends on the responses from OEMs and Tier 1 suppliers.

Introduction

HCCI has elevated the need for SOC sensors. HCCI engines have been the exciting focus of engine research recently, primarily because HCCI offers higher thermal efficiency than conventional spark ignition engines and significantly lower oxides of nitrogen (NOx) and soot emissions than conventional compression ignition engines. HCCI has the potential to combine the best features of internal combustion engine technology to achieve high efficiency and low emissions. However, these advantages do not come easily. It is well known now that the problems encountered with HCCI combustion center on the difficulty of controlling the start of combustion. The emergence of a durable and effective SOC sensor will solve what is arguably the most critical challenge to the viability of HCCI engine platforms. The SOC sensor could be an enabler for a new breed of engines saving 15-20% of petroleum used in transportation, while meeting or exceeding 2010 emission targets.

Approach

The objective of the Phase II research is to refine the design of the SOC sensor and algorithm into a production-ready prototype and position it for hand-off to a commercialization partner. The Phase II research will identify any potential soft spots in the algorithm and allow the team to implement and test a solution. During the Phase II effort, the team will work to make sure the processing code efficiency (response time of control system) is rapid enough that control decisions may be made and implemented. The interface with the HCCI actuation/control mechanism (variable valve actuation, fuel injection, etc.) must be rapid and robust enough to allow the control mechanisms an opportunity to change engine conditions, so as to effectively manage short transients.

Results

During Phase I of the project, data was gathered from the test engine in the vehicle and the Wayne State University Engine Test setup to prove the feasibility and repeatability of the SOC algorithm for select operating

points. As Phase I transitioned into Phase II, the algorithm was coded to run on a real-time platform. As the second phase of the project continues, further data is actively being recorded to ensure algorithm accuracy and robustness over low to medium speed and low to medium load engine operation. Figure 1 shows the three test platforms.

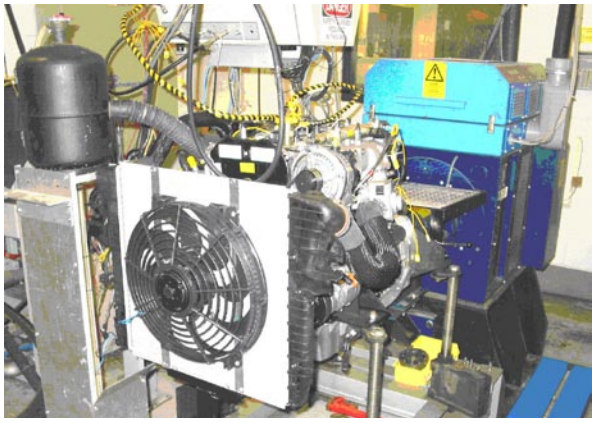

Engine Test Setup at TIAX

Wayne State University Engine Test Setup

Test Engine in Vehicle

FIGURE 1. Photographs of the three engine test setups (same engine model, different serial numbers) designed to test engine to engine repeatability of the sensor system.

Since the effectiveness and robustness of the accelerometer-based sensor system depends on its ability to work across multiple engine blocks, installation and testing of these three similar engines was a key accomplishment.

The algorithm developed has shown promise for the detection of the SOC. Shown in Figure 2 is the pressure trace (the top plot) during the same time period as two accelerometer traces (the bottom two plots). The red circle on the pressure trace shows the calculated SOC based upon the industry standard practice of heat release analysis (an off-line laboratory approach for combustion analysis). This circle is also shown on the raw accelerometer trace next to a green circle, which is the SOC determined independently from the algorithm analyzing the accelerometer trace. The agreement between the two methods is very good, as may be seen from their close proximity.

Conclusions

- Three engine setups are being used to determine engine-to-engine repeatability of the sensor/algorithm system, and progress to date is encouraging.
- The algorithm has being coded in a real-time embodiment and is undergoing testing.
- Low-temperature combustion work will enhance the work done to date with diesel SOC detection.

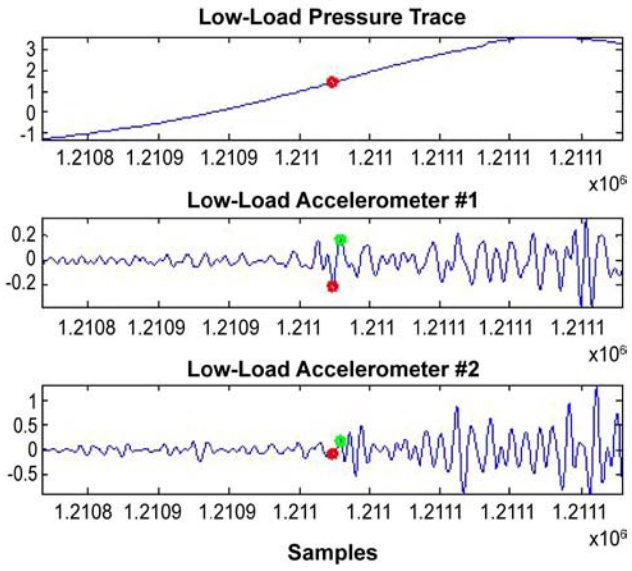

FIGURE 2. Comparison of the identification of the start of combustion using the developed algorithm with the industry standard method.

II.C.5 The Development of a Robust Accelerometer-Based Start of Combustion Sensing System

David Mumford (Primary Contact), Jim Huang
Westport Power, Inc.
1691 West 75th Ave.
Vancouver, BC V6P 6P2
Canada

DOE Technology Development Manager:
Roland Gravel

NETL Project Manager: Jason Conley

Objectives

- Development of an accelerometer-based start-of-combustion (SOC) sensing system.
- Develop a method to minimize sensor-to-sensor variation for the accelerometer-based SOC sensing system.

Accomplishments

- Exceeded initial target to achieve sensor-to-sensor variation of 0.5 crank angle degree (CA°). The average sensor-to-sensor variation over all modes has been reduced to 0.36 CA° with 98.9% confidence level.
- Exceeded the initial target to achieve total error of measured SOC timing of 0.5 CA°. The mode-averaged total error (based on one standard deviation) was reduced to 0.41 CA°.
- Extended the capability of the accelerometer-based combustion sensing system to capture not only the SOC timing but also the complete in-cylinder pressure trace.
- Significant improvement in the robustness of the processing method indicates as few as three knock sensors are required for a six-cylinder engine.
- On-road testing has demonstrated that the knock-sensor based combustion sensing method and the algorithm developed from the test cell studies are applicable to on-road application without major modification.

Future Directions

This project is complete.

Introduction

The development of modern combustion systems increasingly relies on detailed knowledge of the combustion event. As the limits of combustion are approached, tight control of combustion leads to improved emissions and higher efficiencies, while retaining and even improving engine reliability and durability.

While developing a novel homogeneous charge compression ignition (HCCI) technology for large natural gas engines, Westport found that there was no reliable cost-effective technology to monitor the combustion event. As a result, Westport began to develop a solution based on commercially-available knock sensors. While initially developed around HCCI, Westport has identified that numerous other forms of combustion (high exhaust gas recirculation [EGR] systems, homogeneous charge direct injection, etc) will require combustion sensors. This requirement is also reflected in the development of other technologies in this field. However, the potential low system cost and the lack of intrusion into the cylinder head area are significant benefits for the Westport approach.

Previous work by Westport has proven the method on two different large compression ignition gas engines. The objective of the current work is to improve robustness of this technology; particularly, to identify and reduce the sensor-to-sensor variations.

Approach

Experimental study has been carried out on a Cummins ISB 5.9L HPCR diesel engine. Accelerometer (knock sensor) data were collected under 6 of 13 European Stationary Cycle (ESC) testing modes, which cover a wide range of engine loads and speeds. After obtaining the initial signal from the sensors, physical models that describe the correlation between the sensor signal and in-cylinder pressure change were established. An algorithm was developed based on these models to obtain the timing for the SOC using the data from the accelerometers. This timing was compared with the SOC determined from the in-cylinder pressure measurement.

To further explore the potential of the sensing system, another algorithm was developed to reconstruct the in-cylinder pressure and heat release rate from

the raw knock sensor data. The algorithm allows in situ compensation of sensor-to-sensor variation as well as variation of sensitivity over a wide range of operating conditions; the algorithm also compensates for variations in dynamic response of the sensors.

Results

Data have been collected using two sets of Siemens knock sensors with integrated cables on an ISB325 HPCR diesel engine. Engine tests were carried out at 6 of the 13 ESC modes covering a relatively wide range of engine operating conditions. The test conditions are summarized in Table 1. At each mode, a three-point SOC timing swing (with advanced, nominal and retarded timing) was performed by varying the diesel injection timing. For each test mode and timing, two injection pressures were used to simulate normal and "soft" combustion. The purpose of varying injection pressure is to examine the capability of the current sensor configuration and processing method for capturing the SOC with high EGR combustion. Since the current ISB engine is not equipped with an EGR system, we used reduced injection pressure to achieve the lower peak heat release rate and prolonged the combustion duration similar to high EGR combustion.

A second model of Siemens knock sensor (with integrated connector) was also tested on the same engine. It was found that the signal from this sensor model is significantly different from the previous model under identical engine operating conditions. In particular, the high frequency oscillation associated with the ignition observed in the signal from the previous sensor model was not present in this model. As a result, the SOC sensing method developed with the first model could not be applied to the second model, which required a different approach for signal processing.

TABLE 1. Engine Test Modes

ESC Mode	% Load	Torque (Nm)	RPM	Power (BHP)	SOI[1]
5	50	305	1,885	109	a, n, r
6	75	457.5	1,885	164	a, n, r
8	100	610	2,292	266	a, n, r
9	25	152.5	2,292	67	a, n, r
12	75	457.5	2,698	235	a, n, r
13	50	305	2,698	157	a, n, r

[1] Start of Injection: advanced, nominal, retarded

The knock sensor data from the ISB testing are distinct from those of the previous study on the larger ISX engines. In particular, the knock sensor signal shows high frequency oscillations with significant magnitude at the SOC, whereas previous studies with ISX engines showed predominantly low-frequency signals. This is probably due to a lower structural stiffness of the smaller ISB engines when compared with the larger ISX engines. Analysis of the high-frequency signal established the reproducibility of a characteristic frequency between the engines. It was decided that both the high and low frequency signals should be used in the current work as independent measures for determining SOC.

There are three main steps to the processing algorithm:

- pre-process the raw accelerometer data;
- extract SOC information from the accelerometer signals; and
- select the SOC timing with the highest confidence level.

First, the raw accelerometer data is manipulated to increase the combustion signal-to-noise ratio. Standard finite impulse response filters were applied to the raw accelerometer signal to reduce noise. Both the high and low frequency signals were extracted using filters with different bands. The phase shift among different ignition timings was observed in the high-frequency, low-frequency and reconstructed data, so attempts were made to extract the SOC from all of them and examine which one had the best correlation with the actual SOC measured from the in-cylinder pressure. A global method and a local method were used to obtain the phase shift of SOC from the calibration signal. Both methods can provide an independent SOC estimate, and the results were crosschecked with each other to improve the reliability.

A set of data were acquired at a number of engine operating modes to determine how well the accelerometer-based system could measure the SOC. These data include SOC timing swings at advanced, nominal, and slow combustion rates to test SOC detection at the widest expected range of heat release rates. Figure 1 shows a global correlation between the measured and actual SOC from all test points.

Figure 2 shows the total error (standard deviation) for individual modes. It can be seen that the total error was significantly lower than the 0.5 degree target for all modes. The total error averaged over all modes is 0.41 CA°.

The engine-to-engine variability was modeled as the reproducibility of the measurement system. For most modes, the variability is significantly less than 0.5 CA°. The results are also shown graphically in Figure 3. The average sensor-to-sensor variability with 98.9% confidence level is 0.36 degrees, which meets the 0.5 degree target. Thus the conclusion was drawn that the current accelerometer method can meet the performance requirement for SOC detection.

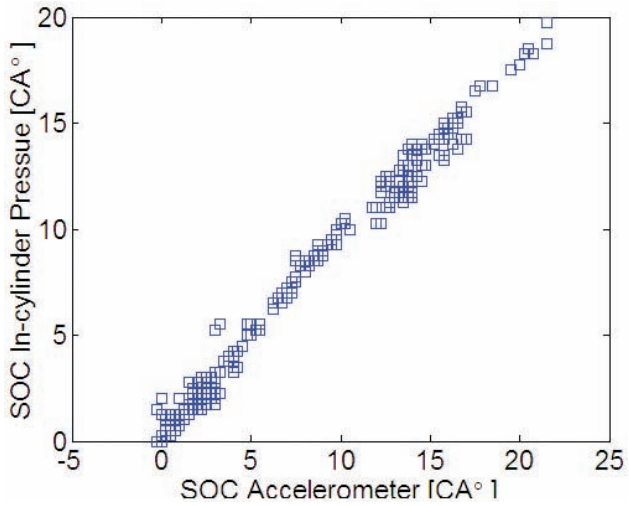

FIGURE 1. Comparison of SOC Determined from Knock Sensor Signal with In-Cylinder Pressure SOC

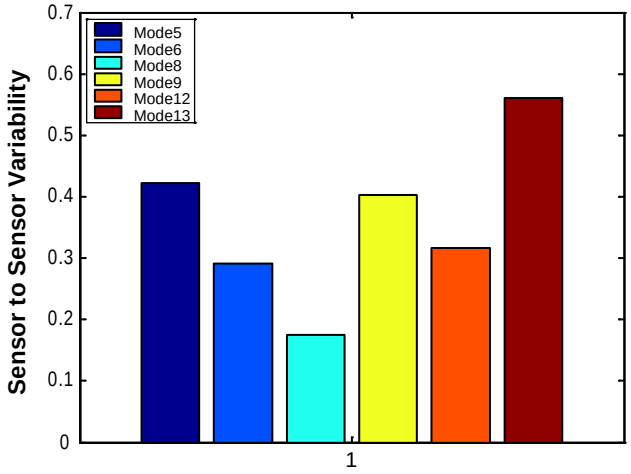

FIGURE 2. Mean Sensor-to-Sensor Variability based on Two Sets of Siemens Knock Sensors (3σ – 0.36 °CA)

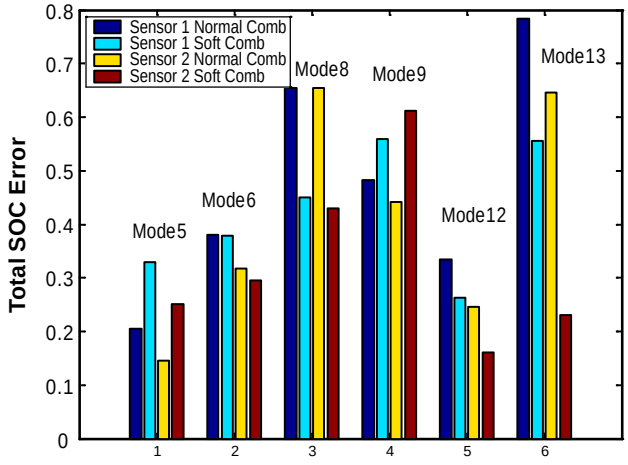

FIGURE 3. Mean SOC Error (1σ – 0.41 °CA)

An algorithm was also developed to reconstruct the in-cylinder pressure and heat release rate from the raw knock sensor signal. The algorithm allows in situ compensation of sensor-to-sensor variation as well as variation of sensitivity over different operating points; the algorithm also compensates for decay in the signal due to the dynamic response of the sensors. Figure 4 shows a comparison of in-cylinder pressure from a research grade in-cylinder pressure sensor and a knock sensor mounted on one of the two adjacent bearing caps. It can be seen that good agreement is achieved between the reconstructed and the actual pressure data.

Conclusions

A knock sensor based combustion sensing technology has been developed. Engine test results shows that the system easily meets the initial target of 0.5 degree sensor-to-sensor variation. The average sensor-to-sensor variation over all modes is reduced to 0.36 CA° with 98.9% confidence level.

The system has exceeded the initial target to achieve total error of measured SOC timing of 0.5 degree. The mode-averaged total error (based on one standard deviation) was reduced to 0.41 degree.

Another algorithm was developed to reconstruct the in-cylinder pressure and heat release rate from the raw knock sensor data. This algorithm allows in situ compensation of sensor-to-sensor variation as well as variation of sensitivity over a wide range of operating conditions; the algorithm also compensates for variations in dynamic response of the sensors. A reasonable agreement has been achieved between the reconstructed in-cylinder pressure and that measured by research-grade in-cylinder sensors for both single and multiple injection modes over a wide range of test conditions.

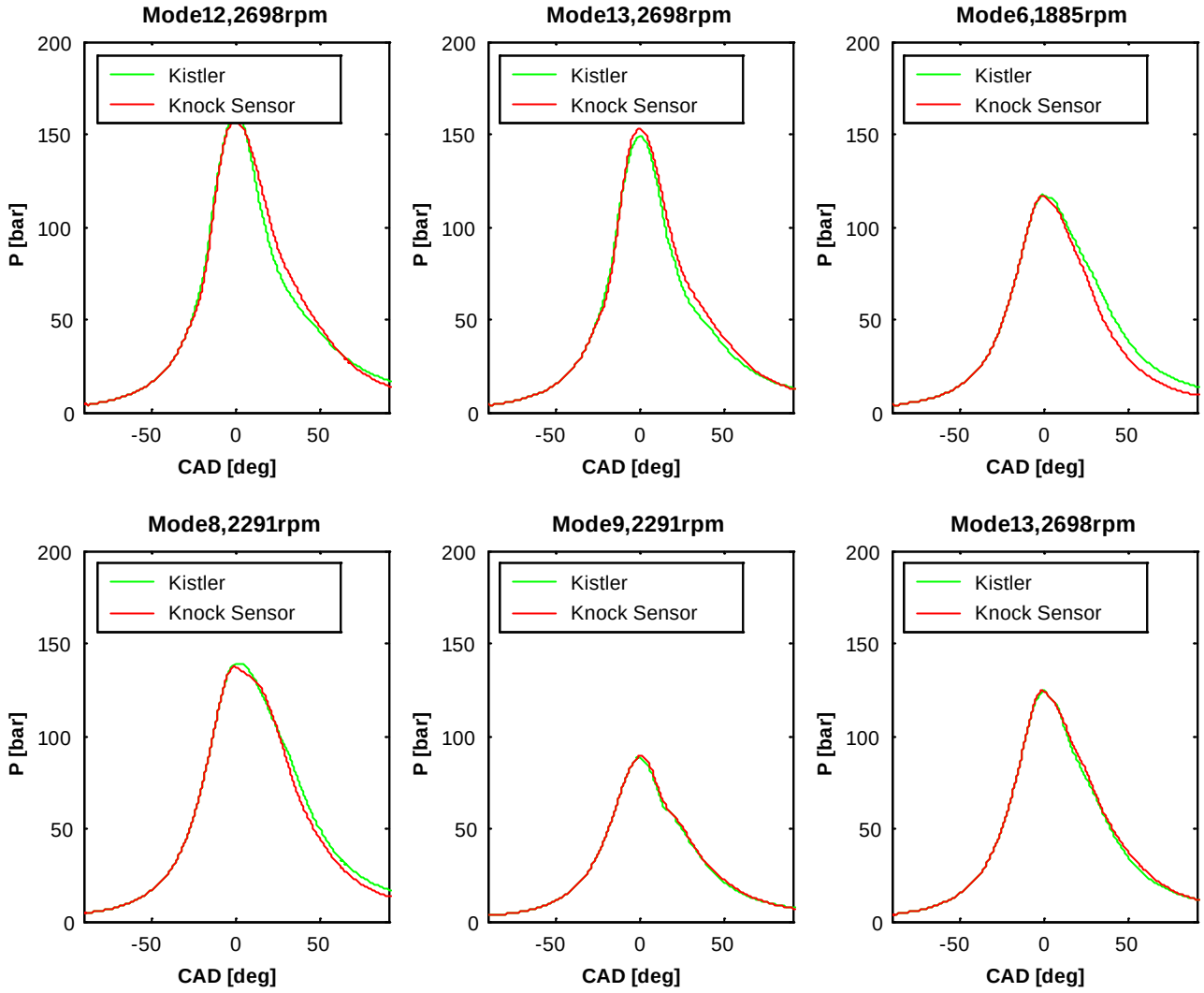

FIGURE 4. Comparison of Actual and Reconstructed In-Cylinder Pressure (data for cylinder #2, knock sensor data from bearing cap #2)

II.C.6 Variable Compression Ratio Engine

Charles Mendler
Envera LLC
7 Millside Lane
Mill Valley, CA 94941

DOE Technology Development Manager:
Roland Gravel

NETL Program Manager: Jason Conley

Objective

Phase I

- Design, build and bench-test a proof-of-concept variable compression ratio (VCR) actuator system.
- Optimize the actuator system where practical within the scope of Phase I funding.

Phase II

- Optimize the actuator hydro-mechanical design and its control system.
- Production-intent design optimization of the VCR engine crankcase with imbedded VCR actuator system.
- Rig testing of the VCR actuator hardware.

Accomplishments

- Hydraulic pressures in the actuator system were reduced by 86% through system optimization. The reduction in pressure significantly relaxes the demands that will be placed on the hydraulic system and enables cost to be reduced.
- A test rig was designed and built for evaluating actuator response. Test results indicate that compression ratio can be reduced from 18:1 to 8.5:1 in ~0.35 seconds, and increased from 8.5:1 to 18:1 in ~0.70 seconds. On average 0.074 seconds is projected to elapse for each point increase in compression ratio.
- Finite element analysis (FEA) of the Envera production intent 4-cylinder VCR engine was conducted. Modeling results indicate that the crankcase meets all stiffness, robustness and durability requirements for mass production.
- Production-intent design optimization of the VCR engine crankcase with imbedded VCR actuator system. The upper crankcase has been optimized for low-cost mass production.

Future Directions

- Optimize the hydro-mechanical system crankcase for improved performance and manufacturability.
- Rig-test the VCR actuator and demonstrate low-cost, fast response and mass production practicality.

VCR Overview

VCR is an innovative technology for improving the fuel economy of engines used in passenger cars, sport utility vehicles (SUV) and trucks. Fleet operators of light-duty vans are potential early adopters of the VCR engine. Fleet operated vans are used for package delivery, and telephone and cable service and repair.

VCR enables the compression ratio of the engine to be changed from a diesel-like value of approximately 18:1 during normal driving conditions to approximately 8.5:1 when the engine is generating high power levels with the aid of supercharging or turbocharging. The low compression ratio permits the engine's power output to be more than doubled.

Large gains in fuel economy can be attained by replacing a large naturally-aspirated engine with a small supercharged or turbocharged VCR engine of similar power and torque. In some cases fuel economy can be improved by more than 50% when a large V8 engine is replaced with a supercharged or turbocharged 4-cylinder engine having the same power and torque as the V8. In Figure 1 the target efficiency of the Envera 4-cylinder VCR engine is compared to the efficiency of a 4.6 L V8. Most of the fuel consumed by light-duty trucks and SUVs occurs at small power levels, as indicated by the blue step curve in Figure 1. The efficiency of the

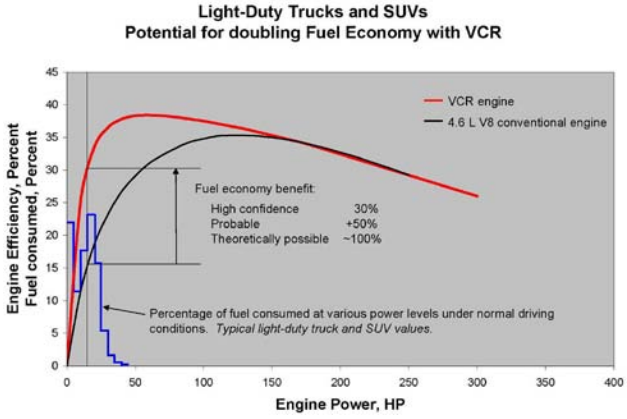

FIGURE 1. Efficiency of 4-Cylinder VCR Engine Compared to a 4.6 L V8

Envera VCR engine is double that of the V8 engine at 15 horsepower.

VCR enables boosted engines to attain significantly greater power levels by lowering compression ratio when the engine is under boost. Virtually all passenger car diesel engines sold in Europe are now turbocharged. Advanced supercharging technology is expected to be available in the near term that provides very high torque values for vehicle launch.

VCR provides high fuel efficiency by enabling a smaller 4-cylinder engine to do the work previously preformed by a V8, without any loss of power or torque. The smaller 4-cylinder engine operates much more efficiently at the relatively small power levels where most of the fuel is consumed during normal driving. Boosting combined with VCR provides the higher power levels needed for acceleration and hill climbing.

Table 1 compares the target power and torque values of the Evera 4-cylinder VCR engine to that of the Ford 4.6 L V8, currently sold in the Model Year 2009 F150 pickup truck. It can clearly be seen that the VCR 4-cylinder has greater power and torque than the Ford 4.6 L V8.

Attaining high power levels from a small engine requires a robust VCR mechanism. Envera's VCR mechanism is exceptionally robust and reliable. Envera's VCR mechanism can support engine speeds of over 8,000 rpm. Envera's VCR mechanism has a low manufacturing cost.

TABLE 1. Power and Torque Comparison

	Power	Torque
Ford 4.6 L V8	248 hp @ 4750 rpm	294 ft lb @ 4000 rpm
Envera VCR 4-cylinder	320 hp @ 6000 rpm 280 hp @ 4750 rpm	320 ft lb @ 4000 rpm

At light power levels the Envera VCR engine operates at the same compression ratio setting as diesel engines, and attains similar in-cylinder combustion efficiency. The Envera VCR engine, however, has lower internal frictional losses than the diesel. VCR also enables higher exhaust gas recirculation dilution values to be employed – in the order of 30%. The net result is that in some cases the Envera VCR engine can return higher efficiency and much greater power that diesel engine of the same size (e.g., the same displacement). When downsizing is used, VCR engines return significantly greater fuel economy benefits.

When the benefits of improved engine efficiency attained using VCR are combined with other fuel saving technologies (hybrid drive, reduced vehicle weight, aerodynamics) the fuel economy of some light-duty trucks could be doubled.

NETL Program Introduction

The current DOE/NETL/Envera effort is directed towards reducing VCR system cost and providing a fast actuator response. The technology has three main cost areas; the VCR mechanism; the actuator system for adjusting compression ratio; and the supercharging or turbocharging hardware.

The Envera VCR mechanism comprises an eccentric carrier that holds the crankshaft of the engine. Pivoting of the eccentric carrier raises and lowers the crankshaft relative to the engine's cylinder head, and adjusts engine compression ratio. The Envera VCR eccentric carrier presently has a low cost.

A hydraulic actuator system is used to pivot the eccentric carrier. The current effort is directed towards reducing the cost of the actuator system and engine crankcase, and providing a fast actuator response. Another goal is to provide a durable compact VCR actuator design.

Prior to the Phase I contract award Envera anticipated that actuator response and cost would be optimized primarily through hydraulic control circuit system design and computer software. The results of Phase I have shown, however, that hydraulic cylinder sizing and mechanical design changes are of primary importance for attaining project and commercialization objectives. Specifically, hydro-mechanical design changes realized in Phase I have resulted in an 86% reduction in projected peak hydraulic system pressure. The lower pressure will enable a simpler more robust hydraulic control circuit system to be used. In consideration of the performance gains realized in Phase I of the initiative, work is currently focused on hydro-mechanical design, system hardware, and a low-cost production intent crankcase. The hydraulic cylinder is located vertically adjacent to engine cylinder bore 3 to provide a compact and stiff crankcase.

Approach

The current effort is directed towards the development of the actuator used for adjusting the pivot angle of the eccentric carrier. Development goals include low cost and a fast response. At the beginning of the NETL program mechanical loading on the VCR eccentric carrier and hydraulic system were evaluated using:

ProEngineer Wildfire 2.0	Part and mechanism assembly
MDO Extension	Dynamic force analysis
GTPower	Gas force on the piston (Prior data)
Origin 7.5	Data conversion

Dynamic loads were modeled at five conditions, from 2,000 rpm 4 bar bmep to 6,000 rpm 12 bar bmep. The 2,000 rpm 12 bar bmep condition causes the highest loading on the hydraulic system of about 2,250 psi. In Phase I of the project Envera pursued reducing the size of the hydraulic pressure spikes through system optimization. Through this effort peak hydraulic pressures have now been reduced to an estimated 314 psi, an 86 percent reduction in peak pressure. This reduction in peak pressure is a huge improvement.

A test rig was designed and built for evaluating actuator response. Test results indicate that compression ratio can be reduced from 18:1 to 8.5:1 in ~0.35 seconds, and increased from 8.5:1 to 18:1 in ~0.70 seconds. On average 0.074 seconds is projected to elapse for each point increase in compression ratio.

In consideration of the performance gains realized through geometry optimization, development work was focused on hydro-mechanical design, system hardware, and low-cost packaging within the crankcase. Figure 2 shows an Envera crankcase with integrated hydraulic actuator.

Envera ran FEA of the crankcase/cylinder head assembly. The analysis, shown in Figure 3, was performed using ProEngineer Mechanica software and high-performance quad-core hardware. Simulation run time was approximately 54 hours. Results were excellent. Bottom-end structure is sound and stiff.

Current efforts have been directed toward low-cost production-intent development of the crankcase and integrated VCR mechanism.

With success of the FEA analysis, Envera anticipates using the new crankcase on the current project for rig testing. The decision on whether or not to use the new crankcase will be made after successful cast, machine and assembly of the new crankcase. If problems are encountered Envera will continue with the current project plan of using the existing modified Mercedes M271 VCR engine crankcase. The feasibility assessment of the new crankcase also included production of the machine drawings. The machine drawings show that the new crankcase can be mass produced using tolerances and machining operations that are compatible with low-cost mass production.

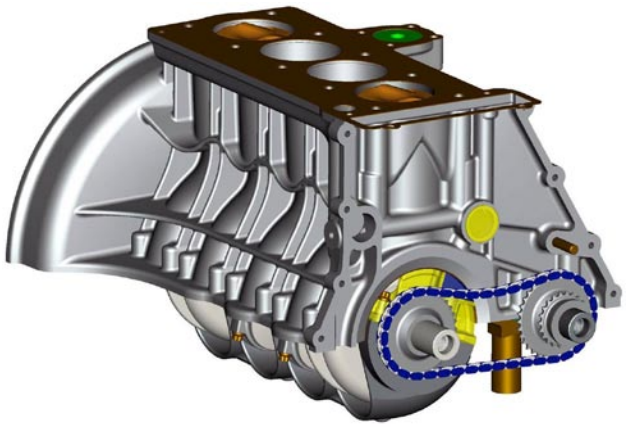

FIGURE 2. VCR Crankcase, with Hydraulic Cylinder located Vertically next to the 3rd Engine Cylinder

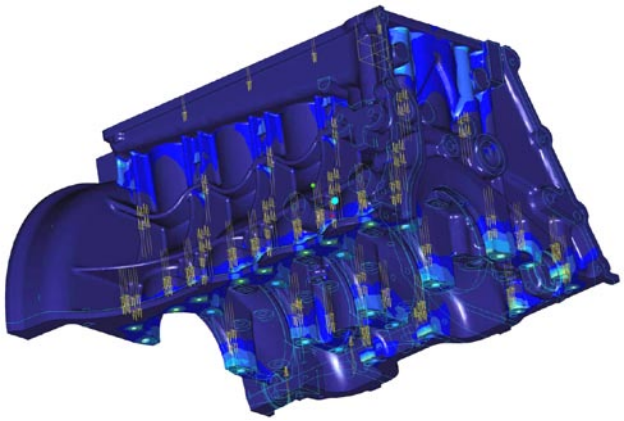

FIGURE 3. FEA Analysis of VCR Upper Crankcase Assembly

Results

Hydraulic pressures in the actuator system were reduced by 86% through system optimization. The reduction in pressure significantly relaxes the demands that will be placed on the hydraulic system and enables cost to be reduced.

A test rig was designed and built for evaluating actuator response. Test results indicate that compression ratio can be reduced from 18:1 to 8.5:1 in ~0.35 seconds, and increased from 8.5:1 to 18:1 in ~0.70 seconds. On average 0.074 seconds is projected to elapse for each point increase in compression ratio.

FEA analysis indicates that the production-intent crankcase design is rigid and durable.

Design development of the crankcase indicates that the upper crankcase will have a low manufacturing cost due to low casting and low machining costs.

Conclusion

- During Phase I of the project hydraulic pressures in the actuator system were reduced by 86% through system optimization. The reduction in pressure will significantly relax the demands placed on the hydraulic actuator system.
- The fuel economy of some light-duty trucks and SUVs can be improved by over 50% with down-sized gasoline boosted-VCR engines. Stringent tailpipe emission standards can be attained using

proven catalytic converter technology. The spark-ignited VCR engine can be operated on alternative fuels such as natural gas, ethanol, liquefied petroleum gas and other alternative fuels.

- FEA of the Envera production-intent 4-cylinder VCR engine was conducted. Modeling results indicate that the crankcase meets all stiffness, robustness and durability requirements for mass production.
- Design development of the crankcase indicates that the upper crankcase will have a low manufacturing cost due to low casting and low machining costs.

II.D.1 Health Effects from Advanced Combustion and Fuel Technologies

John Storey (Primary Contact), Teresa Barone, Jim Parks, Sam Lewis, Maggie Connatser
Oak Ridge National Laboratory (ORNL)
P.O. Box 2008, MS 6472
Oak Ridge, TN 37831-6472

DOE Technology Development Manager:
James J. Eberhardt

Objectives

- Understand potential impact of developing fuel, combustion, and aftertreatment technologies on air quality and, thereby, human health.
- Quantify mobile source air toxic emissions from advanced technologies.
- Link emissions measured in laboratory setting to air quality impact, and thereby, health impact.

Accomplishments

- Completed measurements of mobile source air toxics (MSATs) from light-duty vehicles operating on intermediate blends of ethanol (E10, E15 and E20):
  - Higher ethanol blends decrease emissions of benzene, toluene, ethylbenzene, and xylenes (BTEX) over a driving cycle.
  - BTEX reduction proportionally higher than what would be expected from simple mixtures with ethanol which does not contain BTEX.
- Completed an intensive campaign to measure the morphology and effective density of diesel particulate matter (PM) from conventional and premixed charge compression ignition (PCCI) operation:
  - The difference in effective density of conventional diesel and PCCI PM depended on particle diameter.
  - Transmission electron microscopy (TEM) analysis of diesel particle morphology was conducted and compared to the particles generated using high-efficiency clean combustion (HECC) modes.
- Characterized particle size and number concentration emissions from a homogeneous charge compression ignition (HCCI) engine operating on surrogate gasoline fuels:
  - Combustion phasing for reduced fuel consumption and particle number concentration emissions was affected by fuel chemical composition.

Future Directions

- Characterize particulate emissions from a direct-injection spark ignition vehicle operating on gasoline and intermediate blends of ethanol.
- Examine mixed mode diesel particulate filter/lean-NOx trap/selectic catalytic reduction catalytic effects on MSATs.
- Reconcile idealized aggregate theory with PM samples collected under conventional and HECC conditions.

Introduction

Scientists and engineers at national laboratories, universities, and industrial companies are developing new fuels and energy efficient technologies for transportation, and the U.S. DOE is actively involved in this innovative research. However, care must be taken to insure that any new fuel or technology developed for transportation must not adversely directly impact human health or impact the health of the environment, which subsequently may impact human health. To address this need, DOE sponsors research studies on the potential health impacts of advanced technologies for transportation including advanced fuels, combustion techniques, and emissions controls (also known as "aftertreatment" or, more commonly, "catalytic converters"). DOE sponsored health impact research activities at ORNL are presented in this report.

ORNL conducts research on advanced fuel, combustion and emissions control technologies at the Fuels, Engines, and Emissions Research Center. As the research is being conducted on engine and chassis dynamometers, specific studies of the potential health impacts of the technologies are conducted by the ORNL team for DOE's health impacts activity. Results from ongoing ORNL studies in Fiscal Year 2009 are presented here. A major focus has been the impact of ethanol blends on emerging gasoline vehicle technologies. A second focus has been on the impact of advanced combustion regimes on the emissions of PM and MSATs. In the first study reported here, several in-use vehicles operating on intermediate ethanol blends were analyzed for emissions of gaseous MSATs. In the second

study, PM emissions from two engines operating in the advanced diesel combustion modes of HCCI and PCCI were characterized.

Approach

Gaseous MSATs from Vehicles Fueled with Intermediate Blends of Ethanol

A series of in-use light-duty vehicles (model years from 1999–2007) were acquired by ORNL and evaluated as part of a larger study on the use of intermediate blends of ethanol in the existing fleet [1]. The vehicles were driven over the LA92, also known as the Unified Cycle, a driving cycle that is commonly used for emissions inventory and other in-use studies. The LA92 is considered to be more representative of in-use driving than the Federal Test Procedure (FTP). In addition to standard emissions, gaseous MSAT emissions were collected in canisters and analyzed with gas chromatography/mass spectrometry.

PM Characteristics for PCCI Diesel Engines

A Mercedes 1.7-liter 4-cylinder diesel engine was operated at 1,500 rpm, and 2.6 brake mean effective pressure (BMEP), a point representative of light-duty vehicle cruise operation, on an engine dynamometer. The engine operated in both production calibration conditions and under PCCI combustion conditions. The engine was not equipped with any aftertreatment. Utilizing a special aerosol mass analyzer (Kanomax APM-3600) in combination with a differential mobility analyzer (DMA; TSI 3081), the effective density of the PM in both conventional and PCCI modes was measured. At the same time, size selected PM was collected for morphological studies and analyzed by TEM.

PM and MSATs from an HCCI Engine Operating on Surrogate Gasoline Fuels

The effect of fuel chemical composition on engine efficiency and emissions was investigated. A single-cylinder research engine for which performance is dominated by fuel effects was used. Because the chemical composition of gasoline is highly complex, the engine was operated with three surrogate gasoline fuels with representative functional groups, branched alkane, straight chain alkane, aromatic, and alcohol. The fuels had the following compositions: 87% iso-octane and 13% n-heptane (iso-octane reference fuel); 58% iso-octane, 9% n-heptane and 33% ethanol (iso-octane reference fuel with ethanol); and 73% toluene and 27% n-heptane (toluene reference fuel). Thermal efficiency and fuel consumption were investigated by combustion phasing experiments in which the intake air and fuel mixture temperature was decreased such that the combustion event was delayed. PM number concentration and diameter were measured with a nano-scanning mobility particle sizer (TSI 3085 DMA, TSI 3025 condensation particle counter) following dilution in a microtunnel. The dilution ratio was factored into the calculation for the emissions. Fuel consumption and PM emissions were compared for varying crank angle degree at which 50% of the fuel mass fraction burned.

Results

Gaseous MSATs from Vehicles Fueled with Intermediate Blends of Ethanol

Example gaseous MSAT emissions with intermediate blends of ethanol are shown for two different vehicles in Figure 1. The only measurable emissions essentially occurred in Bag 1 of the driving cycle. The presence of ethanol definitely lowers the emissions of BTEX by amounts beyond the simple substitution percentages. This result is consistent with previous work on an E85 vehicle showing dramatic reductions in BTEX [2].

PM Characteristics for PCCI Diesel Engines

Previous studies have indicated that unburned hydrocarbon (HC) emissions are higher for PCCI than conventional combustion [3,4]. Some HC species in the gas phase may condense on soot present in the exhaust or nucleate to form semi-volatile PM. Soot coated with condensed liquid HCs may act as a vehicle for transporting biologically active HC compounds into the lung. Furthermore, if the soot is immersed in liquid hydrocarbons, the soot effective density will be greater than if the soot were dry. Thus, we expected to find

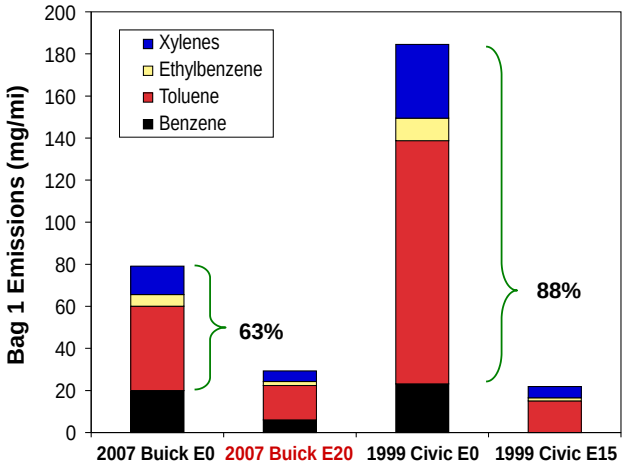

FIGURE 1. Intermediate ethanol blends substantially lower MSATs such as benzene, toluene, ethylbenzene and xylenes. Note that these are calculated for Bag 1 only of the FTP cycle since virtually no emissions of these compounds are detected in Bags 2 and 3.

higher effective densities for PCCI soot. However, our results show that the effective density of PCCI PM was similar to conventional diesel PM for 50 and 100 nm particles and less than conventional diesel PM for 150 nm particles (Figure 2). In addition, a liquid HC layer was not present on PCCI soot as indicated by TEM analysis (Figure 3). However, it is possible that the liquid hydrocarbons may be present in the pores of the soot primary particles [5]. Idealized aggregate theory predicts that PCCI PM may have a lower effective density than conventional diesel PM if the primary particle diameters are smaller. To test this hypothesis, the diameter of approximately 13,000 primary particles was measured using the image analysis technique of Xiong and Friedlander [6]. The average primary particle diameter of PCCI soot (21 ± 3 nm) was less than that for conventional diesel soot (25 ± 4) for 150 nm particles, consistent with Idealized Aggregate Theory. A report of these results is being prepared for publication.

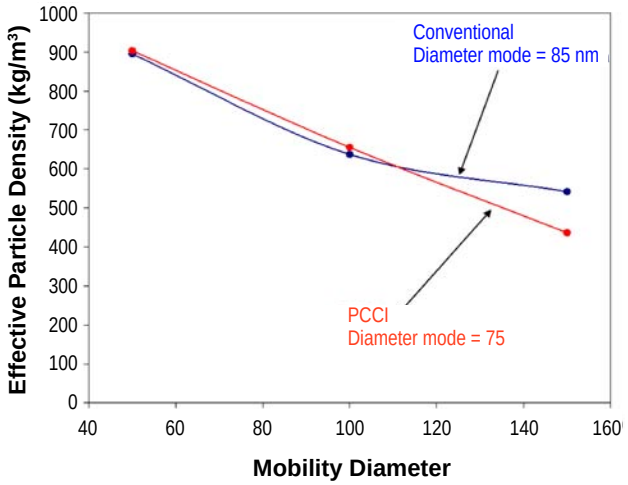

FIGURE 2. Comparison of PCCI (red) and conventional (blue) particle effective densities for 50, 100, and 150 nm electrical mobility diameters. (Engine conditions: 1,500 rpm, 2.6 BMEP)

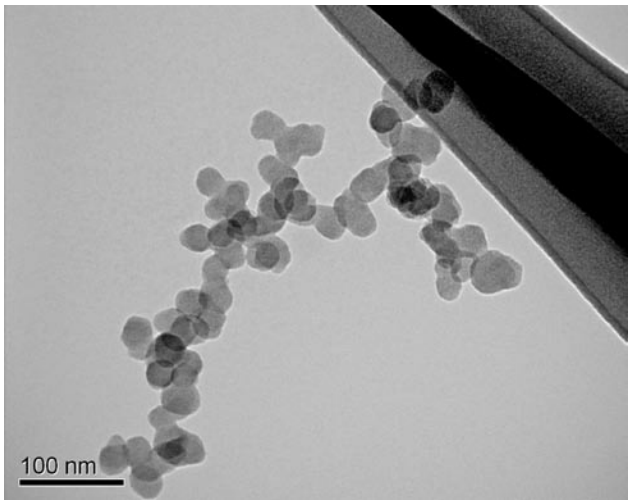

FIGURE 3. TEM image of PCCI soot with 100 nm electrical mobility diameter. (Engine conditions: 1,500 rpm, 2.6 BMEP)

PM and MSATs from an HCCI Engine Operating on Surrogate Gasoline Fuels

The effect of fuel chemical composition on HCCI engine efficiency and emissions was compared for the iso-octane reference fuel, iso-octane reference fuel with ethanol, and toluene reference fuel. The results indicated that combustion phasing for minimum fuel consumption differs depending on the fuel chemical composition. The lowest fuel consumption was achieved with the iso-octane reference fuel. Because the energy content of ethanol is lower than the other fuels, a comparison was made in terms of thermal efficiency, and the iso-octane reference fuel was again the most efficient. At the crank angle degree for 50% mass fraction burned and the minimum in fuel consumption for each fuel, the iso-octane reference fuel had the lowest PM number concentration emissions ($1.0 \pm 0.4 \times 10^5$ part./cm^3). Delaying the combustion event of the ethanol and toluene fuels, resulted in significant reduction of PM number concentration and only a slight rise in fuel consumption, such that the emissions were close to that for the iso-octane reference fuel. The fuel consumption and PM number concentration emissions results are shown in Figure 4 for the iso-octane reference fuel. For all fuels and conditions, the particle geometric mean diameter ranged from 10 to 30 nm. At the minimum fuel consumption point, the iso-octane reference fuel PM emissions had geometric mean diameter of 14 ± 1 nm. These findings

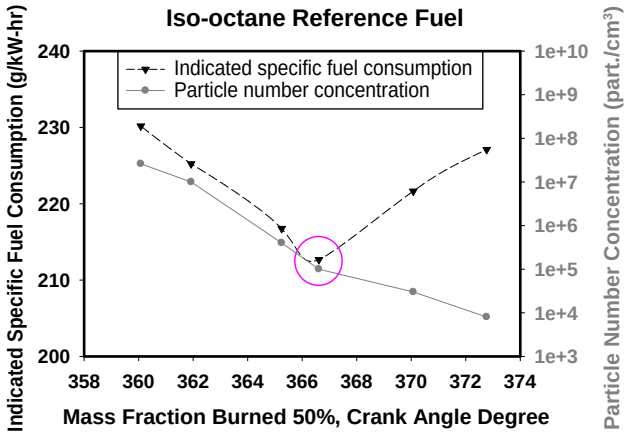

FIGURE 4. HCCI engine cycle timing for minimum fuel consumption (black) and particle number concentration emissions for each operating point (grey). The operating point for simultaneous low emissions and fuel consumption is circled (pink). (Engine conditions: 1,800 rpm, nominal 3.0 indicated mean effective pressure)

may be of use in future models of fuel effects on engine efficiency and emissions.

Conclusions

- Intermediate Blends:
  - Benzene, toluene, ethylbenzene and xylenes decrease with increasing ethanol content.
- PCCI and Conventional Diesel PM Effective Density:
  - The effective density of 50 and 100 nm PCCI PM was nearly the same as conventional diesel PM. For 150 nm particles, PCCI PM effective density was lower than conventional diesel PM.
  - The lower effective density of 150 nm PCCI PM may be the result of smaller soot primary particle diameters; based on TEM and image analysis, the average primary particle diameter of PCCI soot was 21 ± 3 nm and of conventional diesel soot 25 ± 4 nm.
- HCCI Gasoline Surrogate Fuels:
  - The lowest PM number concentration emissions and highest thermal efficiency occurred for the iso-octane reference fuel.
  - For the ethanol and toluene fuels, delaying the combustion event past the point of minimum fuel consumption reduced PM number concentration emissions substantially while only increasing fuel consumption slightly.
  - The PM geometric mean diameter for all fuels and combustion phasing conditions ranged from 10 to 30 nm.

References

1. Knoll, Keith, Brian West, Wendy Clark, Ronald Graves, John Orban, Steve Przesmizki, Timothy Theiss, "Effects of Intermediate Ethanol Blends on Legacy Vehicles and Msall Non-Road engines, Report 1 – Updated," ORNL/TM-2008-117, February 2009.

2. West, B., Lopez, A., Theiss, T., Graves, R., Storey, J., Lewis, S., "Fuel Economy and Emissions of the Ethanol-Optimized Saab 9-5 Biopower", SAE Paper Number 2007-01-3994. Society of Automotive Engineers, Warrendale. 2007.

3. Sluder, C.S., Wagner, R.M., Lewis, S.A., Storey, J.M., "Fuel Property Effects on Emissions From High Efficiency Clean Combustion in a Diesel Engine," SAE Paper Number 2006-01-0080. Society of Automotive Engineers, Warrendale, 2006.

4. Storey, J.M.E., Lewis, S.A. Sr., Parks, J.E. II, Szybist, J.P., Barone, T.L., Prikhodko, V.Y., "Mobile Source Air Toxics (MSATs) from High Efficiency Clean Combustion in Diesel Engines", *SAE Int. J. Engines*, Vol. 1, pp. 1157-1166, 2008.

5. Ishiguro, T., Suzuki, N., Fujitani, Y. and Morimoto, H. (1991) Microstructural changes of diesel soot during oxidation. Combustion and Flame, 85, 1-6.

6. Xiong, C. and Friedlander, S.K. "Morphological properties of atmospheric aerosol aggregates." Proc. Natl. Acad. Sci., 98, 11851-11856. 2001.

FY 2009 Publications/Presentations

1. John Storey, James Parks II, Sam Lewis, Laura Kranendonk, and Teresa Barone, "Measurement and Characterization of Unregulated Emissions from Advanced Technologies," *Presentation at the DOE Vehicle Technologies Merit Review* on May 21, 2009.

2. Teresa Barone, Anshuman Lall, John Storey, Michael Zachariah, Vitaly Prikhodko, James Parks, "A Comparison of Advanced and Conventional Diesel Combustion Particulate Matter Emissions: Particle Effective Density," In preparation.

3. Teresa Barone, John Storey, Scott Eaton, Bruce Bunting, Raynella Connatser, and Samuel Lewis, "The Influence of Fuel Chemical Composition on Particle Emissions from an Advanced Combustion Engine," *Poster Presentation at the* American Association of Aerosol Research 28th Annual Conference. Minneapolis, MN. October 2009.

4. Teresa Barone, John Storey, and Norberto Domingo, "Durability Analysis of a Field-Aged Diesel Particulate Filter Used in a School Bus Retrofit Program" *Oral Presentation* at the American Institute of Chemical Engineers Annual Meeting in Nashville, TN in November, 2009.

II.D.2 Collaborative Lubricating Oil Study on Emissions (CLOSE) Project

Dr. Douglas R. Lawson
National Renewable Energy Laboratory (NREL)
1617 Cole Boulevard
Golden, CO 80401

DOE Technology Development Manager:
Dr. James J. Eberhardt

Subcontractors:
- Southwest Research Institute®, San Antonio, TX
- Desert Research Institute, Reno, NV

Objective

The objective of this project is to quantify the relative roles of fuels and engine lubricating oil on particulate matter (PM) and semi-volatile organic compound (SVOC) emissions from in-use motor vehicles fueled with gasoline, 10% ethanol in gasoline (E10), diesel, biodiesel, and compressed natural gas (CNG) while operating on fresh and used crankcase lubricants.

Accomplishments

- Continued Cooperative Research and Development Agreement between NREL and the South Coast Air Quality Management District (SCAQMD) and the California Air Resources Board for project funding.
- Obtained additional funding from the Coordinating Research Council (sponsored by the automotive and petroleum industries), Lubrizol and the SCAQMD for project support.
- The American Chemistry Council Petroleum Additives Product Approval Protocol Task Group provided new and aged engine lubricating oils for all vehicles tested in the project.
- Completed all medium-duty vehicle ("normal" and high emitter) emissions testing in September 2009. Heavy-duty vehicle testing will begin in October 2009.

Future Directions

A variety of light-, medium-, and heavy-duty (LD, MD, HD) vehicles are being tested over different driving test cycles at room (72°F) and cold (20°F) temperatures on chassis dynamometers. The test matrix depicting the vehicles and test conditions is shown in Table 1. The complete vehicle and emissions testing project will be completed during Fiscal Year 2010.

The engine lubricating oil used in the project is labeled with deuterated hexatriacontane ($C_{36}D_{74}$). This tracer, along with other naturally-occurring compounds found in lubricating oil, such as hopanes and steranes, is used to quantify the relative contributions of PM formed from the fuels and the lubricants in the vehicles in the CLOSE Project.

TABLE 1. CLOSE Project Test Matrix

Test Temperature	72°F (nominal)				20°F			
Test Lubricant	Fresh		Aged		Fresh		Aged	
Vehicle / Sample Number	1	2	1	2	1	2	1	2
LD gasoline ("normal" PM emitter)	√	√	√	√	√	√	√	√
LD gasoline (high PM emitter)	√	√	√	√	√	√	√	√
LD E10 ("normal" PM emitter)	√	√	√	√	√	√	√	√
LD E10 (high PM emitter)	√	√	√	√	√	√	√	√
MD diesel ("normal" PM emitter)	√	√	√	√	√	√	√	√
MD diesel (high PM emitter)	√	√	√	√	√	√	√	√
MD biodiesel ("normal" PM emitter)	√	√	√	√	√	√	√	√
MD biodiesel (high PM emitter)	√	√	√	√	√	√	√	√
HD CNG ("normal" PM emitter)	√	√	√	√				
HD CNG (high PM emitter)	√	√	√	√				
HD diesel ("normal" PM emitter)	√	√	√	√				
HD diesel (high PM emitter)	√	√	√	√				

"Normal" and high-emitting vehicles representing gasoline, diesel, and CNG-powered vehicles are being tested. Lubricants used in each technology are representative of those currently on the market, with both new and aged lubricants being tested in the project. The fuels used in the vehicles will be gasoline containing no ethanol, E10, TxLED diesel, biodiesel, and CNG. Room temperature and cold temperature testing will be performed on all of the light- and medium-duty vehicles. Cold temperature testing will not be conducted on the heavy-duty vehicles due to funding limitations.

The data collected throughout the study are being chemically analyzed with detailed speciation to quantify the relative importance of the fuel and lubricant to PM

and SVOC emissions from these vehicles under the variety of testing conditions specified in the study design.

Introduction

Air quality studies conducted in Denver, Phoenix, Washington D.C., Pittsburgh, Portland, and the Office of Vehicle Technology's (OVT's) Gasoline/Diesel PM Split Study in Los Angeles have shown that PM from gasoline engines is a more significant contributor to ambient air quality than PM from diesel engines [1,2]. For example, data collected in Washington, D.C., over a ten-year period suggest that PM from gasoline exhaust is ten times more important to the emission inventory than diesel exhaust, as shown in Figure 1 [3].

OVT's comparative toxicity studies have also shown that the toxicity from gasoline exhaust on a per-unit-mass basis is at least as toxic as that from diesel exhaust, and that high emitters' toxicity is even greater than that from normal emitters [4].

Because PM and SVOC emissions from both gasoline and diesel exhaust are so important to human health and ambient air quality, it is important to understand their source – whether it derives from the fuel, the lubricant, or both, and to understand the engine operating conditions that are responsible for PM emissions. That is the objective of the CLOSE Project.

Approach

The CLOSE Project is conducting extensive chemical and physical characterizations of PM and SVOC emissions from vehicles fueled with gasoline, E10, diesel, biodiesel, and CNG while operating on fresh and used crankcase lubricants in an effort to improve our current understanding of the impact of crankcase lubricant formulations on vehicle emissions. In-use light- and heavy-duty vehicles are being recruited, including both "normal" and high-PM emitters, and operated on chassis dynamometers at room temperature (72°F nominal) and cold temperature (20°F). Gaseous (total hydrocarbons, non-methane hydrocarbons, carbon monoxide, oxides of nitrogen) and real-time particle emissions are being measured, and PM and SVOC samples are being collected for subsequent chemical analyses. Physical PM characterization is being conducted to obtain data on particle size and count, which will be investigated over the various driving test cycles run on the chassis dynamometers.

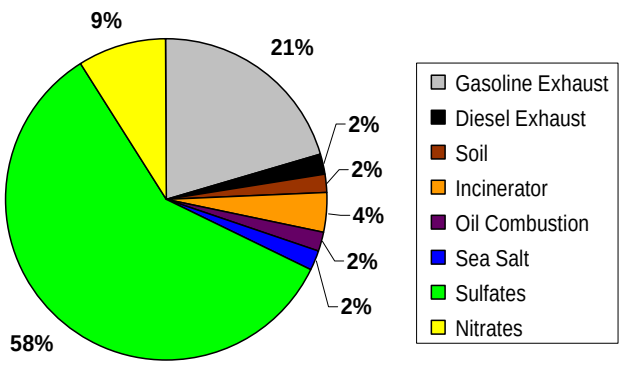

FIGURE 1. Source apportionment of $PM_{2.5}$ in the Washington, D.C., area, samples collected between 1988 and 1997 [3].

Results

At the time of this report, vehicle testing has been completed on the light-duty and medium-duty "normal" and high-emitting vehicles. Figures 2 and 3 show the "normal" emitter vehicle on the dynamometer, along with the sampling ports and equipment used in the sampling tunnel.

Conclusions

There is much national interest in the results coming from the CLOSE Project. In FY 2008, the Environmental Protection Agency asked for a presentation of the CLOSE Project at its Mobile Source Technical Review Subcommittee meeting in Arlington, VA, in May 2008, and additional presentations have been made to the Health Effects Institute and the annual DOE Merit Review Meeting. Because this project is not completed, there are no conclusions at the time of this report. The CLOSE Project will be completed by August 2010, and results will be available at that time.

References

1. Fujita, E.M., D.E. Campbell, W.P. Arnott, B. Zielinska, J.C. Chow. Evaluations of Source Apportionment Methods for Determining Contributions of Gasoline and Diesel Exhaust to Ambient Carbonaceous Aerosols, *J. Air & Waste Manage. Assoc.*, Vol. 57, pp. 721-740 (2007).

2. Lough, G.C. and J.J. Schauer. Sensitivity of Source Apportionment of Urban Particulate Matter to Uncertainty in Motor Vehicle Emissions Profiles, G.C. Lough and J.J. Schauer, *J. Air & Waste Manage. Assoc.*, Vol. 57, pp. 1200-1213 (2007).

3. Kim, E. and P. K. Hopke. Source Apportionment of Fine Particles in Washington, D.C., Utilizing Temperature-Resolved Carbon Fractions, *J. Air & Waste Manage. Assoc.*, Vol. 54, pp. 773-785 (2004).

FIGURE 2. Light-duty "normal" emitter tested in the CLOSE Project, a 2006 Chevrolet Impala.

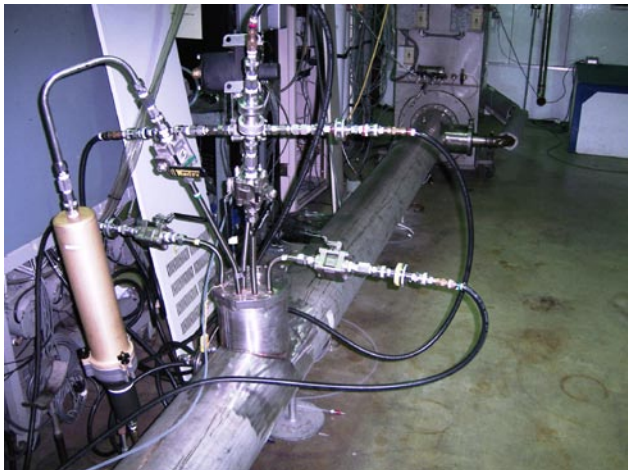

FIGURE 3. Sampling probes used to collect exhaust emissions samples from the dilution tunnel.

4. McDonald, J.D., I. Eide, J.C. Seagrave, B. Zielinska, K. Whitney, D.R. Lawson, J.L. Mauderly. Relationship between Composition and Toxicity of Motor Vehicle Emission Samples, *Environ. Health Persp.*, Vol. 112, pp. 1527-1538 (2004).

FY 2009 Publications/Presentations

1. "The Collaborative Lubricating Oil Study on Emissions (CLOSE) Project," progress reports presented at CRC AVFL meetings and at Infineum, February, May and October 2009.

2. "The Collaborative Lubricating Oil Study on Emissions (CLOSE) Project," presented at DOE Merit Review Meeting, Arlington, VA; May 2009.

II.D.3 The Advanced Collaborative Emissions Study (ACES)

Dan Greenbaum (Primary Contact),
Robert O'Keefe, Maria Costantini,
Annemoon van Erp
Health Effects Institute (HEI)
101 Federal Street, Suite 500
Boston, MA 02110

DOE Technology Development Manager:
James Eberhardt

NETL Project Manager: Carl Maronde

Subcontractors:
- Coordinating Research Council (CRC), Alpharetta, GA
- Lovelace Respiratory Research Institute (LRRI), Albuquerque, NM

Objectives

- Phase 1: Extensive emissions characterization at Southwest Research Institute® (SwRI®) of four production-intent heavy-duty diesel engine and control systems designed to meet 2007 standards for particulate matter (PM) and nitrogen oxides (NOx). One engine/aftertreatment system will be selected for health testing.
- Phase 2: Extensive emissions characterization of a group of production-intent engine and control systems meeting the 2010 standards (including more advanced NOx controls to meet the more stringent 2010 NOx standards).
- Phase 3: One selected 2007-compliant engine will be installed and tested in a specially-designed emissions generation and animal exposure facility at LRRI (Phase 3A) and used in chronic and shorter-term health effects studies to form the basis of the ACES safety assessment (Phases 3B and 3C). This will include periodic emissions characterization during both a core 24-month chronic bioassay of cancer endpoints in rats and biological screening assays in both rats and mice (Phase 3B) as well as emissions characterization during a set of shorter animal exposures and biological screening using accepted toxicological tests after the end of the chronic bioassay (Phase 3C). (NOTE: Only the emissions characterization and biological screening activities during Phase 3 are components of the DOE ACES contract).

Accomplishments

Key Accomplishment

Issued and widely distributed on the Web and in media the first major report of ACES – the results of the extensive emissions characterization of 2007-compliant Class 8 heavy-duty engines from each of the four major manufacturers. The report highlighted dramatic improvements (>90% reduction of many emissions) in the new technology compared to 2004 technology.

General Oversight

- Held a combined meeting of the HEI ACES Oversight and Advisory Committees to review the data on exposure chamber concentrations in Phase 3A and make a final recommendation on dilution levels for the bioassay (June 2009).
- Communicated the recommendations about the dilution levels and other suggestions about exposure characterization during Phase 3A to the investigators at LRRI (June 2009).
- Communicated with Oversight Committee members and the investigators at LRRI about remaining issues regarding the protocols for Phases 3A (emissions characterization) and 3B (chronic bioassay) (July 2009).
- Held a conference call meeting of the ACES Steering Committee to review progress on disseminating Phase 1 results and implementing Phase 3, and to begin planning for Phase 2 (the detailed emissions characterization of the 2010-compliant heavy-duty engines) (July 2009).
- Shared with the ACES Oversight and Advisory Committees data from Phase 3A and planned a conference call to discuss them (August 2009).
- Sent the near-final Phase 3B protocol to the Advisory Committee for their input (August 2009).
- Held a conference call with the Oversight and Advisory Committees and the LRRI team to discuss initial Phase 3A results and plans for completion of Phase 3A and starting Phase 3B; during the call agreement was reached to use the slightly newer engine/aftertreatment combination B' for the animal exposures during the chronic bioassay because it is more representative of engine systems currently in the market than the original engine B (September 2009).
- Communicated with the LRRI team the requirements for completing emissions and animal chamber exposure characterization with engine

B' before receiving permission to start Phase 3B (September 2009).

Phase 1

- Completed emissions characterization of a duplicate selected engine ("fifth engine") at SwRI® under high altitude conditions as will be encountered at LRRI (October 2008).
- Received a draft final report on Phase 1 including an emissions characterization data set for all five engines (February 2009).
- Issued and widely disseminated the Phase 1 final report by SwRI® on June 18, 2009, including the Air & Waste Management Association meeting in Detroit, MI.
- Phase 1 results were already integrated into the latest U.S. Environmental Protection Agency (EPA) assessment of emissions, exposure, and health for consideration in the particulate matter National Ambient Air Quality Standards process.
- Made plans for publication of Phase 1 results in the peer-reviewed literature.

Phase 3

- Approved the protocol for Phase 3A, characterization of engine emissions and inhalation atmosphere at LRRI (October 2008).
- Installed the test engine (engine B) at LRRI, completed an initial set of emissions characterization, and commissioned the test cell (November 2008).
- Conducted further emissions characterization of the test engine B at LRRI under various operating conditions to ensure proper operation according to manufacturer specifications (December 2008).
- Shipped the duplicate engine (B′) from SwRI® to LRRI and secured the remainder of the original fuel batch used in Phase 1 for use in Phase 3 and arranged for delivery to LRRI (December 2008).
- Finalized the contract with LRRI for conduct of work in Phases 3A and 3B that falls within DOE funding (January 2009).
- Discussed a proposal from LRRI and collaborators to fill remaining gaps in biological screening regarding measurements of immune responses in mice with the ACES Oversight Committee, who did not approve funding (February 2009).
- Resumed detailed emissions and exposure chamber characterization of the test engine B at LRRI for Phase 3A after both dynamometers were repaired (April 2009).
- Completed detailed emissions and exposure chamber characterization of the test engine B at LRRI in Phase 3A and commenced characterization of the back-up engine B' (July 2009).

Future Directions

Phase 1

- Publish Phase 1 results in a peer-reviewed journal.
- Continue to promote and disseminate results at professional and other meetings and to ensure their integration into key decision documents.

Phase 2

- Review feasibility and develop and implement timeline for beginning Phase 2 characterization of 2010-compliant engines.

Phase 3

- Complete Phase 3A emissions and exposure chamber characterization at LRRI (October 2009).
- Agree upon final protocol for Phase 3B (October 2009).
- Receive a draft final report on Phase 3A (November 2009).
- Complete review of Phase 3A results and approve start of Phase 3B (November 2009).
- Complete contract negotiations for the additional biological screening studies (November 2009).
- Start chronic bioassay in rats and associated biological screening studies in rats and mice (December 2009/January 2010).
- Expose rats for 24 months and mice for 3 months at three selected diesel exhaust exposure concentrations (high, medium, and low) or clean air and obtain results from biological screening in rats and mice (2010 and 2011).

Introduction

The ACES is a cooperative, multi-party effort to characterize the emissions and assess the safety of advanced heavy-duty diesel engine and aftertreatment systems and fuels designed to meet the 2007 and 2010 emissions standards for PM and NOx. It is utilizing established emissions characterization and toxicological test methods to assess the overall safety of production-intent engine and control technology combinations that will be introduced into the market during the 2007-2010 time period. This is in direct response to calls in the U.S. EPA Health Assessment Document for Diesel Engine Exhaust (U.S. EPA 2002) for assessment and

reconsideration of diesel emissions and health risk with the advent of new cleaner technologies.

The characterization of emissions from representative, production-intent advanced compression ignition (CI) engine systems will include comprehensive analyses of the gaseous and particulate material, especially those species that have been identified as having potential health significance. The core toxicological study will include detailed emissions characterization at its inception, and periodically throughout a two-year chronic inhalation bioassay similar to the standard National Toxicology Program bioassay utilizing two rodent species. Other specific shorter-term biological screening studies also will be undertaken, informed by the emissions characterization information, to evaluate these engine systems with respect to carefully selected respiratory, immunologic, and other effects for which there are accepted toxicologic tests. It is anticipated that these emissions characterizations and studies will assess the safety of these advanced CI engine systems, will identify and assess any unforeseen changes in the emissions as a result of the technology changes, and will contribute to the development of a data base to inform future assessments of these advanced engine and control systems.

Approach

Experimental work under ACES is being conducted in three phases, as outlined in the Objectives. Detailed emissions characterization (Phases 1 and 2) is performed by an existing engine laboratory (SwRI®) that meets the U.S. EPA specifications for 2007 and 2010 engine testing. In Phase 1, emissions from four 2007-compliant engine/control systems have been characterized. One engine has been selected for health testing in Phase 3. In Phase 2, emissions from four 2010-compliant engine/control systems will be characterized. In Phase 3, the selected 2007-compliant engine/control system has been installed in a specially designed emission generation facility connected to a health testing facility at LRRI to conduct a chronic inhalation bioassay and shorter term biological screening in rats and mice. During the 2-year bioassay, emissions will be characterized at regular intervals throughout the testing.

The emissions characterization work is overseen by CRC and its ACES Panel. The health effects assessment is overseen by HEI and its ACES Oversight Committee (a subset of the HEI Research Committee augmented by independent experts from several disciplines), with advice from an Advisory Committee of ACES stakeholder experts. The overall effort is guided by an ACES Steering Committee consisting of representatives of DOE, engine manufacturers, EPA, the petroleum industry, the California Air Resources Board, emission control manufacturers, and the Natural Resources Defense Council. Set-up of the emission generation facility at LRRI (for Phase 3) and establishment of periodic emissions characterization throughout Phase 3 has been done with input from the team of investigators who conducted Phase 1 and the CRC ACES Panel.

Results

The results obtained during this reporting period pertain to (1) the Phase 1 characterization of emission rates of a fifth engine at high altitude conditions at SwRI®, and (2) Phase 3A characterization of engine emissions and inhalation chamber exposure atmosphere prior to the start of Phase 3B at LRRI.

Phase 1. Engine 5 (back-up engine for the chronic bioassay) was tested at SwRI® to verify that its regulated emissions were similar to those of the selected engine. Tests were conducted using the Federal Test Procedure (FTP) test cycle and three steady-state tests modes. The emission rate of NOx was slightly higher than that of the selected engine while the emissions of CO and PM were lower. To facilitate the comparison with the emissions characterization that will be done at LRRI using the selected engine, a set of tests was conducted under simulated high-altitude conditions (the same as encountered at the LRRI facility). Higher altitude led to a small increase in NOx and CO emissions relative to emissions at sea level under some of the test conditions (see Table 1). Full results were included with the Phase 1 report with results from the four original test engines.

TABLE 1. NOx Emissions of Five 2007-Compliant Test Engines

		NOx, g/hp-hr					
		SwRI® Elevation					LRRI Elevation
Test Cycle[a]		Engine A	Engine B	Engine C	Engine D	Engine B′	Engine B′-Altitude
FTP-w	Avg	1.26	0.89	1.03	1.12	0.98	1.33
	Stdev	0.01	0.01	0.03	0.01	0.01	0.01
FTP-wo	Avg	1.25	0.90	1.05	1.11	0.97	1.31
	Stdev	0.01	0.01	0.01	0.02	0.01	0.03

[a]FTP-w includes crank case blow-by, FTP-wo is without blowby.

Phase 3A. Emissions characterization of engines B (main engine) and engine B' (back-up engine) commenced in late 2008. Due to complications with the test set-up–most notably with the dynamometer and its back-up–testing was delayed by several months. Testing of engine B was completed in July 2009; basic emissions and operating specifications were met and approved by the engine manufacturer. Initial testing of the exposure atmosphere in the animal inhalation chambers (without animals present) was conducted at a target NO_2 concentration of 4.2 ppm (lowest dilution level or highest diesel engine exhaust [DEE] concentration), 0.8 at the mid level and 0.01 ppm at the highest dilution level (Table 2).

The tests revealed some concerns regarding chamber temperature at the highest diesel exhaust concentration, which was close to what is allowed under animal care guidelines (data not shown). Levels of particles in the exposure chamber were very low except during trap regeneration (Figure 1).

Testing continued with engine B' at all dilution levels with additional room cooling in place to reduce the exposure chamber temperature. Based on the initial test results with both engines, final requirements for completion of Phase 3A were negotiated, including more detailed recording of trap regeneration events.

A decision was made to conduct the Phase 3B health testing with engine B' because it is a newer version of engine B with updated emission controls and has a larger share in today's marketplace. Thus, the remaining inhalation chamber characterization is being done with engine B' and is expected to be completed by the end of October 2009. At that time, the data will be reviewed and a decision to start Phase 3B will be made.

Conclusions

First, the publication and dissemination of the Phase 1 report in June 2009 was an important milestone in the project. Phase 1 results were well received at several conferences and a Webinar, and efforts to disseminate the results continue. Second, despite some technical delays, characterization of emissions and exposure atmosphere at LRRI in Phase 3 has made important progress. Completion of Phase 3A is expected very soon, allowing the main health effects testing during Phase 3B to go forward by the end of 2009. All this work has been conducted with input from the ACES stakeholders.

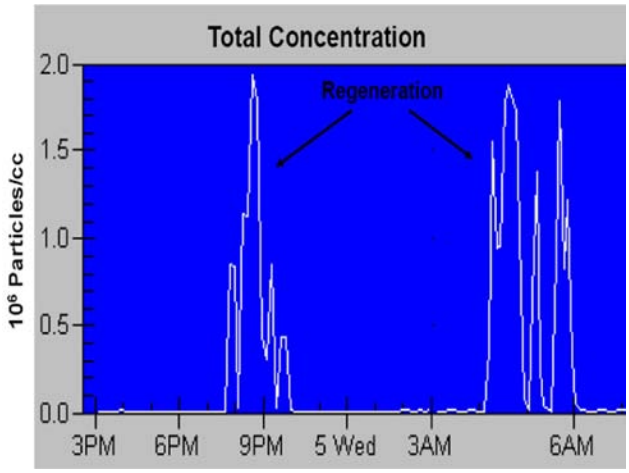

FIGURE 1. Real-Time Particle Number Concentrations in Inhalation Chamber during 16-hr Cycle

References

1. U.S. Environmental Protection Agency. 2002. Health Assessment Document for Diesel Engine Exhaust. EPA/600/8-90/057F. U.S. Environmental Protection Agency, National Center for Environmental Assessment, Office of Research Development, Washington, D.C.

FY 2009 Publications/Presentations

1. CRC Report: ACES Phase 1. Phase 1 of the Advanced Collaborative Emissions Study. June 2009. Coordinating Research Council, Alpharetta GA. Available from http://www.crcao.org/reports/recentstudies2009/ACES%20Phase%201/ACES%20Phase1%20Final%20Report%2015JUN2009.pdf.

2. Poster presentation at the CRC On-Road Vehicle Emissions Workshop in San Diego CA, March 2009: "Phase 1 of the Advanced Collaborative Emissions Study: Highlights of Project Findings."

3. Platform and poster presentations at the HEI Annual Conference in Portland OR, May 2009: "Advanced Collaborative Emissions Study (ACES)"; "Status of ACES

TABLE 2. Initial Characterization of Exposure Chamber Atmosphere during 16-hr Cycle at Three Dilution Levels

	High DEE						Mid DEE		Low DEE	
	CO_2 (ppm)	CO (ppm)	HC (ppm)	PM ($\mu g/m^3$)	NO (ppm)	NO_2 (ppm)	NO (ppm)	NO_2 (ppm)	NO (ppb)	NO_2 (ppb)
Avg	2786	-0.004	0.190	9.19	3.18	4.77	0.53	0.86	28.48	92.01
Stdev	121	0.262	0.233	3.62	0.082	0.273	0.013	0.026	1.917	10.93

Phase 3: Chronic Inhalation Bioassay"; and "Advanced Collaborative Emissions Study (ACES): Additional Studies of Genotoxicity and Vascular Endpoints Funded Under RFA 06-2".

4. Platform presentation at the annual DOE Vehicle Technologies Program Annual Merit Review, Arlington, VA, May 2009: "Advanced Collaborative Emissions Study (ACES)."

5. Platform presentations at the Air & Waste Management Association's 102nd Annual Conference & Exhibition in Detroit MI, June 2009:

- "Overview of the Advanced Collaborative Emissions Study (ACES)";
- "Advanced Collaborative Emission Studies - Regulated Emissions from 2007 Diesels";
- "Advanced Collaborative Emission Studies (ACES) - Unregulated Emissions from 2007 Diesel Engines";
- "Heavy-Duty Diesel Engine Test Cycles for the Advanced Collaborative Emissions Study";
- "Particle Number and Size Measurement Principles"; and
- "Particle Number Measurements from Filter-Equipped 2007 On-Highway Diesel Truck Engines."

6. Platform presentation at the ETH-Conference on Combustion Generated Nanoparticles June 2009, Zurich, Switzerland: "Particle Emissions from 2007 Heavy-Duty On-Highway Diesel Engines During Active Regeneration of Catalyzed DPF."

7. Platform and poster presentations at the Directions in Engine-Efficiency and Emissions Research (DEER) conference in Dearborn MI, August 2009:

- "Update on Phase 1 of the Advanced Collaborative Emissions Study (Aces Phase 1)"; and
- "Advanced Collaborative Emissions Study (ACES): Phase 3."

8. Webinar organized by the Diesel Technology Forum: "Heavy-Duty Diesel Engine Emissions Research Webinar" (September 2009). Available at http://www.dieselforum.org/multimedia.

III. Solid State Energy Conversion

III.1 Develop Thermoelectric Technology for Automotive Waste Heat Recovery

Gregory P. Meisner (Primary Contact),
Jihui Yang, James R. Salvador,
Michael G. Reynolds
General Motors Research and Development (GM R&D)
MC 480-106-224
30500 Mound Road
Warren, MI 48090

DOE Technology Development Manager:
John W. Fairbanks

NETL Project Manager: Carl Maronde

Subcontractors:
- Marlow Industries, Dallas, TX
- University of Michigan, Ann Arbor, MI
- Michigan State University, East Lansing, MI
- Brookhaven National Laboratory, Upton, NY
- Oak Ridge National Laboratory, Oak Ridge, TN
- University of Nevada, Las Vegas, NV

Objectives

- Construct and assemble thermoelectric (TE) generator heat exchanger subassemblies.
- Begin fabrication of lead telluride (PbTe) TE modules.
- Acquire and install electronics and control systems in vehicle.
- Continue optimization of cost-effective bulk TE materials.

Accomplishments

- Completed the TE generator design and commenced fabrication of heat exchanger subassemblies.
- Completed detailed design of the power electronics necessary for integrating the thermoelectrically generated power into the vehicle electrical system.
- Evaluated braze alloys and braze reflow methods for electrical connections to the PbTe materials in the TE modules.
- Designed tooling for fabricating ceramic headers for the TE modules.
- Synthesized several n-type PbTe ingots, and explored processing variables to reduce cracking and fragility and to improve adhesion of electrical and thermal contacts.
- Explored optimization of preferred materials for use in TE modules, including non-equilibrium grown skutterudites.
- Achieved a figure of merit (ZT) = 1.6 for multiple filled skutterudites, the highest value yet reached for any n-type filled skutterudite material.
- Validated experimental results on material properties and performance at high temperature, and demonstrated consistence of results among the various laboratories and measurement techniques used in this work.
- Developed a method for improving the TE properties of type I clathrates by doping transition metals on the gallium sites.
- Demonstrated improvement in the synthesis, processing, and transport properties of Yb-filled skutterudites associated with specifically created nano-scale precipitates at grain boundaries and within grains.
- Completed a systematic theoretical study of thermodynamic properties of PbTe-, PbSe-, and PbS-based TE materials to determine and thereby better understand their structural, electronic, and lattice dynamic properties.
- Conducted a computational and experimental study of the microstructure and nucleation mechanisms of nanoprecipitates that lead to the superior TE performance of the recently discovered material $(PbTe)_{1-x}(AgSbTe_2)_x$.

Future Directions

- Complete construction and assembly of the TE generator subassemblies.
- Complete fabrication of PbTe modules and validation of their performance.
- Assemble and integrate TE generator into a vehicle exhaust system.
- Integrate TE generator into the controls and electrical system of the test vehicle, and conduct preliminary testing.
- Collect and analyze performance data for TE generator in a test vehicle.
- Develop metal contact layers for skutterudites.

Introduction

During the past year, we have transitioned our focus from design, modeling, and material development work to fabrication, assembly, and implementation of a working TE generator for waste heat recovery. The modeling and simulation work for the TE generator has now yielded a specific engineering design, which

required down-selecting the materials for the heat exchanger and other structural parts, finalizing the geometry of the hot and cold side heat sinks, and resolving joining and other structural issues to ensure that the final unit could be assembled and installed on the vehicle. The development and fabrication of TE modules is progressing with the focus on maintaining good TE material properties while achieving material compatibility with electrical and thermal contacts within the modules. The vehicle modification and TE generator integration is underway, and this includes both adapting the exhaust system to work with the TE generator and installing the power electronics and control systems for interfacing with the generator's output. Our material research effort has focused on further improving material properties, such as higher ZT values and increased mechanical strength.

GM R&D is now completing the fabrication of the generator subassemblies and electrical subsystems, and much of the machine shop work is already completed. Additional circuitry for protection of the TE module assemblies is being designed and will be installed internal to the TE generator during its assembly. Marlow is fabricating and supplying the TE modules. Their work includes developing adequate electrical and thermal contact technology for the PbTe-based TE components within the modules specifically to achieve thermal and chemical stability in the harsh environment of the vehicular exhaust system. Similar work is underway for skutterudite materials. The electrical integration subsystems have been designed, and vehicle modification and integration work has begun. GM Powertrain is focusing on the vehicle modification, installation, and integration of the TE generator. Ultimately, their testing, data collection, and analysis will provide quantitative results for the actual performance of this TE-based waste heat recovery system under various vehicle driving conditions.

Approach

The scope of this project has ranged from the basic physics and chemistry of new and breakthrough TE materials to the modeling and design of a waste heat recovery device for automotive applications and, finally, to the engineering and assembly of a working TE generator. Existing and newly developed materials were carefully studied and selected by the materials research partners. Experimental results for TE material properties were validated by Oak Ridge National Laboratory to help avoid any potential pitfalls associated with material stability and performance at the elevated and cyclical temperatures typical of an automotive exhaust system. Mechanical property experts at Oak Ridge National Laboratory have provided electron microscopy of various materials selected for the project. Based on these results and mechanical property measurements, strength-limiting flaws has been identified that provide critical insight for the materials team in terms of improving the materials processing procedures to achieve better mechanical performance. These results were supplied to the system engineers to include in their TE generator design and optimization modeling. In addition, the cost per watt of electrical power generated was used as one of the primary metrics for design optimization. TE module development and fabrication by Marlow has focused on compatibility, durability, and robustness of the mechanical, thermal, and electrical contacts and connections. Vehicle level electrical and thermal management algorithms have been developed to optimize potential fuel economy gains. The design and modeling engineers worked closely with vehicle engineers to ensure that accurate vehicle level information was used for developing subsystem models and generator design, and this enabled the actual engineering and fabrication of the TE generator.

Throughout this project, we have incorporated costs associated with materials, modules, subsystems, and integration into the selection criteria for all of the aspects of the final generator design and implementation. We use this approach not only as a guide for balancing technology options, but also for providing consumer benefits.

Results

1. TE Generator Design

GM has now finalized the TE generator design, shown in Figure 1. The team ensured that the generator could be machined and assembled, and that it was mechanically compatibility with automotive components. The design is also flexible for swapping out TE modules in case of failure. Improvements were also made to enhance the thermal insulation between the cold and hot side to improve performance. The GM team that included people from GM Powertrain Integration, Exhaust Component Group, exhaust suppliers, and the R&D TE group, have approved the

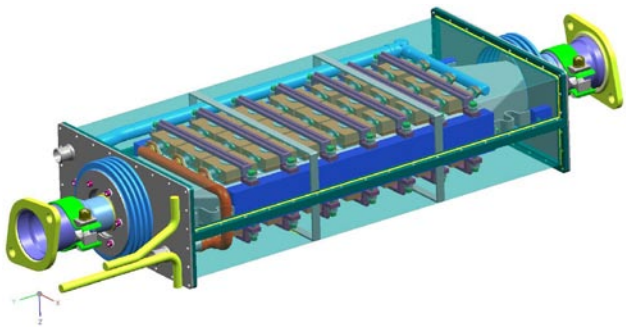

FIGURE 1. Side View of the TE Generator Design

design. Fabrication is underway; various parts and components have been ordered, most of which have been received.

2. Vehicle Integration

The task to identify the direct current (DC)-to-DC power conversion strategy was initiated at the beginning of the year. Based on the results of that study, a generator and power conversion topology was selected. Initial circuit simulation models were developed to examine high-level performance. We have also assessed the lumped element electrical properties and impedance of a typical commercial TE module. The results indicate that the low capacitance and inductance of the module should have no effect on the optimum power-tracking scheme. A simplified transient model was implemented in Matlab Simulink to simulate the dynamic performance of the TE generator system. The model is flexible and allows various drive cycles to be easily assessed. A proportional controller was designed and simulated in the Simulink model to control the exhaust bypass valve. The controller ensures that the TE generator remains within temperature and backpressure service limits. Significant effort has continued on the thermo-mechanical design of the generator. The focus remains on mitigating the significant differences in thermal expansion between the heat exchangers and the module interfaces.

3. TE Module Development

Marlow has evaluated braze alloys and developed braze reflow methods for PbTe modules, designed and ordered braze reflow tooling, and designed tooling for fabricating ceramic headers. An improved formula for p-type PbTe has been evaluated that is more mechanically robust and exhibits improved TE performance over both Na-doped PbTe and $PbSnTe_2$ formulas. Diffusion barrier metals and application methods for the improved P-type TE material have also been investigated. A functioning prototype module, as shown in Figure 2, has been fabricated by Marlow and is now being tested at GM. Marlow has also supplied the Bi-Te modules to GM for characterization and for the assembly of the TE generator.

4. TE Materials Research

The materials research team members continue to explore new materials and to optimize the existing materials. Non-equilibrium grown skutterudites have been characterized, and we attribute the low thermal conductivity values observed to nanostructures in these materials. Improvements in the TE properties of skutterudites have been achieved using three different filling atoms in the guest atom site [1], as shown in Figure 3. This result arises in part because of the different phonon scattering frequencies associated with the different fillers [2-4]. We have also developed a method for improving the TE properties of type I clathrates by transition metal doping on the Ga sites [5], and the results are shown in Figure 4.

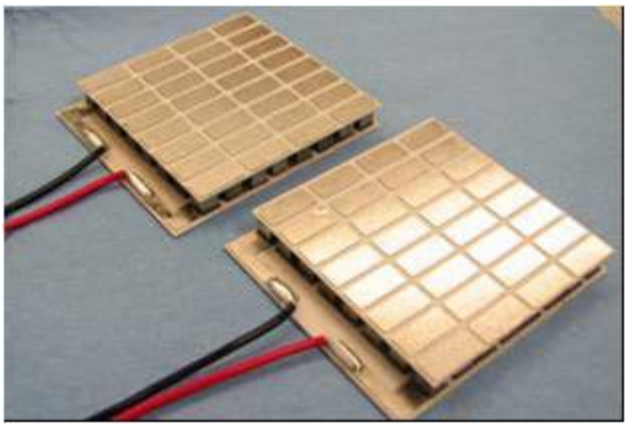

FIGURE 2. Prototype PbTe Modules

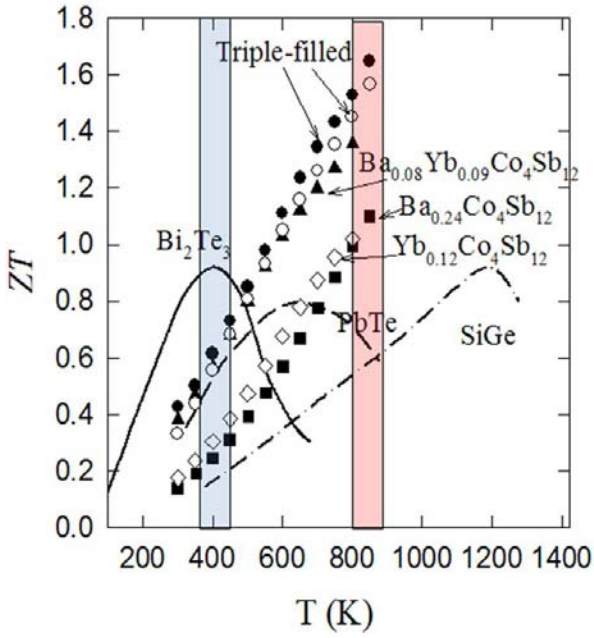

FIGURE 3. Improved Figures of Merit Values for Triple-Filled Skutterudites

Conclusions

We have made substantial progress on developing a TE generator for waste heat recovery from a vehicle exhaust system. This includes advances in the design, engineering, fabrication, and integration of a prototype unit, as well as in the design and fabrication of TE modules.

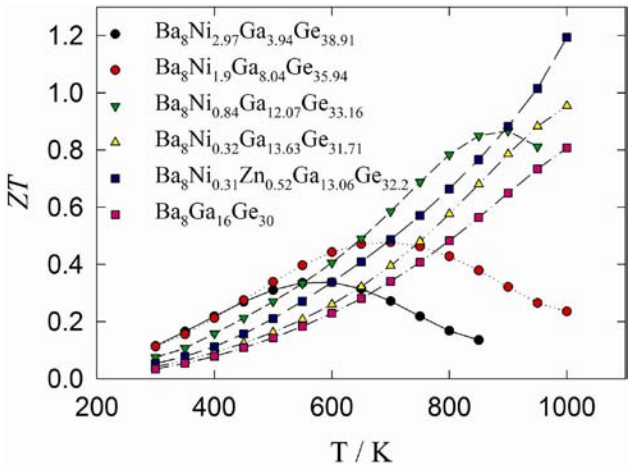

FIGURE 4. Temperature Dependence of the TE Figure of Merit *ZT* for TM-Substituted $Ba_8Ga_{16}Ge_{30}$

References

1. Shi, X., Salvador, J.R., Yang, J., and Wang, H., "Thermoelectric Properties of n-Type Multiple-Filled Skutterudites", J. Electronic Materials 38, 930 (2009).

2. Shi, X., Zhang, X., Chen, L.D., and Yang, J., Phys. Rev. Lett. 95, 185503, 2005.

3. Yang, J., Zhang, W., Bai, S.Q., Mei, Z., and Chen, L.D., Appl. Phys. Lett. 90, 192111, 2007.

4. Shi, X., Kong, H., Li, C.-P., Uher, C, Yang, J., Salvador, J.R., Wang, H., Chen, L., and Zhang, W., Appl. Phys. Lett. 92, 182101, (2008).

5. Shi, X., Yang, Jiong, Bai, S.Q., Yang, J., Salvador, J.R., Wang, H., Chi, M., Zhang, W.Q., Chen, L. and Wong-ng, W., Advanced Functional Materials (accepted).

FY 2009 Publications/Presentations

1. Shi, X., Yang, Jiong, Bai, S.Q., Yang, J., Salvador, J.R., Wang, H., Chi, M., Zhang, W.Q., Chen, L. and Wong-ng, W., "On the Design of High Efficiency Thermoelectric Clathrates through a Systematic Cross-substitution of Framework Elements", Advanced Functional Materials (accepted).

2. Beekman, M., Shi, X., Salvador, J.R., Nolas, G.S., and Yang, J., "Characterization of delafossite-type $CuCoO_2$ prepared by ion exchange", J. Alloys and Compounds (accepted).

3. Ke, X., Chen, C., Yang, J., Wu, L., Zhou, J., Li, Q., Zhu, Y., and Kent, P.R.C., "Microstructure and a Nucleation Mechanism for Nanoprecipitates in PbTe-$AgSbTe_2$", Phys. Rev. Lett. 103, 145502 (2009).

4. Pei, Y.Z., Yang, Chen, L.D. , Zhang, W., Salvador, J.R., and Yang, J., "Improving thermoelectric performance of caged compounds through light-element filling", Appl. Phys. Lett. 95, 042101 (2009).

5. Zhang, Y., Ke, X., Chen, C., Yang, J., and Kent, P.R.C., "Thermodynamic properties of PbTe, PbSe, and PbS: First-principles study", Phys. Rev. B 80, 024304 (2009).

6. Salvador, J.R., Yang, J., Shi, X., Wang, H., Wereszczak, A.A., Kong, H., Uher, C., "Transport and mechanical properties of Yb-filled skutterudites", Phil. Mag. 89, 1517 (2009).

7. Salvador, J.R., Yang, J., Shi, X., Wang, H., and Wereszczak, A.A., "Transport and mechanical property evaluation of (AgSbTe)1-x(GeTe)x (x = 0.80, 0.82, 0.85, 0.87, 0.90)", J. of Solid State Chemistry 182, 2088 (2009).

8. Wu, L., Zheng, J., Zhou, J., Li, Q., Yang, J., and Zhu, Y., "Nanostructures and defects in thermoelectric $AgPb_{18}SbTe_{20}$ single crystal", J. of Appl. Phys. 105, 094317 (2009).

9. Bai, S.Q., Pei, Y.Z., Chen, L.D., Zhang, L.D., Zhao, X.Y., and Yang, J., "Enhanced thermoelectric performance of dual-element-filled skutterudites BaxCeyCo4Sb12", Acta Materialia 57, 3135 (2009).

10. Yang, Jiong, Xi, L., Zhang, W., Chen, L.D., and Yang, Jihui, "Electrical Transport Properties of Filled CoSb3 Skutterudites: A Theoretical Study", J. Electronic Materials 38, 1397 (2009).

11. Yang, J. and Stabler, F. R., "Automotive Applications of Thermoelectric Materials", J. Electronic Materials 38, 1245 (2009).

12. Shi, X., Salvador, J.R., Yang, J., and Wang, H., "Thermoelectric Properties of n-Type Multiple-Filled Skutterudites", J. Electronic Materials 38, 930 (2009).

13. Wang, Y., Xu, X., and Yang, J., "Resonant Oscillation of Misch-Metal Atoms in Filled Skutterudites", Phys. Rev. Lett. 102, 175508 (2009).

14. Xi, L., Yang, Jiong, Zhang, W., Chen, L. and Yang, J., "Anomalous Dual-Element Filling in Partially Filled Skutterudites", J. Am. Chem. Soc. 131, 5560, (2009).

15. Yang, J., "Thermoelectric Materials by Design" Materials Science and Engineering Department Colloquium, University of Michigan, Ann Arbor, MI, January 2009 (invited).

16. Yang, J., "Thermoelectric Materials by Design" Materials Science & Engineering Department Colloquium, California Inst. of Tech., Pasadena, CA, May 2009, (invited).

17. Yang, J., "Development of Automotive Thermoelectric Waste Heat Recovery Technology" 2009 DEER Conference, Dearborn, MI: August 2009 (invited).

18. Yang, J., "Improving Energy Efficiency by Developing Components for Distributed Cooling and Heating Based on Thermal Comfort Modeling," 2009 DEER Conference, Dearborn, MI, August 2009, (invited).

19. Yang, J., "Engineering and Materials for Automotive Thermoelectric Applications", 2009 DOE Thermoelectric Applications Workshop, San Diego, CA: September 2009.

20. Yang, J., "Opportunities and Challenges for Automotive Thermoelectric Applications," MS&T Conference, Pittsburg, PA, October 2009 (Invited).

Special Recognitions & Awards/Patents Issued

1. "High Efficiency Transition-Metal-Doped Type I Clathrate Thermoelectric Materials", J. Yang, X. Shi, Jiong, Yang, S. Bai, W. Zhang, and L. Chen, P-008791, 3/6/2009 (pending).

2. "High Efficiency Multiple-Element-Filled Skutterudite Thermoelectric Materials", J. Yang, X. Shi, S. Bai, W. Zhang, and L. Chen, P-008792, 3/7/2009 (pending).

3. "Formation of thermoelectric (TE) elements by net shape sintering for improved mechanical property performance", James R. Salvador, J. Yang, and A. R. Wereszczak, P009885, 7/10/2009 (to be filed).

III.2 High-Efficiency Thermoelectric Waste Energy Recovery System for Passenger Vehicle Applications

J. LaGrandeur[1] (Primary Contact), D. Crane, Steve Ayers[1], C. Maranville[2], Andreas Eder[3], Lee Chiew[4]

[1] BSST LLC
5462 Irwindale Avenue
Irwindale, CA 91706

[2] Ford Motor Company
Scientific Research Lab
Room 2417, MD 3083
201 Village Road
Dearborn, MI 48124

[3] BMW AG
EG-65
Knorrstrasse 147
80788 Munich, Germany

[4] Emcon Technologies LLC
1050 Wilshire Drive
Suite 200
Troy, MI 48084

DOE Technology Development Manager: John Fairbanks

NETL Project Manager: Aaron Yocum

Subcontractors:
- BMW, Palo Alto, CA and Munich, Germany
- Ford Motor Company, Detroit, MI
- Visteon, Van Buren Township, MI
- Emcon Technologies LLC, Troy, MI

2009 Objectives

The primary objective of 2009 is to test a full-scale, high-temperature (600°C) thermoelectric generator (TEG) integrated with a BMW 6-cylinder engine on a dynamometer at the National Renewable Energy Laboratory (NREL) in Golden, Colorado. Through computer modeling and hardware bench testing it is predicted that the TEG will enable a reduction in fuel consumption by as much as 5%. Objectives for 2009 also include:

1. Improving TEG design readiness for commercialization.
2. Preparing for Phase 5 TEG installation in vehicles.

Accomplishments

At the time of this report, the high-temperature TEG subassemblies are in the final stages of build and test and dynamometer testing is planned to occur in January 2010.

- A significant TEG redesign has occurred, in which the planar form has been succeeded by a cylindrical shape, offering significantly improved manufacturability and, as a result, accelerated readiness for commercialization. The cylindrical TEG has been designed to provide a nominal 500 watts electric power during a 130 kph driving condition.
- Emcon has joined the BSST-BMW-Ford team for the 5th and final phase and has designed the TEG into BMW X6 (manufactured in South Carolina) and Ford Fusion exhaust systems.

Future Directions

- In early 2010 BSST is planning to complete dynamometer testing of a high-temperature TEG at NREL to validate the vehicle fuel efficiency performance model and to gain experience operating the TEG with an internal combustion engine.
- By June 2010, BSST, together with Emcon, will install high temperature TEGs into BMW and Ford demonstration vehicles to gain further experience and to show concept readiness.

✧ ✧ ✧ ✧ ✧

Introduction

In 2009 a 125 watt high-temperature TEG was built and successfully bench tested at BSST. The TEG was planar in design, with thermoelectric (TE) engines based on BSST's stack design arranged between flat plate cold (liquid) and hot (gas) heat exchangers. Although the test and thermal cycling results were encouraging, it was believed that the difficulty in maintaining coplanar, flat, smooth and equal separation distance flat plate heat exchangers would inhibit the commercialization of the technology and a decision to adapt the stack-designed TE engines to a cylindrical form factor was made (see Figure 1).

The advantages of a cylindrical TEG include:

1. Internal gas bypass for high-speed engine operation with a reduced TEG subsystem volume compared to planar form factors.
2. Improved heat transfer between hot and cold TE engine substrates and heat exchangers by rigidly attaching hot and cold TE substrates to their respective gas and liquid heat exchangers.

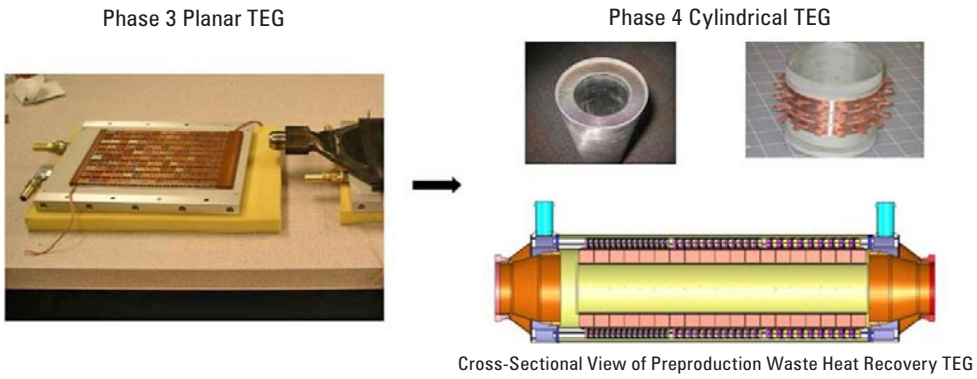

FIGURE 1. BSST TEG Transition, Planar to Cylindrical

The cylindrical TEG was analyzed for electric power production capability, installation volume, pressure drop and acoustic quality in the BMW X6 and Ford Focus and a preliminary design is taking shape for the 5th Phase vehicle demonstration project.

Approach

Due to the difficulties previously mentioned in maintaining tight tolerances in a planar TEG assembly, inconsistent heat transfer, and as a result, inconsistent hot and cold TE substrate temperatures were observed in Phase 3. An approach was taken in Phase 4 to rigidly attach the hot and cold TE substrates to heat exchangers to improve heat transfer which necessitated that coefficient of thermal expansion mismatches be managed within the TE engine subassembly. Thin barrier materials that provided acceptable heat transfer while maintaining electrical isolation between the TE substrates and heat exchangers had to be developed.

The stack design of the TE engine was carried through to the new, cylindrical design; however compliance features had to be developed for the TE engine subassembly to accommodate the required temperature excursions.

The design changes were evaluated through thermal cycling to evaluate robustness in advance of full-scale TEG build and test at a fractional TEG level.

Results

A 500-watt cylindrical TEG was designed including 36 copper rings rigidly attached to a stainless steel tube using a thermally-conductive, electrically-isolating barrier material. Each copper ring includes 15 “flags” which are used to attach TE elements for hot side heat transfer. The stainless steel tube has stainless clad copper wavy fin brazed to its inner circumference and a 55 mm cylindrical internal gas bypass. The TEG design includes three temperature zones to optimize TE material performance across the wide temperature variation in the direction of gas flow through the TEG. The three TE subassemblies optimized for performance in the direction of gas flow are shown in Figure 2.

The full-scale TEG is shown in Figure 3 fully assembled with outer cover and in cross section views.

The cold-side heat transfer is accomplished via flat shunts attached to small diameter tubes running in counter flow to the direction of the exhaust gas (see blue zone in bottom of Figure 3).

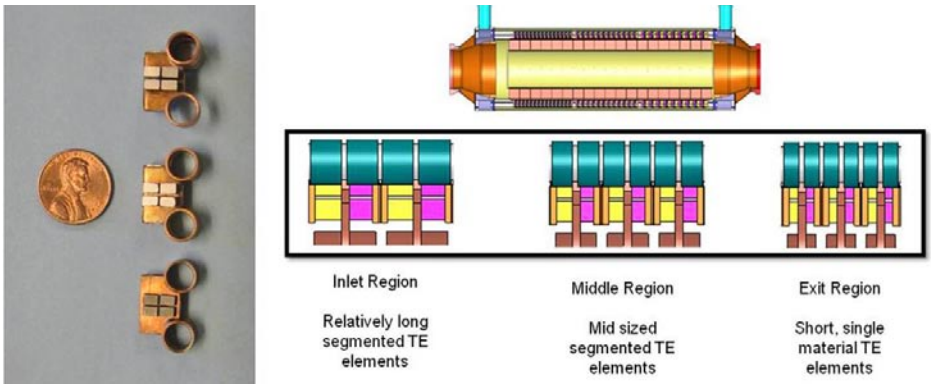

FIGURE 2. TE Subassemblies Optimized for Performance in the Direction of Gas Flow

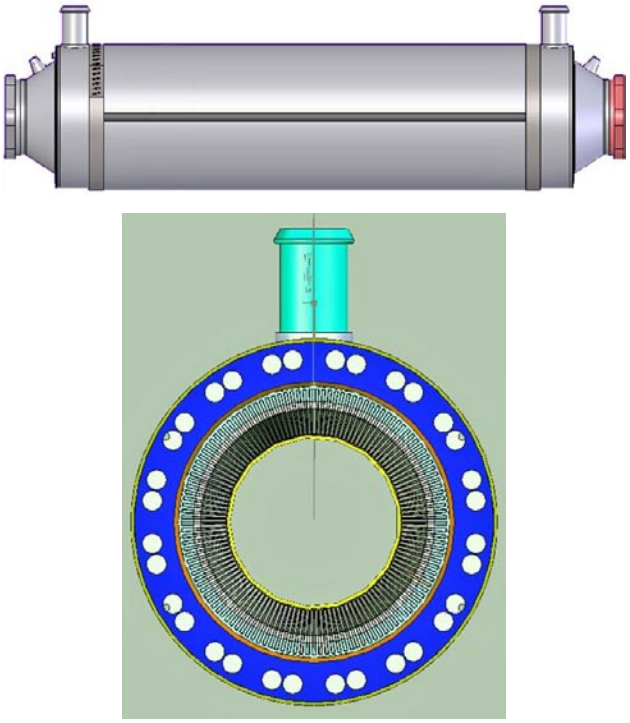

FIGURE 3. TEG Plan and Cross Section Views

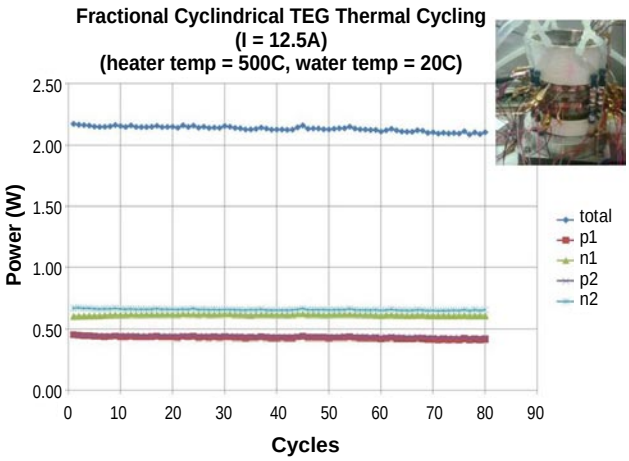

FIGURE 4. Fractional TEG Test Results

A fractional TEG was built including three copper rings with one of the 15 flag-rows populated with high-temperature TE subassemblies (top left in Figure 2). Temperature cycling results showing power produced over 80 temperature cycles for the fractional TEG are shown in Figure 4.

In preparation for Phase 5, modeling of the TEG was performed to determine pressure drop characteristics over a wide range of vehicle operating conditions. The modeling showed a 17% increase in static backpressure for the BMW X6 necessitating TEG design modification. The design modification is not complete, but early results indicate that the TEG outside diameter will need to increase to accommodate a larger internal bypass to manage backpressure during high speed driving events. The backpressure through the X6 exhaust system is shown in Figure 5 with and without the TEG installed.

In addition to the component level work performed in 2009, Ford Motor Company continued to evaluate TEG technology for applications including hybrid electric vehicles (HEVs), where TEG technology compliments regenerative braking and provides highway driving efficiency gains not otherwise achievable in an

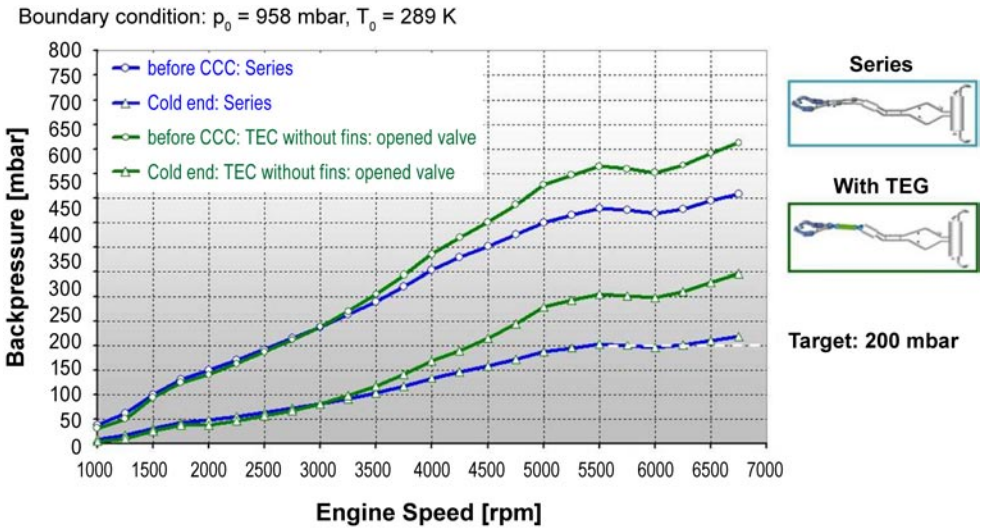

FIGURE 5. Backpressure Through the X6 Exhaust Component, With and Without the TEG Installed

HEV. Ford's analysis was performed by integrating BSST's TEG computer performance model into a vehicle fuel efficiency model and is reported in the following.

Ford Projected Mid-Term Performance Modeling

As reported in the 2008 Advanced Combustion Technologies Report, Ford performed detailed modeling of the benefit of a multilayer TEG in an Escape HEV. Results of that study, assuming materials and process that could be rapidly commercialized, indicated a potential of 90 watts while on the City cycle of the Federal Test Procedure (FTP) and 350 watts while on the Highway cycle of the FTP; and between 1 to 1.5% fuel economy improvement over the combined FTP driving cycles. To determine the amount of improvement in fuel economy achievable in the mid-term, the study results were extrapolated to determine the relative effect of key parameters thought to be achievable in the 6-8 year timeframe, assuming continuing technical and commercial progress. Key parameters included an average 75% improvement in ZT, a significant reduction in heat transfer losses due to thermal bypass, and a 3X improvement in interfacial resistance. With these improvements, power produced was estimated to increase to 240 watts for the City cycle and 1,000 watts for Highway cycle, with fuel economy improvements in the range of 5% to 7%. Costs were not analyzed for these studies. Results are summarized in Table 1.

TABLE 1. Results of TEG in a Escape HEV Using Near-Term (1-3 year) and Mid-Term (6-8 year) Materials and Processes

	Current Design	Mid-Term Design
Material Performance (ZT)	0.97	1.7
Heat Transfer Losses	40% $T_{hot,\ junction}$ = 180 – 250°C	20% $T_{hot,\ junction}$ = 350 – 420°C
TE Mass	1.6 kg	1.1 kg
Interfacial Resistance	2 μΩ-cm²	0.5 μΩ-cm²
% Conversion Efficiency	4.8 % T_h: 215°C, T_c: 90°C	14.4 % T_h: 385°C, T_c: 90°C
Power Generated – M/H EPA Cycle (Watts)	90 / 350	240 / 1000
Fuel Economy Improvement	1.5%	5%-7% (est.)

Conclusions

In 2009 the BSST-led TEG project focused on accelerating the commercialization of the technology by addressing fundamental challenges relating to the fabrication, assembly and integration of a TEG with heat exchangers and the exhaust system. Significant progress was made by converting the planar design to a cylindrical form and early prototype TEG testing shows promising results.

In preparation for the 5th and final phase, in which TEGs will be installed and evaluated in BMW and Ford vehicles, a new partner, Emcon Technologies, was added who brings excellence in exhaust system design, analysis and production. Through analysis of vehicle operating conditions and exhaust system analysis, the design of the TEG will be modified from Phase 4 to accommodate requirements at the vehicle level for Phase 5.

FY 2009 Publications/Presentations

1. Bell, L.E. and Crane, D.T., 2009, "Vehicle Waste Heat Recovery System Design and Characterization", *International Thermoelectric Conference*, Freiburg, Germany.

2. Crane, D.T. and LaGrandeur, J.W., 2009, "Progress Report on BSST Led, US DOE Automotive Waste Heat Recovery Program", *International Thermoelectric Conference*, Freiburg, Germany.

3. Ayers, S., Bell, L.E., Crane, D.T., and LaGrandeur, J.W., 2009, "Development of a 500 Watt High Temperature Thermoelectric Generator", *Directions in Engine-Efficiency and Emissions Research (DEER Conference*, Dearborn, Michigan.

4. LaGrandeur, J.W., 2009, "Automotive Fuel Efficiency Improvement via Exhaust Gas Waste Heat Conversion to Electricity", *Thermoelectrics Application Workshop*, San Diego, California.

Special Recognitions & Awards/Patents Issued

1. U.S. Patent Application, Title: WASTE HEAT RECOVERY SYSTEM, U.S. Application No.: 61/228,528, Filed: July 24, 2009.

III.3 Thermoelectric Conversion of Waste Heat to Electricity in an Internal Combustion Engine Vehicle

- Harold Schock, Professor, Mechanical Engineering, Principal Investigator (Primary Contact)
- Eldon Case, Professor, Chemical Engineering and Material Science
- Tim Hogan, Associate Professor, Electrical and Computer Engineering
- Jeff Sakamoto, Assistant Professor, Chemical Engineering and Material Science
- Fang Peng, Associate Professor, Electrical and Computer Engineering
- Edward Timm, Research Associate, Mechanical Engineering
- Trevor Ruckle, Research Assistant, Mechanical Engineering
- James Winkelman, Research Associate, Mechanical Engineering

Michigan State University (MSU)
450 Hannah Administration Building
East Lansing, MI 48824

DOE Technology Development Manager:
John Fairbanks

NETL Project Manager: Samuel Taylor

Subcontractors:

- Tom Shih, Professor and Chair,
  Department of Aerospace Engineering
  Iowa State University, Ames, IA
- Mercouri Kanatzidis, Professor, Chemistry
  Northwestern University, Evanston, IL
- Thierry Caillat, Senior Member of Technical Staff
  Jean-Pierre Fleurial, Technical Staff
  NASA – Jet Propulsion Laboratory (JPL),
  Pasadena, CA
- Christopher Nelson, Technical Advisor,
  Advanced Engineering
  Cummins Engine Company, Columbus, IN

Objectives

- Evaluate the available thermoelectric materials and develop the capability to build a thermoelectric generator from that material with power output to 1 kW.
- Quantify the potential performance gains possible by implementation of a thermoelectric auxiliary power unit (APU) for this application.
- Demonstrate a generator constructed of the non-heritage thermoelectric material chosen.
- Evaluate the cost to benefit by implementation of a thermoelectric APU.

Accomplishments

- We have evaluated various materials and chosen skutterudite as the non-heritage material for our generator demonstrations.
- We have developed the capability to fabricate thermoelectric generators using non-heritage thermoelectric material.
- We have demonstrated 5-, 25-, 50- and 100-watt generators fabricated from skutterudite and heated with air.
- We have evaluated the cost-to-benefit of implementation of a thermoelectric APU.

Future Directions

Analyze

- Establish the modes of failure experienced during operation of the generators described above and engineer a solution to correct these issues.

Conduct

- Scale up the hot pressing operation to allow for production of a 75 mm diameter n and p type thermoelectric material billets.
- Identify significant barriers relevant to implementation of thermoelectric generators (TEG) in transportation systems.
- Demonstrate the operation of a 1 kW TEG.

Introduction

The previous Phase I effort has described the technology barriers to overcome for successful implementation of thermoelectric technology to extract electric energy from the exhaust gases of an over-the-road Class 8 diesel engine. In Phase I, we evaluated the materials developed at MSU (Kanatzidis-Hogan-Schock). We also considered current materials and module designs of one of our project partners, NASA-JPL. The MSU materials were evaluated in conjunction with engine simulations and TEG thermal analysis. Using a different set of materials based on the skutterudite family, JPL has built high efficiency TEGs with proven reliability and efficiency. The JPL experience provides us the opportunity to leverage

our effort with over 50 years worth of experience in the design, construction and cost analysis related to TEGs. Critical to a realistic evaluation of thermoelectric technology for this application is the calculation of the temperature gradients available in the exhaust stream while maintaining the performance of the engine.

Much work has been devoted to developing thermoelectric materials, calculating theoretical power outputs and researching the most cost-effective applications for these devices. However, there have been very few experiments performed that put these theoretical concepts to the test by measuring the actual power generated by the thermoelectric modules in a semi-realistic environment. In Phase II, our work concentrates on developing the methods to build and test TEGs. These methods included material synthesis, powder processing, hot pressing, unicouple fabrication, modules fabrication and generator testing. The goal of the Phase II generator effort was to design, fabricate and test a 50-W and a 100-W TEG and thus verify the feasibility of using high-temperature TEGs for salvaging energy from waste heat. In addition to fabricating and testing a TEG, we continued parallel studies of new material research, powder processing techniques, mechanical property characterization and power electronics. One of the final objectives was to determine the cost and price model of 1-kW and 5-kW thermoelectric-based APUs on Class 8 trucks.

Module Fabrication

After a batch of Skutterudite unicouples have been fabricated, the unicouples are used to build modules. A 10-leg module (5 n- and p-type unicouples) is fabricated by soldering in series the 5 unicouples to tin-coated copper plates (cold shoes). A copper plate with a brass fastener was soldered onto each end of the module to allow it to be integrated into a generator assembly. The modules contained five 1 W (nominal output for a $\Delta T = 500°C$) skutterudite unicouples connected in series; thus, each module was capable of producing around 5 W under normal testing conditions (shown in Figure 1).

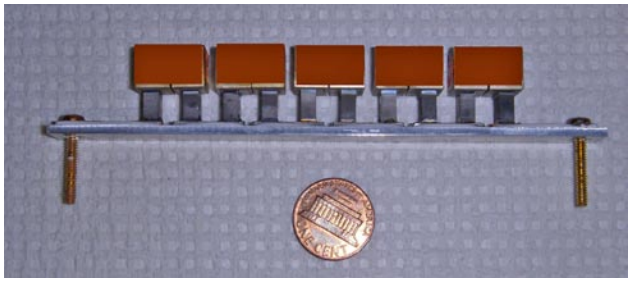

FIGURE 1. A 10-Leg Module Capable of Producing 5 W

TEG System Design

The configuration used to test the modules was divided into three systems, heating, cooling, and electrical, (shown in Figure 2). The heating system starts with nitrogen gas as the working fluid. The nitrogen starts as a compressed gas and is regulated into a heating airtorch system. The nitrogen gas first flows though a Meriam Instruments laminar flow element to measure the flow rate and then into the airtorch. A flow divider is then used to force the nitrogen gas through flow tubes directed onto the TEG. After heating the TEG, the gas is diluted with cold air and exhausted. Temperatures are measured at every stage within the system; before the heater, in the TEG and after the TEG.

The cooling system starts with tap water that flows through four Gems Sensors roto-flowmeters to measure the flow rate and then through copper cold plates which the modules are in contact with to remove heat. The water temperature is measured before entering the cold plate and after exiting to find the ΔT and thus, the energy gained.

The electrical system consists of the TEG, a Kepco power supply that was used to backload the modules, and an Omega OMB-DAQ-56 data acquisition system to monitor and record the voltages of each TEG module.

Prior to testing, the 10- and 20-module TEG, a single 10-leg module was evaluated. An infrared camera was used to estimate the temperature of the each of the hot shoes on the 10-leg module and determine some of the gas flow characteristics that affect the modules performance. This setup was tested two different times to demonstration repeatable power outputs for the module. The nitrogen gas was heated to 685°C with a flow rate of 9.7 cubic feet per minute. Using this temperature and flow rate, the hot shoes reached a

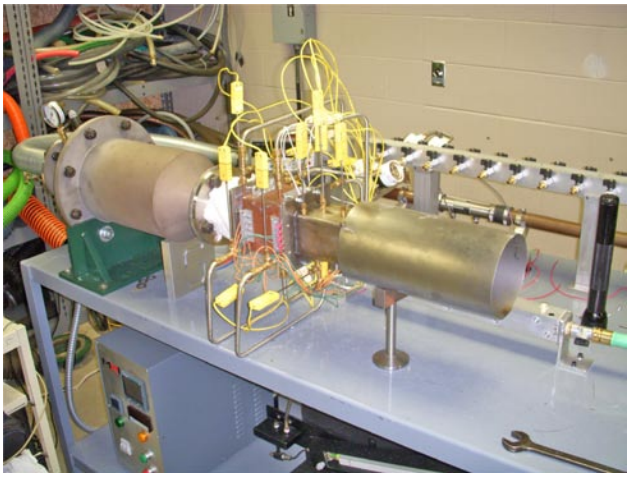

FIGURE 2. System Consisting of a Heater, Cooling System and Electrical Components used for Testing a TEG

temperature of 500-550°C. In both tests, the module produced 5.4 W with an open circuit voltage of 0.725 volts. Both of the power and voltage curves are shown in Figure 3.

The results of the 10-module generator test are shown in Figure 4. At a maximum inlet temperature of 716°C and a ΔT of 550°C between the hot side and the cold side, the generator produced a combined power output of 50.1 W at a steady 13 amps. The maximum power output for the 10 modules ranges from 3.9 to 5.9 W. The sum of the maximum power achieved for each of the 10 modules was about 50.4 W. This was the most successful test of a number of modules conducted by the MSU group to date. Based on an energy balance, and assuming similar energy recovery by adding additional modules, we estimate that the technology demonstrated could be implemented in construction of a TEG which would recover about 4% of the energy in an air (or exhaust) stream. The energy flow rate for this experiment was nominally equal to the output of a four-cylinder engine operating at steady road load conditions.

In the 20-module generator test, several of the modules failed, resulting in a reduced power output. Results of the 20-module test are shown in Figure 5. During this test, the power output was measured only from 10 to 16 amps. At a maximum inlet temperature of 790°C, the ΔT between the hot side and cold side only reached 440°C. This produced a combined power output of 70.4 W at 10 amps. The maximum power output from each module ranged from 1.9 to 5.0 W.

TEG Insulation - Aerogel Activities

Three thrusts comprised the aerogel-insulation activities. First, the first generation aerogel formulation was integrated into multiple unicouples, subassemblies, individual panels and one entire TEG. The formulation was first developed at JPL and has been modified by the Sakamoto group at MSU. It is now compatible with the Skutterudite TEG technology. Secondly, efforts to improve and characterize the next generation aerogel were conducted. Attempts to improve the consistency from batch to batch were conducted and a preliminary test to measure the thermal insulation efficacy was completed. Lastly, efforts to significantly reduce the cost of aerogel encapsulation were initiated. The key to reducing costs will likely require the ability to dry the aerogel under ambient conditions rather than in an autoclave as is currently done.

Cost and Price Model of 1-kW and 5-kW Thermoelectric-Based APUs for Class 8 Trucks

Introduction

This effort is intended to serve as an initial evaluation of the economics associated with the use of

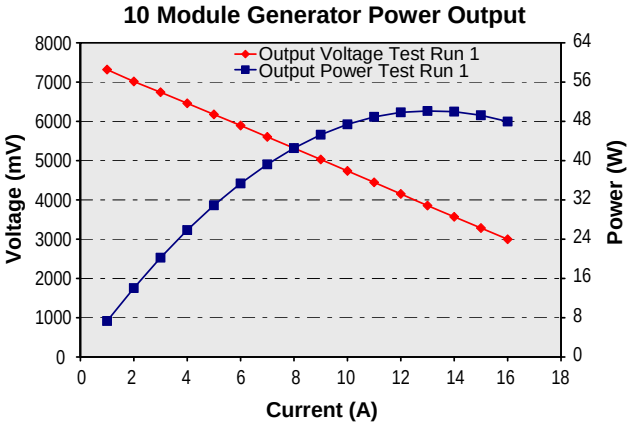

FIGURE 4. Combined Voltage and Power Output Curves for a 10-Module Generator

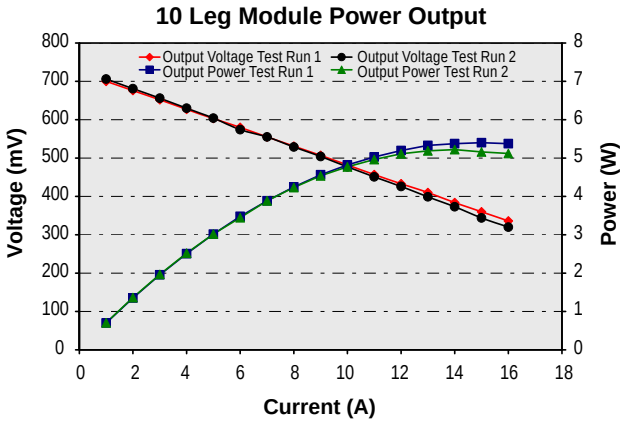

FIGURE 3. Voltage and Power Output Curves for a Single 10-Leg Module for Two Different Test Runs

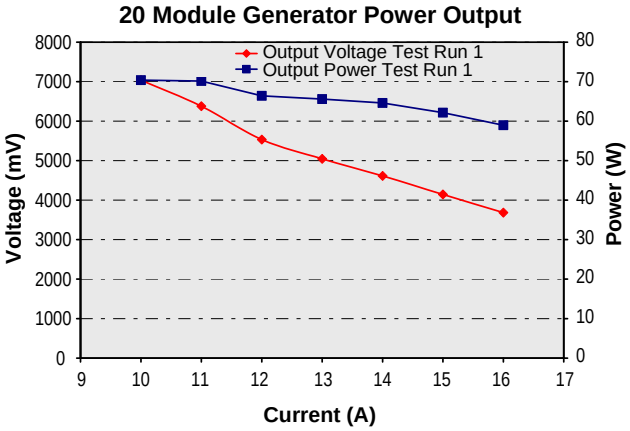

FIGURE 5. Combined Voltage and Power Output Curves for a 20-Module Generator

a waste heat energy recovery system that also provides an APU to the vehicle utilizing solid state TEGs. To facilitate the cost and pricing study, the APU under study was divided into four major subsystems:

- Electrical/Electronics
- Thermoelectric Generator
- Burner
- Cooling Subsystem.

In developing a "retail" price for the whole system, we used a process of establishing a price for each of the subsystems and adding the parts up to establish the total cost. The price number reflects an attempt to include such things as fully accounted for labor, overhead (building cost, cost of capital, etc.), and general and administrative cost. The general rule, the material cost makes up only a certain percentage of the price that is used and the specific percentage varies by subsystem. Thus, by having the material cost and the percent of the price, we can calculate the price of the part.

The early estimate for the price that a manufacturer would have to charge for a 1-kW system to cover his cost and provide a reasonable return is $4,773.77. The estimate for the price of a 5-kW system using the same procedure as for the 1-kW system is $19,276.13. The details for developing these price estimates follow.

Total 1-kW System Price

To develop the price for the 1-kW systems, we totaled the cost for the following four major subsystems:

Electrical/Electron	$943.28
TEG Subsystem:	
TEG devices	$1200.00
Module Assembly	$1124.85
Housing	$400.00
Burner	$717.00
Cooling Subsystem	$388.64
Total	**$4,773.77**

Total 5-kW System Price

To develop the price for the 5-kW systems, we total the cost for the following four major subsystems:

Electrical/Electronics	$4671.68
TEG Subsystem:	
TEG devices	$6000.00
Module Assembly	$5624.25
Housing	$600.00
Burner	$717.00
Cooling Subsystem	$1663.20
Total	**$19,276.13**

These prices are estimates. As the design and process steps become better defined, the assumptions used in developing the cost and prices can be reduced.

Total 1 kW System Price Based on Four Subsystems

- Electrical/Electronics $943.28
- TEG Subsystem
  - TE Materials $1200.00
  - Module Assembly $1124.85
  - Housing $400.00
- Burner $717.00
- Cooling Subsyste $388.64

Total Price $4773.77

Total 5 kW System Price $19276.13

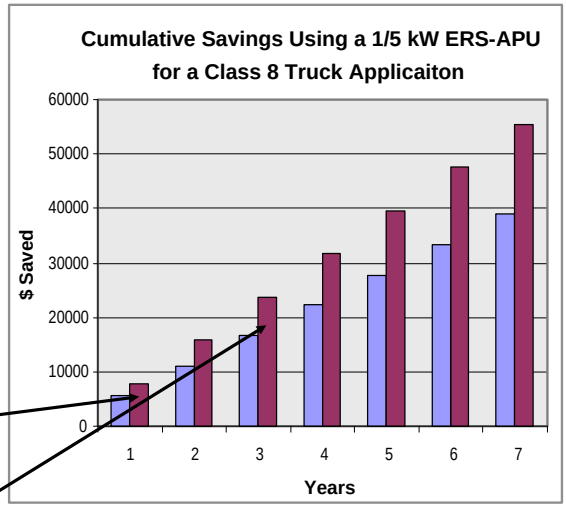

FIGURE 6. TEG cost to benefit for a 1- and 5-kW Thermoelectric APU

Cost-to-Benefit Anticipated for 1- and 5-kW, Thermoelectric APU Systems

Figure 6 shows the cost-to-benefit anticipated with 1- and 5-kW, thermoelectric APU systems. The benefits come from energy recovery while the vehicle is in operation and by a savings during idling periods by allowing one to turn the engine off. Assumptions are a 10% efficient thermoelectric generator APU operation as it can operate at a higher temperature than in the exhaust heat recovery mode, and 1 and 5 kW recovered during these modes. The vehicle is assumed to operate 150,000 miles per year in 300 days with eight hours of idling each day. This savings is likely the upper limit that could be anticipated for this configuration.

FY 2009 Publications

1. "Heat Transfer Enhancement in Thermoelectric-Power Generation," Hu, K., Chi, X., Shih, T.I-P. and Schock, H.J., AIAA 2009-1210, January 2009.

Technical Publications, DOE 2009

1. "Agglomeration during wet milling of LAST (Lead-Antimony-Silver-Tellurium) powders," B.D. Hall, E.D. Case., F. Ren, J. Johnson and E.J. Timm, Materials Chemistry and Physics, 113[1]: 497 – 502, 2009.

2. "Temperature-dependent elastic moduli of lead-telluride based thermoelectric materials," F. Ren, E.D. Case, J.E. Ni, E.J. Timm, E. Lara-Curzio, R.M. Trejo, C.-H. Lin, M.G. Kanatzidis, Philosophical Magazine, 89[2]: 143- 167, 2009.

3. "Room temperature mechanical properties LAST (Pb-Sb-Ag-Te) thermoelectric materials as a function of cooling rate during ingot casting," F. Ren, E.D. Case, B.D. Hall, J.E. Ni, E.J. Timm, C-I. Wu, T. Hogan, and E. Lara-Curzio, Philosophical Magazine Letters, 89: 267 – 275, 2009.

4. "Temperature dependent thermal expansion of cast and hot pressed LAST (Pb-Sb-Ag-Te) thermoelectric materials," F. Ren, B.D. Hall, E.D. Case, E.J. Timm, R.M. Trejo, R. Meisner, and E. Lara-Curzio, Philosophical Magazine, 89: 1439-1455, 2009.

5. "Porosity dependence of elastic moduli in LAST (Lead-antimony-silver-tellurium) thermoelectric materials," Jennifer E. Ni, Fei Ren, Eldon D. Case, Edward J. Timm, accepted for publication, Materials Chemistry and Physics.

6. "Anomalous temperature-dependent Young's modulus of a cast LAST (Pb-Sb-Ag-Te) thermoelectric material," F. Ren, E.D. Case, E.J. Timm, E. Lara-Curzio and R.M. Trejo, accepted for publication, Acta Materialia, 2009.

7. "Room Temperature Young's modulus, shear modulus, Poisson's ratio and hardness of $Ce_{0.9}Fe_{3.5}Co_{0.5}Sb_{12}$ and $Co_{0.95}Pd_{0.05}Te_{0.05}Sb_3$ skutterudite materials," Robert Schmidt, Jennifer E. Ni, Eldon D. Case, Jeffery Sakamoto, Daniel Kleinow, Bradley Wing, Ryan Stewart, Edward J. Timm, to be submitted, Journal of Alloys and Compounds.

Technical Presentations, 2009

1. "Thermoelectric Generators Made with Novel Lead Telluride Based Materials," Chun-I Wu, Steven N. Girard, Joe Sootsman, Ed Timm, Robert Schmidt, Mercouri G. Kanatzidis, Harold Schock, Eldon D. Case, Duck Young Chung, Timothy P. Hogan, abstract submitted, Materials Research Society Fall meeting, Boston, MA, Nov. 30 – Dec. 4, 2009.

2. "Opacified, Reinforced Aerogel for Thermal Insulation of Thermoelectric Generators and Other Advanced Energy Systems," Jeff Sakamoto and Ryan Maloney, Materials Science and Technology Conference, Pittsburgh, PA., Oct. 27, 2009.

3. Powder Processing and Mechanical Properties of n- and p-type skutterudites, R.D. Schmidt, J.E. Ni, F. Ren, E.D. Case, J.S. Sakamoto, D.C. Kleinow, E.J. Timm, abstract accepted Materials Science and Technology Conference, Pittsburgh PA, October 2009.

4. "Thermoelectric Conversion of Waste Heat to Electricity in an IC Engine Powered Vehicle," Presented by Harold Schock, in collaboration with: Eldon Case, Thierry Caillet, Charles Cauchy, Jean-Pierre Fleurial, Tim Hogan, Mercouri Kanatzidis, Ryan Maloney, Christopher Nelson, Jennifer Ni, James Novak, Fang Peng, Trevor Ruckle, Jeff Sakamoto, Robert Schmidt, Tom Shih, Ed Timm, and James Winkelman. Presented at the DOE sponsored Thermoelectrics Workshop, San Diego, September 30, 2009.

5. 'Thermoelectric Conversion of Waste Heat to Electricity in an IC Engine Powered Vehicle,' Presented by Harold Schock, in collaboration with: Eldon Case, Thierry Caillet, Charles Cauchy, Jean-Pierre Fleurial, Tim Hogan, Mercouri Kanatzidis, Ryan Maloney, Christopher Nelson, Jennifer Ni, James Novak, Fang Peng, Trevor Ruckle, Jeff Sakamoto, Robert Schmidt, Tom Shih, Ed Timm, and James Winkelman. Presented at the DEER Conference on August 5, 2009.

6. "Fabrication and Testing of Skutterudite-based Thermoelectric Devices for Power Generation Applications," from MSU: Jeff Sakamoto, Ryan Maloney, Trevor Ruckle, Ed Timm, Harold Schock, from JPL: Thierry Caillat, J. Cheng, I. Chi, Jean-Pierre Fleurial, J. Paik, S. Jones, and from Iowa State: Tom Shih. Presented at the International Conference on Thermoelectrics, Freiburg Germany, July 2009.

7. "Aerogel Encapsulation of Thermoelectric Generators," Jeff Sakamoto and Ryan Maloney, MSU Chemical Engineering and Materials Science Annual Research Forum (Poster), June 3, 2009. East Lansing, MI.

8. "Mechanical Characterization and Powder Processing of PbTe-Based Thermoelectric Materials," Jennifer E. Ni, Dan Kleinow, Fei Ren, Eldon Case, Harold Schock, Ed Timm, Tim Hogan, Chun-I Wu, Mercouri Kanatzidis, 6th Annual CHEMS Research Forum 2009, MSU University Club and Henry Center, Lansing, MI, June 3, 2009.

9. "Powder Processing and Mechanical Characterization of Skutterudite Thermoelectric Materials," Robert D. Schmidt, Jennifer E. Ni, Eldon D. Case, Jeffrey S. Sakamoto, Edward J. Timm, Sixth Annual Research Forum 2009, MSU University Club and Henry Center, Lansing, MI, June, 2009.

10. "Fabrication and Testing of Skutterudite-based Thermoelectric Devices for Power Generation Applications," from MSU: Jeff Sakamoto, Ryan Maloney, Trevor Ruckle, Ed Timm, Harold Schock, from JPL: Thierry Caillat, J. Cheng, I. Chi, Jean-Pierre Fleurial, J. Paik, S. Jones, and from Iowa State: Tom Shih. Presented at the Materials Research Society meeting April 2009 San Francisco.

11. "Thermoelectric Generators Made with Novel Lead Telluride Based Materials," Materials Research Society Spring meeting, San Francisco, CA, April 2009. T.P. Hogan, C.-I Wu, J. D'Angelo, N. Matchanov, M. Farhan, M. Khan, F. Ren, B.D. Hall, J.E. Ni, E.D. Case, E. Timm, H. Schock, J. Sootsman, S. Girard, M.G. Kanatzidis.

IV. University Research

IV.1 University Consortium on Low-Temperature Combustion For High-Efficiency, Ultra-Low Emission Engines

Dennis Assanis
University of Michigan (UM)
Mechanical Engineering
2045 W.E.Lay Auto. Lab.
1231 Beal Avenue
Ann Arbor, MI 48109-2133

DOE Technology Development Manager:
Gurpreet Singh

NETL Project Manager: Samuel Taylor

Subcontractors:
- Massachusetts Institute of Technology (MIT), Cambridge, MA
- Stanford University (SU), Stanford, CA
- University of California, Berkeley (UCB), Berkeley, CA

Objectives

- Investigate the fundamental processes that determine the practical boundaries of low-temperature combustion (LTC) engines.
- Develop methods to extend LTC boundaries to improve the fuel economy of homogeneous charge compression ignition (HCCI) engines fueled on gasoline and alternative blends, while operating with ultra low emissions.
- Investigate alternate fuels, ignition and after-treatment for LTC and partially premixed compression ignition (PPCI) engines.

Accomplishments

- The experimental high load limit established last year by supercharging has been extended by more than 2 bar NMEP to 8.7 bar in multi-cylinder tests. The key to this extension is to minimize the ringing index by increasing the overall dilution level as the engine is boosted.
- Extending the low-load limit to near 1 bar net mean effective pressure (NMEP) was shown last year to be achievable through fuel injection during negative valve overlap (NVO). Modeling efforts to understand the relevant kinetic features have now been carried out to show the tradeoffs between prereaction and endothermicity effects; the results show the maximum effect near overall equivalence ratios of $\Phi = 0.8$.
- The GT-Power® modeling tool with a combustion submodel developed previously in the consortium has been used to generate performance maps for various proposed valve actuation schemes subject to ignition, NOx and knock constraints. The model was coupled to a drive cycle simulation to assess the in-vehicle fuel economy potential of several variable valve timing strategies.
- A multi-mode combustion diagram has been established to delineate the characteristic regimes of combustion including spark ignition (SI), HCCI and spark-assisted compression ignition (SACI). Together with experimental optical engine observations reported previously, the analysis indicates that spark assist is likely to be primarily useful as an ignition helper when not enough sensible heat is available for autoignition.
- A comprehensive analytical exploration of flame propagation at spark assist conditions has been carried out. Based on the results a flame speed correlation has been developed and is the subject of a publication currently being prepared. The study supports the experimental engine observations that viable flame propagation is possible at SACI conditions not normally encountered in conventional SI engines, i.e. highly dilute but high unburned temperature.
- Previous ignition delay studies of small biofuels esters carried out in the UM Rapid Compression Facility (RCF) have been extended to include speciation studies of the intermediates formed during ignition of methylbutanoate and air mixtures. The results are the first of their kind to provide quantitative insight into the reaction pathways important during ester combustion and have been used to improve available kinetic models.

Future Directions

- Carry out extensive thermodynamic and system analyses of new mixed combustion modes and their potential benefit for lean-burn, high-pressure engine operation.
- Explore fuel and thermal stratification and its interaction with fuel properties and heat transfer for improving and controlling combustion.
- Investigate advanced multi-mode ignition and combustion under lean, high-pressure conditions.
- Explore opportunities for improved engine efficiency through novel fuel chemistry.

Introduction

LTC is a new technology for internal combustion engines which promises to provide improved fuel economy with low emissions. With this technology, the engine is operated lean and cool enough to drastically reduce NOx emissions and reduce particulate matter (PM). In addition, operating lean allows high compression ratios for gasoline and reduces particulate emissions in diesels. The overall effect is to offer potential fuel economy gains for gasoline applications of up to 20%, and in the case of diesel engines, provide the means of satisfying the new, more stringent emissions regulations.

Because LTC implies operation at low temperatures near the limit of flame propagation, reliable combustion is usually initiated by autoignition which requires successful control of the thermal history of the gas charge and the engine. In principle this can be achieved with adequate thermal management control; various methods have been suggested for accomplishing this. However, as seen in Figure 1, full use of LTC has been limited at both high and low loads. At low load there is not enough heat in the charge to keep combustion healthy, while at high load the combustion is too rapid and may damage the engine structure. This situation threatens to reduce the ultimate fuel economy benefit that can be achieved in a vehicle system. The main focus of this consortium is to investigate the limit phenomena and to propose methods of extending the limits. As indicated in Figure 1, consortium experiments (square data points) have demonstrated extended operation at both high and low loads. Details will be discussed below.

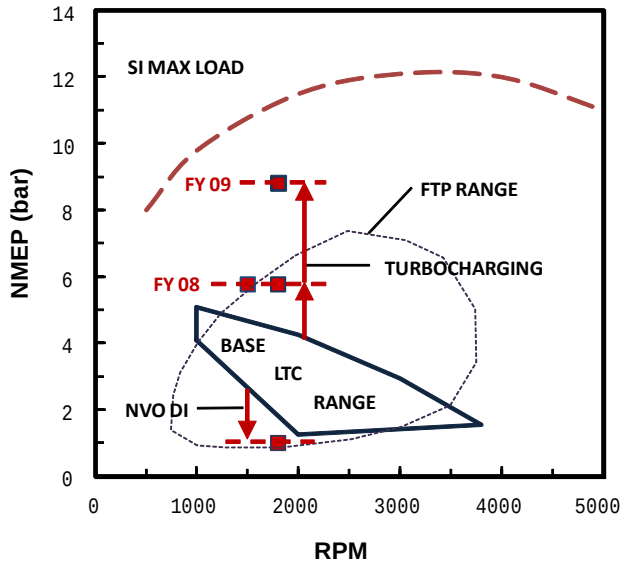

FIGURE 1. Speed/load map for a naturally aspirated automotive engine showing maximum load line, desired region for Federal Test Procedure (FTP) cycle operation (dashed oval), and base LTC range limited by knock at high load and misfire at low load. Square data points denote consortium engine experiments demonstrating expanded operation limits for previous year and current year.

Approach

Our research project, now at the end of its third year, combines experiments and modeling at four university research centers in order to acquire the knowledge and technology to extend the load range of LTC engines. To accomplish this, both single-cylinder and multi-cylinder engine experiments investigate direct fuel injection strategies, turbo/supercharging, and fast thermal management as possible approaches. Other tasks concentrate on spark-assisted LTC, and the ignition characteristics of alternate and bio-fuels. Recognizing the role of emission constraints particularly in the context of transient vehicle operation, studies of after-treatment devices have been carried out with specific application to the low exhaust temperatures typical of LTC both for HCCI and for PPCI systems and have been described in previous reports.

An array of modeling tools are being developed and refined, and brought to bear on the specific limit problems of importance. These models cover a range of detail from system models for engines and after-treatment devices, through fully coupled computational fluid dynamics/kinetic models, to detailed and reduced chemical mechanisms. Our intent is to take advantage of the broad range of capabilities of the university partners and the collaborative relationships among them.

Results

High-Load HCCI

At higher loads, combustion in HCCI engines becomes progressively more rapid and eventually results in undesirable pressure rise rates. It is accepted practice to measure the acoustic radiation of the combustion event by the Ringing Index (R.I.) defined as:

$$R.I. \equiv \frac{1}{2\gamma}\frac{\left(\beta \left(\frac{dP}{dt}\right)_{MAX}\right)^2}{P_{MAX}}\sqrt{\gamma R T_{MAX}} \quad (\mathrm{MW/m^2})$$

One way of decreasing the pressure rise rate is by dilution either with air or with residual gases. This effectively reduces the temperature rise during combustion and the rate of energy release. By boosting, the overall pressure in the cylinder is increased thus

decreasing the ringing index. Previous experimental work in the consortium utilized both turbocharging and cooled external exhaust gas recirculation (EGR) to achieve ~ 6 bar NMEP (MIT, UCB). Recently this limit has been pushed to 8.7 bar while still satisfying a R.I. limit of 5 MW/m^2. This was achieved by boosting to 1.7 bar while at the same time leaning the mixture to $\Phi = 0.35$ at 1,800 rpm as shown in Figure 2 (UCB). Further optimization with respect to combustion phasing and external/internal EGR fraction is underway.

Low-Load HCCI

Previously Song et al., [1] demonstrated experimentally that injecting fuel during the NVO period, resulted in achieving lower loads as shown in Figure 1 (SU). To understand this phenomenon better, a single-zone model has been employed using detailed chemical kinetics. The model assumes perfect mixing of the fuel and air during the overlap period and then tracked the subsequent evaporation, cooling and chemical reactions. In the simulations, detailed kinetic mechanisms of two pure chemicals (n-heptane and i-octane) were adopted to elucidate both chemical and thermal consequences of the recompression reactions on the following combustion event [2].

The computed results in Figure 3 show that at near-stoichiometric operation, the endothermicity of fuel pyrolysis during NVO reduces overall mixture temperature, which counteracts the improved mixture ignitability. At equivalence ratios near 0.8, the transformed fuel mixture combined with modest exothermicity leads to the shortest ignition delays. Finally, near the leanest conditions (equivalence ratio ~0.6), significant oxidation of fuel during NVO results in relatively long ignition delay due to low fuel chemical energy available, while increased temperature from

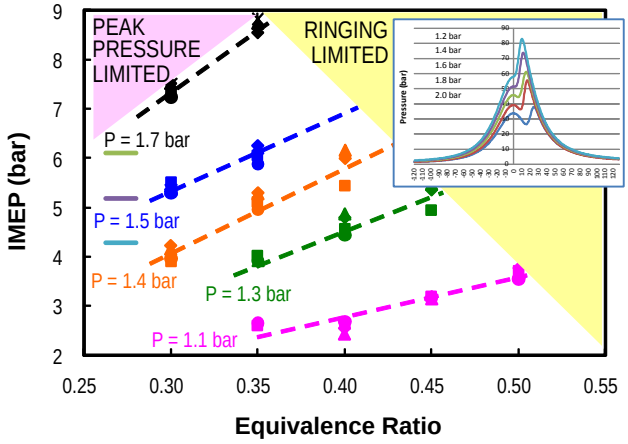

FIGURE 2. Extended high-load LTC operation achieved by leaning the mixture along with boosting to maintain acceptable R.I. values below ~ 5.0 MW/m^2.

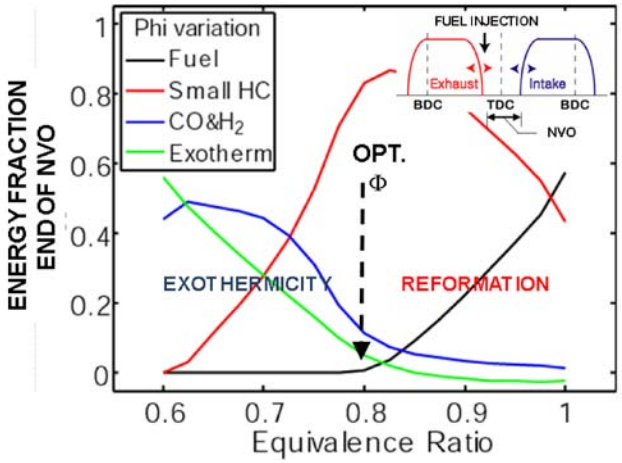

FIGURE 3. Computed energy breakdown of recompression reaction products as a function of overall equivalence ratio. Optimum effect on subsequent ignition timing is a result of tradeoff between endothermic reformation reactions and exothermic oxidation reactions.

exothermicity partially compensates for the lengthening of ignition delay. The competing effects of reformation and exothermicity on mixture ignitability leads to an optimum oxygen concentration (here near equivalence ratio 0.8) for the shortest ignition delay.

System Modeling for Improved Fuel Economy

The UM-developed HCCI engine and system model described by Babajimopoulos et al. [3] has been used extensively over the past year to explore the operating range of engines equipped with various valve actuation schemes which regulate the amount of internal residual and the combustion timing. The model allows the limits in LTC operating regimes to be established based on ringing index, NOx, and stability constraints. This year within the framework of GT-Power® we have made in-vehicle assessments of fuel economy gains possible relative to a conventional SI engine for two candidate valve strategies: one, a rebreathing scheme which depends on a dual event exhaust cam and phasing of the intake event; the other, a recompression strategy which relies on lost motion to increase the amount of negative valve overlap. The results in Figure 4 are for a midsize passenger car operated over the FTP driving cycle. Both strategies show improved fuel economy relative to the base SI engine. Rebreathing shows 8% improvement while recompression shows an additional 3% due to the fact that its range extends to lower load where HCCI gains over SI are more pronounced. The model has been used to support the efforts to increase the high-load limit by boosting noted previously. Current work is focused on developing a suitable combustion model for dilute stoichiometric conditions at high pressure levels.

Combustion Modes for LTC

Current SI engines operate under stoichiometric conditions to ensure three-way catalyst treatment of both HC and NOx emissions. HCCI promises to operate lean enough to achieve low NOx emissions without aftertreatment, thereby opening up the possible fuel efficiency gains of lean-burn engines. However, HCCI engines are limited by rapid combustion rates at high loads and timing control issues brought about by their reliance on autoignition. SACI may ease these difficulties by offering timing control and combustion rate moderation.

In an attempt to better understand spark assist, analytical work was carried out to delineate typical combustion regimes in terms of the local thermodynamic conditions (Lavoie et al., [4]). Figure 5 shows the regimes mapped according to unburned (T_U), and adiabatic burned gas temperatures (T_B). Constant equivalence ratio lines progress from lower left to upper right. When EGR is present, equivalence ratio refers to the total diluents ratio, i.e. Φ' represents Φ (1-residual gas fraction, RGF) as a relative measure of energy content of the charge. The rectangular HCCI region to the lower right of the figure is determined by ignition, misfire and NOx constraints. The SI region on the upper left is determined by requirements of good laminar flame propagation, lean or stoichiometric mixtures and borderline knock limits. The region where spark assist is feasible lies between the HCCI and the SI zones. In this zone both flame and autoignition processes are possible. The dashed oval indicates the area where spark assist has been observed in HCCI engines, both in metal engines and in optical engines. The trend toward boosted, leaner, i.e., high pressure lean burn (HPLB) and more efficient engines can be visualized on the diagram by the green arrow moving from SI toward the leaner HCCI region.

Because little or no experimental flame speed data are available in this region we carried out an analytical study of flame speeds in this regime with the one dimensional transient Hydrodynamics, Chemistry, Thermodynamics flame code. The range of initial conditions included T_U up to 1,000 K; $0.1 \le \Phi \le 1.0$; and pressures up to 250 bar. The results show that the flame and autoignition process are relatively independent until noticeable exothermicity begins as a result of the autoignition process; further, viable laminar flames should be possible down to equivalence ratios of ~ 0.3-0.4 provided that the unburned temperature is high enough to ensure a flame temperature of ~ 1,750 K. The model generated flame speed has been correlated into a practical set of numerical expressions for general use over the portion of the range where viable flames were achieved in the simulated data set (Martz et al, [5]).

PPCI and Kinetics

Flamelet Modeling of PPCI Combustion – Fundamental characterization of autoignition in LTC engine environments was conducted using high-fidelity direct numerical simulations (DNS) with non uniform H_2-Air mixtures. Based on the full-cycle KIVA-3v data, three representative parametric cases were considered in order to represent the range between early and late start of injection (SOI) conditions. It was found that initially uncorrelated temperature and mixture fluctuation fields, which correspond to an early SOI scenario, lead

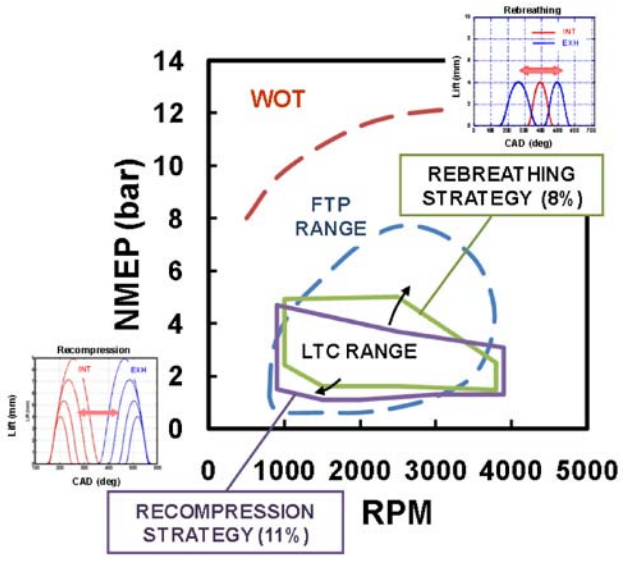

FIGURE 4. GT-Power®-based model results showing projected vehicle fuel economy gains for two valve strategies over the FTP driving cycle.

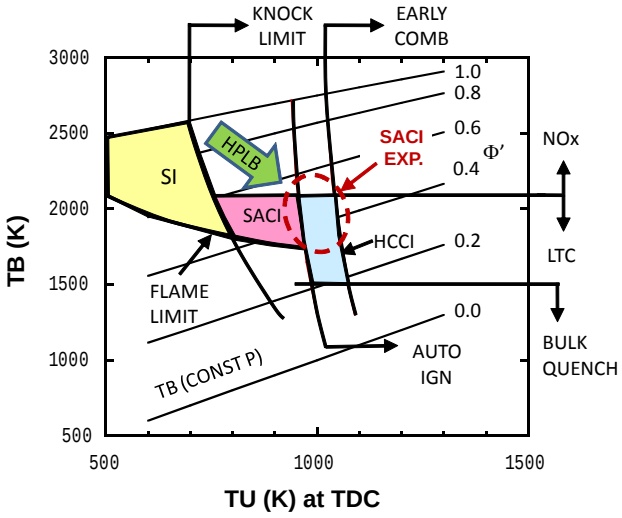

FIGURE 5. Schematic map of combustion regimes for SI, SACI, and HCCI determined by constraints on unburned temperature (autoignition, combustion phasing and knock); and on burned gas temperature (flame limit, quenching, and NOx limit). Dashed oval denotes available experimental data on SACI.

to a thin front-like propagation mode. On the other hand, negatively-correlated temperature-mixture fields, as would be the case in a late SOI condition because of evaporation, result in homogeneous autoignition. A numerical diagnostic algorithm was developed to automatically identify different ignition modes.

Towards an advanced combustion submodel applicable to LTC engine combustion, a novel principal component analysis (PCA) approach was used to identify intrinsic low-dimensional manifolds in the complex autoigniting system. PCA was applied to a DNS database of autoignition in inhomogeneous mixtures. It was observed that only two principal components were sufficient to describe temporal and spatial evolution of all the reactive scalars, offering a promising strategy to reduce the chemical complexity of the LTC combustion modeling. A PCA-based turbulent combustion closure model is currently being investigated.

Kinetics of Alternative Fuels – During the last year speciation studies were carried out on intermediates formed during ignition of methylbutanoate/air mixtures using the UM RCF. The results are the first of their kind to provide quantitative insight into the reaction pathways important during ester combustion. These data are also the first of their kind and provide understanding of the fundamental reaction chemistry important during combustion of oxygenated compounds. We also continue to work with Dr. Charlie Westbrook, our partner at Lawrence Livermore National Laboratory (LLNL) to develop new chemical reaction mechanisms to represent combustion of these compounds. Figure 6 shows recent RCF data for the intermediate ethane compared to the predictions of the LLNL model for methylbutanoate autoignition. In addition, we conducted preliminary UM RCF ignition studies of ester/n-heptane blends. Methyl 3-hexanoate was used as the reference ester compound due to the larger hydrocarbon chain and because methyl-3-hexanoate represents an unsaturated ester (which are typically more prevalent in biodiesels than saturated esters). The results indicate negative temperature coefficient behavior for blends containing larger amounts of n-heptane.

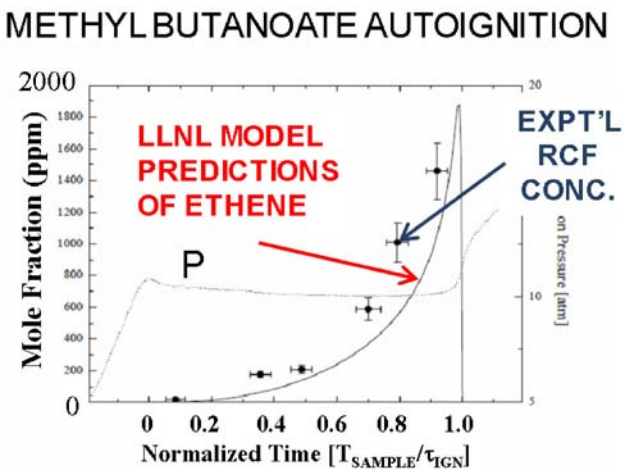

FIGURE 6. Concentration measurements of the intermediate species ethane, during autoignition of methylbutanoate in the UM RCF compared to predictions using the LLNL detailed kinetic model.

Recently we have focused on understanding the specific reactions controlling oxygenate ignition for our reference fuel methylbutanoate, and developing reaction sensitivity coefficients. The results for the sensitivity analysis of methylbutanoate show that HO_2 and H_2O_2 reactions are the most important reactions controlling ignition at HCCI conditions. Rate of production analyses show that the fuel is consumed primarily by H-atom abstraction via the hydroxyl radical. Together these results indicate potential pathways to further control HCCI ignition using OH chain carriers (e.g. fuel blends, fuel additives, etc.). We are now working to extend our capabilities to heavier (higher molecular weight) fuels which are more representative of real fuels and real fuel blends.

Conclusions

- Experimentally the high load limit defined by an R.I. constraint of 5 MW/m^2 has been extended to 8.7 bar NMEP in multi-cylinder tests by boosting to 1.7 bar and by operating lean at $\Phi = 0.35$. Expectations are that this can be extended further by optimizing external EGR, pressure level and combustion phasing.
- The mechanism of low-load extension by fuel injection during NVO has been explored using a chemical kinetic model for n-heptane and iso-octane to simulate the reactions and heat release. In agreement with last year's experimental results it was found that lowest loads can be achieved at overall equivalence ratios near $\Phi = 0.8$ because of the tradeoff between fuel reformation reactions and exothermicity.
- An analysis of the combustion regimes for SACI indicates that the regime for SACI exists between normal SI operation and HCCI. Because robust flame propagation requires somewhat higher burned gas temperatures than HCCI, spark assist appears to function as an ignition helper at higher loads when not enough sensible heat is available for auto ignition.
- Rapid compression measurements of intermediate species have been made during the autoignition of the biofuel methylbutanoate. These measurements have been compared with the LLNL models and have been useful in improving those models.

References

1. Song, H.H., Padmanabhan, A., Kaahaaina, N.B., and Edwards, C.F. (2009) Experimental study of recompression reaction for low-load operation in direct-injection homogeneous charge compression ignition engines with n-heptane and i-octane fuels. International Journal of Engine Research, Vol. 10, No. 4, 215-229.

2. Song, H.H., and Edwards, C.F. (2009) Understanding chemical effects in low-load-limit extension of homogeneous charge compression ignition engines via recompression reaction. International Journal of Engine Research, Vol. 10, No. 4, 231-250.

3. Babajimopoulos, A., Challa, P., Lavoie, G.A., and Assanis, D.N. (2009) Model-based assessment of two variable cam timing strategies for HCCI engines: recompression vs. rebreathing. Proceedings of the ASME Internal Combustion Engine Division 2009 Spring Technical Conference, ICES2009, May 3–6, 2009, Milwaukee, Wisconsin, USA, Paper ICES2009-76103,

4. Lavoie, G., Martz, J., Wooldridge, M., and Assanis, D., "A Multi-Mode Combustion Diagram for Spark Assisted Compression Ignition," submitted to Combustion and Flame, July 2009, accepted September 2009.

5. Martz, J., Middleton, R., Lavoie, G., Babajimopoulos, A., Assanis, D., (2009) "A Computational Study and Correlation of Premixed Isooctane Air Laminar Flame Properties under SI and Spark Assisted Compression Ignition Engine Conditions", in preparation.

FY 2009 LTC Consortium Publications

1. Babajimopoulos, A., Challa, P., Lavoie, G.A., and Assanis, D.N. (2009) Model-based assessment of two variable cam timing strategies for HCCI engines: recompression vs. rebreathing. Proceedings of the ASME Internal Combustion Engine Division 2009 Spring Technical Conference, ICES2009, May 3–6, 2009, , Milwaukee, Wisconsin, USA, Paper ICES2009-76103.

2. Keros, P., Zigler, B.T., Wiswall, J.T., Walton, S.M., Wooldridge, M.S., (2009) "An Experimental Investigation of the Exhaust Emissions from Spark.

3. Keum, S., Im, H.G., Assanis, D.N., (2008) "A Spray-Interactive Reduced Dimensional Model (SIRDM) for Direct Injection, Partially Premixed, Compression Ignition Engine Combustion," SAE paper 09PFL-1115, submitted.

4. Lavoie, G., Martz, J., Wooldridge, M., and Assanis, D., "A Multi-Mode Combustion Diagram for Spark Assisted Compression Ignition," submitted to Combustion and Flame, July 2009, accepted September 2009.

5. Martz, J., Middleton, R., Lavoie, G., Babajimopoulos, A., Assanis, D., (2009) "A Computational Study and Correlation of Premixed Isooctane Air Laminar Flame Properties under SI and Spark Assisted Compression Ignition Engine Conditions", in preparation.

6. Saxena, S., Mack, J.H. and Dibble, R.W. "Increasing Indicated Mean Effective Pressure (IMEP) of a Homogeneous Charge Compression Ignition (HCCI) Engine", Combustion Institute US National Meeting, May 2009.

7. Saxena, S., Dillstrom, T., Chen, J-Y, and Dibble, R.W., "Increasing Signal-to-Noise Ratio of Spark-plug Ion Sensors through Addition of Salt-based Fuel Additives", Combustion Institute Western States Meeting, October 2009.

8. Saxena, S., Chen, J-Y., and Dibble, R.W., "A Survey of Experimental HCCI Research at U.C. Berkeley", Combustion Institute Australian Combustion Symposium, Dec 2009.

9. Scaringe, R.J., Wildman, C., Cheng, W., "On the High Load Limit of Boosted Gasoline HCCI Engine Operating in NVO Mode," Paper submitted to the 2010 SAE Congress.

10. Song, H. H., Padmanabhan, A., Kaahaaina, N. B., and Edwards, C. F. (2009) Experimental study of recompression reaction for low-load operation in direct-injection homogeneous charge compression ignition engines with n-heptane and i-octane fuels. International Journal of Engine Research, Vol. 10, No. 4, 215-229.

11. Song, H.H., and Edwards, C.F. (2009) Understanding chemical effects in low-load-limit extension of homogeneous charge compression ignition engines via recompression reaction. International Journal of Engine Research, Vol. 10, No. 4, 231-250.

12. Walton, S. M., Wooldridge, M. S., and Westbrook, C.K., (2009) "An Experimental Investigation of Structural Effects on the Auto-Ignition Properties of Two C_5 Esters" *Proceedings of the Combustion Institute*, **32**, pp. 255-262.

13. Wildman, C., Scaringe, R.J., Cheng, W., "On the Maximum Pressure Rise Rate in Boosted HCCI Operation," SAE Paper 2009-01-2727, 2009.

IV.2 Kinetic and Performance Studies of the Regeneration Phase of Model Pt/Ba/Rh NOx Traps for Design and Optimization

Michael P. Harold (Primary Contact) and Vemuri Balakotaiah
University of Houston
Department of Chemical and Biomolecular Engineering
S222 Engineering Building 1
Houston, TX 77204-4004

DOE Technology Development Manager: Ken Howden

NETL Project Manager: Chris Johnson

Objectives

- Carry out studies of regeneration kinetics on lean-NOx trap (LNT) catalysts.
- Evaluate and compare the effect of different reductants on LNT performance.
- Incorporate the kinetics findings and develop and analyze a first-principles-based predictive LNT model for design and optimization.
- Test the new LNT designs in a heavy-duty diesel vehicle dynamometer facility.

Accomplishments

- Conducted isotopic temporal analysis of products (TAP) studies which show that the transport of stored NOx is an important rate limiting process during regeneration/reduction (Task 1).
- Completed comprehensive cyclic studies using H_2 which reveals a significant effect of the Pt dispersion on the storage and reduction rates as well as product distribution (Task 2).
- Developed a global reaction-based LNT trap model which predicts most of the spatio and temporal data using H_2 as the reductant (Task 3).
- Incorporated crystallite level description that accounts for stored NOx gradients and predicts most of the trends in the dependence of conversion and selectivity on Pt/BaO catalysts with a wide range of Pt dispersions (Task 3).
- Developed a microkinetic model of NOx storage which predicts most of the trends including the effect of Pt loading (Task 3).
- Completed the construction of a second bench-scale reactor system that enables the use of actual diesel engine exhaust feeds (Task 4).
- Developed low-dimensional models that can be used for real time simulations of catalytic after-treatment systems.

Future Directions

During the final months of the project we will focus our efforts on the following activities:

- Conduct bench-scale and isotopic TAP (using ^{15}NO) experiments on additional catalyst types:
  - Quantify the stored NOx diffusion coefficient as function of temperature.
  - Evaluate effect of Rh and CeO_2 with H_2 as reductant.
- Carry out analysis of coupled thermal and concentration fronts using the global LNT model.
- Carry out testing of selected LNTs with engine exhaust in dynamometer facility.
- Complete microkinetic model development for the regeneration and compare with data.
- Use LNT model to investigate different NOx trap operating strategies and designs.

Introduction

During the fourth year of the four-year grant, we utilized bench-scale and TAP reactors to assess the coupling between the precious metal (Pt) and storage (BaO) functions of model LNT catalysts. Using catalysts provided by BASF Catalysts LLC, we quantified the effect of Pt dispersion and identified evidence for a shift in rate limiting processes. Both micro-kinetic and global reaction models were developed, refined, and utilized to predict many of the features of the bench-scale data, such as the effect of Pt loading on storage kinetics, and the effects of temperature and Pt dispersion on the regeneration rate and product distribution. Current modeling efforts are focused on completing the treatment of the interfacial chemistry during the regeneration. Finally, we have completed the construction of a second reactor system at the Diesel Center that enables the use of actual diesel engine exhaust in addition to synthetic mixtures.

Activities to be carried out during the final several months of the project will involve Tasks 1, 3b, and 4. We will complete efforts related to Task 1 (isotopic TAP

experiments with model Pt/BaO catalysts), Task 3a (microkinetic model of storage and reduction), Task 3b (optimization studies using global reaction LNT model), and Task 4 (performance evaluations of model NOx storage and reduction [NSR] catalysts using exhaust from actual diesel engine).

Approach

We utilize a combination of experimental and theoretical tools to advance LNT technology. Fundamental kinetics studies are carried out on model LNT catalysts containing variable loadings of precious metals (Pt, Rh), and storage components (BaO, CeO_2). A TAP reactor provides transient data under well-characterized conditions of both powder and monolith catalysts, enabling the identification of key reaction pathways and estimation of the corresponding kinetic parameters. The performance of model NSR monolith catalysts are evaluated in a bench-scale NOx trap using synthetic exhaust, with attention placed on the effect of the pulse timing and composition on the instantaneous and cycle-averaged product distributions. From these measurements we formulate a mechanistic-based microkinetic model that incorporates a detailed understanding of the chemistry, and incorporate the kinetic model into a LNT model. The NOx trap model is used to determine its ability to simulate bench-scale data and ultimately to evaluate alternative LNT designs and operating strategies.

Results

NO Oxidation Studies

Modeling and experimental studies on model Pt/Al_2O_3 and Pt/BaO/Al_2O_3 catalysts are performed to elucidate the kinetics of NO oxidation, which is a key step during the lean phase of NOx trap operation. Experiments show that a steady-state is never truly achieved during NO oxidation; a continuous decrease in the reaction rate with time is observed on both the catalysts. This decrease is distinct from and beyond the prompt inhibition of the NO oxidation reaction observed with NO_2 in the feed or product. NO oxidation carried out after catalyst pretreatments with H_2, O_2 and NO_2 indicates that NO_2 is responsible for the deactivation while NO_2 storage plays a negligible role. Experiments with NO_2 as the feed elucidate its role in the production of NO, either by storage or decomposition, for a wide range of temperatures. The highly oxidizing nature of NO_2 suggests that the Pt surface could be covered with oxygen, either as chemisorbed O or as Pt oxides, which results in slow poisoning of the catalyst. Microkinetic analysis of the NO oxidation reaction shows O_2 adsorption as the rate determining step and predominant surface species to be adsorbed NO and O. Based on the microkinetic studies, a global kinetic model is proposed which includes the inhibiting effect of NO_2 on the NO oxidation reaction. The importance of including coverage of NO in the global model at low temperatures is shown, which is neglected in the current literature global models. The model predicts the experimental observations for a wide range of temperatures within acceptable error limits. However, prediction of the transient data requires modeling of NO_2 storage, decomposition and the complex NO_2 inhibition chemistry in addition to other surface reactions. Further details are in publication 8 listed at the end of the report.

Global LNT Model

A global kinetic model for NOx storage and reduction for the case of anaerobic regeneration with hydrogen is developed, based on parallel experimental studies. The existence of two different types of BaO storage sites on the catalyst is proposed, which differ in their storage as well as regeneration activity. The two-site model explains the close to complete NOx storage at the start of the storage phase and the gradual emergence of NO and NO_2 during later storage times. The effluent concentrations and concentration fronts of the reactants and products within the monolith are predicted by the model, providing insight into the mechanisms of regeneration and storage. An example comparison of experimental data and model predictions is shown in Figure 1. The H_2 front velocities are predicted to increase as the H_2 front propagates down the length of the monolith, thus showing the presence of more stored NOx in the front of the reactor. The simulations show that even though regeneration is fast, H_2 concentration fronts are not very steep, which is attributed to the lower regeneration activity of the "slow" sites. The model captures the formation of NH_3 and the NH_3 concentration fronts, which reveal the reaction of NH_3 formed upstream with the stored NOx downstream of the H_2 front. The lower diffusivity of NH_3 as compared to H_2 is shown to be responsible for the wider width of the NH_3 front and earlier appearance of NH_3 in the effluent than H_2. Further details are in publication 9 listed at the end of the report.

Pt Dispersion Experiments

This study provides insight into the effect of Pt dispersion on the overall rate and product distribution during NOx storage and reduction. The storage and reduction performance of Pt/BaO/A_2O_3 monoliths with varied Pt dispersion (3, 8, and 50%) and fixed Pt (2.36 wt%) and BaO (12.7 wt%) loadings is reported. At low temperature (<200°C), the differences in storage and reduction activity were the largest between the three catalysts. The amount of NOx stored increased with increased dispersion, as did the amount of stored NOx

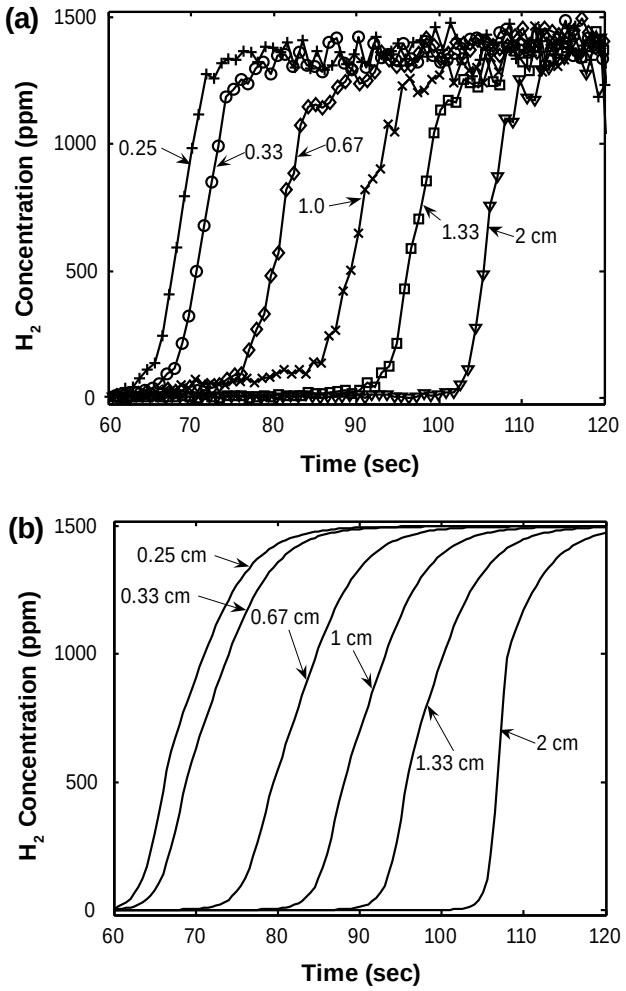

FIGURE 1. Comparison of experimental data (top figure) with global LNT model predictions (bottom figure) for H_2 effluent concentration as a function of time for several monolith lengths.

that was reduced. These trends are attributed to larger Pt surface area and Pt-BaO interfacial perimeter, the latter of which enhances the spillover of surface species between the precious metal and storage components. At high temperature (370°C), the stored NOx was almost completely regenerated for the three catalysts. However, the regeneration of the 3% dispersion catalyst was much slower, suggesting a rate limitation involving the reverse spillover of stored NOx to Pt and/or of adsorbed hydrogen from Pt to BaO. The results indicate that the catalyst dispersion and operating conditions may be tuned to achieve the desired ammonia selectivity. For the aerobic regeneration feed, the most (net) NH_3 was generated by the 50% dispersion catalyst at the lowest temperature (125°C), by the 3% dispersion catalyst at the highest temperature (340°C), and by the 10% dispersion catalyst at the intermediate temperatures (170-290°C). Similar trends were observed for the net production of NH_3 with an anaerobic regeneration feed. A phenomenological picture is proposed that describes the effects of Pt dispersion consistent with the established spatio-temporal behavior of the lean LNT. Further details are in publications 6 and 13 listed at the end of the report.

Isotopic TAP Experiments

A systematic isotopic study over $Pt/BaO/Al_2O_3$ powder catalyst was carried out using TAP to elucidate the role of the Pt/BaO interface and spillover processes during NOx storage and reduction. The sequential pre-nitration of $Pt/BaO/Al_2O_3$ using NO and ^{15}NO followed by reduction with H_2 results in the preferential evolution of ^{15}N containing species during initial H_2 pulses. The evolution shifts towards N containing species in later H_2 pulses. The data suggest that NOx storage proceeds radially outward from the Pt crystallites and that some mobility of the stored NOx species exists. The subsequent reduction is limited by transport of stored NOx from BaO storage phase to the Pt/BaO interface. The evolution of N_2 and ^{15}NN during $^{15}NO–H_2$ pump-probe on a pre-nitrated (using unlabeled NO) catalyst confirms the involvement of spillover processes at the Pt/BaO interface. The evolution of nitrogen takes place by NO decomposition as well as by the reaction of stored NOx with H_2 to form adsorbed N and eventually N_2. A significant fraction of N_2 is also produced via NH_3 serving as an intermediate. The results suggest that the local gradients at the Pt/BaO interface in the stored NOx are important and that these should be taken into account in NSR catalyst design and modeling. Further details are in publications 5 and 12 listed at the end of the report.

Modeling Studies on Monolith Reactors

(a) Low-Dimensional Models for Real Time Simulations of Catalytic After-treatment Systems

We present accurate low-dimensional models for real time simulation, control and optimization of monolithic catalytic converters used in automobile exhaust treatment. These are derived directly by averaging the governing equations and using the concepts of internal and external mass transfer coefficients. They are expressed in terms of three concentration and two temperature modes and include washcoat diffusional effects without using the concept of the effectiveness factor. The models reduce to the classical two-phase models in the limit of vanishingly thin washcoat. The models are validated by simulating the transient behavior of a three-way converter for various cases and comparing the predictions with detailed solutions. It is shown that these new models are robust and accurate with practically acceptable error, speed up the computations by orders of magnitude, and can be used with confidence for the real time simulation and control of monolithic

and other catalytic reactors. Further details are in publication 7 listed at the end of the report.

(b) Internal Mass Transfer Coefficients in Catalytic Monoliths

We utilize the recently developed concept of internal or intraphase mass transfer coefficient to simplify the problem of diffusion and reaction in more than one spatial dimension for a washcoated monolith of arbitrary shape. We determine the dependence of the dimensionless internal mass transfer coefficient (Sh_i) on washcoat and channel geometric shapes, reaction kinetics, catalyst loading and activity profile. It is also reasoned that the concept of intraphase transfer coefficient is more useful and fundamental than the classical effectiveness factor concept. The intraphase transfer coefficient can be combined with the traditional external mass transfer coefficient (Sh_e) to obtain an overall mass transfer coefficient (Sh_{app}) which is an experimentally measurable quantity depending on various geometric and transport properties as well as kinetics. We present examples demonstrating the use of Sh_{app} in obtaining accurate macro-scale low-dimensional models of catalytic reactors by solving the full three-dimensional convection-diffusion-reaction problem for a washcoated monolith and comparing the solution with that of the simplified model using the internal mass transfer coefficient concept. Further details are in publication 10 listed at the end of the report.

(c) Controlling Regimes in Catalytic Monoliths

It is well known that the performance of a catalytic monolith is bounded by two limits: the kinetic regime at low temperatures (or before the ignition for the case of exothermic reactions) and the external mass transfer controlled regime at sufficiently high temperatures (or after the ignition). The washcoat diffusional resistance can also be significant over an intermediate range of temperatures. The transition temperatures at which the controlling regime changes from kinetic to washcoat diffusion to external mass transfer depend on the various geometric properties of the monolith, flow properties, the catalyst loading and washcoat properties. We present analytical criteria for determining these transition temperatures. These are derived using the recently developed low-dimensional model and the concepts of internal and external mass transfer coefficients. The criteria are more general than those in the literature and are useful in analyzing the experimental data. Further, we present an explicit expression for the experimentally measurable dimensionless apparent mass transfer coefficient (Sh_{app}) in terms of individual transfer coefficients in each phase. It is shown that Sh_{app} can be lowered by orders of magnitude compared to the theoretical upper bound obtained in the limit of external mass transfer control. Low values of Sh_{app} are obtained due to a small value of effective diffusivity in the washcoat, low catalyst loading or a reaction with low activation energy. The analytical criteria may be used for the design of monolith properties and experimental conditions so that the performance of the monolith approaches the upper limit defined by the external mass transfer controlled limit. Further details are in publication 15 listed at the end of the report.

Microkinetic Models for NOx Storage on BaO/Al_2O_3 and $Pt/BaO/Al_2O_3$ Catalysts

A NOx storage model with two types of barium sites was systematically developed. A kinetic model for NO_2 storage on BaO via gas-surface reactions was evaluated by comparing with the experimental measurements. The model parameters were modified by a fit of the data. Then a parametric sensitivity study was carried out to identify the relative importance of different gas-surface reactions. It was shown that several of the reactions are slow and can be neglected. The formation of $Ba(NO_3)_2$ on BaO (without Pt) is a slow process and can be neglected for the practical storage time during an NSR operation.

The sensitivity study also provided clues for the development of the spillover chemistry at the Pt-BaO interface. Two spillover reaction steps were proposed without increasing the number of surface species, and an estimation of the rate constants were carried out based on a series of assumptions. A storage model was constructed to include NO oxidation on Pt, NOx storage reactions between gas and barium surface species, and spillover reactions between platinum and barium surface species. Barium sites in the proximity of Pt and far from Pt particles were also differentiated during the model development. The model captured the major trends of experimental measurements. Specifically, the Pt promoted NOx storage and nonmonotonic NO (NO_2) effluent concentration as a function of Pt loading in the short time range of NO_2 (NO) storage were predicted. The dependence of surface reaction rates on catalyst loading was discussed based on physical analysis. Two qualitative contradictions between the model predictions and experimental observations were investigated. One experimental observation missed by the model predictions is the high NO formation peak in the short time range, which indicates that the dependence of proximal barium sites on Pt concentration is not linear but of a lower order. An upper bound of proximal barium concentration was estimated to be in the range of 140–180 mol/m^3. The other contradiction is a secondary NO storage feature probably due to support effects.

The present model is able to predict an accurate NOx breakthrough point and significant nitrate formation of NO storage on B3 catalyst in the presence of O_2, and meets the requirements of the current study. This storage model, without further modifications, was

used to simulate the cyclic NSR experiments conducted on B3 catalyst. Good agreements with experimental data were obtained and the result will be presented in a forthcoming publication (in preparation).

Modeling of Pt Crystallite Size Effect on NOx Storage and Reduction

A crystallite-scale model is incorporated into a reactor-scale model to study the effect of Pt dispersion and temperature during the regeneration of a LNT, based on a parallel experimental study [1]. It is shown that for a fixed Pt loading, an increase in the Pt dispersion results in an increase in the interfacial perimeter between Pt and Ba, where the reduction of NOx takes place. The rate determining process during the regeneration is found to be the diffusion of stored NOx within the Ba phase towards the Pt/Ba interface. The transient product distribution for three catalysts having varied Pt dispersions (3.2%, 8% and 50%) is explained by the localized stored NOx gradients in the Ba phase. Temperature-dependent NOx diffusivities in the Ba phase are used to predict the breakthrough profiles of H_2, N_2 and NH_3 over a range of catalyst temperatures. Figure 2 compares experimental data with model predictions. Finite gradients in the stored NOx concentration are predicted in the Ba phase, thus showing that the nitrate ions are not sufficiently mobile at lower temperatures for the low dispersion catalysts. The model predicts that the highest amount of NH_3 is produced by the low dispersion catalyst (3.2% dispersion) at high temperatures, by the high dispersion catalyst (50% dispersion) at low temperatures, and by the medium dispersion catalyst (8% dispersion) at intermediate temperatures, which is consistent with the experimental data. The model considers the consumption of chemisorbed oxygen on Pt by H_2, which is used to predict the low effluent N_2 concentration for the 50% dispersion catalyst as compared to the 8% dispersion catalyst. Finally, a novel design is proposed to maximize the amount of NH_3 in the effluent of a LNT, which can be used as a feed to a selective catalytic reduction unit placed downstream of the LNT. Further details are in publication 13 listed at the end of the report.

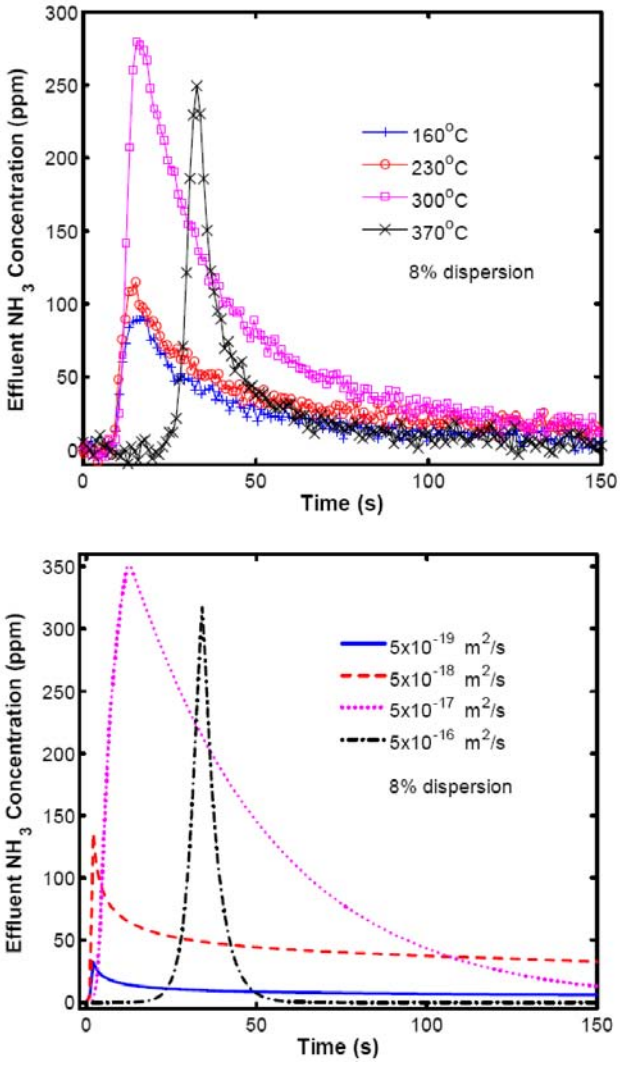

FIGURE 2. Comparison of experimental data (top figure) with crystallite level LNT model predictions (bottom figure) for NH_3 effluent concentration as function of time for several different temperatures using the intermediate dispersion Pt/BaO monolith catalyst.

Conclusions

During the fourth year we have made very good progress towards completing the project objectives. During a six-month no-cost extension, efforts will be focused on completing the microkinetic and crystallite-level models of NOx storage and reduction, bench-scale studies of Pt/Rh/BaO/CeO_2 catalysts, isotopic TAP experiments to quantify the extent of rate limitations associated with stored NOx transport, bench-scale studies of model NSR catalysts using actual diesel vehicle exhaust and development of software for real time simulations of catalytic after-treatment systems.

References

1. R.D. Clayton, M.P. Harold, V. Balakiotaiah, C.Z. Wan, Appl. Catal., B 90 (2009) 662.

FY 2009 Publications/Presentations

Refereed Journal Publications (from project start)

1. Clayton, R.D.., M.P. Harold, and V. Balakotaiah, "Performance Features of Pt/BaO Lean NOx Trap with Hydrogen as Reductant," *AIChE J.*, **55**, 687-700 (2009).

2. Kumar, A., V. Medhekar, M.P. Harold, and V. Balakotaiah, "NO Decomposition and Reduction on Pt/Al_2O_3 Powder and Monolith Catalysts Using the TAP Reactor," *Appl. Catal. B. Environmental*, **90**, 642-651 (2009).

3. Xu, J., M.P. Harold, and V. Balakotaiah, "Microkinetic Modeling of Steady-State $NO/H_2/O_2$ on $Pt/BaO/Al_2O_3$ Monolith Catalysts," *Appl. Catal. B. Environmental*, **89**, 73-86 (2009).

4. Bhatia, D., V. Balakotaiah and M.P. Harold, "Kinetic and Bifurcation Analysis of the Co-Oxidation of CO and H_2 in Catalytic Monolith Reactors." *Chem. Eng. Sci.*, **64**, 1544-1558 (2009).

5. Kumar, A., V. Medhekar, M.P. Harold, and V. Balakotaiah, "NO Decomposition and Reduction on Pt/Al_2O_3 Powder and Monolith Catalysts Using the TAP Reactor," *Appl. Catal. B. Environmental*, **90**, 642-651 (2009).

6. Clayton, R.D., M.P. Harold, V. Balakotaiah, and C.Z. Wan "Effect of Pt Dispersion on NOx Storage and Reduction in $Pt/BaO/Al_2O_3$ Catalyst," *Appl. Catal. B. Environmental*, **90**, 662-676 (2009).

7. Joshi, S.Y., M.P. Harold, and V. Balakotaiah, "Low-dimensional Models for Real Time Simulations of Catalytic Monoliths", *AIChE Journal*, **55**, 1771-1783 (2009).

8. Bhatia, D., V. Balakotaiah, M.P. Harold, and R. McCabe, "Experimental and Kinetic Study of NO Oxidation on Model Pt Catalysts," *J. Catalysis*, **266**, 106-119 (2009).

9. Bhatia, D., R.D. Clayton, M.P. Harold, and V. Balakotaiah, "A Global Kinetic Model for NO_x Storage and Reduction on $Pt/BaO/Al_2O_3$ Monolithic Catalysts," *Catalysis Today*, **147S**, S250-S256 (2009).

10. Joshi, S., M.P. Harold, and V. Balakotaiah, "On the use of Internal Mass Transfer Coefficients in Modeling of Diffusion and Reaction in Catalytic Monoliths", *Chem. Eng. Sci.*, **64**,4976-4991 (2009).

11. Harold, M.P., and V. Balakotaiah, "Catalytic After-treatment of NOx from Diesel Exhaust," to appear in McGraw-Hill 2010 Yearbook of Science and Technology, to appear (2010).

12. Kumar, A., M.P. Harold, and V. Balakotaiah, "Isotopic TAP Studies of NO Decomposition and Reduction on $Pt/BaO/Al_2O_3$ Catalysts," *J. Catalysis*, revisions pending (December, 2009).

13. Bhatia, D., V. Balakotaiah and M.P. Harold, "Modeling the Effect of Pt Dispersion and Temperature During Anaerobic Regeneration of a Lean NOx Trap Catalyst". *Catalysis Today*, submitted for publication (October, 2009).

14. Joshi, S., Ren, Y., M.P. Harold, and V. Balakotaiah, "Theoretical and Experimental Investigation of the Controlling Regimes in Catalytic Monoliths", *Chem. Eng. Sci.*, in press (December, 2009).

15. Joshi, S., M.P. Harold, and V. Balakotaiah, "Overall Mass Transfer Coefficients and Controlling Regimes in Catalytic Monoliths, *Chem. Eng. Sci.*, accepted for publication (October, 2009).

Conference and Other Presentations

1. AIChE National Meeting, *Microkinetic Modeling of Steady-State $NO/H_2/O_2$ on $Pt/BaO/Al_2O_3$ NOx Storage and Reduction Monolith Catalysts: The Role of NH_3*, Philadelphia, PA, 11/08 (with Jin Xu, presenter, V. Balakotaiah).

2. AIChE National Meeting, *Elucidating the Role of the Pt/Ba Interface During NO_X Storage and Reduction on Model $Pt/BaO/Al_2O_3$ Catalyst*, Philadelphia, PA, 11/08 (with Ashok Kumar, presenter, V. Balakotaiah).

3. AIChE National Meeting, *Bifurcation Analysis of CO and H_2 Oxidation on Pt/Al_2O_3 Monolith Reactors*, Philadelphia, PA, 11/08 (with Divesh Bhatia, presenter, V. Balakotaiah).

4. AIChE National Meeting, *Modeling of Spatio-Temporal Effects in a Lean NOx Trap Using Global Kinetics*, Philadelphia, PA, 11/08 (with Divesh Bhatia, presenter, V. Balakotaiah).

5. Department of Mechanical Engineering, University of Houston, *Reduction of NO_x from Lean Burn Vehicle Exhaust: Technology Solutions from Simple to Complex,* 2/09.

Division of Research, University of Houston, *Clean Diesel*, 2/09.

6. CLEERS Conference, *Elucidating the Mechanism of NOx Storage and Reduction*, Dearborn, MI, 4/09.

7. North American Catalysis Society Meeting, *Experimental and Kinetic Investigations of NO_x reactions on Model Pt Catalysts*, San Francisco, CA, 6/09 (with D. Bhatia, speaker; R. McCabe, V. Balakotaiah).

8. North American Catalysis Society Meeting, *Isotopic Studies of NO_X Storage and Reduction over $Pt/BaO/Al_2O_3$ using Temporal Analysis of Products*, San Francisco, CA, 6/09 (with A. Kumar, speaker; V. Balakotaiah).

9. CLEERS Working Group, *Mechanistic and Kinetics Studies of NOx Storage and Reduction on Model Catalysts, Isotopic Studies of NOx Storage and Reduction over $Pt/BaO/Al_2O_3$ using Temporal Analysis of Products*, 6/09.

10. AIChE South Texas Section, *Catalytic Solutions to Achieve Clean Diesel Power*, 9/09.

11. International Conference on Structured Catalysts and Reactors, Ischia, Italy, *A Global Kinetic Model for NO_x Storage and Reduction on $Pt/BaO/Al_2O_3$ Monolithic Catalysts*, 9/09.

12. AIChE Annual Meeting, Nashville, TN, November, 2009, "Effects of Rh, CeO2 and Regeneration Conditions during NOx Storage and Reduction on $Pt/BaO/Al_2O_3$ Monolith Catalysts", paper #547a (Y. Ren, R.D. Clayton, V. Balakotaiah and M.P. Harold).

13. AIChE Annual Meeting, Nashville, TN, November, 2009, "Modeling of Spatiotemporal Effects in a NOx trap using Global Kinetics", paper #547f (D. Bhatia, R.D. Clayton, V. Balakotaiah and M.P. Harold).

14. AIChE Annual Meeting, Nashville, TN, November, 2009, "Isotopic Studies of NOx Storage and Reduction Over $Pt/BaO/Al_2O_3$ Monolith Catalysts", paper #560c (A. Kumar, V. Balakotaiah and M.P. Harold).

15. AIChE Annual Meeting, Nashville, TN, November, 2009, "Modeling Studies on the Effect of Ceria on the Performance of a Lean NOx Trap using H2 as Reductant", paper #487ak (with D. Bhatia, R.D. Clayton, V. Balakotaiah and M.P. Harold).

16. AIChE Annual Meeting, Nashville, TN, November, 2009, "Low-dimensional Models for Real Time Simulations of Catalytic Monoliths", paper #487am (S.Y. Joshi and M.P. Harold and V. Balakotaiah).

17. AIChE Annual Meeting, Nashville, TN, November, 2009, "Internal Mass Transfer Coefficients for Modeling Multi-component Diffusion and Reaction in Washcoated Catalytic Monoliths", paper #487an (S.Y. Joshi, M.P. Harold and V. Balakotaiah).

IV.3 Investigation of Aging Mechanisms in Lean-NO_X Traps

Mark Crocker (Primary Contact), Yaying Ji, Vence Easterling, Jin Wang
University of Kentucky
Center for Applied Energy Research
2540 Research Park Drive
Lexington, KY 40511

DOE Technology Development Manager:
Ken Howden

NETL Project Manager: Christopher Johnson

Subcontractor:
Todd J. Toops, Jae-Soon Choi, John M. Storey
Oak Ridge National Laboratory (ORNL), Oak Ridge, TN

Partners:
- Bob McCabe, Ford Motor Co., Dearborn, MI
- Owen Bailey, Umicore Autocat USA, Inc., Auburn Hills, MI

Objectives

- Examine the effect of washcoat composition on lean-NO_X trap (LNT) catalyst aging characteristics. To this end, prepare model Pt/Rh/CeO_2(-ZrO_2)/BaO/Al_2O_3 catalysts with systematic variation of the main component concentrations.
- Study the physical and chemical properties of the model catalysts in the fresh state and after aging.
- Investigate transient phenomena in the fresh and aged catalysts during lean-rich cycling using spatially-resolved capillary-inlet mass spectrometry (SpaciMS).
- Investigate the kinetics and mechanism of desulfation in fresh and aged catalysts using chemical ionization mass spectrometry for the simultaneous analysis of evolved sulfur species.
- Correlate evolution of catalyst microstructure to NO_X storage and reduction characteristics.

Accomplishments

- Steady-state data for NO_X reduction over fresh and aged model LNT catalysts have been obtained in order to gain insights into the effect of catalyst aging on the kinetics of NO_X reduction.
- Analytical data have been acquired for the fresh and aged catalysts which provide insights into the physico-chemical changes that occur in the washcoat during aging.
- A detailed high resolution transmission electron microscopy (TEM) study has been performed on the fresh and aged catalysts which reveals that two main factors can be held responsible for the degradation in LNT performance, *viz*., (i) Pt particle sintering and (ii) sulfur accumulation in the washcoat (associated with the Ba phase) resulting from repeated sulfation-desulfation cycles.
- Spectacular improvement in LNT durability through the incorporation of CeO_2 or CeO_2-ZrO_2 in the washcoat has been demonstrated and the factors responsible for this improvement elucidated.

Future Directions

- Perform additional high resolution TEM (HRTEM) studies aimed at visualization of Pt-Ba phase segregation during LNT thermal aging.
- Derive a quantitative model that describes LNT catalyst performance as a function of aging time.
- Complete project reporting.

Introduction

LNTs represent a promising technology for the abatement of NO_X under lean conditions. Although LNTs are starting to find commercial application, the issue of catalyst durability remains problematic. LNT susceptibility to sulfur poisoning is the single most important factor determining effective catalyst lifetime. The NO_X storage element of the catalyst has a greater affinity for SO_3 than it does for NO_2, and the resulting sulfate is more stable than the stored nitrate. Although this sulfate can be removed from the catalyst by means of high-temperature treatment under rich conditions, the required conditions give rise to deactivation mechanisms such as precious metal sintering, total surface area loss, and solid-state reactions between the various oxides present. The principle objective of this project is to improve understanding of the mechanisms of LNT trap aging, and to understand the effect of washcoat composition on catalyst aging characteristics.

Approach

The approach utilized makes use of detailed characterization of model catalysts prior to and after aging, in tandem with measurement of catalyst performance in NO_X storage and reduction. In this manner, NO_X storage and reduction characteristics can be correlated with the evolution of catalyst

microstructure upon aging. The effect of washcoat composition on catalyst aging characteristics is studied by systematic variation of the concentration of the four main active components: Pt, Rh, CeO_2 (or CeO_2-ZrO_2) and BaO (supported on alumina). In addition to the use of standard physico-chemical analytical techniques for studying the fresh and aged model catalysts, use is made of advanced analytical tools for characterizing their NO_X storage/reduction and sulfation/desulfation characteristics, such as SpaciMS and in situ diffuse reflectance infrared fourier transform spectroscopy (DRIFTS).

Results

Effect of LNT Aging on NO_X Reduction Activity

In order to study the effect of washcoat composition on catalyst aging characteristics, fully formulated monolithic catalysts were prepared containing varying amounts of La-stabilized CeO_2 (5 wt% La_2O_3) and CeO_2-ZrO_2 mixed oxide (Ce:Zr = 70:30), at fixed loadings of Pt (3.5 g/L), Rh (0.7 g/L) and BaO (30 g/L) [1]. The BaO phase was supported on alumina. Core samples were then aged on a bench reactor to the equivalent of ca. 75,000 miles of road aging, using a published accelerated aging protocol [2]. As detailed in a previous report [3], subsequent evaluation of these catalysts on a bench reactor under lean-rich cycling conditions revealed the beneficial effects of ceria incorporation with respect to the NO_X reduction performance of the aged catalysts. However, the transient nature of lean-rich cycling experiments, coupled with the integral nature of the monolith core sample, results in complex spatial and temporal concentration variations within the catalyst during these measurements. These variations make it difficult to directly relate the outlet gas composition to the chemistry taking place inside the catalyst. Steady-flow experiments have therefore been performed in an effort to avoid the difficulties associated with transient LNT behavior, the aim being to decouple the NO_X storage/release process from the reduction reactions. This was accomplished by flowing NO_X and reductant species simultaneously over the catalyst.

The results of one such experiment are summarized in Figure 1, in which NO reduction with H_2 was examined over fresh and aged samples of catalysts 30-0 (containing 30 g BaO/L of catalyst and 0 g CeO_2/L) and 30-100Z (containing 30 g BaO/L of catalyst and 100 g CeO_2-ZrO_2/L). As shown, in the fresh state both catalysts show excellent NO reduction activity, achieving 100% conversion to reduction products (N_2, NH_3 and N_2O) at 225°C. After aging, catalyst 30-100Z shows a slight decline in NO conversion in the temperature range 125-175°C, whereas a significant decline is observed for 30-0 over the range 125-300°C. Striking too is the fact

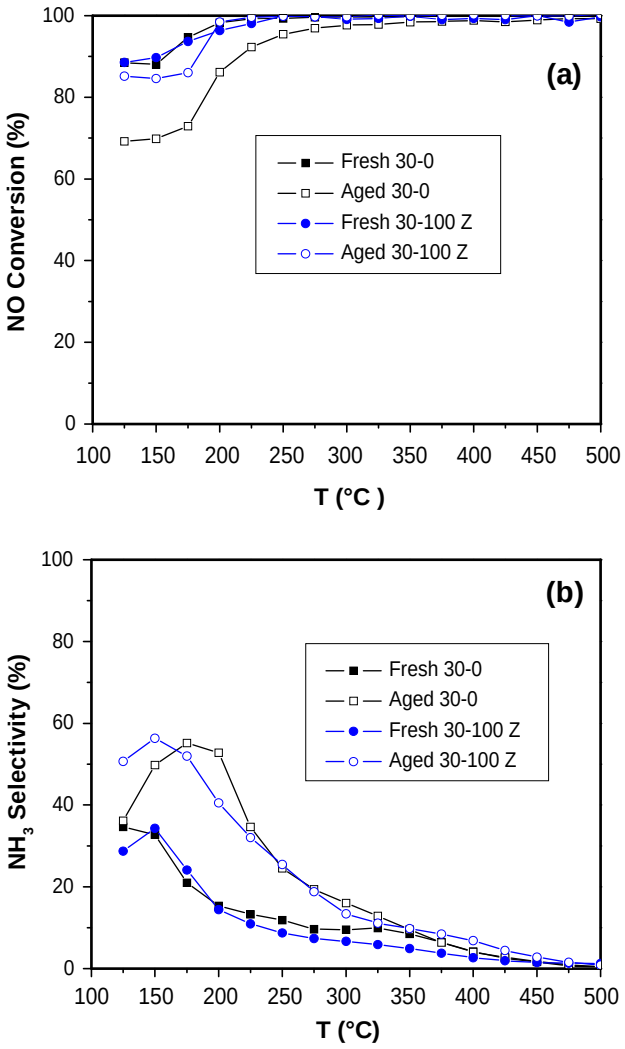

FIGURE 1. NO reduction with H_2 over fresh and aged catalysts 30-0 and 30-100Z: (a) NO conversion, (b) selectivity to NH_3. Reaction conditions: 300 ppm NO, 300 ppm H_2, 5% H_2O, 5% CO_2, balance N, gas hourly space velocity = 120,000 h^{-1}.

that both catalysts show increased selectivity to NH_3 between 125 and 300°C after aging (Figure 1b), which mirrors the result obtained under lean-rich cycling [3].

It is generally agreed that the functioning of LNT catalysts involves four sequential steps [2]: (i) NO oxidation to NO_2, (ii) NO_X storage, (iii) NO_X release (i.e., nitrate decomposition) and (iv) NO_X reduction. In previous work, performed under lean-rich cycling conditions, it was found that simulated road aging resulted in significant deterioration of catalyst performance in steps (ii) and (iii) [3]. For catalyst 30-0, containing no ceria, the decline in NO_X conversion after aging could be attributed mainly to the deterioration in cycle-averaged NO_X storage efficiency, which in turn is determined by the intrinsic NO_X storage efficiency and the extent to which the catalyst is regenerated

during rich purging. From the data shown in Figure 1, it is apparent that for 30-0, catalyst activity for NO_X reduction is also compromised after aging (step iv). Indeed, this is consistent with increased rich phase NO_X release observed for 30-0 after aging, although we note that a decrease in the rate of the reverse spillover process (i.e., NO_X migration to Pt) due to Pt-Ba phase segregation could also contribute to the overall decrease in the rate of NO_X reduction (and hence increased rich phase NO_X slip).

In the remainder of this project, data obtained for the fresh and aged monolith catalysts will be fitted to ORNL's LNT model. Initial fitting will be performed using the steady-state data shown in Figure 1, along with data acquired for other relevant reactions (e.g., $NO_2 + H_2$, NO + CO, NO_2 + CO, NO + NH_3, etc.), after which lean-rich cycling data will be used to fine tune the model. This exercise should help to provide further insights into the catalyst functions which are most affected by aging.

Correlation of Catalyst Performance with Evolution of Washcoat Structure Upon Aging

Analytical data for the aged catalysts reveal two main physico-chemical changes which can explain the degradation in LNT performance. First, residual sulfur was observed in the catalyst washcoats. According to X-ray photoelectron spectroscopy (XPS), TEM and X-ray diffraction (XRD) data, sulfur accumulated during the aging process as $BaSO_4$, thereby decreasing catalyst NO_X storage capacity. Second, sintering of the precious metals in the washcoat was inferred from H_2 chemisorption and TEM data, which can be expected to lessen the contact between the Ba and Pt phases, resulting in less efficient NO_X spillover from Pt to Ba during NO_X adsorption (and hence decreased NO_X storage efficiency). Similarly, decreased rich phase nitrate decomposition suggests that Pt-Ba phase segregation adversely affected the rate of reductant spillover from Pt to Ba.

These physico-chemical changes in the catalyst washcoats are readily apparent from HRTEM data. Figure 2, which shows TEM images of aged catalyst 30-0, illustrates the growth in Pt particle size that results from catalyst aging. In the fresh catalyst (not shown), Pt particles on Al_2O_3 surfaces display a narrow size range with the majority of particles ~2 nm in size, while Pt on Ba-rich surfaces show a broader size range from 1 to 4 nm. In contrast, Figure 2 reveals the presence of rather large Pt crystals, some as big as 25 nm. There is evidence that Pt particle growth occurred due to migration and coalescence as evidenced in Figure 2a, where Pt particles are shown that clearly have fused together. The energy dispersive spectroscopy (EDS) spectrum in Figure 2c shows that Ba and S occur together in the washcoat, consistent with sulfation of the Ba NO_X storage component.

Shown in Figure 3 are TEM images of aged catalyst 30-100 (containing 100 g/L of CeO_2). After aging, large (up to 30 nm) Pt particles are again present, although the majority of Pt particles are in a size range from 3 to 15 nm. Pt particles on CeO_2 have grown to a size of up to 5 nm, suggesting significantly less sintering of Pt on the ceria support in contrast to Al_2O_3 surfaces. There are also dense sulfur-rich Ba nodules present on the Al_2O_3 surface (Figure 3a). The EDS spot analysis in Figure 3b was performed at the area marked in Figure 3a and identified Ba, S, Al and Pt, pointing toward the fact that the $BaSO_4$ nodules were present on the surface of the Al_2O_3 support. The electron energy loss spectroscopy (EELS) spectrum taken over the entire sulfur-rich nodule clearly shows two sharp peaks for Ce M_5 M_4 and also for Ba M_5 M_4 (Figure 6c), as well as signals for O and Al (note that the signal for Al appears outside of the energy range depicted in Figure 6c). This suggests that the beam penetrated the ceria particles and also probed underlying BaO/Al_2O_3 particles. The EELS line scan results indicate that sulfur is only observed in the presence of barium, but does not occur where only ceria is located.

Effect of Ceria on LNT Durability

Overall, this study shows the spectacular improvement in LNT durability which can be achieved through the incorporation of CeO_2 or CeO_2-ZrO_2 (particularly the latter). Based on the foregoing, combined results from our previous work, several factors are believed to be responsible for this improvement, *viz.*:

(i) Ceria can be directly involved in NO_X storage/reduction as a supplement to the main NO_X storage component (Ba); hence, even if the NO_X storage capacity of the $Pt/Ba/Al_2O_3$ component is degraded as a result of aging, NO_X storage can still proceed on the $Pt/CeO_2(-ZrO_2)$ component. Similarly, the $Pt/CeO_2(-ZrO_2)$ component can contribute to NO_X reduction.

(ii) Unlike the $Pt/Ba/Al_2O_3$ component, for which segregation of the Pt and Ba can occur during aging, migration and sintering of Pt in the $Pt/CeO_2(-ZrO_2)$ component does not lead to the same degree of segregation, i.e., the Pt and $CeO_2(-ZrO_2)$ remain in intimate contact, which should be beneficial for the retention of NO_X storage efficiency, as well as efficient nitrate decomposition.

(iii) Ceria-containing catalysts exhibit superior sulfation and desulfation characteristics as compared to their non-ceria analogs; more particularly, the ability of ceria to trap sulfur results in decreased sulfur accumulation on the main Ba NO_X storage component. Further, the ceria can be completely

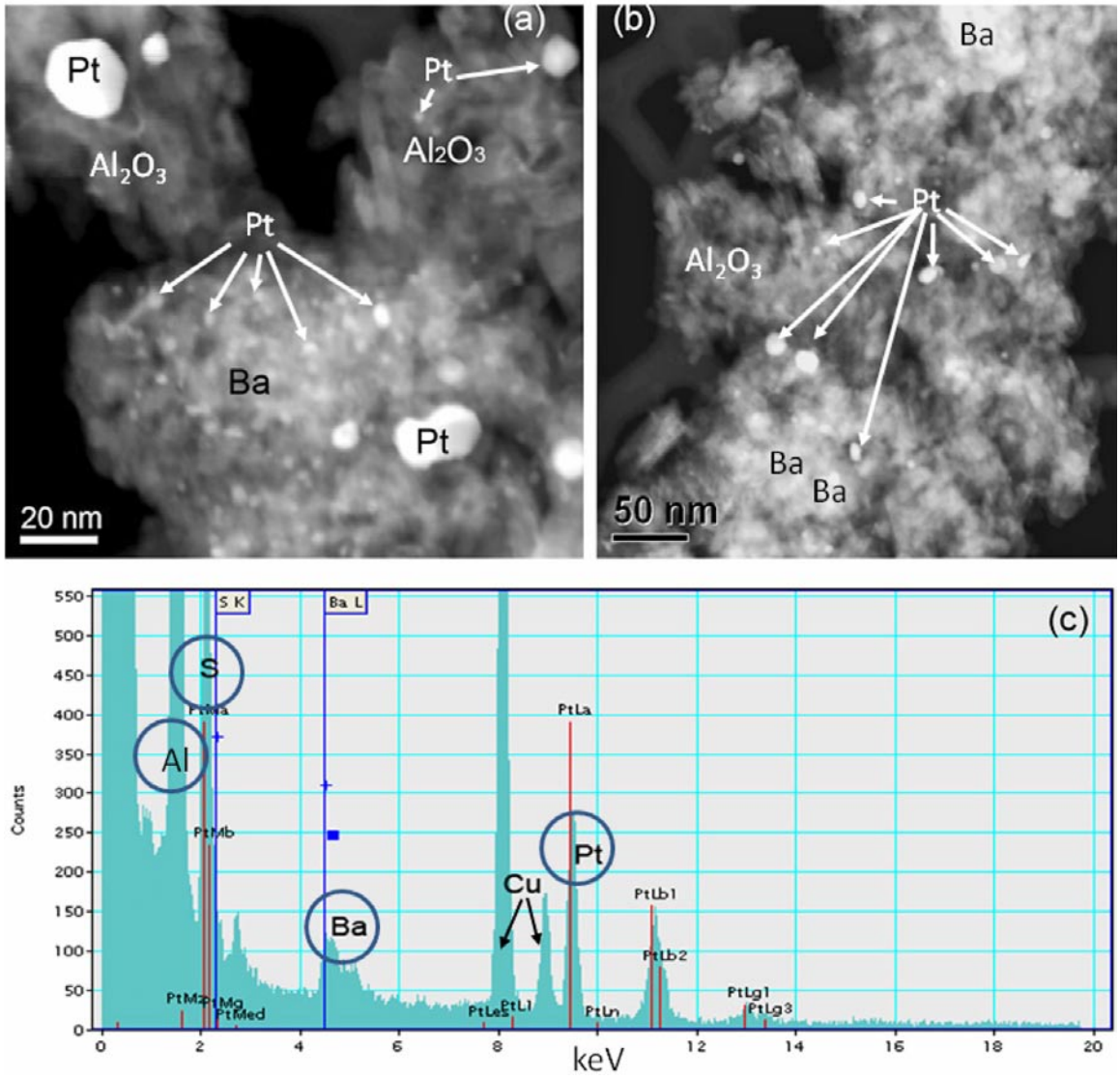

FIGURE 2. Scanning transmission electron microscope (STEM) images for aged 30-0 (a and b) illustrating large particle size range for Pt shown in white; (c) EDS spectrum.

desulfated, unlike the Ba phase on which sulfur accumulation is observed over the course of repeated sulfation-desulfation cycles.

Conclusions

- Steady-state and lean-rich cycling data acquired for aged model LNT catalysts indicate that the decline in cycle averaged NO_X conversion after aging can be attributed to deterioration of three key catalyst functions, *viz.*, NO_X storage, NO_X release and NO_X reduction.
- HRTEM data reveal the occurrence of significant Pt sintering on Al_2O_3 after LNT aging, whereas Pt supported on CeO_2 is sintered to a lesser degree.
- XPS, XRD and TEM/EDS/EELS data reveal that sulfur accumulates in the washcoat as $BaSO_4$ over the course of repeated sulfation-desulfation cycles. Sulfur accumulation on CeO_2 is not observed.
- Based on the analytical data, LNT degradation is attributed to two main factors: (i) Pt sintering, resulting in Pt-Ba phase segregation, and (ii) sulfation of the Ba NO_X storage material (which degrades NO_X storage capacity).
- Spectacular improvement in LNT durability is observed for catalysts containing CeO_2 or CeO_2-ZrO_2 relative to their non-ceria containing analog. This is attributed to (i) the ability of ceria to participate in NO_X storage/reduction as a supplement to the main Ba NO_X storage component; (ii) the fact that Pt and

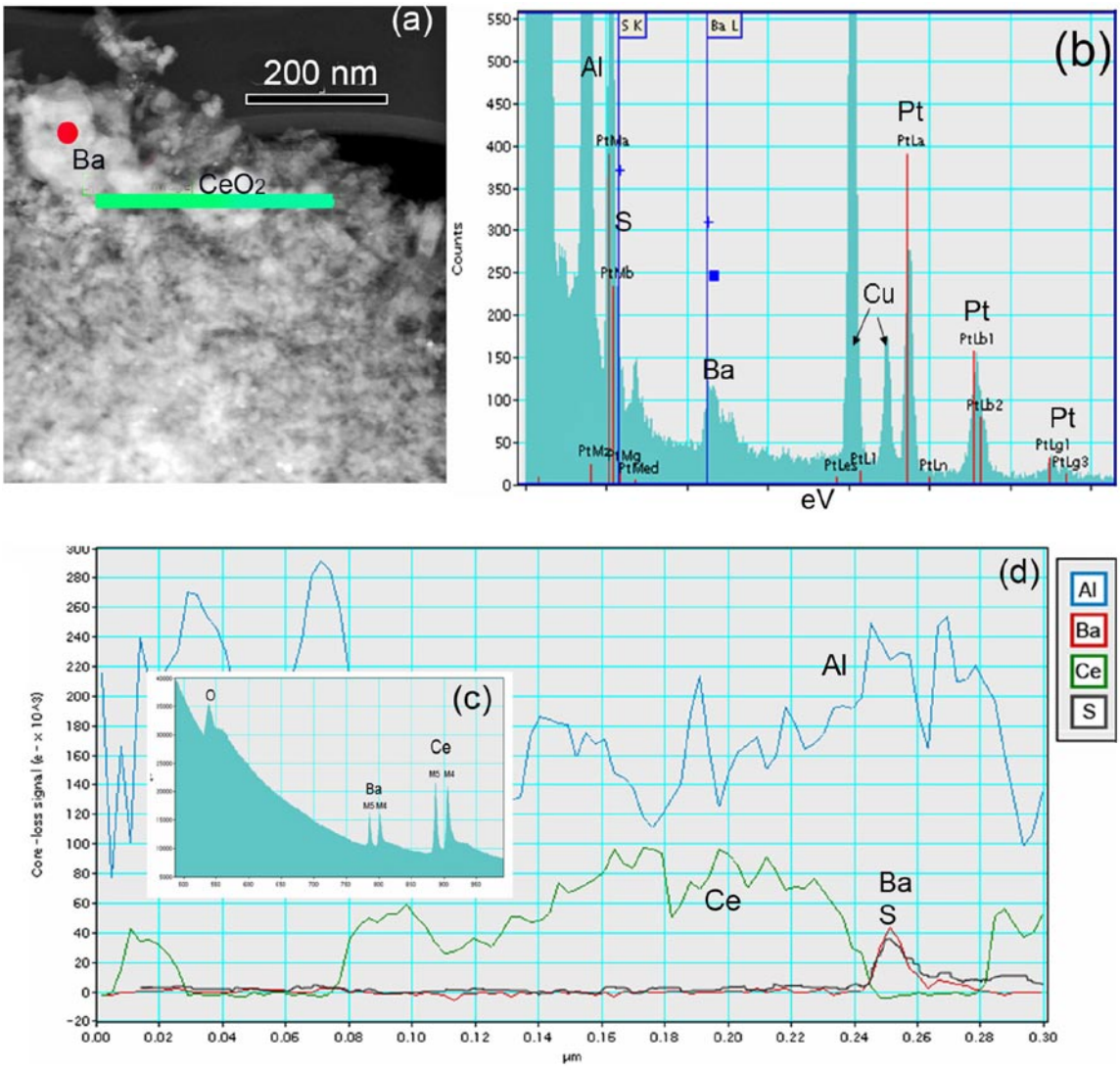

FIGURE 3. (a) STEM image for aged 30-100 showing Al_2O_3 support and Ba-rich nodules, as well as a CeO_2-rich area. The solid line indicates the EELS line scan region; (b) EDS spectrum recorded at the marked dotted area shown in (a); (c) EELS spectrum taken at the dotted area in (a); (d) EELS trace-line: the line is shown in (a). The trace line included 30 EELS measurements along the distance. S-enrichment is seen at the interface between Al_2O_3 and CeO_2.

CeO_2(-ZrO_2) are not subject to the same degree of phase segregation as Pt and Ba; and (iii) the ability of ceria to trap sulfur, resulting in decreased sulfur accumulation on the Ba component.

References

1. Y. Ji, J.-S. Choi, T.J. Toops, M. Crocker, M. Naseri, Catal. Today 136 (2008) 146.

2. L. Xu, R. McCabe, W. Ruona, G. Cavataio, SAE Technical Paper Series 2009-01-0285 (2009).

3. "Investigation of Aging Mechanisms in Lean NOx Traps", FY2008 Progress Report, Advanced Combustion Engine Technologies, Office of Vehicle Technologies Program, U.S. Department of Energy.

FY 2009 Publications/Presentations

1. Y. Ji, T.J. Toops, J.A. Pihl, M. Crocker, " NO_x storage and reduction in model lean NO_x trap catalysts studied by in situ DRIFTS", *Appl. Catal. B* 91 (2009) 329.

2. Y. Ji, T.J. Toops and M. Crocker, "Effect of Ceria on the Sulfation and Desulfation Characteristics of a Model Lean NO_x Trap Catalyst", *Catal. Lett.* 127 (2009) 55.

3. Yaying Ji, Courtney Fisk, Vence Easterling, Mark Crocker, Jae-Soon Choi, William Partridge, "NO_x Storage-Reduction Characteristics of Ba-Based Lean NO_x Trap Catalysts Subjected to Simulated Road Aging", paper presented at the 21st North American Catalysis Society Meeting, San Francisco, CA, June 7–11, 2009, paper OB19.

4. Vencon Easterling, Mark Crocker, Justin Ura, Joseph Theis, Robert McCabe, "Effect of Ceria on the Desulfation Characteristics of Model Lean NO_x Trap Catalysts", paper presented at the 21st North American Catalysis Society Meeting, San Francisco, CA, June 7–11, 2009, paper P-M-18.

5. M. Crocker, "Investigation of Aging Mechanisms in Lean NOx Traps", Office of Vehicle Technologies 2009 Annual Merit Review Meeting, Crystal City, VA, May 18–21, 2009.

6. M. Crocker and Y. Ji, "NOx Storage-Reduction Characteristics of Lean NOx Trap Catalysts Subjected to Simulated Road Aging", 12th DOE Crosscut Workshop on Lean Emissions Reduction Simulation, Dearborn, MI, April 28–30, 2009.

7. V. Easterling, J. Ura, J. Theis, R.W. McCabe, M. Crocker, "Effect of Ceria on the Desulfation Characteristics of Model Lean NOx Trap Catalysts", Tri-State Catalysis Society annual meeting, Lexington, KY, April 20, 2009.

IV.4 On-Board Engine Exhaust Particulate Matter Sensor for HCCI and Conventional Diesel Engines

Matthew Hall (Primary Contact) and Ronald Matthews
University of Texas at Austin
1 University Station, C2200
Austin, TX 78712-0292

DOE Technology Development Manager: Roland Gravel

NETL Project Officer: Ralph Nine

Subcontractor:
Cummins Engine Co., Columbus, IN

Objectives

- The primary goal of the research is to refine and complete development of an on-board particulate matter (PM) sensor, bringing it to a point where it can be commercialized and marketed. The work is performed through a joint effort between the University of Texas at Austin and the Cummins Engine Company. The research is to be completed in two phases.
- The objective of Phase 1 is to refine the current PM sensor system, adapting it to account for the velocity dependence of the PM sensor signal response, and to further improve and verify the accuracy, durability, and sensitivity of the sensor.
- The objectives of Phase 2 are to determine whether the sensor can be successfully used for diesel engines, including the diesel particulate filter (DPF) and determine if the sensor has the potential to provide useful sensing for individual cylinder control of homogenous charge compression ignition (HCCI) engines. The sensor will also be tested upstream and downstream of a DPF to determine whether it would be useful as a diagnostic of the need for DPF regeneration and DPF failure.

Accomplishments

We have just completed the third year of this three-year and three-month project. During the third year, we made significant progress in understanding the fundamental operation of the sensor. The sensor was applied to a high PM emitting vehicle to characterize its response in an actual vehicle. The characteristics of the sensor were also characterized for the first time on a modern multi-cylinder diesel engine having a diesel oxidation catalyst (DOC) and DPF. Throughout the third year we have been working closely with our industrial partner, EmiSense, a division of Ceramatec, Inc. on the development of a commercial product.

Light-Duty Vehicle Application

- The PM sensor was used to make time-resolved measurements of non-volatile PM mass concentrations in the exhaust of a light-duty diesel vehicle that was without exhaust after-treatment. The sensor's output correlated well with exhaust opacity for both very high PM emission concentrations and for lower concentrations approaching the resolution limit of the opacity meter.
- PM emissions were found to be highest for rapid accelerations, and were strongly correlated with pedal position, which for a given engine speed, can be taken as a surrogate for the fuel delivery per cycle. Peak PM concentrations for these high emission events were in the range of 1,000 mg/m^3.
- Vehicle PM emissions at idle were approximately 10 mg/m^3 and were resolvable by the sensor for the stationary vehicle.
- The measured PM concentrations were found to be affected by the exhaust gas velocity past the sensor electrodes, but the effect could be minimized using sensor orientations or installation configurations that minimized the change in flow velocity past the sensor as engine speed changed.

Cummins 6.7 Liter Diesel Engine Application

- The PM sensor was found to be more sensitive in the exhaust of the Cummins engine by several orders of magnitude over that of the single-cylinder Yanmar engine used previously for testing. This is thought to be due to a much higher number density of nucleation size particles in the exhaust of the Cummins.
- The physical mechanisms underlying the sensor's principle of operation have been further elucidated. For the Cummins 6.7 liter engine, the PM sensor's output signal was dominated by the response to induced charge carriers rather than to particles naturally charged in-cylinder during the combustion process. It is suggested that where the electric field between the two sensor electrodes is maximum, a Townsend mechanism ionizes molecules creating molecular ions and charged particles which are

then driven by the strong electric field toward the sensing electrode. The limited mobility of the particles, however, suggests that the ions contribute to the signal more significantly. This is supported by measurements that show the PM sensor signal is symmetric for positive versus negative voltages applied to the field electrode, i.e., the shape and magnitude of the output voltage is the same but of opposite sign for the two different polarities.

- Gravimetric measurements of particulate mass concentration in the exhaust of the Cummins were substantially lower than those previously measured in the exhaust of the Yanmar diesel engine that we had been using. This older engine had no emissions control and an older mechanical fuel pump. Based on the literature, the overall reduction of particulate mass emission in a common-rail emissions-controlled engine is accompanied by a substantial decrease in the mean particle diameter and an increase in the number density of particulates. The far greater sensitivity of the PM sensor for the Cummins engine versus the Yanmar engine is strong evidence of sensitivity to number density rather than particulate mass concentration.
- The sensor orientation was found to affect its sensitivity in the exhaust of the Cummins engine. PM sensor sensitivity was lower when the field electrode was upstream and higher when the sensing electrode was upstream, consistent with a theory of an active charging region near the surface of the field (high voltage) electrode. A dip in sensitivity when the field electrode is masked from upstream flow and the lack of a corresponding dip in sensitivity when the sensing electrode is masked, strongly suggests that charging only occurs at the field electrode.
- Exhaust flow velocity was found not to have a significant effect on sensor sensitivity, all other factors being constant. This is evidence that the migration velocity of the charge carriers is much higher than the free stream velocities seen in this study, suggesting that the charge is carried by molecular ions rather than charged soot particles.
- The PM sensor sensitivity was found to decrease with increasing rate of exhaust gas recirculation (EGR). The literature shows that while overall particle number density increases with increasing EGR, the mean particle diameter also increases, and the number density of the smallest (<20 nm diameter) particles decreases substantially with EGR. This strongly suggests that the PM sensor sensitivity is highest for the nucleation-mode primary particles that fall into this size category.
- The PM sensor output increased linearly with engine fueling rate for fixed EGR rate. This suggests that the PM number concentration in the exhaust of the Cummins engine scaled linearly with the amount of fuel for a given EGR rate.
- The sensor was shown capable of detecting a simulated DPF failure at the level set by U.S. federal emission standards. The sensor is most sensitive at higher load and speed conditions, but even at the least sensitive operating condition (700 RPM idle – 150 kPa brake mean effective pressure, BMEP), it detected a simulated DPF failure: the resolution for failure detection was about 0.7 mg/m^3, or 10 mg/bhp-hr, with a signal-to-noise ratio of 36:1 for a pre-DPF PM concentration level of 20 mg/m^3 (280 mg/bhp-hr). At a higher load condition (800 kPa BMEP) the resolution for failure detection was 0.005 mg/m^3 with signal-to-noise ratio of 220:1 for a pre-DPF PM concentration level of 6 mg/m^3.
- A licensing agreement to commercialize the PM sensor technology was signed in February 2008 with Emisense, Inc. a division of Ceramatec, Inc., which is a division of Coorstek, Inc. We are currently pursuing joint development of the technology and are working in support of original equipment manufacturer (OEM) trials of the PM sensor system.

Future Directions

- Continue commercialization efforts in cooperation with Emisense. We will continue evaluating sensor response, durability and velocity sensitivity for the commercially manufactured sensors and electronics, and we will work to support OEM trials of the PM sensor.
- Future work measuring particle size and morphology using transmission electron microscopy to accompany the existing sensitivity data will shed more light on the sensor response and allow quantification of its sensitivity to particle size.

Introduction

In view of the tightening restrictions on engine emissions of PM there has been increased interest in developing a fast, inexpensive sensor for measuring PM concentrations in engine exhaust flows. Numerous applications can be envisioned for diesel, HCCI, and direct-injection gasoline engines. These include: feedback for control of engine operating parameters, failure detection of DPFs, and as an indicator of the need for DPF regeneration.

Approach

The first 15 months of the project comprised Phase 1. The following 24 months comprise Phase 2. A major focus of Phase 2 was the refinement of PM sensor designs and electronics, especially in cooperation

with our commercialization partner. The other major efforts were to test the sensor on-board a vehicle and with a 2008 model year 6.7 liter engine from Cummins to study sensor behavior with this modern engine.

Results

Seven tasks comprise the third-year budget period as outlined in the original proposal and shown below (Please note that Tasks 3.2 and 3.7 are redundant). The original work plan had to be revised somewhat because Cummins was not able to provide us with the 6.7 liter engine within the time-frame originally specified. This impacted several of the second-year tasks (Task 2.2, 2.3, and 2.4). We did finally receive the engine in October 2008 and completed these tasks in Year 3. Fortunately, the delay in receiving the Cummins engine did not substantially slow our PM sensor development efforts as mentioned under *Accomplishments*. Because of the delay, however, we were not able to evaluate the use of the sensor for HCCI measurements. This impacts Tasks 3.4-3.6 as outlined below. The other Year 3 tasks have been completed, however.

- **Task 3.1.** Examine PM sensor suitability as an on-board diagnostic for regeneration of a diesel particulate filter and detection of filter failure.
- **Task 3.2.** Optimize electronics package.
- **Task 3.3.** Assist commercialization partner (as yet unidentified) with design of production version of PM sensor system, and assist with licensing agreements.
- **Task 3.4.** Document sensitivity, time response, suitability, and durability for application to a heavy-duty diesel HCCI engine - in HCCI mode.
- **Task 3.5.** Document sensitivity, time response, suitability, and durability for application to a heavy-duty diesel HCCI engine - in transition (mode-switching) mode.
- **Task 3.6.** Examine PM sensor installation in HCCI exhaust manifold for suitability for individual cylinder control.
- **Task 3.7.** Optimize electronics package.
- **Task 3.8.** Identify most commercially-viable design for PM sensor and electronics.

Sensor Design

The sensor design has evolved greatly over the last year. Figure 1 shows a prototype commercial sensor built by Emisense. Most of our Year 3 work was done with these pre-production sensors.

The engine was fitted with a combined DOC/DPF unit for installation in the exhaust system to enable full testing of the onboard diagnostics function of the sensor. Plumbing was installed to allow part or all of the exhaust

FIGURE 1. Typical EmiSense electronic soot sensor with electrode and shrouds on the left, M18 threads, and sensor body on the right.

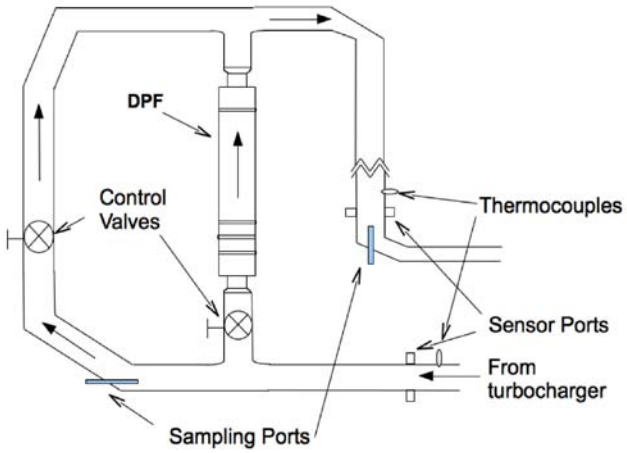

FIGURE 2. Arrangement of the Diesel Particulate Filter and Bypass Loop

gas to flow around the DOC/DPF. In this way, a DPF failure could be simulated by allowing unfiltered exhaust to reach a sensor installed downstream of the DPF. Valves were installed at the DPF inlet and in the bypass to provide no- partial- or full-diversion of exhaust gas through the bypass. A schematic diagram of the DPF-bypass arrangement is shown in Figure 2.

Simulation of DPF Failure

To simulate the failure of a DPF by leakage of unfiltered exhaust gas, sensors were installed in the upstream and downstream ports. The engine was warmed up and brought to thermal equilibrium. Initially, all of the exhaust flow was directed through the DPF. At a specified time, the valve to the bypass loop was slowly opened. After 20 seconds, the valve to the DPF was closed, thus diverting all of the flow through the bypass. Then after 20 seconds, the process was reversed, first by opening the valve to the DPF, and then by closing the valve to the bypass. Steady-state averages were calculated for the initial state, the intermediate state, and the full bypass state. Figure 3a shows the signal history from one such test at a high-speed, low load condition at 2,200 RPM. The signal from the upstream sensor is shown for comparison.

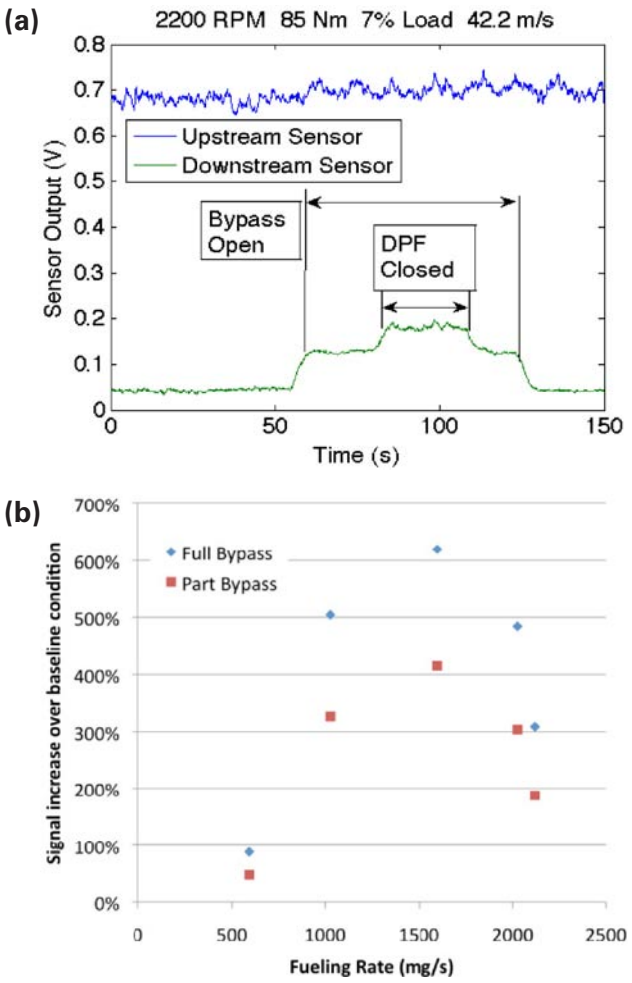

FIGURE 3. (a) Simulation of DPF leak at 2,200 RPM at light load, (b) increase in PM sensor output during DPF leak event at various fueling rates.

Several such tests were conducted ranging from idle condition (where the sensor has the least sensitivity) to partial load (50%, 1,800 RPM) to assess the ability of the sensor to detect leakage of unfiltered exhaust gas through the DPF. At each condition, the mean value of the sensor signal was calculated for the initial, DPF-filtered state, and for the partial and full bypass states. A percent increase in the signal over the initial, post-DPF baseline condition ($V_{mean,DPF}$) could then be calculated for the partial and full bypass conditions as follows:

$$\%\ increase = \frac{V_{mean} - V_{mean,\ DPF}}{V_{mean,\ DPF}}$$

These percentage increases are shown plotted against fueling rate in injection mass per second in Figure 3b. Note that the increase for the partial bypass condition is about half the increase for the full bypass. In the case with the greatest sensitivity, the full-bypass produces a signal increase of 620% over the baseline condition. In the least sensitive case, at 700 RPM idle, the increase was 88% for full bypass.

Conclusions

Development of the University of Texas electronic particulate matter sensor is proceeding well. Testing in a 2008 model year Cummins 6.7 liter engine showed that at least for some operating conditions, it has the sensitivity to detect DPF failures and the time resolution for feedback control applications. Sensitivity decreased with increasing EGR levels. The sensor was found to be most sensitive to the number density of the smallest (nucleation mode) particles. Because of this the sensor's sensitivity is affected by any engine operating condition that changes the particle size distribution, particularly of the smallest particles. These conditions may include engine load, EGR level and downstream location in the exhaust. The effect of gas velocity on sensor sensitivity is complex and may be compensated for by sensor orientation. Commercialization efforts are proceeding.

FY 2009 Publications/Presentations

1. Hall, M.J., U.S. DOE Merit Review Meeting, Washington, D.C., May 22, 2009.

2. Diller, T.T., Osara, J., Hall, M.J., and Matthew, R.D. "Electronic Particulate Matter Sensor – Mechanisms and Application in a Modern Light-Duty Diesel Vehicle," Society of Automotive Engineers Paper 2009-01-0647, 2009.

Special Recognitions & Awards/Patents Issued

Patent Pending: 2443 - A Sensor to Measure Time-Resolved Particulate (soot) Exhaust Emissions from Internal Combustion Engines has been patented with coverage in the U.S. in the form of a PCT that was nationalized in the U.S.

Provisional: 7/19/2002

PCT conversion: 7/18/2003

V. New Projects

The following are brief abstracts of newly instituted Advanced Combustion Engine Technologies projects. These projects have not been in effect a sufficiently long period of time to accumulate results worthy of reports similar to those in the previous sections. These projects will have full-length reports in the FY 2010 Annual Progress Report.

V.1 Optimization of Advanced Diesel Engine Combustion Strategies

Engine Research Center,
University of Wisconsin-Madison

PI: Prof. R.D. Reitz

This project addresses DOE's program goals of a 20-40% improvement in fuel economy in a light-duty vehicle and the attainment of 55% brake thermal efficiency in heavy-duty engine systems. Over the three-year duration of this work, fundamental science and engineering concepts and tools will be developed to support the development and commercialization of clean, efficient internal combustion engine powertrains operating on both nonpetroleum- and petroleum-based fuels. To achieve DOE's brake thermal efficiency goals it is necessary to improve the efficiency of expansion work extraction, and this requires optimized combustion phasing and minimized in-cylinder heat transfer losses. There is also a need to minimize the fuel needed for after-treatment system regeneration, and thus, it is necessary to minimize pollutant emissions. Because of the complex nature of the combustion process this project will use high-fidelity computing and high-resolution engine experiments synergistically to create, apply and advance the tools (i.e., fast accurate predictive models) needed for low emission, fuel efficient engine designs. The experiments will be conducted using representative research automotive and truck diesel engines. Combustion technologies to be considered include operation on partially premixed charge compression ignition (PCCI) with transition to advanced compression ignition direct injection combustion strategies, including lifted flame operation at higher loads and starting conditions, and PCCI at moderate to light loads ("mixed-mode" operation). Advanced fueling strategies, including variable injection pressure, multiple injections and dual fueling can help control combustion phasing and reduce wall-wetting and soot and hydrocarbon emissions, and will be explored using novel injection hardware. In addition to in-cylinder combustion technologies, methods for reducing the overall system fuel consumption will be explored. System technologies to be considered include reducing urea required for selective catalytic reduction exhaust after-treatment, minimizing the need for exhaust after-treatment using optimized dual (gasoline/diesel) fuel for combustion phasing control for improved fuel efficiency and extended load range, developing system optimization models for engine and after-treatment operation, and developing transient mode switching concepts.

V.2 A University Consortium on High Pressure Lean Combustion for Efficient and Clean IC Engines

University of Michigan,
Massachusetts Institute of Technology,
and University of California, Berkeley

PI: Prof. Dennis N. Assanis

The goal of this work is to explore new high-pressure, lean-burn (HPLB) combustion that can enable future gasoline engines with 20-40% improved fuel economy. Achieving such breakthrough efficiencies in an engine system is a very challenging objective. Nonetheless, the combination of HPLB unthrottled operation in a stratified charge, highly dilute combustion system points to a promising pathway for attaining these objectives.

The challenges of HPLB operation are significant, with previous attempts unsuccessful due to fuel injection repeatability, ignition reliability and emission problems. Fortunately, a wide range of new enabling technologies on the horizon including advanced turbochargers, multiple pulse fuel injectors, and inexpensive pressure transducers for active combustion control open up new opportunities to push beyond the present constraints. Mixed-mode options also offer the potential to couple the strengths of both conventional and advanced combustion modes. The key objective of this work is to explore low-temperature HPLB regimes and determine the fuel economy benefits of engines and engine cycles designed to take advantage of these advanced combustion modes.

V.3 Experimental Studies for DPF and SCR Model, Control System, and OBD Development for Engines Using Diesel and Biodiesel Fuels

Michigan Technological University

PI: Dr. John Johnson

The focus of this research is to develop experimentally validated diesel particulate filter (DPF) and selective catalytic reduction (SCR) models with real-time internal state estimation strategies that support future onboard diagnostics (OBD), advanced control system, and system optimization objectives for diesel oxidation catalyst-DPF-SCR aftertreatment systems that minimize the energy penalty of meeting emission regulations. Although SCR and DPF devices have fundamentally different objectives, there is commonality in the model requirements from an OBD/controls perspective. To make optimal use of these devices in current and advanced engine and vehicle technologies there must exist (1) internal state estimation strategies (2) methods to quantify state uncertainty, (3) adaptation to aging, and (4) fundamental and applied knowledge of the effects of alternative fuels. This research project addresses these issues while also providing fundamental knowledge that will support aftertreatment development and control activities for low oxides of nitrogen diesel engines.

V.4 Development of Optimal Catalyst Designs and Operating Strategies for Lean NOx Reduction in Coupled LNT-SCR Systems

University of Houston

PI: Dr. Michael P. Harold

This project, a collaboration between the University of Houston, University of Kentucky, Ford Motor Company, Oak Ridge National Laboratory, and BASF Catalysts LLC, involves the research and development of coupled oxides of nitrogen (NOx) storage and reduction and selective catalytic reduction (SCR) that enables a high conversion of NOx under lean conditions typical of a diesel or lean burn gasoline vehicle. The project goal is to identify the mechanisms responsible for the synergy of coupled lean-NOx trap (LNT) and SCR catalysts, and to use this knowledge to design optimized LNT-SCR systems in terms of catalyst architecture and operating strategies. The following specific objectives will be pursued:

1. The mechanisms and kinetics of NOx reduction in LNT-SCR systems will be elucidated. This will involve the study of both NH_3 and non-NH_3-based mechanisms.
2. LNT selectivity to NH_3 will be mapped as a function of catalyst composition (ceria content and type, precious metal loading) and relevant process parameters (NOx loading, purge duration, purge fuel/air ratio and space velocity). The resulting data will be used to develop a microkinetic model capable of predicting LNT NOx reduction conversion and product selectivities.
3. The optimal catalyst architecture and operating strategy of LNT-SCR catalyst systems will be determined, with the goal of maximizing the NOx conversion level with minimum fuel penalty.
4. The extent for precious metal reduction in LNT-SCR catalyst systems will be ascertained (at equivalent performance to the corresponding LNT-only system).
5. A low dimensional LNT-SCR model will be developed, to assist with system optimization.
6. Using bench-scale and full-scale vehicle exhaust testing, the optimal operating strategy for LNT-SCR systems will be validated with respect to NOx conversion level and fuel penalty. These tests will be extended to include aged LNT-SCR systems, with the aim of assessing system durability and sulfation-desulfation protocols and their effects on performance.

V.5 Flex Fuel Optimized SI and HCCI Engine

Michigan State University

PI: Dr. Gouming Zhu

The objective of this research is to demonstrate a closed-loop combustion controlled engine system with smooth combustion mode transition between spark-ignited (SI) and homogenous charge compression ignition (HCCI) operations adapted to a given gasoline and ethanol blend. The first deliverable is a concept SI and HCCI dual-combustion mode engine optimized for flex fuel; and the second deliverable is a control oriented SI and HCCI dual combustion mode engine model that is developed and calibrated based upon both combustion analysis and test data obtained during optical and metal engine experiments.

In order to assemble a well configured SI and HCCI dual-mode engine with proper combustion controllability, a number of advanced engine subsystems will be used. A port fuel injection (PFI) and direct injection (DI) dual-fuel system will be used to control charge mixture temperature through DI injection timing and PFI/DI fueling ratio. An electro-pneumatic valve actuator (EPVA) will be used for both intake and exhaust valves. The EPVA is mainly used for adjusting intake and exhaust valve timing to regulate both the charge air and the residual exhaust gas amount. Ionization sensing of combustion feedback will be performed in both SI and HCCI combustion modes. During the SI combustion mode, ionization will be used for detecting engine partial burn, knock, minimal advance for the best torque timing, and combustion stability; and during the HCCI combustion mode, it will be used for detecting two key combustion parameters, the start of combustion and burn duration.

Closed-loop combustion control (CLCC), based upon individual cylinder ionization feedback signals, will be used for fixed combustion mode operation. For the SI combustion mode the CLCC control regulates engine spark timing, EPVA intake and exhaust valve timings, and the dual-fuel system to achieve the best fuel economy possible with desired engine output torque. CLCC will also be used during the HCCI combustion mode to control the start of combustion and burn duration and to maximize the operating range of the HCCI combustion using ionization feedback under different gasoline and ethanol blends. Pressure measurements will be used to guide the system development.

Combustion mode transitions from HCCI to SI combustion and from SI to HCCI combustion have different physical and chemical characteristics. The transition from SI to HCCI mode is more difficult than the reversed transition due to higher SI exhaust temperature than that in HCCI operational mode. A smooth transition from SI to HCCI mode requires accurate control of the physical properties of the trapped in-cylinder gas mixture. This research will divide the combustion mode transition into two stages. First, the SI combustion condition is adjusted to create a favorable combustion condition for mode transition to HCCI; and then, mode transition will be regulated using a model-based predictive control of trapped gas properties while maintaining a smooth torque output.

V.6 Three-Dimensional Composite Nanostructures for Lean NOx Emission Control

University of Connecticut

PI: Dr. Puxian Gao

This project will explore the synthesis, characterization, and modeling of a new class of vehicle emission control nanocatalysts based on a three-dimensional (3D) composite nanoarchitecture that consists of a semiconductor nanowire/nanodendrite core, a mesoporous perovskite shell doped with functional metals. The composite nanostructure inherits complimentary multi-functionalities resulting from the combination of a de-sulfur semiconducting oxide core (such as CeO_2, ZnO, SnO_2 and TiO_2) and a de-NOx mesoporous perovskite thin film (such as La-based transition metal oxides, $LaMO_3$, M= Co, Cr, Fe, Mn, and Ni). Precious metals (Pt, Pd) and lean-NOx trap (LNT) metal doping (Ba, K, Sr, Ce) will be conducted on the grown 3D composite nanostructures to form a new class of lean-NOx emission control catalysts. The formed 3D nanocatalysts are expected to have hybrid, tunable and synergistic functions in terms of nitrate storage, simultaneous conversion of CO and NOx into CO_2 and N_2, minimization of NH_3 emission, as well as the de-sulfation process. Both two-dimensional flat substrates and 3D monolith substrates such as Al_2O_3, SnO_2 and TiO_2, will be used for demonstrating the capability of this unique nanostructure as efficient lean NOx emission control devices.

One of the focuses is to rationally design, fabricate and control the 3D composite nanoarchitectures through the nanostructure control and composite layering during a two-step synthesis combining solution approaches and vapor phase growth processes. Hydrothermal synthesis or thermal evaporation is employed to synthesize semiconductor nanowire/dendrite arrays as the 3D nanocatalyst skeletons, while a pulsed laser deposition, or magnetron sputtering process, or sol-gel wash-coating will be used to form the catalytic active mesoporous perovskite shells. The selective precious metals (Pt, Pd) and LNT metals (Ba, K, Sr, Ce) doping will be conducted using chemical impregnation or physical sputtering techniques.

To find the best multi-functional combination, a kinetic control study will be conducted on the growth of 3D composites, and the metal doping process. A systematic characterization of nanostructures will be conducted on their structure, morphology, chemical properties and catalytic behavior via a range of microscopy, thermal analysis and spectroscopy techniques. To understand the nanostructure-property relationship, a systematic and complementary ab initio theoretical study will be conducted on the thermal/mechanical stability and catalytic behavior of the multi-functional core-shell nanocomposites. The surface/interface structural and chemical properties will be correlated to the surface catalytic behavior in terms of nitrate storage, CO oxidation, NOx reduction, hydrocarbon, and particular matter filtering.

V.7 Improving Energy Efficiency by Developing Components for Distributed Cooling and Heating Based on Thermal Comfort Modeling

General Motors

PI: Jeff Boseman

General Motors (GM) improved energy efficiency by developing components for distributed cooling and heating based on thermal comfort modeling. GM has partnered with Delphi Thermal Systems and the University of California, Berkeley (UCB) to create a team that is uniquely qualified to accomplish the DOE's stated program objectives. The primary objectives of this project are the following:

- Use human subject testing to characterize the response to localized cooling and heating of body segments in a thermal comfort model. This math model will identify the optimal locations for energy-efficient distributed cooling and heating components by selecting occupant body segments that are sensitive to thermal comfort and can offset the effects of higher or cooler cabin temperatures.
- Develop distributed heating, ventilation and air conditioning (HVAC) components to supplement the central HVAC system and integrate them in a 5-passenger demonstration vehicle. These will reduce the energy required by current compressed gas air conditioners by at least one-third. Thermoelectric (TE) HVAC components will have a coefficient of performance (COP) greater than 1.3 for cooling and greater than 2.3 for heating.

A secondary objective is to improve the efficiency of TE generators for directly converting engine waste heat to electricity. GM will collaborate with the University of Nevada, Las Vegas on TE material research to accomplish this objective as part of the project. This research will build directly on GM's existing DOE project for automotive waste heat recovery.

A National Renewable Energy Laboratory (NREL) study identified the potential for a 7% reduction in air conditioning (AC) compressor power from the application of ventilated seats. Using their model, NREL estimated a fuel savings of 522 million gal/year or a 7.5% reduction in U.S. AC fuel usage based on that 7% reduction. Our approach will optimize the selection of distributed HVAC components, which should further improve the AC power reduction beyond 7%. This would provide a corresponding increase in the estimates for fuel savings and CO_2 reduction versus the study of ventilated seats.

V.8 Ford Thermoelectric HVAC Project

Ford Motor Company

PI: Clay Maranville

Current light-duty vehicles provide passenger thermal comfort primarily through the use of a centralized heating, ventilation, and air conditioning (HVAC) unit that distributes conditioned air to vent locations throughout the vehicle. A substantial portion of the air energy content is spent conditioning various elements of the vehicle's interior structures. This is not an overwhelming issue in today's vehicles, but as pressure builds to improve powertrain efficiency, the energy available to provide occupant comfort will decrease.

The objective of this project is to identify a technical and business approach that will accelerate the deployment of light-duty automotive thermoelectric (TE) HVAC technology. The use of this technology is expected to result in improved energy efficiency by advancing the methods of climate control design and execution. A solid-state TE solution, which allows for evolution with changing vehicle propulsion technologies, is proposed. The approach addresses many challenges faced by climate control system designers. These challenges include: increasing federal and state regulatory pressure focused on reducing greenhouse gas (GHG) pollutants, increased vehicle electrification, increased powertrain efficiencies, and rising societal expectations that automobile manufacturers address climate change, foreign oil dependency, and high fuel prices.

The Ford TE HVAC Project will develop a zonal HVAC system that is optimized to provide comfort to each occupant, while reducing the overall power consumed by the HVAC system compared with a baseline system. Project success will be evaluated using occupant comfort metrics, based on a novel comfort-modeling approach, and empirical testing. The ability to produce and market the technologies developed in this project will be assessed by a business analysis, which will result in recommendations regarding the steps required for a self-sustaining TE HVAC market. This entails a value analysis for the original equipment manufacturer, system suppliers, and the customer, while helping to achieve national goals for reduced petroleum consumption and GHG emissions.

A key enabler to the success of this project will be the development of a distributed, localized, TE-based heating and cooling system for passenger vehicles. This system will provide the basis for a down-sized central HVAC unit, provide equivalent comfort and equivalent heating/cooling time-to-comfort at startup, and reduce the energy consumed to provide these functions. The long range goal is to provide a commercially viable climate solution that optimizes comfort for every vehicle occupant. Key attributes will be explored to determine how they contribute to the commercialization potential of the technology.

To accomplish the goals of the TE HVAC Project, Ford Motor Company has established partnerships with key stakeholders whose expertise will be vital to the success of the project. Visteon Corp. is a leading integrator of HVAC systems in automobiles and brings expertise in HVAC system modeling, design, test and commercialization. BSST, a research subsidiary of Amerigon, Inc., brings a deep knowledge of TE device implementation in the automotive industry and proprietary TE technology. The National Renewable Energy Laboratory brings expertise in the area of vehicle occupant comfort and HVAC load reduction. The Ohio State University brings expertise in development of advanced TE materials for heating and cooling. The Ford TE HVAC Project is a novel approach to developing more efficient and effective vehicle climate control systems. The project, for the first time, brings together experts in a broad range of disciplines to address this large systems design and engineering problem.

VI. Acronyms, Abbreviations and Definitions

Φ	Fuel air equivalence ratio
γ	Ratio of Specific Heats (c_p/c_v)
µs	Micro-second
°C	Degrees Celsius
°F	Degrees Fahrenheit
ΔP	Pressure drop
ΔT	Delta (change in) temperature
0-D	Zero-dimensional
1-D	One-dimensional
2-D	Two-dimensional
3-D	Three-dimensional
4Q	Fourth quarter
a.u.	Arbitrary units
AC	Alternating current
ACES	Advanced Collaborative Emissions Study
ACM	Acicular ceramic material
AEI	After end of injection
AEOs	Alkaline earth oxides
A/F	Air to fuel ratio
Ag	Silver
Agro15	The name of a fuel consisting of 85% Swedish Environmental Class 1 Diesel (having low aromatic content), 10% heavy alcohols (with an average of 6 carbon atoms) made from bio source and 5% rapeseed methyl ester
a.k.a.	Also known as
Al	Aluminum
Al_2O_3	Aluminum oxide
ANL	Argonne National Laboratory
APU	Auxiliary power unit
ASC	Ammonia slip catalyst
ASI	After start of injection
ASME	American Society of Mechanical Engineers
atdc, ATDC, aTDC	After top dead center
atm	Atmosphere
Au	Gold
Avg.	Average
B	Boron
Ba	Barium
$BaAl_2O_4$	Barium aluminate
$Ba(NO_3)_2$	Barium nitrate
BaO	Barium oxide
bar	unit of pressure (14.5 psi or 100 kPa)
BCAC	Bounce chamber air control
BDC	Bottom dead center
BES	Basic Energy Sciences
BET	Named after Brunauer, Emmett and Teller, this method for determining the surface area of a solid involves monitoring the adsorption of nitrogen gas onto the solid at low temperature and, from the isotherm generated, deriving the volume of gas required to form one monolayer adsorbed on the surface. This volume, which corresponds to a known number of moles of gas, is converted into a surface area though knowledge of area occupied by each molecule of adsorbate.
BFC	Boundary-fitted cells
bhp-hr	Brake horsepower hour
BMEP	Brake mean effective pressure
Bsfc, BSFC	Brake specific fuel consumption
bsNOx, BSNOx	Brake specific NOx emissions
BSSoot	Brake specific soot
BSTC	Brake specific total fuel consumption
BTDC, btdc	Before top dead center
BTE	Brake thermal efficiency
BTEX	Benzene, toluene, ethylbenzene, and xylenes
C_2H_4	Ethene
C_2H_6	Ethane
C_3H_6	Propylene
ca.	about, approximately
CA	Crank angle
CA50	Crank angle at which 50% of the combustion heat release has occurred
CAC	Charge air cooler
CAD	Crank angle degrees
CAE	Computer-aided engineering
CARB	California Air Resources Board
CBS	Characteristic-based split
cc	Cubic centimeter
CCD	Charge coupled device
CDI	Compression direct injection
Ce	Cerium
CeO_2	Cerium oxide
CFD	Computational fluid dynamics
CH_4	Methane
CI	Compression ignition

CIDI	Compression ignition direct injection
CLCC	Closed-loop combustion control
CLEAN	Trademark for Detroit Diesel low-temperature combustion strategy
CLEERS	Cross-Cut Lean Exhaust Emissions Reduction Simulations
CLOSE	Collaborative Lubricating Oil Study on Emissions
cm	Centimeter
cm^3	Cubic centimeters
CMOS	Complementary metal–oxide–semiconductor
CN	Cetane number
CNG	Compressed natural gas
CO	Carbon monoxide
CO_2	Carbon dioxide
COP	Coefficient of performance
COV	Coefficient of variation
CPF	Catalyzed particulate filter
cpsi	Cells per square inch
CPU	Central processing unit
Cr	Chromium
CR	Compression ratio
CRADA	Cooperative Research and Development Agreement
CRF	Combustion Research Facility
Cu	Copper
DC	Direct current
DDC	Detroit Diesel Corporation
DEE	Diesel engine exhaust
deg	Degrees
°CA	Degrees crank angle, 0° = TDC intake
ΔT	Delta (change in) temperature
DI	Direct injection, direct-injected
DME	Dimethyl ether
DNPH	2,4-dinitorophenylhydorazine
DNS	Direct numerical simulation
DOC	Diesel oxidation catalyst
DOE	U.S. Department of Energy
DOHC	Double overhead camshaft
DP	Pressure differiential
DPF	Diesel particulate filter
DPNR	Diesel Particulate NOx Reduction
DRIFTS	Diffuse reflectance infrared Fourier-transform spectroscopy
DST	Dual-stage turbo
E10	10% ethanol, 90% gasoline fuel blend
E15	15% ethanol, 85% gasoline fuel blend
E20	20% ethanol, 80% gasoline fuel blend
EC1	Swedish Environmental Class 1 diesel fuel (<10 ppm sulfur, by weight)
ECM	Electronic control module
ECN	Engine Combustion Network
ECU	Electronic control unit
EDS	Energy dispersive spectroscopy
EDX	Energy dispersive X-ray
EELS	Electron energy loss spectroscopy
EERE	Energy Efficiency and Renewable Energy
EEVO	Early exhaust valve opening
EGR	Exhaust gas recirculation
EOI	End of injection
EPA	U.S. Environmental Protection Agency
EPMA	Electron probe microanalysis
EPR	Electron paramagnetic resonance
EPVA	Electro-pneumatic valve actuator
ERC	Engine Research Center
ESC	European Steady State Cycle
ES&H	Environment, safety, and health
EVC	Exhaust valve closing
EVO	Exhaust valve opening
EWHR	Exhaust waste heat recovery
FAME	Fatty acid methyl ester
FCVT	FreedomCAR and Vehicle Technologies
FDML	Fourier Domain Mode Locked
Fe	Iron
FEA	Finite-element analysis
FEERC	Fuels, Engines and Emissions Research Center
FEM	Finite-element method
FFVA	Fully flexible valve actuation
FMEA	Failure mode and effects analysis
fmep	Friction mean effective pressure
FMG	Flywheel-integrated motor-generator
FSN	Filter smoke number
FTIR	Fourier transform infrared
ft-lb	Foot-pound
FTP	Federal Test Procedure
FTP-75	Federal Test Procedure for LD vehicles
FVVA	Full variable valve actuation
FWHM	The full width at half the maximum activity as a function of temperature
FY	Fiscal year
g, G	Gram
GATE	Graduate Automotive Technology Education
g/bhp-hr	Grams per brake horsepower-hour

GC	Gas Chromatography
GC-FID	Gas chromatograph combined with a flame ionization detector
GC-MS	Gas chromatography – mass spectrometry
GDC	Gadolinium-Doped Cerium Oxide
GDI	Gasoline direct injection
Ge	Germanium
g/hphr	Grams per horsepower-hour
GHSV	Gas hourly space velocity
GM	General Motors
g/mi	Grams per mile
H_2	Diatomic (molecular) hydrogen
H_2CO	Formaldehyde
H_2O	Water
H_2O_2	Hydrogen peroxide
H2ICE	Hydrogen-fueled internal combustion engine
HAADF STEM	High angle annular dark field scanning transmission electron microscopy
HC	Hydrocarbons
HCCI	Homogeneous charge compression ignition
HC-SCR	Hydrocarbon selective catalytic reduction
HDCC	Heavy duty corporate composite
He	Helium
HECC	High-efficiency clean combustion
HEI	Health Effects Institute
HEV	Hybrid electric vehicle
HFPE	Hydrogen free-piston engine
HHV	Higher heating value
HMN	Heptamethylnonane
hp	Horsepower
HPL	High pressure loop
HPLB	High-pressure, lean-burn
HPLC	High-performance liquid chromatography
HPT	High performance turbo
hr	Hour
HR	Heat release
HRR	Heat release rate
HSDI	High-speed direct-injection
HTML	High Temperature Materials Laboratory
HTR	High-temperature reaction
HVAC	Heating, ventilation and air conditioning
HWFET	Highway Fuel Economy Test
HXN	Heat exchanger
Hz	Hertz
IC	Internal combustion
I/C	Intercooler
ICCD	Intensified charged-coupled device
ICE	Internal combustion engine
ID	Injection delay
ID	Internal diameter
IEGR	Internal exhaust gas recirculation
IMEP	Indicated mean effective pressure
$IMEP_g$	Indicated mean effective pressure, gross
IMT	Inlet manifold temperature
INCITE	Innovative and novel computational impact on theory and experiment
IR	Infrared
ISFC	Indicated specific fuel consumption
ISX	Cummins Inc. 15-liter displacement, inline, 6-cylinder heavy duty diesel engine
IVC	Intake valve closing
IVO	Intake valve opening
J	Joule
k	thousand
K	Kelvin
K	Potassium
kg	Kilogram
kHz	Kilohertz
KIVA	Combustion analysis software developed by Los Alamos National Laboratory
kJ	Kilojoules
kJ/L	Kilojoules per liter
kJ/m^3	Kilojoules per cubic meter
kPa	Kilopascal
kW	Kilowatt
L	Liter
La	Lanthanum
LANL	Los Alamos National Laboratory
LAST	Lead, antimony, silver, and tellurium, an n-type TE material
LAST/T	LAST/Tin, a p-type TE material
LB	Lattice-Boltzmann
L/D	Length-to-diameter ratio
lb ft	Pound foot
lb/min	Pounds per minute
lbs	Pounds
lbs/sec	Pounds per second
LD	Light-duty
LDT	Light-duty truck
LES	Large eddy simulation
LHV	Lower heating value
LIF	Laser-induced fluorescence

LII	Laser-induced incandescence
LLNL	Lawrence Livermore National Laboratory
LNT	Lean-NOx trap
LP	Low pressure
LPEGR	Low pressure exhaust gas recirculation
LPL	Low pressure loop
LRRI	Lovelace Respiratory Research Institute
LTC	Low-temperature combustion
LTR	Low-temperature reaction
m^2	Square meters
m^2/gm	Square meters per gram
m^3	Square meters
mA	Milliamps
MAS	Magic-angle spinning
MB	Mercedes-Benz
mbar	Millibar
MBT	Minimum (spark advance) for best torque; Maximum brake torque
Mg	Magnesium
mg/cm^2	Milligrams per square centimeter
mg/mi	Milligram per mile
mg/mm^2	Micrograms per square millimeter
mg/scf	Milligrams per standard cubic foot
mi	Mile
µs	Micro-second
min	Minute
MIT	Massachusetts Institute of Technology
MPI	Message-passing interface
µm	Micrometer
mm	Millimeter
mmols	Micro-moles
Mn	Manganese
Mo	Molybdenum
mol	Mole
mol/s	Moles per second
MPa	Megapascals
mph	Miles per hour
ms	Millisecond
MS	Mass spectrometry
MSATs	Mobile source air toxics
MSU	Michigan State University
MTU	Michigan Technological University
N_2	Diatomic nitrogen
N_2O	Nitrous oxide
N_2O_3	Nitrogen trioxide
Na	Sodium
NAAQS	National Ambient Air Quality Standards
Nd:YAG	Neodymium-doped yttrium aluminium garnet
NETL	National Energy Technology Laboratory
NExBTL	A patented Neste Oil (Finland) biodiesel fuel produced by a vegetable oil refining process; US-D – U.S. diesel fuel
NH_3	Ammonia
NIR	Near-infra-red
nm	Nanometer
Nm	Newton meter
NMEP	Net mean effective pressure
NMHC	Non-methane hydrocarbon
NMOG	Non-methane organic gases
NMR	Nuclear magnetic resonance
NO	Nitric oxide
NO_2	Nitrogen dioxide
NOP	Nozzle opening pressure
NOx	Oxides of nitrogen (NO and NO_2)
NRE	NOx reduction efficiency
ns	Nanosecond
NSE	NOx storage efficiency
NSR	NOx storage and reduction
NVH	Noise, vibration, and harshness
NVO	Negative valve overlap
O_2	Diatomic (molecular) oxygen
O_3	Ozone
OBD	On-board diagnostics
OC	Organic carbon
OEM	Original Equipment Manufacturer
OFCVT	Office of FreedomCAR and Vehicle Technologies
OH	Hydroxyl
OH*	Hydroxyl radical that emits ultraviolet photons
OHC	Oxygenated hydrocarbons
OH PLIF	Planar laser-induced fluorescence of OH
ORC	Organic Rankine Cycle
ORNL	Oak Ridge National Laboratory
OVT	Office of Vehicle Technologies
P	Pressure
PAH	Polycyclic aromatic hydrocarbon
PbTe	Lead telluride thermoelectric material
PCA	Principal component analysis
PCCI	Premixed charge compression ignition
PCI	Premixed compression ignition
PDF	Probability density function
P_{in}	Intake pressure
PIV	Particle image velocimetry

PLII	Planar laser-induced incandescence
PLIF	Planar laser induced fluorescence
PM	Particulate matter
PNNL	Pacific Northwest National Laboratory
PP	Plug position
ppb	Parts per billion
PPC	Partially premixed combustion
PPCI	Partially premixed compression ignition
ppi	Pores per square inch
ppm	Parts per million
Pr	Praseodymium
PRF	Primary Reference Fuels (iso-octane and n-heptane),
PRF80	PRF mixture with an octane number of 80 (i.e., 80% iso-octane and 20% n-heptane)
PRR	Pressure-rise rate
PSAT	Powertrain Systems Analysis Toolkit
psi	Pounds per square inch
psig	Pounds per square inch gauge
Pt	Platinum
PV	Pressure-volume
PWM	Pulse width modulated
Q	Heat
Q1, Q2, Q3, Q4	First, second, third and fourth quarters
QW	Quantum well
R&D	Research and development
RAPTR	Regenerative air preheating with thermochemical recuperation
RCF	Rapid compression facility
Redox	Reduction-oxidation
RGF	Residual gas fraction
Rh	Rhodium
RME	Rapeseed methyl ester
RPM, rpm	Revolutions per minute
RSNIR	Rapid scanning near-infra-red
RT	Room temperature
RV	Reed valve
S	Seebeck coefficient
S	Sulfur
SA	Spark assist(ed)
SAIC	Spark-assisted compression ignition
SCAQMD	South Coast Air Quality Management District
sccm	Standard cubic centimeters
SCF/min	Standard cubic feet per minute
SCORE	Sandia Compression-ignition Optical Research Engine
SCR	Selective catalytic reduction
sec	Second
SEM	Scanning electron microscopy
Si	Silicon
SI	Spark ignition, spark-ignited
SiC	Silicon carbide
SIDI	Spark ignition direct injection
SFC	Specific fuel consumption
SFTP	Supplemental Federal Test Procedure
SGS	Subgrid-scale
SLPM	Standard liters per minute
SNL	Sandia National Laboratories
SO_2	Sulfur dioxide
SOC	Start of combustion; soluble organic compound
SOI	Start of injection
SOF	Soluble organic fraction
SO_x	Oxides of sulfur
SpaciMS	Spatially resolved capillary inlet mass spectrometer
Sr	Strontium
SST	Single-stage turbo
Stdev	Standard deviation
STL	stereo-lithographic
SU	Stanford University
SULEV	Super ultra low emissions vehicle
SUV	Sports utility vehicle
SVOC	Semivoltaic organic compound
SwRI®	Southwest Research Institute®
T	Temperature
TAP	Temporal Analysis of Products
TCD	Thermal conductivity detector
TCR	Thermo-chemical recuperation
TDC	Top dead center
TE	Thermoelectric
TEG	Thermoelectric generator
TEM	Transmission electron spectroscopy
TEOM	Tapered element oscillating microbalance
TER	Thermal energy recovery
TGA	Thermal gravimetric analysis
TGM	Thermoelectric generator module
THC	Total hydrocarbon
T_{in}	Intake temperature
TNF	Turbulent nonpremixed flames
TPD	Temperature-programmed desorption
TPO	Temperature programmed oxidation
TPR	Temperature-programmed reduction or reaction

TPRX	Temperature-programmed reaction
TP-XRD	Temperature programmed X-ray diffraction
TR-XRD	Time resolved X-ray diffraction
TTW	Tank-to-wheels
TWC	Three-way catalyst
UCB	University of California Berkeley
UEGO	Universal exhaust gas oxygen
UHC	Unburned hydrocarbons
ULSD	Ultra-low sulfur diesel
UM	University of Michigan
US06	Supplemental Federal Test Procedure (SFTP) drive cycle
UV	Ultraviolet
UW	University of Wisconsin
UW-ERC	University of Wisconsin Engine Research Center
V	Volt
VAC	Volts, alternating current
VCR	Variable compression ratio
VDC	Volts – direct current
VGC	Variable geometry compressor
VGT	Variable geometry turbocharger
VIGV	Variable inlet guiding vane
VNT	Variable nozzle turbine
VOCs	Volatile organic compounds
VSD10	Volvo standard diesel (<10 ppm sulfur, by weight)
VTG	Variable turbine geometry
VVA	Variable valve actuation
VVT	Variable valve timing
W	Watt
WGS	Water-gas shift
WGSR	Water-gas-shift reaction
WHC	World harmonized cycle
WHR	Waste heat recovery
WNTE	Within not-to-exceed limit
WOT	Wide open throttle
wt%	Weight percent
WTT	Well-to-tank
XAFS	X-ray aborption fine structure
XANES	X-ray absorption near-edge spectroscopy
XPS	X-ray photoelectron spectroscopy
XRD	X-ray diffraction
Y	Yttrium
yr	Year
YTZP	Yttrium oxide (Y_2O_3) partially stabilized zirconia (Zr)
YSZ	Ytrria-stabilized zirconia
Zn	Zinc
Zr	Zirconium
ZT	Dimensionless thermoelectric figure of merit; equal to: (electrical conductivity) (Seebeck coefficient)^2(temperature)/ (thermal conductivity)

VII. Index of Primary Contacts

U.S. DEPARTMENT OF ENERGY | Energy Efficiency & Renewable Energy

For more information
1-877-EERE-INF (1.877.337.3463)
programname.energy.gov